Introduction to Vascular Neurosurgery

Justin R. Mascitelli
Mandy J. Binning
Editors

Springer

Introduction to Vascular Neurosurgery

Justin R. Mascitelli • Mandy J. Binning
Editors

Introduction to Vascular Neurosurgery

Springer

Editors
Justin R. Mascitelli
Department of Neurosurgery
University of Texas Health Science Center at San Antonio
San Antonio, TX, USA

Mandy J. Binning
Global Neurosciences Institute
Drexel University
Pennington, NJ, USA

ISBN 978-3-030-88195-5 ISBN 978-3-030-88196-2 (eBook)
https://doi.org/10.1007/978-3-030-88196-2

This Springer imprint is published by the registered company Springer Nature Switzerland AG
The registered company address is: Gewerbestrasse 11, 6330 Cham, Switzerland

Preface

We strove to cover the majority of neurovascular diseases and management in our textbook. In planning the content, we felt it was important that we covered both endovascular and microsurgical management. The first part reviews neurovascular anatomy, the basics of angiography, and the basics of craniotomies for neurovascular diseases. Next, an entire part is devoted to intracranial aneurysms, covering the natural history, subarachnoid hemorrhage, endovascular management, microsurgical management, and vasospasm. Following this, a number of chapters are devoted to stroke including natural history, mechanical thrombectomy, intracranial stenosis, Moyamoya disease, bypass surgery, vertebrobasilar insufficiency, intracerebral hemorrhage, sinus thrombosis, and the surgical and endovascular management of extracranial carotid disease. Next, we move on to vascular malformations including arteriovenous malformation, arteriovenous fistulas, carotid cavernous fistulas, vein of Galen malformations, spinal malformations, and cavernous malformations. Finally, we cover a few miscellaneous topics including more recent advances in neurovascular care such as venous sinus stenting for idiopathic intracranial hypertension and middle meningeal artery embolization for subdural hematoma. We hope that our textbook provides a comprehensive summary of neurovascular disease and management and will be of interest to medical students, residents, fellows, and young attendings.

The authors of the ensuing chapters were chosen as experts in their field. They are from centers across the country, and all have very busy practices. The reader will enjoy a great depth and breadth of knowledge from surgeons who are at the top of their fields. They are using the most recent advancements in endovascular techniques, while still having expertise and skill in open microvascular surgery. It was important that a book on vascular disorders of the brain and spine was written by surgeons who are experts in all available modalities to treat those disorders. Therefore, you will find explanations in the following chapters of open microvascular and endovascular approaches as well as discussions of radiosurgery, or no

treatment at all. We hope that this book will be comprehensive enough to be used as a daily reference, but also basic enough to be useful for residents and fellows for use in training.

San Antonio, TX, USA — Justin R. Mascitelli
Pennington, NJ, USA — Mandy J. Binning

Contents

Part III Stroke

Part IV Vascular Malformations

Contributors

Rami O. Almefty, MD Department of Neurosurgery, Temple University Hospital, Philadelphia, PA, USA

Neil Almeida, BS School of Medicine and Health Sciences, The George Washington University, Washington, DC, USA

Ali Al Balushi, MD Department of Neurological Surgery, Weill Cornell Medical College/New York Presbyterian Hospital, New York City, NY, USA

Sujani Bandela, MD Department of Neurology, Division of Vascular Neurology, University of Texas Health San Antonio, San Antonio, TX, USA

Jacob F. Baranoski, MD Department of Neurosurgery, Barrow Neurological Institute, St. Joseph's Hospital and Medical Center, Phoenix, AZ, USA

Daniel L. Barrow, MD Department of Neurosurgery, Emory University School of Medicine, Atlanta, GA, USA

Joshua Bederson, MD Department of Neurological Surgery, Mount Sinai Health System, New York, NY, USA

Bernard R. Bendok, MD, MSCI Department of Neurological Surgery, Mayo Clinic, Phoenix, AZ, USA

Precision Neuro-therapeutics Innovation Lab, Mayo Clinic, Phoenix, AZ, USA

Neurosurgery Simulation and Innovation Lab, Mayo Clinic, Phoenix, AZ, USA

Department of Otolaryngology, Mayo Clinic, Phoenix, AZ, USA

Department of Radiology, Mayo Clinic, Phoenix, AZ, USA

Lee A. Birnbaum, MD, MS Department of Neurology, Division of Vascular Neurology, University of Texas Health San Antonio, San Antonio, TX, USA

Jan-Karl Burkhardt, MD Department of Neurosurgery, Hospital of the University of Pennsylvania, Philadelphia, PA, USA

Joshua D. Burks, MD University of Miami Miller School of Medicine, Department of Neurosurgery, Miami, FL, USA

Bryan E. Buster, MD Department of Neurosurgery, Emory University School of Medicine, Atlanta, GA, USA

Justin M. Cappuzzo, MD Department of Neurosurgery, Jacobs School of Medicine and Biomedical Sciences, University at Buffalo, Buffalo, NY, USA

Department of Neurosurgery, Gates Vascular Institute at Kaleida Health, Buffalo, NY, USA

Daniel D. Cavalcanti, MD, PhD Department of Neurosurgery, Ayer Neuroscience Institute, St. Vincent's Medical Center, Bridgeport, CT, USA

Neeraj Chaudhary, MD Department of Radiology, University of Michigan, Ann Arbor, MI, USA

Nader Delavari, MD Department of Neurosurgery, New York University School of Medicine, New York, NY, USA

Dale Ding, MD Department of Neurological Surgery, University of Louisville School of Medicine, Louisville, KY, USA

Rimal H. Dossani, MD Department of Neurosurgery, Jacobs School of Medicine and Biomedical Sciences, University at Buffalo, Buffalo, NY, USA

Department of Neurosurgery, Gates Vascular Institute at Kaleida Health, Buffalo, NY, USA

Ehsan Dowlati, MD, MS Department of Neurosurgery, MedStar Georgetown University Hospital, Washington, DC, USA

Augusto Elias, MD Interventional Neuroradiology, Metro Health- University of Michigan Health, Grand Rapids, MI, USA

Alejandro Enriquez-Marulanda, MD Neurosurgery Service, Beth Israel Deaconess Medical Center, Harvard Medical School, Boston, MA, USA

Sheila R. Eshraghi, MD Department of Neurosurgery, Emory University School of Medicine, Atlanta, GA, USA

Daniel R. Felbaum, MD Department of Neurosurgery, MedStar Georgetown University Hospital, Washington, DC, USA

Department of Neurosurgery, MedStar Washington Hospital Center, Washington, DC, USA

Christina Feller, BS, BA Department of Neurological Surgery, Medical College of Wisconsin, Milwaukee, WI, USA

Justin F. Fraser, MD Departments of Neurosurgery, Neurology, Radiology, and Neuroscience, University of Kentucky, Lexington, KY, USA

Joseph J. Gemmete, MD Department of Radiology, University of Michigan, Ann Arbor, MI, USA

Santiago Gomez-Paz, MD Department of Neurological Surgery, Mount Sinai Health System, New York, NY, USA

Vaidya Govindarajan, BS University of Miami Miller School of Medicine, Department of Neurosurgery, Miami, FL, USA

Jonathan A. Grossberg, MD Department of Neurosurgery, Emory University School of Medicine, Atlanta, GA, USA

Vivek P. Gupta, MD Washington University in St. Louis, Department of Neurosurgery, St. Louis, MO, USA

Zakaria Hakma, MD, FACS, FAANS Global Neuroscience Institute (GNI), Chester, PA, USA

Hirad Hedayat, MD Department of Neurological Surgery, Medical College of Wisconsin, Milwaukee, WI, USA

Daniel A. Hoit, MD University of Tennessee/Semmes-Murphey Clinic Department of Neurosurgery, Knoxville, TN, USA

Brian M. Howard, MD Department of Neurosurgery, Emory University School of Medicine, Atlanta, GA, USA

Department of Radiology and Imaging Sciences, Emory University School of Medicine, Atlanta, GA, USA

Anna L. Huguenard, MD Washington University in St. Louis, Department of Neurosurgery, St. Louis, MO, USA

Aria M. Jamshidi, MD University of Miami Miller School of Medicine, Department of Neurosurgery, Miami, FL, USA

Peter Kan, MD Department of Neurosurgery, University of Texas Medical Branch, Galveston, TX, USA

Anand Kaul, MD Department of Neurosurgery, Temple University Hospital, Philadelphia, PA, USA

Christopher P. Kellner, MD Department of Neurosurgery, Icahn School of Medicine at Mount Sinai, New York, NY, USA

Jared Knopman, MD Department of Neurological Surgery, Weill Cornell Medical College/New York Presbyterian Hospital, New York City, NY, USA

Svetlana Kvint, MD Department of Neurosurgery, Hospital of the University of Pennsylvania, Philadelphia, PA, USA

Michael T. Lawton, MD Department of Neurosurgery, Barrow Neurological Institute, St. Joseph's Hospital and Medical Center, Phoenix, AZ, USA

Neuroscience Publications, Phoenix, AZ, USA

Elad I. Levy, MD, MBA Department of Neurosurgery, Jacobs School of Medicine and Biomedical Sciences, University at Buffalo, Buffalo, NY, USA

Department of Neurosurgery, Gates Vascular Institute at Kaleida Health, Buffalo, NY, USA

Department of Radiology, Jacobs School of Medicine and Biomedical Sciences, University at Buffalo, Buffalo, NY, USA

Canon Stroke and Vascular Research Center, University at Buffalo, Buffalo, NY, USA

Jacobs Institute, Buffalo, NY, USA

Kenneth M. Liebman, MD, FACS, FAANS Global Neurosciences Institute, Pennington, NJ, USA

Evan M. Luther, MD University of Miami Miller School of Medicine, Department of Neurosurgery, Miami, FL, USA

Bianca Marquez, MS Drexel University College of Medicine, Philadelphia, PA, USA

Justin R. Mascitelli, MD Department of Neurosurgery, University of Texas Health Science Center at San Antonio, San Antonio, TX, USA

Abigail P. McCallum, MD Department of Neurological Surgery, University of Louisville School of Medicine, Louisville, KY, USA

J Mocco, MD, MS Department of Neurosurgery, Icahn School of Medicine at Mount Sinai, New York, NY, USA

Alina Mohanty, BA Department of Neurosurgery, Baylor College of Medicine, Houston, TX, USA

Aaisha S. Mozumder, MD Department of Neurology, Division of Vascular Neurology, University of Texas Health San Antonio, San Antonio, TX, USA

William Muñoz, MD, PhD Department of Neurosurgery, Massachusetts General Hospital and Harvard Medical School, Boston, MA, USA

Stanislav Naydin, MD, Pharm BS Global Neurosciences Institute, Pennington, NJ, USA

Matías Negrotto, MD Hospital Maciel, Montevideo, Uruguay

Hospital Universitario de Clínicas, Montevideo, Uruguay

Vincent N. Nguyen, MD University of Tennessee/Semmes-Murphey Clinic Department of Neurosurgery, Knoxville, TN, USA

Felix Nwajei, MD, PhD Department of Neurosurgery, Boston Medical Center, Boston, MA, USA

Christopher S. Ogilvy, MD Neurosurgery Service, Beth Israel Deaconess Medical Center, Harvard Medical School, Boston, MA, USA

Endovascular and Operative Neurovascular Surgery, BIDMC Brain Aneurysm Institute, Professor of Neurosurgery, Harvard Medical School, Boston, MA, USA

Joshua W. Osbun, MD Washington University in St. Louis, Department of Neurosurgery, St. Louis, MO, USA

Aditya S. Pandey, MD Department of Neurosurgery, University of Michigan, Ann Arbor, MI, USA

Aman B. Patel, MD Department of Neurosurgery, Massachusetts General Hospital and Harvard Medical School, Boston, MA, USA

Nicole De La Pena, BS Mayo Clinic Alix School of Medicine, Mayo Clinic, Scottsdale, AZ, USA

Eric Quach, MD Department of Neurosurgery, Temple University Hospital, Philadelphia, PA, USA

Rudy J. Rahme, MD Department of Neurological Surgery, Mayo Clinic, Phoenix, AZ, USA

Precision Neuro-therapeutics Innovation Lab, Mayo Clinic, Phoenix, AZ, USA

Neurosurgery Simulation and Innovation Lab, Mayo Clinic, Phoenix, AZ, USA

Department of Neurosurgery, Global Neuroscience Institute, Philadelphia, PA, USA

Gary Rajah, MD Interventional Neurosurgery, Munson Health, Traverse City, MI, USA

Howard A. Riina, MD Department of Neurosurgery and Radiology, New York University School of Medicine, New York, NY, USA

Andrew J. Ringer, MD Mayfield Clinic, Cincinnati, OH, USA

Christina P. Rossitto, BS Department of Neurosurgery, Icahn School of Medicine at Mount Sinai, New York, NY, USA

Mithun G. Sattur, MD Medical University of South Carolina, Mt Pleasant, SC, USA

Fazeel M. Siddiqui, MD Interventional Neurology, Metro Health- University of Michigan Health, Grand Rapids, MI, USA

Vasu A. Sinai, MD University of Miami Miller School of Medicine, Department of Neurosurgery, Miami, FL, USA

Rohin Singh, BS Mayo Clinic Alix School of Medicine, Mayo Clinic, Scottsdale, AZ, USA

R. Christopher Spears, MD Department of Neurosurgery, University of Kentucky, Lexington, KY, USA

Alejandro M. Spiotta, MD Medical University of South Carolina, Mt Pleasant, SC, USA

Anja I. Srienc, MD, PhD Washington University in St. Louis, Department of Neurosurgery, St. Louis, MO, USA

Christopher J. Stapleton, MD Department of Neurosurgery, Massachusetts General Hospital and Harvard Medical School, Boston, MA, USA

Robert M. Starke, MD University of Miami Miller School of Medicine, Department of Neurosurgery, Miami, FL, USA

Mohanad Sulaiman, MD Global Neuroscience Institute (GNI), Chester, PA, USA

Halima Tabani, MD Department of Neurological Surgery, Mount Sinai Health System, New York, NY, USA

Ryan Tackla, MD Mayfield Clinic, Cincinnati, OH, USA

Evelyn L. Turcotte, BS Department of Neurological Surgery, Mayo Clinic, Phoenix, AZ, USA

Precision Neuro-therapeutics Innovation Lab, Mayo Clinic, Phoenix, AZ, USA

Neurosurgery Simulation and Innovation Lab, Mayo Clinic, Phoenix, AZ, USA

Erol Veznedaroglu, MD, FAHA, FACS, FAANS Department of Neurosurgery, Drexel University College of Medicine, Drexel Neurosciences Institute, Global Neurosciences Institute, Philadelphia, PA, USA

Muhammad Waqas, MBBS Department of Neurosurgery, Jacobs School of Medicine and Biomedical Sciences, University at Buffalo, Buffalo, NY, USA

Department of Neurosurgery, Gates Vascular Institute at Kaleida Health, Buffalo, NY, USA

Kurt Yaeger, MD Department of Neurological Surgery, Mount Sinai Health System, New York, NY, USA

Tianzan Zhou, MD Department of Neurosurgery, MedStar Georgetown University Hospital, Washington, DC, USA

Part I
Basics of Vascular Anatomy and Neurosurgical Treatment

Chapter 1
Vascular Anatomy of the Brain

Stanislav Naydin, Bianca Marquez, and Kenneth M. Liebman

Introduction

This chapter describes the vascular anatomy of the brain including the arterial supply and venous drainage. The arterial supply is robust, composed of an anterior circulation and posterior that anastomose via the circle of Willis. The anterior circulation is supplied by the internal carotid arteries (ICAs). The ICA terminates below the anterior perforated substance by bifurcating into the anterior cerebral artery (ACA) and middle cerebral artery (MCA). The ACA divides into separate segments derived upon its anatomic relationship to the corpus callosum and the anterior communicating artery. MCA forms as a terminal branch of the ICA to run initially at the floor of the middle cranial fossa. As the artery continues, giving off branches of subsequent diminutive and progressively smaller in caliber vessels. The posterior communicating artery (PCOM) arises from the most posterior segment of the intradural ICA and serves to connect the ICA to the posterior cerebral artery (PCA). PCA arises ventrally from the basilar artery (BA) as terminal branches bilaterally. The vertebral arteries project superiorly and enter through the foramen magnum to enter the dura to become the intradural segment (V4). It is V4 that unites bilaterally at the pontomedullary junction to form the basilar artery (BA). The BA spans from its origin within the prepontine cistern to the interpeduncular cistern where it bifurcates into terminal branches as the PCAs.

The surface of the brain is drained by the three major superficial veins: the superior, the superficial middle, and the inferior cerebral veins. These veins drain

S. Naydin (✉) · K. M. Liebman
Global Neurosciences Institute, Pennington, NJ, USA
e-mail: snaydin@gnineuro.org; kliebman@gnineuro.org

B. Marquez
Drexel University College of Medicine, Philadelphia, PA, USA
e-mail: bsm72@drexel.edu

J. R. Mascitelli, M. J. Binning (eds.), *Introduction to Vascular Neurosurgery*,
https://doi.org/10.1007/978-3-030-88196-2_1

into the dural venous sinus system. Dural venous sinuses are intracranial venous channels between the two layers of the dura. Unlike other veins in the body, they run alone, not parallel to arteries. Venous sinuses are valveless, allowing for bidirectional blood flow. This consists of the superior sagittal sinus, inferior sagittal sinus, straight sinus, transvers sinus, sigmoid sinus, occipital sinus, and cavernous sinus.

Internal Carotid Artery

C1, Cervical

The anterior circulation is supplied by the internal carotid arteries (ICA). Several nomenclature schemes exist; Bouthillier segmental nomenclature is most clinically useful and is composed of seven segments ascending with the course of the artery. (Figs. 1.1 and 1.2) The internal carotid artery forms at the bifurcation of the common carotid artery (CCA), most commonly occurring at C4, with some variation. At its origin, the internal carotid artery is somewhat dilated. This part of the artery is known as the carotid sinus or the carotid bulb. The carotid sinus is sensitive to pressure changes in the arterial blood at this level. It is the major baroreceptor site in humans and most mammals.

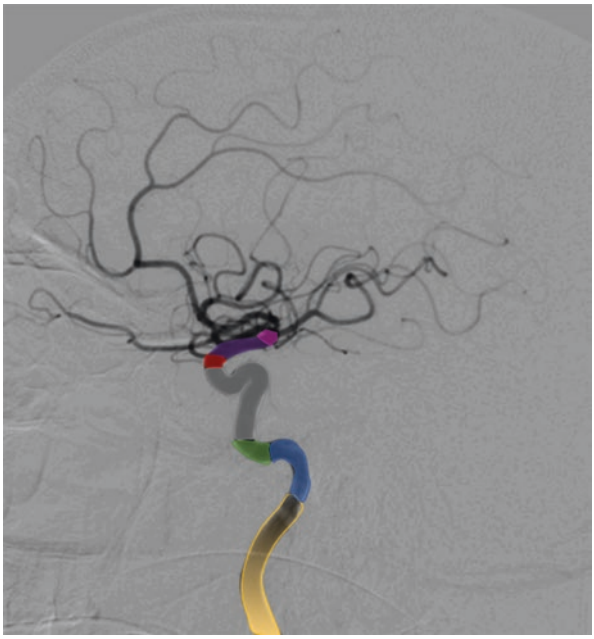

Fig. 1.1 Lateral angiogram of the right internal carotid artery: yellow – C1 (cervical), blue – C2 (petrous), green – C3 (lacerum), gray – C4 (cavernous), red – C5 (clinoidal), purple – C6 (ophthalmic), pink – C7 (communicating)

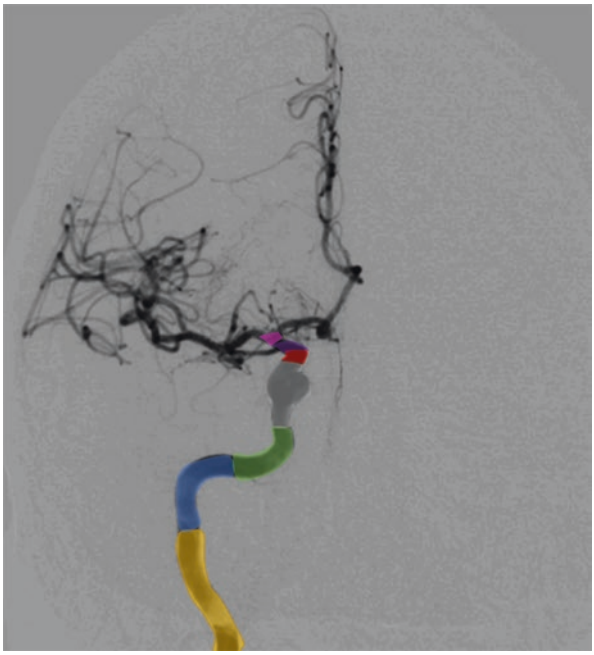

Fig. 1.2 AP angiogram of the right internal carotid artery: yellow – C1 (cervical), blue – C2 (petrous), green – C3 (lacerum), gray – C4 (cavernous), red – C5 (clinoidal), purple – C6 (ophthalmic), pink – C7 (communicating)

The internal carotid runs vertically in the carotid sheath and enters the skull through the carotid canal. The ICA is relatively superficial at its start where it is contained in the carotid triangle of the neck and lies behind and lateral to the external carotid. It courses superiorly where it passes beneath the parotid gland being crossed by the hypoglossal nerve, the digastric muscle, the stylohyoid muscle, the occipital artery, and the posterior auricular artery.

The ICA runs in the carotid sheath medial to the internal jugular vein (IJV). The vagus nerve lies on a plane posterior and lateral to the artery, essentially between and posterior to the ICA and IJV.

Unlike the external carotid artery, the internal carotid artery normally has no branches in the neck.

C2, Petrous

At the skull base, C1 transitions to the C2 portion as it courses through the carotid canal. Here, the petrous ICA ascends, and the artery turns medially in the skull base. The artery continues superiorly toward foramen lacerum not traveling through it as it exits the carotid canal with an anterior trajectory to become C3, the lacerum segment. The petrous portion has three portions: an ascending or vertical part, the genu (bend), and the horizontal portion.

C3, Lacerum

The C3 portion is a short segment that begins above the foramen lacerum (again, not traveling through lacerum) and terminates at the petrolingual ligament, transitioning into the cavernous segment, C4.

C4, Cavernous

The cavernous ICA travels through the cavernous sinus, exiting superiorly through the inner, proximal dural ring. The artery has a distinct trajectory; first, ascending toward the posterior clinoid process, then traveling forward, horizontally by the side of the body of the sphenoid bone, then again curving upward, medial to the anterior clinoid process. This creates an "s" shape referred to as the carotid siphon.

There are two main branches emanating from this portion, the meningohypophoseal artery and the inferior lateral trunk. The artery of Bernasconi and Cassinari, also known as medial or marginal tentorial artery, is a 2 cm long branch from the meningohypophoseal artery. Due to their small size, these arteries are not well depicted on angiography in the absence of pathological increased flow through them. More common disorders that result in engorgement of these arteries, especially the Bernasconi and Cassinari artery, are tentorial meningiomas and tentorial dural arteriovenous fistulas.

The cavernous sinus also gives off small capsular branches that supply the wall of the cavernous sinus.

C5, Clinoidal

C5, the clinoidal segment, starts as the ICA exits the cavernous segment at the proximal dural ring and courses the distance extending to the outer or distal dural ring. This is an important segment because at this point the artery is considered intradural, in the subarachnoid space. Aneurysms arising from this portion are considered intradural and often are referred to as "junctional" aneurysms. Although not common, the ophthalmic artery may arise from this portion.

C6, Ophthalmic

C6, the ophthalmic segment, originates at the distal dural ring and extends to the posterior communicating artery origin. Aneurysms at or above this point that rupture would occupy the subarachnoid space. This forms the superior aspect of the

anterior genu, projecting posteriorly and superiorly. Two branches arise from this segment, the ophthalmic artery and superior hypophyseal artery.

C7, Communicating

C7, the communicating segment, spans to include the formation of the posterior communicating artery to the ICA termination, just prior to the anterior perforated substance. It divides into anterior and middle cerebral arteries. This bifurcation occurs in the proximal Sylvian fissure. The C7 segment is bordered by the optic nerve (CNII) in the superior medial direction and oculomotor nerve (CNIII) inferiorly.

Intracranial Branches of ICA

Ophthalmic Artery

The ophthalmic artery (OA) is most commonly the first major intradural branch of the ICA. Researchers have found that in 83.6% of the cases the ophthalmic artery arises above the dura to follow an intradural course. In 6.6% of cases, it arises just above dura, and in 10% it arises below dura to follow a totally or partial extradural course [2–5]. The ophthalmic artery originates from the ICA anteriorly or sometimes anteromedially as the ICA emerges from the cavernous sinus. This artery projects anteriorly to enter the orbit following the optic nerve in the optic canal. The ophthalmic artery travels with the optic nerve (CNII) superiormedially. The oculomotor (CNIII) and abducens nerves (CNIV) pass laterally. Eventually the OA takes a more superior medial path to the medial orbital wall by passing between the optic nerve and the superior rectus muscle.

The first branch, and the most critical branch, is the central retinal artery that vascularizes the retina and is of essential importance for vision [38]. It is one of the smaller branches from the ophthalmic. This artery enters the optic nerve, traveling along the center of the nerve, ending in the eye supplying the blood to the inner retinal layers. The next branch is the lacrimal artery, along several minor arteries to supply the extraocular muscles as well as periosteum in the region. The lacrimal artery follows the course of the lateral rectus muscle along its superior border to supply the lacrimal gland as well as conjunctiva. A notable branch emanating from the lacrimal artery is the recurrent meningeal artery. This branch travels in the reverse direction to pass through the superior orbital fissure to provide anastomosis with the middle meningeal artery. Additional branches off the ophthalmic artery include: supraorbital, medial palpebral, infratrochlear, supratrochlear, and dorsal nasal artery.

The terminal branches also establish extensive anastomoses with branches of the facial, maxillary, and superficial temporal arteries, all of which arise from the external carotid artery. Thereby, the ophthalmic artery establishes a connection between the internal and external carotid artery systems.

Superior Hypophyseal Artery

The superior hypophyseal artery (or arteries) is (are) medial or posterior-medial branch(s) off the internal carotid artery. In 85% of cadaveric dissections it arises within 5 mm of the ophthalmic artery. There are two distinct patterns of this artery. In 42% cases there is a large dominant artery that branches like a candelabra supplying the pituitary stalk, optic nerve (CNII), and chiasm. When a large trunk is not present, two or three smaller, medial projecting vessels are found [5].

Anterior Choroidal Artery

The anterior choroidal artery (AChA) is the last named branch given off the ICA prior to its bifurcation into the anterior cerebral artery and the middle cerebral artery. This artery is relatively small, but AchA can be visualized in 95% of angiograms, at times as a plexus of small vessels. AchA has a distinct "check" shape at its origin off the ICA (Fig. 1.3). The cisternal segment projects toward the choroid plexus of the lateral ventricle. The artery first courses postero-medially below the optic tract with the temporal lobe uncus lying inferior-laterally and then taking a more posterior lateral course after curving around the cerebral peduncle within the

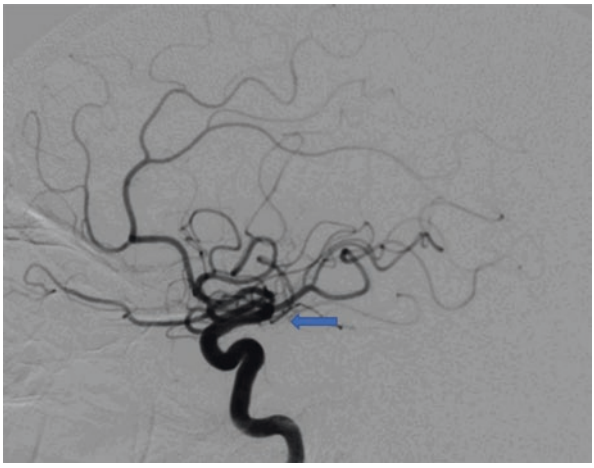

Fig. 1.3 Lateral ICA angiogram; blue arrow pointing to the "check" sign at the origin of the anterior choroidal artery

crural cistern. After continuing to the lateral geniculate body, the AchA generally takes a sharp angle to enter the temporal horn through the choroidal fissure.

As the distal segment or intraventricular AchA continues at the choroidal fissure, it wraps around the pulvinar of the thalamus. Following the choroid plexus in the supracornual cleft. It may continue anteriorly here for a short distance and some have reported AchA extension to the foramen of Monro to anastomose with the medial posterior choroidal artery [6].

Anterior Cerebral Artery

The ICA terminates below the anterior perforated substance by bifurcating into the anterior cerebral artery (ACA) and middle cerebral artery (MCA). The ACA is divided into separate segments derived upon its anatomic relationship to the corpus callosum and the anterior communicating artery.

A1, Pre-communicating

The proximal A1 is the pre-communicating or at times referred to as the horizontal segment. A1 starts immediately from the bifurcation of the ICA forming and extending to the anterior communicating artery complex. The A1 courses straight and medially to the interhemispheric fissure. A1 passes over the optic nerve (CNII) 70% or optic chiasm in 30% of cadaveric dissections. The A1 connects with the anterior communicating artery (Acom) just inferiorly or at the interhemispheric fissure.

The A1 segment provides small perforating branches in the inferior direction for blood supply to the optic chiasm, hypothalamus, and anterior corpus collosum. The horizontal segment also contributes the medial lenticulostriate arteries in the posterosuperior direction through the anterior perforated substance to supply globus pallidus and medial portion of the putamen. These perforating arteries are unpaired with little to no collateral flow, any occlusion or decrease in flow leaves little opportunity for collateral flow to provide adequate perfusion [7].

Anterior Communicating Artery

Anterior communicating artery (ACom) is a horizontal interconnection between the bilateral ACAs within or inferiorly to the interhemispheric fissure. This provides a clinically significant anastomosis between the two hemispheres and ICAs, comprising the anterior portion of the circle of Willis. Along with A1, ACom can contribute perforating arteries to the basal ganglia. There are no cortical branches formed at ACom.

A2, Post-communicating

The A2 segment continues medially and anteriorly as the infracallosal segment also known as the post-communicating segment. This portion travels from ACom along the rostrum of the corpus callosum to the genu in a vertical direction.

A2 is commonly the site of the formation of the recurrent artery of Heubner. Cadaveric dissections demonstrate variance up to 45% from A1 and 5% from ACom. This is the largest and only named branched artery gaining its name from the course it takes by retracing the ACA in the reverse direction at a sharp angle to terminate dorsally and laterally to the carotid terminus. At times, Heubner will continue to the anterior perforated substance close to or just anterior to the Sylvian fissure [6, 8].

Additional branches of the ACA are generally small and demonstrate irregularity, as a result named after the areas that are supplied. These include the orbital, frontal, orbitofrontal, and frontopolar arteries. The orbitofrontal artery, frequently the first branch of the A2 segment, passes anteriorly and inferiorly toward the anterior cranial fossa to terminate in the orbitofrontal cortex. The orbitofrontal artery provides bloody supply to gyrus rectus, medial orbital gyrus, olfactory bulb, as well as tract. When identifiable, the frontopolar artery can be seen forming below the corpus collosum to flow anteriorly to the frontal pole to supply the ventromedial surface of the frontal pole as well as parts of the frontal convexity.

A3, Precallosal

The ACA continues superiorly to wrap around the genu of the corpus callosum to become the precallosal segment. A3 runs until the artery turns directly posterior to lie above the corpus collosum within the interhemispheric fissure. A3 terminates as a bifurcation into pericallosal and callosomarginal arteries, at times referred to as the A4 and A5 segments, respectively. The ACA continues as the pericallosal artery to course over the body of the corpus callosum. The callosomarginal artery passes in the cingulate gyrus and also continues posteriorly. Both of these terminal branches run under the falx cerebri and provide collateral circulation with the MCA and PCA territories; referred to as the “watershed zone.”

Pericallosal Artery

The pericallosal artery is the distal portion of the ACA that courses over the superior surface of the body of the corpus callosum in the pericallosal cistern. It gives off many small branches to the corpus callosum.

Some authors describe the pericallosal artery as the entire distal portion of the ACA beginning at the anterior communicating artery, segments A2–A5. This includes the portion anterior to the lamina terminalis, the rostrum, and genu of the

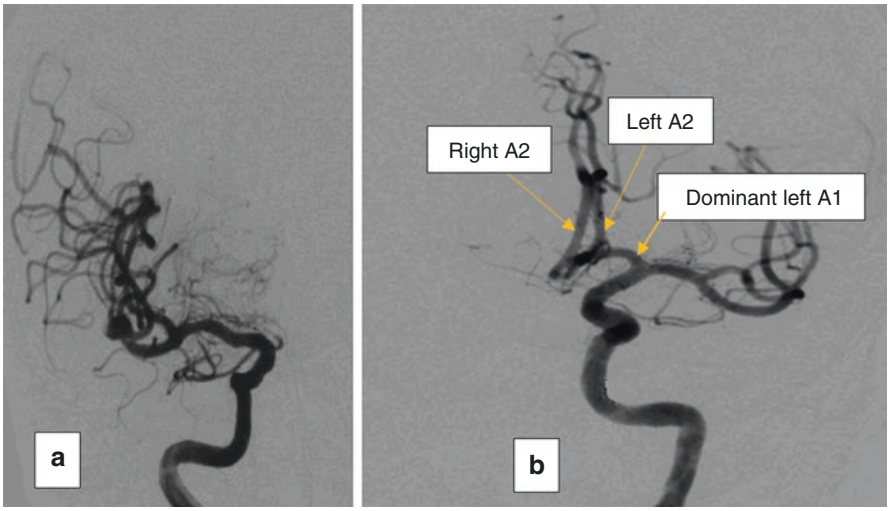

Fig. 1.4 (**a**) Selective right internal carotid artery angiogram depicting an absent right A1. (**b**) A selective left internal carotid artery angiogram. One can see the left A1 is quite robust filling both A2s, right and left

corpus callosum [38, 39]. Other authors define it as the artery created at the bifurcation of the ACA near the genu of the corpus callosum after giving off the callosomarginal artery, segments A3–A5 [38].

ACA can exist as several different normal variants. A1 can be hypoplastic on one side with the contralateral side compensating (Fig. 1.4). The ACA can also form as an azygous artery. In this case a single large artery running in the interhemispheric fissure provides necessary bilateral vasculature.

Middle Cerebral Artery

The middle cerebral artery (MCA) forms as a terminal branch of the ICA to initially run along the floor of the middle cranial fossa. As the artery continues, giving off branches of subsequent diminutive and progressively smaller caliber vessels, the MCA nomenclature changes.

M1, Horizontal

The most proximal MCA segment from the ICA branch point is the M1 or horizontal segment running almost perfectly perpendicular from the ICA to its bifurcation and then the Sylvian fissure. The optic chiasm lies medially, and the olfactory trigone remains anterior. M1 consists of the pre-bifurcation segment and

post-bifurcation segment, approximately 10 mm from ICA terminus. Studies have shown that division of M1 results in a bifurcation in 78%, trifurcation in 12%, and > 3 trunks in 10% of cases. Following this division, the arteries continue to travel in parallel just below the anterior perforating substance to the genu of the Sylvian fissure.

The pre-bifurcation portion of M1 produces the anterior temporal artery tracking anteriorly and inferiorly to run over the temporal lobe to provide vascular supply to the anterior third of the superior, middle, and inferior temporal gyri [12].

It is the proximal M1 segment that gives off the lateral lenticulostriate arteries which serve as perforating arteries supplying the internal capsule via the perforating substance. More distally, still within the horizontal segment, the lateral lenticulostriate arteries form and ascend in the external capsule to pass through the basal ganglia medially to supply the caudate nucleus.

M2, Insular

The M2 segment begins in the Sylvian fissure at the genu where the post-bifurcation segment turns superiorly in its course at the limen insulae and continues to pass over around the insula. Along this path dividing further into up to eight stem arteries which travel around the insula in the cerebrospinal cistern to become M3 (Fig. 1.5).

M3, Opercular

M3 or opercular segment is the superior portion of the circular sulcus as M2 courses more laterally within the Sylvian fissure and to the surface of the lateral cerebral fissure. The MCA continues to form M3 branches which travel to frontal, parietal, and temporal operculum. The artery forms a loop over the top of the Sylvian fissure as the branches turn laterally to exit the fissure to run over the hemisphere.

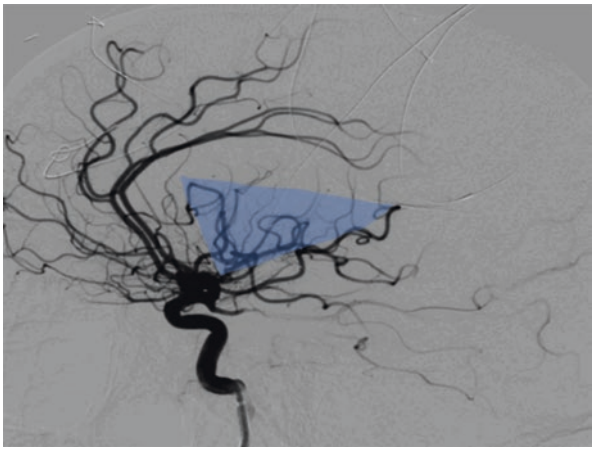

Fig. 1.5 Lateral view cerebral angiogram. Internal carotid artery injection with the blue shaded area demonstrating filling of Sylvian triangle within Sylvian fissure by branches of MCA

M4, Cortical Branches

M4 is the distal most portion of the MCA forming the terminal branches which begin at the surface of the Sylvian fissure as the distal M4 branches to pass over the cortical surface. Up to 12 named branches can be observed. These are generally divided into three groups: anterior, intermediate, and posterior branches based on the territory that they supply.

Anterior Branches

The anterior group of branches consists of the orbitofrontal and prefrontal arteries that supply the frontal lobe in an overlapping pattern, with the prefrontal forming a candelabra to provide arterial vasculature to lateral frontal lobe in front of the Sylvian triangle. The orbitofrontal arteries, as their name implies, give supply to the inferior surface of the frontal lobe overlying the orbits.

Intermediate Branches

Intermediate branches span the distance between the precentral sulcus and postcentral sulcus with nomenclature derived from each branch's relationship to the sulci. Precentral, also referred to as the prerolandic artery, courses superficially between the posterior part of the frontal lobe and anterior edge of the parietal operculum supplying small branches within the precentral and central sulci.

The central sulcus is further supplied by a dedicated branch, or rolandic artery (at times several branches), that project between the precentral and postcentral sulci.

Finally, the postcentral sulcus artery flows within the corresponding sulcus and continues in the intraparietal sulcus.

Posterior Branches

Posterior branches of M4 provide vasculature to the remaining MCA territory consisting of parietal, temporal, and occipital lobes named for each corresponding lobe.

The posterior parietal artery travels in the posterosuperior path over the end of the Sylvian fissure and then anteriorly along the posterior of the parietal lobe. The posterior parietal artery then continues to the supramarginal gyrus.

The temporo-occipital artery travels in the superior temporal sulcus in the dorsal direction to the superior temporal gyrus with branches to the occipital region.

The posterior temporal artery passes the superior temporal gyrus to run superiorly with a sudden downward turn into the superior temporal sulcus to continue to the inferior temporal sulcus to provide vasculature to the posterior portion of the temporal lobe.

Medial Temporal Artery

The medial temporal artery crosses the superior temporal gyrus to supply the inferior temporal sulcus.

Posterior Cerebral Artery

The posterior cerebral artery (PCA) arises ventrally from the basilar artery as terminal branches bilaterally, traveling in either the interpeduncular cistern or the suprasellar cistern.

P1, Pre-communicating

The most proximal segment forms at the basilar artery junction (P1) called the precommunicating or mesencephalic segment. P1 can form in the interpeduncular cistern, posterior to the dorsum sellae or inferior to the third ventricular floor in the suprasellar cistern. P1 extends to the anastomosis with the posterior communicating artery. P1 follows the midbrain and curves around it. At times the PCA can be found in a variant type. In a fetal origin of the posterior cerebral artery the posterior communicating artery (PCOM) branching off the ICA is larger than the posterior cerebral artery (PCA) originating from the basilar. Subsequently the larger fetal type supplies the bulk of the blood to the PCA distribution. Alternatively, the PCA can come directly off of the ICA and there is no PCA from the basilar. This is a common variant in the posterior cerebral circulation, estimated to occur in 20–30% of individuals (Figs. 1.5 and 1.6).

P1 provides perforating arteries to the brainstem and thalamus, the posterior thalamoperforating arteries (PTPAs). The PTPAs initially course posterosuperiorly within the interpeduncular fossa. They pass in the posterior perforated substance posterior to the mammillary bodies. Up to 42% of studied specimens demonstrated that the posterior thalamoperforating arteries were the largest branches from P1 [16]. It has been observed in 80% of occurrences that the posterior thalamoperforating arteries have anastomoses within themselves [17].

The artery of Percheron (AoP) is a rare anatomical variation of the posterior circulation in which a single arterial trunk arises from the posterior cerebral artery (PCA) to supply both sides of the thalamus and midbrain.

P2, Ambient

The second segment, P2, gains its name from the ambient cistern within which it lies. The ambient segment starts from the PCOM branch point spanning to the dorsal midbrain. Its path is parallel to the optic tract and basal vein of Rosenthal.

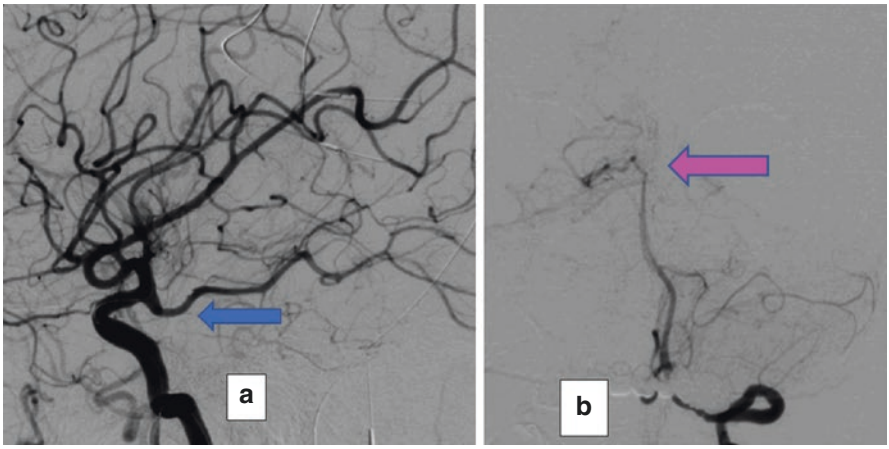

Fig. 1.6 (**a**) A lateral angiogram of the left ICA. The blue arrow points to the PCA emanating from the ICA. (**b**) Angiogram is a left vertebral injection. The pink arrow points to where the left PCA should project originating off the basilar apex. It is absent, again arising from the ICA

Perforating Arteries

Thalamogeniculate perforating arteries generally branch from P2, with up to 20% originating from P3. The number of perforating branches has a high variance from 2 to 12. Cadaveric dissection demonstrates the formation of these vessels in 66% of cases as individual vessel, and in the remaining as a common trunk that then branches into small perforating vessels.

The peduncular perforating arteries branch from P2 and again have many variations, from zero to six vessels, to supply the cerebral peduncle [15].

The medial posterior choroidal artery has been shown to originate from P2 in 70% of cadaveric dissections, from P1 in 12%, or the parietooccipital artery in 12%. However, it is worthwhile to mention that of cadavers investigated it was only present in 10–45% of cases [15]. From the parent vessel the medial posterior choroidal artery circumvents the brainstem to then flow in the superior medial direction through the roof the third ventricle running in between the bilateral thalami to supply the choroid plexus in the lateral ventricle by passing through foramen of Monro.

Lateral posterior choroidal arteries most commonly form as several vessels from P2. The lateral posterior choroidal arteries enter the choroid plexus of the temporal horn via the choroidal fissure to wrap around the thalamic pulvinar in the lateral ventricle. These small perforating arteries anastomose with both the medial posterior choroidal arteries and anterior choroidal artery from ICA.

Cortical

P2 has two commonly accepted cortical artery branches. The first branch is the anterior temporal artery which at times can also exist as several branches. In either

case, the artery projects in the anterolateral direction to pass under the hippocampal gyrus. The anterior temporal artery provides anastomoses with the MCA with its anterior temporal branches [14].

The second cortical branch from P2 supplies the inferior posterior temporal lobe. This branch courses from the middle of P2 to follow the hippocampal gyrus laterally. Along its path it gives off several small branches that can extend as far as the occipital cortex to supply the visual cortex [14].

P3, Quadrigeminal

The PCA continues to curve around the midbrain on the lateral aspect and then takes on a medial course. The two sides project toward each other. P3 lies within the perimesencephalic cistern with the transition from P3 to P4 occurring as the artery reaches the calcarine fissure.

P4, Calcarine

The PCA terminates as P4 (calcarine segment) within the calcarine fissure as it bifurcates into terminal branches, medial and lateral occipital arteries.

The medial PCA trunk further branches into smaller splenic arteries to supply the dorsal surface of the corpus callosum. These provide anastomoses with the ACA via its pericallosal branches, earning the name posterior pericallosal artery.

The parietooccipital artery and calcarine artery form together as a fork of the medial PCA trunk. The parietooccipital artery continues in the superior lateral direction into the parietooccipital sulcus of the occipital lobe to supply the visual cortex. The sibling vessel, the calcarine artery, also takes a posterior path. It courses deep in the calcarine sulcus to supply the visual cortex.

Posterior Communicating Artery

The posterior communicating artery (PCom) arises from the most posterior segment of the intradural ICA and serves to connect the ICA to the posterior cerebral artery (PCA), serving as a vital anastomosis of the anterior and posterior circulation. The PCom courses posteriorly just below the edge of the tentorium, above the oculomotor (CN III) nerve (an essential anatomic relationship). Several tiny branches are given off by the PCom. These thalamoperforating arteries form in many variations. Generally, the largest of these is the premamillary, also named the anterior thalamoperforating artery. These also include the anterior and posterior thalamoperforating arteries that traveling through the anterior perforated substance to provide blood supply to the posterior limb of the internal capsule, anterior thalamus, posterior hypothalamus, anterior one-third of the optic tract, and subthalamic nucleus [1]. It

is worthwhile to note that these perforating branches render blood supply to the wall of the lateral ventricle.

Basilar Artery

The vertebral arteries project superiorly and enter through the foramen magnum to enter the dura to become the intradural segment (V4). It is V4 that unites bilaterally at the pontomedullary junction to form the basilar artery (BA). The BA spans from its origin within the prepontine cistern to the interpeduncular cistern where it bifurcates into terminal branches as the PCAs. The BA takes this course with its location being medial and posterior to the clivus and running anterior to the pons. Along the BA's course, the abducens nerves (CNVI) course directly in front, at the lower pontine border. The oculomotor nerve (CNIII) also courses anteriorly to the BA at the upper pons.

Labyrinthine Arteries

The labyrinthine arteries provide vascular supply to the internal acoustic meatus and inner ear via long projections. These projections can be seen coursing into the internal acoustic meatus with the facial nerve (CNVII) and vestibulocochlear nerve (CNVIII). These arteries form with tremendous variation, 16% as direct projections from BA. The remainder, as branches from other branches of BA, 25% from superior cerebellar and 45% from anterior inferior cerebellar arteries.

Cerebellar Arteries

Posterior Inferior Cerebellar Artery

The posterior inferior cerebellar artery (PICA) is the largest artery that provides arterial supply to the lower medulla, inferior aspects of the fourth ventricle, tonsils, vermis, and inferolateral cerebellar hemisphere. This artery has tremendous variability and is formed from the distal vertebral arteries above the foramen magnum at or below the level of the inferior olive in 80% of studied cases [45].

PICA forms from the bilateral vertebral arteries anterior-laterally and follows the medullary cistern as the anterior medullary segment. PICA then continues in the cerebellomedullary fissure as the lateral medullary segment in the posterior direction, often passing between the roots of the glossopharyngeal (CNIX), vagus (CNX), and spinal accessory (CNXI) nerves. Here, PICA makes its first of two loops. It is not uncommon for the loop to extend below the foramen magnum and return to run

intracranially. PICA continues anteriorly along the lateral surface of the medulla. The next segment (supratonsilar) forms when PICA reaches the posterior border of the medulla as it passes superiorly, posterior to the medullary velum, sometimes across the cerebellar tonsil. Finally, the PICA completes a second loop to terminate by dividing into hemispheric branches: tonsilohemispheric and vermian branches.

Anterior Inferior Cerebellar Artery

Anterior inferior cerebellar artery (AICA) is a small artery that arises from the proximal BA in up to 30% of cases, arising as two or three branches. The artery travels within the cerebellopontine angle cistern continuing posteriorly, inferiorly, and laterally. As AICA courses, the facial nerve (CNVII) remains posterior-lateral to the artery. As discussed above, AICA can give off labyrinthine arteries. One of the more common variants is an absent right PICA with a compensatory robust AICA on the ipsilateral side, sometimes called AICA-PICA [46] (Fig. 1.7).

Superior Cerebellar Artery

The superior cerebellar artery (SCA) forms on both sides of the basilar artery distally, just prior to PCA formation. SCA courses laterally within the prepontine cistern along with the oculomotor nerve, to the ambient cistern and turning posteriorly. SCA continues over the middle cerebellar peduncle and turns medially towards the SCA of the contralateral side near the midline, in the quadrigeminal cistern. The SCA provides vascular supply to the superior portion of the cerebellum

Fig. 1.7 A/P projection of a right vertebral artery angiogram. There is no right PICA, and the red arrow points to a compensatory robust AICA on the ipsilateral side

as well as the inferior vermis. SCA originates to pass below the oculomotor nerve (CNIII) and then passes between the trochlear nerve (CNIV) and the trigeminal nerve (CNV). SCA is in contact with the trigeminal nerve in 50% of studied specimens [18].

The basilar artery gives off many important perforating branches. In the prepontine cistern, it produces the median pontine perforating, paramedian pontine perforating, and later pontine arteries. The former two are given off posteriorly to travel dorsally and penetrate the pons all the way to the fourth ventricular floor. The lateral pontine arteries are also called circumferential branches because of the path in which they travel. They also forming on the posterior aspect but then wrap around the brainstem giving off many tiny perforating arteries to supply the brainstem and pons [19].

Remnants of the Embryonic Arterial System

The persistent trigeminal artery (PTA) is a rare remnant of the embryonic circulatory system that unites the proximal intracavernous segment of internal carotid artery (ICA) with the middle or distal portion of the basilar artery (BA). The origin of the PTA is usually in the posterior or lateral surface of the intracavernous ICA just proximal to the origin of the meningohypophyseal trunk (Fig. 1.8).

A persistent hypoglossal artery is another persistent carotid-vertebrobasilar anastomoses (Fig. 1.9). It is second in frequency to the trigeminal artery. It arises from the distal cervical ICA, usually between C1 and C3. After passing through an enlarged hypoglossal canal, it joins the basilar artery inferiorly. If large, the ipsilateral vertebral artery and PCOM are often hypoplastic or absent.

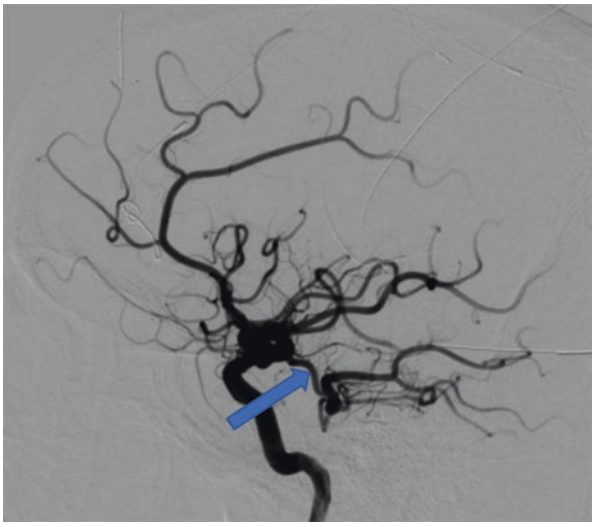

Fig. 1.8 Lateral angiogram of the ICA. The blue arrow points to the persistent trigeminal artery, a rare remnant of the embryonic circulatory system that unites the proximal intracavernous segment of ICA with the middle or distal portion of the basilar artery

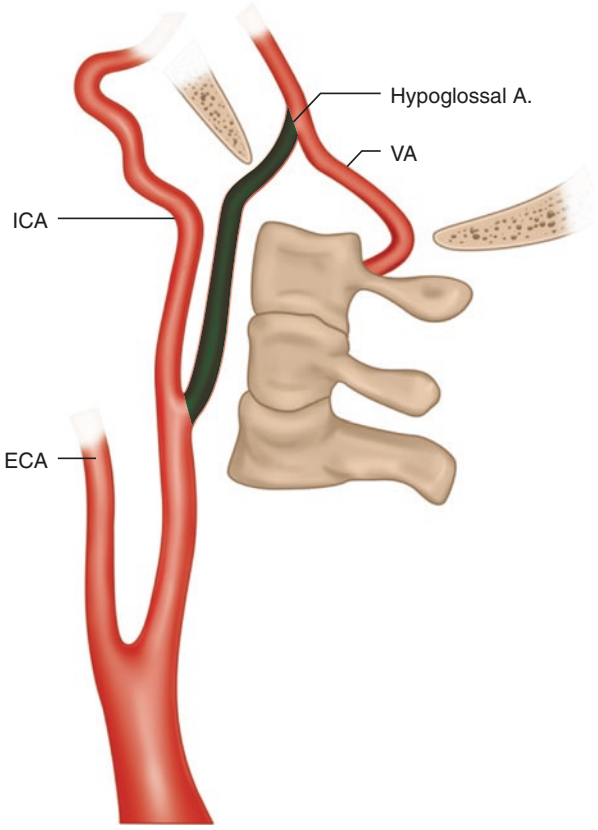

Fig. 1.9 Diagram of persistent hypoglossal artery (in yellow) from internal carotid artery (ICA) to posterior circulation anastomosis with vestibular artery (VA) often hypoplastic or absent

A persistent otic artery is one of the persistent carotid-vertebrobasilar anastomoses, although there is considerable controversy in regard to its existence. It is said to arise from the C2 (petrous) segment of the internal carotid artery, within the carotid canal. This artery emerges from the internal acoustic meatus and joins the basilar artery, inferiorly.

The first three arteries are also known as presegmental arteries and are named after the cranial nerves they follow [40, 41].

The persistent proatlantal artery can be subdivided into two types depending on its origin. Type I, also known as the proatlantal intersegmental artery, arises from the internal carotid artery. This is similar to the hypoglossal artery, but instead of heading for the hypoglossal canal, it joins the vertebral artery at the V4 segment through the foramen magnum [40]. Type II arises from the external carotid artery or rarely from the common carotid artery, and joins the V3 segment of VA [42, 43] (Fig. 1.10).

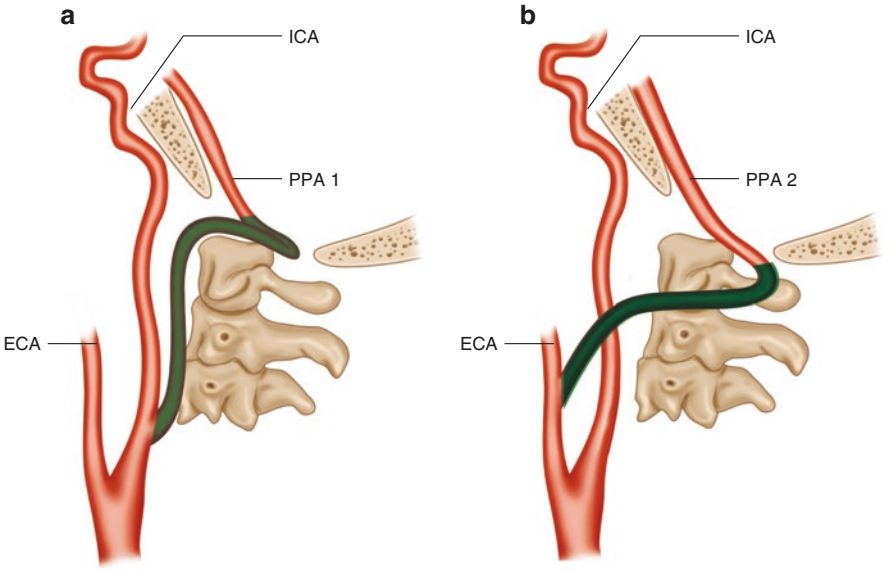

Fig. 1.10 (**a**) Diagram of Type I persistent proatlantal artery (PPA1) (yellow) or proatlantal intersegmental artery arises from the internal carotid artery to join the vertebral artery at the V4 segment through the foramen magnum. (**b**) Diagram of Type II persistent proatlantal artery (PPA 2) (yellow) arises from the external carotid artery or rarely from the common carotid artery to join the vertebral artery at the V3 segment through the foramen magnum

Venous System

Superficial Veins

The surface of the brain is drained by the three major superficial veins: the superior, the superficial middle, and the inferior cerebral veins. The superior cerebral veins drain the superior, lateral, and inferior surfaces of the hemisphere and then drain into the superior sagittal sinus. The middle cerebral vein is located on the lateral surface of each hemisphere, running along the lateral sulcus and to the cavernous sinus. The middle cerebral vein has two important anastomoses: the vein of Trolard and the vein of Labbe. These veins connect to the superior sagittal sinus and the lateral transverse sinus, respectively. Finally, the inferior cerebral vein, as its name implies, drains the inferior surface of the cortex and empties into the cavernous and transverse sinuses.

Dural Venous Sinuses

Dural venous sinuses are intracranial venous channels between the two layers of the dura mater (endosteal layer and meningeal layer). Unlike other veins in the body, they run alone, not parallel to arteries. Venous sinuses are valveless, allowing for

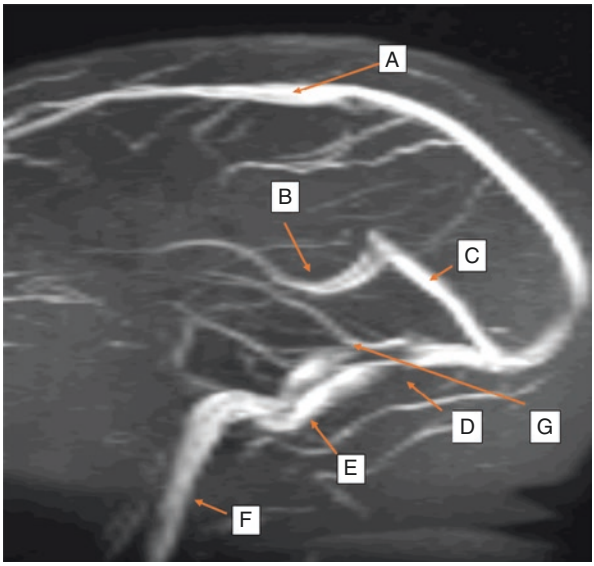

Fig. 1.11 Lateral magnetic resonance venography (MRV). A superior sagittal sinus, B internal cerebral veins, C straight sinus, D transverse sinus, E sigmoid sinus, F jugular vein, G vein of Labbe

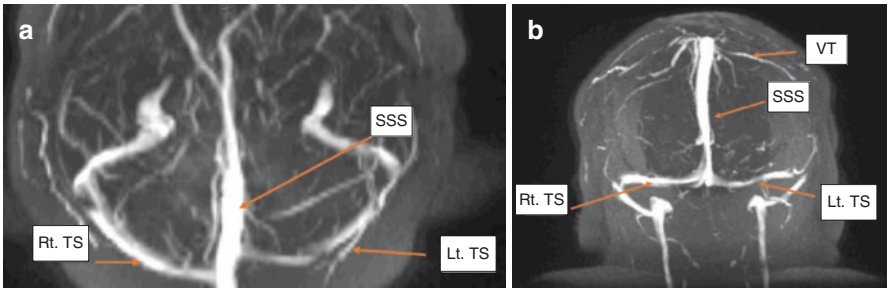

Fig. 1.12 (**a**) An axial MRV, (**b**) coronal MRV: The right transverse sinus (Rt. TS) is dominant and is a continuation of the superior sagittal sinus (SSS). The left transverse sinus (Lt. TS) is the continuation of the straight sinus. Vein of Trolard (VT) draining into the SSS

bidirectional blood flow in intracranial veins. The draining territories of intracranial veins are different from those of major cerebral arteries [36] (Figs. 1.11 and 1.12).

Superior Sagittal Sinus (SSS)

The superior sagittal sinus is formed by the superior portion of the falx cerebri, a fold in the meningeal dura that separates the two hemispheres. Its course begins in the midline of the shallow groove on the inner table of the cranium and grows larger as it traverses posteriorly. Next, it extends backwards from the crista galli (attachment point of the falx cerebri) all the way to the confluence of the sinuses, and thereafter turns right to become continuous with the right transverse sinus. It

receives blood from the veins of the frontal sinus anteriorly and the veins of the nasal cavity (foramen caecum). Additionally, the sinus connects to the superior cerebral vein, the parietal emissary veins, and the venous lacunae.

SSS drains blood from the lateral aspects of anterior cerebral hemispheres to the confluence of sinuses. Cerebrospinal fluid drains through arachnoid granulations into the superior sagittal sinus and is returned to venous circulation.

Ligation of the anterior third of the superior sagittal sinus is generally presumed to be safe and is commonly performed to gain access to the anterior skull base. In contrast to this teaching, studies have demonstrated complications associated with this maneuver. One study describes a morbidity of 8.06% and a mortality of 1.6% from bifrontal venous infarcts [23]. It is important to understand the drainage pattern of the frontal veins draining into the anterior third of the SSS before ligating, especially for tumors of the anterior skull base [28].

The anterior portion of this sinus is atretic in 1% of the population.

Inferior Sagittal Sinus

The inferior sagittal sinus (ISS) runs in the free margin of the falx cerebri and joins posteriorly with the great cerebral vein of Galen. ISS receives blood from the falx cerebri and small veins near the medial surface of the cerebral hemispheres. The sinus drains the blood coming from the deeper medial surface of the cerebrum. ISS joins the great cerebral vein of Galen (VoG) progressing into the straight sinus.

Straight Sinus

The straight sinus is formed by the junction of the inferior sagittal sinus and the VoG. As it courses posteriorly at the junction of the falx cerebri and the tentorium cerebelli, some superior cerebellar veins drain into the straight sinus. The straight sinus then continues its course posterior-inferiorly to drain into the confluence of the sinuses. The exact drainage of is variable, draining into the confluence of sinuses 56% of the time, into the left transverse sinus 21%, and right transverse sinus 13% of the time. The confluence is located deep into the internal occipital protuberance, receiving blood from the straight sinus, the great cerebral vein of Galen, and the superior cerebellar vein [31].

Transverse Sinus

The transverse sinus (TS) begins at the confluence of the sinuses by the internal occipital protuberance. The sinus has right and left segments. Most commonly, the right segment is a continuation of the superior sagittal sinus and is the larger of the

two. The left segment is usually continuous with the straight sinus. Each portion (right and left) travels along the tentorium cerebelli. In greater detail, both portions of the transverse sinus traverse anteriorly and laterally to eventually reach the posterolateral end of the petrous bone. From the petrous bone TS becomes the sigmoid sinus, which continues as the jugular bulb in the base of the skull, receiving blood from the inferior cerebral, inferior cerebellar, diploic, inferior anastomotic veins, and superior petrosal sinus. To note, the sphenoparietal sinus (see cavernous sinus) can drain into the transverse sinus. TS drains the superior sagittal, the occipital, and the straight sinuses.

The anatomy of the transverse sinus is highly variable. The left is hypoplastic 39% and aplastic 20% of the time. The right is hypoplastic and aplastic in 6% and 4% of cases, respectively. The two are symmetrical 31% of the time [32].

Sigmoid Sinus

Similar to the transverse sinus, the sigmoid sinus occurs bilaterally. Both sides curve inferomedially in an S-shaped groove within the mastoid process. It then crosses the jugular process of the occipital bone where the sinus migrates forward to end in the superior jugular bulb (part of the internal jugular vein) at the jugular foramen. In the posterior half of the foramen, the pars vascularis, the sigmoid sinus receives blood from the mastoid and condylar emissary veins. This sinus is distinctive because it has a direct connection to the superior petrosal sinus (SPS) (see cavernous sinus) at the transverse sinus junction. In addition, the sigmoid sinus connects to the inferior petrosal sinus (IPS) (see cavernous sinus) to eventually become the internal jugular vein. The sigmoid sinus drains the transverse sinus.

Occipital Sinus

The occipital sinus (OS), one of the smallest dural sinuses, runs cranially and posteriorly along the margin of the falx cerebelli and stops at the confluence of the sinuses. It receives tributaries from the margins of the foramen magnum where it originates.

The OS also receives blood from the veins of the hypoglossal canal, the basilar plexus, the occipital emissary, and the diploic veins. This sinus drains the blood into the confluence of sinuses. In rare occasions, the OS (oblique sinus) will run on one side as opposed to midline and connect with the sigmoid sinus. The OS can be quite large and may even replace one of the sigmoid sinuses. This is especially true in cases of an absent transverse sinus [22, 34]. In most cases, a single occipital sinus is observed, but double occipital sinuses and total absence of the sinus are not uncommon [22, 34].

Cavernous Sinus

The cavernous sinuses (CS) are two sinuses located on either side of the sella turcica. Their course starts anteriorly up to the medial end of the superior orbital fissure and goes posteriorly all the way up to the apex of the petrous bone. Several vital structures run through this sinus, specifically cranial nerves III, IV, VI, V1, and V2 and the internal carotid artery. CS receives blood from the superior and inferior ophthalmic vein, the superficial middle vein, inferior cerebral vein, the sphenoparietal sinus, and the middle meningeal vein. The CS drains into the TS (via the superior petrosal sinus), the internal jugular vein (via the inferior petrosal sinus), the pterygoid plexus (via the emissary veins), and the facial vein (via the superior ophthalmic veins). Communication between the left and right cavernous sinuses is made by the intercavernous sinuses anterior and posterior to the infundibulum of the pituitary gland [23–25].

Both cavernous sinuses drain the orbit and the anterior portion of the cerebral hemispheres.

Superior Petrosal Sinus

The superior petrosal sinus (SPS) is also a paired structure originating within the cavernous sinus, extending along the superior border of the petrous bone and draining into the sigmoid sinus at the transverse sigmoid junction. It receives blood from the vein of vestibular aqueduct, petrosal vein, and the superior veins of the cerebellum. This sinus drains blood from the medulla, pons, superior cerebellum, and internal ear.

Inferior Petrosal Sinus

The IPS is often a plexus of venous channels rather than a true sinus and drains blood from the cavernous sinus to the jugular bulb through the jugular foramen (pars nervosa) or sometimes via a vein passing through the hypoglossal canal to the suboccipital venous plexus. The IPS extends along the inferior border of the petrous bone.

Basilar Venous Plexus

The basilar venous plexus is postulated to arise from a continuation of the cranial part of the anterior internal vertebral venous plexus or arise as its own entity. It is composed of many interconnecting venous channels located between the layers of

the dura mater. The plexus has a large number of tributaries such as the IPS, internal vertebral venous plexus, SPS, marginal sinus, veins of the hypoglossal canal, condylar emissary veins, and inferior surface of clivus. This plexus has some anomalies such as two intraosseous connections; one between the plexus itself and the inferior side of the clivus through the basilar canal and the other between the veins of the hypoglossal canal and the condylar emissary veins.

Deep Veins

Internal Cerebral Veins

The internal cerebral veins (ICV) are paired and are the first major deep intracerebral veins. These veins form from the thalamostriate vein, septal vein, and the choroidal vein at the foramen of Monro. The ICV courses posteriorly between the tela choridea of the third ventricle and underneath the splenium. These veins drain the deep cerebral hemisphere and join the basal vein to form the great cerebral vein.

Basal Vein

The basal veins of Rosenthal (BVR), of which there are two, are the third deep intracerebral veins. They lie paramedian and originate on the medial surface of the temporal lobe. The BVR is created by the combination of the inferior striate veins, deep middle cerebral veins, and small anterior cerebral vein. They course posteriorly and medially to pass through the ambient cistern lying lateral to the midbrain before joining with the internal cerebral veins.

Great Cerebral Vein of Galen

The great cerebral vein of Galen (VoG) is the last of the three main deep intracerebral veins. It is a short vein that is formed by the three deep veins of the basal aspect of the brain: the BVRs, ICVs, and some superior cerebellar veins. It is situated in the quadrigeminal cistern, posterior to the brainstem and third ventricle.

The main function of the vein of Galen is to drain blood from the superior cerebellum, interpeduncular fossa, inferior horn of the lateral ventricle, parahippocampal gyrus, corpus callosum, midbrain, and choroid plexuses of the third and lateral ventricles. Its course runs caudally between the splenium and the pineal gland. Subsequently the vein merges with the inferior sagittal sinus to create the straight sinus.

Middle Meningeal Veins

The middle meningeal veins (MMV) follow the course of the middle meningeal artery. MMV passes through the foramen spinosum and the vein empties into the maxillary vein or the pterygoid plexus.

Conclusion

The vascular anatomy of the brain consists of arterial supply and venous drainage. The anterior circulation is supplied by the internal carotid arteries bilaterally. The arterial supply is robust with significant anastomose via the circle of Willis. The vertebral artery enters through the foramen magnum to enter the dura to become the intradural segment (V4). V4 unites bilaterally at the pontomedullary junction to form the basilar artery (BA). BA spans from its origin within the prepontine cistern to the interpeduncular cistern where it bifurcates into terminal branches as the PCAs again into the circle of Willis. The venous system is composed of surface veins and deep veins that drain to the venous sinuses. Ultimately, the venous system flows into the jugular veins.

References

1. Drake RL, McBride JM, Lachman N, Pawlina W. Medical education in the anatomical sciences: the winds of change continue to blow. Anat Sci Educ. 2009;2:253–9.
2. Hayreh SS, Dass R. The ophthalmic artery: I. Origin and intra-cranial and intra-canalicular course. Br J Ophthalmol. 1962;46:65–98.
3. Nishio S, Matsushima T, Fukui M, Sawada K, Kitamura K. Microsurgical anatomy around the origin of the ophthalmic artery with reference to contralateral pterional surgical approach to the carotid-ophthalmic aneurysm. Acta Neurochir. 1985;76:82–9.
4. Perrini P, Cardia A, Fraser K, Lanzino G. A microsurgical study of the anatomy and course of the ophthalmic artery and its possibly dangerous anastomoses. J Neurosurg. 2007;106:142–50.
5. Louw L. Different ophthalmic artery origins: embryology and clinical significance. Clin Anat. 2014;28:576–83.
6. Marinković S, Milisavljević M, Kovačević M. Anatomical bases for surgical approach to the initial segment of the anterior cerebral artery. Surg Radiol Anat. 1986;8:7–18.
7. Jabbour PM. Neurovascular Surgical Techniques. New Delhi: Jaypee Brothers Medical Publisher (P) Ltd.; 2013.
8. Mercier P, Fournier D, Brassier G, Cronier P, Papon X, Velut S, Pillet J. The perforating arteries of the anterior part of the circle of Willis. Riv Neuroradiol. 1994;7:79–83.
9. Gloger S, Gloger A, Vogt H, Kretschmann HJ. Computer-assisted 3D reconstruction of the terminal branches of the cerebral arteries. I Anterior cerebral artery. Neuroradiology. 1994;36:173–80.
10. van der Zwan A, Hillen B, Tulleken CA, Dujovny M, Dragovic L. Variability of the territories of the major cerebral arteries. J Neurosurg. 1992;77:927–40.

11. Hayman LA, Taber KH, Hurley RA, Naidich TP. An imaging guide to the lobar and arterial vascular divisions of the brain. Part I: sectional anatomy. JJNR. 1997;3:175–9.
12. Osborn AG, Jacobs JM. Diagnostic cerebral angiography. Philadelphia: Lippincott-Raven; 1999.
13. Brassier G, Morandi X, Fournier D, Velut S, Mercier P. Origin of the perforating arteries of the interpeduncular fossa in relation to the termination of the basilar artery. Interv Neuroradiol. 1998;4:109–20.
14. Margolis MT, Newton TH, Hoyt WF. Cortical branches of the posterior cerebral artery. Anatomic-radiologic correlation. Neuroradiology. 1971;2:127–35.
15. Van Overbeeke JJ, Hillen B, Tulleken CA. A comparative study of the circle of Willis in fetal and adult life. The configuration of the posterior bifurcation of the posterior communicating artery. J Anat. 1991;176:45–54.
16. Zeal AA, Rhoton AL. Microsurgical anatomy of the posterior cerebral artery. J Neurosurg. 1978;48:534–59.
17. Saeki N, Rhoton AL. Microsurgical anatomy of the upper basilar artery and the posterior circle of Willis. J Neurosurg. 1977;46:563–78.
18. Marinkovic SV, Milisavljevic MM, Kovacevic MS. Anastomoses among the thalamoperforating branches of the posterior cerebral artery. Arch Neurol. 1986;43:811–4.
19. Hardy DG, Rhoton AL. Microsurgical relationships of the superior cerebellar artery and the trigeminal nerve. J Neurosurg. 1978;49:669–78.
20. Marinkovic SV, Gibo H. The surgical anatomy of the perforating branches of the basilar artery. Neurosurgery. 1993;33:80–7.
21. Awad IA, Jafar JJ, Rosenwasser RH. Vascular malformations of the central nervous system. Philadelphia: Lippincott Williams & Wilkins; 1999.
22. Caplan LR, Biller J, Leary M, Lo E, Thomas A, Yenari M, Zhang J. Primer on cerebrovascular diseases. 2nd ed. San Diego: Elsevier, Academic Press; 2017.
23. Gaillard F. Transverse sinus: Radiology Reference Article [Internet]. Radiopaedia Blog RSS. [cited 2021Mar9]. Available from: https://radiopaedia.org/articles/transverse-sinus.
24. Gibo H; Carver CC; Rhoton AL; Lenkey C; Mitchell RJ. Microsurgical anatomy of the middle cerebral artery. In: Journal of neurosurgery. 1981. https://pubmed.ncbi.nlm.nih.gov/7452329/. Accessed 17 Mar 2021.
25. Ipsalali HO, Ciftci AC, Kilic D, Sendemir G, Seyhan S, Kaya I, Ortug G. Variations of the 6th cranial nerve (nervus abducens) in the petroclival region: a microsurgical study. In: Morphologie: bulletin de l'Association des anatomistes. 2019. https://www.ncbi.nlm.nih.gov/pubmed/30713002. Accessed 17 Mar 2021.
26. Krisht AF, Barrow DL, Barnett DW, Bonner GD, Shengalaia G. The microsurgical anatomy of the superior hypophyseal artery. In: Neurosurgery. 1994. https://pubmed.ncbi.nlm.nih.gov/7838339/. Accessed 17 Mar 2021.
27. Lasjaunias PL, Berenstein A, ter Brugge KG. Surgical neuroangiography: clinical vascular anatomy and variations. 2nd ed. New York: Springer; 2001.
28. Morris P. Practical neuroangiography. 3rd ed. Wolters Kluwer/Lippincott Williams & Wilkins: Philadelphia etc.; 2013.
29. Nakamura M, Struck M, Roser F, Vorkapic P, Samii M. Olfactory groove meningiomas: clinical outcome and recurrence rates after tumor removal through the frontolateral and bifrontal approach. Neurosurgery. 2007;60:844–52.
30. Ngnitewe RM, Minutello K, Mesfin F. Neuroanatomy, cavernous sinus. In: National Center for Biotechnology Information. 2020. https://pubmed.ncbi.nlm.nih.gov/29083662/. Accessed 17 Mar 2021.
31. Rhoton AL. Cranial anatomy and surgical approaches. Schaumburg: Lippincott Williams & Wilkins; 2003.
32. Rhoton AL, Fuji K, Fradd B. Microsurgical anatomy of the anterior choroidal artery. In: Surgical neurology. 1979. https://pubmed.ncbi.nlm.nih.gov/515913/. Accessed 17 Mar 2021.

33. Salunke P, Sodhi HB, Aggarwal A, Ahuja CK, Dhandapani SS, Chhabra R, et al. Is ligation and division of anterior third of superior sagittal sinus really safe? Clin Neurol Neurosurg. 2013;115(10):1998–2002.
34. Tubbs RS, Bosmia AN, Shoja MM, et al. The oblique occipital sinus: a review of anatomy and imaging characteristics. Surg Radiol Anat. 2011;33:747–9. https://doi-org.ezproxy2.library.drexel.edu/10.1007/s00276-011-0831-9
35. Standring S, Gray H, Griffiths PD. Gray's anatomy: the anatomical basis of clinical practice. 41st ed. Philadelphia: Elsevier; 2016. p. 280–90.
36. Gaillard F. Dural venous sinuses: radiology reference article. In: Radiopaedia Blog RSS https://radiopaedia.org/articles/dural-venous-sinuses?lang=us. Accessed 19 Mar 2021.
37. Perlmutter D, Rhoton AL. Microsurgical anatomy of the distal anterior cerebral artery. J Neurosurg. 1978;49:204–28.
38. Kakou M, Destrieux C, Velut S. Microanatomy of the pericallosal arterial complex. J Neurosurg. 2000;93:667–75.
39. Purkayastha S, et al. Proatlantal intersegmental arteries of external carotid artery origin associated with Galen's vein malformation. AJNR Am J Neuroradiol. 2005;26(9):2378–83.
40. Raybaud C. Normal and abnormal embryology and development of the intracranial vascular system. Neurosurg Clin N Am. 2010;21:399–426.
41. Choudhary G, Ahuja K, Khan R, Kubal W. Bilateral persistent primitive hypoglossal artery presenting with hemiplegia. Radiol Case Rep. 2018;13:1072–5.
42. Kolbinger R, Heindel W, Pawlik G, Erasmi-Körber H. Right proatlantal artery type I, right internal carotid occlusion, and left internal carotid stenosis: case report and review of the literature. J Neurol Sci. 1993;117:232–9.
43. Menshawi K, Mohr JP, Gutierrez J. A functional perspective on the embryology and anatomy of the cerebral blood supply. J Stroke. 2015;17:144.
44. Gumus T, Önal B, Ilgit ET. Bilateral persistence of type 1 proatlantal arteries: report of a case and review of the literature. Am J Neuroradiol. 2004;25:9.
45. Morris P. Practical neuroangiography. Wolters Kluwer/Lippincott Williams &; Wilkins, Philadelphia etc.; 2013.
46. Akgun V, Battal B, Bozkurt Y, Oz O, Hamcan S, Sari S, Akgun H. Normal anatomical features and variations of the vertebrobasilar circulation and its branches: an analysis with 64-detector row CT and 3T MR angiographies. Sci World J. 2013;2013:1–7.

Chapter 2
Vascular Anatomy of the Neck/Spine

Christina Feller and Hirad Hedayat

Introduction

In this chapter, we address the extracranial arterial and venous anatomy of the head, neck, and spine. Angiographic depictions and common variants are also included to serve as quick reference when preparing for an open or endovascular approach to these regions. We specifically address the vessels that are most pertinent to neurosurgical pathologies which are addressed in other chapters of this text and include small points to bear in mind with respect to the vessels covered.

Aortic Arch

The aortic arch is the portion of the aorta that connects the ascending aorta to the descending aorta within the thoracic cavity. It wraps around the pulmonary aorta in the thoracic cavity [1] with, typically, three main branches emanating from the arch. The branches listed in the antegrade direction of flow are as follows: right brachiocephalic (or innominate) trunk (BT), left common carotid artery (CCA), and left subclavian artery (SubA) (Fig. 2.1).

The right brachiocephalic (innominate) artery branches into the right subclavian and right common carotid arteries. The right vertebral artery (VA) emanates off the right SubA, and the right internal (ICA) and external carotid (ECA) arteries branch off the right CCA. On the left, the CCA branches into the left ICA and ECA. The left SubA gives off the left VA. In 2–5% of the population the left VA emerges directly from the aortic arch and in 4% of the population the VA branches

C. Feller · H. Hedayat (✉)
Department of Neurological Surgery, Medical College of Wisconsin, Milwaukee, WI, USA
e-mail: cfeller@mcw.edu; hhedayat@mcw.edu

J. R. Mascitelli, M. J. Binning (eds.), *Introduction to Vascular Neurosurgery*,
https://doi.org/10.1007/978-3-030-88196-2_2

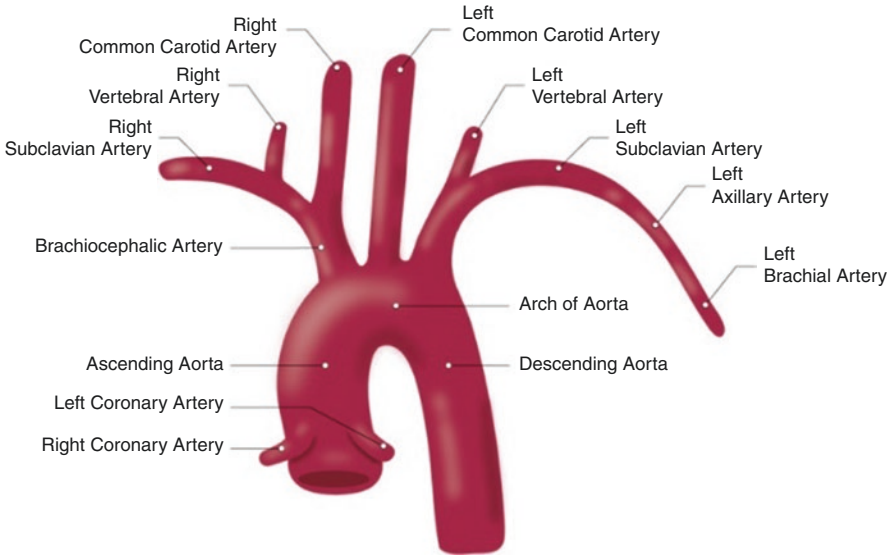

Fig. 2.1 Aortic arch branches. (Reproduced with permission from Ref. [7], https://www.ncbi.nlm.nih.gov/books/NBK441947/)

off the left CCA [2, 3]; variants to keep in mind when attempting to catheterize the left VA from the left SubA and a SubA angiogram reveals that there is no left VA present (or to take note of on pre-procedure CTA [computed tomography angiography] or MRA [magnetic resonance angiogram]). Both the left and right SubAs give off internal thoracic, thyrocervical, and costocervical trunk arteries which may be involved in fistulas and arteriovenous malformations of the spine [4].

Aortic Arch Variants

Bovine arch conformation is the most common variant occurring with a frequency of 27% and describes the variant wherein the right brachiocephalic trunk and left CCA emanate from the aortic arch in a common trunk [3]. A bicarotid trunk is usually seen in the setting of an aberrant origin of the right SubA in which the left CCA may have a deep recurrent course. During angiographic cases often an aortic arch angiogram may have to be performed to elucidate the takeoff of the great vessels.

Radiographic classification of aortic arch variants fall into three types based on the vertical distance from the origin of the brachiocephalic trunk (BT) to the top of the arch in the parasagittal "stretched-out" projection and affect the catheterization of these vessels with respect to angle of approach, catheter choice, and vessel used for their access (e.g., femoral versus radial) (Fig. 2.2a–c). Type

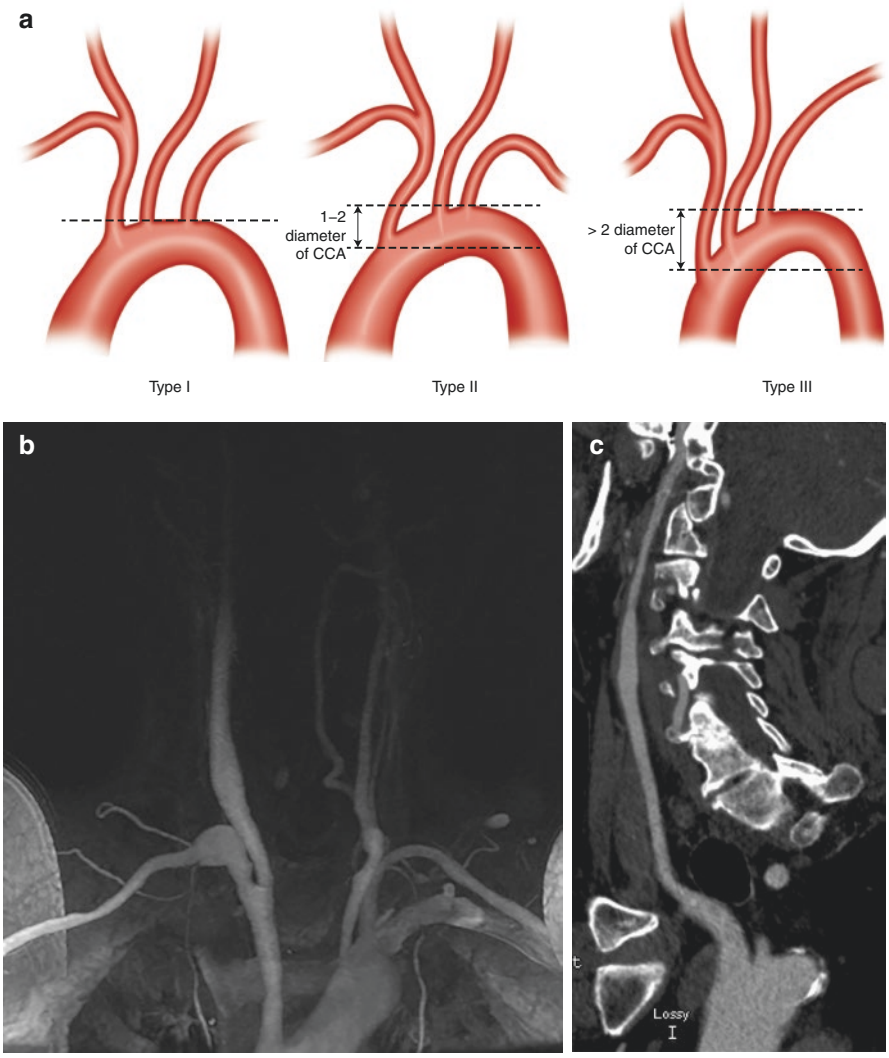

Fig. 2.2 (**a**) Aortic arch diagram and angiogram. (Reproduced with permission from Ref. [6]). (**b**) Coronal rotational CTA reconstruction demonstrating a type I arch. (**c**) Coronal MRA demonstrating a type III arch

I occurs when all the great vessels arise within the arc segment of the aortic arch and the BT occurs within <1 vessel diameter of the left CCA. Type II anatomy has a BT vertical distance between 1 and 2 diameters of the left CCA and Type III anatomy has a vertical distance greater than 2 diameters of the left CCA [5, 6].

Carotid and Jugular Vasculature

Common Carotid Artery

The *common carotid artery* travels within the carotid sheath with the internal jugular vein (IJ), vagus nerve, and Ansa Cervicalis. It eventually bifurcates into external carotid (ECA) and internal carotid (ICA) arteries typically at the level of C3-C5 vertebral bodies [4].

Internal Carotid Artery

The *internal carotid artery (ICA)* arises posterolateral to the ECA and travels distally to enter the cranial cavity via the carotid canal of the petrous temporal bone. The cervical portion of the ICA has no branches and delivers blood to the intracranial space (discussed in a different chapter). The bifurcation and takeoff of the ICA are often the focal point of progressive atherosclerotic stenosis development and embolic events related to progressively turbulent flow (Fig. 2.3).

Fig. 2.3 Surgical exposure for a left carotid endarterectomy. Note the posterolateral location of the ICA in relation to ECA with surgical exposure

External Carotid Artery

The *external carotid arteries (ECA)* are bilateral arteries supplying the skin and superficial soft tissues of the head and neck, cranial nerves, and the supporting structures associated with the upper airway and pharyngeal regions. There are eight branches emanating from the ECA (Fig. 2.4): superior thyroid, ascending pharyngeal, lingual, facial, occipital, posterior auricular, superficial temporal, and internal maxillary arteries.

The ECA arises anterior to the ICA and lies lateral to the pharynx and medial to the sternocleidomastoid muscle, reliable and consistent anatomical landmarks used when dissecting the neck to locate the carotid system. At the angle of the mandible, the ECA lies deep to the posterior belly of the digastric and stylohyoid muscles before entering the parotid gland. As it runs superiorly, it rises more posteriorly and eventually lays lateral to the ICA beneath the neck of the mandible where it divides into superficial temporal and maxillary arteries after passing through the parotid gland. The reversing of the ECA and ICA orientation is relative to the plane in which an image is taken of the vasculature. For example, a frontal angiogram will demonstrate a more medial ECA inferiorly and more lateral ECA superiorly while a lateral angiogram will portray the ECA as anterior to the ICA throughout its course [1] (Fig. 2.5).

Superior Thyroid Artery

The *superior thyroid artery* is the first branch off the ECA; branching anteriorly and remarkably close to the ECA origin. It conforms to a concave curve as it runs medially to the superior apex of the thyroid to supply the larynx and upper thyroid gland. Further branches off the superior thyroid artery (from proximal to distal) are: a small infrahyoid artery (contributing to the submental anastomoses), a branch to the sternocleidomastoid muscle, the superior laryngeal artery (supplying the mucosa), a cricothyroid branch, and finally, anterior and posterior branches (terminal branches supplying the thyroid gland) [1].

Lingual Artery

The second branch off the ECA is the *lingual artery* which supplies the tongue. Further branches from it are the small suprahyoid artery, sublingual artery, and the dorsal artery of the tongue (deep lingual artery) (Fig. 2.6).

Ascending Pharyngeal Artery (APA)

The third branch of the ECA is the *ascending pharyngeal artery (APA)* which supplies the pharynx, dura, and lower cranial nerves at the skull base. The trunk divides into two divisions distal to its origin with further branches arising from proximal

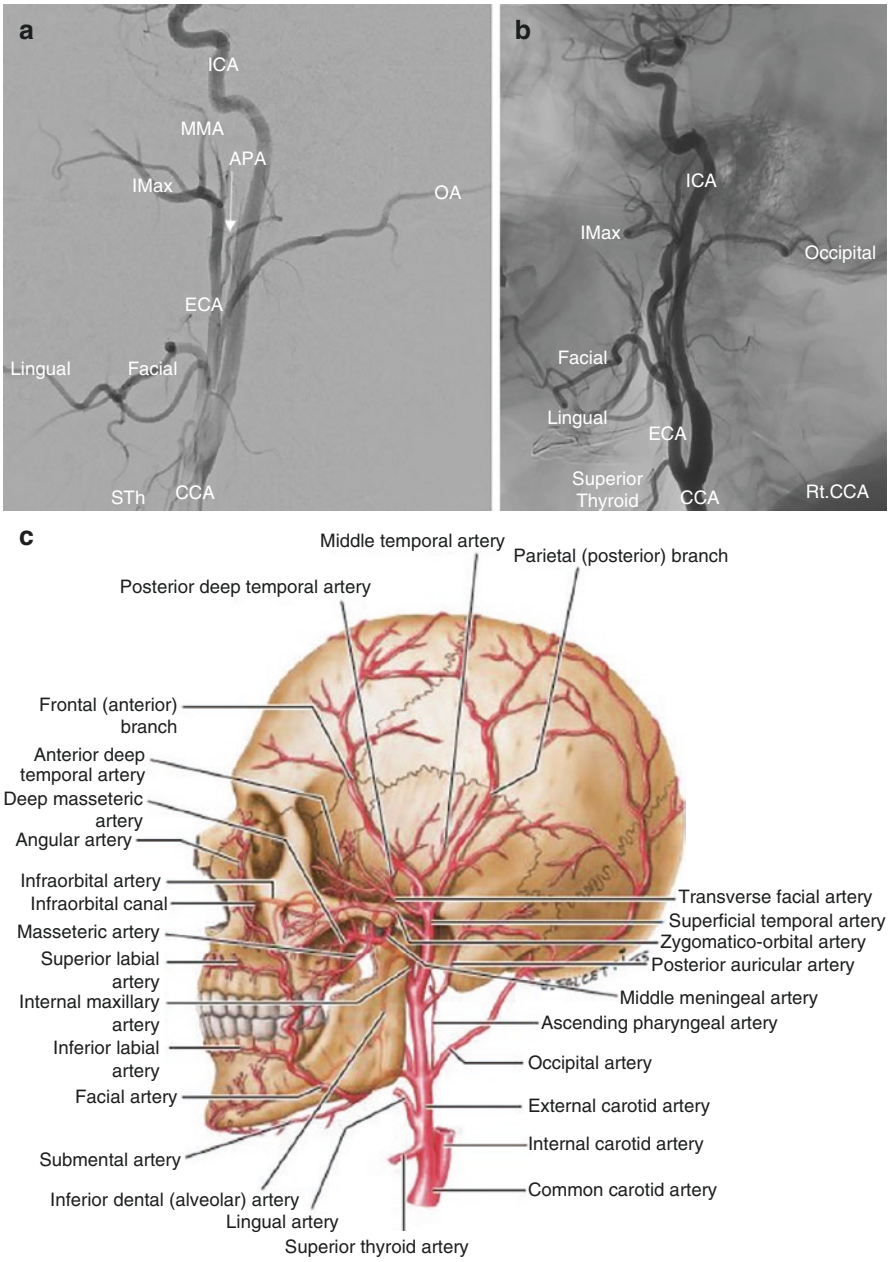

Fig. 2.4 (**a**) CCA lateral angiogram demonstrating the branches of the ECA and their overlapping appearance upon the ICA. (**b**) Unsubtracted CCA lateral angiogram demonstrating the branches of the CCA with respect to the bony anatomy of the region. Of note, a fibromuscular dysplasia appearance of the ICA is seen distal to the carotid bifurcation. (**c**) Arterial supply to the head and neck with ECA branches. (Reproduced with permission from Ref. [8])

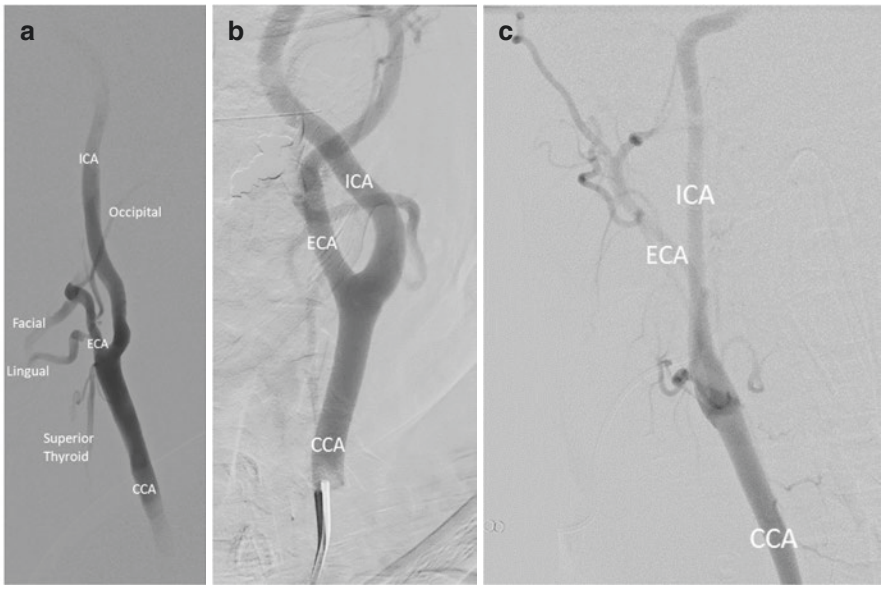

Fig. 2.5 (**a**) Lateral CCA angiogram demonstrating the branches of the ECA more proximally in the neck. (**b**) AP angiogram of the CCA demonstrating the normal anatomic location of the branching of ECA and ICA, where ECA initially lays medial to ICA, and more distally lays lateral to ICA which is coursing medially to enter the carotid canal of the petrous temporal bone. (**c**) Lateral CCA angiogram demonstrating the reversal of ECA and ICA position, where the ECA appears more anterior than the ICA

portions of either division or the main trunk. The anterior division (composed of the pharyngeal trunk/branches) branches into the inferior pharyngeal artery, middle pharyngeal artery, superior pharyngeal artery, palatine branches, and prevertebral branches. The posterior division (composed of the neuromeningeal trunk supplying the dura) includes the hypoglossal artery (clival branches, branches to the meninges, and prevertebral arteries), and jugular artery. The main trunk is composed of the musculospinal arteries (arising from the main APA trunk or the posterior division/neuromeningeal trunk) and the inferior tympanic artery [1]. The APA is often difficult to see on routine angiograms but may often play a prominent role in the supply of dural arteriovenous fistulae.

Facial Artery (FA)

The fourth branch of the ECA is the *facial artery (FA)* supplying most of the face, palate, lip, and cheek. Branches of the facial artery include the ascending palatine artery (supplying the pharynx, soft palate, tonsil, and Eustachian tube), tonsillar branch or small branches to the palatine tonsil, the submandibular arteries, submental artery, inferior and superior labial arteries, small branches to the facial muscles

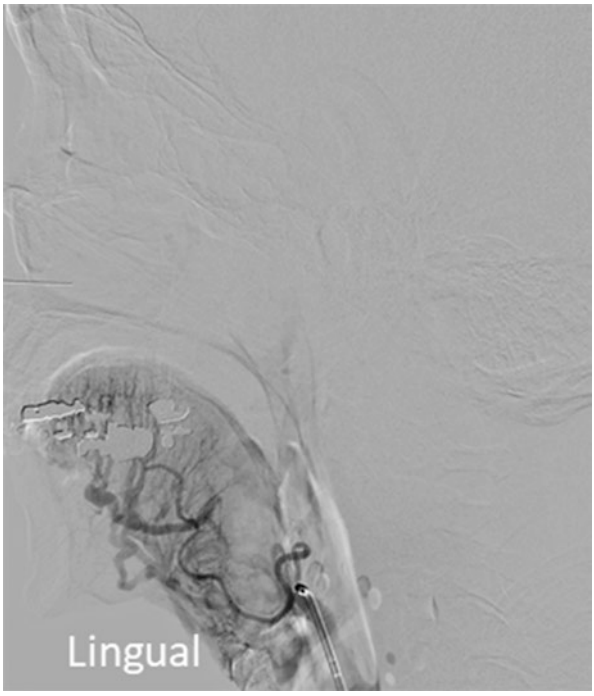

Fig. 2.6 Lateral angiogram of the lingual artery demonstrating a hypertrophic lingual artery in a patient with contralateral lingual cancer

as well as the buccinator and masseter muscles, lateral nasal artery, and angular and alar artery terminations (located around the orbit which anastomoses with branches of the ophthalmic artery from ICA) [1].

Occipital Artery (OA)

The fifth branch of the ECA is the *occipital artery (OA)* with further branches including muscular arteries, stylomastoid artery, and transmastoid or artery of the mastoid foramen. The OA may act as a donor for extracranial-intracranial revascularization cases.

Posterior Auricular Artery (PAA)

The next branch of the ECA is the *posterior auricular artery (PAA)*. Branches of the PAA include muscular branches, parotid branches, the stylomastoid artery, auricular branches (supplying the posterior pinna), and occipital branches (supplying the scalp posterior to the ear, in a reciprocal relationship with the OA) [1]. The PAA may also act as a donor for extracranial-intracranial revascularization cases.

Superficial Temporal Artery (STA)

The seventh branch of the ECA is the *superficial temporal artery (STA)*. The STA branches into the transverse facial artery, anterior auricle artery, posterior deep temporal artery, zygomatico-orbital artery, and frontal and parietotemporal scalp arteries [1]. The latter two branches are the most commonly harvested vessels for extracranial-intracranial bypass procedures and their diameter ideally should be evaluated at the time of catheter angiogram in cases which may benefit from bypass (Fig. 2.7).

Internal Maxillary Artery (IMax)

The eighth and final branch of the ECA is the *internal maxillary artery (IMax)* which branches anteriorly. Branches of the IMA are the ascending intracranial and extracranial arteries, five descending arteries (supplying the viscerocranium—face, mouth, and jaw), recurrent arteries supplying the skull base, anterior branches to the face, and finally the terminal sphenopalatine artery [1]. The sphenopalatine arteries are often the site of endovascular embolization for epistaxis which has failed medical and surgical treatments. The middle meningeal (MMA) is a terminal branch of the ascending intracranial arteries and is often involved with dural arteriovenous fistulas and, recently, with embolization for the treatment of chronic subdural hematoma.

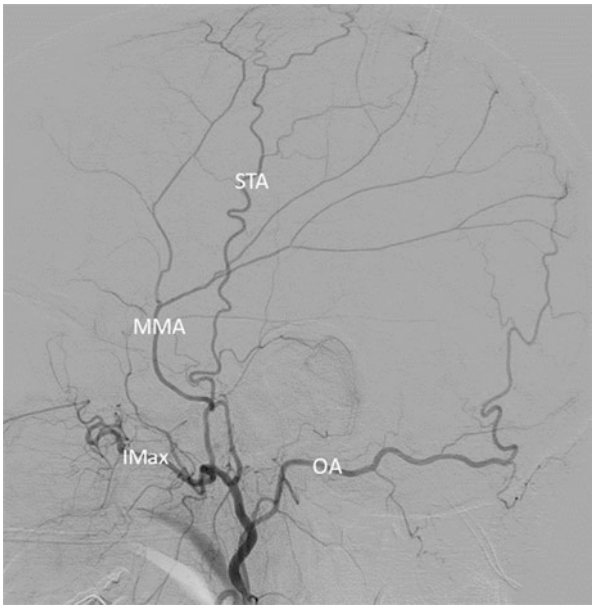

Fig. 2.7 Lateral ECA angiogram demonstrating the distal branches of the ECA perfusing the soft tissues of the face and scalp along with the dura (middle meningeal artery (MMA))

Jugular Veins

The corresponding anatomical venous system to the carotid arteries is the paired jugular veins. The internal and external jugular veins drain directly into the brachiocephalic vein and subclavian vein, respectively.

Internal Jugular Vein

The *internal jugular vein (IJ)*, the larger of the two, drains the venous blood from the brain, cranium, face, and majority of the neck. The vein runs from the sigmoid sinus in the posterior portion of the jugular foramen and travels within the carotid sheath to reach the brachiocephalic vein. Its contributors from cranial to caudal are (Fig. 2.8): inferior petrosal sinus, anterior condylar vein, facial, lingual, pharyngeal, superior thyroid, middle thyroid, and posterior jugular veins [1].

Anterior Condylar Vein

The *anterior condylar vein* connects the IJV with the venous plexus of the hypoglossal canal and acts as a communication channel between the IJV and vertebral epidural venous system.

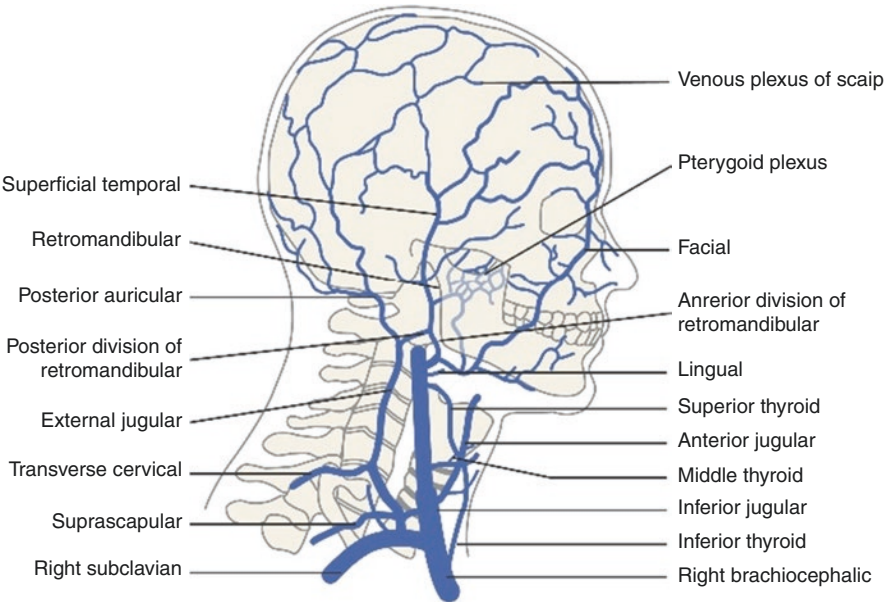

Fig. 2.8 Cervical venous drainage pathway. (Reproduced with permission from Ref. [9])

Facial Vein

The *facial vein* concentrates the venous drainage from most of the face, mouth, and muscles of mastication. It originates at the medial angle of the orbit and runs across the cheek to the ramus of the mandible where it terminates by joining the IJV at the level of the greater cornu of the hyoid [1]. During exposure of the carotid arteries for endarterectomy, the facial vein is often lying over the region of the bifurcation as an anatomical landmark; it is typically divided to allow exposure of the arterial system.

Lingual Vein

The *lingual vein* drains the tongue and sublingual and submandibular glands. It joins the IJV at the level of the great cornu of the hyoid, sometimes with the facial vein (common thyrolingual vein).

Pharyngeal Vein

The *pharyngeal veins* are a series of two or three short veins which drain the pharyngeal plexus. The *superior thyroid vein* originates at the superior aspect of the lateral lobe of the thyroid and accompanies its corresponding artery. The *middle thyroid vein* originates lateral to the thyroid gland and terminates in the IJV at the latter's midpoint. The *posterior jugular vein* arises from the occipital vein and drains the superficial structures of the posterior neck where it runs beneath the SCM to join the distal IJV with its equivalent in the anterior neck, the anterior jugular vein.

External Jugular Vein

The *external jugular vein (EJ)* drains deeper regions of the face, the mid and posterior scalp, and posterolateral neck (Fig. 2.9). It courses from the confluence of the retromandibular vein and smaller posterior auricular vein and/or superficial temporal vein inferiorly to join the subclavian vein, traveling superficial to the platysma [1]. The *anterior jugular vein* is a smaller neck vein that arises from superficial submental veins and descends in the anterior neck to drain into the subclavian or external jugular vein. It forms a venous arcade with the contralateral anterior jugular vein across the midline—a site of potential hemorrhagic complications during tracheostomy procedures. The posterior neck is drained via the suboccipital plexus which connects occipital veins with the vertebral artery venous plexus.

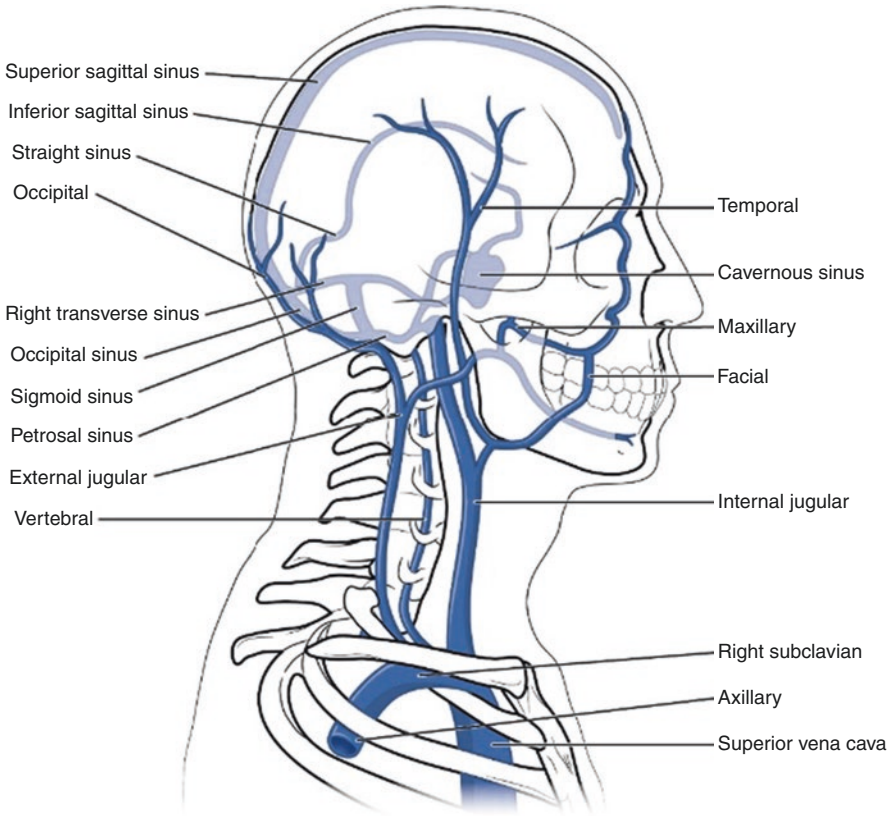

Fig. 2.9 External jugular veins. (Reproduced with permission from Ref. [10], access for free at https://openstax.org/books/anatomy-and-physiology/pages/1-introduction)

Scalp Veins

The drainage of the scalp, apart from the major dural sinuses, follows the regional arteries. For example, the forehead drains to the supratrochlear and supraorbital veins and then to the facial and ophthalmic veins while the temporal region drains to the superficial temporal vein leading to the EJ vein. The posterior scalp drains to the posterior auricular and occipital veins which also drain to the EJ vein. They communicate with veins in the diploe of the skull and via emissary veins with the dural sinuses and veins of the pericranium and meninges. In the region of the major dural sinuses, emissary veins are common and venous blood flow may be directed intracranially into the parasagittal, mastoid, and occipital regions [1]. The mastoid emissary vein is commonly transected during the approach for retrosigmoid craniotomies and easily controlled.

External Carotid-Internal Carotid Artery Collaterals

Normal anatomic anastomoses occur between EC and IC circulations that one must be mindful of when performing endovascular embolization procedures, with liquid embolics particularly, which may pass from EC to IC circulations, or vice versa, and lead to therapeutic misadventures and potential neurological compromise. The most important anastomosis is via the ophthalmic artery (Fig. 2.10). The OA is connected to both the ICA (directly) and the ECA (via the angular artery then IMax or Facial artery). Another collateral may occur between the MMA of the ECA and anterior cerebral artery of the ICA [11–14]. Collaterals between the STA and supratrochlear and supraorbital arteries commonly occur; one must be mindful of this when treating arteriovenous fistulas of the scalp. The STA is long and relatively exposed on the scalp. After crossing the zygomatic arch, the STA is only cushioned by the superficial temporal muscle in some regions, while there is no muscular cushion after crossing the superior temporal line [15]; thus, it is particularly vulnerable to superficial trauma and 75–90% of post-traumatic scalp fistula cases involve the STA [15–17]. Possible complications include hemorrhage, thrombosis, ulceration, and aesthetic complications [18].

The inferolateral trunk (ILT) of the ICA also provides a collateral route in proximal ICA occlusion via the foramen rotundum branch, accessory, and cavernous

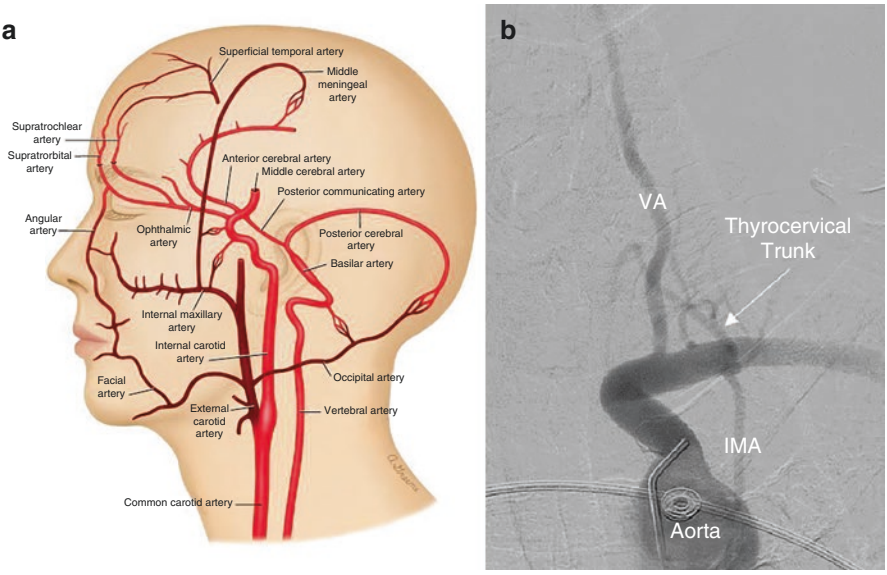

Fig. 2.10 (**a**) External carotid-internal carotid collaterals. (Reproduced with permission from: Gillespie DL, Doyle A. Overview of blunt and penetrating thoracic vascular injury in adults [19]). (**b**) Left subclavian artery AP angiogram demonstrating the branch points of the VA and thyrocervical trunk, vessels often involved in AVM and fistulae of the subaxial cervical spine and spinal cord (internal mammary artery (IMA))

branches of the accessory and middle meningeal arteries. The superior thyroid artery from the ECA to contralateral ECA and further ICA may provide another anatomic collateral routing. Similarly, the ipsilateral thyrocervical trunk supplies the inferior thyroid artery and then the superior thyroid artery to the ECA and ICA [12]. Additionally, the OA may develop anastomoses with the posterior cerebral artery or extradural vertebral artery [11, 12].

Vertebral Vasculature

The paired *vertebral arteries (VA)* are around 3–4 mm in diameter with the left vertebral artery typically being larger or dominant (Fig. 2.11). They are the first branch from the SubA, bilaterally arising superiorly and traveling vertically and posteriorly to the level of the sixth cervical vertebral body (C6) (see common variants under aortic arch). They travel rostrally through the vertebral canal via foramen in the transverse processes of all the upper cervical vertebrae (foramen transversarium). After leaving the superior border of the foramen of the axis (C2), the arteries run horizontally and posteriorly to the more lateral foramen of the atlas (C1) and then return medially to reach the foramen magnum. To reach the brain cavity, the arteries penetrate the dura and run vertically and medially to eventually join in creating the basilar artery (BA) anterior to the upper border of the medulla at the pontomedullary junction.

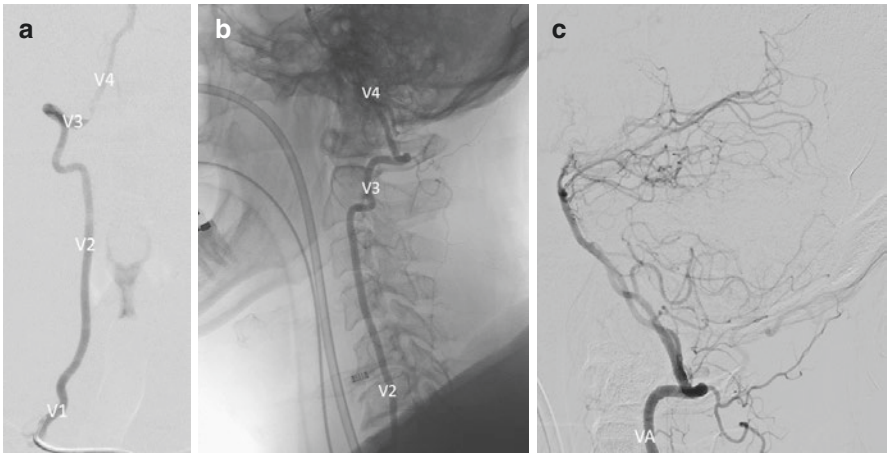

Fig. 2.11 (**a**) AP angiogram of the right VA demonstrating the four segments of the vessel. (**b**) Lateral unsubtracted VA angiogram demonstrating the segments of the vessel and their relation to the bony anatomy. Note the straight course of the V2 segment as it travels through the foramen transversarium of the visualized vertebral bodies from C3 to C6. (**c**) Lateral VA angiogram demonstrating the distal portion of the vessel with a muscular branch emanating from the V3 segment as well as the visualized contralateral V4 segment overlapping the originally injected vessel

Based on this anatomical course the vertebral arteries are divided into four segments: V1 (running from the subclavian to the foramen transversarium), V2 (from the foramen transversarium to C2), V3 (from C2 to the dura), and V4 (intradural portion).

The extracranial branches of the vertebral arteries supply the spinal cord and its dura, cervical vertebrae and muscles, as well as the dura of the inferior posterior fossa. From proximal to distal, they include (Fig. 2.11): branches to the stellate ganglion, anterior (2) and posterior (1) spinal branches from C6 to C1 (the VA along with deep cervical arteries from the costocervical trunk and ascending cervical artery contributes to the supply of the roots and their sheaths), and odontoid arterial arcade together with collaterals from the ascending pharyngeal artery and occipital artery. The arteries of the cervical expansion (spinal radiculomedullary arteries arising between C4 and C6 to supply the lower cervical spine along with the anterior spinal artery) additionally branch from the VA, although they may also arise from the thyrocervical trunk. Finally, muscular branches to the paraspinal muscles may also arise and anastomose with branches of the deep cervical and occipital arteries and may become major feeders for cervical AVMs. The anterior meningeal artery is a very small artery supplying the dura of the anterior foramen magnum and inferior clivus with anastomoses forming the odontoid arterial arcade.

Vertebral Artery Variants

Anatomical variants of the VA are related to the varying levels at which the artery enters the foramen transversarium. Typically, this occurs at C6; however, the most common variant entry is at C4 in relation to a left VA arising directly from the aortic arch [20]. Note should also be made of posterior inferior cerebellar artery (PICA) takeoffs which begin in the V3 segment of the VA rather than the typical V4 portion, a matter which needs to be appreciated on preoperative imaging studies before proceeding with open surgery in the region leading to PICA injury.

More rare variants are termed proatlantal artery Type I and Type II (Fig. 2.12). Proatlantal artery Type I describes the proatlantal intersegmental artery origin of the VA from the ICA which then joins the usual course of the vertebral artery at C1, corresponding to the first segmental artery. In proatlantal artery Type II the VA arises from the ECA (rarely from the CCA) and travels into the posterior fossa, corresponding to the second segmental artery (C2) [20].

Vertebral Veins

The vertebral veins are paired and drain directly into the brachiocephalic veins to drain into the superior vena cava (Fig. 2.13).

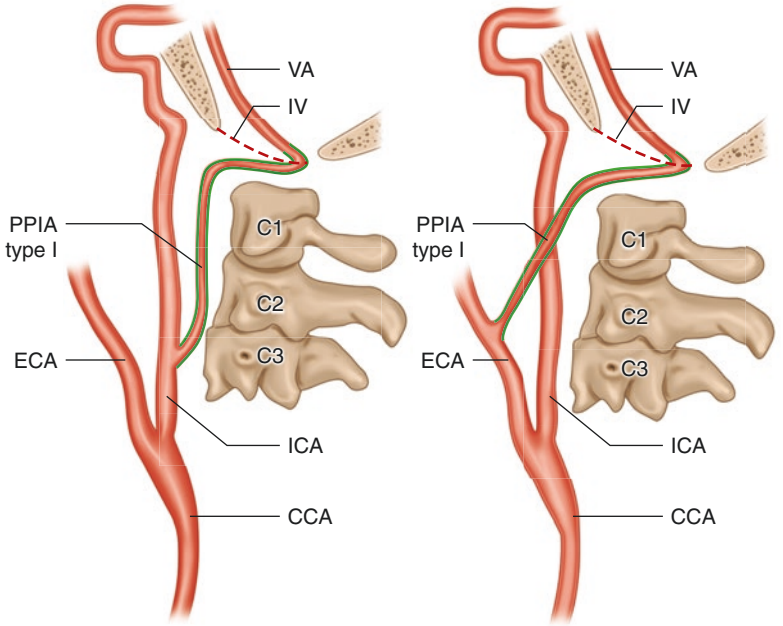

Fig. 2.12 Proatlantal artery Type I (left) and Type II (right). (Reproduced with permission from Ref. [21])

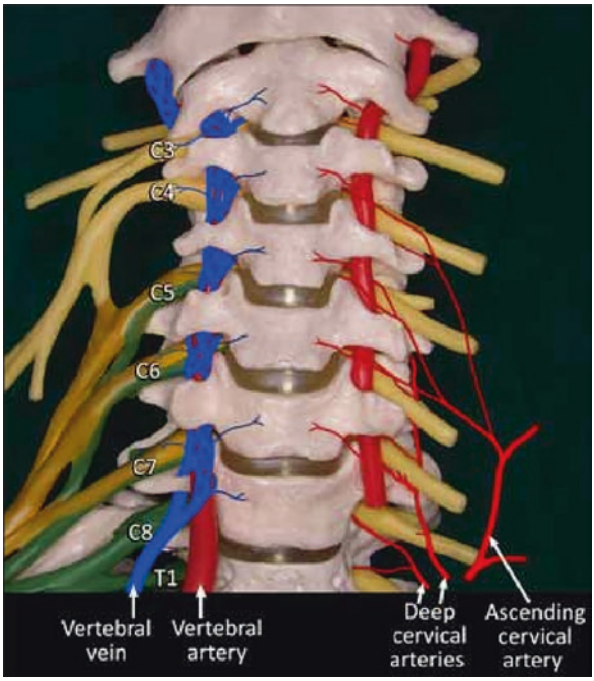

Fig. 2.13 Vertebral arteries and veins. Note the course of the VA and vertebral veins travelling within the foramen transversarium. (Reproduced with permission from Ref. [22])

Spinal Vascular Anatomy

Spinal Arteries

The blood supply to the spine includes paired intersegmental and intercostal arteries (numbered by the rib under which it travels) emanating from the thoracic aorta and running posteriorly on each side of the vertebral body, in turn, giving short osseous branches to the vertebral body before dividing into ventral and dorsal branches (Figs. 2.14, 2.15, and 2.16). An anterior intersegmental anastomosis may be seen before a division where the ventral or lateral branch becomes an intercostal or lumbar artery (depending on the level in the spine). In the rostral most portion of the descending aorta when catheterizing the intercostal vessels, one may encounter a supreme intercostal artery emanating from the aorta (where it usually branches from the costocervical trunk) which supplies multiple intercostal levels at the top of the thoracic cavity along with intersegmental anastomoses providing this supply. The vessel continues as the ventral branch of the spinal segmental artery and enters the spinal foramen to give an anterior epidural branch to supply the bone and dura and then anastomoses with its counterpart at the midline. The dorsal spinal segmental branch then travels into the intervertebral foramen and passes under the transverse process of the vertebral body to supply the posterior muscles and bones of the lamina and spinous processes.

The *radiculospinal artery (spinal segmental artery)* usually terminates in reticular spinal branches which supply the nervous elements itself as will be described next. The vessel divides to irrigate the respective tissues after which it is named and thereby anatomically located in the anterior-posterior plane. These arteries are termed radicular (supplying nerve root only), radiculopial (nerve root and pial plexus; i.e., white matter), and radiculomedullary (nerve root, pial plexus, and cord medulla; i.e., gray matter).

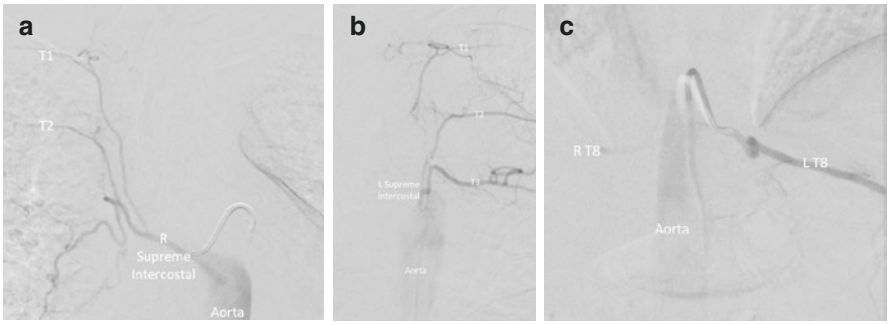

Fig. 2.14 (**a**) AP angiogram of the right supreme intercostal artery providing supply to the right T1 and T2 intercostal arteries. (**b**) AP angiogram of the left supreme intercostal artery demonstrating the anastomotic network providing supply to the T1–3 intercostal arteries. (**c**) AP angiogram of the left T8 intercostal artery with its characteristic appearance running on the underside of the corresponding rib

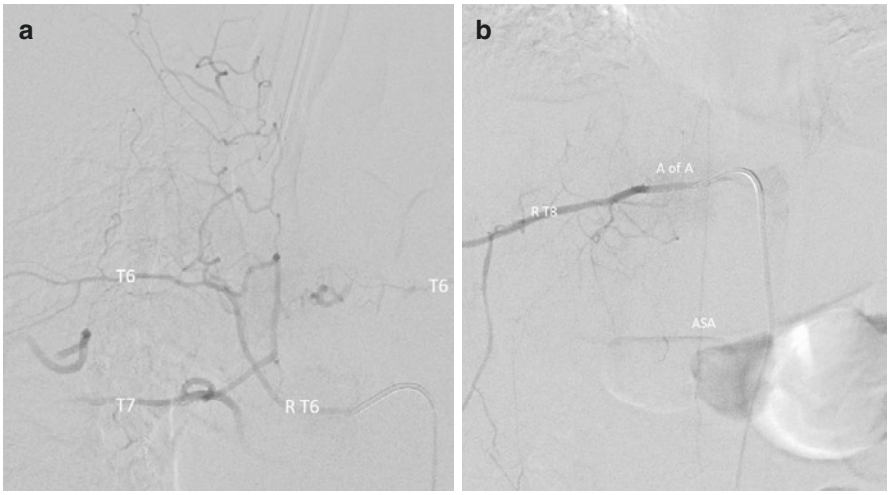

Fig. 2.15 (**a**) AP angiogram of the right T6 intercostal artery. Note filling of the right T7 intercostal artery as well via the anterior intersegmental anastomosis. Additionally, there is filling of the left T6 intercostal artery via a midline anastomotic network. (**b**) AP angiogram of the right T8 intercostal artery demonstrating the characteristic hairpin loop of the artery of Adamkiewicz (A of A) and its filling of the anterior spinal artery (ASA)

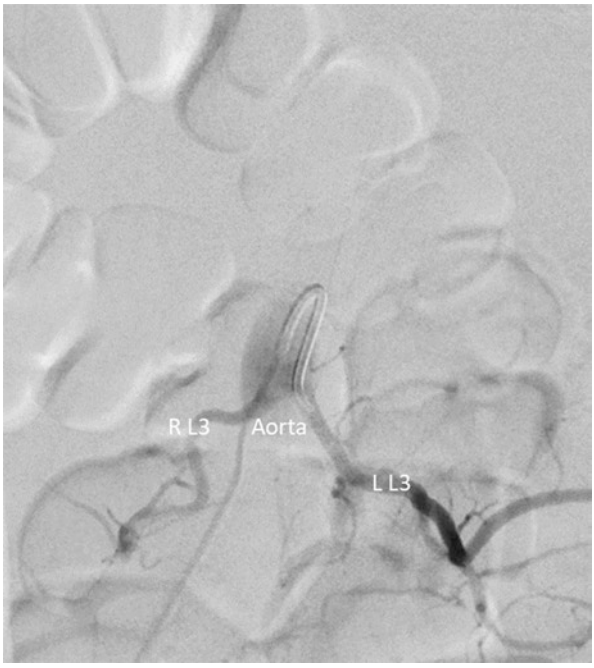

Fig. 2.16 AP angiogram of the left L3 lumbar artery catheterized with aortic reflux demonstrating the right L3 lumbar artery as well. The ventral and dorsal segmental branches can also be traced where the ventral branches appear more proximally and travel medially in this projection

The *anterior spinal artery (ASA)* runs from the vertebrobasilar junction to the filum terminale. It arises from two small branches of the intracranial vertebral artery conjoining at the level of the medullary olives in the midline. It then runs on the ventral surface of the spinal cord and continues to the conus where it is termed the artery of the filum terminale. On the spinal cord, it lies at the entrance of the anterior median sulcus and deep to the anterior median vein. It supplies the anterior 2/3 of the spinal cord and most of its gray matter which includes the anterior and lateral corticospinal and anterior and lateral spinothalamic tracts. These tracts are associated with movement and pain and temperature sensation, respectively. The artery of the lumbar enlargement, or *artery of Adamkiewicz*, usually arises between T9 and T12 on the left side. It is also known as the great anterior radiculomedullary artery or arteria radicularis anterior magna and is the name given to the dominant thoracolumbar segmental artery that supplies the spinal cord in forming a characteristic hairpin loop where it adjoins the ASA. When the artery of Adamkiewicz arises below L2 or above T8, a second ventral radiculomedullary artery exists cranially or caudally to supply the thoracolumbar region [23]. This anatomic configuration of the ventral supply to the spinal cord creates watershed regions of parenchymal perfusion leaving the thoracic spinal cord particularly susceptible to injury from occlusions or compressive pathology as there is no significant redundant supply to the ventral cord.

There are two paired *posterior spinal arteries (PSA)* supplying the ipsilateral posterior one-third of the spinal cord. These posterior arteries are fed by smaller posterior radicular arteries at nearly every spinal level. The PSAs supply the posterior columns and dorsal column medial lemniscus system (gracile fasciculus and cuneate fasciculus) which are associated with sensation (vibration and proprioception).

Spinal Veins

The veins of the spinal cord include the internal cord veins, longitudinal cord veins, and radicular (or radiculomedullary) veins (Fig. 2.17). The *internal cord veins* drain centrifugally with a radiating pattern of symmetric venous capillaries which drain to two *longitudinal midline veins*—the anterior and posterior median spinal veins. In the lower thoracic cord (at the lumbar enlargement), this symmetry varies with a modest dominance of drainage to central veins in the median sulcus. The anterior and posterior median veins drain to the internal and external plexuses, which in turn empty into the systemic segmental veins. The internal vertebral plexus also empties into the dural venous sinuses superiorly. The anterior median vein is continuous with the anterior medullary vein and thus connects cranially with the veins of the posterior fossa. These latter points should be considered with spinal fistulae or arteriovenous malformations (AVMs) and their drainage patterns before and after treatment.

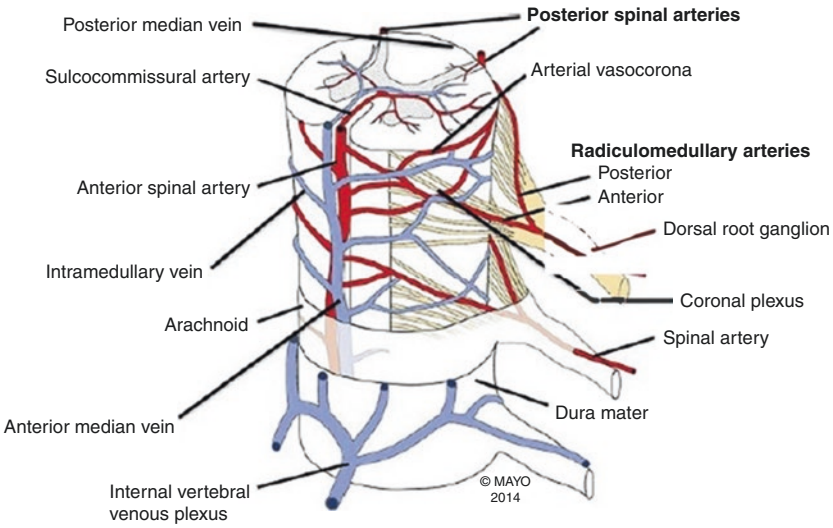

Fig. 2.17 Diagram of the spinal arteries and veins in relation to the spinal cord parenchyma and bony anatomy. (Reproduced with permission from Ref. [24])

The *radicular veins* appear at most, but not all, spinal levels. The anterior and posterior radicular veins are equally numerous (15–50 with 5–8 in cervical, 10 in the upper thoracic, and 1–2 in the lumbar regions). Most of the radicular veins follow the anterior spinal nerve root to pierce the dura (where type 1 dural AV fistula are located), but about 40% leave via separate openings. They do not occur in association with segmental arteries, and a larger vein, from the lumbar expansion is said never to travel with the artery of Adamkiewicz [1].

The internal vertebral plexus lies between the thecal lining of the spinal cord and the bony canal, extending from the skull base to sacrum. It receives venous drainage from the radicular veins and veins from the vertebral bodies. The internal vertebral plexus drains into the external vertebral plexus which connects with the azygous and hemiazygous veins via intercostal and lumbar veins. In the neck, the plexus drains to the vertebral vein and deep cervical veins [1].

In summary, the venous drainage of the spinal cord consists of internal cord veins, longitudinal cord veins, and radicular veins. Internal cord vein anatomy differs depending on the spinal segment; however, most drain centrifugally (with a radiating pattern) into the two longitudinal midline veins. These longitudinal veins, draining along the entire spinal cord, include the anterior median vein and posterior median vein. Finally, the anterior radicular vein (along the ventral nerve root) and the posterior radicular vein (along the dorsal nerve root) track horizontally at almost every spinal segment. The anatomy of the venous drainage of the spinal cord typically varies more widely than the arterial supply.

Conclusion

The arteries and veins of the head and neck are often only thought of as the roadways for our entrée into the intracranial space where our primary focus as neurosurgeons is usually targeted. However, as witnessed by the diversity of anatomic variants or pathologies that may exist in these vessels, and the challenges with navigation or treatment they pose, they may often be even more formidable to deal with than intracranial pathologies. The secure knowledge of this anatomy, its variants, and anastomotic networks open up wide arrays of creative combinations toward approaches and treatments that can combine open and endovascular modalities, leading to the safest and most durable treatments we can offer our patients.

References

1. Byrne JV. Tutorials in endovascular neurosurgery and interventional neuroradiology. Berlin, Heidelberg: Springer; 2012.
2. Lemke AJ, et al. Anomalous origin of the right vertebral artery: review of the literature and case report of right vertebral artery origin distal to the left subclavian artery. AJNR Am J Neuroradiol. 1999;20(7):1318–21.
3. Case D, et al. Neuroangiography: review of anatomy, periprocedural management, technique, and tips. Semin Intervent Radiol. 2020;37(2):166–74.
4. Prince EA, Ahn SH. Basic vascular neuroanatomy of the brain and spine: what the general interventional radiologist needs to know. Semin Interv Radiol. 2013;30(3):234–9.
5. Demertzis S, et al. Aortic arch morphometry in living humans. J Anat. 2010;217(5):588–96.
6. Madhwal S, et al. Predictors of difficult carotid stenting as determined by aortic arch angiography. J Invasive Cardiol. 2008;20(5):200–4.
7. Qaja E, Theetha Kariyanna P. Carotid artery surgery. In StatPearls. 2020, StatPearls Publishing Copyright © 2020, StatPearls Publishing LLC.: Treasure Island (FL).
8. Uflacker R. Atlas of vascular anatomy: an angiographic approach. 2nd edn. Philadelphia: Lippincott Williams & Wilkins; 2007. Copyright © 2007 Lippincott Williams & Wilkins.
9. Bezyanova, Image 6092729. 2021, VectorStock. https://www.vectorstock.com/royalty-free-vector/human-facial-vein-in-vector-6092729.
10. Betts JG, Young KA, Wise JA, et al. Anatomy and physiology. 2013, OpenStax. https://openstax.org/books/anatomy-and-physiology/pages/20-5-circulatory-pathways.
11. Geibprasert S, et al. Dangerous extracranial-intracranial anastomoses and supply to the cranial nerves: vessels the neurointerventionalist needs to know. AJNR Am J Neuroradiol. 2009;30(8):1459–68.
12. Wang J, et al. Four collateral circulation pathways were observed after common carotid artery occlusion. BMC Neurol. 2019;19(1):201.
13. Mokin M, Siddiqui AH. ICA–ECA Collaterals. In: Saba L, Raz E, editors. Neurovascular imaging: from basics to advanced concepts. New York: Springer; 2014. p. 1–11.
14. Uchino A, et al. Persistent dorsal ophthalmic artery and ophthalmic artery arising from the middle meningeal artery diagnosed by MR angiography at 3 T. Surg Radiol Anat. 2013;35(9):775–82.
15. Vargas DA, et al. Cirsoid aneurysms, the arteriovenous fistulae of the scalp: case series and literature review. Rev Colomb Radiol. 2018;29(1):4867–73.

16. Heilman CB, et al. Elimination of a cirsoid aneurysm of the scalp by direct percutaneous embolization with thrombogenic coils. Case report. J Neurosurg. 1990;73(2):296–300.
17. Barnwell SL, et al. Endovascular treatment of scalp arteriovenous fistulas associated with a large varix. Radiology. 1989;173(2):533–9.
18. Morare N, Baloyi E. Post-traumatic arteriovenous malformation of the superficial temporal artery. J Vasc Surg Cases Innov Tech. 2020;6:50–4.
19. *Collateral circulation between external internal carotid arteries*. 2011; Available from: https://somepomed.org/articulos/contents/mobipreview.htm?6/30/6631.
20. Morris P, editor. Practical neuroangiography. 2nd ed. Philadelphia: Lippincott Williams & Wilkins; 2007.
21. Erk H, K.H. Illustrated review of Persistent Primitive Carotico-vertebrobasilar Anastomoses. 2020; Available from: https://doi.org/10.26044/ecr2020/C-14304.
22. Arslan M, et al. The cervical arteries: an anatomical study with application to avoid the nerve root and spinal cord blood supply. Turk Neurosurg. 2017;28:234.
23. Deshaies EM. Handbook of neuroendovascular surgery. New York: Thieme Medical Publishers; 2012.
24. Hanna Al-Shaikh RCL, Eidelman B, et al. Spinal cord infarction. In: StatPearls [Internet]. Treasure Island (FL): StatPearls Publishing; 2021 Jan-. [Figure, Visual depiction of the arterial...] Available from: https://www.ncbi.nlm.nih.gov/books/NBK545185/figure/article-55376.image.f1/.

Chapter 3
Basics of Angiography

Bryan E. Buster and Jonathan A. Grossberg

Indications

Any good discussion of medical testing or intervention typically begins with a list of the indications. Cerebral angiography or digital subtraction angiogram (DSA) still reigns as the gold standard for the evaluation of the cerebral vasculature due to its unparalleled spatial and temporal resolution. The indications for the performance of DSA include evaluation of subarachnoid hemorrhage, ischemic stroke, intracerebral hemorrhage, and further characterization of cerebral vascular disease and abnormalities such as aneurysms, arteriovenous malformations (AVMs), dural arteriovenous fistulas (DAVFs), arterial stenosis, arterial dissection, venous sinus thrombosis, Moyamoya, suspected vasculopathies, and vasospasm [1]. Neuroangiography can also be used to evaluate extracranial disease including carotid and vertebral artery stenosis, carotid artery blowout, epistaxis, oropharyngeal bleeding, and carotid body tumors [2].

With regard to intraparenchymal hemorrhage, any patient under the age of 50 presenting with a spontaneous ICH should undergo evaluation with a DSA. Patients older than 50 with findings on MRI consistent with amyloid angiopathy or classic hypertensive hemorrhage and history of hypertension do not require further evaluation with DSA. Patients older than 50 who do not meet these criteria should be considered for cerebral angiography.

The characterization of cerebral vascular pathology such as aneurysms, AVMs, and DAVFs via DSA is invaluable for risk stratification and treatment (open, endovascular, and radiosurgical) planning. Angiography is also extremely useful for intraoperative and postoperative evaluation of clipped aneurysms, resected AVMs, and ligated DAVFs. Additionally, DSA can help determine pathologies that may be

B. E. Buster · J. A. Grossberg (✉)
Department of Neurosurgery, Emory University School of Medicine, Atlanta, GA, USA
e-mail: Bryan.Edward.Buster@emory.edu; Jonathan.A.Grossberg@emory.edu

J. R. Mascitelli, M. J. Binning (eds.), *Introduction to Vascular Neurosurgery*,
https://doi.org/10.1007/978-3-030-88196-2_3

amenable to endovascular treatment, such as ischemic stroke, ruptured and unruptured cerebral aneurysms, carotid stenosis, AVMs, DAVFs, venous sinus thrombosis, and vasospasm. Angiography and associated preoperative embolization can be used to aid in tumor and AVM resection. Finally, DSA can also be used to deliver targeted intra-arterial chemotherapy for the treatment of tumors such as retinoblastoma.

It is essential for the practitioner to understand the goal of DSA in specific cases prior to beginning the procedure. For example, symptoms or bleed pattern suggestive of a DAVF should prompt investigation of the external carotid arteries (ECAS). Similarly, focal low posterior fossa subarachnoid hemorrhage should be evaluated with bilateral selective vertebral artery injections as relying on reflux into contralateral posterior inferior cerebellar artery (PICA) may not be sufficient to reveal or exclude a dissecting vertebral artery aneurysm.

Pre-procedure Evaluation

Prior to undergoing any diagnostic or interventional endovascular procedures, the patient should undergo careful assessment to determine suitability and to establish baselines. Medical history should screen for any history of kidney disease or dysfunction, presence of atherosclerotic disease, use of antiplatelet or anticoagulant medications, and contrast dye allergies. Physical examination should include neurological examination and palpation (and marking) of pulses. A pre-procedural baseline neurological and pulse exam is critical to both detecting post-procedural complications and avoiding unnecessary anxiety regarding, and evaluation of, pre-existing deficits noted post-procedurally. Doppler ultrasound can be useful in locating difficult to palpate pulses. Basic laboratory tests including CBC, Cr/GFR, and PT/INR need to be obtained and reviewed. If a stent device is to be placed, the patient should be placed on appropriate anti-platelet therapy and platelet function assays may be checked to ensure adequate platelet suppression. Women of childbearing age should undergo pregnancy testing.

Patients with significant comorbidities may require further medical evaluation and physiologic optimization prior to undergoing non-emergent angiographic procedures. Patients taking potentially nephrotoxic drugs such as metformin, NSAIDs, or ACE inhibitors should be asked to discontinue these medications in the days prior to and following their procedure to reduce the risk of contrast induced nephropathy and lactic acidosis. Anticoagulants should be held as permitted to reduce risk of post procedural bleeding or hematoma. For patients with known contrast allergies, pre-treatment with corticosteroids, with or without diphenhydramine can reduce the risk of severe or life-threatening reaction.

If the patient has prior imaging, especially vascular imaging, this should be reviewed in detail. The practitioner should note such features as arch configuration and vertebral artery dominance as this will assist with planning and equipment selection. Note should also be made of the presence of vessel stenosis and calcific

or atheromatous plaques, as this will help modify the procedure goals to reduce patient risk.

In subarachnoid hemorrhage, the distribution of blood on a non-contrast CT can provide clues as to whether the hemorrhage is aneurysmal or non-aneurysmal in nature. If the appearance is consistent with aneurysmal subarachnoid hemorrhage, the distribution can often provide information on where the ruptured aneurysm may be, which can be especially helpful in treating patient with more than one aneurysm. For example, if the hemorrhage is thickest within one of the Sylvian fissures, suspect a ruptured middle cerebral artery (MCA) aneurysm. A flame hemorrhage at the base of the frontal lobe in the setting of SAH is suspicious for a ruptured anterior cerebral artery (ACA) aneurysm. A subdural hemorrhage occurring concurrently with SAH in the absence of trauma is classically associated with a ruptured posterior communicating artery (PCOM) aneurysm.

For subarachnoid hemorrhage confined to the high convexity, aneurysmal origin is less likely. Much higher on the differential is vasculitis/vasculopathy (e.g., reversible cerebral vasoconstrictive syndrome), cortical vein or venous sinus thrombosis, DAVF, or distal atypical aneurysm such as a mycotic or oncotic aneurysm. This differential is important as it keys the operator to look for features of these pathologies (e.g., beaded appearance of vessels in vasculitis) and ensures that the imaging of all appropriate vessels (e.g., ECAs for dAVF).

In summary, careful review of the patient's prior imaging can often guide our expectations and technique in performing the angiogram and inform our differential, increasing the likelihood that we will capture any pathology present.

Consent

The consent process should begin with an explanation of the purpose of the procedure including what is suspected thus far based on history, lab tests, and noninvasive imaging and the goals of the procedure, which can include diagnosis, treatment, or possibly both. Next, the practitioner should explain the procedure itself to the patient using easy to understand language. Setting up expectations is critical to garnering trust and cooperation with patients and their families. It is important to inform the patient regarding what to anticipate before, during, and after the procedure. For patients who are to remain awake during the procedure, the practitioner should walk them through the procedure from start to finish. The physician should discuss the importance of remaining still throughout the procedure for optimal image and diagnostic quality, and rehearse the intraprocedural instructions, such as "take a breath in, hold it, don't move, don't breathe, don't swallow… Okay, you can breathe normally." The patient should be told to expect possible flashing lights or feelings of warmth, flushing, or dizziness during the contrast injections, and that these sensations will all be temporary and brief. Finally, the consent process should discuss the role of different team members and the involvement of residents or fellows if applicable.

After discussing the procedure, there should be a discussion of the potential risks of DSA including bleeding, limb complications, infection, allergy, renal injury, vessel injury, and stroke. Overall, DSA has a low rate of complications. In one study of 19,826 patients undergoing cerebral angiography for various indications from 1981 to 2003, complication rates were as follows: hematoma 4.2% (requiring surgery 0.03%), thrombosis of access vessel 0.05%, headaches 0.8%, nausea, vomiting, or transient hypotension 1.2%, chest pain or arrhythmia 0.3%, anaphylaxis and/or circulatory collapse 0.03%, acute renal failure 0.02%, death (not related to neurologic complication) 0.06%, TIA 2.1%, other reversible neurological deficit 0.36%, permanent neurological complication 0.14%, and death (related to neurological complication) 0.05% [3]. The overall rate of complication in this study was 2.63%. Another study of 1715 patients undergoing cerebral angiography from 2000 to 2008 showed even lower rates of complications [4]. Only one patient suffered TIA and no patients developed any permanent neurological deficits.

Access

Femoral

The common femoral artery is traditionally the most commonly used access site, and until the recent growth of radial access, was used in over 95% of all neurointerventional cases [5]. It is ideal due to its large size, location just under the skin, and compressibility [6]. Since most operators are right handed (and most angiography suites are set up accordingly) the right side is more often accessed than the left, though both sides should be prepped and draped in case difficulty is encountered. The common femoral artery is the extension of the external iliac artery after it passes deep to the inguinal ligament. The inguinal ligament spans between the pubic tubercle and the anterior superior iliac spine. The artery typically crosses at the midpoint of this ligament and traverses over the medial half of the femoral head (usually about 1 cm medial to the center of the femoral head). This can be localized radiographically in the angiography suite prior to puncture using a hemostat or other radiopaque object (Fig. 3.1). Distally the common femoral artery bifurcates into the superficial and deep femoral arteries. Lateral to the artery is the femoral nerve and medial to the artery is the femoral vein.

The artery should be accessed distal to the inguinal ligament, where it is compressible over the femoral head, and proximal to the bifurcation where the vessels are smaller (Fig. 3.2). Puncturing above the inguinal ligament risks retroperitoneal hematoma and potentially hemodynamically significant or even life-threatening blood loss. Accessing the deep or superficial branches distal to the bifurcation increases risks of complications including acute vessel closure, formation of pseudoaneurysm or arteriovenous fistula, and hematoma [6]. Puncturing at or just below the inguinal crease has frequently been offered as a

Fig. 3.1 The hemostat is placed over the medial femoral head to aid in artery localization and to insure compressibility for hemostasis

landmark; however, it should be noted that the bifurcation of the femoral artery is proximal to the inguinal crease in approximately 75% of patients in some studies [6]. When palpating the pulse, the point of maximal impulse overlies the common femoral artery in over 90% of patients [6]. However, many patients have weak pulses or are obese, making locating a pulse difficult. One proposed access technique is to use fluoroscopy to localize the inferior border of the femoral head, marking with a hemostat, and then palpating for the point of maximal impulse just proximal to this. Skin puncture should be made with the needle at a 45° angle so that artery is entered 0.5–1.5 cm below the skin surface along the centerline of the femoral head [6]. Ultrasound can also be employed to localize the artery and guide the needle into the artery in patients where palpation is difficult.

For awake patients, local anesthetics should be used to reduce the discomfort of accessing the artery. Begin with a small wheel of local at the intended puncture site and then inject more deeply, especially laterally where the femoral nerve is located. Avoid puncturing the artery or vein and be sure to aspirate prior to injecting to avoid inadvertent intravascular delivery of local anesthetic. The local use should not contain epinephrine as this can lead to vasoconstriction, complicating vascular access. Moderate sedation can also assist with patient tolerance of the procedure. We typically use 25–50 μg of fentanyl and 0.5–1 mg of midazolam for the average diagnostic cerebral angiogram.

After the local anesthetic has been injected, a scalpel should be used to create a small skin incision sufficient for the diameter of the sheath which will be used (or catheter if no sheath is to be used). This can be done prior to arterial puncture or

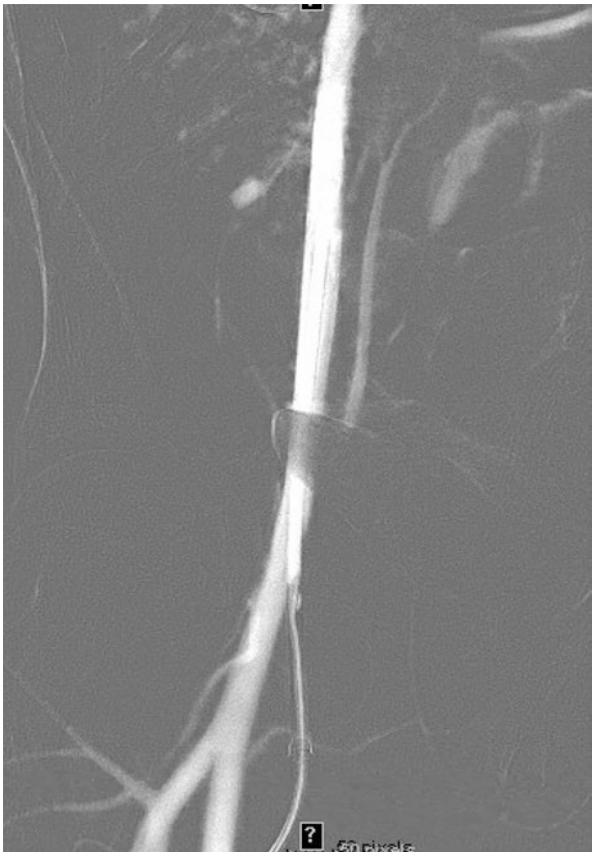

Fig. 3.2 Roadmap image demonstrates sheath placement above the bifurcation in the right common femoral artery

subsequent to puncture once intraluminal positioning has been secured with wire placement as described below.

A single anterior wall puncture is preferred over the previously popular double wall technique where the operator intentionally passed through both the anterior and posterior wall and then slowly withdrew the needle until intraluminal positioning was confirmed with the return of pulsatile blood. We use a 5 French micropuncture kit for the initial access. For a right-handed operator accessing the right common femoral artery, the left hand is used to feel for the pulse or hold the ultrasound probe and the right hand wields the access needle in an underhand fashion with the hub grasped between the thumb and forefinger. The bevel of the needle should be upward facing. Once pulsatile blood is returned, the needle should be stabilized with the left hand and the Cope mandril wire is guided into the needle with the right hand. spinning the wire can help it pass from the hub down the metal shaft of the needle and then smoothly through the vessel. The wire should advance easily and smoothly. If any resistance is met, proceed with caution and consider evaluating under fluoroscopy or withdrawing the wire, to re-establish pulsatile flow. Of note, any withdrawal of the Cope mandril wire should be done under

fluoroscopy to ensure the wire is not sheared as it is being withdrawn. If resistance is felt when withdrawing the wire, the needle and wire should be removed as a unit and pressure held for hemostasis.

Once the microwire is in the vessel, the needle can be withdrawn. A microdilator is then placed over the wire. Always ensure sufficient wire at the distal end of dilators, sheaths, and catheters to maintain access. Once the dilator has been placed, the inner cannula is removed with the Cope mandril wire and pulsatile arterial blood should be noted. A Bentson or other similar braided wire is then inserted into the outer cannula which remained in the artery. Again, this wire should pass smoothly, and if not, it should be investigated with fluoroscopy. Once the Bentson wire is in the descending aorta, the microdilator is removed leaving the Bentson wire in place. The wire is wiped with a moistened telfa and the sheath is then placed over the wire and inserted into the artery. For diagnostic procedures we typically use a 5f short sheath. Longer sheaths which can reach to the level of the carotid or vertebral arteries are available as needed. These catheters are useful for interventional cases when greater support is required for more distal navigation with microcatheters and devices, such as during coil embolization or flow diverter placement. Once in place the wire is withdrawn, and the sheath is connected to a heparinized saline infusion. At our institution, we give heparin once the sheath is in place. We administer 3000 U intravenously for diagnostic procedures. For interventional procedures we typically start with 5000 U and then conduct activated clotting time (ACT) checks every hour, with target ACT of 250–300.

Radial

Radial access is a safe and well-studied alternative to femoral access and has become a favorite of many cardiovascular interventionalists and is growing in popularity in the neurointerventional space. Advantages of radial access include easier vessel selection in patients with bovine arch configuration, facilitated selection of the vertebral arteries, easier access in obese patients, and no need for bed rest post-procedure. Proponents also point to lower rates of major access related complications and major bleeding especially in patients on antiplatelet medications, shorter hospital stays, lower hospital costs, and greater patient satisfaction. Various reasons have been offered to explain the delayed adoption of the transradial approach (TRA) despite its purported advantages and widespread adoption in cardiac procedures. These include a perception that this route offers less favorable vectors for navigation of cerebral vasculature, the smaller diameter of the radial artery may limit size of catheter employed, and a lack of familiarity among current operators, which may result in apprehension regarding potential complications. This includes those involved in teaching fellows, perpetuating the current state of the field [7]. The tide is however changing and there is increased adoption among neurointerventionalists with multiple studies demonstrating the feasibility and quick, though persistent learning curve [8].

The brachial artery bifurcates into the radial and ulnar arteries at the elbow. These two arteries course in parallel down forearm to the wrist where they both give rise to the superficial and deep palmar arches which form distal anastomoses of these arteries in the hand. The palmar digital arteries, princeps pollicis artery, and radialis indicis artery which supply the digits of the hand arise from these arches. As always, there are anatomic variations, and not all individuals have complete arches, though studies have indicated that more than 80% of patients have a complete superficial palmer arch and 90-95% have a complete deep palmer arch.

There is understandably a concern that distal radial artery obstruction following TRA could compromise blood flow to the hand and digits resulting in ischemic complication. Due to this, many operators employ an Allen's test to evaluate collateral perfusion to the hand while compressing the radial artery prior to radial artery access. This technique was first described by Dr. Allen in 1929 and has undergone various modifications and updates over the intervening years. A modern incarnation of the test, the Barbeau test, employs the use of a pulse oximeter applied to a patient's thumb and assessing the waveform for up to 2 minutes with the radial artery compressed. The pulse oximetry tracing is then observed for any damping or drop out (with or without return).

While these tests aim to ensure adequate collateral circulation prior to cannulation and possible inadvertent occlusion of the radial artery, the evidence indicates that such tests do not reliably predict presence (in individuals with abnormal Allen's test) or absence (in individuals with normal Allen's test) of clinically significant hand ischemia in the setting of radial artery occlusion following TRA [7]. Regardless, we still routinely perform an Allen's or Barbeau test prior to TRA at our institution.

When TRA is chosen for access, typically the right side is used due to the more advantageous ergonomics for a right-handed operator and greater ease of selection of the common and internal carotid arteries. In cases where the left vertebral artery is the site of the pathology, then a left radial approach is employed either by reversing the room orientation or using the distal transradial technique described below. The patient's arm can be placed at his/her side or abducted at 70–90°. The wrist is extended over a towel or brace and secured in place. Some operators place topical anesthetics and vasodilators prior to catheterization to increase cross sectional area. The artery is punctured 2–3 cm proximal to the styloid process of the radius, where its diameter is somewhat larger and course straight. An angle of 30–45° between the needle and the skin is recommended. At our center, we routinely employ ultrasound guidance to facilitate access and the same 21G micropuncture kit as for TFA. However, we use a dedicated radial access sheath which is hydrophilic and does not require a skin incision or separate dilator. Typically sheaths up to 6 Fr can be employed without risk of radial artery occlusion. Following sheath placement, a "radial cocktail" consisting of some combination of vasodilators/antispasmotic agents (e.g., nitrates and calcium channel blockers) and heparin is instilled through the sheath after being diluted with the patient's blood (~20 cc).

Other operators have described distal radial access via the dorsal radial artery over the anatomic snuff box (distal transradial approach, dTRA) for diagnostic procedures [9]. For this technique, the wrist is not extended. This technique has the

advantages of using a hand position more comfortable for operator and patient, especially in cases where the left wrist is used as the arm is placed across the chest. The dTRA also has the advantage of employing a puncture distal to the take off of the deep palmer arch, minimizing potential for disruption of the collateral circulation. Finally, in cases of radial artery occlusion, the traditional TRA approach is still an option for a follow-up procedure.

Catheter Selection

There are a wide variety of catheters available and suitable for cerebral angiography, and catheter selection is often based on a particular operator's experience and preference along with the patient's anatomy. Catheters vary in length, shape, and stiffness. Catheters are also classified as diagnostic catheters, guide catheters, and microcatheters. In general, diagnostic catheters are used, as the name suggests, for diagnostic neuroangiography or initial selection of vessels originating off the arch up to the level of the proximal internal/external carotid arteries. At our institution, for diagnostic work, we typically begin with a 5 Fr vertebral or hockey stick catheter for most adult patients. In patients with greater tortuosity or Bovine arch configuration, we often employ a Simmons 3 catheter.

Guide catheters are intermediate sized catheters that can be placed more distally (e.g., into the petro-cavernous carotid or V3-4 segment of the vertebral artery) and provide support and stability for microcatheters used in super selective angiographic procedures and interventional cases. These are often brought into place over an exchange length wire after initial vessel selection has been accomplished with a diagnostic catheter. Some guide catheters have balloon tips, which can be useful for creating flow arrest for thrombectomy.

Finally, microcatheters are used for selection of intracranial vessels. As with diagnostic and guide catheters, there are a large number of commercially available microcatheters with varying properties. Most are designed for use over a microwire, though there are some flow directed microcatheters which are mostly used for AVM embolization. Many microcatheters have tips which can be steam shaped to allow some steerability for accessing vessels or aneurysms and provide more stability during aneurysm treatment. A full discussion of catheters configurations is well beyond the scope of this work.

Catheters for Radial Access

Catheter selection is different when TRA is used. Typically, a type of Simmons catheter is used for vessel selection. The catheter can be formed at various points depending on the configuration of the arch and the vessel to be selected, including at the aortic valve, within the ascending or descending aorta, or within the arch itself.

Aortic Arch

Aortic arches are also classified into types (I-III) based on the vertical distance from the origin of the brachiocephalic artery to the apex of the arch, as observed in a parasagittal projection. A type 1 arch involves a vertical distance of less than 1 diameter of the left common carotid artery, type II between 1 and 2 diameters, and type III greater than 2 diameters. This typically varies with age, with older patients tending toward types II and III.

There are a large number of normal permutations in the arrangement of vessels arising from the aortic arch, and, in some respects, it is instructive to conceptualize these arrangements as a spectrum of variability rather than a collection of discreet configurations. The most frequently encountered configuration of the arch is a "three vessel arch" with the brachiocephalic, left common carotid, and left subclavian originating, from proximal to distal/right to left, off the arch (Fig. 3.3). The brachiocephalic is the largest of these branches and gives rise to the right subclavian and right common carotid artery. The right vertebral artery is typically the first branch off of the right subclavian artery, prior to the origin of the internal thoracic artery, thyrocervical trunk, and costocervical trunk. The left vertebral artery is likewise typically the first branch from the left subclavian artery.

The most common variant is the so-called "Bovine arch" configuration, where left common carotid originates from the brachiocephalic artery. This variant is found in up to 15–20% of patients [10]. Interestingly, this is not the typical

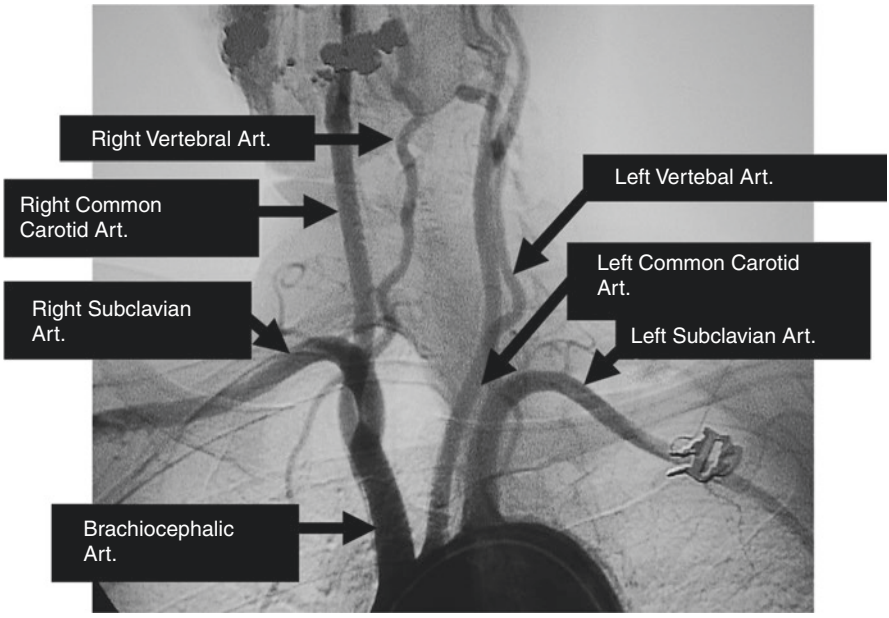

Fig. 3.3 AP angiographic image demonstrates the most common aortic arch configuration

configuration of the aortic arch in cows, where a single brachicephalic trunk trifurcates into a right subclavian artery, left subclavian artery, and bicarotid artery. Another similar configuration is where the left common carotid artery and brachiocephalic artery share a common origin is referred to as truncus bicaroticus. These configurations often require a recurved catheter such as a Simmons or Vitek to access. Alternatively, TRA often provides an advantageous vector for accessing this type of arch with a more simply curved catheter.

Another commonly encountered variant involves the left vertebral artery originating directly off the arch. Approximately 4% of patients will exhibit this anatomy. Again, a spectrum exists from very proximal take off of the left vert from the left subclavian, to common origin, to the aforementioned direct origin from the arch.

More unusual variants include an aberrant right subclavian artery or artery of Lusoria where the right subclavian is the most distal vessel to branch from the arch, occurring in 0.5–2% of patients. Occasionally in this configuration, the right vertebral artery will be a branch of the right common carotid artery. Artery of Lusoria is a variant which makes TRA quite difficult and in our experience is a reason to convert to TFA. A full tabulation and cataloguing of the anatomic variation of the great vessels and their branches are beyond the scope of this work.

Navigation and Initial Vessel Selection

Prior to their introduction into the vasculature, all catheters should be flushed with saline to remove air. At our institution, we place a three-way stopcock on the back of the diagnostic catheter to facilitate connection to a heparinized flush line between diagnostic runs. At other centers, a heparinized flush is constantly infused during the procedure. The guide wire is also placed into the catheter prior to introduction into the sheath, though it is left just short of the tip to allow easy insertion into the sheath. We typically begin with a 0.035” Bentson guidewire. Once the catheter is secure within the sheath, wire is advanced such as to allow for at least 8–10 cm of length beyond the catheter tip. Leading with less than this amount of wire while advancing the catheter and wire together can constrain the guide wire tip resulting in a higher probability of intimal injury and vessel dissection. The catheter and wire are then advanced together under A-P fluoroscopy over the arch. To advance the system, the left hand is positioned at the sheath, and the stopcock at the end of the catheter is held between the thumb and forefinger and fed into the sheath. The right hand is used to control the distal end of the catheter and stabilize the position of the catheter relative to the wire.

Once the catheter is over the arch, the wire is withdrawn to the elbow of the vertebral catheter. The position of the catheter is then optimized for selection of the brachiocephalic artery by gently torquing the catheter counterclockwise until the tip points cranially. Once optimized, the catheter is gently pulled back. Once at the ostium of the brachiocephalic artery, it will “click’ into place. Once at the ostium of

the brachiocephalic artery, the wire is once again advanced under fluoroscopic visualization to the level of the proximal ICA or distal CCA. If the patient has a history of carotid stenosis on noninvasive imaging or if there are any irregular wire movements observed, then the wire is removed, and a roadmap obtained. The wire is then pinned using the fifth digit and hypothenar eminence and the catheter is carefully advanced while torquing. Although we have described selection of the right internal carotid here, generally, many operators like to begin with the vessel of greatest interest.

An alternative to using the guide wire for vessel selection, once over the arch, involves carefully puffing small amounts of contrast from the tip of the catheter while steering the catheter into place. The puffs of contrast serve as a navigational adjunct and potentially push the catheter tip away from the vessel wall, reducing the likelihood of intimal injury. In skilled hands, this method can be very efficient, as it saves time of bringing the wire into and out of the catheter (and consequently, the need to double flush) for subsequent vessel selection.

Roadmapping

Roadmapping creates a negative image of the vessels seen on contrast injection to superimpose on a live fluoroscopic image, thus allowing accurate vessel selection with a guidewire or microwire (Fig. 3.4). It can be useful for selecting extracranial vessels in patients with aberrant anatomy or tortuosity and is essential for safe intracranial navigation. A roadmap is obtained by acquiring a set of images using fluoroscopic subtraction while injecting contrast. The images are summed during the acquisition process; therefore, any motion during the acquisition will distort the roadmap. Alternatively, a "false" roadmap can be created by using an image from an angiographic run for the negative. Since the negative is simply superimposed on the live fluro images, any movement of the patient or detectors or straightening of vessels via catheterization will decrease the roadmap accuracy. To navigate extracranial vessels once we have created a roadmap, we typically use a hydrophilic Terumo Glidewire (Tokyo, Japan).

Double Flushing and Image Acquisition

Once the catheter is in the right internal carotid (or other vessel of interest), the wire is removed. Again, this should be done under fluoroscopy so as to ensure the catheter remains in place. Following wire removal and prior to contrast injection, the catheter should always be "double flushed" to clear any clots or air bubbles from the catheter that may have formed. This is accomplished by aspirating the catheter contents into a 10 cc syringe. This syringe is removed, and a small contrast syringe connected. Again, a small amount of blood is aspirated, and the syringe is tapped

Fig. 3.4 Example of a roadmap image of the left vertebral artery used for wire and catheter navigation

vigorously while being held upright to ensure any air bubbles are removed. Small amount of contrast is injected to clear the catheter of blood and observe to see if the contrast runs off appropriately. If needed, a roadmap can be acquired at this point, as described above. If the catheter is indeed in the vessel of interest, it is then connected to a continuous heparinized saline infusion. This allows the catheter to remain free of blood products while the angiographic projections are being obtained.

Once the catheter is in position, the patient table and detectors are positioned for acquisition of the angiogram images. Biplane image acquisition is the standard for cerebral angiography as it allows for two sets of images, typically orthogonal to each other for diagnostic angiograms, with a single injection of contrast, decreasing procedural time and contrast load for the patient. There are several standard projections used in cerebral angiography. For a standard AP projection, the upper margins

of the orbits are aligned with the petrous ridges. For a straight AP projection, the lower margin of the orbits is aligned with the petrous ridge. Townes and Waters views involve 35° of cranial and 45° of caudal angulation, respectively. For a straight lateral view, the auditory meatus or the two sides of the floor of the anterior fossa should be aligned. In addition to AP and lateral views, the detectors are often rotated together 45° to obtain oblique views. For complete characterization of abnormalities such as aneurysm, 3D rotational images are also typically obtained. These data are then fed into mainframes that allow for a full three-dimensional perspective, accurate measurement, and optimization of detector placement for treatment views.

Injections can be performed either manually or with a power injector, depending upon operator and institutional preference. Manual injections provide tactile and visual feedback, which allows the operator to vary the force of the injections and can be helpful in complex pathology such as AVMs and DAVFs. Manual injections also tend to reduce procedure time compared to use of power injectors. Power injectors reduce the radiation exposure to the operator and lead to a more consistent uniform contrast injection. When injecting manually, the syringe should be held up off the patient to prevent catheter kinking and slightly upright to allow bubbles to rise. The syringes are filled with 70-100% contrast solution based on the anatomy and operator preference. The thenar eminence of the right hand should be used to engage the plunger to ensure adequate force. The thumb of the left hand can be positioned at the upper lip of the syringe to function as a safety, preventing complete expulsion of the contents of the syringe which may include a small amount of air at the top. Typically runs are held through late venous phase, though this can be varied depending on the pathology being evaluated. If a flush is connected to the catheter, it is turned off during the injection and back on once the capillary phase begins.

It goes without saying that regardless of the injection technique used, the upmost care must be taken to ensure that all connections and injections remain free of air. This is done by always connecting “wet to wet” with the flush running through the connector, aspirating, and tapping vigorously to remove air from connections. If, despite all efforts to avoid it, air is injected, rapid action is needed to avoid ischemic injury from gas emboli. If the air embolus is large and detectable on angiogram in an accessible vessel, a catheter can be used to aspirate the air. In addition, induced hypertension may allow for improved collateral perfusion. Hyperbaric chambers can also be used to reduce the size of an air embolus.

Hemostasis and Closure Devices

Once the angiogram or intervention is complete, the catheter and sheath must be withdrawn and hemostasis achieved. The most basic method for achieving hemostasis at the arteriotomy is manual compression. For TFA, once the sheath is removed, the artery is compressed against the femoral head, superior to the skin incision ~1–2 cm. If there are no contraindications, protamine may be used to reverse heparin given for the procedure once the sheath is withdrawn. During compression, the

skin incision should remain visible to ensure adequate pressure is applied to prevent extravasation. If pressure is directed at the site of the incision, this may allow for extravasation of blood but entrapment within the overlying tissue, resulting in formation of a hematoma or pseudoaneurysm. For a 4–5 fr arteriotomy, typically 15 min of pressure is adequate. As a general rule of thumb, increase the time by 5 minutes for each additional French of sheath size. Patients on antiplatelet medications will likely require much greater compression time. The first third of the compression time should employ occlusive pressure. The operator can then slowly and progressively decrease the pressure over the remaining period, being careful to observe for bleeding or hematoma formation. Once manual compression has ended and hemostasis ensured, a dressing is applied, and the patient is instructed to remain on bed rest with the procedure leg straight for at least 2–4 hours for a 5 fr sheath.

To reduce the time that manual pressure must applied and that patients must remain on bed rest with their leg straight, a wide variety of closure adjuncts have been developed including external devices, such as hemostasis pads, and compression devices, and percutaneous devices, such as collagen plug devices, and suture devices. Prior to employing the percutaneous devices, an arteriogram of the puncture site should be done to confirm access within the common femoral artery (below origin of epigastric artery and above the bifurcation). If the puncture is observed to be high or low, use of a percutaneous closure device should be reconsidered.

Hemostasis pads such as Abbot Vasular Chito-Seal (Chicago, Illinois) and Argon Medical V + Pad (Frisco, Texas) contain agents that promote platelet aggregation clot formation and are used in conjunction with manual compression. However, since they are applied over the skin rather than directly over the arteriotomy, their effectiveness may be limited [11]. Additionally, they require occlusion at the skin incision, which may prevent the operator from noting inadequate pressure at the arteriotomy. At our institution, we use the V + Pad as an adjunct to stop minor continued bleeding after successful deployment of another device such as a Cardiva VASCADE (Sunnyvale, California), Terumo Interventional Systems Angio-Seal (Somerset, New Jersey), or Abbott Vascular Perclose Proglide.

External compression devices obviate the need for extended manual pressure at the arteriotomy site, freeing staff up for other duties. However, they tend to be less comfortable for patients and require extended periods of bed rest, just as with manual compression. These devices typically have a clear plastic inflatable bulb that allows for observation of the puncture site and is positioned just above the arteriotomy. They are secured with straps or adhesive wings. Initially the bulbs are inflated above the systolic pressure immediately following sheath removal and then slowly deflated over time according to the manufacturer's specifications.

Devices such as VASCADE and Angio-Seal deliver a collagen plug to the outer wall of the artery. The Angio-Seal device additionally deploys an absorbable intravascular anchor which secures the collagen plug in place against the vessel. Both systems' manufacturers claim faster time to hemostasis and ambulation. These plugs tend to dissolve over a few months, and it is important to note that these devices can limit repeat access in that time period. Other devices which employ a suture, such as the Perclose Proglide, allow immediate arterial reaccess if needed,

and accordingly are our institution's choice for patients with subarachnoid hemorrhage who may require repeat angiography for vasospasm or aneurysm management. After the use of a percutaneous closure device, we typically only require 2 hours of bed rest with the procedure leg straight compared with 4 or more hours with manual compression.

For radial access, there are several commercially available inflatable compression devices. We typically use the Terumo TR Band. The band is applied around the wrist prior to sheath removal. A marker on the device is used to line up the puncture site. The compression balloon is inflated with 15–18 mL of air as the sheath is withdrawn. Air is slowly withdrawn until bleeding is seen and then 1–2 mL of air are re-injected until bleeding ceases. In the recovery room, 3–5 mL of air are removed every 10–15 minutes unless fully deflated.

Complications and Their Management

Neurologic Complications

Perhaps the most feared complication of a cerebral DSA is neurological compromise. Reported rates of permanent neurological deficit following diagnostic cerebral angiography vary widely, with some dedicated neurovascular specialist reporting rates <1% and other series claiming rates from 0.3% to 5.7% [4]. Patients with symptomatic atherosclerotic disease have been reported to have higher rates of stroke than those without. Some authors advocate routine use of roadmapping to identify danger areas with atherosclerotic plaques or tortuous vessels so as to avoid disruption of these plaques or vessel dissection. Dissection resulting in lower grade stenosis can be treated with oral anti-platelet or anticoagulants, whereas patients with high grade stenosis following dissection will likely require stenting [12]. In addition to disruption of plaques and arterial dissection, other sources of emboli can include thrombus forming in or on catheters and inadvertent air injection. At our center, we administer heparin after sheath placement to minimize potential thromboembolic complications. We administer 3000 U for diagnostic procedures and for interventional procedures we administer 5000 U and conduct ACT checks every hour with target ACT 250–300. In addition, catheters must be double flushed following wire removal and should be connected to continuous heparinized flush between injections. As discussed previously, great care must be taken to ensure air is purged from all lines and connections. In-line air filters can serve as additional safety measures.

Access Site Complications

Poor hemostasis at the puncture site can result in the formation of a hematoma. For punctures inadvertently made above the inguinal ligament, this can lead to life-threatening retroperitoneal hemorrhage. For any patient exhibiting signs of shock including tachycardia and hypotension, consider STAT evaluation with CT of the abdomen and pelvis and have a low threshold for administering volume and blood replacement. For punctures below the inguinal ligament, development of hematoma is typically noted on physical exam. If recognized early, direct pressure along with correction of any coagulopathy can be sufficient. However, once a large hematoma has formed, direct pressure can be inadequate to stop the hemorrhage. Large hematomas can cause compression and injury to surrounding structures. Compression of the femoral vein can result in venous stasis and potential DVT formation. Additionally, a large hematoma could result in overlying skin necrosis. Pulses should be regularly checked to ensure adequate distal perfusion. Any evidence of compromise of distal circulation or surrounding structures should prompt surgical consultation for possible evacuation and open repair of the arteriotomy.

Development of hematoma can also lead to formation of a pseudoaneurysm, a cavity within the hematoma continuously fed by the arteriotomy. Any significant hematoma should be evaluated with duplex ultrasound to screen for pseudoaneurysm. Smaller pseudoaneurysms, less than 1-3 cm, may thrombose spontaneously. For larger pseudoaneurysm, treatment is often required. Often, ultrasound guided injection of thrombin into the pseudo aneurysm or proximal arterial compression is sufficient. Occasionally, surgical consultation is required for endovascular stenting or even open repair.

Arteriovenous fistula can also form between the femoral artery and femoral or saphenous vein in rare case. Typically these are small and self-resolving. Occasionally they can become symptomatic with resulting lower extremity edema. For subacute fistula, compression at the site may be sufficient. For persistent fistula, open or endovascular treatment may be required.

Acute limb ischemia is a rare but morbid complication of arterial access. It can be caused by underlying atherosclerosis, vessel dissection, closure device misadventure, or simply thrombosis of a relatively small artery used for access. Rapid recognition is paramount. The classic findings include pain, pulselessness, parathesis, poikilothermia, and paralysis. If found, early surgical consultation should be sought, along with potential initiation of anticoagulation with intravenous heparin. CT angiogram of the aorta with runoff can provide additional information for the vascular surgeons but should not delay operative intervention.

Conclusion

Cerebral angiography is a powerful diagnostic and treatment tool for cerebrovascular disease. It can be performed safely if proper history, precautions, and techniques are employed. It is important for all interventionalists to understand the potential complications and how to best avoid and manage them.

References

1. Sawiris N, Venizelos A, Ouyang B, Lopes D, Chen M. Current utility of diagnostic catheter cerebral angiography. J Stroke Cerebrovasc Dis. 2014;23:e145–e50.
2. Case D, Kumpe D, Roark C, Seinfeld J. Neuroangiography: review of anatomy, periprocedural management, technique, and tips. Semin Interv Radiol. 2020;37:166–74.
3. Kaufmann TJ, Huston J, Mandrekar JN, Schleck CD, Thielen KR, Kallmes DF. Complications of diagnostic cerebral angiography: evaluation of 19 826 consecutive patients1. Radiology. 2007;243:812–9.
4. Thiex R, Norbash AM, Frerichs KU. The safety of dedicated-team catheter-based diagnostic cerebral angiography in the era of advanced noninvasive imaging. Am J Neuroradiol. 2010;31:230–4.
5. Starke RM, Snelling B, Al-Mufti F, et al. Transarterial and transvenous access for neurointerventional surgery: report of the SNIS Standards and Guidelines Committee. J NeuroInt Surg. 2020;12:733–41.
6. Irani F, Kumar S, Colyer WR Jr. Common femoral artery access techniques: a review. J Cardiovasc Med (Hagerstown). 2009;10:517–22.
7. Zalocar LAD, Doroszuk G, Goland J. Transradial approach and its variations for neurointerventional procedures: literature review. Surg Neurol Int. 2020;11:248.
8. Snelling BM, Sur S, Shah SS, et al. Transradial cerebral angiography: techniques and outcomes. J NeuroInt Surg. 2018;10:874–81.
9. Brunet M-C, Chen SH, Sur S, et al. Distal transradial access in the anatomical snuffbox for diagnostic cerebral angiography. J NeuroInt Surg. 2019;11:710–3.
10. Shapiro M, Raz E, Peter. Aortic arch variants: a practical guide to safe and timely catheterization. Int Neurol. 2018;7:544–55.
11. Nguyen N, Hasan S, Caufield L, Ling FS, Narins CR. Randomized controlled trial of topical hemostasis pad use for achieving vascular hemostasis following percutaneous coronary intervention. Catheter Cardiovasc Interv. 2007;69:801–7.
12. Goeggel Simonetti B, Hulliger J, Mathier E, et al. Iatrogenic vessel dissection in endovascular treatment of acute ischemic stroke. Clin Neuroradiol. 2019;29:143–51.

Chapter 4
Basics of Craniotomy

Santiago Gomez-Paz, Alejandro Enriquez-Marulanda, Felix Nwajei, and Christopher S. Ogilvy

General Principles

The treatment of intracranial aneurysms is an ever-changing field that reacts and accommodates new treatment strategies based on endovascular techniques considered equally efficacious and with similar or better outcomes compared to performing open surgery. However, less invasive is not always lower risk. Specific aneurysm configuration, location, and failure to obtain a good endovascular treatment response are some of the facts that make lesions amenable to open surgical treatment. Proper patient selection requires understanding the unique aneurysm characteristics and a successful craniotomy can provide the field of view needed for performing a safe and effective treatment [1]. The basic craniotomies used for obliterating an intracranial aneurysm are essential surgical techniques in the arsenal acquired by training neurosurgeons.

S. Gomez-Paz
Department of Neurological Surgery, Mount Sinai Health System, New York, NY, USA
e-mail: Santiago.GomezPaz@mountsinai.org

A. Enriquez-Marulanda
Neurosurgery Service, Beth Israel Deaconess Medical Center, Harvard Medical School, Boston, MA, USA
e-mail: aenriqu1@bidmc.harvard.edu

F. Nwajei
Department of Neurosurgery, Boston Medical Center, Boston, MA, USA
e-mail: felix.nwajei@bmc.org

C. S. Ogilvy (✉)
Neurosurgery Service, Beth Israel Deaconess Medical Center, Harvard Medical School, Boston, MA, USA

Endovascular and Operative Neurovascular Surgery, BIDMC Brain Aneurysm Institute, Professor of Neurosurgery, Harvard Medical School, Boston, MA, USA
e-mail: cogilvy@bidmc.harvard.edu

J. R. Mascitelli, M. J. Binning (eds.), *Introduction to Vascular Neurosurgery*,
https://doi.org/10.1007/978-3-030-88196-2_4

A number of the craniotomies discussed in this chapter have one or more variations modeled based on a few approaches to minimize unnecessary intracranial exposure [2, 3]. It is the training neurosurgeons' task to expand upon these techniques and master different approaches to avoid a fixed use of a single approach. Expertise in performing open surgery begins with a thorough understanding and visualization of the surgical corridor needed to optimize each step of the intradural dissection and aneurysm manipulation, finalized with a complete neck occlusion upon clip deployment. This chapter will provide a review of the primary surgical approaches used to access and obliterate aneurysms within the intracranial vasculature, as well as insight into the selection process of each surgical window and its benefits and inherent limitations. The array of treatment options is an ever-evolving field. However, the training neurosurgeon must understand the essential anatomical principles and develop a step-wise approach to selecting a specific surgical corridor.

Approaches for Anterior Circulation Aneurysms (e.g., AComA, PComA, MCA, ICA, Paraophthalmic, and Distal ACA)

In this section, we discuss the basic craniotomies commonly used to treat aneurysms arising from the anterior circulation and posterior circulation. The first and most commonly used approach is the pterional craniotomy [4]. This classic approach is usually but not necessarily modified by adjunctive drilling of the lateral orbit and/or the zygomatic process. Adjunctive drilling serves to expand the available corridors and angles available for dealing with a given aneurysm. However, drilling extensions should be based on the anatomical characteristics of the aneurysm (i.e., location and projection), which influences the anatomical relationship between the aneurysm and perforating arteries or nearby branches (e.g., AChoA and Pcomm aneurysms). The main craniotomies we will discuss are the pterional, orbitozygomatic, supraorbital, and lateral supraorbital.

General principles such as brain relaxation techniques via CSF release, proximal and distal parent vessel control, and temporary clip application when necessary and proper dissection are all to be considered and performed as needed in each craniotomy that will be discussed below. This section will discuss the critical principles of each craniotomy presented; this includes patient positioning, landmarks used, skin incision, the sequence of dissection, the pathway for the osteotomy and burr holes, dural opening, and closure. Microsurgical steps specific to each aneurysm and its configuration are beyond the intended scope of this chapter.

Pterional Craniotomy (Frontotemporal Sphenoidal)

This operative corridor is composed of an osteotomy that runs through the frontal and temporal bone and the greater wing of the sphenoid bone. It is considered one of the key supratentorial approaches. A pterional craniotomy provides a versatile set

of corridors with excellent exposure to the main aneurysms harbored within the anterior portion of Circle of Willis [1, 5]. Exposure to some aneurysms at the basilar apex and superior cerebellar artery origin can also be reached through this approach [6]. The craniotomy is performed with the patient in a supine position. The head is turned so that the ipsilateral malar eminence remains at the highest point of the heads' surgical field. Slightly different angulations to the head depend on the projection of the target aneurysm.

Patient Positioning

Generally, a supine position with the head turned between 20 and 45° after rigid pin fixation works well. The head is extended to 15–20% to facilitate frontal lobe relaxation away from the cranial base, allowing for a better field of view and less need for tissue retraction.

Skin Incision, Temporal Muscle, and Scalp Handling

The incision is planned based on two anatomic landmarks, the tragus and the ipsilateral mid-pupillary line. One should extend the incision marking from the root of the zygomatic arch (1 cm anterior to the tragus; to avoid injuring the frontalis branch of the facial nerve) in a curvilinear fashion until reaching the point leveled at the ipsilateral pupil (Fig. 4.1). The incision, cutting from the skin deep into the periosteum, should start medially behind the hairline and toward the zygoma, interrupted once reaching the temporal muscle fascia just below the superior temporal line. The muscular fascia (temporoparietal fascia) is then opened with scissors toward the zygoma. The temporal muscle is incised parallel to the skin/galeal incision. Both the muscle and the skin are reflected anteriorly as a unit while conserving the fascia [7].

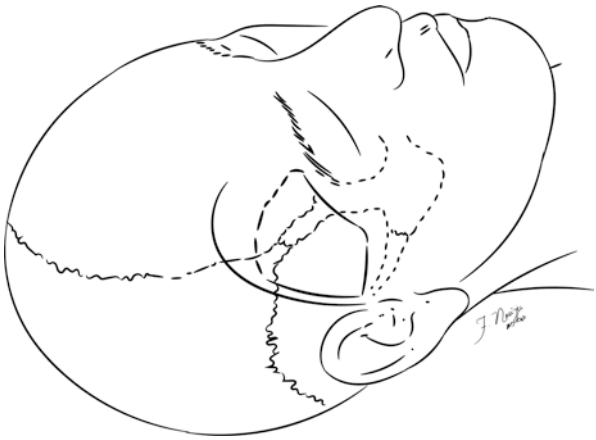

Fig. 4.1 Pterional approach: skin incision (thick line) and outline of craniotomy (dashed line) for a pterional approach

A periosteal elevator is used to dissect the sub-periosteum to reflect the muscle as a subfascial subpericranial flap. The fascia must be separated from the skull, and this should be reflected as low as needed to expose the area behind the frontal process of the zygomatic bone at the level of the frontozygomatic recess (key burr hole area). The myocutaneous flap is secured with fish-hook retractors or sutures and folded over a sponge or gauze to avoid skin necrosis. This subfascial subpericranial flap comprises both a subpericranial mobilization medial to the superior temporal line and a subfascial mobilization lateral to the superior temporal line. This method protects the fat pad located between the interfascial plane just anterior to the key burr hole area, therefore, preserving the frontalis branch of the facial nerve [8].

Bone Flap, Dural Opening, and Pterional Closure

Between 1 and 3 burr holes are made before the osteotomy. A temporal burr hole along the side of the pterion can be used to dissect the dura from the skulls' inner table with a Penfield dissector (no. 3). The additional pair of burr holes can be placed more anteriorly at the key burr hole level in the frontozygomatic recess, with the second burr hole superior to the key burr hole and just above the superior temporal line. A powered drill with a B1 bit and footplate or a craniotome can be used for the osteotomy. An alternative technique is to use a "matchstick" cutting bit to create the craniotomy without burr holes. We have found this produces a good cosmetic result.

The first bony cut extends from the key burr hole along the floor of the anterior cranial fossa and superiorly just lateral to the supraorbital rim, following a curvilinear pattern until reaching the superior burr hole (Fig. 4.2). The basal aspect of the resulting bone flap is made by extending the osteotomy from the key burr hole toward the basal frontal bone in a curvilinear direction toward the superior burr hole. A rongeur is used to cut down the lateral wing of the sphenoid bone. The bone flap is then elevated, allowing it to fracture away from the pterion. The resulting dimensions of this craniotomy are usually around 6×6 cm but can be much smaller for specific aneurysms. The dura should be separated from the roof of the orbit and the lateral sphenoid wing. Once we remove the bone flap, a drill is used to flatten these bony prominences to reach the lateral orbit close to the superior orbital fissure. With a drill, one can extend the bone flap and drill away any residual attachments to the pterion, further flattening its surface and the lateral surface of the sphenoid wing until reaching the lateral edge of the superior orbital fissure. This sequence of techniques should result in a surgical corridor with a flat base to which we then reflect the dural opening anteriorly.

One should take care to avoid exposing the frontal sinus while performing these maneuvers; however, if entered, prompt repair should be performed by stripping away the mucosal lining of the sinus and filling its cavity with antibiotic Gelfoam and bone wax. If a larger entry is encountered, fat should be used to fill the exenterated sinus. Closure of the sinus entry can be done with a portion of pericranium obtained from the scalp flaps' inner surface. The dura is opened with a curvilinear

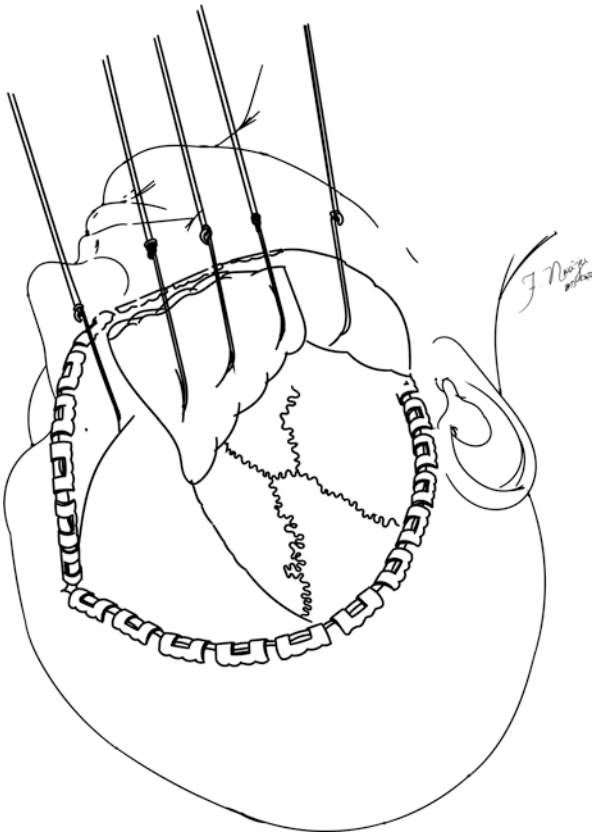

Fig. 4.2 Pterional extradural exposure: exposure of the cranium for a pterional approach by reflecting the galea and temporalis muscle anteriorly

incision, starting at the posterior-inferior limits of the surgical window toward the floor of the anterior cranial fossa at the anterior-inferior limit. The dural flap is then reflected anteriorly and secured with low-lying sutures close to the brain surface so that there is a maximal reflection of the dura away from the surgical field. Microsurgical dissection and exposure of the lesion in question follow at this point.

Supraorbital Craniotomy

The supraorbital craniotomy provides a subfrontal corridor to the anterior skull base, useful for treating lesions within the sellar and suprasellar region, as well as the majority of aneurysms from the anterior circulation (AComA, PComA, MCA) [9]. While narrow viewing angles are the main limit to the resulting corridor, this opening provides enough surgical depth to treat deep-seated lesions such as basilar apex aneurysms [10]. This approach is most commonly used to treat wide-neck ACommA aneurysms whenever the dome has an anterior or inferior pointing

direction. Complex aneurysms in the anterior circulation are treated more efficiently with a pterional craniotomy due to the wider range of operative corridors available (e.g., better lateral access and manipulation).

Patient Positioning

The anatomical configuration of the aneurysm and its dome projection play an essential role in patient positioning. The patient is positioned supine in the operative table with the head rotated 15–20° contralateral to the side of the lesion. The head is slightly extended with the zygoma at the highest level in the field to provide enough gravitational assistance for the ipsilateral frontal lobe to suspend away from the anterior cranial fossa. A head fixation system can be used with parallel pins at the level of the superior temporal line. Several adjunctive measures (e.g., lumbar drainage and ventriculostomy) to relax the brain tissue and improve the surgical fields' working space can be performed on a case-by-case basis.

Skin Incision, Temporal Muscle, and Scalp Handling

A 3–4 cm skin incision just above the eyebrow and lateral to the supraorbital notch works very well. This approach can be performed through either a bicoronal or preferably, an eyebrow incision as shown in Fig. 4.3. The structures below this skin incision, including the frontalis and corrugator supercili muscle, should be incised deep into the pericranium, followed by blunt dissection in the area of the craniotomy. In contrast with the pterional approach, a supraorbital craniotomy only dissects the temporalis fascia overlying the frontobasal lateral burr hole. There is minimal manipulation of the temporalis muscle and its' fascia, which ultimately aids in avoiding permanent frontalis palsy.

Bone Flap, Dural Opening, and Closure

The inferior edge of the supraorbital craniotomy is the roof of the orbit, and the bone flap measures approximately 2 cm in diameter. The inner edge of the orbital rim is drilled and flattened. Additional drilling of the sphenoid ridge or the frontal bony prominences depends on the aneurysm location. The dural opening is performed in a U shape with its base at the level of the orbital rim. The dura is then fixed with low lying tenting sutures. After the surgeon finishes the intradural microsurgery, the dura is closed, and the bone flap is placed back in position, using simple plates and screws with or without cranioplasty material to level any bone defect. To maximize the available corridor from a supraorbital craniotomy, one should carefully retract the frontal lobe to liberate CSF and dissect the surrounding cisterns as well as the Sylvian fissure. This sequence of steps will allow the frontal lobe to relax and fall away from the anterior cranial fossa, maximizing the available exposure.

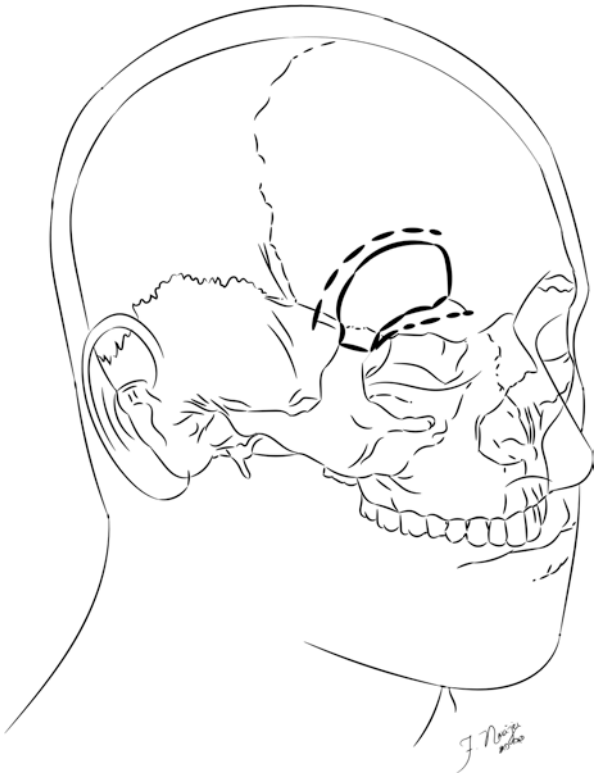

Fig. 4.3 Supraorbital approach: skin incision (dashed lines; options for above or below the eyebrow incision) and outline of craniotomy region for a supraorbital approach (thick line)

Lateral Supraorbital Craniotomy

This craniotomy is made with a series of osteotomies more lateral than those performed in a regular supraorbital craniotomy. This approach has a similar reach than the SOC, and it is used to access aneurysms of the anterior circulation and the basilar apex. However, it is slightly larger than a SOC, and its lateralized corridor enables a wider range of angles for surgical manipulation. Compared to the pterional approach, the bony resection in a lateral supraorbital craniotomy differs by incorporating less of the temporal bone into its final bone flap (Fig. 4.4) [11, 12].

Positioning

The patient is placed in a supine position and the head is hold with rigid fixation with the neck extended and a slight head rotation of 15–20° contralateral to the site of the lesion. Final head positioning and specific angulations are selected based on careful examination of the aneurysms anatomical configuration seen with preprocedural imaging (e.g., dome projection or incorporated branch vessels). While this approach is more lateral than the SOC, it is essential to remember that it is still

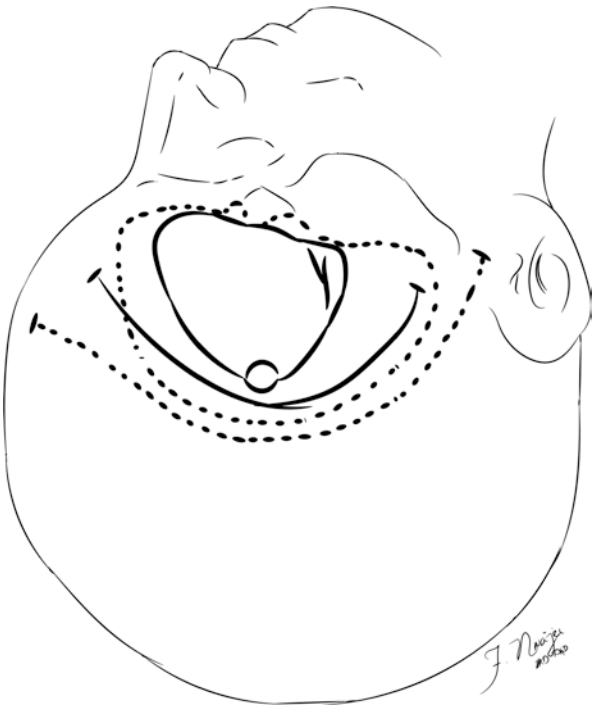

Fig. 4.4 Lateral supraorbital approach: skin incision and outline of craniotomy region for lateral supraorbital (thick lines) versus a pterional approach (dashed lines)

a medial approach, and excessive head rotation can lead to obstructed access into the Sylvian fissure.

Skin Incision, Temporal Muscle, and Scalp Handling

The myocutaneous flap from this craniotomy is more straightforward to obtain than the resulting subperiosteal subcutaneous flap from a pterional approach. It is reflected as a single unit containing skin, subcutaneous tissue, and a portion of the temporalis muscle, which avoids extensive dissection of the temporalis fascia. The skin incision is done behind the hairline and follows the same curvilinear path of a pterional incision; however, it is shorter, starting above the zygoma with its medial end landing just above the level of the ipsilateral supraorbital notch. Once the temporal muscle is exposed, a straight cut is made through the muscle to reflect it anteriorly with the skin flap as a single unit. The retraction is made with low lying spring hooks until we reveal the orbital rim and the frontozygomatic bone. The final size of the craniotomy is usually between 2.5 and 3.5 cm in diameter. This approach needs a single burr hole, placed below the superior temporal line (i.e., level of temporal muscle insertion). Additional burr holes will depend on the patients' age and the degree of dural adherence to the craniums' inner Table. A side-cutting craniotome is used for the osteotomy, starting at the burr hole and directed superiorly and

anteriorly toward the frontozygomatic bone. This osteotomy joins a second one that starts at the burr hole and travels inferiorly through the temporal bone and then superiorly toward the sphenoid ridge.

After bone removal, additional drilling can be made over the sphenoid ridge to maximize the inferior-to-superior view in the operative field. The exchange between high-speed drilling and diamond tip drilling is a technique used when drilling away parts of the sphenoid ridge. It allows for controlled hemostasis from local bony bleeding. To open the dura, we perform a curvilinear incision with its base over the lateral orbital rim and frontozygomatic bone. Elevation of the dura with stitches helps in excluding epidural bleeding from getting into the operative field. A subfrontal corridor is used to start the intradural dissection, which begins by using dynamic and gentle retraction of the frontobasal surface, followed by CSF release from the basal cisterns. After the intradural procedure, the dura is closed in a watertight fashion. If the frontal sinus is exposed, careful repair should follow (mucosa extirpation, cavity filling with temporalis muscle or fat, and cranioplasty closure).

Frontotemporal Orbitozygomatic Craniotomy

The orbitozygomatic extension of the frontotemporal craniotomy provides a wide corridor made through a series of osteotomies that connect the orbital roof, the lateral orbital wall, and the zygoma. This extended craniotomy is often used to treat deep-seated skull base lesions and complex vascular pathologies (e.g., giant carotid bifurcation aneurysms and basilar apex aneurysms) [13, 14]. The extension of this exposure allows the surgeon to decrease the need for manipulation or retraction of brain tissue. Patient positioning, head rotation, and neck extension are done similar to the pterional approach, and changes are based on the type of lesion involved. Precautions during the extradural dissection portion of the procedure include those depicted in the pterional approach. Associated risks specific to this approach include orbital entrapment, vision, or eye movement changes.

Skin, Fascial Flap, and Temporal Muscle Dissection

The skin is incised in the same fashion as with the pterional approach, starting at the level of the tragus with a superior-anterior direction toward the ipsilateral midpupillary line behind the hairline. The skin flap is retracted anteriorly to provide adequate exposure of the zygoma and the orbital rim. Temporal muscle dissection is similar to the pterional exposure, and this includes a subfascial dissection technique with a final fascial cuff separated from the temporal muscle for retraction. This is accomplished by performing an incision along the course of the lateral orbital rim and zygomatic bone. This cut will allow the surgeon to mobilize the flap of the

temporalis fascial layers as a single unit directed anteriorly and inferiorly toward the orbital rim. This will uncover the orbital rim and the zygomatic bone for performing a series of osteotomies to separate the orbitozygomatic unit (either as a single piece with the frontotemporal bone or as a separate cranial flap with one or two additional pieces).

We proceed next by dissecting the superficial fascia toward the orbital cavity, where it becomes the periorbita. Further dissection of the periorbita is made by separating its content laterally from the orbital notch housing the supraorbital nerve. The periorbita is dissected free from the frontozygomatic suture starting laterally and toward the inferior orbital fissure, with an approximate depth of 3 cm. Similar to the pterional approach, a temporal muscle cuff may or may not be left behind its superior incision just below the superior temporal line; However, we have seen less postoperative temporalis atrophy when no cuff is left behind. An additional cut is made parallel to the superiorly oriented skin incision that starts at the tragus. Manipulation of the final temporal muscle flap differs from the pterional approach by displacing it inferiorly for a broader unobstructed field of view (Fig. 4.5).

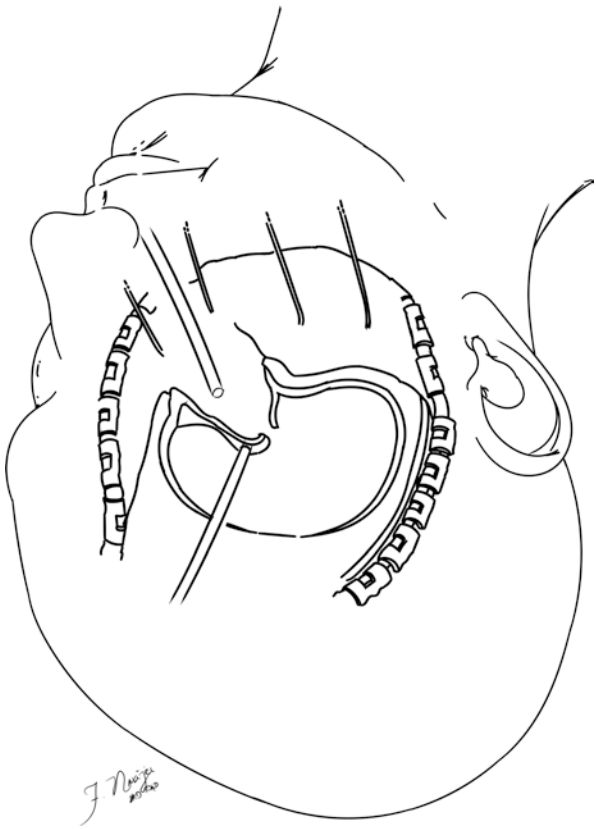

Fig. 4.5 Frontotemporal orbitozygomatic approach: this figure shows the resulting intradural exposure of a frontotemporal orbitozygomatic craniotomy

Bone Flap and Modifications, Dural Opening, and Pterional Closure

Once the temporalis muscle flap is reflected infero-posteriorly and the scalp flap anteriorly (along with the superficial temporal fascia, the periorbita, and the supraorbital nerve), we proceed with placing a pair of burr holes. These burr holes will serve to disjoint part of the orbit and the zygoma through a sequence of osteotomies, obtaining a final orbitozygomatic bone flap as a single unit for removal. These osteotomies can be performed to obtain from 1 to 3 bone units, but the authors prefer the 1-piece approach, to be described as follows. A properly placed McCarty keyhole is crucial to this exposure [15]. This keyhole should reveal through its inner surface, both the periorbita and the frontal dura matter. To accomplish this, we place the craniotome just above and posterior to the frontozygomatic suture. The craniotome is positioned at a 45° angle to reach the surface of both the orbital roof and the frontal dura. A second burr hole is placed posteriorly just below the superior temporal line. The frontotemporal portion of the bone flap is made through the same technique used for the pterional approach. The first orbitozygomatic osteotomy starts at the posteriorly located burr hole and it is extended toward the posterior border of the orbital rim. This osteotomy connects with a pair of additional bony cuts; one starting close to the inferior orbital fissure, inferior to the orbit and toward a mid-point at the zygomatic bone, and a second osteotomy starting at the inferolateral border of the zygomatic process, connected in an oblique angle with the previous osteotomy at the mid-point of the zygomatic process. This sequence can be simplified by skipping the zygomatic osteotomy in the setting of certain aneurysm projections (i.e., superiorly projecting Acomm aneurysms). The orbital portion of the bone flap is connected with the frontotemporal component through an osteotomy just lateral to the supraorbital notch directed anteriorly and posteriorly toward the medial orbital roof. An additional osteotomy is made over the pterion and the lateral aspect of the orbital rim, joining both the orbital and frontotemporal components of the bone flap.

The supraorbital modification of the frontotemporal orbitozygomatic approach is made by omitting the inferolateral osteotomy made at the level of the zygomatic process and including an additional osteotomy at the level of the frontozygomatic suture. A subtemporal modified craniotomy eliminates the osteotomies intended to include the orbital rim and the zygomatic bone, thereby incorporating into its bone flap the frontotemporal bone alone. A separate osteotomy is made in the zygomatic bone at the level of the superior zygomatic arch. This creates a bone gap between the superior and inferior portions of the zygomatic arch, used to retract the dural and muscular flaps, providing a greater level of exposure into the middle cranial fossa.

At this point, an osteotome can be used to apply pressure through the keyhole to fracture the roof of the orbit. The final view offers an expanded set of trajectories toward the subfrontal area without excessive retraction of the frontal lobe. Any remaining component of the orbital roof and lateral aspect of the sphenoid wing can be further dissected, including the sphenoid wing toward the superior orbital fissure. Further exposure for thinning of the clinoid process can be accomplished through an extradural clinoidectomy, reflecting the dura lying over the temporal bone anterior surface, ultimately exposing the clinoid process. This bony dissection unroofs the

optic nerve, a technique often needed for prompt release of localized pressure whenever the underlying pathology involves the optic nerve. Next, a dural opening is made in a curvilinear fashion, similar to the pterional craniotomy. Low-lying retention sutures are placed for both anterior traction and depression of the orbital components, away from the field of view.

Approaches for Posterior Circulation Aneurysms (e.g., Used for Basilar Artery Bifurcation, Trunk and Branches, Vertebrobasilar Junction, Vertebral Artery, PICA, AICA, SCA, and Distal PCA)

Aneurysms in the posterior circulation account for 15–20% of all intracranial aneurysms and are particularly challenging as they are located in the posterior cranial fossa with narrow surgical working avenues (Fig. 4.6) [16]. In addition, these aneurysms arise from arteries which feed the brainstem. Given the improving safety and efficacy of new endovascular therapies, many of the open surgical approaches to these aneurysms are less utilized and surgical experience among young neurosurgeons has declined [17–19]. However, there are some situations in which open surgery might be preferred over endovascular therapies and cerebrovascular trainees should therefore be familiar with these approaches.

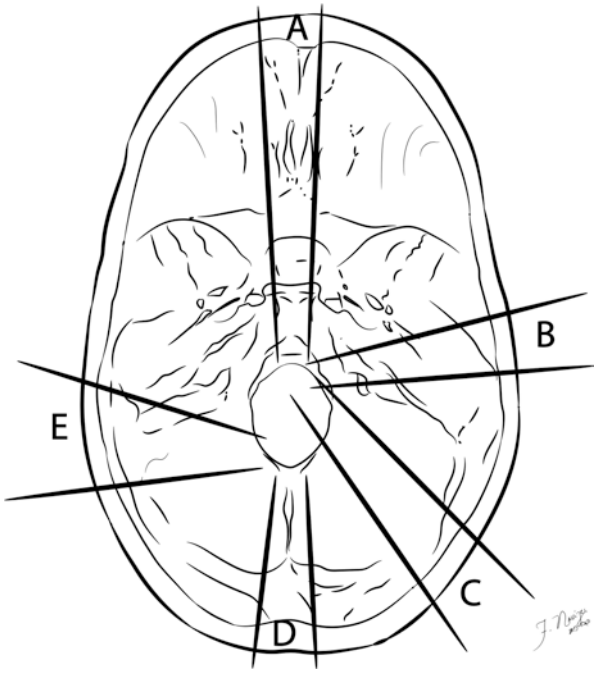

Fig. 4.6 Angle views of craniotomies for surgical treatment of aneurysms within the posterior fossa: approaches used for a posterior fossa aneurysm in
a clockwise manner
A. transfacial;
B. subtemporal; C. far lateral suboccipital,
D. midline suboccipital;
E. combined subtemporal transtentorial

This section will discuss these surgical approaches and nuances, focusing on the subtemporal and the suboccipital far lateral approaches, which are the ones most frequently used (Fig. 4.7 Panel a and b). To choose the best approach to these lesions a computed tomography angiogram (CTA), and in some cases magnetic resonance angiography (MRA) in addition to conventional catheter-based cerebral angiography should be performed for preoperative planning. CTA is preferred on most occasions as it details the nearby bony anatomy. Based on neuroimaging, it can be decided if a basilar tip aneurysm is better suited to be approached through a transylvian approach, such as the frontotemporal orbitozygomatic approach described in the previous section. This approach is best if the lesion is located between the midsella and 1 cm above the posterior clinoids. A subtemporal approach is recommended when lesions are below the area shown in Fig. 4.8. Many neurosurgeons elect to place either a lumbar drain or an external ventricular drain (in ruptured aneurysms) to aid with brain and posterior fossa relaxation.

Subtemporal

This approach allows a wide approach to the middle cranial fossa and the upper petroclival region. The approach is good for low-riding (1 cm below the dorsum sella) or posteriorly projected basilar apex aneurysms. These aneurysms are not

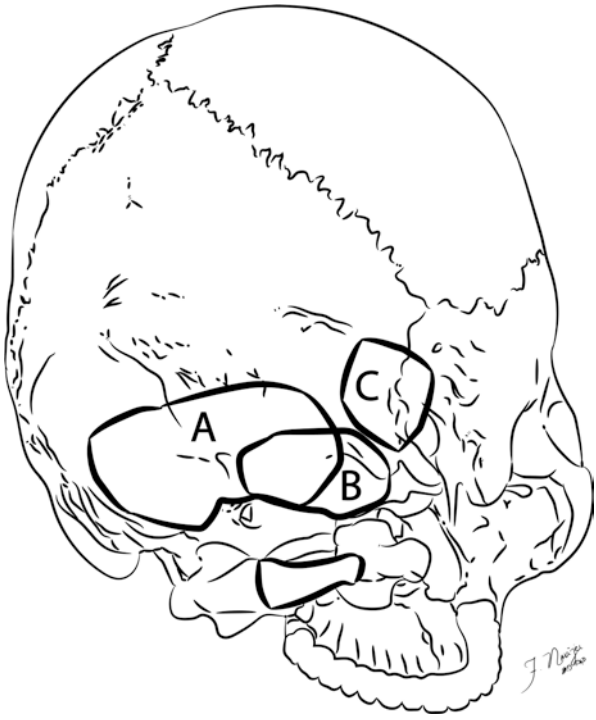

Fig. 4.7 Most common craniotomies used for treating posterior fossa aneurysms: common craniotomies used to access aneurysms within the posterior fossa:
A. midline suboccipital,
B. far lateral, and
C. retrosigmoid

Fig. 4.8 High-riding basilar aneurysm: sagittal section of the skull revealing a large high-riding basilar tip aneurysm (in relation to the posterior clinoid process) amenable to surgical treatment via an anterior approach

recommended to be approached through standard transylvian approaches as critical thalamoperforators near the aneurysm may not be visible and could be placed in jeopardy.

One disadvantage of the subtemporal approach is the need for significant temporal lobe retraction. This is an important drawback in ruptured aneurysms, in which the significant lobar edema may challenge the accessibility to the point to require an inferior temporal gyrus resection or an anterior temporal lobectomy to open the path to the interpeduncular cistern. Another critical issue to consider before starting this approach is avoiding the vein of Labbé to prevent its injury and development of temporal lobe venous infarction [20]. The course of the vein of Labbé can be determined with preoperative venous magnetic resonance venography and venous phase of the angiogram. The surgeon should always be prepared to preserve this vessel. Other disadvantages described for this approach include the occurrence of transient CNIII palsy and that the microsurgical field is narrow, which can make intraoperative bleeding difficult to control.

Preparation and Positioning

All patients should be considered for lumbar drain placement preoperatively to facilitate temporal lobe retraction. For surgery, the patient is placed in the supine position with a shoulder roll underneath the ipsilateral shoulder or in the lateral position. After pinning, the head is placed parallel to the floor and then tilted 20° downward (Fig. 4.9). With this position the zygoma would be the highest point of the field and the temporal lobe will fall with gravity facilitating the lobe retraction.

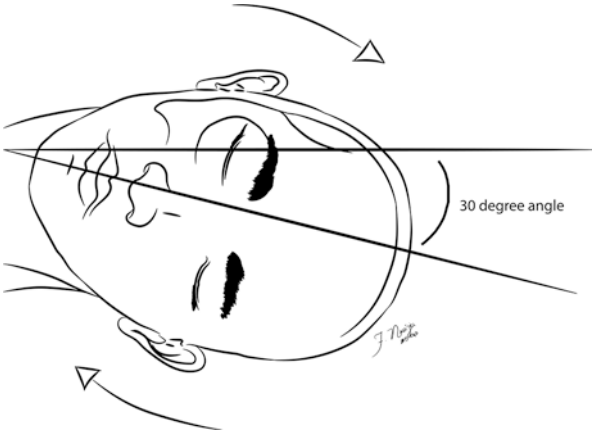

Fig. 4.9 Head position for a subtemporal approach: a slight 30° tilt toward the floor

Incision, Dissection, and Craniotomy

A horseshoe-shaped incision is usually performed, starting from the root of the zygoma to the superior temporal line and going posteriorly to the end of the asterion. Preservation of the superior temporal artery should be attempted as it may be of use if an extracranial to intracranial bypass is needed. The myocutaneous flap is elevated and retracted inferiorly, avoiding injuries to the external auditory meatus. The craniotomy should be performed as close to the floor of the middle cranial fossa as possible. If possible, the craniotomy should cross the area where the vein of Labbé joins with the transverse sinus. A rongeur or drill is used after craniotomy removal to remove the overhanging bone at the inferior edge of the craniotomy at the middle cranial fossa floor level. Mastoid cells are waxed if encountered. After removal of the bone flap, an inferiorly based U-shaped dural incision is made, which should be performed cautiously to avoid vein of Labbé injuries.

After this, subtemporal dissection is performed with gentle elevation of the temporal lobe. A malleable retractor can be used in conjunction with other brain relaxation techniques (draining CSF from the lumbar drain, hyperventilation, or diuresis with mannitol/Lasix). Dissection with loop magnification is continued until the edge of the tentorium is visualized. Greenberg or other self-retaining retractors are used to maintain retraction and the operating microscope is now used for the remainder of the dissection and aneurysm clipping.

Far Lateral Suboccipital

This approach provides adequate access to the vertebral artery, vertebrobasilar junction, and proximal posterior inferior cerebellar artery (PICA) aneurysms as well as lesions located in the ventral or ventrolateral aspect of the brainstem in the inferior cervicomedullary region.

Preparation and Positioning

The patient is positioned either in the true lateral position with a shoulder roll placed under the axilla or in the "park bench" lateral position with the side of the aneurysm (ipsilateral) facing upward. The ipsilateral arm is put to rest on a pillow, and the ipsilateral shoulder is pulled down with tape. The skull clamp is placed with the single pin positioned 2 cm superior and anterior to the ipsilateral ear pinna and the paired pins are placed, so the posterior pin is above the contralateral ear pinna by 2 cm. The head is then flexed gently, leaving two fingerbreadths from the chin to the clavicle, then it is flexed laterally to the contralateral side about 30°, and the head is then rotated to the contralateral side (nose toward the floor). These head movements in conjunction with a slight reverse Trendelenburg position of the surgical table help place the head above the level of the heart, aiding in venous drainage and flattening of the incision plane along the surgical fields' highest point ultimately providing an adequate working space.

Incision, Dissection, and Craniotomy

Many incisions are described for the far lateral approach, but the senior author prefers a curved incision. This incision starts approximately three fingerbreadths medial to the mastoid at the superior aspect. It is then carried inferiorly, curving at a 45° angle toward the midline under the inion and terminating at the spinous process of C2 in the midline (Fig. 4.10 Panel a). This provides a broad exposure of the operative field, but it requires significant muscle splitting, thus increasing postoperative discomfort. Other incisions described include the "hockey-stick" incision, which starts at the spinous process of C2, running superiorly along the midline, and then moving laterally at the inion through the horizontal plane until it reaches the pinna. This incision has less muscle splitting but leaves a greater muscle bulk retracted laterally, which can obstruct the operative working avenue.

Fig. 4.10 Far lateral suboccipital approach. Panel **a** demonstrates the positioning of the head and mapping of the skin incision used for a far lateral suboccipital approach. Panel **b**, the resulting exposure to the posterior fossa through a far lateral suboccipital approach

If a bypass is anticipated, the occipital artery is dissected and harvested after the scalp and muscular flaps are turned. The myocutaneous flap is retracted inferolaterally. Pericranium is then harvested, which would be useful if primary dural closure is not feasible. Subperiosteal dissection is performed to expose the subocciput until reaching the mastoid process all the way to the arch of C1 and the lamina of C2. A lateral suboccipital craniotomy is then performed from the asterion, which marks the transverse-sigmoid sinus complex, to just past the midline and including the foramen magnum in a teardrop fashion. The senior author's preference is to place a burr hole away from the transverse-sigmoid complex, strip the dura with a Penfield No. 3 dissector, and then use the craniotome footplate to create the bone flap. Also, Leksell rongeurs or drill are used to remove the inferior rim of bone to allow access to the cisterna magna. Generally, bony removal is extended in the standard approach to one-third of the occipital condyle. The lateral portion of the C1 arch may also be removed completing a hemilaminectomy (Fig. 4.10 Panel b). After this, the dura is incised in a reverse "K" opening, in which the backbone of the "K" is placed laterally in parallel to the sigmoid sinus and the two arms are projected medially. Dural tack up sutures are placed, and later gentle medial and superior retraction of the cerebellar hemisphere and tonsil exposes the proximal vertebral artery.

Extended Far Lateral Suboccipital Approach

Transcondylar Extension

This modification of the standard far lateral approach aims to have improved exposure of the inferior clivus, the anterolateral medulla, the vertebrobasilar junction, and lower basilar artery trunk, without the need for lower brainstem retraction. In this approach, the occipital condyle is removed without violating the atlantooccipital joint, and the hypoglossal canal is skeletonized. The initial positioning and dissection are similar to the standard far lateral approach. Because of greater invasiveness, there is a higher morbidity rate which includes occipitocervical junction instability, vocal cord paralysis, and aspiration pneumonia due to injury of lower cranial nerves. Given this, the extended far lateral approach is reserved for giant lesions of the vertebrobasilar junction or distal vertebral artery.

Supracondylar Extension (Transtubercular)

This modification aims to remove the jugular tubercle, a bony structure located above the occipital condyle, allowing better visualization of the brainstem's anterolateral region. By drilling the jugular tubercle, the dura covering can be pushed forward to gain access to the pontomedullary junction. This approach is used for PICA aneurysms in which the PICA originates in the distal vertebral artery.

Midline Suboccipital Approach

This approach is used for PICA aneurysms in the telovellar or cortical segments (distal to the PICA's cranial loop and plexal point). The patient is placed prone on chest rolls, and after the placement of the skull clamp, the chin is tucked in by flexing the head as much as possible to open the foramen magnum-C1 interval and facilitate bony work. A midline incision is performed from above the inion to the spinous process of C2. Dissection is performed in the avascular midline and the musculature is retracted. Burr holes are placed just inferior to the nuchal line on either side of the midline, and then a free bone flap craniotomy is created. Leksell Rongeurs are used to open the foramen magnum and usually there is no need to remove the C1 arch. After midline durotomy, the aneurysm is approached by applying lateral retraction to the cerebellar tonsils.

Retrosigmoid

Although this approach is frequently used for non-cerebrovascular diseases in neurosurgery, particularly for posterior fossa tumoral lesions in the cerebellopontine angle, it is very uncommon to be used in isolation for aneurysm surgery. This approach is useful for low-riding distal superior cerebellar artery aneurysms, anterior inferior cerebellar artery aneurysms, or even high-riding posterior inferior cerebellar aneurysms [21].

Other Approaches

There are several approaches described for reaching the basilar trunk, vertebrobasilar junction, or distal vertebral artery aneurysms. For example, the transfacial transclival approach is used for aneurysms affecting the previously mentioned arterial segments that are midline oriented. Other approaches include combinations and are the subtemporal-presigmoid transtentorial, far lateral-transpetrosal, retrosigmoid-transpetrosal, and anterior and posterior pretrosectomies. Review of each of these techniques is beyond the scope of this chapter as they are not commonly used.

References

1. Wong JH, Tymianski R, Radovanovic I, Tymianski M. Minimally invasive microsurgery for cerebral aneurysms. Stroke. 2015;46(9):2699–706.
2. Fischer G, Stadie A, Reisch R, Hopf NJ, Fries G, Bocher-Schwarz H, et al. The keyhole concept in aneurysm surgery: results of the past 20 years. Neurosurgery. 2011;68(1 Suppl Operative):45–51; discussion.

3. Radovanovic I, Abou-Hamden A, Bacigaluppi S, Tymianski M. A safety, length of stay, and cost analysis of minimally invasive microsurgery for anterior circulation aneurysms. Acta Neurochir. 2014;156(3):493–503.
4. Yasargil MG, Fox JL. The microsurgical approach to intracranial aneurysms. Surg Neurol. 1975;3(1):7–14.
5. Figueiredo EG, Deshmukh P, Nakaji P, Crusius MU, Crawford N, Spetzler RF, et al. The minipterional craniotomy: technical description and anatomic assessment. Neurosurgery. 2007;61(5 Suppl 2):256–64; discussion 64–5
6. Yasargil MG, Antic J, Laciga R, Jain KK, Hodosh RM, Smith RD. Microsurgical pterional approach to aneurysms of the basilar bifurcation. Surg Neurol. 1976;6(2):83–91.
7. Kadri PA, Al-Mefty O. The anatomical basis for surgical preservation of temporal muscle. J Neurosurg. 2004;100(3):517–22.
8. Yasargil MG, Reichman MV, Kubik S. Preservation of the frontotemporal branch of the facial nerve using the interfascial temporalis flap for pterional craniotomy. Technical article. J Neurosurg. 1987;67(3):463–6.
9. Jallo GI, Bognar L. Eyebrow surgery: the supraciliary craniotomy: technical note. Neurosurgery. 2006;59(1 Suppl 1):ONSE157–8; discussion ONSE-8.
10. Stamates MM, Wong AK, Bhansali A, Wong RH. Supraorbital keyhole craniotomy for basilar artery aneurysms: accounting for the "cliff" effect. Oper Neurosurg (Hagerstown). 2017;13(2):182–7.
11. Hernesniemi J, Ishii K, Niemela M, Smrcka M, Kivipelto L, Fujiki M, et al. Lateral supraorbital approach as an alternative to the classical pterional approach. Acta Neurochir Suppl. 2005;94:17–21.
12. Cha KC, Hong SC, Kim JS. Comparison between lateral supraorbital approach and pterional approach in the surgical treatment of unruptured intracranial aneurysms. J Korean Neurosurg Soc. 2012;51(6):334–7.
13. Zabramski JM, Kiris T, Sankhla SK, Cabiol J, Spetzler RF. Orbitozygomatic craniotomy. Technical note. J Neurosurg. 1998;89(2):336–41.
14. Seckin H, Avci E, Uluc K, Niemann D, Baskaya MK. The work horse of skull base surgery: orbitozygomatic approach. Technique, modifications, and applications. Neurosurg Focus. 2008;25(6):E4.
15. Aziz KM, Froelich SC, Cohen PL, Sanan A, Keller JT, van Loveren HR. The one-piece orbitozygomatic approach: the MacCarty burr hole and the inferior orbital fissure as keys to technique and application. Acta Neurochir. 2002;144(1):15–24.
16. Day JD, Fukushima T, Giannotta SL. Cranial base approaches to posterior circulation aneurysms. J Neurosurg. 1997;87(4):544–54.
17. Sorkin GC, Dumont TM, Eller JL, Mokin M, Snyder KV, Levy EI, et al. Cerebrovascular neurosurgery in evolution: the endovascular paradigm. Neurosurgery. 2014;74(Suppl 1):S191–7.
18. Spetzler RF, McDougall CG, Albuquerque FC, Zabramski JM, Hills NK, Partovi S, et al. The barrow ruptured aneurysm trial: 3-year results. J Neurosurg. 2013;119(1):146–57.
19. Pierot L, Wakhloo AK. Endovascular treatment of intracranial aneurysms: current status. Stroke. 2013;44(7):2046–54.
20. Avci E, Dagtekin A, Akture E, Uluc K, Baskaya MK. Microsurgical anatomy of the vein of Labbe. Surg Radiol Anat. 2011;33(7):569–73.
21. Zhao X, Tayebi Meybodi A, Naeem K, Belykh E, Labib MA, Baranoski JF, et al. The Glossopharyngo-Cochlear triangle-part I: quantitative anatomic analysis of high-riding posterior inferior cerebellar artery aneurysms exposed through the extended retrosigmoid approach. Oper Neurosurg (Hagerstown). 2021;20(3):242–51.

Part II
Aneurysms

Chapter 5
Presentation and Natural History

Kurt Yaeger, Halima Tabani, and Joshua Bederson

Background

Intracranial aneurysms (IAs) manifest as abnormal outpouchings of the intracranial arteries, typically at bifurcation points on the outside curve of a parent vessel as well as other regions of high hemodynamic stress. IAs vary in morphology, size, and anatomical location. They can be broadly classified into saccular, fusiform, and mycotic subtypes, with saccular being the most common. Typically, aneurysms develop spontaneously and gradually enlarge over time, as pathological changes to the smooth muscle layer in the tunica media allow weakening of the arterial wall and subsequent ballooning of the intimal layer [1]. While most intracranial aneurysms arise sporadically, certain individuals are predisposed to aneurysm formation due to a genetic or familial propensity [2].

Overall, the prevalence of unruptured IAs in the general population has been reported as high as 3% [3], a rate that has increased over time due to a greater frequency and higher resolution of neurological imaging [4, 5]. The prevalence increases with age and is higher in women as compared to men (female to male ratio of 3:1) [3], in patients with autosomal dominant polycystic kidney disease (ADPKD) and those with family history of aneurysmal subarachnoid hemorrhage. Other modifiable risk factors for aneurysm development include smoking and hypertension [4], characteristics that also increase overall IA rupture rates.

Rapid diagnosis and treatment of ruptured intracranial aneurysms are quintessential topics for the vascular neurosurgeon, and thus requires a thorough understanding of the typical modes of presentation. However, treatment of unruptured IA is more subtle and requires a thoughtful consideration of the natural history of

K. Yaeger (✉) · H. Tabani · J. Bederson
Department of Neurological Surgery, Mount Sinai Health System, New York, NY, USA
e-mail: Kurt.yaeger@mountsinai.org; Halima_Tabani@mountsinai.org; Joshua_Bederson@mountsinai.org

J. R. Mascitelli, M. J. Binning (eds.), *Introduction to Vascular Neurosurgery*,
https://doi.org/10.1007/978-3-030-88196-2_5

unruptured or incidental IAs. This chapter attempts to parse these topics in an effort to inform the cerebrovascular neurosurgeon, neuro-interventionalist, and neurologist on indications for management of intracranial aneurysms.

Presentation

The clinical presentation of IAs varies, depending on whether the IA is ruptured or unruptured (Table 5.1). Unruptured IAs are most commonly asymptomatic [3]; however, they can present with symptoms such as headache, cranial nerve deficits, or focal neurologic deficits due to rapid aneurysm growth or thromboembolic events. Ruptured IAs, on the other hand, usually have a more severe presentation, with symptoms ranging from a thunderclap headache to obtundation and coma.

Screening and Incidental

Unruptured IAs can be discovered on screening in individuals with certain congenital or connective tissue disorders, with an increased risk of IAs as compared to the general population. These include ADPKD, neurofibromatosis Type I, Marfan syndrome, Ehlers-Danlos syndrome, multiple endocrine neoplasia Type I, pseudoxanthoma elasticum, and hereditary hemorrhagic telangiectasia. In addition, individuals with a family history of aneurysms (first-and second-degree relatives) also have a higher frequency of IAs (up to 10%) which may be revealed on screening.

The vast majority (up to 91%) of unruptured IAs are asymptomatic and thus are discovered incidentally on imaging performed for nonspecific symptoms or unrelated causes.

Between 20% and 30% of individuals have multiple aneurysms [5]; therefore, unruptured IAs can also be incidentally discovered during imaging performed during evaluation of another ruptured IA.

Table 5.1 Clinical presentation of intracranial aneurysms

Clinical presentation of intracranial aneurysms	
Unruptured	Ruptured
Asymptomatic Headache Cranial nerve deficits Thromboembolic events Seizures	Severe “thunderclap” headache or worst headache of life (WHOL) Nausea and vomiting Altered mental status (spectrum ranging from confusion, lethargy to obtundation, and coma) Meningismus and nuchal rigidity Symptoms of increased intracranial pressure (i.e., blurred vision and alteration of consciousness) Seizures Focal neurologic deficits (especially if associated with intraparenchymal hemorrhage)

Headache

The most common presenting symptom that leads to imaging and subsequent discovery of unruptured IAs is headache [6, 7]. The presenting features and severity of headaches in patients with unruptured IAs varies. Although sudden, severe headache (aka thunderclap headache) has been most commonly associated with ruptured IAs, patients with unruptured IAs can also present with thunderclap headache, with negative CT and lumbar puncture and symptom resolution within 72 hours (aka sentinel headache). It has been postulated that such headaches may occur due to rapid aneurysm growth, thrombosis within the aneurysm, intramural bleeding, formation of a new bleb or daughter sac, or a small contained bleed that is not detected by imaging or spinal tap. Thus, thorough evaluation for IAs in patients with such symptoms is warranted.

More commonly, patients with unruptured IAs have been reported to have symptoms of nonspecific chronic headaches, which can be the presenting symptom in up to 18% of individuals. The pathophysiology of such headaches is not entirely clear, but proposed mechanisms include intrasaccular bleeding due to rupture of vasa vasorum or perivascular innervation due to aneurysm wall distension. These support the observation that patients with symptomatic, unruptured IA have an increased risk of rupture [8]. Furthermore, it has been observed that treatment of unruptured IAs in such patients leads to marked symptomatic improvement in about 65% of the patients [9].

Mass Effect

IAs may clinically manifest due to mass effect on adjacent neural structures, especially if the aneurysm is large (>10 mm) in size. Most commonly, enlarging IA may cause cranial nerve palsies, for example, oculomotor nerve palsy resulting from compression of the third cranial nerve by a posterior communicating artery aneurysm. It is important to note that the initial manifestation of third nerve palsy secondary to aneurysmal mass effect may only be mydriasis, as the peripherally located parasympathetic pupillary fibers are initially affected. Less commonly, compression of the oculomotor nerve can be caused by basilar artery aneurysms as well, particularly if they are large and/or calcified, as well as by aneurysms arising from the junction of basilar and superior cerebellar artery or posterior cerebral artery aneurysms.

Other common cranial neuropathies resulting from aneurysm-related mass effect include abducens, trochlear, and trigeminal (V1 and V2) nerve palsies caused by aneurysms of the cavernous segment of the internal carotid artery. In addition to extraocular movement impairment leading to double vision, such compression can present with retrobulbar and facial pain due to involvement of the branches of the trigeminal nerve. Rarely, distal anterior inferior cerebellar artery aneurysms projecting into the

internal acoustic meatus can cause compression of the facial and/or vestibulocochlear nerve resulting in facial weakness or hearing loss, respectively [10, 11].

Sudden onset of cranial nerve palsy might be a harbinger of imminent aneurysm rupture as it indicates a rapid increase in the size of the aneurysm, or formation of a daughter sac in the aneurysm. This scenario is generally considered an indication for urgent treatment. Ruptured posterior inferior cerebellar artery (PICA) aneurysms can cause isolated abducens nerve (CN VI) palsy. It has been postulated that CN VI irritation can result either due to the jet of blood flow from the ruptured aneurysm or via subarachnoid blood causing irritation of CN VI in Dorello's canal [10]. Interestingly, as opposed to ipsilateral deficits in the case of cranial neuropathies due to mass effect, CN VI deficits in patients with ruptured PICA aneurysms can be ipsilateral, contralateral, or even bilateral.

Other clinical symptoms related to aneurysmal mass effect include sudden vision loss or visual field deficits (e.g., inferomedial quadrantanopsia with superiorly projecting ophthalmic segment ICA aneurysms due to compression of the superolateral optic nerve fibers against the falciform ligament) [12], and seizures due to compression and edema on brain cortical structures.

Thromboembolic Events

The alteration of hemodynamic forces within the aneurysmal sac can lead to stasis and formation of thrombi which can potentially be a source of emboli, resulting in symptoms of transient ischemic attacks (more common) or stroke distal to the aneurysm. Interestingly, it has been observed that thromboembolic events are more commonly associated with small aneurysms (<10 mm diameter), despite the fact that larger aneurysms have a higher predisposition of thrombus formation. This could be explained in part by higher shear forces that appear to occur within smaller aneurysms, which could lead to embolus formation and downstream migration. Small aneurysms may also be less likely than larger aneurysms to contain a thrombus simply because there is less room in the sac. Thromboembolic events are most commonly associated with aneurysms of the middle cerebral artery and internal carotid artery [13]. Observational studies have shown that treatment of the aneurysm leads to a decrease in the recurrence of such thromboembolic events.

Rupture

While the overall prevalence of IAs in the adult population is 1–3%, the incidence of aneurysmal rupture leading to subarachnoid hemorrhage is between 6 and 8 per 100,000, resulting in between 16,000 and 30,000 cases of aneurysmal subarachnoid hemorrhage (aSAH) in the United States annually [14, 15]. Most, but not all, cases of spontaneous subarachnoid hemorrhage (75–80%) are due to aneurysm rupture.

Clinical presentation of patients with aSAH can range in severity from severe, acute onset headache to obtundation and coma. As many as 12% of patients with ruptured IAs die before reaching medical attention [16]. Headaches due to aneurysmal rupture are typically described as worst-of-life or thunderclap in nature. The differential diagnosis for such an acute, paroxysmal headache includes migraine, benign orgasmic cephalalgia, idiopathic thunderclap headache, all of which can be associated with blurry vision, photophobia, and nausea. Overall, a minority (25%) of patients presenting with worst-headache-of-life have an aSAH on further workup [17]. Meningismus or neck stiffness frequently accompanies aSAH as the subarachnoid blood products irritate the meninges of the cervical spine. The pathophysiology of headache in aneurysmal subarachnoid hemorrhage involves irritation of the meninges by blood products between the pial and arachnoid spaces. A "sentinel headache" often precedes aneurysm rupture by hours or days [7].

Patients with thick cisternal subarachnoid hemorrhage or with intraventricular extension may develop acute hydrocephalus. Hematoma directly obstructing the ventricular foramina may lead to obstructive hydrocephalus, whereas diffuse subarachnoid hemorrhage may impair arachnoid granulation reabsorption of CSF, leading to communicating hydrocephalus. The clinical presentation of hydrocephalus ranges in severity from headache to complete obtundation and often requires emergent CSF diversion with ventriculostomy.

Less commonly, patients with aneurysmal rupture may also present with seizure, a result of cerebral cortical irritability due to presence of subarachnoid blood products. Seizures can occur in nearly 8% of patients with subarachnoid hemorrhage and often predict a poor long-term outcome [18].

Several clinical grading systems have been validated for patients with aneurysmal subarachnoid hemorrhage, including Hunt-Hess and World Federation of Neurosurgical Societies (WFNS) (Table 5.2). The modified Fisher scale uses CT imaging to assess degree of cisternal subarachnoid and intraventricular hemorrhage (Fig. 5.1) and is used to predict rates of vasospasm following aneurysmal rupture (Table 5.2).

Ruptured intracranial aneurysms may present with intraparenchymal hemorrhage, intraventricular hemorrhage, or subdural hematoma. Intraparenchymal hemorrhage may occur when the aneurysm dome rupture point is adjacent to cerebral or cerebellar parenchyma and may or may not be associated with cisternal subarachnoid hemorrhage. For example, middle cerebral artery aneurysm rupture may result in frontal or temporal intracerebral hematomas depending on the location of the aneurysm. Ruptured anterior communicating artery aneurysms and occasionally distal anterior cerebral artery aneurysms are associated with characteristic frontal flame hemorrhages also referred to as "jet hematoma."

Intraparenchymal hemorrhage may be more likely to occur with aneurysm rerupture because of adhesions between the healing rupture site and adjacent brain that limits bleeding into the subarachnoid space. Rebleeds are associated with higher mortality rates than first bleeds. Various focal neurological deficits, from hemiparesis to aphasia, may be observed in these cases, given focal mass effect by the hematoma. Acute subdural hematoma is a rare finding after rupture of an

Table 5.2 Clinical and radiographic grading scores for aneurysmal subarachnoid hemorrhage

Hunt-Hess		
1	Minimal symptoms	70% survival
2	Moderate headache, cranial nerve palsy	60% survival
3	Drowsy, neurological deficit	50% survival
4	Stuporous, hemiparesis, possible decerebrate posturing	20% survival
5	Deep coma, decerebrate posturing, moribund	10% survival
WFNS		
1	GCS 15, no motor deficit	
2	GCS 13–14, no motor deficit	
3	GCS 13–14, with motor deficit	
4	GCS 7–12, +/− motor deficit	
5	GCS <7, +/− motor deficit	
Modified fisher		
0	No SAH, no IVH	0% vasospasm
1	Thin SAH, no IVH	24% vasospasm
2	Thin SAH, with IVH	33% vasospasm
3	Thick SAH, no IVH	33% vasospasm
4	Thick SAH, with IVH	40% vasospasm

GCS Glascow Coma Scale, *IVH* intraventricular hemorrhage, *SAH* subarachnoid hemorrhage, *WFNS* World Federation of Neurosurgical Societies

internal carotid or posterior communicating artery aneurysm and can cause lateralizing neurological deficits such as contralateral hemiparesis, posturing, or cerebral herniation. Vascular imaging, such as CT angiography, is required in cases of spontaneous, non-traumatic intraparenchymal or subdural hematoma to rule out a ruptured aneurysm. Both intraparenchymal and subdural hematoma related to aneurysm rupture are associated with poor long-term outcomes [19].

Despite recent advances in the diagnosis and management of ruptured IAs, the reported case fatality rates for ruptured IAs within the first few months remain high, at 35–39% with approximately 10% reported rate of sudden death [6, 7].

Natural History

Intracranial aneurysms (IAs) are abnormal dilations in intracranial vessel walls result from a complex relationship between hemodynamic factors, intrinsic vessel wall characteristics (arteriosclerosis, lipid accumulation, etc.), genetic predisposition (i.e., type III collagen deficiency, other familial genotypes), and environmental factors (smoking, hypertension, etc.) [4]. IAs occur most commonly in the anterior circulation, particularly at branch points or bifurcation sites: most commonly internal carotid artery bifurcation, origin of posterior communicating artery, junction of the anterior communicating artery with the anterior cerebral artery, and proximal

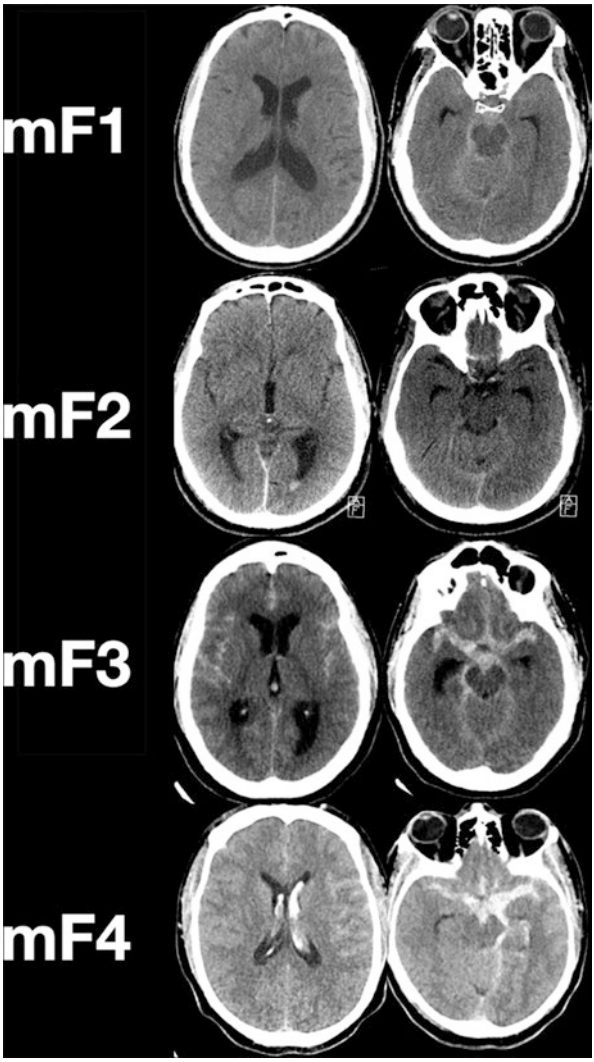

Fig. 5.1 CT images depicting the modified Fischer score (1–4) for aneurysmal subarachnoid hemorrhage (mF modified Fischer)

middle cerebral artery. Common sites of aneurysm formation in the posterior circulation include the basilar tip, and the posterior inferior cerebellar artery origin.

Risks of Aneurysm Formation

Intracranial vessels are distinct from extracranial arteries in that there are fewer elastic fibers and a thinner tunica adventitia. Moreover, instead of being surrounded by connective tissue, these vessels are submerged in cerebrospinal fluid. These

factors increase the susceptibility of intracranial vessels to aneurysm formation. The key inciting event in aneurysm formation is thought to be the weakening and disruption of the internal elastic lamina at a branch point or on the lateral wall of a curving vessel due to hemodynamic stresses. Another important factor in the formation of IAs is the presence of anatomical variations in the circle of Willis such as bifurcations with sharp angles or this with hypoplastic arteries. These can result in increased flow and shear forces leading to vessel wall weakening and subsequent outpouching [4].

As discussed previously, the risk of IAs is significantly higher in certain genetic disorders and clinical syndromes such as APKD, Ehlers Danlos syndrome, Marfan syndrome, α1-antitrypsin deficiency, fibromuscular dysplasia, neurofibromatosis 1, and several others. In addition, individuals with a family history of subarachnoid hemorrhage (SAH) or those with two or more family members with IAs have a higher risk of developing IAs. There are several unique characteristics of IAs in the familial subgroup: they often have more than one aneurysm, there is a predilection for middle cerebral artery as the most common site of aneurysms in this subgroup, the mean age of rupture leading to SAH is younger, and they tend to have poorer outcomes [20].

To date, no specific genetic abnormality associated with sporadic intracranial saccular aneurysm formation has been identified. However, in a large meta-analysis of genetic studies for etiology of sporadic IAs, three single nucleotide polymorphism (SNP) sites were identified: on chromosome 9 within the CDKN2B-AS1 gene, on chromosome 8 near the SOX17 transcription regulator gene, and on chromosome 4 near the endothelin receptor gene [21].

Risks of Aneurysm Progression

A variety of factors can contribute to the progression of aneurysmal size over time. Various patient factors include younger age, female sex, smoking, and history of previous thromboembolic events (TIAs or stroke). As previously mentioned, symptomatic patients have a higher risk of aneurysm growth. Specific aneurysm features related to higher propensity for aneurysm growth are increasing size, branch point location, and multiplicity of aneurysms [22].

Risks of Aneurysm Rupture

Factors associated with aneurysm progression also portend a higher risk of aneurysmal rupture. Broadly, they can be grouped into patient factors (age, female sex, and hypertension), environmental factors (smoking, cholesterol, and alcoholism), and aneurysm features (size, location, shape, morphology, presence of a daughter sac, or evidence of recent growth).

A positive family history of IAs is a strong risk factor for aneurysmal rupture with the annual rupture rate being 17 times higher in such individuals as compared to those without a family history of IAs [2]. Certain triggering factors such as physical exercise, sexual intercourse, and maneuvers leading to increase in intracranial pressure (for example, Valsalva during coughing or defecation) have been postulated to be associated with aneurysmal rupture, but no causality has been established till date [23].

Conversely, a reduced risk of aneurysmal rupture has been observed in patients with IAs taking aspirin [24, 25]. Although aspirin use has been shown to be associated with reduced risk of SAH, there has been no difference observed in the outcomes of patients presenting with SAH and concomitant aspirin use.

One of the most monumental studies establishing the natural history of IAs was the International Study of Unruptured Intracranial Aneurysms (ISUIA) [3]. The first phase of this study (1998) was a retrospective analysis of over 1400 patients, divided into two groups: those with and those without a prior history of aneurysmal SAH. The results revealed that for aneurysms less than 10 mm in diameter, the risk of rupture in individuals with no prior history of SAH was very low (0.05% per year). However, it was almost 11-fold higher (0.5% per year) in those with history of previous SAH. For aneurysms 10 mm or larger, the risk of rupture was 0.7% per year. In terms of aneurysm location, the highest risk of rupture was found for aneurysms in the basilar tip, vertebrobasilar location, and in the posterior communicating artery location. However, this study has received criticisms due to its retrospective design and patient selection criteria, leading to possible selection bias.

The results of the prospective arm of the ISUIA trial revealed that small aneurysms (<7 mm in diameter) in the anterior circulation rarely rupture. The rate of rupture increases with increasing size and posterior circulation aneurysms have a higher tendency to rupture as compared to those in the anterior circulation (Table 5.3) [26].

In addition to aneurysm size and location, certain morphological features of the aneurysm have been postulated to contribute toward risk of rupture (neck width, dome width, and aspect ratio [height/neck width]). Higher rupture risk is associated with an aspect ratio of >1.6 and presence of surface irregularity or daughter sacs/blebs. Features impacting flow dynamics within the aneurysm such as angle of the aneurysm to the parent artery and aneurysm size to parent artery ratio have also been shown to important determinants of risk of rupture [27].

Based on a large meta-analysis, the six independent risk factors predictive of aneurysm rupture have been identified [28]. These include the following: age over 70 years, history of hypertension, history of prior SAH, aneurysm size, aneurysm location, and patient geographical background (North American, European, Japanese, or Finnish). These risk factors have been developed into the PHASES score for prediction of rupture risk, which ranges from 0.3% to ≥15%. Aneurysms that have demonstrated recent growth, for example, an incidental posterior communicating artery aneurysm that suddenly enlarges to cause a third nerve palsy should be considered high risk for rupture and should be treated immediately.

Table 5.3 Rates of aneurysm rupture based on size and location (5-year cumulative rupture rates), based on results from the ISUIA trial

Aneurysm size					
	<7 mm		*7–12 mm*	*13–24 mm*	*>25 mm*
Location	Group 1	Group 2			
Cavernous carotid artery	0%	0%	0%	3%	6.4%
Anterior circulation[a]	0%	1.5%	2.5%	14.5%	40%
Posterior circulation[b]	2.5%	3.4%	14.5%	18.4%	50%

Reproduced with permission from Wiebers et al. [26]. [Group 1: patients with no history of subarachnoid hemorrhage, Group 2: patients with history of subarachnoid hemorrhage due to different aneurysm rupture]

[a]Includes anterior cerebral artery, anterior communicating artery, middle cerebral artery, and internal carotid artery aneurysms

[b]Includes posterior cerebral, vertebrobasilar, and posterior communicating artery aneurysms

Conclusion

Understanding the natural history of IAs is imperative in guiding management decisions. A careful assessment of the risk of progression and rupture (both short and long term) should be made based on the factors discussed and weighed against risks of intervention (either surgical clipping or endovascular obliteration). Such multidisciplinary assessments can aid clinicians as well as patients in informed decision-making regarding the management of intracranial aneurysms.

References

1. Jung K-H. New pathophysiological considerations on cerebral aneurysms. Neurointervention. 2018;13(2):73–83. https://doi.org/10.5469/neuroint.2018.01011.
2. Broderick JP, Brown RD, Sauerbeck L, et al. Greater rupture risk for familial as compared to sporadic unruptured intracranial aneurysms. Stroke. 2009;40(6):1952–7. https://doi.org/10.1161/STROKEAHA.108.542571.
3. Unruptured intracranial aneurysms — risk of rupture and risks of surgical intervention. N Engl J Med. 1998;339(24):1725–33. https://doi.org/10.1056/nejm199812103392401.
4. Etminan N, Rinkel GJ. Unruptured intracranial aneurysms: development, rupture and preventive management. Nat Rev Neurol. 2016;12(12):699–713. https://doi.org/10.1038/nrneurol.2016.150.
5. Weir B. Unruptured intracranial aneurysms: a review. J Neurosurg. 2002;96(1):3–42. https://doi.org/10.3171/jns.2002.96.1.0003.
6. The natural course of unruptured cerebral aneurysms in a Japanese cohort. N Engl J Med. 2012;366(26):2474–82. https://doi.org/10.1056/nejmoa1113260.
7. Alessandro C, Emanuele P, Roberto DB, Silvia TC, Giusepp B. Clinical presentation of cerebral aneurysms. Eur J Radiol. 2013;82(10):1618–22. https://doi.org/10.1016/j.ejrad.2012.11.019.
8. Gilard V, Grangeon L, Guegan-Massardier E, et al. Headache changes prior to aneurysmal rupture: a symptom of unruptured aneurysm? Neurochirurgie. 2016;62(5):241–4. https://doi.org/10.1016/j.neuchi.2016.03.004.

9. Kong DS, Hong SC, Jung YJ, Kim JS. Improvement of chronic headache after treatment of unruptured intracranial aneurysms. Headache. 2007;47(5):693–7. https://doi.org/10.1111/j.1526-4610.2006.00630.x.
10. Burkhardt JK, Winkler EA, Lasker GF, Yue JK, Lawton MT. Isolated abducens nerve palsy associated with subarachnoid hemorrhage: a localizing sign of ruptured posterior inferior cerebellar artery aneurysms. J Neurosurg. 2018;128(6):1830–8. https://doi.org/10.3171/2017.2.JNS162951.
11. Lv X, Ge H, He H, Jiang C, Li Y. Anterior inferior cerebellar artery aneurysms: segments and results of surgical and endovascular managements. Interv Neuroradiol. 2016;22(6):643–8. https://doi.org/10.1177/1591019916656474.
12. Park W, Park JC, Han K, Ahn JS, Kwun BD. Anterior optic pathway compression due to internal carotid artery aneurysms: neurosurgical management and outcomes. J Stroke. 2015;17(3):344–53. https://doi.org/10.5853/jos.2015.17.3.344.
13. Qureshi AI, Mohammad Y, Yahia AM, et al. Ischemic events associated with unruptured intracranial aneurysms: Multicenter clinical study and review of the literature. Neurosurgery. 2000;46(2):282–90. https://doi.org/10.1097/00006123-200002000-00006.
14. Zacharia BE, Hickman ZL, Grobelny BT, et al. Epidemiology of aneurysmal subarachnoid hemorrhage. Neurosurg Clin N Am. 2010;21(2):221–33. https://doi.org/10.1016/j.nec.2009.10.002.
15. Linn FHH, Rinkel GJE, Algra A, Van Gijn J. Incidence of subarachnoid hemorrhage: role of region, year, and rate of computed tomography: a meta-analysis. Stroke. 1996;27(4):625–9. https://doi.org/10.1161/01.STR.27.4.625.
16. Huang J, Van Gelder JM, Haines SJ, et al. The probability of sudden death from rupture of intracranial aneurysms: a meta-analysis. Neurosurgery. 2002;51(5):1101–7. https://doi.org/10.1097/00006123-200211000-00001.
17. Linn FHH, Wijdicks EFM, van Gijn J, Weerdesteyn-van Vliet FAC, van der Graaf Y, Bartelds AIM. Prospective study of sentinel headache in aneurysmal subarachnoid haemorrhage. Lancet. 1994;344(8922):590–3. https://doi.org/10.1016/S0140-6736(94)91970-4.
18. Butzkueven H, Evans AH, Pitman A, et al. Onset seizures independently predict poor outcome after subarachnoid hemorrhage. Neurology. 2000;55(9):1315–20. https://doi.org/10.1212/WNL.55.9.1315.
19. Biesbroek JM, Rinkel GJE, Algra A, Van Der Sprenkel JWB. Risk factors for acute subdural hematoma from intracranial aneurysm rupture. Neurosurgery. 2012;71(2):264–8. https://doi.org/10.1227/NEU.0b013e318256c27d.
20. Brown RD, Broderick JP. Unruptured intracranial aneurysms: epidemiology, natural history, management options, and familial screening. Lancet Neurol. 2014;13(4):393–404. https://doi.org/10.1016/S1474-4422(14)70015-8.
21. Alg VS, Sofat R, Houlden H, Werring DJ. Genetic risk factors for intracranial aneurysms: a meta-analysis in more than 116,000 individuals. Neurology. 2013;80(23):2154–65. https://doi.org/10.1212/WNL.0b013e318295d751.
22. Molenberg R, Aalbers MW, Mazuri A, et al. UIATS as a predictor of aneurysm growth or rupture. Eur J Neurol. 2020;28(3). https://doi.org/10.1111/ene.14636.
23. Reynolds MR, Willie JT, Zipfel GJ, Dacey RG. Sexual intercourse and cerebral aneurysmal rupture: potential mechanisms and precipitants: a review. J Neurosurg. 2011;114(4):969–77. https://doi.org/10.3171/2010.4.JNS09975.
24. Gross BA, Rosalind Lai PM, Frerichs KU, Du R. Aspirin and aneurysmal subarachnoid hemorrhage. World Neurosurg. 2014;82(6):1127–30. https://doi.org/10.1016/j.wneu.2013.03.072.
25. Hasan DM, Mahaney KB, Brown RD, et al. Aspirin as a promising agent for decreasing incidence of cerebral aneurysm rupture. Stroke. 2011;42(11):3156–62. https://doi.org/10.1161/STROKEAHA.111.619411.

26. Wiebers DO. Unruptured intracranial aneurysms: natural history, clinical outcome, and risks of surgical and endovascular treatment. Lancet. 2003;362(9378):103–10. https://doi.org/10.1016/S0140-6736(03)13860-3.
27. Lall RR, Eddleman CS, Bendok BR, Batjer HH. Unruptured intracranial aneurysms and the assessment of rupture risk based on anatomical and morphological factors: sifting through the sands of data. Neurosurg Focus. 2009;26(5):1–7. https://doi.org/10.3171/2009.2.FOCUS0921.
28. Greving JP, Wermer MJH, Brown RD, et al. Development of the PHASES score for prediction of risk of rupture of intracranial aneurysms: a pooled analysis of six prospective cohort studies. Lancet Neurol. 2014;13(1):59–66. https://doi.org/10.1016/S1474-4422(13)70263-1.

Chapter 6
Subarachnoid Hemorrhage Management and External Ventricular Drain Placement

Ehsan Dowlati, Tianzan Zhou, and Daniel R. Felbaum

Introduction

Subarachnoid hemorrhage (SAH) refers to the presence of blood in the subarachnoid space of the central nervous system. Though the most common reason for SAH is trauma, aneurysmal rupture is the most common cause of non-traumatic SAH making up about 85% [1]. It is a much more serious condition than traumatic SAH requiring prompt diagnosis, medical attention, and timely intervention (Table 6.1). SAH patients are one of the most critical and complex patient populations. Centers managing less than 10 SAH patients per year are recommended to transfer these patients to tertiary high-volume centers with dedicated neurocritical care physicians [2, 3]. The management of SAH patients represents a continuum of care through several stages of pathophysiology. The early phase of SAH injury is critical and is typically defined by the first 72 hours from ictus. Multiple steps are taken simultaneously to stabilize, diagnose, and treat the patient [4]. We will be discussing the early phase of management in this chapter.

E. Dowlati · T. Zhou
Department of Neurosurgery, MedStar Georgetown University Hospital, Washington, DC, USA

D. R. Felbaum (✉)
Department of Neurosurgery, MedStar Georgetown University Hospital, Washington, DC, USA

Department of Neurosurgery, MedStar Washington Hospital Center, Washington, DC, USA
e-mail: daniel.r.felbaum@gunet.georgetown.edu

J. R. Mascitelli, M. J. Binning (eds.), *Introduction to Vascular Neurosurgery*,
https://doi.org/10.1007/978-3-030-88196-2_6

Table 6.1 Quick facts and pearls of SAH

Morbidity and mortality	Grading	Re-rupture	Vasospasm
10–15% dead before arrival, 1/3 die in hospital, 1/3 moderate to severe deficit, 1/3 mild to none 10–15% go back to prior occupation	HH score (1–5) corresponds with morbidity and mortality WFNS includes treatment of hydrocephalus first before final grade	5% re-rupture in first 24 hours 2.5% the following 24 hours 0.5% each day thereafter	Vasospasm peaks 5–10 days Modified fisher grade corresponds with vasospasm risk 75% radiographic 25% clinical

Epidemiology and Risk Factors

Aneurysmal subarachnoid hemorrhage (SAH) comprises 5% of all stroke cases. The overall incidence of SAH is estimated to be 2–22.5 per 100,000 people with a mean age at presentation of 55 [3, 5–7]. There are differences in incidence between regions and across racial/ethnic groups with African Americans and Hispanics having a higher incidence than white Americans [8]. The incidence of SAH increases with increasing age, and women are more affected [5]. There has been a slight decrease in the incidence of SAH of 0.6% per year, reflecting better control of known risk factors [5]. The incidence and lifetime risk of SAH in the general population are highly variable based on the presence or absence of known risk factors with a lifetime risk between 0.2% and 7.2% based on the various risk factors [9].

Aneurysmal SAH carries considerable morbidity and mortality, with some studies reporting mortality of up to 30–45% at 30 days [10]. It is responsible for 8–12% of all out-of-hospital deaths [3, 11, 12]. About 35–55% of those surviving achieve a good functional outcome as defined by modified Rankin Scale of 0–3 [11]. Many, however, suffer from cognitive dysfunction, which affects quality of life [13]. Due to baseline comorbidities and risk factors associated with the SAH patient population, those that survive have a considerable decrease in life expectancy compared to age-matched control population [14]. These patients are also at higher risk of subsequent SAH, recurrent aneurysms, and new aneurysm formation (15-fold higher than controls) [15].

Modifiable risk factors for harboring aneurysms include current and former smoking (more than twofold increased risk) [16], hypertension, and heavy alcohol intake [17]. Adrenergic stimulants such as cocaine also increase risk in the younger population. Non-modifiable risk factors include increased age, female sex (1.6 times more common in women above the age of 50), coarctation of the aorta, some connective tissue disorders (Ehlers-Danlos Syndrome and Marfan Syndrome), familial intracranial aneurysm syndrome, and adult polycystic kidney disease [5]. About one in five SAH patients has a positive family history of aneurysms. This should be documented on presentation as other first-degree relatives may need screening for aneurysms. The risk associated with female sex is seen in patients above 50 years of age. A meta-analysis showed an increased risk of SAH with patients using oral contraceptives and post-menopausal women compared to pre-menopausal women of the same age [18].

Perimesencephalic SAH accounts for 10% of all SAH. The bleed is confined to the midbrain/perimesencephalic cisterns without hemorrhage into interhemispheric or Sylvian fissures. The source of the bleed is typically from primitive veins around the midbrain. These patients have better outcomes with fewer neurologic sequelae and may present with milder symptoms than aneurysmal SAH patients [20]. Nonetheless, these patients still require optimal treatment and management warranting a formal cerebral angiogram to rule out aneurysmal source and monitoring in the ICU.

Clinical Presentation

Clinical presentation largely depends on the amount of extravasation of blood from the aneurysm upon rupture. This can be negligible to large amounts which may cause sudden death [21]. Of those that are conscious and make it to medical attention, a classic presenting symptom involves a "thunderclap" or "worst headache of my life" that comes on suddenly. Despite the characteristic presentation, headache symptoms may be variable. Unawareness of the acute onset and prior history of headaches may delay referral for further evaluation [22]. Even still, some patients may not seek medical attention for days at which point the headache become intolerable, or patient develops hydrocephalus and/or vasospasm [23]. The severe headache can be preceded by strenuous activity in some cases (especially within 2 hours of onset), although it may also occur at rest [24]. It can also be preceded by a prior sentinel headache in up to 43% of patients, characterized as an insidious less severe headache that may occur up to 6 weeks before SAH [25, 26]. The sentinel headache can denote a small leak, hemorrhage into the wall of the aneurysm or acute expansion in size. Photophobia and visual disturbances from ocular hemorrhages (Terson's syndrome) [27], nuchal rigidity from irritation of the subarachnoid space, nausea/vomiting, depressed consciousness, cranial nerve palsies depending on location, seizures, and focal deficits from intraparenchymal hemorrhage (IPH) are also common presentations [28, 29]. Atypical symptoms may lead to misdiagnosis and delayed treatment in up to 12% [30]. Given the range of symptomatology and the critical importance of a prompt diagnosis, the Ottawa SAH rule may be applied to identify patients in whom further CT and lumbar puncture are warranted. The rules include patients above 40 years, with neck pain/stiffness, loss of consciousness, onset with exertion, thunderclap nature of headache, and limited neck range of motion [31]. Patients who do not make it to medical attention typically die from sequela of increased ICP leading to cerebral circulatory arrest or cardiac dysrhythmia [32]. Vital sign abnormalities patients may present with include severe hypertension, fever, and relative bradycardia. The surge in catecholamines also produces a systemic inflammatory response syndrome [33]. Neurologic decline early after presentation is seen in up to one-third of patients and related to increased age and clot burden [34].

Imaging and Diagnosis

Computed Tomography

Non-contrast computed tomography (CT) of the head is the primary method of SAH diagnosis and it detects above 95% of SAH cases with a 97% sensitivity in the first 72 hours and 50% sensitivity after 5 days [35, 36]. Volume and location of SAH on CT are significant independent risk factors for death and disability. Additionally, a CT may help with localization of the aneurysm or source of hemorrhage, specifically when there is an associated IPH [37]. Additional findings noted on CT scan include intraventricular hemorrhage (IVH) in 20%, IPH in 19%, ventriculomegaly in 16%, midline shift from mass effect in 8%, subdural hematoma (SDH) in 2%, and in cases of large aneurysms, the aneurysm itself (5%) [38] (Fig. 6.1).

Lumbar Puncture

A lumbar puncture (LP) is performed in cases where SAH is suspected but the CT is negative. This can be done at bedside or in the fluoroscopy suite. Contraindications

Fig. 6.1 Non-contrast axial view of a CT head showing diffuse subarachnoid hemorrhage, ventriculomegaly as well as intraventricular hemorrhage in the fourth ventricle

to an LP include coagulopathy, increased ICP from a space-occupying lesion, suspected arteriovenous malformation (AVM), and infection in the lumbar area. SAH is confirmed by the presence of similar number of red blood cells (RBCs) in the first and final tube, while in a traumatic tap, the CSF should clear of blood in subsequent tubes and typically forms clots. An RBC count of greater than 2000×10^6/L in the final tube is concerning for SAH [39]. If unsure if traumatic tap was obtained, a repeat LP may be done at a higher level. An LP performed in the first 6 hours is not as sensitive or specific and xanthochromia typically appears after 12 hours due to lysis and degradation of RBCs and hemoglobin products [35, 40]. Additionally, spectrophotometry may be most reliable though it is difficult to perform since CSF needs to be stored at a certain temperature and centrifuged immediately. Cellular polymorphonuclear reaction can be seen in the first few hours after SAH and this transitions into a predominantly monocytic reaction with elevated proteins levels that may persist up to 3 weeks [32].

In addition to laboratory studies of CSF, opening pressure should be obtained with a lumbar puncture. A high pressure with clear CSF can suggest a dural venous thrombosis or meningitis, whereas a low opening pressure and clear CSF place intracranial hypotension further up the differential [37].

Magnetic Resonance Imaging

In the acute setting of less than 6 hours onset, magnetic resonance imaging (MRI) without contrast can play a role in diagnosis. MRI also has a role in cases where the angiogram is negative, especially when fluid-attenuated inversion recovery (FLAIR) and T2 sequences are used [15]. An MRI of the brain and cervical spine with and without gadolinium can evaluate for angiographically occult lesions, dissections, tumors, or lesions in the upper cervical spine.

Noninvasive Vascular Imaging

A CT angiogram (CTA) of the head (and neck) may be performed for aneurysm diagnosis in situations where an angiogram is not possible or for operative planning. It is up to 94% accurate in detecting aneurysms greater than 3 mm [42] (Fig. 6.2). In 5% of cases, patients may show contrast extravasation which is associated with high risk of mortality.

Magnetic resonance angiography (MRA) is another option like CTA for noninvasive diagnosis of aneurysms; however, it is not as practical to obtain in the acute setting. It has slightly lower sensitivity compared to CTA and accuracy increases

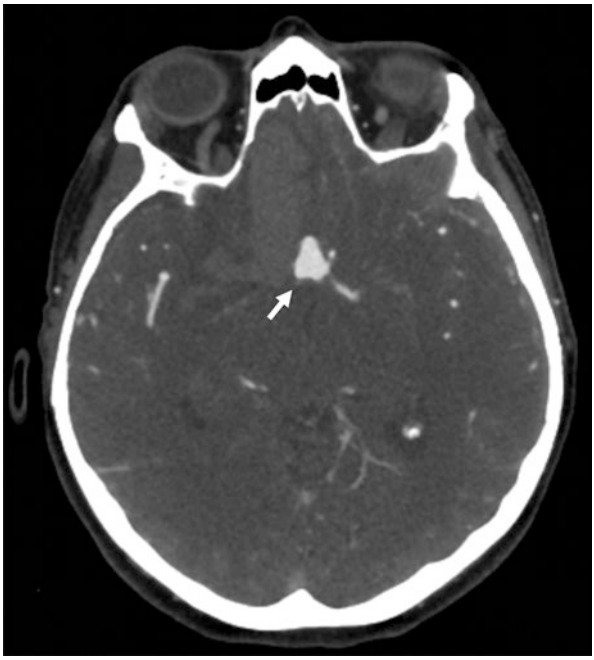

Fig. 6.2 Axial view of CTA head done on a patient with ruptured anterior communicating artery aneurysm (arrow) with associated right frontal intraparenchymal hemorrhage

with aneurysms greater than 3 mm [43, 44]. Newer technology and 3-Tesla imaging or greater have increased this sensitivity [43].

Angiography

A six-vessel digital subtraction angiography (DSA) is performed once the diagnosis of SAH is established (Fig. 6.3). This is the gold-standard for aneurysm diagnosis approaching 100% sensitivity and specificity and a three-dimensional rotation angiogram allows for even better spatial resolution. DSA also allows for therapeutic intervention to be pursued at the time of diagnosis in the form of endovascular occlusion. The angiogram will also allow for diagnosis of any early vasospasm, which may be treated accordingly. In negative angiograms where no source of SAH is identified (15% of patients undergoing DSA for SAH), a repeat DSA or other vascular study such as a CTA or MRA is performed within 1–2 weeks as the aneurysm may be small enough to have completely thrombosed after bleeding. In most cases, negative angiograms will be due to a perimesencephalic SAH, for which further vascular imaging is controversial [45]. In cases where multiple aneurysms are diagnosed, we closely examine the CT for the presence of focal SAH, and treat the aneurysm with higher risk factors, such as larger or irregularly shaped aneurysms [46]. If possible, we attempt to treat all aneurysms as to mitigate the risk of rupture or re-rupture.

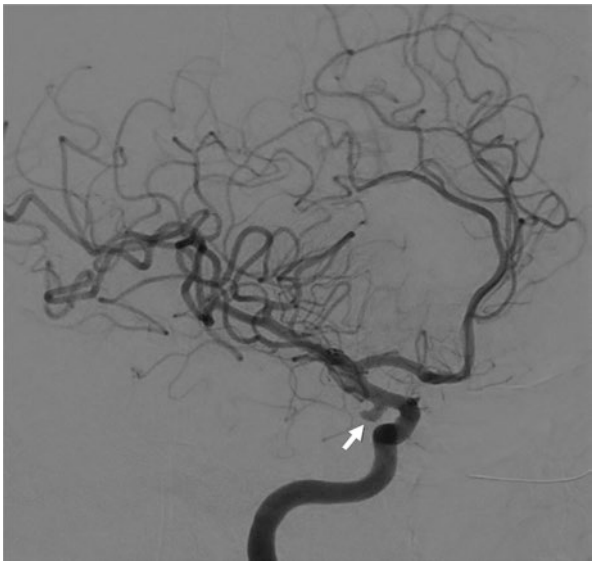

Fig. 6.3 Digital subtraction angiogram with oblique view of right internal carotid artery injection shown here. There is a 5.5 × 3.9 mm boot-shaped posterior communicating artery aneurysm noted (arrow)

Grading

There are multiple scales used to define clinical status and prognosticate outcome. Although primarily established for trauma, the well-known Glasgow Coma scale (GCS) is used in SAH grading to establish the severity of the initial neurologic insult and to assist with immediate neurocritical care needs. The Hunt Hess (HH) score is a widely used clinically defined scale determined by neurologic examination and shown to correlate with mortality [47]. The World Federation of Neurological Surgeons Scale (WFNS) is another clinical scale used for SAH patients and has better positive and negative predictive values related to outcomes and also provides a more objective measure [48]. Use of both scales provides best prediction of outcome when used after patient is stabilized and resuscitation measures have been completed, including ventricular drainage [49, 50]. Other scales that exist but less commonly used include the Prognosis on Admission of Aneurysmal Subarachnoid Hemorrhage scale and Botterell scale [51, 52].

Radiographic features such as volume of SAH on CT scan is also an important predictor of outcome. The Fisher grade is a radiologically defined scale determined by amount of subarachnoid blood and location. The scale should be used on initial CT of the head. However, this scale starts at 1 and is not linear in its prediction of outcome or vasospasm. The more widely adopted modified Fisher grading scale carries a predictive correlation with risk for vasospasm and overall patient outcome [53]. The Hijdra scale is more detailed but less practical. It grades based on subarachnoid blood in 10 cisterns and IVH in each ventricle [54]. These grading schemes have been used for many years to provide a common method of communicating SAH severity so that providers may have objective measures, follow exams, and render prognosis on patients with SAH.

Pathophysiology of Early Brain Injury

Chemical injury is derived from the release of oxyhemoglobin and bilirubin oxidation products which acts as a vasoconstrictor and iron which may induce apoptosis. In the acute setting, SAH causes a transient global ischemia that results from disturbed metabolism and temporary cerebral circulatory arrest. This is seen in patients with altered consciousness. Factors that contribute to this early brain injury and transient global ischemia include endothelial injury, excitotoxicity, and impaired ionic channels. These events occur in part due to failure of ATP-dependent channels and ionic derangements including increased in intracellular calcium, which leads to failure of smooth muscle relaxation. This failure of energy metabolism has been shown in cerebral microdialysis studies [55]. The molecular cascade of events leads to impaired autoregulation, cell death, inflammation, oxidative stress, and edema [56]. The cascade of energy failure, ionic disturbance, and oxidative stress leads to an increase in ICP. There is a concomitant global decrease in cerebral blood flow (CBF) and cerebral metabolic rate of oxygen which has been correlated with SAH grade and the decline can be seen for days after the SAH. This decrease is due to decreased demand.

Initial Management

SAH patients may be neurologically intact or very ill and comatose. First steps in assessment include a systematic evaluation of airway, breathing, circulation, and hemodynamic parameters. Then a neurological assessment should be done to assess consciousness, awareness, speech, motor exam, and cranial nerves. All patients should be admitted to the intensive care unit and placed on bed rest. Frequent monitoring of vital signs and neurological assessments should be undertaken at least once every hour. The proceeding sections go over the main aspects of acute SAH patient care.

Airway

SAH patients are at risk for respiratory failure due to depressed level of consciousness, seizures, elevated ICP, brainstem compression, and hydrocephalus. Endotracheal intubation is indicated for any patient presenting with a GCS of less than 8, compromised airway, HH score greater than 2, and Fisher grade greater than 2. We also prefer to intubate all patients who need an external ventricular drain (EVD). During intubation, the blood pressure should be monitored as to not provoke sudden changes. Both hypertension and hypotension should be avoided.

The primary goal of mechanical ventilation is airway protection in the setting of impaired consciousness. Other goals, equally as important, include adequate oxygenation and adequate ventilation as to avoid hypercarbia. Continuous end-tidal CO_2 monitoring is necessary in all patients. Induced hypocapnia is not currently recommended and is reserved as a temporary measure during cases of malignant intracranial hypertension [57]. Additionally, long-term hypocapnia with a pCO_2 of less than 25 mmHg may lead to vasoconstriction, metabolic alkalosis, and hypoperfusion since autoregulation may be impaired in SAH patients [58]. Typically, the recommended goal range is partial pressure of arterial CO_2 ($PaCO_2$) from 30 to 40 mmHg and a PaO_2 of 90 to 100 mmHg.

Blood Pressure Management

Hypertension in SAH is common and likely related to the sympathetic surge from cerebral injury along with factors such as pain, agitation, and anxiety. Blood pressure should be promptly treated immediately after airway is stabilized and hydrocephalus is addressed. The primary goal of blood pressure control is preventing a rebleed event [3]. One must assume an unsecure vascular lesion at risk of rebleeding with any SAH patient. Guidelines currently recommend a systolic blood pressure (SBP) of less than 160 [3]. On the other end, one must also avoid hypotension as to not compromise cerebral perfusion pressure (CPP). A central venous catheter/line (CVC) and an arterial line may be indicated for close hemodynamic monitoring. Variability in blood pressure may be as important as absolute blood pressure [59].

The most effective method of blood pressure control is use of a continuous infusion and the preferred agents of choice include nicardipine, labetalol, or esmolol. Beta blocker use, however, may be limited by symptomatic bradycardia and/or bronchospasm. Additionally, nimodipine, a calcium-channel blocker, is initiated on all SAH patients at 60 mg every 4 hours. Nitrates such as nitroglycerin and nitroprusside are vasodilating agents that should be avoided as to prevent increase in intracranial pressure (ICP) [60].

Administration of agents to control pain and agitation may be indicated as long as they are short-acting so the patient may be neurologically assessed. Later in the patient's hospital course, induced hypertension may be needed to provide increase in CPP in the setting of vasospasm. After aneurysm treatment, we prefer to keep SBP between 100 and 180.

Intracranial Hypertension

Intracranial hypertension is the most common cause of death in the immediate post-bleed period. Causes include hydrocephalus, global cerebral edema from transient global ischemia, and mass effect from concurrent IPH or

SDH. Mechanical means of injury relate to the subarachnoid blood stretching the subarachnoid space and compressing arteries leading to an increase in ICP. Additionally, blood products may block the subarachnoid space impeding cerebrospinal fluid (CSF) flow, leading to communicating hydrocephalus. There is also some contribution from disruption of the blood–brain barrier (BBB), worsening edema [61]. ICP is monitored in a variety of ways, most commonly through an EVD catheter given that it is also therapeutic. Multimodal monitoring can also be achieved with intraparenchymal/subdural ICP monitors which may provide additional information regarding brain temperature and partial pressure brain tissue oxygen (Fig. 6.4).

Intraparenchymal or Intraventricular Hemorrhage

IPH is seen in about one-third of aneurysmal SAH [62, 63], typically in patients with middle cerebral artery (MCA) or distal anterior cerebral artery aneurysms. IPH size, location, and degree of midline shift are predictors of outcome [64]. Hemorrhage

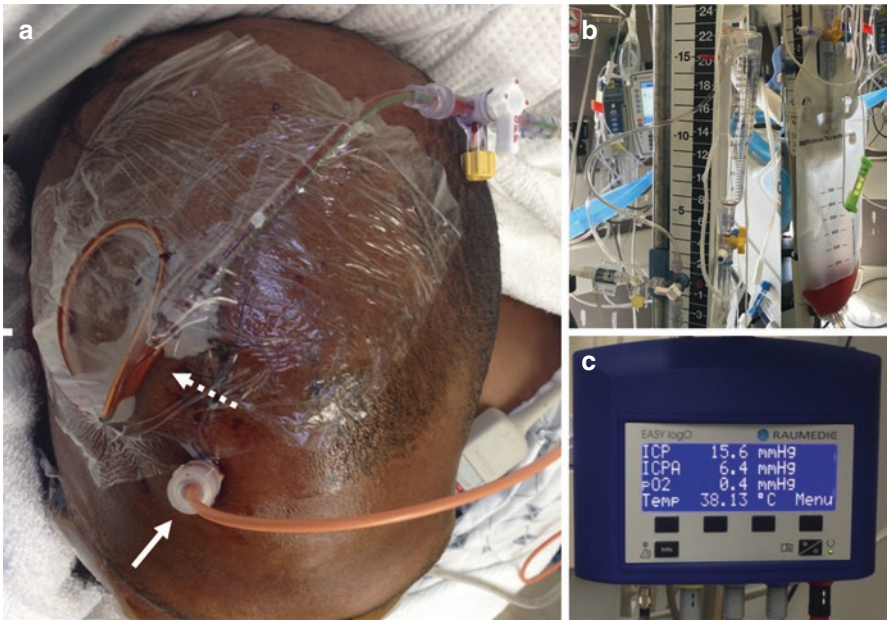

Fig. 6.4 (**a**) Subarachnoid hemorrhage patient with a right external ventricular drain (solid arrow) as well as a right intraparenchymal Neurovent-P-tel ICP monitor (Raumedic, Helmbrechts, Germany) in place for multimodal monitoring. (**b**) The buretrol for CSF diversion and drainage reservoir containing blood-tinged CSF is seen. (**c**) Raumedic display monitor showing values for ICP, partial pressure of brain tissue oxygen, and brain temperature

location and size vary due to a number of factors. Differentiating between an aneurysmal and hypertensive IPH is important and can be done based on presence of SAH in the cisterns or location of the IPH near the skull base as well as patterns of IVH. SDH can also be seen in SAH patients, typically from MCA and posterior communicating artery aneurysms. In cases of significant mass effect from the hemorrhage, a craniotomy or craniectomy can be performed for clot evacuation, decompression, and aneurysm clipping. Others propose securing the aneurysm with coiling followed by surgical clot evacuation [65].

IVH is an independent risk factor for worse clinical grade and poor outcome. Some degree of IVH is seen in almost half of patients and 13–28% experience major IVH [66]. Anterior communicating artery aneurysms and basilar tip aneurysms are the most common to produce larger volumes of IVH and mortality in these patients can reach 64% [67]. With a large IVH, increased ICP should be presumed even in the setting of no significant ventriculomegaly.

ICP Management

Management of elevated ICP, defined as exceeding 20 mmHg for more than 5 minutes, in the acute setting focuses on optimizing venous return and reduction of CSF volume typically with an EVD. In the case of large IVH, intraventricular thrombolytics may be administered to speed clearance [68]. If an EVD is not possible, an intraparenchymal ICP monitor should be placed in patients with GCS less than 8. Over one-third of patients will display ICPs greater than 20 mmHg at some point during monitoring [69]. Positioning with the head neutral and midline and the head of bed at 30° optimized venous return from the head. Additionally, medical management after or in lieu of surgery may occur through multiple methods [70]. Fevers, seizures, and agitation or pain should be identified and addressed if present as they increase metabolic demand of the brain. Osmotic diuretics through a CVC such as mannitol and hypertonic saline can be used to create an osmotic shift across the BBB [71]. Suppressing global cerebral demand with propofol or barbiturates can also reduce ICP in refractory cases [72, 73]. Hyperventilation is used only as a temporizing measure as chronic hypocapnia can negatively affect cerebral hypoperfusion and when stopping hyperventilation, one must be aware of rebound intracranial hypertension that may ensue. Hypothermia is another option that has been explored in these patients, during their procedure or for refractory ICP control with mixed results and associated with increased complications [3, 74]. If there is mass effect that can be surgically addressed, such as an IPH or SDH, evacuation with or without clipping of the aneurysm is indicated. If lesions do not exist, a hemicraniectomy is also a surgical option in refractory cases. Components of ICP management are shown in Table 6.2.

Table 6.2 ICP crisis management tactics

Positioning	HOB at 30° and head midline
Airway	Make sure secured Hyperventilate (temporary measure only)
CSF	EVD if possible If present, drain 5–10 cc
Imaging	Head CT to evaluate for re-rupture and for any surgical lesions that can be addressed
Hyperosmolar therapy	Mannitol 1 g/kg 23% hypertonic saline via central venous line
Hypothermia	Treat fevers Prophylactic hypothermia not indicated
Surgery	If mass lesion exists, surgical resection with or without decompressive craniectomy

Acute Hydrocephalus

Acute hydrocephalus is caused by subarachnoid blood interfering with CSF circulation within the ventricular system and subarachnoid space. It can also block absorption at the arachnoid granulations. One objective measure of ventriculomegaly is calculating the ventriculocranial ratio and comparing that to 95th percentile for certain age group [75]. There are a number of factors associated with increased risk of hydrocephalus including increasing age, hypertension, IVH, volume of SAH, posterior circulation aneurysms, and worse clinical grade [76]. Treatment in the acute setting is with CSF diversion via an EVD typically placed in sterile fashion at bedside with a twist drill for cranial access. If indicated, this should be done before any operative or endovascular procedure. We prefer to place an EVD in all intubated patients at our institution. Clinical improvement is reported in 80% of patients who undergo EVD placement [77]. Details regarding placement and nuances of management of an EVD are discussed later in this chapter.

Seizure Management

Seizure activity may be a presenting feature in 8% of patients and up to a quarter of SAH patients may develop seizures before treatment [78]. Risk factors associated with seizures include IPH (especially in an MCA location), intracranial hypertension, poor HH grade, and electrolyte imbalances such as hyponatremia [79]. Seizure is associated with increased brain swelling, increased oxygen demand, blood pressure variability, and risk of rebleeding [80]. In one study, 11% of patients had a generalized tonic-clonic seizure within 6 hours of presentation and this was associated with higher incidence of in-hospital seizures and complications.[81] Another study showed seizure association with poor clinical grade on presentation and greater hematoma burden. In cases of new-onset seizures that occur after

presentation, imaging should be done after stabilization to assess for rebleed, hydrocephalus, or ischemia. Labs should be drawn to evaluate for electrolyte and glucose level abnormalities.

Seizure management begins with benzodiazepines and intravenous (IV) antiepileptic medication (AEDs) such as fosphenytoin. Airway must be stabilized, especially if the patient proceeds to status epilepticus. High doses of AEDs may precipitate respiratory depression. Additional sedatives such as propofol are indicated to achieve seizure control. Currently, there are no randomized control trials to assess the effect of prophylactic AEDs. In high-grade SAH, continuous electroencephalogram (EEG) monitoring is recommended to diagnosis and monitor therapy. Although high-quality evidence for routine AED use in SAH is lacking and a systematic review showed no effect [82], short-term prophylactic antiepileptic therapy (typically 3–7 days) is still commonly used due to the detrimental effects of seizures in these ill patients [3, 83]. Eventually, epilepsy will develop in 12% at 5-year follow-up [84] although endovascular treatment is less associated with epilepsy than microsurgical clipping [85].

Volume Status

Hypovolemia can be seen with SAH and patients require volume repletion and expansion in the first 24 hours of presentation. This functional dehydration, if not corrected, may lead to end-organ dysfunction. Volume status during the course of the ICU stay may be monitored by central venous pressure (CVP) through a CVC. Methods of assessment include use of pulmonary artery catheter, although not commonly used anymore. Instead, one may use continuous cardiac output monitoring and stroke volume variation through less- or noninvasive means [86, 87]. A Foley catheter should be placed for monitoring of output and ensure adequate urine output of greater than 0.5 mL/kg/hr. Fluid intake should be 3 L per day once the aneurysm is secured, although overall goal should be euvolemia [88].

Laboratory Studies

Labs including a complete blood count with differential, comprehensive metabolic panel, coagulation studies, arterial blood gas, and troponin should be obtained once patient is stabilized.

The common electrolyte disturbances following SAH in order of frequency are hyponatremia, hypomagnesemia, hypokalemia, and hypernatremia [89]. Hyponatremia can exacerbate cerebral swelling. It is frequently encountered during the course of the hospitalization rather than in the acute presenting period. Accurate assessment of intake and output is essential in diagnosing the etiology of hyponatremia: euvolemic or hypervolemic syndrome of inappropriate antidiuretic hormone

versus hypovolemic cerebral salt wasting [90]. Hyperglycemia is also common in SAH patients and glucose management is essential in preventing poor outcomes and minimizing infection risk [91]. Though hyperglycemia is more common on presentation, it is important to avoid hypoglycemia in treating these patients as that could have deleterious effects on a compromised brain [92]. Anemia is a common medical complication requiring transfusion. It is typically developed over days into the hospitalization and not typically an acute concern [93].

Coagulation studies and platelet count are critical to have before starting any procedures. At our institution, patients also obtain thromboelastography studies to quantify clotting ability. Patient's medications should also be reviewed, and any antithrombotic medication or coagulopathy should be reversed appropriately. Each medication will have their own reversal algorithm, and this may differ between institutions. For warfarin, we administer fresh frozen plasma (10 mL/kg) or inactivated prothrombin-complex concentrate (factors II, VII, IX, and X) along with 3 days of 10 mg of vitamin K. Some medications including dabigatran have specific reversal agents: idarucizumab [94]. The recently US Food and Drug Administration approved drug, Andexxa (coagulation factor Xa), can be used for apixaban and rivaroxaban [95]. Thrombocytopenia should be addressed by treating the underlying cause and if a quantitative deficiency exists, it should be treated with platelet transfusions, especially if the patient is to undergo procedures or surgical intervention.

Acute Cardiac Complications

The SAH patient should have continuous electrocardiographic (EKG) monitoring upon presentation to obtain a baseline rhythm and monitor for any changes. The cardiac manifestations in a SAH patient include EKG changes in T waves, elevations in troponin and/or B-type natriuretic peptide levels, arrhythmias, and ischemic heart failure [96]. Cardiac arrhythmias can occur immediately upon ictus and are life threatening in 5–10% of cases [97]. Up to 30% of patients may experience a serious cardiac disorder in the form of neurocardiogenic stunning during their admission. Troponin leaks are associated with demand ischemia or abnormal left ventricular wall motion. Transient left ventricular dysfunction may occur due to myocardial stunning, apical ballooning syndrome, or Takotsubo cardiomyopathy. Etiology is pointed toward failure of myocardial contractility from calcium overload from increased sympathetic surge that results in oxygen free radicals [98]. An echocardiogram is indicated to diagnose and evaluate severity. It will typically show reduced ejection fraction and regional hypokinesis [99, 100]. In severe cases, the use of an intra-aortic balloon pump has been described for management [101]. Neurogenic stunned myocardium is reversible and timely intervention supports the mean arterial pressure (MAP), reduces need for vasopressors, and thus reduces delayed neurologic deficits [102]. The need for acute cardiac intervention and the need for anti-platelet or anti-coagulation therapy must be weighed against the risks in the setting of a subarachnoid hemorrhage.

Acute Pulmonary Complications

Pulmonary complications in the acute setting in SAH patients are typically due to aspiration from an unprotected airway and depressed consciousness or pulmonary edema from neurogenic insult or cardiogenic in etiology. In the acute case, pulmonary edema is typically neurogenic and associated with poor grade SAH. Mechanisms behind development of neurogenic pulmonary edema differ. A sudden increase in ICP leads to sympathetic surge causing hypertension and pulmonary artery vasoconstriction which builds pressure in alveolar capillaries leading to leakage of transudate. It may also involve direct neural mechanisms leading to disruption of the alveolar-endothelial barrier [103]. Most patients recover from it when identified early and managed appropriately with mechanical ventilation [104]. Another manifestation is ensuing pulmonary edema from cardiac failure previously described or iatrogenic aggressive volume expansion in the setting of hyperdynamic therapy. Overall, pulmonary complications have been estimated to be the cause of death in 50% of medical deaths in SAH patients [105].

Sedation and Pain Management

Continuous IV sedation is commonly used in intubated patients to address ventilator-associated discomfort or agitation. Because frequent neurologic assessments are essential in the acute period, short-acting sedatives should be used. Common agents include propofol, fentanyl, or midazolam. Although propofol has rapid-onset and short duration of action, it can still impair neurologic status for some time and affect blood pressure [106]. Dexmedetomidine is another option and has been effective in minimizing neurologic dysfunction although side effects of bradycardia limit its use [107].

Pain is experienced by most patients with SAH and it can independently increase cerebral oxygen consumption by 30%. Short-acting narcotics such as fentanyl may be used as long as patients are closely monitored and not over-sedated. Short courses of dexamethasone may also be indicated to alleviate persistent nuchal inflammatory symptoms.

Rebleeding

Rebleeding is the primary cause of death in patients who present to medical attention after initial SAH [108, 109]. It is associated with significant morbidity and 80% mortality, making rebleeding the most preventable cause of poor outcome [37]. The risk is increased in patients who have a delay in their time to diagnosis, time to treatment, and those with incompletely secure aneurysms. This risk peaks in the first

2–12 hours occurring between 4% and 13.6% [3]. It then occurs at a rate of about 1–2% per day during the following month [110]. In situations where a treatment needs delay, aminocaproic acid or tranexamic acid has been studied as antifibrinolytic agents to prevent rebleeding [111]. In untreated patients, the cumulative risk of a rebleed within first 30 days is 20–30%, within 6 months is 50% and approach 80% within the first year, the incidence is 3% per year after that [37, 112, 113]. Risk factors associated with increased frequency of rebleeding include history of hypertension, poor clinical grade, IPH, IVH, larger aneurysms, and posterior circulation aneurysms [114]. Although no randomized control exists, blood pressure control is a common practice to prevent rebleeding [3]. Ultimately, ruptured aneurysms should undergo definitive treatment by coiling or clipping as soon as possible.

External Ventricular Drain

Indications

The rate of acute hydrocephalus has been reported in 15–85% of patients presenting with aneurysmal subarachnoid hemorrhage. Most recent studies have demonstrated rates of 20–30%.[115] The use of an EVD to manage hydrocephalus in the setting of aneurysmal SAH was first reported in 1973 by Kusske et al. and it has since become the standard approach for treatment of acute hydrocephalus [116, 117]. Common considerations for EVD insertion in the setting of SAH include GCS $\leq$ 12 [118], HH grade $\geq$ 3 [76], or inability to follow commands [119]. Prospective studies have suggested that the majority of patients presenting with radiographic ventriculomegaly and headache improve without drainage and may be observed [118]. However, the natural course for patients with fluctuating cognition is less well defined and some propose for more aggressive management with an EVD.

Preparation

As with any procedure, efficiency is dictated by thoughtful preparation prior to the procedure. The patient's clinical status and the need for airway management in the non-intubated patient should be addressed prior to proceeding with EVD insertion. Depending on the patient's coagulation status, a specific reversal algorithm may need to be addressed prior to insertion. Adequate sedation and analgesia should also be ensured for the patient. Pre-procedural antibiotics should also be used to decrease the incidence of ventriculostomy-related infections [120].

The patient should be maintained in a supine position with head of bed elevated at 45°. This elevation may be lowered to aid the trajectory of the EVD if necessary. The patient's hair on the side of insertion should be removed using clippers. A donut

headrest may be used and the head can be taped to the bed to minimize movement during the procedure. An aggressive skin preparation should be performed using an anti-septic agent. At our institution, a povidone-iodine solution is preferred. Subsequently, sterile drapes should be used to isolate the non-sterile areas from the procedural field.

Technique

A freehand technique is commonly used for the insertion of EVDs. The right frontal cerebral cortex is non-dominant for language function in >90% of patients and therefore is the preferred site of entry [121]. However, based on the characteristics of the SAH or presence of IVH, it may be necessary to move the insertion site to the left frontal cerebral cortex. A burr hole should be placed at Kocher's point to avoid the superior sagittal sinus and the motor cortex. This point is located 11 cm posterior to the nasion and 3 cm lateral from midline. It should be located along the ipsilateral midpupillary line (Fig. 6.5).

After the site is marked, it is injected with local anesthesia; 1% lidocaine with epinephrine 1:100,000 is preferred to assist with hemostasis. A 1–2 cm linear incision along the midpupillary line centered on Kocher's point should be made down to bone. The periosteum is subsequently scraped from the bone using a blunt instrument to prevent the drill tip from migrating during initialization. A twist drill should then be aimed perpendicular to the skull at Kocher's point and used to penetrate bone. The cortical and cancellous layers of the bone should be easily felt, with a rise in resistance in the latter stages of drilling indicating the inner cortical layer. At this point, care should be taken not to apply excessive pressure on the drill and risk cortical injury if the cortical layer were to suddenly give way. A sharp drop in resistance indicates that the bone has been completely penetrated. The dura should subsequently be pierced sharply. A blunt instrument can be used to confirm penetration of the dura.

The ventricular catheter is put into position and passed to no more than 7 cm deep from the skin into the ventricle. The traditional trajectory for the catheter is toward the ipsilateral medial canthus in the coronal plane and the ipsilateral tragus in the sagittal plane. However, a more medial trajectory in the coronal plane toward the nasion or the contralateral medial canthus may provide better accuracy in a subset of patients, especially those with mild radiographic ventriculomegaly [122]. The CT scan should be studied to ensure the optimum trajectory on a patient-by-patient basis.

Successful insertion of the catheter into the ventricle can be confirmed by assessing for spontaneous CSF flow from the catheter. Subsequently, the catheter should be tunneled in a posterior and medial direction to avoid the path of a possible future ventriculoperitoneal shunt (VPS) and exit the skin at least 4 cm away from the site of insertion. The incision site is closed, and the drain is secured to the scalp using

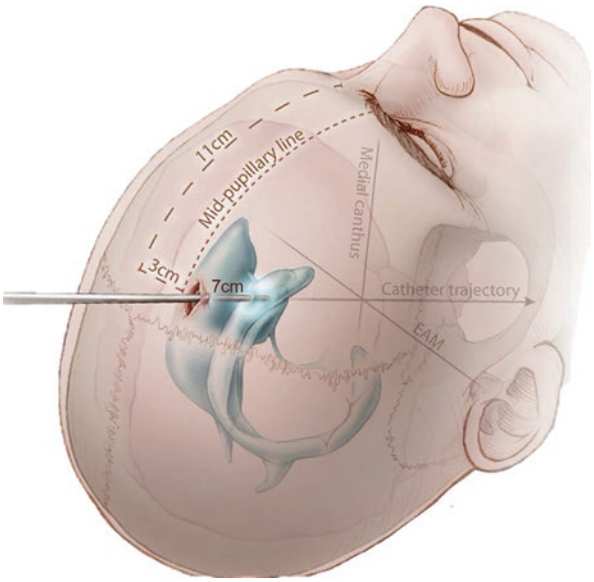

Fig. 6.5 Ventricular access via Kocher's point. The burr hole should be placed 11 cm superior and posterior to the nasion and 3 cm lateral to the midline. The catheter is aimed at an angle that is perpendicular to the intersection of lines drawn from the ipsilateral medial canthus and the ipsilateral external auditory meatus. The catheter is passed to a depth of approximately 7 cm from the skin or until the frontal horn of the ipsilateral lateral ventricle is reached. (Obtained and modified with permission from Oxford University Press. Morone PJ, Dewan MC, Zuckerman SL, Tubbs RS, Singer RJ. Craniometrics and Ventricular Access: A Review of Kocher's, Kaufman's, Paine's, Menovksy's, Tubbs', Keen's, Frazier's, Dandy's, and Sanchez's Points. *Oper Neurosurg* (Hagerstown). 2020;18(5):461–469)

multiple stitches, with care being taken not to puncture or occlude the catheter at this stage. It is subsequently connected to a buretrol in sterile fashion.

EVD Management

Aneurysm rebleeding is a concern after EVD placement and provides the rationale for limited CSF drainage in the setting of an unsecured aneurysm. In a meta-analysis evaluating aneurysm rebleeding after EVD placement, rebleeding was observed in 18.4% of patients who were treated with EVD placement versus 6.4% in patients who did not receive an EVD. The average time between EVD placement and rebleeding was 1 hour. Factors associated with rebleeding include large size (>10 mm) and high Fisher grade (III-IV) [123]. In one study, patients who experienced rebleeding after EVD placement had a mean level of drainage of 2.5 cm H_2O compared to 14 cm H_2O in patients in whom re-hemorrhage did not occur [124]. It is important to note, however, that the association between EVD and aneurysm

rebleeding may be an epiphenomenon associated with large aneurysmal ruptures presenting with high grade hemorrhage and poor neurological status.

There currently exists a consensus on limiting CSF drainage in the setting of an unsecured ruptured aneurysm. The majority of institutions favor continuous drainage at either 15 or 20 cm H_2O [125]. This is due to the fear that the pressure gradient formed by aggressive CSF drainage may increase the risk of re-rupture based on historical data that demonstrated re-rupture being associated with relatively low ICP [126]. Patients with secured aneurysms are largely managed via continuous CSF drainage at 10 cm H_2O [125]. There are multiple rationales for continuous drainage: (1) to treat symptomatic hydrocephalus, (2) to clear blood, and (3) to improve cerebral perfusion pressure. The practice of continuous CSF drainage is also based on an extrapolation from the 2016 Brain Trauma Foundation Level III recommendation stating that continuous CSF drainage may lower the ICP burden more effectively than intermittent drainage [127]. However, some proponents argue for intermittent drainage based on a randomized trial by demonstrating that intermittent drainage is associated with a lower incidence of catheter occlusion as well as a trend toward lower rates of ventriculitis and CSF leak or hemorrhage in the intermittent drainage group [128]. There is also a theoretical argument that the earlier and higher pressures caused by intermittent drainage may promote resumption of natural CSF absorption pathways. However, all major studies to date have demonstrated comparable rates of eventual VPS placement in patients undergoing intermittent versus continuous CSF drainage.

The symptoms of EVD-related infections may be masked by the patient's primary pathology. Furthermore, most causative organisms only cause mild inflammatory responses. Several institutions have therefore instituted routine sampling of CSF. However, opponents of this practice argue that routine CSF sampling may increase the risk of contamination of the drainage system. Observational studies regarding CSF sampling have noted that a decreased frequency of sampling is associated with a decreased risk of culture-positive infections [129]. Furthermore, each CSF sample increases the relative likelihood of ventriculostomy-related infection by 8.3% [130]. The current recommendation from the Neurocritical Care Society is to avoid routine CSF sampling and only obtain CSF for analysis when clinically indicated [120].

There is currently no consensus regarding the routine administration of prophylactic antibiotics in the periprocedural setting versus throughout the duration that the EVD is in place. The largest randomized controlled trial to date by Poon et al. demonstrated a lower rate of ventriculostomy-related infections in the group treated with prophylactic antibiotics for the duration of the EVD. However, there are methodological issues that confound this finding; the duration arm received broader spectrum antibiotics than the periprocedural group. There was also a larger incidence of resistant organisms in the duration arm [131]. In contrast, a number of smaller studies have demonstrated no difference in infection rate between periprocedural antibiotic administration versus antibiotic administration for the duration of the EVD. Furthermore, long-term antibiotic administration is also associated with an increased incidence of resistant organisms and *C. difficile* colitis. It is therefore a reasonable to limit antibiotic administration to the periprocedural period.

Patients with acute neurological injuries are at an increased risk of venous thromboembolisms (VTE). A retrospective study found a VTE rate of 7.2% in patients who had undergone an EVD placement [132]. Neurosurgical patients with elastic stockings alone and no other forms of VTE prophylaxis exhibit VTE between 14% and 16% [133]. Administration of prophylactic doses of unfractionated heparin (UFH) or low-molecular-weight heparin (LMWH) is associated with a 45% relative risk reduction compared to no prophylaxis [134]. A retrospective analysis of VTE prophylaxis with UFH reported a new intracranial hemorrhage on CT in 18% of patients, although only 4.5% of these were determined to be clinically significant [132]. A decision analysis found that in neurosurgical patients with no additional risk factors for pulmonary embolism, mechanical prophylaxis alone is most efficacious as the benefits of UFH and LMWH were outweighed by an increased incidence of intracranial hemorrhage [135]. However, given the critically ill state of patients presenting with SAH who undergo EVD placement, it is reasonable to institute chemical prophylaxis placement utilizing either UFH or LMWH after the hemorrhage has been ruled stable and new hemorrhages have been ruled out.

EVD Wean Protocol

Given the tenuous clinical state of many patients after SAH, we recommend keeping the EVD in place through the window of vasospasm risk. Once this window has passed, the timing for initiating a wean of the EVD can be based on clinical status, drainage volume, presence of blood in drained CSF, and EVD duration [136]. Different strategies for weaning an EVD exist. A gradual wean involves step-wise increase in the drain height over several days prior to clamping the drain. A rapid wean involves immediate clamping of the drain. There currently exists only one randomized controlled trial comparing gradual to rapid wean of an EVD. No difference in VPS placement was found between the two groups, but the rapid wean group had significantly lower ICU and in-hospital days [137]. A large observational study by Jabbarli et al. demonstrated that rapid wean was associated with a higher incidence of VPS placement in their cohort and VPS placement was inversely associated with length of external ventricular drainage. However, patients who underwent gradual wean have a higher risk of a delayed development of shunt-dependency [138]. Currently, the majority of institutions utilize a gradual wean protocol [125].

Complications

Ventriculostomy-related infections are the most common complication associated with EVD placement and occur with an average rate of 7.3%. These are associated with a significant increase in inpatient mortality, length of stay, and cost of care [139]. CSF sampling and antibiotic prophylaxis strategies to minimize infections

were discussed earlier in the chapter. In the past, there was a recommendation for exchanging ventriculostomy catheters after 5 days to decrease the risk of infection [140]. However, the use of anti-microbial impregnated catheters has been associated with a significant reduction in infection rates and have rendered the practice of catheter exchange obsolete [141]. Many centers are reporting ventriculostomy-related infection rates of 2% or lower with anti-microbial impregnated catheters without changing catheter sites [142].

Hemorrhage associated with EVD placement can potentially cause devastating and irreversible injury. Radiographic evidence of hemorrhage has been reported in over 20% of patients following EVD placement, although only 2% of these required further interventions. Factors associated with an increased risk of hemorrhage include low platelet count upon admission and an increased number of EVD placement attempts [143]. Similarly, a meta-analysis reported an overall hemorrhage rate of 5.7% and clinically significant hemorrhages occurring in <1% of patients [144]. In evaluating risk factors associated with hemorrhage following EVD placement, nonsignificant increase in hemorrhage rates was found in patients receiving antiplatelet agents or on anticoagulation with for VTE prophylaxis [145].

Treatment Preparation

Early treatment goal should be to secure the aneurysm and prevent re-hemorrhage. Efforts to treat aneurysms within a 24-hour window can help improve outcomes versus within 72 hours (a 10.2% absolute risk reduction in poor outcome) [146]. This is done through microsurgical clipping or more commonly endovascular coiling. A recent meta-analysis on outcomes between endovascular and surgical treatment of rupture aneurysms showed lower chance of functional dependency in endovascular patients [147]. Regardless of treatment modality, the SAH patient should be prepared to undergo maximal intervention if need be. At our institution, the patient or family member is counseled on all treatment options and they are consented for EVD, diagnostic angiogram, coiling, craniotomy for clipping, and possible craniectomy at once, so they are aware of all options and can have the opportunity to discuss alternatives with the surgeon rather than having the discussion in the middle of an emergent crisis (e.g., aneurysm re-rupture during endovascular coiling).

Although the specifics of interventions for rupture aneurysms is beyond the scope of this chapter, important considerations should be made with respect to planning and preparation. Before going into the interventional radiology suite or operating room, all laboratory studies, including type and cross and coagulation factors, should be resulted. The patient should have good IV access, preferably with a central line, and an arterial line for continuous monitoring. If indicated, an EVD should be in place. The patient will be intubated for the procedure, lying flat, without any assessment of the neurologic status other than physiologic neuromonitoring. Therefore, even in cases of mild ventriculomegaly or lower grade patients, an EVD should still

be considered. At least one unit of packed RBCs should be made available. For the angiography suite, proper equipment such as catheter types are reviewed by the angiographer. A CTA of the head and neck done beforehand may assist in planning for access difficulties and potential need for adjunct coiling devices.

Conclusion

Aneurysm rupture is a common cause of non-traumatic SAH and remains a serious diagnosis with significant morbidity and mortality even with optimal measures. Prompt recognition, diagnosis, and critical care management are key in the acute phase of the disease as the initial trajectory of the disease dictates the patient's eventual outcome. Specifically, airway protection, blood pressure management, seizure management, and control of intracranial hypertension are main modalities of management that should be addressed in parallel within the first few hours. A large component of this is relief of hydrocephalus and addressing increased ICP with an EVD placed in a timely manner. The appropriate management of the EVD both in the acute phase and further into the hospitalization of the patient is critical.

References

1. van Gijn J, Rinkel GJ. Subarachnoid haemorrhage: diagnosis, causes and management. Brain. 2001;124:249–78.
2. Samuels O, Webb A, Culler S, Martin K, Barrow D. Impact of a dedicated neurocritical care team in treating patients with aneurysmal subarachnoid hemorrhage. Neurocrit Care. 2011;14:334–40.
3. Connolly ES, Rabinstein AA, Carhuapoma JR, Derdeyn CP, Dion J, Higashida RT, et al. Guidelines for the management of aneurysmal subarachnoid hemorrhage: a guideline for healthcare professionals from the American Heart Association/American Stroke Association. Stroke. 2012;43:1711–37.
4. Raya AK, Diringer MN. Treatment of subarachnoid hemorrhage. Crit Care Clin. 2014;30:719–33.
5. de Rooij NK, Linn FHH, van der Plas JA, Algra A, Rinkel GJE. Incidence of subarachnoid haemorrhage: a systematic review with emphasis on region, age, gender and time trends. J Neurol Neurosurg Psychiatry. 2007;78:1365–72.
6. Epidemiology of aneurysmal subarachnoid hemorrhage in Australia and New Zealand: incidence and case fatality from the Australasian Cooperative Research on Subarachnoid Hemorrhage Study (ACROSS). Stroke. 2000;31:1843–50.
7. Feigin VL, Lawes CMM, Bennett DA, Barker-Collo SL, Parag V. Worldwide stroke incidence and early case fatality reported in 56 population-based studies: a systematic review. Lancet Neurol. 2009;8:355–69.
8. Eden SV, Meurer WJ, Sánchez BN, Lisabeth LD, Smith MA, Brown DL, et al. Gender and ethnic differences in subarachnoid hemorrhage. Neurology. 2008;71:731–5.
9. Vlak MHM, Rinkel GJE, Greebe P, Greving JP, Algra A. Lifetime risks for aneurysmal subarachnoid haemorrhage: multivariable risk stratification. J Neurol Neurosurg Psychiatry. 2013;84:619–23.

10. Broderick JP, Brott TG, Duldner JE, Tomsick T, Leach A. Initial and recurrent bleeding are the major causes of death following subarachnoid hemorrhage. Stroke. 1994;25:1342–7.
11. Nieuwkamp DJ, Setz LE, Algra A, Linn FHH, de Rooij NK, Rinkel GJE. Changes in case fatality of aneurysmal subarachnoid haemorrhage over time, according to age, sex, and region: a meta-analysis. Lancet Neurol. 2009;8:635–42.
12. Huang J, van Gelder JM. The probability of sudden death from rupture of intracranial aneurysms: a meta-analysis. Neurosurgery. 2002;51:1101–5; discussion 1105–7
13. Rinkel GJE, Algra A. Long-term outcomes of patients with aneurysmal subarachnoid haemorrhage. Lancet Neurol. 2011;10:349–56.
14. Korja M, Silventoinen K, Laatikainen T, Jousilahti P, Salomaa V, Kaprio J. Cause-specific mortality of 1-year survivors of subarachnoid hemorrhage. Neurology. 2013;80:481–6.
15. Wermer MJH, Greebe P, Algra A, Rinkel GJE. Incidence of recurrent subarachnoid hemorrhage after clipping for ruptured intracranial aneurysms. Stroke. 2005;36:2394–9.
16. Koskinen L-OD, Blomstedt PC. Smoking and non-smoking tobacco as risk factors in subarachnoid haemorrhage. Acta Neurol Scand. 2006;114:33–7.
17. Sandvei MS, Romundstad PR, Müller TB, Vatten L, Vik A. Risk factors for aneurysmal subarachnoid hemorrhage in a prospective population study: the HUNT study in Norway. Stroke. 2009;40:1958–62.
18. Algra AM, Klijn CJM, Helmerhorst FM, Algra A, Rinkel GJE. Female risk factors for subarachnoid hemorrhage: a systematic review. Neurology. 2012;79:1230–6.
19. van der Schaaf IC, Velthuis BK, Gouw A, Rinkel GJE. Venous drainage in perimesencephalic hemorrhage. Stroke. 2004;35:1614–8.
20. Dupont SA, Lanzino G, Wijdicks EFM, Rabinstein AA. The use of clinical and routine imaging data to differentiate between aneurysmal and nonaneurysmal subarachnoid hemorrhage prior to angiography. Clinical article. J Neurosurg. 2010;113:790–4.
21. Whitmore RG, Grant RA, LeRoux P, El-Falaki O, Stein SC. How large is the typical subarachnoid hemorrhage? A review of current neurosurgical knowledge. World Neurosurg. 2012;77:686–97.
22. Visser F, Rinkel GJE. Isolated headache in general practice: determinants for delay in referral in patients with subarachnoid haemorrhage. Eur J Gen Pract. 2012;18:149–53.
23. Spetzler RF, Kalani YS, Nakaji P. Neurovascular surgery. 2nd ed. New York: Thieme; 2015.
24. Anderson C, Ni Mhurchu C, Scott D, Bennett D, Jamrozik K, Hankey G, et al. Triggers of subarachnoid hemorrhage: role of physical exertion, smoking, and alcohol in the Australasian Cooperative Research on Subarachnoid Hemorrhage Study (ACROSS). Stroke. 2003;34:1771–6.
25. Polmear A. Sentinel headaches in aneurysmal subarachnoid haemorrhage: what is the true incidence? A systematic review. Cephalalgia. 2003;23:935–41.
26. Beck J, Raabe A, Szelenyi A, Berkefeld J, Gerlach R, Setzer M, et al. Sentinel headache and the risk of rebleeding after aneurysmal subarachnoid hemorrhage. Stroke. 2006;37:2733–7.
27. Sung W, Arnaldo B, Sergio C, Juliana S, Michel F. Terson's syndrome as a prognostic factor for mortality of spontaneous subarachnoid haemorrhage. Acta Ophthalmol. 2011;89:544–7.
28. Becker KJ. Epidemiology and clinical presentation of aneurysmal subarachnoid hemorrhage. Neurosurg Clin N Am. 1998;9:435–44.
29. Behrouz R, Birnbaum LA, Jones PM, Topel CH, Misra V, Rabinstein AA. Focal neurological deficit at onset of aneurysmal subarachnoid hemorrhage: frequency and causes. J Stroke Cerebrovasc Dis. 2016;25:2644–7.
30. Kowalski RG, Claassen J, Kreiter KT, Bates JE, Ostapkovich ND, Connolly ES, et al. Initial misdiagnosis and outcome after subarachnoid hemorrhage. JAMA. 2004;291:866–9.
31. Perry JJ, Stiell IG, Sivilotti MLA, Bullard MJ, Hohl CM, Sutherland J, et al. Clinical decision rules to rule out subarachnoid hemorrhage for acute headache. JAMA. 2013;310:1248–55.
32. Loftus CM. Neurosurgical Emergencies [Internet]. 3rd ed. Thieme; 2017 [cited 2020 Jun 4]. Available from: https://medone%2D%2Dneurosurgery-thieme-com.eu1.proxy.openathens.net/ebooks/2022748?fromSearch=true#/ebook_2022748_SL78074758.

33. Chen S, Li Q, Wu H, Krafft PR, Wang Z, Zhang JH. The harmful effects of subarachnoid hemorrhage on extracerebral organs. Biomed Res Int. 2014;2014:858496.
34. Helbok R, Kurtz P, Vibbert M, Schmidt MJ, Fernandez L, Lantigua H, et al. Early neurological deterioration after subarachnoid haemorrhage: risk factors and impact on outcome. J Neurol Neurosurg Psychiatry. 2013;84:266–70.
35. Backes D, Rinkel GJE, Kemperman H, Linn FHH, Vergouwen MDI. Time-dependent test characteristics of head computed tomography in patients suspected of nontraumatic subarachnoid hemorrhage. Stroke. 2012;43:2115–9.
36. Boesiger BM, Shiber JR. Subarachnoid hemorrhage diagnosis by computed tomography and lumbar puncture: are fifth generation CT scanners better at identifying subarachnoid hemorrhage? J Emerg Med. 2005;29:23–7.
37. van Gijn J, Kerr RS, Rinkel GJE. Subarachnoid haemorrhage. Lancet. 2007;369:306–18.
38. Byyny RL, Mower WR, Shum N, Gabayan GZ, Fang S, Baraff LJ. Sensitivity of noncontrast cranial computed tomography for the emergency department diagnosis of subarachnoid hemorrhage. Ann Emerg Med. 2008;51:697–703.
39. Perry JJ, Alyahya B, Sivilotti MLA, Bullard MJ, Émond M, Sutherland J, et al. Differentiation between traumatic tap and aneurysmal subarachnoid hemorrhage: prospective cohort study. BMJ. 2015;350:h568.
40. Nagy K, Skagervik I, Tumani H, Petzold A, Wick M, Kühn H-J, et al. Cerebrospinal fluid analyses for the diagnosis of subarachnoid haemorrhage and experience from a Swedish study. What method is preferable when diagnosing a subarachnoid haemorrhage? Clin Chem Lab Med. 2013;51:2073–86.
41. Rabinstein AA, Lanzino G. Aneurysmal subarachnoid hemorrhage: unanswered questions. Neurosurg Clin N Am. 2018;29:255–62.
42. Lubicz B, Levivier M, François O, Thoma P, Sadeghi N, Collignon L, et al. Sixty-four-row multisection CT angiography for detection and evaluation of ruptured intracranial aneurysms: interobserver and intertechnique reproducibility. AJNR Am J Neuroradiol. 2007;28:1949–55.
43. HaiFeng L, YongSheng X, YangQin X, Yu D, ShuaiWen W, XingRu L, et al. Diagnostic value of 3D time-of-flight magnetic resonance angiography for detecting intracranial aneurysm: a meta-analysis. Neuroradiology. 2017;59:1083–92.
44. Sailer AMH, Wagemans BAJM, Nelemans PJ, de Graaf R, van Zwam WH. Diagnosing intracranial aneurysms with MR angiography: systematic review and meta-analysis. Stroke. 2014;45:119–26.
45. Agid R, Andersson T, Almqvist H, Willinsky RA, Lee S-K, ter Brugge KG, et al. Negative CT angiography findings in patients with spontaneous subarachnoid hemorrhage: when is digital subtraction angiography still needed? AJNR Am J Neuroradiol. 2010;31:696–705.
46. Nehls DG, Flom RA, Carter LP, Spetzler RF. Multiple intracranial aneurysms: determining the site of rupture. J Neurosurg. 1985;63:342–8.
47. Hunt WE, Hess RM. Surgical risk as related to time of intervention in the repair of intracranial aneurysms. J Neurosurg. 1968;28:14–20.
48. Report of World Federation of Neurological Surgeons Committee on a universal subarachnoid hemorrhage grading scale. J Neurosurg. 1988;68:985–6.
49. Giraldo EA, Mandrekar JN, Rubin MN, Dupont SA, Zhang Y, Lanzino G, et al. Timing of clinical grade assessment and poor outcome in patients with aneurysmal subarachnoid hemorrhage. J Neurosurg. 2012;117:15–9.
50. Rosen DS, Macdonald RL. Subarachnoid hemorrhage grading scales: a systematic review. Neurocrit Care. 2005;2:110–8.
51. Botterell EH, Lougheed WM, Scott JW, Vandewater SL. Hypothermia, and interruption of carotid, or carotid and vertebral circulation, in the surgical management of intracranial aneurysms. J Neurosurg. 1956;13:1–42.
52. van Heuven AW, Dorhout Mees SM, Algra A, Rinkel GJE. Validation of a prognostic subarachnoid hemorrhage grading scale derived directly from the Glasgow Coma Scale. Stroke. 2008;39:1347–8.

53. Kramer AH, Hehir M, Nathan B, Gress D, Dumont AS, Kassell NF, et al. A comparison of 3 radiographic scales for the prediction of delayed ischemia and prognosis following subarachnoid hemorrhage. J Neurosurg. 2008;109:199–207.
54. Hijdra A, Brouwers PJ, Vermeulen M, van Gijn J. Grading the amount of blood on computed tomograms after subarachnoid hemorrhage. Stroke. 1990;21:1156–61.
55. Fein JM. Brain energetics and circulatory control after subarachnoid hemorrhage. J Neurosurg. 1976;45:498–507.
56. Sehba FA, Friedrich V. Early events after aneurysmal subarachnoid hemorrhage. Acta Neurochir Suppl. 2015;120:23–8.
57. Curley G, Kavanagh BP, Laffey JG. Hypocapnia and the injured brain: more harm than benefit. Crit Care Med. 2010;38:1348–59.
58. Voldby B, Enevoldsen EM. Intracranial pressure changes following aneurysm rupture. Part 1: clinical and angiographic correlations. J Neurosurg. 1982;56:186–96.
59. Ascanio LC, Enriquez-Marulanda A, Maragkos GA, Salem MM, Alturki AY, Ravindran K, et al. Effect of blood pressure variability during the acute period of subarachnoid hemorrhage on functional outcomes. Neurosurgery. 2020;87:779.
60. Bederson JB, Sander CE, Hunt BH, Dacey Ralph G, Dion Jacques E, Diringer Michael N, et al. Guidelines for the management of aneurysmal subarachnoid hemorrhage. Stroke. 2009;40:994–1025.
61. Mocco J, Prickett CS, Komotar RJ, Connolly ES, Mayer SA. Potential mechanisms and clinical significance of global cerebral edema following aneurysmal subarachnoid hemorrhage. Neurosurg Focus. 2007;22:E7.
62. Pasqualin A, Bazzan A, Cavazzani P, Scienza R, Licata C, Da Pian R. Intracranial hematomas following aneurysmal rupture: experience with 309 cases. Surg Neurol. 1986;25:6–17.
63. Güresir E, Beck J, Vatter H, Setzer M, Gerlach R, Seifert V, et al. Subarachnoid hemorrhage and intracerebral hematoma: incidence, prognostic factors, and outcome. Neurosurgery. 2008;63:1088–93; discussion 1093–4
64. Benoit BG, Cochrane DD, Durity F, Ferguson GG, Fewer D, Hunter KM, et al. Clinical - radiological correlates in intracerebral hematomas due to aneurysmal rupture. Can J Neurol Sci. 1982;9:409–14.
65. Jeong JH, Koh JS, Kim EJ. A less invasive approach for ruptured aneurysm with intracranial hematoma: coil embolization followed by clot evacuation. Korean J Radiol. 2007;8:2–8.
66. Kassell NF, Torner JC, Haley EC, Jane JA, Adams HP, Kongable GL. The international cooperative study on the timing of aneurysm surgery. Part 1: overall management results. J Neurosurg. 1990;73:18–36.
67. Mohr G, Ferguson G, Khan M, Malloy D, Watts R, Benoit B, et al. Intraventricular hemorrhage from ruptured aneurysm. Retrospective analysis of 91 cases. J Neurosurg. 1983;58:482–7.
68. Kramer AH, Roberts DJ, Holodinsky J, Todd S, Hill MD, Zygun DA, et al. Intraventricular tissue plasminogen activator in subarachnoid hemorrhage patients: a prospective, randomized, placebo-controlled pilot trial. Neurocrit Care. 2014;21:275–84.
69. Zoerle T, Lombardo A, Colombo A, Longhi L, Zanier ER, Rampini P, et al. Intracranial pressure after subarachnoid hemorrhage. Crit Care Med. 2015;43:168–76.
70. Ropper AH. Management of raised intracranial pressure and hyperosmolar therapy. Pract Neurol. 2014;14:152–8.
71. Horn P, Münch E, Vajkoczy P, Herrmann P, Quintel M, Schilling L, et al. Hypertonic saline solution for control of elevated intracranial pressure in patients with exhausted response to mannitol and barbiturates. Neurol Res. 1999;21:758–64.
72. Eisenberg HM, Frankowski RF, Contant CF, Marshall LF, Walker MD. High-dose barbiturate control of elevated intracranial pressure in patients with severe head injury. J Neurosurg. 1988;69:15–23.
73. Ravishankar N, Nuoman R, Amuluru K, El-Ghanem M, Thulasi V, Dangayach NS, et al. Management strategies for intracranial pressure crises in subarachnoid hemorrhage. J Intensive Care Med. 2020;35:211–8.

74. Bernard SA, Gray TW, Buist MD, Jones BM, Silvester W, Gutteridge G, et al. Treatment of comatose survivors of out-of-hospital cardiac arrest with induced hypothermia. N Engl J Med. 2002;346:557–63.
75. van Gijn J, Hijdra A, Wijdicks EF, Vermeulen M, van Crevel H. Acute hydrocephalus after aneurysmal subarachnoid hemorrhage. J Neurosurg. 1985;63:355–62.
76. Dorai Z, Hynan LS, Kopitnik TA, Samson D. Factors related to hydrocephalus after aneurysmal subarachnoid hemorrhage. Neurosurgery. 2003;52:763–9; discussion 769–71
77. Roitberg BZ, Khan N, Alp MS, Hersonskey T, Charbel FT, Ausman JI. Bedside external ventricular drain placement for the treatment of acute hydrocephalus. Br J Neurosurg. 2001;15:324–7.
78. Pinto AN, Canhao P, Ferro JM. Seizures at the onset of subarachnoid haemorrhage. J Neurol. 1996;243:161–4.
79. Ibrahim GM, Fallah A, Macdonald RL. Clinical, laboratory, and radiographic predictors of the occurrence of seizures following aneurysmal subarachnoid hemorrhage. J Neurosurg. 2013;119:347–52.
80. Butzkueven H, Evans AH, Pitman A, Leopold C, Jolley DJ, Kaye AH, et al. Onset seizures independently predict poor outcome after subarachnoid hemorrhage. Neurology. 2000;55:1315–20.
81. De Marchis GM, Pugin D, Lantigua H, Zammit C, Tadi P, Schmidt JM, et al. Tonic-clonic activity at subarachnoid hemorrhage onset: impact on complications and outcome. PLoS One. 2013;8:e71405.
82. Raper DMS, Starke RM, Komotar RJ, Allan R, Connolly ES. Seizures after aneurysmal subarachnoid hemorrhage: a systematic review of outcomes. World Neurosurg. 2013;79:682–90.
83. Chumnanvej S, Dunn IF, Kim DH. Three-day phenytoin prophylaxis is adequate after subarachnoid hemorrhage. Neurosurgery. 2007;60:99–102; discussion 102–3
84. Huttunen J, Kurki MI, von Und Zu Fraunberg M, Koivisto T, Ronkainen A, Rinne J, et al. Epilepsy after aneurysmal subarachnoid hemorrhage: a population-based, long-term follow-up study. Neurology. 2015;84:2229–37.
85. Molyneux AJ, Kerr RSC, Yu L-M, Clarke M, Sneade M, Yarnold JA, et al. International subarachnoid aneurysm trial (ISAT) of neurosurgical clipping versus endovascular coiling in 2143 patients with ruptured intracranial aneurysms: a randomised comparison of effects on survival, dependency, seizures, rebleeding, subgroups, and aneurysm occlusion. Lancet. 2005;366:809–17.
86. Simonassi F, Ball L, Badenes R, Millone M, Citerio GM, Zona G, et al. Hemodynamic monitoring in patients with subarachnoid hemorrhage: a systematic review and meta-analysis. [review]. J Neurosurg Anesthesiol. 33:285.
87. Mutoh T, Ishikawa T, Suzuki A, Yasui N. Continuous cardiac output and near-infrared spectroscopy monitoring to assist in management of symptomatic cerebral vasospasm after subarachnoid hemorrhage. Neurocrit Care. 2010;13:331–8.
88. Hasan D, Vermeulen M, Wijdicks EF, Hijdra A, van Gijn J. Effect of fluid intake and antihypertensive treatment on cerebral ischemia after subarachnoid hemorrhage. Stroke. 1989;20:1511–5.
89. Wartenberg KE, Schmidt JM, Claassen J, Temes RE, Frontera JA, Ostapkovich N, et al. Impact of medical complications on outcome after subarachnoid hemorrhage. Crit Care Med. 2006;34:617–23; quiz 624
90. Hannon MJ, Thompson CJ. Neurosurgical hyponatremia. J Clin Med. 2014;3:1084–104.
91. Latorre JGS, Chou SH-Y, Nogueira RG, Singhal AB, Carter BS, Ogilvy CS, et al. Effective glycemic control with aggressive hyperglycemia management is associated with improved outcome in aneurysmal subarachnoid hemorrhage. Stroke. 2009;40:1644–52.
92. Naidech AM, Levasseur K, Liebling S, Garg RK, Shapiro M, Ault ML, et al. Moderate hypoglycemia is associated with vasospasm, cerebral infarction, and 3-month disability after subarachnoid hemorrhage. Neurocrit Care. 2010;12:181–7.

93. Le Roux PD. Participants in the international multi-disciplinary consensus conference on the critical care management of subarachnoid hemorrhage. Anemia and transfusion after subarachnoid hemorrhage. Neurocrit Care. 2011;15:342–53.
94. Pollack CV, Reilly PA, Eikelboom J, Glund S, Verhamme P, Bernstein RA, et al. Idarucizumab for Dabigatran reversal. N Engl J Med. 2015;373:511–20.
95. Momin JH, Candidate P, Hughes GJ. Andexanet Alfa (Andexxa®) for the reversal of direct oral anticoagulants. P T. 2019;44:530–49.
96. Wybraniec MT, Mizia-Stec K, Krzych Ł. Neurocardiogenic injury in subarachnoid hemorrhage: a wide spectrum of catecholamin-mediated brain-heart interactions. Cardiol J. 2014;21:220–8.
97. van der Kleij FG, Henselmans JM, van de Loosdrecht AA. Cardiac arrhythmia as initial presentation of aneurysmal subarachnoid hemorrhage. Neth J Med. 1999;55:242–6.
98. Rose JJ, Vanhecke TE, McCullough PA. Subarachnoid hemorrhage with neurocardiogenic stunning. Rev Cardiovasc Med. 2010;11:254–63.
99. van der Bilt IAC, Hasan D, Vandertop WP, Wilde AAM, Algra A, Visser FC, et al. Impact of cardiac complications on outcome after aneurysmal subarachnoid hemorrhage: a meta-analysis. Neurology. 2009;72:635–42.
100. Zhang L, Zhang B, Qi S. Impact of echocardiographic wall motion abnormality and cardiac biomarker elevation on outcome after subarachnoid hemorrhage: a meta-analysis. Neurosurg Rev. 2020;43:59–68.
101. Kerro A, Woods T, Chang JJ. Neurogenic stunned myocardium in subarachnoid hemorrhage. J Crit Care. 2017;38:27–34.
102. Ducruet AF, Albuquerque FC, Crowley RW, Williamson R, Forseth J, McDougall CG. Balloon-pump counterpulsation for management of severe cardiac dysfunction after aneurysmal subarachnoid hemorrhage. World Neurosurg. 2013;80:e347–52.
103. Vespa PM, Bleck TP. Neurogenic pulmonary edema and other mechanisms of impaired oxygenation after aneurysmal subarachnoid hemorrhage. Neurocrit Care. 2004;1:157–70.
104. Kimura T, Kamide T, Onodera K, Tabata S, Shibata A, Suzuki K, et al. Clinical features of neurogenic pulmonary edema in patients with subarachnoid hemorrhage. World Neurosurg. 2020;135:e505–9.
105. Solenski NJ, Haley EC, Kassell NF, Kongable G, Germanson T, Truskowski L, et al. Medical complications of aneurysmal subarachnoid hemorrhage: a report of the multicenter, cooperative aneurysm study. Participants of the Multicenter Cooperative Aneurysm Study. Crit Care Med. 1995;23:1007–17.
106. Kowalski SD, Rayfield CA. A post hoc descriptive study of patients receiving propofol. Am J Crit Care. 1999;8:507–13.
107. Pandharipande PP, Pun BT, Herr DL, Maze M, Girard TD, Miller RR, et al. Effect of sedation with dexmedetomidine vs lorazepam on acute brain dysfunction in mechanically ventilated patients: the MENDS randomized controlled trial. JAMA. 2007;298:2644–53.
108. Laidlaw JD, Siu KH. Ultra-early surgery for aneurysmal subarachnoid hemorrhage: outcomes for a consecutive series of 391 patients not selected by grade or age. J Neurosurg. 2002;97:250–8; discussion 247–9
109. van Donkelaar CE, Bakker NA, Veeger NJGM, Uyttenboogaart M, Metzemaekers JDM, Luijckx G-J, et al. Predictive factors for rebleeding after aneurysmal subarachnoid hemorrhage: rebleeding aneurysmal subarachnoid hemorrhage study. Stroke. 2015;46:2100–6.
110. Kassell NF, Torner JC. Aneurysmal rebleeding: a preliminary report from the cooperative aneurysm study. Neurosurgery. 1983;13:479–81.
111. Starke RM, Kim GH, Fernandez A, Komotar RJ, Hickman ZL, Otten ML, et al. Impact of a protocol for acute antifibrinolytic therapy on aneurysm rebleeding after subarachnoid hemorrhage. Stroke. 2008;39:2617–21.
112. Jane JA, Kassell NF, Torner JC, Winn HR. The natural history of aneurysms and arteriovenous malformations. J Neurosurg. 1985;62:321–3.

113. Winn HR, Richardson AE, Jane JA. The long-term prognosis in untreated cerebral aneurysms: I. the incidence of late hemorrhage in cerebral aneurysm: a 10-year evaluation of 364 patients. Ann Neurol. 1977;1:358–70.
114. Tang C, Zhang T-S, Zhou L-F. Risk factors for rebleeding of aneurysmal subarachnoid hemorrhage: a meta-analysis. PLoS One. 2014;9:e99536.
115. Garton T, Keep RF, Wilkinson DA, Strahle JM, Hua Y, Garton HJL, et al. Intraventricular hemorrhage: the role of blood components in secondary injury and hydrocephalus. Transl Stroke Res. 2016;7:447–51.
116. Fountas KN, Kapsalaki EZ, Machinis T, Karampelas I, Smisson HF, Robinson JS. Review of the literature regarding the relationship of rebleeding and external ventricular drainage in patients with subarachnoid hemorrhage of aneurysmal origin. Neurosurg Rev. 2006;29:14–8; discussion 19–20
117. Kusske JA, Turner PT, Ojemann GA, Harris AB. Ventriculostomy for the treatment of acute hydrocephalus following subarachnoid hemorrhage. J Neurosurg. 1973;38:591–5.
118. Hasan D, Vermeulen M, Wijdicks EF, Hijdra A, van Gijn J. Management problems in acute hydrocephalus after subarachnoid hemorrhage. Stroke. 1989;20:747–53.
119. Mack WJ, King RG, Ducruet AF, Kreiter K, Mocco J, Maghoub A, et al. Intracranial pressure following aneurysmal subarachnoid hemorrhage: monitoring practices and outcome data. Neurosurg Focus. 2003;14:e3.
120. Fried HI, Nathan BR, Rowe AS, Zabramski JM, Andaluz N, Bhimraj A, et al. The insertion and management of external ventricular drains: an evidence-based consensus statement: a statement for healthcare professionals from the Neurocritical Care Society. Neurocrit Care. 2016;24:61–81.
121. Bisnaire D, Robinson L. Accuracy of levelling intraventricular collection drainage systems. J Neurosci Nurs. 1997;29:261–8.
122. Muirhead WR, Basu S. Trajectories for frontal external ventricular drain placement: virtual cannulation of adults with acute hydrocephalus. Br J Neurosurg. 2012;26:710–6.
123. Cagnazzo F, Gambacciani C, Morganti R, Perrini P. Aneurysm rebleeding after placement of external ventricular drainage: a systematic review and meta-analysis. Acta Neurochir. 2017;159:695–704.
124. McIver JI, Friedman JA, Wijdicks EFM, Piepgras DG, Pichelmann MA, Toussaint LG, et al. Preoperative ventriculostomy and rebleeding after aneurysmal subarachnoid hemorrhage. J Neurosurg. 2002;97:1042–4.
125. Chung DY, Leslie-Mazwi TM, Patel AB, Rordorf GA. Management of external ventricular drains after subarachnoid hemorrhage: a multi-institutional survey. Neurocrit Care. 2017;26:356–61.
126. Nornes H. The role of intracranial pressure in the arrest of hemorrhage in patients with ruptured intracranial aneurysm. J Neurosurg. 1973;39:226–34.
127. Carney N, Totten AM, O'Reilly C, Ullman JS, Hawryluk GWJ, Bell MJ, et al. Guidelines for the management of severe traumatic brain injury, fourth edition. Neurosurgery. 2017;80:6–15.
128. Olson DM, Zomorodi M, Britz GW, Zomorodi AR, Amato A, Graffagnino C. Continuous cerebral spinal fluid drainage associated with complications in patients admitted with subarachnoid hemorrhage. J Neurosurg. 2013;119:974–80.
129. Williams TA, Leslie GD, Dobb GJ, Roberts B, van Heerden PV. Decrease in proven ventriculitis by reducing the frequency of cerebrospinal fluid sampling from extraventricular drains. J Neurosurg. 2011;115:1040–6.
130. Williamson RA, Phillips-Bute BG, McDonagh DL, Gray MC, Zomorodi AR, Olson DM, et al. Predictors of extraventricular drain-associated bacterial ventriculitis. J Crit Care. 2014;29:77–82.
131. Poon WS, Ng S, Wai S. CSF antibiotic prophylaxis for neurosurgical patients with ventriculostomy: a randomised study. Acta Neurochir Suppl. 1998;71:146–8.

132. Tanweer O, Boah A, Huang PP. Risks for hemorrhagic complications after placement of external ventricular drains with early chemical prophylaxis against venous thromboembolisms. J Neurosurg. 2013;119:1309–13.
133. Agnelli G, Piovella F, Buoncristiani P, Severi P, Pini M, D'Angelo A, et al. Enoxaparin plus compression stockings compared with compression stockings alone in the prevention of venous thromboembolism after elective neurosurgery. N Engl J Med. 1998;339:80–5.
134. Iorio A, Agnelli G. Low-molecular-weight and unfractionated heparin for prevention of venous thromboembolism in neurosurgery: a meta-analysis. Arch Intern Med. 2000;160:2327–32.
135. Danish SF, Burnett MG, Ong JG, Sonnad SS, Maloney-Wilensky E, Stein SC. Prophylaxis for deep venous thrombosis in craniotomy patients: a decision analysis. Neurosurgery. 2005;56:1286–92; discussion 1292–4
136. Capion T, Lilja-Cyron A, Bartek J, Forsse A, Logallo N, Juhler M, et al. Discontinuation of external ventricular drainage in patients with hydrocephalus following aneurysmal subarachnoid hemorrhage – a Scandinavian Multi-institutional Survey. Acta Neurochir. 2020;162:1363–70.
137. Klopfenstein JD, Kim LJ, Feiz-Erfan I, Hott JS, Goslar P, Zabramski JM, et al. Comparison of rapid and gradual weaning from external ventricular drainage in patients with aneurysmal subarachnoid hemorrhage: a prospective randomized trial. J Neurosurg. 2004;100:225–9.
138. Jabbarli R, Pierscianek D, RÖlz R, Reinhard M, Darkwah Oppong M, Scheiwe C, et al. Gradual external ventricular drainage weaning reduces the risk of shunt dependency after aneurysmal subarachnoid hemorrhage: a pooled analysis. Oper Neurosurg (Hagerstown). 2018;15:498–504.
139. Poblete R, Zheng L, Raghavan R, Cen S, Amar A, Sanossian N, et al. Trends in ventriculostomy-associated infections and mortality in aneurysmal subarachnoid hemorrhage: data from the Nationwide inpatient sample. World Neurosurg. 2017;99:599–604.
140. Mayhall CG, Archer NH, Lamb VA, Spadora AC, Baggett JW, Ward JD, et al. Ventriculostomy-related infections. A prospective epidemiologic study. N Engl J Med. 1984;310:553–9.
141. Harrop JS, Sharan AD, Ratliff J, Prasad S, Jabbour P, Evans JJ, et al. Impact of a standardized protocol and antibiotic-impregnated catheters on ventriculostomy infection rates in cerebrovascular patients. Neurosurgery. 2010;67:187–91; discussion 191
142. McLaughlin N, St-Antoine P, Bojanowski MW. Impact of antibiotic-impregnated catheters on the timing of cerebrospinal fluid infections in non-traumatic subarachnoid hemorrhage. Acta Neurochir (Wien). 2012;154:761–6; discussion 767
143. Miller C, Tummala RP. Risk factors for hemorrhage associated with external ventricular drain placement and removal. J Neurosurg. 2017;126:289–97.
144. Bauer DF, Razdan SN, Bartolucci AA, Markert JM. Meta-analysis of hemorrhagic complications from ventriculostomy placement by neurosurgeons. Neurosurgery. 2011;69:255–60.
145. Leschke JM, Lozen A, Kaushal M, Oni-Orisan A, Noufal M, Zaidat O, et al. Hemorrhagic complications associated with ventriculostomy in patients undergoing endovascular treatment for intracranial aneurysms: a single-center experience. Neurocrit Care. 2017;27:11–6.
146. Phillips TJ, Dowling RJ, Yan B, Laidlaw JD, Mitchell PJ. Does treatment of ruptured intracranial aneurysms within 24 hours improve clinical outcome? Stroke. 2011;42:1936–45.
147. Chai CL, Pyeong Jeon J, Tsai Y-H, Whittaker P, Macdonald RL, Lindgren AE, et al. Endovascular intervention versus surgery in ruptured intracranial aneurysms in equipoise: a systematic review. Stroke. 2020;51:1703–11.

Chapter 7
Endovascular Aneurysm Treatment

Daniel D. Cavalcanti, Nader Delavari, and Howard A. Riina

For the last few decades, the endovascular treatment of intracranial aneurysms has escalated from an adjuvant position to a main therapeutic role. In order to provide a minimally invasive method that avoided craniotomies, minimized brain exposure, and manipulation, practitioners invested years of work developing catheters and devised new ways to make endovascular treatment feasible. Werner et al. [1] pioneered the intravascular occlusion of an intracranial aneurysms in 1941 after exposing an ICA aneurysm, puncturing it, introducing 9 m (cm, or meter?) of a silver-enameled wire and then heating the wire to 80°C. Later, based on a foundation of landmark works conducted by Gallagher, Serbineko, Guglielmi, and others, undoubtedly, there was witnessed an evolution of devices and improvements resulting in occlusion rates that were critically necessary for such paradigm change. Neuroendovascular surgery is now the most commonly practiced therapeutic approach for most vascular conditions affecting the central nervous system [2].

The results of both the International Subarachnoid Aneurysm Trial (ISAT) and the Barrow Ruptured Aneurysm Trial (BRAT) led to a steady increase in the use of endovascular treatment for not only ruptured aneurysms, but also unruptured aneurysms worldwide [3–6]. The percentage of patients with unruptured aneurysms

D. D. Cavalcanti
Department of Neurosurgery, Ayer Neuroscience Institute, St. Vincent's Medical Center, Bridgeport, CT, USA
e-mail: daniel.cavalcanti@hhchealth.org

N. Delavari
Department of Neurosurgery, New York University School of Medicine, New York, NY, USA
e-mail: nader.delavari@nyulangone.org

H. A. Riina (✉)
Department of Neurosurgery and Radiology, New York University School of Medicine, New York, NY, USA
e-mail: howard.riina@nyulangone.org

J. R. Mascitelli, M. J. Binning (eds.), *Introduction to Vascular Neurosurgery*,
https://doi.org/10.1007/978-3-030-88196-2_7

treated with coiling ranged from 19.8% in 2001 to approximately 63.3% by 2008; decreasing periprocedural morbidity and mortality was observed concurrently among those treated in the United States [7]. As a result of this surge in patient treatment, interventionalists, community and academic hospitals, and industry have been directing enormous resources into the field. This has led to an expanding interest in device design using new technologies. The last two decades witnessed a major evolution in the development of different and better devices, microcatheters, and microwires, reducing recurrence rates, allowing a massive growth of endovascular therapy for the management of intracranial aneurysms in every location. The is now in the neuroendovascular armamentarium for different techniques such as direct coiling, balloon-remodeling, stent-coiling, flow diversion technology, and now intrasaccular devices. The possibility of success in aneurysm protection from these techniques resulting in the prevention of rupture or rebleeding has increased dramatically. Residents and fellows are now routinely trained in neuroendovascular techniques, graduating a new generation of hybrid vascular neurosurgeons.

Coiling

Inserting coils into intracranial aneurysms initiates a process that ultimately leads to aneurysm thrombosis and occlusion. Guglielmi et al. [8] developed the idea of applying an electric current to detach coils and thrombose aneurysms in the beginning of the 1980s. The first patient with an intracranial aneurysm was treated with modern endovascular coil embolization using a transfemoral approach in 1990. In 1995, the Guglielmi detachable coil system received FDA clearance. In 2004, Henkes et al. [9] reported a large retrospective study from a single institution, treating 1811 aneurysms in 1579 patients with endovascular coiling, with a promising 90–100% occlusion rate in 86.5% of the cases. The ischemic complication rate was 9%, early procedural morbidity was 5.3%, while the procedural mortality was a mere 1.5%.

The published results of ISAT in 2002 and BRAT in 2012, which both demonstrated favorable results for coiling when compared to surgical clipping, significantly changed neurosurgical practice worldwide [3–5]. It is interesting to point out that stent-assisted coiling and many contemporary techniques were not available during ISAT. Given equipoise, clipping has been gradually replaced by endovascular procedures for the treatment of aneurysms [10–14]. At the same time, coiling has been also used to treat a wide spectrum of patients with unruptured aneurysms even without the same level of evidence as ruptured aneurysms [15]. It therefore remains unclear whether or not the superior clinical outcomes offered by embolization of ruptured aneurysms will also hold true for patients with unruptured aneurysms.

Early data were cautiously expectant about the results of coiling and long-term stability. The first large series results with embolization of aneurysms with Guglielmi Detachable coils (GDC) included 916 aneurysms; complete occlusion was seen in 55% and overall recanalization was seen in 20.9% [16]. The overall incidence of

delayed rerupture reached 1.6%. Indeed, the CARAT (Cerebral Aneurysm Rerupture After Treatment) Study revealed a lower rate of total occlusion (39%) comparing to clipping (92%); there was a trend to higher rates of rerupture among patients undergoing coil embolization when compared to those undergoing clipping (cumulative hazard 3.4% versus 1.3%; $P = 0.09$) [17]. In a large early multicenter study conducted in France, Gallas et al. [18] found that 74% of ruptured aneurysms treated with coiling were completed occluded after a mean of 36 months of follow-up; they found out that only 4.7% of patients needed retreatment. A large review including more than 8100 coiled aneurysms identified that 20.8% of them recanalized during follow-up, half of these underwent retreatment [19]. Posterior circulation aneurysms tend to have more reopenings. Aneurysms larger than 10 mm are also related to more recurrences when treated with pure coiling, maybe due to the presence of intraluminal thrombus [16, 19–21].

Undoubtedly, the ultimate goal is complete obliteration of a ruptured aneurysm (Fig. 7.1). However, there has been a long discussion about the necessity of pursuing complete occlusion of a ruptured aneurysm especially during emergency endovascular coiling; it is a common practice to intentionally partially coil ruptured aneurysms to prevent intra-procedural rupture or complication due to dense packing of the sac [22]. This technique may provide protection until a second stage more definitive occlusion can be performed (with either stent or flow divertor placement) in the same admission or later subacute follow-up period. Waldau et al. [22] demonstrated excellent results with this technique as seen in late follow-up angiograms. However, CARAT demonstrated that incomplete occlusion of an aneurysm was a powerful predictor of rebleeding. Indeed, the authors found that the risk of rupture in aneurysms that were partially occluded (<70%) was 24.5% in the first year, equivalent to rebleeding rates previously reported for untreated aneurysms, suggesting that retreatment should be performed early.

Indeed, the durability of isolated coiling has been called into question in long-term observation demonstrated by in both ISAT (34%) and BRAT (52%) [23, 24]. Coil compaction can lead to development of a recurrent neck and/or lumen. It is noteworthy that aneurysm occlusion is commonly evaluated using the modified Raymond–Roy classification (Class I: complete obliteration, Class II: residual neck, Class IIIa: residual aneurysm: contrast within coil interstices, Class IIIb: residual aneurysm: contrast along aneurysm wall) [25]. Even outcomes using the newer coil designs have similar findings. For instance, the combined success rate in the Cerecyte Coil Trial reached 57% (245/433) for both ruptured and unruptured aneurysms after 6 months [26]. Both the HELPS (Hydrogel-Coated Coils versus Bare Platinum Coils for the Endovascular Treatment of Intracranial Aneurysms) Trial and the MAPS (Matrix and Platinum Science) Trial noted complete occlusion in fewer than 60% of treated aneurysms [27, 28].

Rebleeding has been one of the main concerns with isolated coiling; coiled aneurysms rebled 2.5 times more often than after clipped aneurysms in ISAT (however, the overall rebleed number was low). Nevertheless, in the 6-year follow-up analysis of BRAT, no rebleeding had occurred in the patients with aneurysmal remnants and recurrences after coiling. Moore et al. [29] recently reported a 7.7% rerupture rate

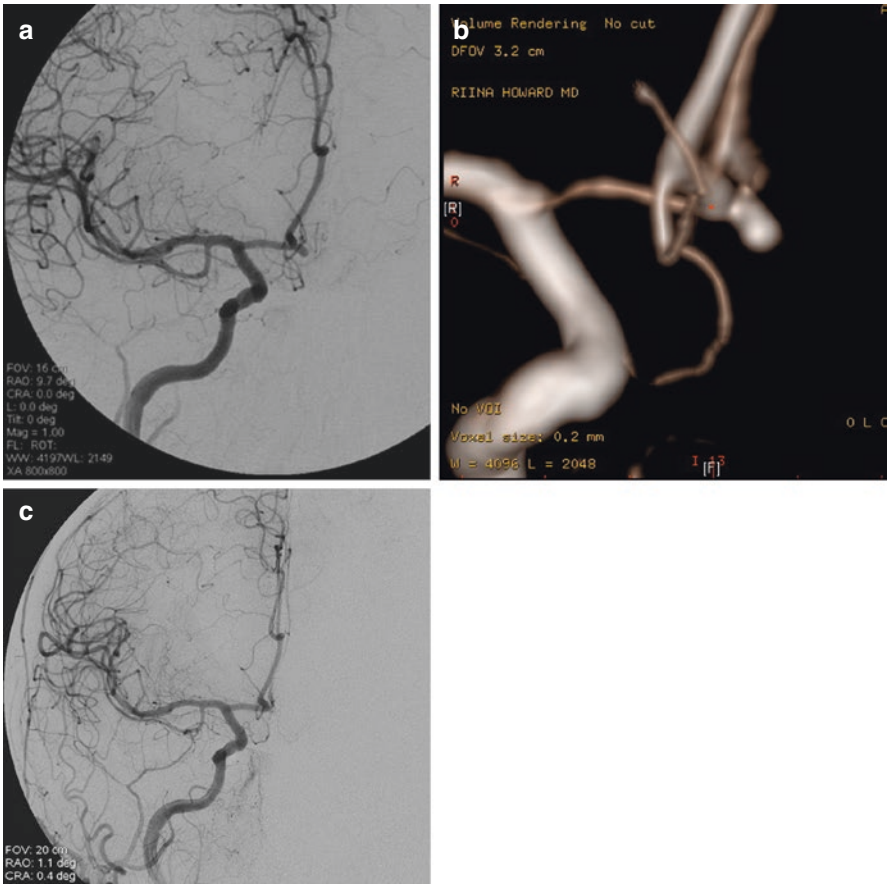

Fig. 7.1 Endovascular coiling of a small anterior communicating artery aneurysm. (**a**) Digital subtraction angiography showing a small aneurysm of the anterior communicating artery. (**b**) 3D rotational angiography better demonstrates the anatomy of the neck and the relationship with all vessels of the anterior communicating artery. (**c**) Coiling of an anterior communicating artery aneurysm leading to modified Raymond Roy type II

in previously ruptured small ACoA aneurysms after embolization, with remnant or recurrent rate that reached 82%. The ACoA location was also noted by Schuette et al. [30] as bearing a higher rerupture rate during the embolization itself, with aneurysms smaller than 4 mm having a rerupture rate almost five times greater than larger ACoA aneurysms, most likely secondary to technical considerations. All of these data shed some light on the need for other endovascular devices or techniques to manage aneurysms.

In fact, approximately 17% of patients needed retreatment in the ISAT and BRAT trials [23, 24]. Campi et al. [23] demonstrated that in ISAT patients late retreatments were performed nearly seven times more frequently after coiling than after clipping. Notably, retreatments have been shown to reach as high as 47% when managing

ruptured ACoA aneurysms endovascularly, even in a high-volume institution [29]. Unfortunately, as many as half of cases undergoing a second endovascular procedure may also require more interventions [31]. Patients' exposure to radiation during repeated procedures and during subsequent follow-up imaging should not be overlooked. However, despite procedural radiation exposure being a theoretical risk factor for developing cancer following a latency period between 10 and 20 years, radiation associated cancers are considered rare and extremely unlikely [32, 33]. The value of a diagnostic or therapeutic use of radiation in this setting far exceeds the rate risk of an associated malignancy.

Balloon-Remodeling Technique

Undoubtedly, management of complex wide-necked aneurysms is challenging for both clipping and coiling techniques. The wide-neck morphology offers up front limitations for coil retention within the aneurysm sac during and after deployment, introducing a risk of coil herniation. Wide-necked bifurcation aneurysms also present additional difficulties, as branch vessels may be incorporated into the aneurysm neck and make treatment at the neck more complicated. The temporary occlusion of the aneurysm neck with an inflatable balloon, the balloon remodeling technique, provides improved coiling deposition within the dome and at the neck by forcing the coil mass to better conform the aneurysm sac morphology, allowing better occlusion results and management of more diverse aneurysm configurations (Fig. 7.2) [34, 35]. The technique can be also used to protect a side branch or as a "rescue" technique in cases of coil prolapse or frank herniation [36]. The additional advantage of balloons is that balloons can work as an immediate temporary occlusion solution to quickly control intraprocedural rupture. With the technique, a nondetachable balloon is temporarily inflated covering the extension of the neck of the aneurysm for every coil placement. Following coil placement but prior to detachment, the balloon is deflated and stability is assessed. It can be a very straightforward technique for sidewall aneurysms, once the balloon is navigated into the parent vessel, both the proximal and distal markers are aligned with the neck extension, and then the 0.0165″ microcatheter is then navigated over a 0.014″ microguidewire to catheterize the aneurysm dome. The balloon can be then inflated only during the initial critical coiling, once the framing coils are placed, or for delivering every coil, when the herniation of part of the balloon into the neck of the aneurysm will enhance coil packing. The inflation of the balloon also has a role in stabilizing the coiling microcatheter. With a bifurcation aneurysms, the compliant balloon is inflated in the parent vessel and one of the branches covering the neck of the aneurysm; two balloons can also be used like for basilar apex aneurysms and finally a transcirculation technique can be utilized, using the anterior circulation approach [37, 38].

Controversially, the ATENA (Analysis of Treatment by Endovascular Approach of Nonruptured Aneurysms) study found similar total occlusion rates for aneurysms treated with pure coiling and remodeling technique (63.7% and 65.9%,

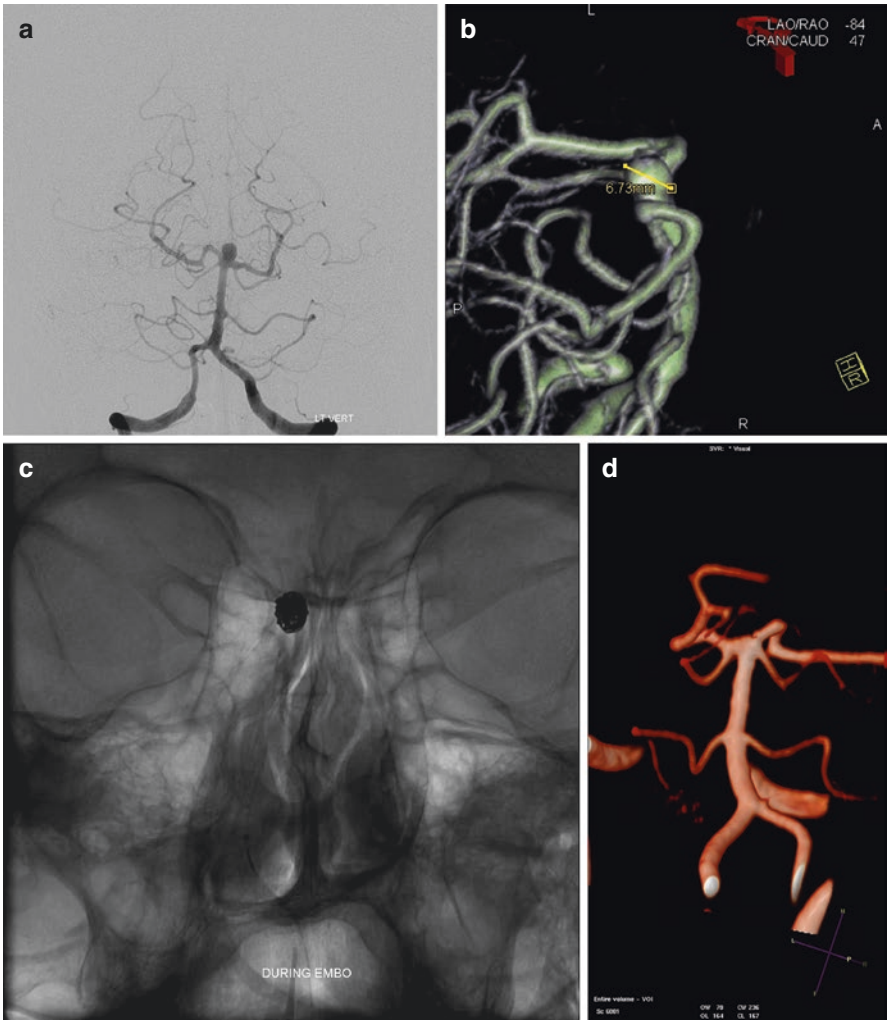

Fig. 7.2 Balloon-assisted coiling of a basilar apex aneurysm. (**a**) Digital subtraction angiography (DSA) showing a saccular aneurysm of the basilar apex. (**b**) 3D rotational angiography demonstrating the maximum diameter of 6.73 mm. (**c**) Unsubtracted image depicts a solid coil mass that completely occluded the saccular aneurysm assisted by a temporary inflation of a balloon. The balloon remodeled the neck as well protected the origin of the left posterior cerebral artery. (**d**) Late follow-up tridimensional angiogram revealing stable complete occlusion of the aneurysm

respectively) in a large series. But this series was important to confirm that safety in performing the remodeling technique was similar to that of primary coiling. The CLARITY (Clinical and Anatomic Results In the Treatment of Ruptured Intracranial Aneurysms) series demonstrated an equivalent safety pattern as well, with treatment morbidity being 3.9% for the coiling group and 2.5% for the remodeling group; mortality rates were 1.2% and 1.3%, respectively [38]. Additionally, Shapiro et al.

[39] found that balloon remodeling is not associated with higher rates of thromboembolic complication when compared to pure coiling.

A more recent series, using a double-lumen balloon technology, demonstrated a Raymond-Roy 1 occlusion rate of 56.5% and a Raymond-Roy 2 of 35.6% in a cohort of 219 patients; retreatment reached 12.6%. In a retrospective series, Pop et al. [40] were able to show a higher initial occlusion rate using the Eclipse 2 L double-lumen balloon (Balt USA, Irvine, CA), reaching 81.7%, probably due to an improved compliance, better navigability, and more variety in lengths.

Comaneci Temporary Aneurysm Embolization Assist Device

New technology has been developed in order to treat those wide-necked aneurysms, with the same goals of optimizing coil packing and preventing coil prolapse, however, avoiding temporary flow arrest and its implicated thromboembolic and ischemic risks. The Comaneci device (Rapid Medical, Israel) is a retrievable, non-detachable stent made of a compliant radiopaque mesh composed of 12 nitinol wires mounted on a 182-cm-core wire, with a distal end consisting of a 7-mm flexible tip [41]. The neurointerventionalist can gradually expand and compress the device's mesh with a slider mechanism controlled by a button at the device handle. Another advantage is that this device can be used in the setting of subarachnoid hemorrhage to obviate the need for an intracranial stent, preventing the use of antiplatelets. Sirakov et al. [42] recently reviewed their series of 118 ruptured aneurysms treated with the assistance of the Comaneci device; immediate total occlusion rates were 70.3% with a Raymond-Roy class II of 27.1%. In 6 months, 66.9% of the aneurysms had complete occlusion. Other smaller series have demonstrated similar safe acquisition of a stable bridging position offered by the Comaneci device while opened along the aneurysm neck and satisfactory occlusion results (81.8–88.8%) [43, 44].

Stent-Assisted Coiling

Stent-assisted coiling has been routinely used to assist immediate occlusion as well as improving longevity of aneurysm obliteration by allowing better initial packing and greater stability [39]. Besides improving results in wide-neck aneurysms (Fig. 7.3), as an alternative to balloon-assisted techniques, it has been a critical technology in the treatment of side-wall, fusiform, and dissecting aneurysms, especially prior the introduction and later popularization of flow diversion technology [45].

The Neuroform stent was the first nitinol self-expandable stent approved by the FDA, under a humanitarian device exemption, in the treatment of wide-neck aneurysms as an adjuvant to endovascular coiling. Fiorella et al. [46] reported one of the first results with this device treating complex aneurysms; the immediate rate of

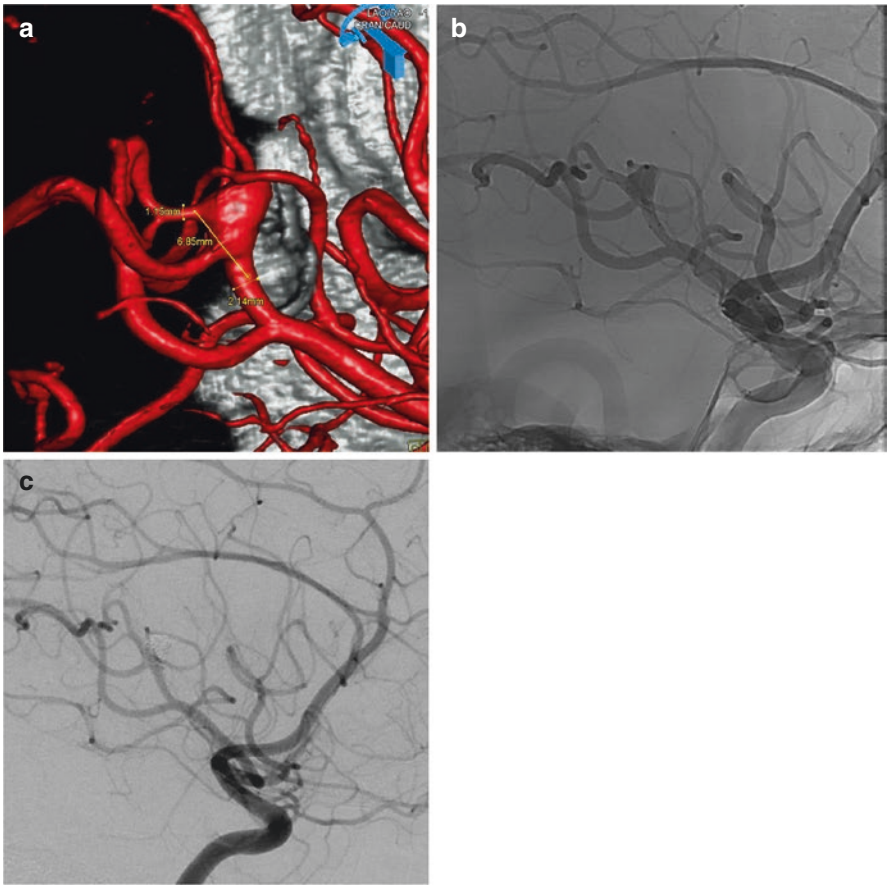

Fig. 7.3 A stent-assisted coiling of a right middle cerebral artery aneurysm. (**a**) Tridimensional rotational angiogram revealing a side-wall aneurysm of a M2 segment, demonstrating the acquisition of different measurements, mainly length from estimated proximal landing zone to distal landing zone, and vessel diameters. Measurements are taken usually in 2D and 3D images to improve accuracy. (**b**) Unsubtracted image of a right ICA injection demonstrating the stent already in place and the coiling microcatheter crossing one of its cells immediately before starting the actual aneurysm coiling. (**c**) Control angiogram showing complete obliteration of the aneurysm and patency of the stent and branches

complete or near-complete occlusion (>95%) was approximately 46% and the recanalization rate at 3–6 months was 23%; delayed and severe in-stent stenosis was present in 7%. Most of the studies revealed a risk of in-stent stenosis of 4–10%. Biondi et al. [47] also revealed later, initial (35%) and late (57%) occlusion rates in a retrospective study of 42 patients undergoing stent-assisted coiling with Neuroform.

Shapiro et al. [39] reviewed 39 studies dealing with stent-assisted coiling that included a total of 1517 patients, and found that only 45% of aneurysms were

completely occluded initially, reaching 61% after 6 months of follow-up. Despite historically increasing the spectrum of aneurysms amenable to coiling, stenting requires a period of dual antiplatelet therapy, increasing the likelihood of hemorrhagic complications especially in elderly patients as well as limiting its use in the setting of a ruptured aneurysm. Moreover, the neurointerventionalist needs to monitor patients for delayed stent-related complications like the development of in-stent stenosis and parent vessel occlusion, though exceedingly rare with open celled and less dense stent device construction. Indeed, using stents to assist coiling trades some increase in thromboembolic complications and mortality risk for improved occlusion durability [22, 39, 48–50].

Stent technology has continued to evolve and focus on the dedicated creation and manufacturing of specifically designed intracranial stents. The LVIS (low profile visualized intraluminal support) stent is a self-expanding closed cell stent, braided with a single nickel titanium wire. It has distal radiopaque markers, and double helical tantalum strands to assist full length visualization. One of its main benefits is its high metal to surface coverage (23% on average) allowing improved flow diversion over other stents. Analyzing a registry with 78 unruptured intracranial aneurysms treated by stent-assisting coiling with LVIS or LVIS Jr. stents (MicroVention Terumo, Tustin, California, USA), being 19 of them in the posterior circulation, the initial complete occlusion rate was 85%, with 82% being occluded after 6 months. Morbidity included a 3% rate of transient ischemic attacks [51]. In a Chinese series with 97 patients treated with the LVIS stent, with 100% technical success rate and no mortality, complete occlusion was seen in 84.2% of patients available for late follow-up [52].

The Neuroform Atlas Stent (new generation of the Neuroform stent) has an open cell design and is a laser cut nitinol self-expanding microstent. This allows a lower profile delivery system (0.0165″ microcatheter versus 0.027″ microcatheter), better trackability, and higher conformability to the vessel wall [53, 54]. The Atlas Investigational Device Exemption (IDE) demonstrated exciting results, with 86.7% of Raymond class I results with aneurysms measuring a mean of 5.3 ± 1.7 mm [53]. A single-center retrospective study revealed a complete occlusion rate of approximately 84% with the Atlas stent at mean follow-up of 8.7 months [55]. It is important to note that the new technology allowed a procedural technical success of 100% in deployment.

All stent patients are pretreated with aspirin (81–325 mg) daily and clopidogrel 75 mg daily for at least 5 days; platelet function assays can be used to confirm patient responsiveness to these drugs though many practitioners do not use them for this type of device. During the procedure, IV, weight-based is given and activated coagulation time (ACT), if monitored, is maintained between 250 s and 300 s. In those cases where stent placement is required unexpectedly, intraprocedurally, a bolus dose of eptifibatide or cangrelor can be administered in addition to 300 mg of aspirin as a rectal suppository or via OG tube.

There are different techniques that are equally effective for stent-assisted coiling. Many practitioners will “jail” a microcather in the aneurysm dome. The jailing technique consists of navigating the stent microcatheter to its optimal place spanning

across the neck of the aneurysm, and then the coiling microcatheter into the aneurysm sac. The stent is then delivered across the aneurysm neck, jailing the coiling microcatheter in the aneurysm dome. Alternatively, the stent can be deployed and a coiling microcatheter over a 0.014″ microguidewire can be used to navigate within the stent and then cross the stent cells catheterizing the aneurysm sac. Finally, the coil-then-stent technique can also be used. Some aneurysm morphologies may require creative stent constructs. For example, basilar apex aneurysms may demand complex constructs, mainly the so-called "Y-stent" construct [56, 57]. This includes both the kissing-Y and the crossing-Y techniques. The crossing-Y technique can be completed in one stage or two stages, crossing the first deployed stent later, after endothelization has occurred, preventing its dislodgement. High occlusion rates (82–96%) and low complications rates have been reported with the Y-stent techniques [57, 58].

Flow Diversion

The concept of diverting flow was initially explored by Wakhloo and colleagues in 1997, when two fundamental principles were described: [1] variation in flow patterns could promote flow stasis within the aneurysm leading to stable thrombus formation; and [2] a porous stent works as a scaffold for neointimal growth, remodeling the affected arterial segment [59]. Nelson and colleagues were simultaneously looking into the concept of telescoping stents as a way of achieving neo-intimal growth over devices to serve as endothelial scaffolding to obliterate aneurysms [60].

In flow diversion, the minimized porosity endoluminal devices modify the character of fluid exchange between the parent vessel and the aneurysm, and facilitate reestablishment of the mural integrity of the parent artery. Thus, endovascular flow diversion represented a paradigm shift, focusing on treating the parent vessel without the necessity of catheterizing the aneurysm dome most of the times (Figs. 7.4 and 7.5). Nelson and colleagues subsequently developed the first commercially available flow diverter, the Pipeline Embolization Device (PED) [59, 61–63]. The Pipeline Embolization Device for the Intracranial Treatment of Aneurysm Trial (PITA) was the pioneer prospective, multi-center trial, with 31 wide-neck aneurysms measuring 11.5 mm in average (18 treated with one device and 11 with two) [63]. Total occlusion reached a solid rate of 93.3% after 6 months.

The PUFS trial granted the PED premarket approval by the FDA in 2011 [61]. PUFS was a prospective, multi-center, single-arm trial including 109 large and giant wide-neck internal carotid artery aneurysms proximal to the communicating segment of the ICA; 22 aneurysms were giant (≥25 mm). An average of three devices was used per aneurysm. An 87% total occlusion rate was achieved after 12 months of follow-up. There were five cases of intracranial hemorrhage, four ischemic strokes, and two carotid-cavernous fistulas. No late aneurysm rupture was seen. The 5-year analysis showed that total occlusion rates increased, for the first time when compared to existing technology in the follow-up period, to 95.2% [64]. Retreatment

Fig. 7.4 Combination of flow-diversion and adjuvant coil embolization. (**a**) 3D angiogram shows an unruptured aneurysm of the right terminal ICA. (**b**) Unsubtracted image showing partial coiling of the aneurysm and the initial deployment of a PED , covering the proximal M1 segment. (**c**) Six-month follow-up angiogram revealing complete occlusion of the aneurysm, no in-stent stenosis. The left A1 segment had a normal diameter and the anterior communicating artery had been always patent, leading to normal flow into the right distal anterior cerebral artery. (Figures **b** and **c** were published on: Riina [2]. Retrieved May 6, 2021, from https://thejns.org/view/journals/j-neurosurg/131/6/article-p1690.xml)

with additional flow diverters devices was needed in 5.7% of the cases after 1 year of follow-up. The device itself demonstrated an excellent safety profile, with 96.3% of patients seen in 5-year clinical follow-up having a modified Rankin scale ≤2. The excellent results in large and giant aneurysms led some authors to use flow diversion off-label in small aneurysms with promising results [65]. The PREMIER (prospective study on embolization of intracranial aneurysms with the pipeline device) was

a prospective, multicenter, single arm trial that included 141 patients treated with PEDs with an average size of 5.0 ± 1.92 mm [66]. The successful placement rate was 99.3%, with a single device used in 93% of patients; Raymond grade I without major parent vessel stenosis was seen in 76.8% of patients. Practitioners then began exploring flow diversion for aneurysms associated with a large end vessel. In a small cohort of 15 patients with 16 aneurysms incorporating an end vessel, Kan

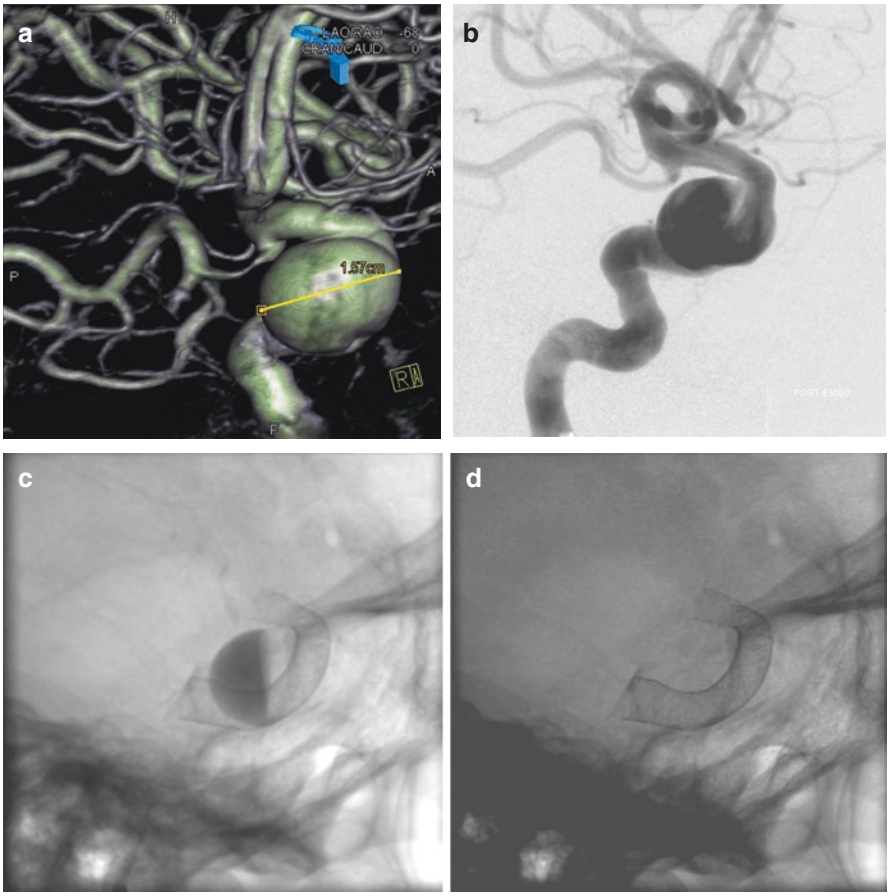

Fig. 7.5 Flow diversion embolization io a large unruptured aneurysm of the cavernous segment of the left internal carotid artery. (**a**) Tridimensional rotational angiography demonstrating the maximal diameter of the aneurysm (15.7 mm). (**b**) Immediate control angiogram revealing full patency of the flow diverter construct and flow stagnation within the aneurysm sac. (**c**) Unsubtracted lateral projection image demonstrating the multidevice PED construct in place and remaining stagnated flow within the aneurysmal sac. (**d**) Unsubtracted single-shot image taken during a 6-month follow-up angiogram demonstrating the multidevice PED construct stent in place, no in-stent stenosis and no stagnation of contrast within the aneurysmal sac. (**e**) Left common carotid artery injection, cranial view, lateral projection, during a 6-month follow-up cerebral angiogram revealing complete obliteration of the aneurysm

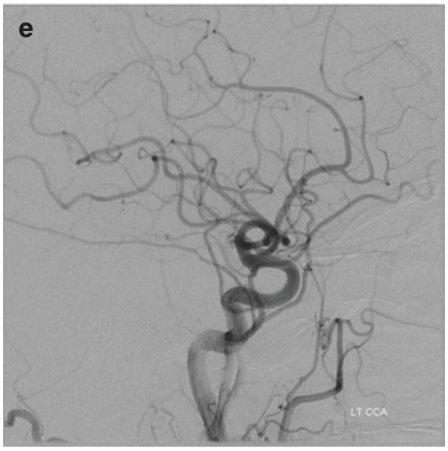

Fig. 7.5 (continued)

et al. [67] reported that the off-label use of flow diverters in small and medium saccular aneurysms has proven itself ineffective, not seeing occlusion after a mean of 24 months of follow-up. Most of the patients, except for 2, had only one PED placed. Tsang et al. [68] also found aneurysms of fetal-type posterior communicating artery to be refractory for treatment with flow diverter therapy, chiefly when the aneurysm incorporates a significant part of the vessel. The use of multidevice constructs would eventually demonstrate that end vessel associated aneurysms could be considered for treatment in select cases.

The International Retrospective Study of the Pipeline Embolization Device (IntrePED) would go on to demonstrate that besides all the excellent occlusion rates observed in different trials and initial series, the procedure was not risk-free [69]. Composite rate of neurologic morbidity and mortality reached 8.4%, greater than half of which was related to ischemic stroke. Neurologic morbidity and mortality rates were highest among patients harboring posterior circulation aneurysms (16.4%) and those with subarachnoid hemorrhage (18.4%), where tiny perforating vessels might be covered by the construct. Spontaneous post-treatment rupture, however, was only seen in 5 of 793 patients (0.6%) [69].

Numerous anatomic and technical variables can impact both flow diversion and associated occlusion rates (Fig. 7.6). It has been shown that failures in aneurysm obliteration have been associated with insufficient neck coverage, unsatisfactory device apposition, and incorporation of a branch vessel into the aneurysm wall or fundus [70]. Other series also identified the incorporation of a branch vessel arising from the aneurysm wall or fundus as predictor of failed treatment or delayed aneurysmal occlusion [71]. Interestingly, Bhogal et al. [72] reviewed the fate of covered side branches during the follow-up of patients undergoing endovascular flow diversion, analyzing 140 patients harboring 147 aneurysms; the overall side branch occlusion rate was roughly 20%. The slowly progressive occlusion of some of these branches with redirection of flow during the endothelization of the device allowing

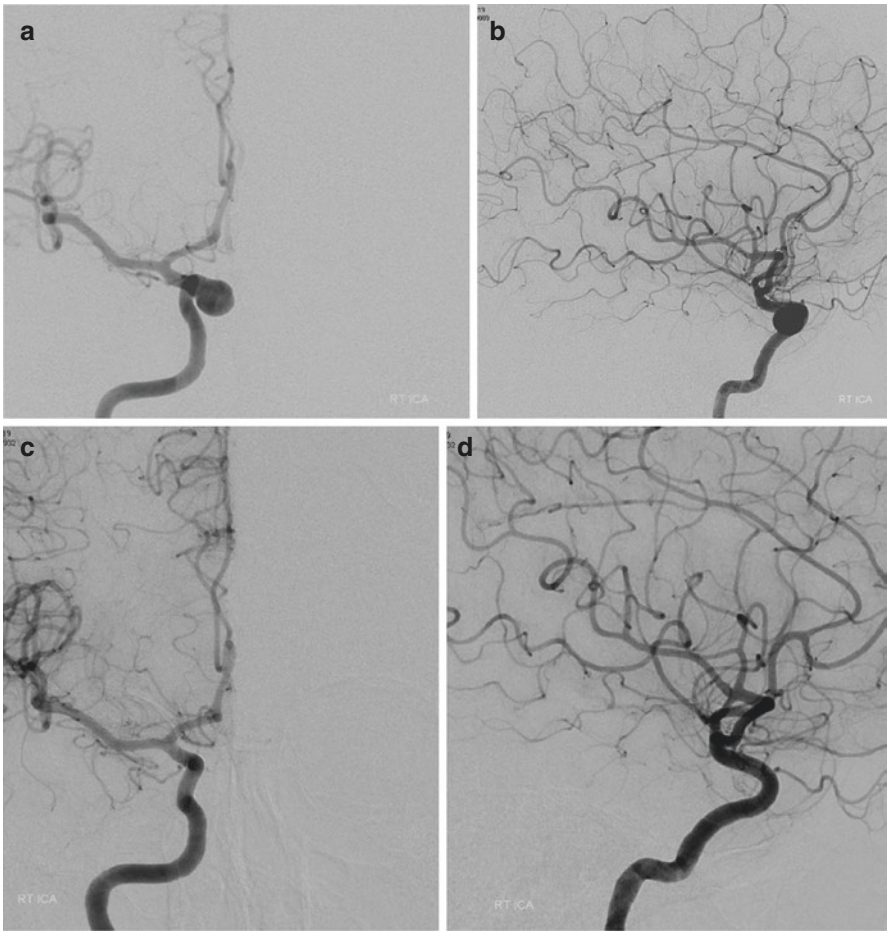

Fig. 7.6 The flow diversion embolization changed dramatically the way carotid-ophthalmic aneurysms are currently treated. (**a**, **b**) DSA with a right internal carotid artery injection showing a moderated-sized saccular aneurysm of the ophthalmic segment pointing medially and caudally. (**c**, **d**) Six-month follow-up DSA revealing complete obliteration of the aneurysm, no in-stent stenosis and patency of the ophthalmic artery

for natural revascularization may be a more tolerated process compared to acute flow arrest. The posterior communicating artery was the vessel most often occluded, followed by the ophthalmic artery. Interestingly, the anterior choroidal artery was extremely resistant, remaining open in all 91 patients when it was covered, with the same flow pattern after long-term coverage. More studies have demonstrated an incidence of silent occlusion of the ophthalmic artery varying between 0 and 21.6%, with revascularization via branches of the external carotid artery [73, 74].

The flow diverter device can be delivered using a coaxial technique, when a 0.070–0.071″ guide catheter and a 0.027″ microcatheter are utilized in combination, especially for PEDs and the Surpass Evolve (Stryker Neurovascular, Fremont, CA).

One of the main benefits of the FRED device (Microvention, Aliso Viejo, CA) is that a 0.021″ microcatheter can be used to deliver the devices with the two smallest diameters (2.5 and 3.0 mm). A larger guide catheter (0.088″ inner diameter) may be needed when a coiling microcatheter is used in parallel, or when a triaxial system with a distal access catheter (0.044″ or 0.058″) is added, to allow high-standard control injections. Standard radial or snuffbox approaches have been used more recently to complete flow diversion embolization with success [75].

Device selection is critical, and measurements need to be carefully obtained, including the diameter of the parent vessel and specific landing zones. Some foreshortening should be expected and varies according to the diameter of the device and vessel as well as the device itself. The optimal wall-apposition can be achieved by the deft alternation of movements of unsheathing (retracting the microcatheter) and pushing the flow diversion wire, specifically with the PED and FRED [76]. The device cell area will vary to the same device size according to the amount of compression and constraint, changing the degree of metal coverage; this property of the device can be exploited to obtain aneurysm coverage or to reduce coverage when over an important associated branch. For the Surpass device, one stabilizes the delivery wire while microcatheter retraction unsheathes the flow diverter. A cone-beam computed tomography can be performed at the end of the case to evaluate optimal implantation of the flow diverter device and rule out endovascular leaks. When observed, a microwire with a J-shaped tip (0.014″ or 0.016″) advanced through the incompletely opened segment of stent will often suffice, making sure the wire is within the device and the proximal edges are not damaged. Ultimately, an in-stent balloon angioplasty can be utilized to optimize apposition when the J-wire technique is insufficient.

Intrasaccular Devices

The Woven Endoluminal Bridge (WEB) device (Microvention, Aliso Viejo, CA) is an intra-aneurysmal flow-disruption device designed to alter the blood flow at the aneurysm neck, leading to subsequent obliteration (Fig. 7.7). It was specially designed to embolize wide-neck bifurcation aneurysms, which can represent 26–26% of all intracranial aneurysms [77]. Despite the current body of literature on the topic, the first WEB-DL (double layer) device was used in France in 2011. Papagiannaki et al. [78] conducted a prospective, multicenter study in France including 85 treated aneurysms, with an aneurysm size varying from 4.6 to 13.8 mm (mean, 7.4 ± 1.4 mm), unveiling a technical success of 93%, thromboembolic events in 11.7% of them, but with a permanent neurologic deficit in 3.9% of patients. Complete occlusion was seen in only 56.9%. Another European trial, the WEB Clinical Assessment of Intrasaccular Aneurysm Therapy (WEBCAST) trial, also found a complete occlusion rate after 6 months of only 56.1%. Modifications of the design of the product were introduced, and lower profile, single-layer versions were rapidly employed (WEB-SL and WEB-SLS – single layer spherical). The WEBCAST 2 results were unveiled in 2017, including 55 patients with the same

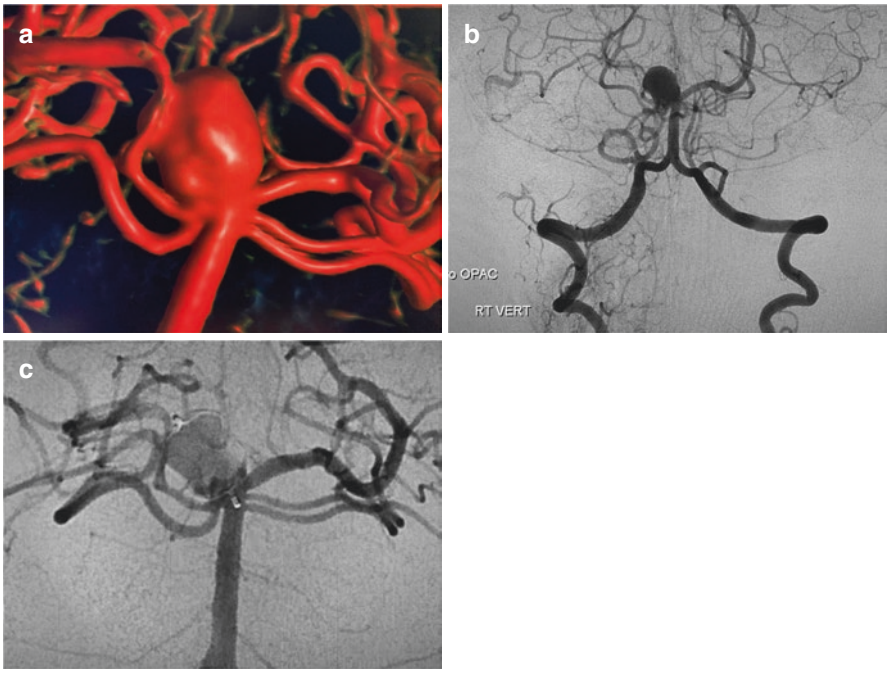

Fig. 7.7 Endovascular embolization of a basilar apex aneurysm with an intrasaccular flow-disrupting device. (**a**) Tridimensional rotational angiography image reveals a large saccular aneurysm of the basilar apex. The right superior cerebellar artery branches off the proximal right P1 segment. (**b**) Right vertebral artery injection reveals codominant vertebral arteries, and demonstrates the intricate relationship with the proximal right P1 segment. (**c**) Immediate control angiogram after deploying a WEB device in this basilar apex aneurysm, occupying completely the aneurysm neck, and most of the dome, showing immediate optimal result with flow stagnation seen in most of the aneurysm sac

number of aneurysms; the total occlusion rates again reached slightly above the 50% mark, with a neck remnant seen in other 26% [79]. Global morbidity was 3.9% in 1 year and mortality rate was 2%. The Woven EndoBridge Intrasaccular Therapy (WEB-IT) Study was a pivotal, prospective, single-arm, investigational device exemption study including 21 centers in the United States and six other international centers managing 148 patients [80]. Following a specific angiographic scale specific to this device, like in the previous studies, "adequate" occlusion included complete aneurysm occlusion and a residual neck. Adequate occlusion was seen in 84.6% of the subjects and 53.8% had a complete occlusion, a similar result to the European trials. To better understand the application of intrasaccular flow disruption in ruptured aneurysms, Cortez et al. [81] studied the use of the WEB device in 94 ruptured intracranial aneurysms, 83% being wide-necked. Most of them were located in the anterior communicating artery (44.6%), 17% in the middle cerebral artery, and 16% in the basilar artery. Successful treatment was accomplished in 97.8% of patients, with most of the patients not receiving any antiplatelets (86.8%).

Intraprocedural rupture occurred in 3.2% and intraoperative thrombus formation in 6.7%. At a median follow-up of 3.4 months, complete occlusion was seen in 48% and residual neck in 32%. Finally, some authors have recently reported the application of the WEB device in small and very small aneurysms; treating 128 aneurysms, Girot et al. [82] found a more promising complete occlusion rate (71%), with an adequate occlusion rate of 90% in the follow-up angiograms, widening the spectrum of indications of intrasaccular flow disruption. More data are needed on the long-term results of this first generation device. The intrasaccular device concept is an exciting possible future application for aneurysm occlusion.

Undoubtedly, one of the main advantages to the WEB device usage is that antiplatelet medications are not required, more specifically dual antiplatelet medications. Also, one cannot underestimate the importance of correct device selection based on accurate aneurysm measurements; oversizing the device width is the rule in order to obtain adequate secure positioning and to prevent later device compression. To deliver a WEB device, a triaxial system is utilized most of time, starting with a 6-French long sheath with an inner diameter of 0.088″. A distal access catheter (0.058″ inner diameter) offers more support in advancing one of the VIA microcatheters (Microvention, Aliso Viejo, CA), 0.017″, 0.021″, 0.027″, or 0.033″. It is important to notice the relative stiffness of the system, moreover, the rigidity of the leading portion of the constrained device. Excess pushing in the early phase can lead to rupture. Careful unsheathing of the WEB is required to allow the device to begin to expand prior to advancing it into position within the aneurysm dome. Once partially blossomed, the device becomes much more malleable and additional pushing of the device against the aneurysm wall is safer. By unsheathing more device, the inferior margin of the device is then aligned with the neck of the aneurysm. The device tends to self-center. Compression is applied to advance the device against the dome, filling more of the sac. Gentle traction will now allow the device to maximally expand in height under compression, filling also the neck. Any slack is removed and catheters are kept in a neutral position before detachment to prevent device displacement. Smaller low profile intrasaccular devices that can be delivered through smaller catheters are currently under development by several manufacturers.

Conclusion

From modest beginnings with detachable coils to flow diversion and now successful and safe intrasaccular flow disruption, dramatic changes have expanded how both ruptured and unruptured intracranial aneurysms are treated. The current variety of techniques in the neuroendovascular armamentarium and constant advances in device design and development have expanded how neurosurgeons, neurointerventional radiologists, and neurologists safely treat any kind of intracranial aneurysm. With every new device, initial enthusiasm is sometimes met with sobering feedback but ultimately intelligent practice. Continued evaluation and research are

continuously warranted to aid our understanding of endovascular devices, their applications, and their limitations. What can be sure is that endovascular treatment will continue to evolve and give physicians additional tools to best serve our patients.

References

1. Werner S, AH B, King B. Aneurysm of the internal carotid artery within the skull: wiring and electrothermic coagulation. J Am Med Assoc. 1941;116(7):578–82.
2. Riina HA. Neuroendovascular surgery. J Neurosurg. 2019;131(6):1690–701.
3. Molyneux A, Kerr R, Stratton I, Sandercock P, Clarke M, Shrimpton J, et al. International subarachnoid aneurysm trial (ISAT) of neurosurgical clipping versus endovascular coiling in 2143 patients with ruptured intracranial aneurysms: a randomised trial. Lancet. 2002;360(9342):1267–74.
4. Molyneux AJ, Kerr RS, Yu LM, Clarke M, Sneade M, Yarnold JA, et al. International subarachnoid aneurysm trial (ISAT) of neurosurgical clipping versus endovascular coiling in 2143 patients with ruptured intracranial aneurysms: a randomised comparison of effects on survival, dependency, seizures, rebleeding, subgroups, and aneurysm occlusion. Lancet. 2005;366(9488):809–17.
5. McDougall CG, Spetzler RF, Zabramski JM, Partovi S, Hills NK, Nakaji P, et al. The Barrow ruptured aneurysm trial. J Neurosurg. 2012;116(1):135–44.
6. Spetzler RF, McDougall CG, Albuquerque FC, Zabramski JM, Hills NK, Partovi S, et al. The Barrow ruptured aneurysm trial: 3-year results. J Neurosurg. 2013;119(1):146–57.
7. Brinjikji W, Rabinstein AA, Nasr DM, Lanzino G, Kallmes DF, Cloft HJ. Better outcomes with treatment by coiling relative to clipping of unruptured intracranial aneurysms in the United States, 2001–2008. AJNR Am J Neuroradiol. 2011;32(6):1071–5.
8. Guglielmi G, Vinuela F, Dion J, Duckwiler G. Electrothrombosis of saccular aneurysms via endovascular approach. Part 2: preliminary clinical experience. J Neurosurg. 1991;75(1):8–14.
9. Henkes H, Fischer S, Weber W, Miloslavski E, Felber S, Brew S, et al. Endovascular coil occlusion of 1811 intracranial aneurysms: early angiographic and clinical results. Neurosurgery. 2004;54(2):268–80; discussion 80–5
10. Huang MC, Baaj AA, Downes K, Youssef AS, Sauvageau E, van Loveren HR, et al. Paradoxical trends in the management of unruptured cerebral aneurysms in the United States: analysis of nationwide database over a 10-year period. Stroke. 2011;42(6):1730–5.
11. Koh KM, Ng Z, Low SY, Chua HZ, Chou N, Low SW, et al. Management of ruptured intracranial aneurysms in the post-ISAT era: outcome of surgical clipping versus endovascular coiling in a Singapore tertiary institution. Singap Med J. 2013;54(6):332–8.
12. Kozba-Gosztyla M, Czapiga B, Jarmundowicz W. Aneurismal subarachnoid hemorrhage: who remains for surgical treatment in the post-ISAT era? Arch Med Sci. 2015;11(3):536–43.
13. Lin N, Cahill KS, Frerichs KU, Friedlander RM, Claus EB. Treatment of ruptured and unruptured cerebral aneurysms in the USA: a paradigm shift. J Neurointerv Surg. 2012;4(3):182–9.
14. Niemela M, Koivisto T, Kivipelto L, Ishii K, Rinne J, Ronkainen A, et al. Microsurgical clipping of cerebral aneurysms after the ISAT study. Acta Neurochir Suppl. 2005;94:3–6.
15. Darsaut TE, Jack AS, Kerr RS, Raymond J. International Subarachnoid Aneurysm Trial – ISAT part II: study protocol for a randomized controlled trial. Trials. 2013;14:156.
16. Murayama Y, Nien YL, Duckwiler G, Gobin YP, Jahan R, Frazee J, et al. Guglielmi detachable coil embolization of cerebral aneurysms: 11 years' experience. J Neurosurg. 2003;98(5):959–66.
17. Johnston SC, Dowd CF, Higashida RT, Lawton MT, Duckwiler GR, Gress DR, et al. Predictors of rehemorrhage after treatment of ruptured intracranial aneurysms: the Cerebral Aneurysm Rerupture After Treatment (CARAT) study. Stroke. 2008;39(1):120–5.

18. Gallas S, Pasco A, Cottier JP, Gabrillargues J, Drouineau J, Cognard C, et al. A multicenter study of 705 ruptured intracranial aneurysms treated with Guglielmi detachable coils. AJNR Am J Neuroradiol. 2005;26(7):1723–31.
19. Ferns SP, Sprengers ME, van Rooij WJ, Rinkel GJ, van Rijn JC, Bipat S, et al. Coiling of intracranial aneurysms: a systematic review on initial occlusion and reopening and retreatment rates. Stroke. 2009;40(8):e523–9.
20. Henkes H, Fischer S, Mariushi W, Weber W, Liebig T, Miloslavski E, et al. Angiographic and clinical results in 316 coil-treated basilar artery bifurcation aneurysms. J Neurosurg. 2005;103(6):990–9.
21. Raymond J, Guilbert F, Weill A, Georganos SA, Juravsky L, Lambert A, et al. Long-term angiographic recurrences after selective endovascular treatment of aneurysms with detachable coils. Stroke. 2003;34(6):1398–403.
22. Waldau B, Reavey-Cantwell JF, Lawson MF, Jahshan S, Levy EI, Siddiqui AH, et al. Intentional partial coiling dome protection of complex ruptured cerebral aneurysms prevents acute rebleeding and produces favorable clinical outcomes. Acta Neurochir. 2012;154(1):27–31.
23. Campi A, Ramzi N, Molyneux AJ, Summers PE, Kerr RS, Sneade M, et al. Retreatment of ruptured cerebral aneurysms in patients randomized by coiling or clipping in the International Subarachnoid Aneurysm Trial (ISAT). Stroke. 2007;38(5):1538–44.
24. Spetzler RF, McDougall CG, Zabramski JM, Albuquerque FC, Hills NK, Russin JJ, et al. The Barrow ruptured aneurysm trial: 6-year results. J Neurosurg. 2015;123(3):609–17.
25. Mascitelli JR, Moyle H, Oermann EK, Polykarpou MF, Patel AA, Doshi AH, et al. An update to the Raymond-Roy Occlusion Classification of intracranial aneurysms treated with coil embolization. J Neurointerv Surg. 2015;7(7):496–502.
26. Molyneux AJ, Clarke A, Sneade M, Mehta Z, Coley S, Roy D, et al. Cerecyte coil trial: angiographic outcomes of a prospective randomized trial comparing endovascular coiling of cerebral aneurysms with either cerecyte or bare platinum coils. Stroke. 2012;43(10):2544–50.
27. White PM, Lewis SC, Gholkar A, Sellar RJ, Nahser H, Cognard C, et al. Hydrogel-coated coils versus bare platinum coils for the endovascular treatment of intracranial aneurysms (HELPS): a randomised controlled trial. Lancet. 2011;377(9778):1655–62.
28. McDougall CG, Johnston SC, Gholkar A, Barnwell SL, Vazquez Suarez JC, Masso Romero J, et al. Bioactive versus bare platinum coils in the treatment of intracranial aneurysms: the MAPS (Matrix and Platinum Science) trial. AJNR Am J Neuroradiol. 2014;35(5):935–42.
29. Moore N, Lang M, Bain M. 603. Rehemorrhage and recurrence rates of small ACOM aneurysms post embolization. Oral presentations 2016 AANS annual scientific meeting Chicago, IL. J Neurosurg. 2016;124(4):A1152.
30. Schuette AJ, Hui FK, Spiotta AM, Obuchowski NA, Gupta R, Moskowitz SI, et al. Endovascular therapy of very small aneurysms of the anterior communicating artery: five-fold increased incidence of rupture. Neurosurgery. 2011;68(3):731–7; discussion 7
31. Raymond J, Darsaut TE. An approach to recurrent aneurysms following endovascular coiling. J Neurointerv Surg. 2011;3(4):314–8.
32. Jones C, Badger SA, Boyd CS, Soong CV. The impact of radiation dose exposure during endovascular aneurysm repair on patient safety. J Vasc Surg. 2010;52(2):298–302.
33. Valentin J. Avoidance of radiation injuries from medical interventional procedures. Ann ICRP. 2000;30(2):7–67.
34. Mericle RA, Wakhloo AK, Rodriguez R, Guterman LR, Hopkins LN. Temporary balloon protection as an adjunct to endosaccular coiling of wide-necked cerebral aneurysms: technical note. Neurosurgery. 1997;41(4):975–8.
35. Moret J, Cognard C, Weill A, Castaings L, Rey A. The "Remodelling Technique" in the treatment of wide neck intracranial aneurysms. Angiographic results and clinical follow-up in 56 cases. Interv Neuroradiol. 1997;3(1):21–35.
36. Moret J, Cognard C, Weill A, Castaings L, Rey A. Reconstruction technic in the treatment of wide-neck intracranial aneurysms. Long-term angiographic and clinical results. Apropos of 56 cases. J Neuroradiol. 1997;24(1):30–44.

37. Albuquerque FC, Gonzalez LF, Hu YC, Newman CB, McDougall CG. Transcirculation endovascular treatment of complex cerebral aneurysms: technical considerations and preliminary results. Neurosurgery. 2011;68(3):820–9; discussion 9–30
38. Pierot L, Cognard C, Spelle L, Moret J. Safety and efficacy of balloon remodeling technique during endovascular treatment of intracranial aneurysms: critical review of the literature. AJNR Am J Neuroradiol. 2012;33(1):12–5.
39. Shapiro M, Becske T, Sahlein D, Babb J, Nelson PK. Stent-supported aneurysm coiling: a literature survey of treatment and follow-up. AJNR Am J Neuroradiol. 2012;33(1):159–63.
40. Pop R, Harsan O, Martin I, Mihoc D, Richter JS, Manisor M, et al. Balloon-assisted coiling of intracranial aneurysms using the eclipse 2L double lumen balloon. Interv Neuroradiol. 2020;26(3):291–9.
41. Gupta R, Kolodgie FD, Virmani R, Eckhouse R. Comaneci neck bridging device for the treatment of cerebral aneurysms. J Neurointerv Surg. 2016;8(2):181–5.
42. Sirakov A, Minkin K, Penkov M, Ninov K, Karakostov V, Sirakov S. Comaneci-assisted coiling as a treatment option for acutely ruptured wide neck cerebral aneurysm: case series of 118 patients. Neurosurgery. 2020;87:1148.
43. Fischer S, Weber A, Carolus A, Drescher F, Gotz F, Weber W. Coiling of wide-necked carotid artery aneurysms assisted by a temporary bridging device (Comaneci): preliminary experience. J Neurointerv Surg. 2017;9(11):1039–97.
44. Molina-Nuevo JD, Lopez-Martinez L, Pedrosa-Jimenez MJ, Julia-Molla E, Hernandez-Fernandez F. Comaneci device-assisted embolization of wide-necked carotid aneurysms with an unfavorable ratio. BMC Neurol. 2020;20(1):384.
45. Cavalcanti DD, Delavari N, Riina HA, Endovascular Neurosurgery Research G. Stent-assisted coiling of a sidewall aneurysm of the distal middle cerebral artery: 2-dimensional operative video. Oper Neurosurg (Hagerstown). 2020;20(1):E37–E8.
46. Fiorella D, Albuquerque FC, Deshmukh VR, McDougall CG. Usefulness of the Neuroform stent for the treatment of cerebral aneurysms: results at initial (3-6-mo) follow-up. Neurosurgery. 2005;56(6):1191–201; discussion 201–2
47. Biondi A, Janardhan V, Katz JM, Salvaggio K, Riina HA, Gobin YP. Neuroform stent-assisted coil embolization of wide-neck intracranial aneurysms: strategies in stent deployment and midterm follow-up. Neurosurgery. 2007;61(3):460–8; discussion 8–9
48. Hetts SW, Turk A, English JD, Dowd CF, Mocco J, Prestigiacomo C, et al. Stent-assisted coiling versus coiling alone in unruptured intracranial aneurysms in the matrix and platinum science trial: safety, efficacy, and mid-term outcomes. AJNR Am J Neuroradiol. 2014;35(4):698–705.
49. Piotin M, Blanc R, Spelle L, Mounayer C, Piantino R, Schmidt PJ, et al. Stent-assisted coiling of intracranial aneurysms: clinical and angiographic results in 216 consecutive aneurysms. Stroke. 2010;41(1):110–5.
50. Bechan RS, Sprengers ME, Majoie CB, Peluso JP, Sluzewski M, van Rooij WJ. Stent-assisted coil embolization of intracranial aneurysms: complications in acutely ruptured versus unruptured aneurysms. AJNR Am J Neuroradiol. 2016;37(3):502–7.
51. Poncyljusz W, Bilinski P, Safranow K, Baron J, Zbroszczyk M, Jaworski M, et al. The LVIS/LVIS Jr. stents in the treatment of wide-neck intracranial aneurysms: multicentre registry. J Neurointerv Surg. 2015;7(7):524–9.
52. Feng Z, Fang Y, Xu Y, Hong B, Zhao W, Liu J, et al. The safety and efficacy of low profile visualized intraluminal support (LVIS) stents in assisting coil embolization of intracranial saccular aneurysms: a single center experience. J Neurointerv Surg. 2016;8(11):1192–6.
53. Jankowitz BT, Hanel R, Jadhav AP, Loy DN, Frei D, Siddiqui AH, et al. Neuroform atlas stent system for the treatment of intracranial aneurysm: primary results of the atlas humanitarian device exemption cohort. J Neurointerv Surg. 2019;11(8):801–6.
54. Ten Brinck MFM, de Vries J, Bartels R, Grotenhuis JA, Boogaarts HD. NeuroForm atlas stent-assisted coiling: preliminary results. Neurosurgery. 2019;84(1):179–89.
55. Cay F, Peker A, Arat A. Stent-assisted coiling of cerebral aneurysms with the Neuroform atlas stent. Interv Neuroradiol. 2018;24(3):263–9.

56. Lozen A, Manjila S, Rhiew R, Fessler R. Y-stent-assisted coil embolization for the management of unruptured cerebral aneurysms: report of six cases. Acta Neurochir. 2009;151(12):1663–72.
57. Zhao KJ, Yang PF, Huang QH, Li Q, Zhao WY, Liu JM, et al. Y-configuration stent placement (crossing and kissing) for endovascular treatment of wide-neck cerebral aneurysms located at 4 different bifurcation sites. AJNR Am J Neuroradiol. 2012;33(7):1310–6.
58. Samaniego EA, Mendez AA, Nguyen TN, Kalousek V, Guerrero WR, Dandapat S, et al. LVIS Jr device for Y-stent-assisted coil embolization of wide-neck intracranial aneurysms: a multicenter experience. Interv Neurol. 2018;7(5):271–83.
59. Aenis M, Stancampiano AP, Wakhloo AK, Lieber BB. Modeling of flow in a straight stented and nonstented side wall aneurysm model. J Biomech Eng. 1997;119(2):206–12.
60. Canton G, Levy DI, Lasheras JC, Nelson PK. Flow changes caused by the sequential placement of stents across the neck of sidewall cerebral aneurysms. J Neurosurg. 2005;103(5):891–902.
61. Becske T, Kallmes DF, Saatci I, McDougall CG, Szikora I, Lanzino G, et al. Pipeline for uncoilable or failed aneurysms: results from a multicenter clinical trial. Radiology. 2013;267(3):858–68.
62. Fiorella D, Lylyk P, Szikora I, Kelly ME, Albuquerque FC, McDougall CG, et al. Curative cerebrovascular reconstruction with the pipeline embolization device: the emergence of definitive endovascular therapy for intracranial aneurysms. J Neurointerv Surg. 2009;1(1):56–65.
63. Nelson PK, Lylyk P, Szikora I, Wetzel SG, Wanke I, Fiorella D. The pipeline embolization device for the intracranial treatment of aneurysms trial. AJNR Am J Neuroradiol. 2011;32(1):34–40.
64. Becske T, Brinjikji W, Potts MB, Kallmes DF, Shapiro M, Moran CJ, et al. Long-term clinical and angiographic outcomes following pipeline embolization device treatment of complex internal carotid artery aneurysms: five-year results of the pipeline for uncoilable or failed aneurysms trial. Neurosurgery. 2017;80(1):40–8.
65. Chalouhi N, Theofanis T, Starke RM, Zanaty M, Jabbour P, Dooley SA, et al. Potential role of granulocyte-monocyte colony-stimulating factor in the progression of intracranial aneurysms. DNA Cell Biol. 2015;34(1):78–81.
66. Hanel RA, Kallmes DF, Lopes DK, Nelson PK, Siddiqui A, Jabbour P, et al. Prospective study on embolization of intracranial aneurysms with the pipeline device: the PREMIER study 1 year results. J Neurointerv Surg. 2020;12(1):62–6.
67. Kan P, Srinivasan VM, Mbabuike N, Tawk RG, Ban VS, Welch BG, et al. Aneurysms with persistent patency after treatment with the pipeline embolization device. J Neurosurg. 2016;126:1894–8.
68. Tsang AC, Fung AM, Tsang FC, Leung GK, Lee R, Lui WM. Failure of flow diverter treatment of intracranial aneurysms related to the fetal-type posterior communicating artery. Neurointervention. 2015;10(2):60–6.
69. Kallmes DF, Hanel R, Lopes D, Boccardi E, Bonafe A, Cekirge S, et al. International retrospective study of the pipeline embolization device: a multicenter aneurysm treatment study. AJNR Am J Neuroradiol. 2015;36(1):108–15.
70. Shapiro M, Becske T, Nelson PK. Learning from failure: persistence of aneurysms following pipeline embolization. J Neurosurg. 2017;126(2):578–85.
71. Chiu AH, Cheung AK, Wenderoth JD, De Villiers L, Rice H, Phatouros CC, et al. Long-term follow-up results following elective treatment of Unruptured intracranial aneurysms with the pipeline embolization device. AJNR Am J Neuroradiol. 2015;36(9):1728–34.
72. Bhogal P, Ganslandt O, Bazner H, Henkes H, Perez MA. The fate of side branches covered by flow diverters-results from 140 patients. World Neurosurg. 2017;103:789–98.
73. Puffer RC, Kallmes DF, Cloft HJ, Lanzino G. Patency of the ophthalmic artery after flow diversion treatment of paraclinoid aneurysms. J Neurosurg. 2012;116(4):892–6.
74. Rangel-Castilla L, Munich SA, Jaleel N, Cress MC, Krishna C, Sonig A, et al. Patency of anterior circulation branch vessels after pipeline embolization: longer-term results from 82 aneurysm cases. J Neurosurg. 2017;126(4):1064–9.

75. Chen SH, Snelling BM, Shah SS, Sur S, Brunet MC, Starke RM, et al. Transradial approach for flow diversion treatment of cerebral aneurysms: a multicenter study. J Neurointerv Surg. 2019;11(8):796–800.
76. Cavalcanti DD, Nelson PK, Raz E, Shapiro M, Nossek E, Tanweer O, et al. Endovascular treatment of aneurysms using flow-diversion embolization: 2-dimensional operative video. Oper Neurosurg (Hagerstown). 2021;20(4):E284–E5.
77. De Leacy RA, Fargen KM, Mascitelli JR, Fifi J, Turkheimer L, Zhang X, et al. Wide-neck bifurcation aneurysms of the middle cerebral artery and basilar apex treated by endovascular techniques: a multicentre, core lab adjudicated study evaluating safety and durability of occlusion (BRANCH). J Neurointerv Surg. 2019;11(1):31–6.
78. Papagiannaki C, Spelle L, Januel AC, Benaissa A, Gauvrit JY, Costalat V, et al. WEB intrasaccular flow disruptor-prospective, multicenter experience in 83 patients with 85 aneurysms. AJNR Am J Neuroradiol. 2014;35(11):2106–11.
79. Pierot L, Gubucz I, Buhk JH, Holtmannspotter M, Herbreteau D, Stockx L, et al. Safety and efficacy of aneurysm treatment with the WEB: results of the WEBCAST 2 study. AJNR Am J Neuroradiol. 2017;38(6):1151–5.
80. Arthur AS, Molyneux A, Coon AL, Saatci I, Szikora I, Baltacioglu F, et al. The safety and effectiveness of the Woven EndoBridge (WEB) system for the treatment of wide-necked bifurcation aneurysms: final 12-month results of the pivotal WEB Intrasaccular Therapy (WEB-IT) Study. J Neurointerv Surg. 2019;11(9):924–30.
81. Cortez GM, Akture E, Monteiro A, Arthur AS, Peterson J, Dornbos D, et al. Woven EndoBridge device for ruptured aneurysms: perioperative results of a US multicenter experience. J Neurointerv Surg. 2021;13:1012.
82. Girot JB, Caroff J, Cortese J, Mihalea C, Rouchaud A, Da Ros V, et al. Endovascular treatment of small and very small intracranial aneurysms with the woven Endobridge device. AJNR Am J Neuroradiol. 2021;42:1276.

Chapter 8
Microsurgical Aneurysm Treatment

Sheila R. Eshraghi, Brian M. Howard, and Daniel L. Barrow

Introduction

The basic tenets for treatment of intracranial aneurysms (IAs) are to eliminate the aneurysm from the circulation completely, to preserve the patency of the parent vessels and associated branches, and to maintain or improve the patient's neurologic function. Because of the complexity of aneurysm treatment, better outcomes are achieved in large volume centers where neurosurgical, endovascular, neurointensive care, and neuroanesthesia teams work together to care for these patients [1, 2]. The decision to treat and by which modality depends on factors of the patient (i.e., age, clinical status, and risk factors for hemorrhage) and the aneurysm (i.e., size, shape, configuration, multiplicity, and presence of thrombus). This chapter will focus on indications for surgical treatment of IAs in this era of rapid endovascular advancements.

Supplementary Information The online version of this chapter (https://doi.org/10.1007/978-3-030-88196-2_8) contains supplementary material, which is available to authorized users.

S. R. Eshraghi · D. L. Barrow
Department of Neurosurgery, Emory University School of Medicine, Atlanta, GA, USA
e-mail: sheila.eshraghi@emory.edu; dbarr01@emory.edu

B. M. Howard (✉)
Department of Neurosurgery, Emory University School of Medicine, Atlanta, GA, USA

Department of Radiology and Imaging Sciences, Emory University School of Medicine, Atlanta, GA, USA
e-mail: brian.howard@emory.edu

J. R. Mascitelli, M. J. Binning (eds.), *Introduction to Vascular Neurosurgery*,
https://doi.org/10.1007/978-3-030-88196-2_8

History of Surgical Management of Aneurysms

As early as the 1800s, IAs were surgically treated by Hunterian ligation – or gradual occlusion of the carotid artery – to promote aneurysm thrombosis. Direct exposure of a ruptured IA and muscle wrapping was performed by Sir Norman Dott in 1931. The first aneurysm clip, a Cushing-McKenzie silver clip, was placed on the neck of a saccular IA in 1937 by Walter Dandy, while modern, spring-loaded aneurysm clips were first introduced in 1950 by Frank Mayfield and George Kees. Further design refinements were made by Charles Drake with the fenestrated clip, Thoralf Sundt Jr with the encircling clip, Gazi Yasargil, and Kenichiro Sugita. The pterional craniotomy was refined in the 1960s. In 1969, Yasargil described the superficial temporal artery to middle cerebral artery (STA-MCA) bypass as an adjunct in the treatment of complex IAs [3]. With the introduction of the operating microscope, refinements in microsurgical techniques, improved anesthetic and intensive care management, and development of diagnostic imaging, the risk of surgery for IAs decreased over time. Prior to 1991, when Guglielmi introduced detachable platinum coils, microsurgical clip ligation remained the primary treatment for IAs [1, 4].

Neuro-Imaging Evaluation

Imaging of IAs has improved tremendously over time. While axial angiography using computed tomography (CT) or magnetic resonance imaging (MRI) modalities is frequently used for screening and follow-up of both treated and observed aneurysms, noninvasive imaging is most sensitive for aneurysms >3 mm in size [2, 5]. Axial imaging may also provide complimentary and clinically important information regarding the presence of intraluminal thrombus and calcification of aneurysms [5]. Digital subtraction angiography (DSA) is the "gold standard" to evaluate IAs. Two- and three-dimensional DSAs are critical to evaluate the following features of the aneurysm and the surrounding vasculature: (1) parent vessel, (2) size, shape, and relationship to parent and adjacent arteries, (3) presence and location of vasospasm, (4) displacement of adjacent vessels, and (5) the presence of additional aneurysms or vascular malformations [5, 6].

Indications for Aneurysm Surgery in the Endovascular Era

Pediatric Patients

Considering the life expectancy of young adult and pediatric patients, optimal treatment for cerebral aneurysms remains unclear. Endovascular therapies confer reduced durability with recurrence reported to be as high at 20–40% [7–9].

Furthermore, the long-term outcomes of endovascular devices such as flow diverters are unknown due to lack of sufficient follow-up in the growing child or adolescent. Due to the rarity of pediatric aneurysms, only small clinical series have been published, which makes it difficult to make treatment recommendations.

Aneurysms in pediatric patients are more frequently large or giant or fusiform in morphology than adult aneurysms [7–9]. Complete occlusion of the aneurysm is achieved only for 80–82% after endovascular therapies [7–9]. Sanai et al. demonstrated a 14% recurrence after endovascular treatment (EVT) over a mean follow-up period of just 5.7 years [8]. Recurrence after surgery is documented to be around 2.5% or less [8, 9]. The clinical outcomes did not differ significantly between endovascular and microsurgical treatments with overall 7–14% long-term morbidity and low morality in this pediatric population [7–9].

Multiple Aneurysms

Multiple aneurysms are found in 20–34% of patients with intracranial aneurysms [10–12]. Female sex, smoking, and hypertension are all risk factors for developing multiple intracranial aneurysms [11, 12]. When possible, treatment of all aneurysms simultaneously in one procedure is ideal to reduce the number of invasive procedures. Though the overall length of the procedure and risk of complication is increased when treating multiple aneurysms at once, a one-staged operation has overall lower mortality than treating the patient in multiple stages or leaving an unruptured aneurysm untreated [13]. Additionally, one study compared surgical and endovascular treatment for multiple intracranial aneurysms and found similar complication rates (10.9% and 10.3%, respectively) but higher retreatment rates for the endovascular group (3% vs. 18%, respectively) [14]. In cases of multiplicity, microsurgical clip ligation should be considered to safely treat the highest number of aneurysms in the fewest number of procedures if EVT cannot address all of the aneurysms.

Very Small Aneurysms

Very small aneurysms (VSAs) are defined as aneurysms with a maximum diameter of 3 mm or smaller. Whether to treat unruptured VSAs remains controversial due to low reported risk of rupture in large epidemiological studies [15, 16]. Several reasons that may encourage treatment of unruptured VSAs include high risk patient populations, personal or family history of SAH, multiple aneurysms, and irregular shape or daughter sac, all of which portend higher risk of rupture. The International Subarachnoid Aneurysm Trial (ISAT) excluded small aneurysms ($\leq$3 mm) from the trial, which leaves questions about the best treatment strategy for small ruptured aneurysms [17, 18].

Aneurysms ≤3 mm pose technical endovascular challenges for catheterizing the aneurysm, microcatheter stability, and deploying coils into a small volume. Endovascular failure (9.9–13.7%) or incomplete occlusion often results in cross over to surgery [19, 20]. Studies demonstrate that the risk of intraprocedural rupture during EVT is higher for VSAs (7.7%) than larger aneurysms (3.6%) and for ruptured (10.7%) over unruptured (5%) VSAs [19–23]. These data bias toward surgical management for VSAs when treatment is indicated.

Overall, permanent morbidity and mortality are similar between endovascular and surgical treatment of VSAs, but procedure-related complications may be slightly higher for surgical intervention [19, 24, 25]. Data support that very small posterior circulation aneurysms should preferentially undergo endovascular therapy if amenable due to higher postoperative deficits compared to surgically treated anterior circulation aneurysms (45.5% vs. 3.9%, respectively) [22]. Figure 8.1 and Video 8.1 depict a case of young patient with multiple aneurysms including two VSAs.

Endovascular Treatment Failures

The volume of EVT failures that require retreatment either endovascularly or microsurgically will continue to grow as the number of endovascular procedures performed increases. In ISAT, 191 patients (17.4%) required retreatment in the endovascular cohort, and 54% of these patients required surgery [26]. Hayakawa et al. followed 73 aneurysms with residual necks an average of 17.3 months, and 49% showed recanalization on follow-up. Wide-neck (≥4 mm) and large or giant aneurysms were more likely to recur [27]. In one series of previously coiled aneurysms requiring microsurgical retreatment, 4 of 81 patients presented with

Fig. 8.1 The case of a young patient who was admitted for Hunt and Hess grade 1 subarachnoid hemorrhage is depicted. (**a** and **b**) Anteroposterior and lateral 2-D cerebral angiograms of the right internal carotid artery (ICA) reveal posterior communicating artery (Pcomm) and anterior choroidal artery (AchorA) origin aneurysms (open arrow). A double density at the proximal A1 segment of the ACA is suspicious for an aneurysm. (**c**) Three-dimensional reconstruction of the right ICA angiogram in the surgical orientation shows the Pcomm and AchorA aneurysms (open arrow) and the posterior wall A1 segment aneurysm (broken arrow). (**d**) Posteroanterior three-dimensional reconstruction better shows the A1 segment aneurysm (broken arrow). (**e**) Intraoperative photo of the ICA after dissection of the necks of the Pcomm and AchorA aneurysms. The "shoulder" of both the Pcomm and AchorA are well seen originating at the proximal neck of each aneurysm then taking their typical course behind the ICA. (**f**) Indocyanine green (ICG) video angiography reveals patency of the AchorA (arrow) – inset shows light microscopy of the selected ICG frame. (**g** and **h**) The posterior wall A1 segment aneurysm was occluded with a straight miniclip. (**i** and **j**) Intraoperative angiography reveals complete occlusion of the aneurysms and maintained patency of the normal vasculature, including the Pcomm and AchorA

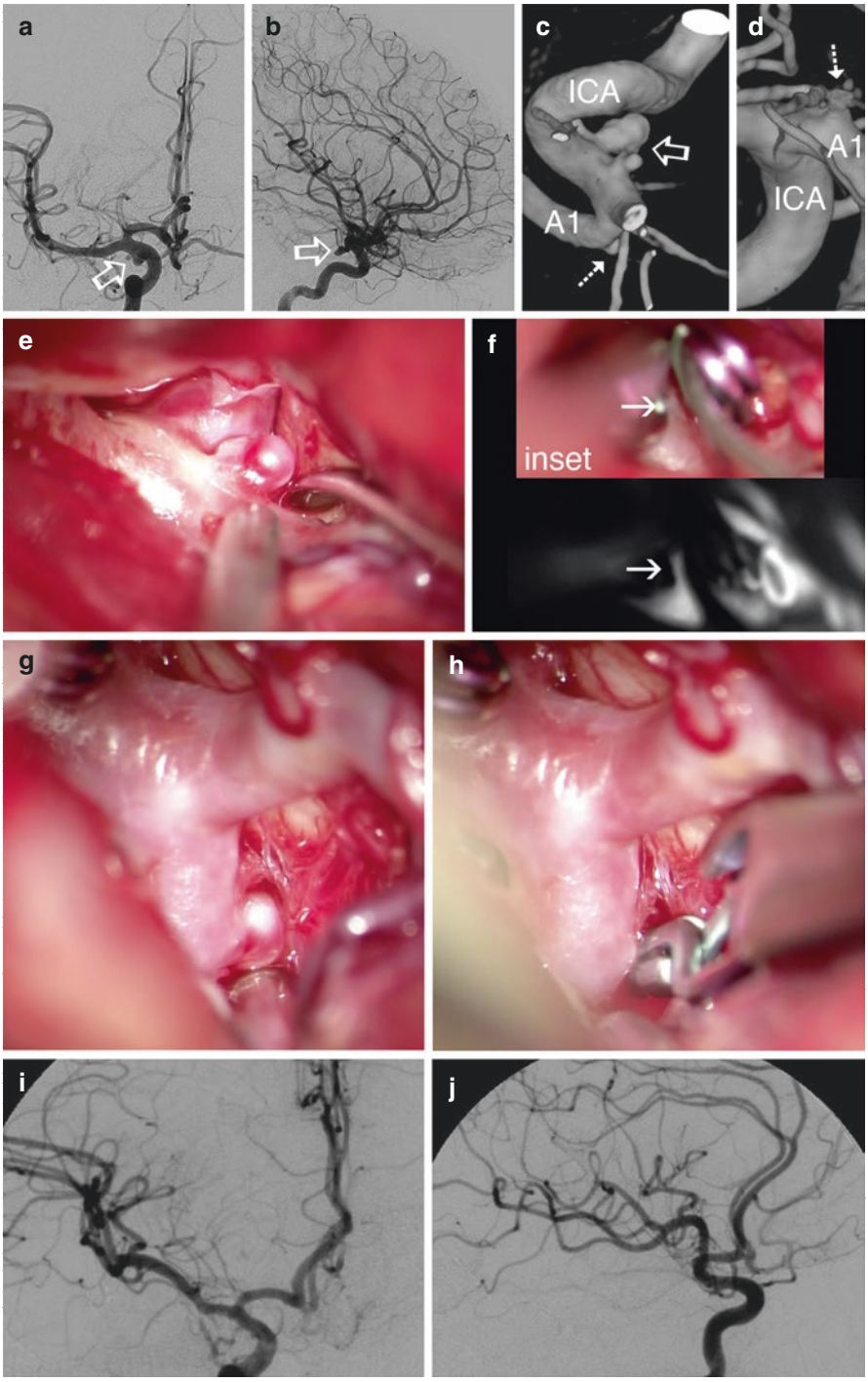
a
b
c
ICA
A1
d
A1
ICA
e
f
inset
g
h
i
j

Contraindications to Dual Antiplatelet Therapies and Noncompliant Patients

Dual antiplatelet therapy (DAPT) is needed for the placement of an intracranial stent or flow diverter to minimize thromboembolic complications. Employing DAPT should be balanced with the risk of bleeding and individualized for each patient. Some patients have contraindications to DAPT which may make microsurgical clip ligation necessary. Contraindications to DAPT include known esophageal varices or gastric ulcers, thrombocytopenia (50,000/μL blood), decompensated liver disease or baseline INR >1.5, other coagulopathy, barriers to compliance (i.e., polysubstance abuse, dementia, and financial constraints), or imminent need for major surgery. While thrombocytopenia and coagulopathy are relative contraindications to cranial surgery, these can typically be corrected and maintained within normal limits in the short term to safely complete surgery.

Many patients presenting with ruptured aneurysms require external ventricular drain (EVD) or ventriculoperitoneal (VP) shunt placement for cerebrospinal fluid diversion. In one series, six of seven patients on DAPT for stent-assisted coiling who required placement of an EVD and/or VP shunt suffered a hemorrhagic complication. Four of these instances were due to placement or exchange of a ventricular catheter, and the remaining two patients suffered rebleeding events [34]. We are, therefore, hesitant to treat patients with aneurysmal SAH by endovascular methods that require DAPT. In the case of flow diversion, the aneurysm may not be immediately secured, which does not mitigate the risk of rebleeding.

Additionally, patients who may be noncompliant with DAPT regimen or unable to maintain the prescribed follow-up after EVT are better candidates for microsurgical treatment. Inability to correctly take a DAPT regimen after stent-assisted coiling or flow diversion could lead to disastrous thromboembolic complications. EVT requires diligent follow-up due to the higher rate of aneurysm recurrence and rerupture when compared to microsurgical treatment [29].

Associated Intracerebral Hemorrhage

Approximately 12–21% of patients with aneurysmal SAH present with concomitant intracerebral hemorrhage (ICH) [35, 36]. Patients with SAH and an associated ICH have worse Hunt and Hess grades on presentation and worse outcomes than those without ICH [36]. Aneurysms with associated ICH are more likely to be located on the middle cerebral artery (MCA) or anterior communicating artery (ACoA) [36]. Studies demonstrate substantial functional and mortality benefit in patients who undergo surgical evacuation of the associated ICH and clip ligation of the offending aneurysm compared to those treated without surgical decompression of the brain [37, 38]. The primary benefit of an endovascular procedure is avoidance of a

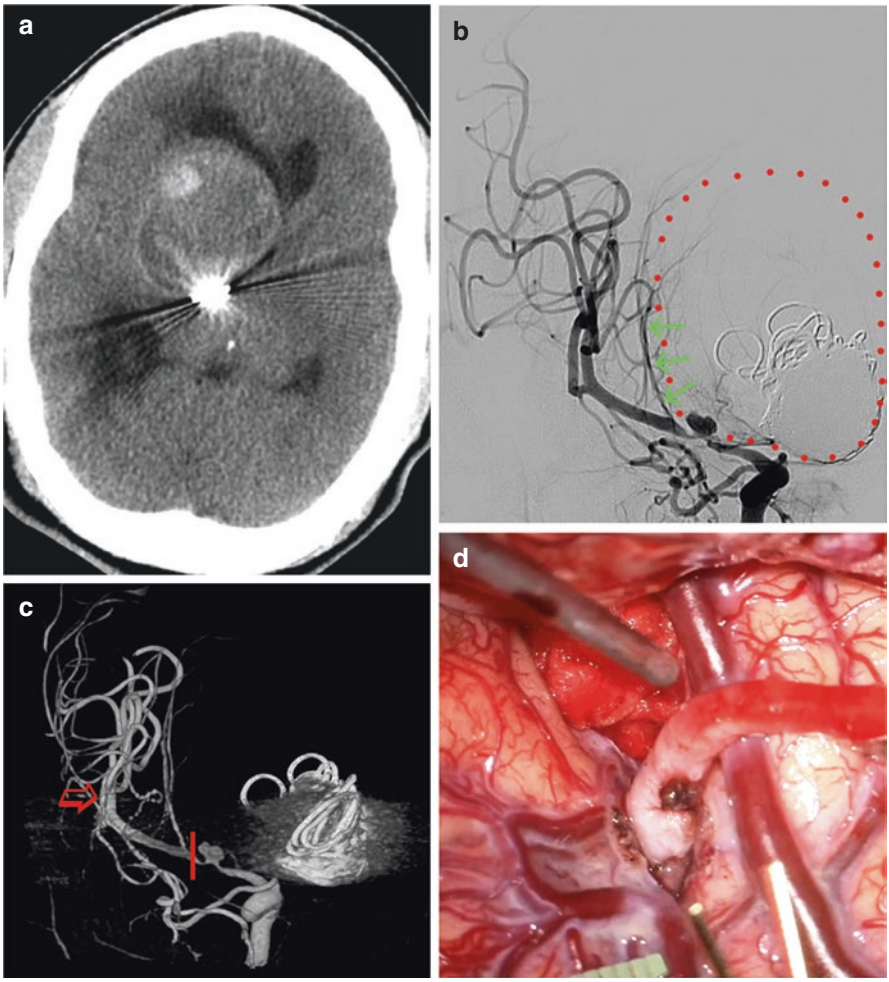

Fig. 8.2 Microsurgical treatment of a giant, partially thrombosed right M1 segment aneurysm after endovascular treatment failure. A 36-year-old man presented with left-sided hemiparesis and 1 week of worsening headache with nausea. (**a**) Computed tomography scan showed a large recurrence of a previously coiled aneurysm with intraluminal hemorrhage. (**b**) Angiography showed only partial filling of the aneurysm and marked stenosis of the middle cerebral artery (MCA) beyond the neck of the aneurysm. The outline of the aneurysm is noted by red dots. Lenticulostriates draped over the lateral margin of the aneurysm are delineated by green arrows. (**c**) The surgical strategy was to perform a radial artery bypass graft from the common carotid artery to an M2 segment (red arrow – recipient site) with clip occlusion distal to the neck of the aneurysm (red bar). (**d**) Intraoperative image of the radial artery to M2 anastomosis. (**e** and **f**) One-month follow-up angiogram demonstrated the radial artery bypass filling the entire MCA distribution with back filling of the lenticulostriate arteries (green arrows), and complete occlusion of the aneurysm. Occlusion of the aneurysm and proximal M1 segment are demonstrated as the delayed angiogram shows that the internal carotid artery terminates at the A1

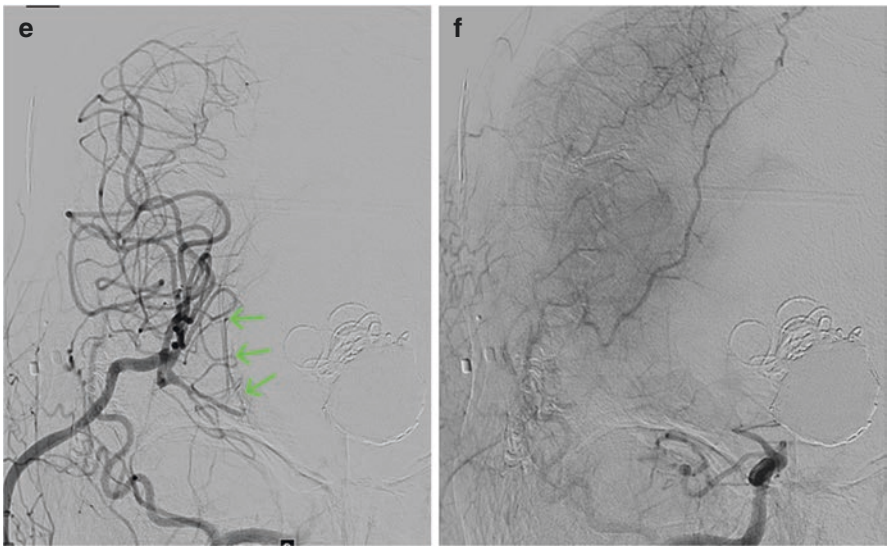

Fig. 8.2 (continued)

craniotomy. If the patient needs surgery for evacuation of a life- or health-threatening hematoma, treatment of the aneurysm at the time of the craniotomy is the most parsimonious therapeutic strategy. Figure 8.3 demonstrates a case of a large, ruptured right MCA aneurysm with an associated ICH.

Large Aneurysms with Mass Effect

Large (13–24 mm) and giant (≥25 mm) IAs pose technical challenges due to development of calcification at the neck and partial thrombosis of the dome, presence of perforators and branch vessels from the aneurysmal walls, and compression of adjacent brain or cranial nerves. Left untreated, giant aneurysms are associated with 70–80% morbidity and mortality rates over 2 years due to rupture, thromboembolic complications, or progressive compressive symptoms [39, 40].

Endovascular vessel sacrifice or surgical trapping is often not feasible for aneurysms that are at or distal to the internal carotid artery (ICA) bifurcation or for patients that fail a balloon test occlusion (BTO). Large and giant aneurysms have a well-documented low complete occlusion rate and high rate of recanalization after endovascular coiling, necessitating subsequent retreatment [41, 42]. Although well established to treat aneurysms of the petrocavernous and paraclinoid segments of the ICA, flow diversion does not immediately address the mass effect of large and giant IAs and can cause compressive symptoms to worsen [6, 43]. Consequently,

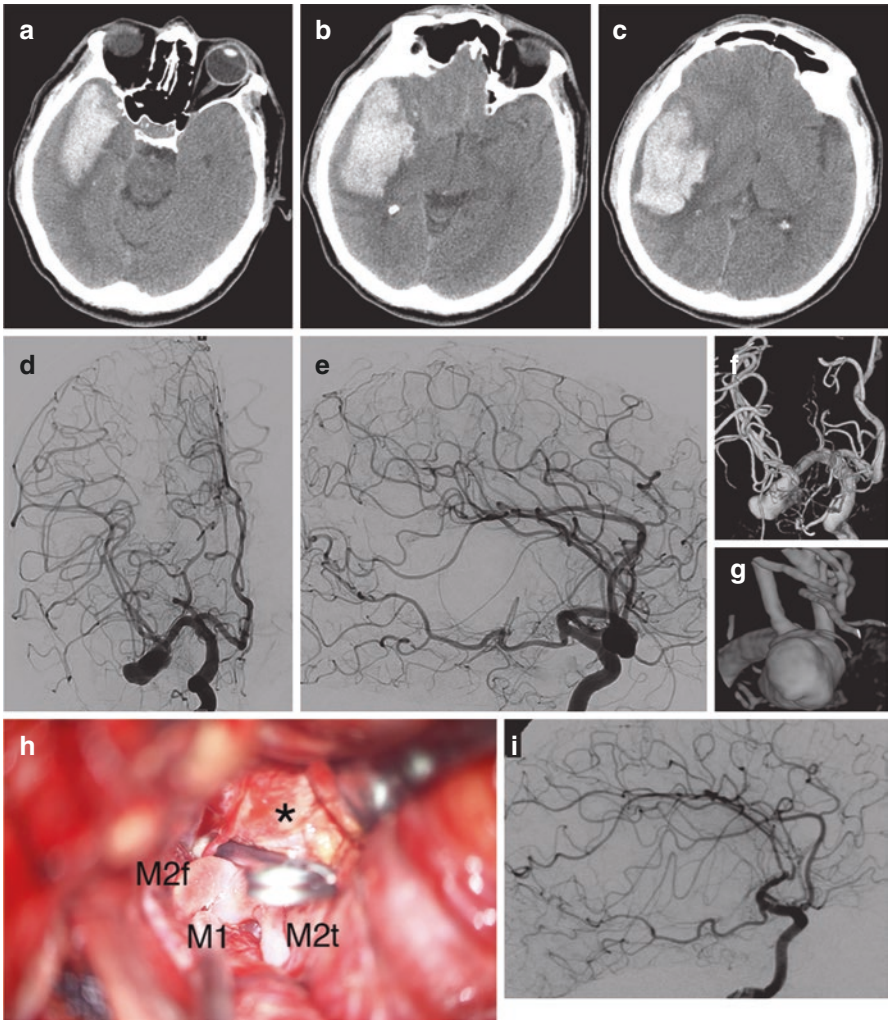

Fig. 8.3 A middle-aged gentleman admitted with a Hunt and Hess grade 3 subarachnoid hemorrhage is shown. (**a**–**c**) Preoperative axial noncontrast computed tomography (CT) of the head shows a large intraparenchymal hemorrhage (IPH) in the right temporal lobe. (**d**–**g**) Two- and three-dimensional cerebral angiography revealed a large right middle cerebral artery (MCA) bifurcation aneurysm. (**h**) Intraoperative photo after clipping shows reconstruction of the MCA bifurcation and obliteration of the aneurysm using a side-angled clip placed parallel to the origins of the M2 segment takeoffs (M2f – frontal division; M2t – temporal division; M1 – M1 segment coming out of the Sylvian fissure). (**i** and **j**) Intraoperative angiography shows complete elimination of the aneurysm from the circulation. (**k**) Intraoperative photo after removal of the IPH. The IPH was removed from the point at which it broke through the temporal lobe surface anteriorly. The dome of the aneurysm is seen in the resection cavity (black arrows). (**l**–**n**) Postoperative CT shows near-complete evacuation of the IPH

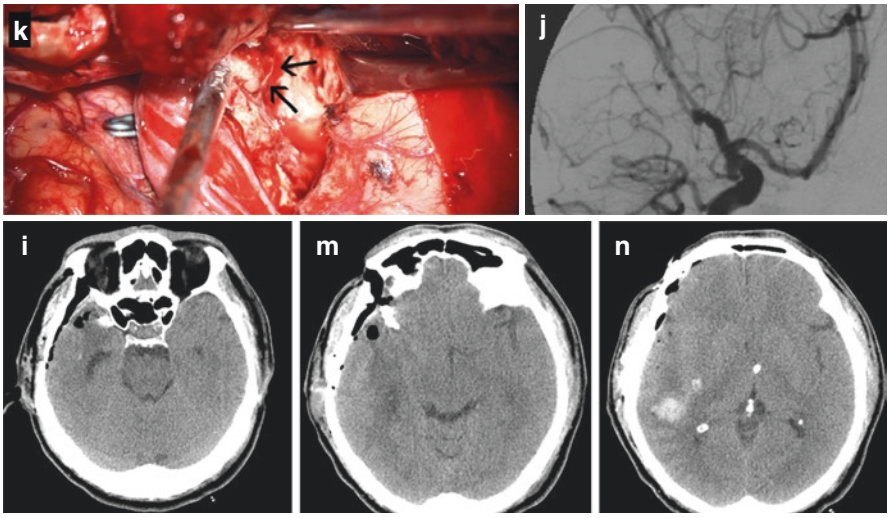

Fig. 8.3 (continued)

surgical management remains a mainstay of treatment of large and giant IAs. Once the aneurysm is surgically occluded, it can be punctured or intrasaccular thrombus can be resected to immediately reduce the mass effect on critical structures, such as cranial nerves, the optic apparatus, or the brainstem. Figure 8.4 and Video 8.2 depict a case of a giant left ophthalmic artery origin ICA aneurysm treated by clipping followed by decompression of the optic apparatus.

Many large and giant aneurysms can be primarily clipped or clip reconstructed (40–60%) [39, 42, 44]. Simple clipping is the preferred treatment strategy but is often prevented by dolichoectatic morphology, aberrant branch anatomy, atherosclerosis at the aneurysm neck, and intraluminal thrombosis. Aneurysms that cannot be directly clipped require alternative techniques to indirectly occlude the aneurysm, which include distal occlusion, proximal occlusion, trapping, or excision with or without bypass. Overall, treatment-related surgical morbidity and mortality for giant IAs is approximately 20–30% with mortality comprising 8–22% [39, 42, 44].

When collateral circulation is inadequate to provide sufficient perfusion after permanent vessel occlusion, a revascularization procedure is required. BTO may be used in selected patients to determine which patients will not tolerate parent vessel occlusion. Many bypass techniques have been described, and the selection of bypass type depends on the location of the aneurysm, the need for low- versus high-flow revascularization, and surgeon preference. Special surgical considerations during bypass procedures include starting aspirin prior to surgery, giving intravenous heparin during the anastomosis, and inducing burst suppression and arterial pressure elevation to 20% above baseline during temporary clip occlusion.

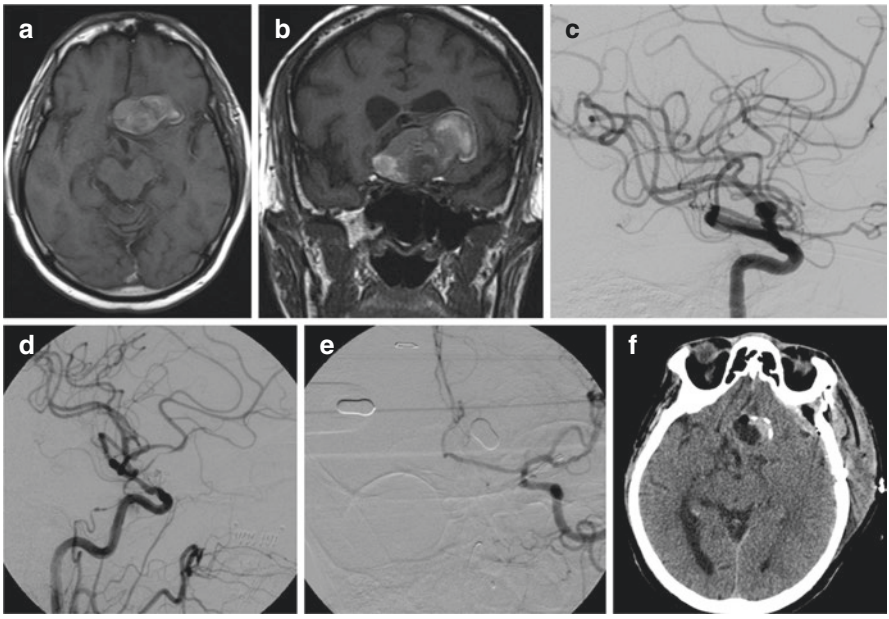

Fig. 8.4 Giant thrombotic internal carotid artery aneurysm arising at the ophthalmic segment causing mass effect. A 59-year-old man presented with progressive vision loss. Axial (**a**) and coronal (**b**) T1 pre-contrast magnetic resonance images with a large heterogeneous mass displacing the optic chiasm. (**c**) Angiography showed a partially thrombosed left ophthalmic artery aneurysm with residual filling measuring 5.3 mm × 6.7 mm × 5.6 mm with a 4.1 mm neck. (**d** and **e**) Intraoperative angiography demonstrated complete occlusion of the aneurysm after placement of single side-angled clip. (**f**) Follow-up computed tomography scan showed decreased mass effect after aneurysm debulking

Wide-Necked Aneurysms

The most commonly used definition for wide-necked aneurysms (WNAs) is neck size ≥4 mm or dome-to-neck ratio <2. Many endovascular techniques exist for the treatment of WNAs including balloon-assisted coiling, stent-assisted coiling, complex neck support devices (i.e., PulseRider and pCONus), parent artery flow diversion (i.e., Pipeline, FRED, and Surpass), and intra-saccular flow diversion (i.e., Woven EndoBridge). Brinjikji et al. found that aneurysms with aspect (height-to-neck) and dome-to-neck ratios >1.6 typically did not require the use of adjunctive techniques during EVT [45]. WNAs are more likely to have a neck remnant and more likely to have recanalization on follow-up than aneurysms with narrow necks after coil embolization [27, 41].

Few studies have examined the results of microsurgical clipping of WNAs while a large number of studies have examined EVT. A post hoc subgroup analysis in the Barrow Ruptured Aneurysm Trial (BRAT) examined WNAs. WNAs comprised

54.1% of the aneurysms treated; were more likely to arise from the MCA, basilar tip, or internal carotid artery (ICA) other than the ICA-posterior communicating artery (PCoA) junction; and were more common in older patients with worse clinical presentation. Complete obliteration on postoperative imaging was lower and retreatment rate was higher for coiling compared with clipping (51.2% vs. 84.3% and 26.8% vs. 0%, respectively), but clinical outcomes after either treatment were not significantly different at any time point [46]. A meta-analysis comparing EVT to surgical clipping for wide-necked bifurcation aneurysms showed similar adverse events (21.1% vs. 24.3%) but lower complete occlusion with EVT (39.8% vs. 52.5%) [47].

Complex Configuration

Numerous factors can make an IA "complex" including deep location, wide neck, large size, inclusion of branching vessels, dolichoectactic morphology, presence of intraluminal thrombus or atherosclerotic walls, or previous endovascular or surgical treatments. Simple aneurysms are readily treated with current endovascular techniques including stand-alone coiling, balloon- or stent-assisted coiling, or parent artery and intra-saccular flow diversion. As this field develops, vascular neurosurgeons are left with more complex aneurysms deemed unsuitable for endovascular therapies. Microsurgical treatment of complex IAs requires careful planning and innovative thinking, expanding the exposure with skull base approaches, temporary occlusion or hypothermic circulatory arrest, the use of a variety of bypass techniques, and, sometimes, the combination of microsurgical and endovascular treatments.

Aneurysms with complex configurations are often located at branch points and have efferent arteries arising from the aneurysm walls. Clip reconstruction is the preferred strategy to obliterate the aneurysm and maintain patency of the parent and branching arteries. When this is not feasible, vessel occlusion (i.e., distal, proximal, or both [trapping]) or aneurysm excision with or without bypass can be performed. Many bypass techniques have been described for the treatment of complex aneurysms including extracranial-intracranial (EC-IC) bypass, EC-IC interpositional bypass, reimplantation, reanastamosis, in situ bypass, IC-IC interpositional bypass, and combination bypass [48]. When microsurgical and endovascular techniques are used together, the number of possible treatment strategies increases drastically to include the following possibilities: coil embolization after partial aneurysm clipping to narrow the neck, endovascular parent vessel and aneurysm occlusion after surgical bypass, proximal endovascular occlusion after distal surgical occlusion and bypass for complete trapping of aneurysm, aneurysm debulking after endovascular parent vessel occlusion, and balloon catheter placement for temporary proximal occlusion and/or suction decompression to allow for surgical clipping [49–53].

Several clinical series have been published examining the combination of endovascular and microsurgical management for complex aneurysms. Aneurysm

occlusion was obtained in 95% of cases [49, 51]. Good or excellent outcomes were seen in 77.1–86% of patients, permanent morbidity occurred in 5.2–8.3%, and procedural mortality was 9.1–14.3% [49, 51, 52]. As seen previously, death or poor outcome was more common after the treatment of a posterior circulation aneurysm than an anterior circulation aneurysm [51, 52].

Thrombotic Aneurysms

Cerebral aneurysms with significant intraluminal thrombus are poorly described in the literature because they are often included in larger series along with fusiform or giant aneurysms, but account for up to 16.8% of aneurysms [54]. These aneurysms should be studied with CT and/or MRI plus catheter angiography due to the discrepancies between aneurysm size and luminal filling. Most patients present with symptoms from mass effect (32%), which is indicative of their predilection to be larger in size. Only 10% of patients with thrombotic aneurysms present with embolic symptoms [55].

Surgical treatment is often preferred to endovascular therapies for thrombosed aneurysms, for which recanalization after coiling is up to five times greater than in non-thrombosed aneurysms [54]. Recurrence of thrombotic aneurysms is multifactorial and likely related to their large or giant size, coil migration into the adjacent thrombus, and failure to endothelialize across the neck [41, 56].

Microsurgical approaches include direct clipping, thrombectomy with clip reconstruction, bypass with aneurysm occlusion, and trapping without bypass. The best surgical results were achieved with direct clipping, which is dependent on compliance of the neck of the aneurysm. Concentric and complete thrombotic aneurysms have noncompliant necks, and canalized thrombotic aneurysms do not have a defined neck. Eccentric thrombotic aneurysms or coiled thrombotic aneurysms with eccentric coil compaction were more likely to be amenable to direct clipping. For unclippable thrombotic aneurysms, better results were achieved with bypass and parent vessel occlusion over thrombectomy with clip reconstruction [55]. Observation is recommended for completely thrombosed aneurysms.

Fusiform or Dolichoectatic Aneurysms

Fusiform aneurysms comprise <0.1% of IAs [57]. They are defined based on appearance of fusiform arterial ectasia at a nonbranching site. In contrast to saccular aneurysms, fusiform aneurysms are more often found in younger patients and more frequently in males [57–59]. The proposed mechanism of formation starts with arterial dissection [58]. The acute dissecting type typically presents with rupture, whereas the chronic type presents with continual growth [60, 61]. Patients may be diagnosed incidentally due to compressive symptoms related to mass effect on the

brain or cranial nerves, thromboembolic events, or rupture. Patients with fusiform aneurysms associated with atherosclerosis, symptomatic presentation, or size >7 mm are at higher risk for progression [62]. A select group of patients can tolerate conservative management or anticoagulation alone with good results.

These lesions are extremely difficult to treat whether by endovascular techniques, microsurgery, or a multidisciplinary approach. Surgical treatment carries a morbidity and mortality rate of approximately 25% [57–59, 62]. Surgical options include clip reconstruction, clip wrapping, bypass and trapping, proximal or distal occlusion only, or excision with reanastomosis [57, 61].

Infectious Aneurysms

Infectious IAs (I-IAs) account for approximately 2% of all IAs [6, 63]. Infective endocarditis is responsible for 70-80% of infectious aneurysms, which typically occur in the distal MCA territory [63, 64]. Extravascular infections such as meningitis, cavernous sinus thrombophlebitis, cerebral abscess, subdural empyema, osteomyelitis of the skull, and sinus infections can also cause infectious aneurysms. These aneurysms typically occur in more proximal locations due to direct infectious spread at the base of the brain.

I-IAs are most commonly due to *Streptococcus* species or *Staphylococcus aureus*, but can be caused by a variety of bacterial, fungal, spirochetal, amebic, or viral pathogens [63, 65]. Pathologic changes show infiltration of the adventitia and tunica media by polymorphonuclear leukocytes, marked intimal proliferation, and destruction of the internal elastic lamina. They are typically friable and thin-walled with a wide or absent neck and are often not easy to separate from the brain parenchyma.

No trials exist comparing surgical and endovascular treatment of I-IAs; therefore, treatment recommendations are based on large case series and systematic reviews. Unruptured infectious aneurysms should initially be treated with appropriate antibiotic therapy for at least 4-6 weeks. Repeat imaging can be performed at 1-week intervals initially to determine stability or change in aneurysm size. Surgical or endovascular treatment should be pursued if an unruptured aneurysm increases in size despite antibiotic therapy, or if a patient presents with a ruptured aneurysm. Rupture of I-IAs may occur in as high as 75% of cases [64]. Morbidity and mortality from infectious aneurysms are 36% and 20%, respectively, though this is likely an underestimate due to death before presentation to neurosurgical attention [63]. If hospitalized for endocarditis, mortality in patients with unruptured I-IAs is 30% but is 80% if ruptured [66]. Fungal etiologies are more frequently fatal despite medical or surgical therapy [65].

Surgical clipping, trapping, or excision of an I-IA is preferred if a symptomatic hematoma is present, if eloquent territory is at risk from parent artery occlusion, or if inaccessible by endovascular means. Surgery offers the opportunity to perform an anastomotic procedure if eloquent, distal circulation will be affected by vessel sacrifice. If the I-IA is proximal to ineloquent brain and is on a sufficiently small vessel, the diseased parent artery may be sacrificed, particularly if a long segment of the artery is diseased, as in the case presented in Fig. 8.5 and Video 8.3.

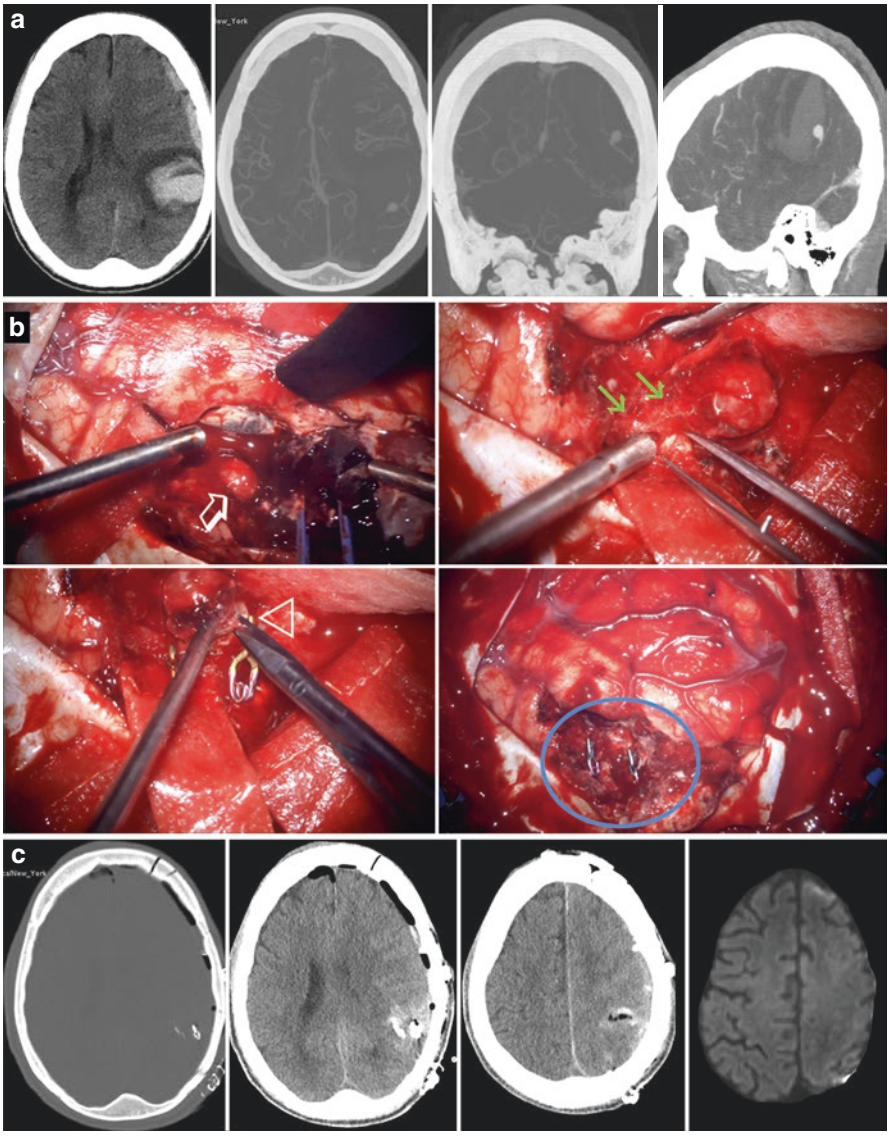

Fig. 8.5 An elderly gentleman with infectious endocarditis was admitted with a left frontoparietal intraparenchymal hemorrhage (IPH). (**a**) Axial noncontrast head computed tomography (CT) shows the IPH, while CT angiography demonstrated a M4 segment middle cerebral artery (MCA) aneurysm. (**b**) Sequential intraoperative photos show removal of the IPH, which unveils the dome of the aneurysm (open arrow). Further dissection reveals the diseased M4 branch proximal to the aneurysm (green arrows). The aneurysm is noted to involve 360° of the vessel lumen with no neck, which rendered clip reconstruction impossible. Aneurysm clips were applied and the aneurysm was excised (open arrowhead). After complete removal of the IPH and sacrifice of the diseased segment the brain is relaxed (blue circle). Shown in the accompanying video, but not here, primary reanastomosis was attempted, but the vessel was under too much tension and given that the branch supplied blood to brain posterior to the primary motor area, the decision was made to excise the aneurysm without reanastamosis. (**c**) Postoperative CT and magnetic resonance images show the clips, complete IPH evacuation, and no ischemic changes distal to the vessel sacrifice

Frameless stereotactic guidance is helpful when the aneurysm is buried within unusual locations. Open surgical treatment confers a higher rate of success than medical therapy and similar complication rate to EVT [64, 65]. EVT may be favored in cases in which the patient has severe cardiac dysfunction and anesthesia risks are too great.

Pseudoaneurysms

Pseudoaneurysms represent <1% of all IAs, but constitute as high as 20% of pediatric IAs [67, 68]. Pseudoaneurysm rupture is associated with mortality as high at 30% [69]. The most common cause of pseudoaneurysms is penetrating or blunt trauma. Other causes include iatrogenic (i.e., trans-sphenoidal surgery, sinus surgery, ventricular taps, stereotactic brain biopsy, endoscopic third ventriculostomy), infectious, radiation-associated, and connective tissue disease. False aneurysms or pseudoaneurysms are distinct from true aneurysms because they are caused by complete disruption of the vessel wall. A contained hematoma outside the vessel then develops a false lumen. The lack of well-formed walls in pseudoaneurysms makes both clipping and coiling difficult.

Despite advancements of EVTs, several limitations remain, including inaccessible distal locations, risk of intraprocedural rupture due to the lack of aneurysm wall, and coil extrusion through the false lumen leading to recurrence of the aneurysm. EVTs are most useful in locations where there are bony confines, like the petrous or cavernous segments of the internal carotid artery, and subacute pseudoaneurysms where the walls are more mature [70]. While the use of DAPT can be limiting, flow diversion has gained traction in the treatment of these lesions, particularly as they provide an intraluminal scaffold for endothelialization.

Many surgical techniques have been used to treat pseudoaneurysms including clipping, vascular reconstruction and revascularization, trapping, wrapping, or simple excision with or without arterial bypass. Direct clipping is possible only in 10–15% [63]. As previously stated, surgery is the preferred treatment strategy for ruptured pseudoaneurysms with associated large ICHs that need urgent evacuation.

Basic Principles of Surgery

Considerations for surgical approach to specific aneurysms are addressed elsewhere; however, the basic tenets of microsurgical clipping of IAs are reviewed in the ensuing text.

Anesthetic Considerations

Optimal management of the patient in the operating room depends on open communication between the surgical and anesthesia teams. Generally, the anesthetic used should be short acting, not reduce cerebral blood flow or increase intracranial pressure, and allow for careful blood pressure control. When using motor and somatosensory evoked potentials, total intravenous anesthesia may be necessary. The anesthesiologist should employ measures to decrease the intracranial pressure including mild hyperventilation, osmotic diuresis with mannitol, and monitoring output from the EVD if present. During temporary occlusion, the blood pressure should be augmented (i.e., goal mean arterial pressure [MAP] >90 mmHg) and burst suppression may be induced to limit the risk of cerebral ischemia [1, 6]. Systemic mild hypothermia is widely used during aneurysm surgery for brain protection. In rare circumstances, deep hypothermic circulatory arrest can prolong the duration of cessation of blood flow during the final aneurysm dissection and clip reconstruction. The anesthesiologist should have adenosine readily available to induce transient cardiac arrest in the event of an untimely intraoperative rupture. Finally, the anesthesia team should closely monitor glucose and electrolytes to prevent hyperglycemia, hyponatremia, or hyperkalemia. Typed and cross-matched blood should be available for all aneurysm surgery.

Positioning and Craniotomy

The chosen craniotomy should maximize surgical exposure and shorten the surgical corridor as much as possible. No matter the surgical approach, the head should be positioned above the heart and as neutral as possible to aid in venous drainage and prevent hyperemia. In addition, the surgeon should use gravity to enhance exposure where possible. Adequate bony exposure minimizes the need for fixed retractors and provides sufficient room to obtain distal and proximal control while providing sufficient degrees of freedom to maximize clip application angle.

Microsurgical Technique

Mannitol is given prior to skin incision to improve rheology and relax the brain to facilitate subarachnoid dissection. The intradural component of aneurysm surgery is completed using a surgical microscope to maximize illumination and magnification. The CSF cisterns are then opened sequentially from superficial to deep taking care not to breach the pia, which may be injurious to the surrounding brain. Microdissection is carried out both sharply, to cut recalcitrant bands of arachnoid, and with gentle

spreading using micro-forceps. Blunt dissection is generally directed along the long axis of the sulcus or fissure to be opened with force applied perpendicular to the brain surfaces (e.g., the Sylvian fissure is opened parallel to its overall course, either distal to proximal, or vice versa, but application of force applied by the tips and shaft of the micro-forceps are directed outward from the middle of the Sylvian fissure to gently separate the frontal and temporal lobes). Temporary clipping is a useful surgical adjunct to make final dissection of the aneurysm neck and clip application safer. In addition, temporary clipping softens large, turgid aneurysms to allow for complete reconstruction. Blind or excessive blunt dissection should be minimized or completely avoided, particularly around the aneurysm neck, to prevent tearing of the aneurysm, which may be challenging to repair. Permanent clips come in a variety of sizes and configurations, making clipping versatile and durable. In general, the simplest possible clipping strategy should be employed to maximize the likelihood of complete aneurysm occlusion while limiting the chance of parent or branch vessel compromise. When possible, the long axis of the clip(s) should be placed parallel to the long access of the parent vessel to limit vessel wall stress at the neck. In the face of intraoperative rupture, calm on the part of the surgeon is paramount. The field is cleared of blood with large-bore suctions, proximal and distal vessel control is achieved, neck dissection is completed, and permanent clips are applied. Cotton tamponade can be gently applied over the site of rupture, either using a suction or by applying light pressure with a fixed retractor to act as a "third hand." The surgeon must consciously avoid the temptation to prematurely "jam" permanent clips across the aneurysm before complete dissection and visualization is achieved. So doing may worsen the rent in the aneurysm and/or parent artery, or avulse small perforating arteries. Once the aneurysm is occluded, temporary clips are removed sequentially from distal to proximal. Each temporary clip is opened partially and the field is closely inspected to assure no residual bleeding before the clip is completely removed. Finally, the surgeon must be prepared for a variety of bailout options, such as cotton-clipping used in the setting of a neck tear, or bypass to revascularize permanently compromised vessels.

Conclusion

As endovascular technology advances, the pool of IAs treated surgically continues to ebb. However, the complexity of aneurysms referred for surgical treatment has increased as a result. Indubitably, the need for well-trained, capable cerebrovascular surgeons will continue into the future. IAs currently considered for microsurgical treatment in the current era include those in the very young, geometries not amenable to EVT, endovascular failures, patients intolerant to or noncompliant with DAPT required for EVT, ruptured aneurysms with associated ICH, very small aneurysms, large and giant aneurysms – particularly those with thrombus – and infectious aneurysms among others.

References

1. Connolly ES, Rabinstein AA, Carhuapoma JR, Derdeyn CP, Dion J, Higashida RT, et al. Guidelines for the management of aneurysmal subarachnoid hemorrhage. Stroke. 2012;43(6):1711–37.
2. Thompson BG, Brown RD Jr, Amin-Hanjani S, Broderick JP, Cockroft KM, Connolly ES Jr, et al. Guidelines for the management of patients with unruptured intracranial aneurysms: a guideline for healthcare professionals from the American Heart Association/American Stroke Association. Stroke. 2015;46(8):2368–400.
3. Lai LT, O'Neill AH. History, evolution, and continuing innovations of intracranial aneurysm surgery. World Neurosurg. 2017;102:673–81.
4. Cowan JA Jr, Ziewacz J, Dimick JB, Upchurch GR Jr, Thompson BG. Use of endovascular coil embolization and surgical clip occlusion for cerebral artery aneurysms. J Neurosurg. 2007;107(3):530–5.
5. Howard BM, Hu R, Barrow JW, Barrow DL. Comprehensive review of imaging of intracranial aneurysms and angiographically negative subarachnoid hemorrhage. Neurosurg Focus. 2019;47(6):E20.
6. Winn HR. Youmans and Winn neurological surgery. Philadelphia: Elsevier; 2017.
7. Gross BA, Smith ER, Scott RM, Orbach DB. Intracranial aneurysms in the youngest patients: characteristics and treatment challenges. Pediatr Neurosurg. 2015;50(1):18–25.
8. Sanai N, Quinones-Hinojosa A, Gupta NM, Perry V, Sun PP, Wilson CB, et al. Pediatric intracranial aneurysms: durability of treatment following microsurgical and endovascular management. J Neurosurg. 2006;104(2 Suppl):82–9.
9. Kakarla UK, Beres EJ, Ponce FA, Chang SW, Deshmukh VR, Bambakidis NC, et al. Microsurgical treatment of pediatric intracranial aneurysms: long-term angiographic and clinical outcomes. Neurosurgery. 2010;67(2):237–49; discussion 50.
10. Rinne J, Hernesniemi J, Puranen M, Saari T. Multiple intracranial aneurysms in a defined population: prospective angiographic and clinical study. Neurosurgery. 1994;35(5):803–8.
11. Juvela S. Risk factors for multiple intracranial aneurysms. Stroke. 2000;31(2):392–7.
12. Jabbarli R, Dinger TF, Darkwah Oppong M, Pierscianek D, Dammann P, Wrede KH, et al. Risk factors for and clinical consequences of multiple intracranial aneurysms: a systematic review and meta-analysis. Stroke. 2018;49(4):848–55.
13. Rinne J, Hernesniemi J, Niskanen M, Vapalahti M. Management outcome for multiple intracranial aneurysms. Neurosurgery. 1995;36(1):31–7; discussion 7–8.
14. Dong QL, Gao BL, Cheng ZR, He YY, Zhang XJ, Fan QY, et al. Comparison of surgical and endovascular approaches in the management of multiple intracranial aneurysms. Int J Surg (London, England). 2016;32:129–35.
15. Greving JP, Wermer MJ, Brown RD Jr, Morita A, Juvela S, Yonekura M, et al. Development of the PHASES score for prediction of risk of rupture of intracranial aneurysms: a pooled analysis of six prospective cohort studies. Lancet Neurol. 2014;13(1):59–66.
16. Wiebers DO, Whisnant JP, Huston J 3rd, Meissner I, Brown RD Jr, Piepgras DG, et al. Unruptured intracranial aneurysms: natural history, clinical outcome, and risks of surgical and endovascular treatment. Lancet (London, England). 2003;362(9378):103–10.
17. Molyneux A, Kerr R, Stratton I, Sandercock P, Clarke M, Shrimpton J, et al. International Subarachnoid Aneurysm Trial (ISAT) of neurosurgical clipping versus endovascular coiling

in 2143 patients with ruptured intracranial aneurysms: a randomised trial. Lancet (London, England). 2002;360(9342):1267–74.
18. Molyneux AJ, Kerr RS, Yu LM, Clarke M, Sneade M, Yarnold JA, et al. International subarachnoid aneurysm trial (ISAT) of neurosurgical clipping versus endovascular coiling in 2143 patients with ruptured intracranial aneurysms: a randomised comparison of effects on survival, dependency, seizures, rebleeding, subgroups, and aneurysm occlusion. Lancet (London, England). 2005;366(9488):809–17.
19. Chalouhi N, Penn DL, Tjoumakaris S, Jabbour P, Gonzalez LF, Starke RM, et al. Treatment of small ruptured intracranial aneurysms: comparison of surgical and endovascular options. J Am Heart Assoc. 2012;1(4):e002865.
20. Pierot L, Barbe C, Spelle L. Endovascular treatment of very small unruptured aneurysms: rate of procedural complications, clinical outcome, and anatomical results. Stroke. 2010;41(12):2855–9.
21. Brinjikji W, Lanzino G, Cloft HJ, Rabinstein A, Kallmes DF. Endovascular treatment of very small (3 mm or smaller) intracranial aneurysms: report of a consecutive series and a meta-analysis. Stroke. 2010;41(1):116–21.
22. Bruneau M, Amin-Hanjani S, Koroknay-Pal P, Bijlenga P, Jahromi BR, Lehto H, et al. Surgical clipping of very small unruptured intracranial aneurysms: a multicenter international study. Neurosurgery. 2016;78(1):47–52.
23. van Rooij WJ, Keeren GJ, Peluso JP, Sluzewski M. Clinical and angiographic results of coiling of 196 very small (< or = 3 mm) intracranial aneurysms. AJNR Am J Neuroradiol. 2009;30(4):835–9.
24. Li J, Su L, Ma J, Kang P, Ma L, Ma L. Endovascular coiling versus microsurgical clipping for patients with ruptured very small intracranial aneurysms: management strategies and clinical outcomes of 162 cases. World Neurosurg. 2017;99:763–9.
25. Zhao B, Xing H, Fan L, Tan X, Zhong M, Pan Y, et al. Endovascular coiling versus surgical clipping of very small ruptured anterior communicating artery aneurysms. World Neurosurg. 2019;126:e1246–e50.
26. Campi A, Ramzi N, Molyneux AJ, Summers PE, Kerr RS, Sneade M, et al. Retreatment of ruptured cerebral aneurysms in patients randomized by coiling or clipping in the International Subarachnoid Aneurysm Trial (ISAT). Stroke. 2007;38(5):1538–44.
27. Hayakawa M, Murayama Y, Duckwiler GR, Gobin YP, Guglielmi G, Viñuela F. Natural history of the neck remnant of a cerebral aneurysm treated with the Guglielmi detachable coil system. J Neurosurg. 2000;93(4):561–8.
28. Romani R, Lehto H, Laakso A, Horcajadas A, Kivisaari R, von und zu Fraunberg M, et al. Microsurgery for previously coiled aneurysms: experience with 81 patients. Neurosurgery. 2011;68(1):140–53; discussion 53–4.
29. CARAT Investigators. Rates of delayed rebleeding from intracranial aneurysms are low after surgical and endovascular treatment. Stroke. 2006;37(6):1437–42.
30. Owen CM, Montemurro N, Lawton MT. Microsurgical management of residual and recurrent aneurysms after coiling and clipping: an experience with 97 patients. Neurosurgery. 2015;62 Suppl 1:92–102.
31. Gurian JH, Martin NA, King WA, Duckwiler GR, Guglielmi G, Viñuela F. Neurosurgical management of cerebral aneurysms following unsuccessful or incomplete endovascular embolization. J Neurosurg. 1995;83(5):843–53.
32. Waldron JS, Halbach VV, Lawton MT. Microsurgical management of incompletely coiled and recurrent aneurysms: trends, techniques, and observations on coil extrusion. Neurosurgery. 2009;64(5 Suppl 2):301–15; discussion 15–7.
33. Zhang YJ, Barrow DL, Cawley CM, Dion JE. Neurosurgical management of intracranial aneurysms previously treated with endovascular therapy. Neurosurgery. 2003;52(2):283–93; discussion 93–5.

34. Tumialán LM, Zhang YJ, Cawley CM, Dion JE, Tong FC, Barrow DL. Intracranial hemorrhage associated with stent-assisted coil embolization of cerebral aneurysms: a cautionary report. J Neurosurg. 2008;108(6):1122–9.
35. Wan A, Jaja BN, Schweizer TA, Macdonald RL. Clinical characteristics and outcome of aneurysmal subarachnoid hemorrhage with intracerebral hematoma. J Neurosurg. 2016;125(6):1344–51.
36. Abbed KM, Ogilvy CS. Intracerebral hematoma from aneurysm rupture. Neurosurg Focus. 2003;15(4):E4.
37. Wheelock B, Weir B, Watts R, Mohr G, Khan M, Hunter M, et al. Timing of surgery for intracerebral hematomas due to aneurysm rupture. J Neurosurg. 1983;58(4):476–81.
38. Heiskanen O, Poranen A, Kuurne T, Valtonen S, Kaste M. Acute surgery for intracerebral haematomas caused by rupture of an intracranial arterial aneurysm. A prospective randomized study. Acta Neurochir. 1988;90(3-4):81–3.
39. Kodama N, Suzuki J. Surgical treatment of giant aneurysms. Neurosurg Rev. 1982;5(4):155–60.
40. Gonzalez NR, Duckwiler G, Jahan R, Murayama Y, Viñuela F. Challenges in the endovascular treatment of giant intracranial aneurysms. Neurosurgery. 2006;59(5 Suppl 3):S113–24; discussion S3–13.
41. Murayama Y, Nien YL, Duckwiler G, Gobin YP, Jahan R, Frazee J, et al. Guglielmi detachable coil embolization of cerebral aneurysms: 11 years' experience. J Neurosurg. 2003;98(5):959–66.
42. Sughrue ME, Saloner D, Rayz VL, Lawton MT. Giant intracranial aneurysms: evolution of management in a contemporary surgical series. Neurosurgery. 2011;69(6):1261–70; discussion 70–1.
43. Malisch TW, Guglielmi G, Viñuela F, Duckwiler G, Gobin YP, Martin NA, et al. Unruptured aneurysms presenting with mass effect symptoms: response to endosaccular treatment with Guglielmi detachable coils. Part I. Symptoms of cranial nerve dysfunction. J Neurosurg. 1998;89(6):956–61.
44. Cantore G, Santoro A, Guidetti G, Delfinis CP, Colonnese C, Passacantilli E. Surgical treatment of giant intracranial aneurysms: current viewpoint. Neurosurgery. 2008;63(4 Suppl 2):279–89; discussion 89–90.
45. Brinjikji W, Cloft HJ, Kallmes DF. Difficult aneurysms for endovascular treatment: overwide or undertall? AJNR Am J Neuroradiol. 2009;30(8):1513–7.
46. Mascitelli JR, Lawton MT, Hendricks BK, Nakaji P, Zabramski JM, Spetzler RF. Analysis of wide-neck aneurysms in the barrow ruptured aneurysm trial. Neurosurgery. 2019;85(5):622–31.
47. Fiorella D, Arthur AS, Chiacchierini R, Emery E, Molyneux A, Pierot L. How safe and effective are existing treatments for wide-necked bifurcation aneurysms? Literature-based objective performance criteria for safety and effectiveness. J Neurointerv Surg. 2017;9(12):1197–201.
48. Lawton MT, Lang MJ. The future of open vascular neurosurgery: perspectives on cavernous malformations, AVMs, and bypasses for complex aneurysms. J Neurosurg. 2019;130(5):1409–25.
49. Lawton MT, Quinones-Hinojosa A, Sanai N, Malek JY, Dowd CF. Combined microsurgical and endovascular management of complex intracranial aneurysms. Neurosurgery. 2003;52(2):263–74; discussion 74–5.
50. Choudhri O, Mukerji N, Steinberg GK. Combined endovascular and microsurgical management of complex cerebral aneurysms. Front Neurol. 2013;4:108.
51. Ponce FA, Albuquerque FC, McDougall CG, Han PP, Zabramski JM, Spetzler RF. Combined endovascular and microsurgical management of giant and complex unruptured aneurysms. Neurosurg Focus. 2004;17(5):E11.
52. Hoh BL, Putman CM, Budzik RF, Carter BS, Ogilvy CS. Combined surgical and endovascular techniques of flow alteration to treat fusiform and complex wide-necked intracranial aneurysms that are unsuitable for clipping or coil embolization. J Neurosurg. 2001;95(1):24–35.
53. Hanel RA, Spetzler RF. Surgical treatment of complex intracranial aneurysms. Neurosurgery. 2008;62(6 Suppl 3):1289–97; discussion 97–9.

54. Kim SJ, Choi IS. Midterm outcome of partially thrombosed intracranial aneurysms treated with guglielmi detachable coils. Interv Neuroradiol. 2000;6(1):13–25.
55. Lawton MT, Quiñones-Hinojosa A, Chang EF, Yu T. Thrombotic intracranial aneurysms: classification scheme and management strategies in 68 patients. Neurosurgery. 2005;56(3):441–54; discussion -54.
56. Molyneux AJ, Ellison DW, Morris J, Byrne JV. Histological findings in giant aneurysms treated with Guglielmi detachable coils. Report of two cases with autopsy correlation. J Neurosurg. 1995;83(1):129–32.
57. Anson JA, Lawton MT, Spetzler RF. Characteristics and surgical treatment of dolichoectatic and fusiform aneurysms. J Neurosurg. 1996;84(2):185–93.
58. Day AL, Gaposchkin CG, Yu CJ, Rivet DJ, Dacey RG Jr. Spontaneous fusiform middle cerebral artery aneurysms: characteristics and a proposed mechanism of formation. J Neurosurg. 2003;99(2):228–40.
59. Drake CG, Peerless SJ. Giant fusiform intracranial aneurysms: review of 120 patients treated surgically from 1965 to 1992. J Neurosurg. 1997;87(2):141–62.
60. Nakatomi H, Segawa H, Kurata A, Shiokawa Y, Nagata K, Kamiyama H, et al. Clinicopathological study of intracranial fusiform and dolichoectatic aneurysms : insight on the mechanism of growth. Stroke. 2000;31(4):896–900.
61. Safavi-Abbasi S, Kalani MYS, Frock B, Sun H, Yagmurlu K, Moron F, et al. Techniques and outcomes of microsurgical management of ruptured and unruptured fusiform cerebral aneurysms. J Neurosurg. 2017;127(6):1353–60.
62. Sacho RH, Saliou G, Kostynskyy A, Menezes R, Tymianski M, Krings T, et al. Natural history and outcome after treatment of unruptured intradural fusiform aneurysms. Stroke. 2014;45(11):3251–6.
63. Quiñones-Hinojosa A, Schmidek HH. Schmidek & Sweet operative neurosurgical techniques: indications, methods, and results. Philadelphia: Elsevier/Saunders; 2012.
64. Alawieh A, Chaudry MI, Turner RD, Turk AS, Spiotta AM. Infectious intracranial aneurysms: a systematic review of epidemiology, management, and outcomes. J Neurointerv Surg. 2018;10(7):708–16.
65. Barrow DL, Prats AR. Infectious intracranial aneurysms: comparison of groups with and without endocarditis. Neurosurgery. 1990;27(4):562–72; discussion 72–3.
66. Bohmfalk GL, Story JL, Wissinger JP, Brown WE Jr. Bacterial intracranial aneurysm. J Neurosurg. 1978;48(3):369–82.
67. Chen R, Zhang S, Guo R, You C, Ma L. Pediatric intracranial pseudoaneurysms: a report of 15 cases and review of the literature. World Neurosurg. 2018;116:e951–e9.
68. Zheng Y, Lu Z, Shen J, Xu F. Intracranial pseudoaneurysms: evaluation and management. Front Neurol. 2020;11:582.
69. Buckingham MJ, Crone KR, Ball WS, Tomsick TA, Berger TS, Tew JM Jr. Traumatic intracranial aneurysms in childhood: two cases and a review of the literature. Neurosurgery. 1988;22(2):398–408.
70. Lempert TE, Halbach VV, Higashida RT, Dowd CF, Urwin RW, Balousek PA, et al. Endovascular treatment of pseudoaneurysms with electrolytically detachable coils. AJNR Am J Neuroradiol. 1998;19(5):907–11.

Chapter 9
Cerebral Vasospasm

William Muñoz, Christopher J. Stapleton, and Aman B. Patel

Background

Throughout the day, as we rest or engage in demanding tasks, our brain activity levels vary widely, and neurons require more or less oxygen and glucose to support the processing demands of the moment. With changing energy demands, the large caliber arteries in our brains, such as the anterior or middle cerebral arteries and their main branches, rapidly change size in order to support their perfused brain territories with increased or decreased blood flow accordingly. This process is elaborate, with multiple chemical messengers entering the perivascular milieu and ultimately influencing the contractility of the arterial wall muscle layer. This muscle layer is also sensitive to a number of insults, such as physical impact to the vessel wall during trauma, or the chemical exposure to extravasated blood and blood breakdown products during subarachnoid hemorrhage. In particular, it has been shown that cerebral arteries can undergo a persistent and severe vasoconstriction in response to such insults, a process termed "vasospasm." It is hypothesized that under these pathological conditions, arterial vasoconstriction is an important strategy to prevent extravasation and promote homeostasis. However, when vasospasm is severe and/or persistent, it can affect brain perfusion and result in neuronal death, or strokes.

The following section explores the clinical and experimental evidence for cerebral vasospasm, as well as outlines the factors associated with its development. In particular, we will emphasize cerebral vasospasm following subarachnoid hemorrhage, as this constitutes a process that has been extensively studied and provides some clues as to the pathological causes of this phenomenon and opportunities for intervention.

W. Muñoz · C. J. Stapleton · A. B. Patel (✉)
Department of Neurosurgery, Massachusetts General Hospital and Harvard Medical School, Boston, MA, USA
e-mail: wmunozmiranda@mgh.harvard.edu; cstapleton@mgh.harvard.edu; ABPATEL@mgh.harvard.edu

J. R. Mascitelli, M. J. Binning (eds.), *Introduction to Vascular Neurosurgery*,
https://doi.org/10.1007/978-3-030-88196-2_9

Discovery

Although cerebral vasospasm following SAH was first clinically demonstrated during the early 1950s, there were a number of clinical observations that suggested its existence, which date back to the late 1890s.

In particular, it was noted that non-comatose patients who survived the initial ictus from a ruptured aneurysmal SAH could deteriorate days later, with development of new neurological deficits, such as paresis, aphasia, or apraxia [1, 2]. These delayed neurological symptoms often fit known stroke syndromes, which in 75% of cases could be attributed to functional impairments of the middle cerebral artery territory, and in approximately 25% of cases to the anterior cerebral artery territory. Indeed, if these patients succumbed to this second phase of their disease, pathological examination of their brains revealed not only the expected blood clot or hemosiderin staining from SAH and associated ruptured aneurysms, but also in 30% of cases, there were strokes of large cortical territories not necessarily fitting the territory supplied by the affected artery [3].

This delayed onset of neurological deficits, or delayed cerebral ischemia (DCI), was noted to occur in one-third of patients after SAH, typically 4–14 days after aneurysm rupture [4–6]. Moreover, these postmortem observations of infarctions of cortical territories often far away from the ruptured aneurysm fueled the notion that while the initial ictus would certainly limit cerebral perfusion focally near the rupture site, subsequent vasospasm of affected cerebral arteries could explain the expansion of the brain territories at risk for stroke. In 1951, Ecker and Riemenschneider published a landmark paper in which they demonstrated for the first time by serial angiography that the caliber of arteries could change over time after SAH [7]. These findings provided evidence of vasospasm near the aneurysmal rupture site, and the methodology became the gold standard for tracking the development of vasospasm.

Angiographic Appearance and Predictors of Vasospasm After SAH

In 70% of patients after SAH, persistent angiographic narrowing of cerebral arteries has been observed. Similar to the clinical timeline of DCI, vasospasm generally starts 3–4 days after aneurysm rupture, peaks at 7–10 days, and resolves by 14–21 days [8, 9]. Importantly, those with the thicker and more widespread subarachnoid clot (modified Fisher scale 2 or higher) on their initial head CT scans are more likely to suffer vasospasm in the days following SAH, whereas in the absence of blood on initial scan (with SAH diagnosed by lumbar puncture) vasospasm is unlikely to happen.

Moreover, it was found that while subarachnoid blood hyperintensities normalize on head CT scans between days 4 and 22 post-SAH, persistent blood on scan by

day 4 was associated with future development of vasospasm [10, 11]. Of note, 83% of the patients with basal cisterns hyperintense blood and in 78% with Sylvian fissure blood develop clinical vasospasm. These investigators concluded that the persistence of the subarachnoid blood clot beyond 5 days post-SAH is likely indicative of either a large initial hemorrhage and/or impaired clearance of red blood cells (RBCs), and more importantly that prolonged exposure to the blood clot could promote the development of vasospasm.

Cerebral vasospasm has been characterized by employing serial catheter angiography, comparing the caliber of affected arteries to that observed in prior imaging, as well as to that observed in the contralateral vasculature. These studies have led to the classification of the degree of vasospasm from severe (more than 50% reduction in vessel caliber) to mild (25–50% reduction in vessel caliber), as well as spatially from diffuse, multisegmental, to localized [12]. Importantly, more severe degrees of vasospasm are increasingly associated with DCI and the development of strokes on serial head CT scans, with mild vasospasm resulting in radiographic strokes in 3% of cases, while moderate in 10% and severe in 46% of cases [5, 13]. Similarly, the mortality rates for patients with higher degrees of vasospasm increase up to 41–45% in patients with severe vasospasm [14].

Other Imaging Modalities for Detecting Vasospasm

While catheter angiography remains the gold standard for detecting and best characterizing vasospasm, the diagnostic value of multiple other noninvasive imaging modalities has been investigated [15, 16], in particular CT angiography (CTA). When compared to catheter angiography, the agreement between observation regarding vasospasm presence and degree was 68% for independent observers. CTA was more in agreement with catheter angiography when there was no observed vasospasm (86%) and when there was severe vasospasm (64%), but was associated with more false negatives when there was mild vasospasm (20%), which might be related to the lower resolution for evaluating blood vessel morphology of CTA compared to catheter angiography (see Management section). A more recent study has shown an accuracy for CTA of 87.0–97.5% and negative predictive value of 95.0–99.5%, compared to catheter angiography [17].

Another imaging modality that has been investigated is transcranial Doppler sonography (TCDs). This is a technique in which ultrasound waves are used to insonate the proximal portion of middle and anterior cerebral arteries in order to evaluate their flow velocities. TCDs were introduced to the armamentarium to assess vasospasm in SAH patients in 1982 [18] under the hypothesis that as the caliber of arteries decreases due to vasospasm, their blood flow velocity should increase. In theory, if a cerebral artery diameter is halved by vasospasm, the velocity of blood flow should increase by 400%. Indeed, a significant inverse relationship between MCA diameters and flow velocities has been described [19]. The mean flow velocity is often trended, as it accounts for systolic/diastolic pressure variations, and thus

is more reliably compared over time [8]. While in healthy subjects, a range of mean velocities 33–90 cm/sec has been described for the middle cerebral artery, for patients with SAH flow velocities are typically elevated by day 5 post-SAH, with usually maximum velocities recorded days 9–13, before normalizing within the following 2 weeks [18]. Notably, rapid increases in flow velocities often precede clinical deterioration due to vasospasm, in particular if velocities increase >50 cm/sec/day [18, 20, 21]. This approach has been reported to have over 95% sensitivity for severe angiographic vasospasm [22]. It is important to highlight that although TCDs can be easily and noninvasively performed by the bedside, its main limitations are inability to diagnose critical vasospasm (>70% diameter reduction) at which point flow velocities will be reduced, as well as inability to insonate distal arterial territories (only accessible large arteries can be visualized) or patients with thick temporal bones. There can also be false positives that can occur when blood pressure is augmented (see Management).

Given the limitations of noninvasive modalities for detecting vasospasm, a retrospective study investigated whether a combinatorial approach could increase the accuracy of noninvasive monitoring. It was found that in a cohort of patients with SAH undergoing concomitant catheter angiography, CTA, TCDs, and CT perfusion protocols (most commonly used for diagnosing stroke), the most accurate combination (93%) was narrowing observed in CTA and mean transit times >6.4 s on CT perfusion [23].

Epidemiology

Approximately one in 10,000 individuals suffers the rupture of an aneurysm and associated SAH each year. These patients are acutely sick with a case fatality close to 40%, and if they survive the initial ictus, their neurological status remains tenuous in part due to the development of DCI from cerebral vasospasm [9]. Approximately two-thirds of patients with SAH will exhibit angiographic arterial narrowing consistent with vasospasm within 3–14 days after the initial rupture [24]. Due to several physiological factors (which will be discussed in the Management section), only one-third of these patients will experience clinical signs of neurological deterioration due to vasospasm [25, 26]. This incidence might be even higher on posterior circulation aneurysmal SAH, for which some studies have found close to 75% of patients developing symptomatic vasospasm (although with perhaps a more protracted course, peaking on the second week post-SAH; [27]).

With increased ease of diagnosis, more accessible and expedited surgical management of ruptured aneurysms, and better neurocritical care, this picture has improved significantly with a decrease in mortality by 50% over the past two decades [28]. However, the development of vasospasm unfortunately continues to double the mortality rate in a susceptible portion of SAH patients [26]. In particular, older patients have a tendency to present with thicker subarachnoid clot on admission CT scans, and although no age-related differences have been appreciated in

terms of overall incidence of angiographic vasospasm, symptomatic vasospasm is more frequently reported in the older age group [29]. Angiographic vasospasm is also more common in females, who also tend to have significantly poorer outcomes [30]. Furthermore, significant association has been found between symptomatic vasospasm and cigarette smoking after aneurysmal SAH [31–33].

Pathophysiology

As shown in Fig. 9.1, several physical, chemical, and cellular processes are initiated after the rupture of an aneurysm in the subarachnoid space. Altogether these processes are thought to be responsible for the ensuing cerebral vasospasm. The following section details our understanding of these processes and points at avenues for potential new therapies.

Blood Extravasation and Local Increases in Subarachnoid Space Pressure

Following the rupture of a cerebral aneurysm, up to 250 mL of blood quickly accumulates in the subarachnoid space over seconds to minutes, until a clot plugs the rupture site. One immediate consequence of this accumulation of blood is an increased pressure in the subarachnoid space, which directly impacts adjacent arteries. Early experiments in animal models (in cats, dogs, and monkeys) and humans showed that this increased local pressure affects the arterial wall and causes vasospasm. In these studies, a gentle stroke was delivered to any vessel of the circle of Willis, which caused a localized narrowing of the tested vessel [34–38].

Interestingly, longer application of the mechanical stimulus, which mimics the persistent presence of blood clot on the subarachnoid space in SAH, not only prolonged the duration of the observed vasospasm, but also resulted in spread of vasospasm distally from the stimulated site. These effects could be reversed by topical application of papaverine and procaine, which implied two mechanisms: stimulating contraction at the level of the muscular layer, as well as indirectly by activating the nerve terminals surrounding these arteries [34–38].

Additionally, it has been hypothesized that the exposure of perivascular nerve terminals to degrading RBCs and hemoglobin (see next subsection) can trigger a denervation of cerebral arteries, which then lack their normal modulatory tone set by various catecholamines, acetylcholine, vasoactive intestinal polypeptide, and substance P [39, 40]. Over time, it is thought that denervated arteries post-SAH in the context of vasospasm become progressively refractory to the vasoconstrictor and vasodilator actions of these numerous neuromodulators and neuropeptides [41].

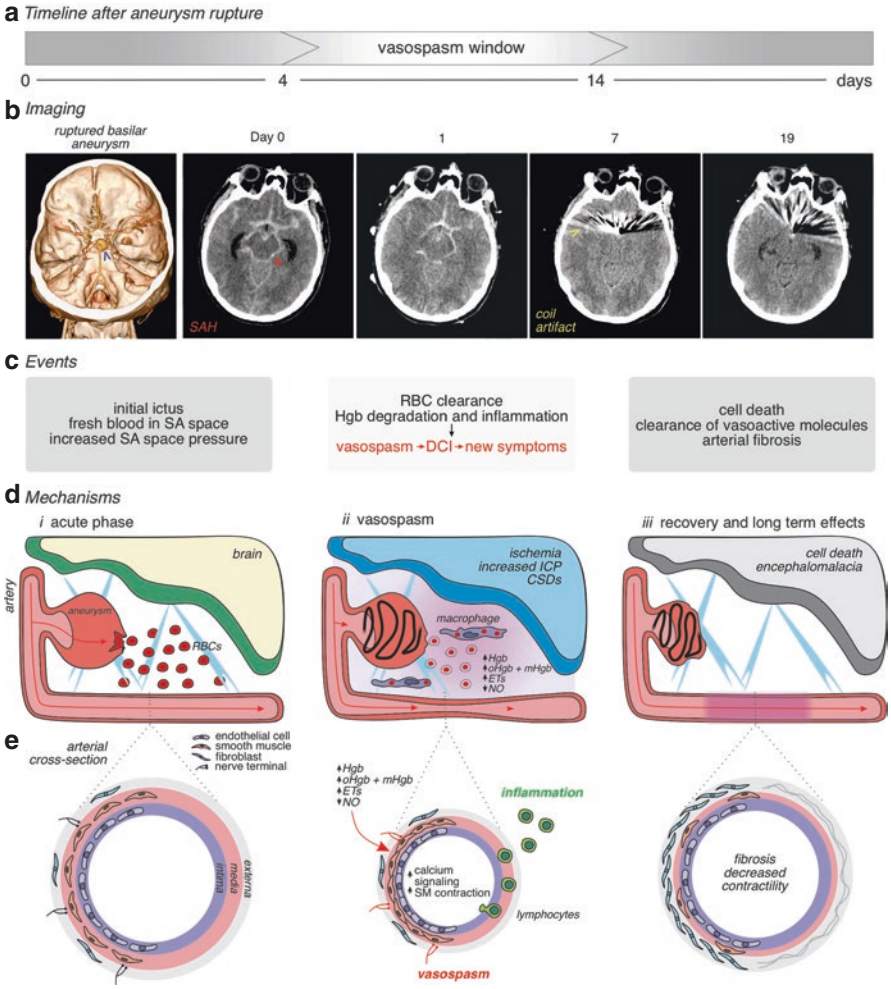

Fig. 9.1 Spatiotemporal dynamics and mechanisms of cerebral vasospasm following SAH. (**a**) The timeline for development of cerebral vasospasm following aneurysmal rupture and SAH is predictable, with most patients experiencing symptoms related to vasospasm within days 4–14 after SAH. (**b**) As specified in the Pathophysiology section, this timeline relates to the clearance of the subarachnoid blood clot following aneurysmal rupture, demonstrated in the head CT series as decreasing intensity of blood products (red arrow, SAH) on major cisterns and fissures over time (second to fifth panel from left to right). In this scan series, the blood intensities on the patient's ambient cistern decreases by 19% on post-SAH day 1, 52% on day 7, and 78% on day 19. Coil artifact (yellow arrow) is seen on the scans on days 7 and 19. This patient had a ruptured basilar tip aneurysm (first panel, reconstruction of CT angiogram on skull base, black arrow points to aneurysm), and developed symptomatic vasospasm, which was treated with intra-arterial verapamil (Fig. 9.3), with recovery back to neurological baseline by discharge. The changes in ventricular size observed in this series relate to the placement of an external ventricular drain on admission, and subsequent management and weaning of this drain. (**c**–**e**) Several cellular, physical, and chemical events after SAH are responsible for the development of cerebral vasospasm. (**d***i*) During the

RBC Clearance, Hemoglobin, and Its Vasoactive Degradation Products

Following the rupture of a cerebral aneurysm, fresh blood gets in contact with cerebrospinal fluid (CSF) in the subarachnoid space, and the extravasated RBCs begin a much faster degradation process than inside blood vessels. The average survival time of RBCs in the subarachnoid space is estimated around 1 week, as opposed to their natural life of 4 weeks inside vessels. Their degradation is aided by a number of cellular and chemical processes that while attempting to clear the blood clot, also release several vasoactive substances that have been implicated in the development of vasospasm.

The role of extravasated RBC clearance and hemoglobin degradation in vasospasm was initially inferred from a number of clinical and experimental observations. On the one hand, as discussed in the Background section, the key prognostic factor for vasospasm is the presence of thick, widespread subarachnoid clot on the initial head CT scan. It was also found that factors shortening the exposure to the blood clot tend to decrease vasospasm incidence, while conversely, the use of antifibrinolytic drugs to prolong the clot exposure of arteries tends to increase the incidence of vasospasm [8]. As the hemolysis of extravasated blood ensues, the concentration of hemoglobin in the subarachnoid fluid increases, and as hemoglobin degrades, its known vasoconstrictive by-products also increase in concentration, which has been hypothesized to trigger vasospasm.

An initial test of this hypothesis was carried out by Echlin who showed the induction of acute vasospasm of monkey cerebral arteries in response to the application

acute phase, fresh blood from the ruptured aneurysm enters the subarachnoid space, increasing the pressure on this space, which triggers early mechanical vasospasm. (**d***ii*) Then, during the vasospasm time window, the persistent blood clot undergoes breakdown by macrophages, which releases hemoglobin (Hgb), with subsequent accumulation of its vasoactive degradation products oxyhemoglobin (oHgb) and methemoglobin (mHgb), two potent vasoconstrictors. Endothelial injury due to initial aneurysmal rupture and subsequent inflammation releases endothelins (ETs) and decreases nitric oxide (NO) signaling, which promotes vasospasm and limits the endogenous vasodilatory response, respectively. Together with these local subarachnoid space processes, the nearby brain parenchyma experiences ischemia due to decreased perfusion by vasospastic arteries, which leads to further increases in intracranial pressure (decreasing the effective cerebral perfusion pressure), and contributing to the generation of cortical spreading depolarizations (also thought to arise due to changes in the chemical composition of cerebrospinal fluid). The arterial wall as seen in associated panels in (**e**) is vasoconstricted by effect of the various effectors described above on the endothelial smooth muscle and increased intracellular calcium signaling. These effectors, in particular Hgb, can also stimulate nerve terminal on the arterial externa, which release catecholamines and further arterial vasoconstriction. The arterial wall is also infiltrated by lymphocytes and other peripheral white blood cells, which initiate inflammatory cascades that also are thought to promote and prolong vasospasm. (**d***iii*) Over time, as the vasospasm window comes to an end, as the blot clot is completely resorbed, the CSF composition normalizes and inflammation subsides, leaving behind structural changes to the arterial wall that limits its contractility, including denervation and fibrosis, as seen in the associated panel in (**e**). If the vasospasm is severe enough and/or untreated, neuronal death and strokes result in persistent neurological deficits, coma, and/or death

of fresh blood in an open arachnoid space [38]. This was further substantiated in a dog basilar artery preparation, which was exposed to a blood-CSF mixture incubated for several days, with maximal arterial vasoconstriction after incubation for 7 days [42]. In agreement with these data and the observed clinical time course of vasospasm, it has been shown in biochemical studies that the breakdown of RBCs peaks around day 7 post-SAH [43, 44]. This has been further investigated in SAH patients by serial lumbar punctures, in which elevated hemoglobin concentrations have been found starting 2 hours post-SAH and up to 26 days post-SAH. In particular, further biochemical analysis of hemoglobin by-products has revealed that CSF containing elevated levels of both oxyhemoglobin and methemoglobin – two vasoconstrictors – coincides with the occurrence of vasospasm in 64% of cases [45].

An important consideration is that extravasated RBCs seem to activate the complement cascade, which is ultimately responsible for RBC lysis and release of hemoglobin into the subarachnoid space. Indeed, CSF from patients with SAH exhibit elevated complement levels. Moreover, the depletion of complement in animal models, which presumably promotes RBC clearance through pathways other than lysis, reduces the incidence of vasospasm after SAH [46].

Another circulating factor that could potentially affect the vasoactive influence is haptoglobin, which is known to bind and potentially neutralize the vasoactive properties of hemoglobin. Haptoglobin occurs in several allelic forms in humans, with different affinities for hemoglobin, and therefore different degrees of protective benefit in reducing the vasoactive effect of hemoglobin after SAH. Indeed, both animal model and human studies had observed different propensities to angiographic vasospasm, as well as degree of inflammation in the subarachnoid space after SAH, depending on the expressed haptoglobin allele of the subject [47, 48].

Other Peripheral Blood Cellular Players and Their Inflammatory Processes

Besides RBCs, several peripheral blood cell types enter the subarachnoid space following SAH, and participate in the clearance of the blood clot, as well as in the repair of the damaged leptomeningeal tissue. During the initial phase, neutrophils accumulate in the subarachnoid space, reaching a maximum within 1 day and then start to dissipate within the next day or so [44, 49]. While neutrophils return to circulation, macrophages tend to persist for up to 2–4 weeks after SAH, as they are largely responsible for clearing RBCs and other cellular debris from their hemolysis [50]. Inflammatory cells have also been observed to infiltrate the walls of vasospastic arteries, where they persist for longer periods of time, with associated local release of immunoglobulins and other inflammatory molecules [51]. While the radiographically observed vasospasm resolves with time, the inflammation within the arterial wall causes fibrosis and reduced compliance, with long-term consequences ([52]; see next subsection).

As RBC lysis ensues, the release of hemoglobin into the subarachnoid space can induce oxygen free radical reactions, further inflammation, and endothelial injury, leading to increased expression and release of endothelins, as well as reduced levels of nitric oxide [53]. Indeed, endothelins, peptides generated by endothelial cells and astrocytes with long-lasting vasoconstrictive effects on cerebral vessels, have been shown to have significant elevations in the CSF of SAH patients, and with highest elevations in those developing vasospasm [54, 55]. Furthermore, nitric oxide signaling, a vasodilator action on the cerebral blood vessels, as measured by the concentration of its metabolites in CSF, appears to be lower in patients with vasospasm on post-SAH days 7–9 [56]. The roles of these two molecular players have been investigated in human clinical trials (as will be discussed in the following section).

Besides endothelins and nitric oxide, several other inflammatory markers have been found on the CSF and/or the serum of patients with SAH with varying associations with the development of radiographic vasospasm and DCI [57, 58]. The role and possible therapeutic utility of these other molecular cascades remains under investigation.

Remodeling of the Arterial Wall

Immediately after endothelial injury, cerebral arteries undergo vasoconstriction in a response that has been thought to prevent blood loss and promote clot formation [59, 60]. The cellular and molecular changes detailed above are thought to ultimately prolong this vasoconstricted phase and potentially remodel cerebral arteries.

These questions have been explored on postmortem examination of cerebral arterial pathological specimens from patients with angiographic vasospasm post-SAH. In these studies, contraction of the medial smooth muscle was observed at the onset of vasospasm, followed by medial thickening, corrugation of the internal elastic lamina, intimal edema due to endothelial injury, and thrombus formation within the subsequent 1 and 2 weeks, with eventual reduction of smooth muscle cells and fibrous thickening of the intima thereafter [61].

Other Contributing Processes That Can Have an Interplay with Vasospasm

Besides hemoglobin, RBC lysis alters the electrolytes composition of CSF in the affected subarachnoid space, which has been associated with the electrographic phenomenon observed in patients with SAH known as cortical spreading depolarization. Notably, in a cohort of SAH patients who developed DCI, the appearance of cortical spreading depolarization on electrocorticography and angiographic vasospasm coincided in space and time. Furthermore, the patient with cortical spreading

depolarization lasting >1 hour developed ischemic changes on subsequent head CTs or MRI [62]. It has been hypothesized that cortical spreading depolarizations and vasospasm can represent a self-reinforcing cycle, in which the vasospasm-triggered ischemia can fuel neuronal depolarization and death, while depolarized neurons can also release several vasoactive neuropeptides that can worsen and spread the vasospastic territory.

Moreover, as a result of severe vasospasm, hemostasis can occur at the points of arterial narrowing and result in thrombus formation, further promoting ischemia and vasoconstriction [63, 64]. Indeed, postmortem brains of SAH patients who developed DCI showed a pathological correlation of increased thrombus formation on the previously identified regions with radiographic vasospasm and/or strokes. The development of these thrombi seemed to correlate as well with the onset of DCI [65].

Management

Interestingly, while two-thirds of patients with SAH exhibit angiographic arterial narrowing consistent with vasospasm, only 50% of those patients develop DCI. This fact speaks to the importance of other local and systemic factors that can affect cerebral perfusion and compensate for the development of vasospasm [5, 13, 66]. As such, DCI symptoms and associated strokes are thought to occur only when vasospasm meets unfavorable pre-existing collateral and anastomotic blood flow in the brain, high cerebral metabolic demand, and/or low systemic blood pressure. This is an important topic with therapeutic implications. In general, the management of patients with SAH at risk of developing DCI is centered in optimizing the balance of cerebral blood perfusion and cerebral metabolic demands.

This balance can be particularly challenging to attain in this patient population in which there is often multisystem involvement, in particular cardiopulmonary dysfunction, due to anoxic injury at the time of presentation from loss of consciousness, and subsequent heightened sympathetic activity and systemic inflammation [67, 68]. The following section explores what we have learnt so far about optimizing the medical management of the SAH patient population, in order to minimize the chances of DCI and prevent permanent brain infarction in the face of clinical vasospasm.

Diagnosis

As noted in the preceding sections, DCI after SAH occurs most commonly on days 3–14 after the initial ictus, with only 5% of cases happening after day 10. During this window of time, the neurological status of SAH patients is frequently assessed in intensive care units. In spite of the highest and most specialized level of care that

can be provided, the detection of DCI remains a challenge, in particular in patients with a poor neurological status after SAH [69].

Most often, vasospasm presents clinically in the awake, interactive SAH patient as a recrudescence of the initial headache which was getting better in the preceding days [70]. In the setting of non-optimal systemic factors, such as hyponatremia and/or hypovolemia, further neurological deficits can emerge over hours or days, in patterns that are expected in accordance with the compromised brain territories with poor perfusion due to vasospasm. If untreated or refractory to medical or surgical management, the neurological deficits can give way to a permanent disability as the stroke process is completed.

It is the clinical standard in major academic medical centers, to take this clinical picture together with careful monitoring of patients at high risk for developing vasospasm with daily TCDs, continuous EEG, fluid balance, and frequent sodium level checks, in order to determine the likelihood of symptomatic vasospasm (see Fig. 9.2). While empiric medical management (as detailed below) should be rapidly instituted in the acute setting, further evaluation for vasospasm and potential therapeutic interventions requires angiographic imaging, as well as evaluation for radiographic stroke development.

Triple H

In 1976, Kosnik and Hunt described a series of SAH patients who developed acute onset of neurological symptoms (DCI) that correlated with drops in systemic blood pressure, and which could be resolved following interventions that restored their blood pressure. In their management scheme, they employed fluid resuscitation and vasopressors to sustain the elevated blood pressure [71]. These concepts conformed the basis for the famous "Triple H" therapy, or hypertensive hypervolemic hemodilution, for SAH patients that were considered at risk of developing vasospasm.

Hypovolemia and relative hypotension can occur due to a number of reasons in these acutely ill patients, including bed rest with peripheral pooling of blood, supine diuresis, and iatrogenic blood loss. Besides their effects on limiting cerebral perfusion, these two factors can lead to hemoconcentration, increasing blood viscosity and further decreasing cerebral blood flow. Altogether, the aim of Triple H therapy is to optimize these three parameters, in order to promote cerebral perfusion and overcome vasospasm.

In practice, SAH patients at risk of developing DCI are maintained euvolemic. Current recommendations are to refrain from using prophylactic hypervolemia, induced hypertension, or hemodilution [72, 73]. If DCI develops, first line treatment for reversing the neurological deficits is the optimization of cerebral perfusion pressure with volume expansion and/or pharmacologically induced hypertension, with target systolic blood pressure above 150 mmHg [74]. The optimal systolic blood pressure in this scheme is typically the lowest blood pressure tolerated by the patient, at which the ischemic symptomatology resolves [71, 75–77]. Although

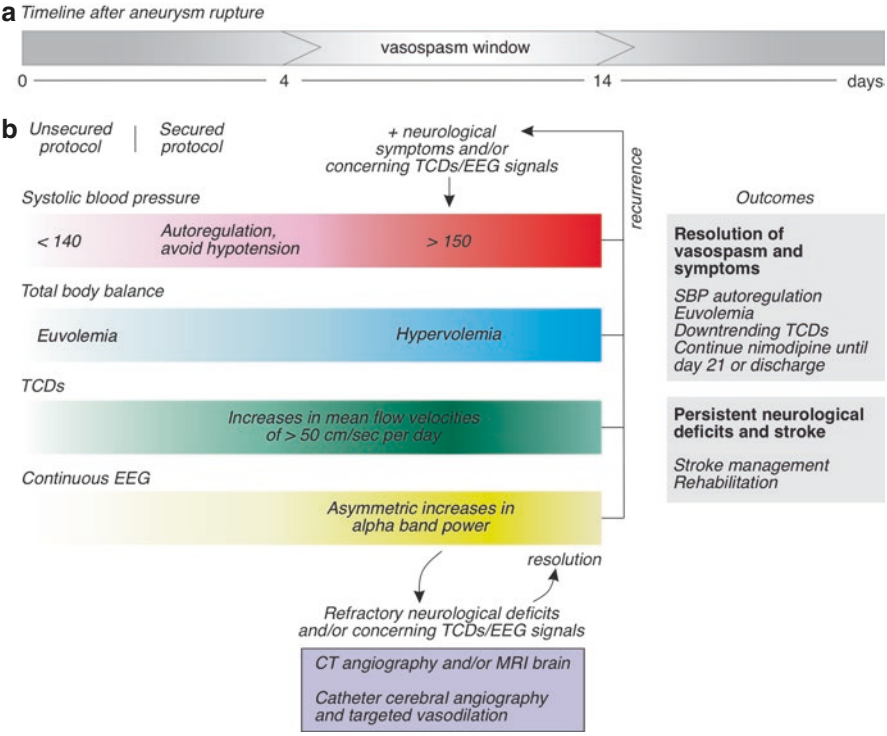

Fig. 9.2 Surveillance and therapeutic algorithm for vasospasm after SAH. A general surveillance and therapeutic algorithm for vasospasm after SAH, followed at our institution, is presented in this figure, and further discussed in the Management section. (**a**) This algorithm takes into consideration the timeline of pathophysiological changes after SAH discussed in Fig. 9.1. (**b**) On admission, patients with ruptured, unsecured aneurysms are monitored carefully in the neurocritical intensive care unit setting. Their systolic blood pressure is continuously measured via an arterial line, and kept under 140 mmHg until the ruptured aneurysm is secured (via coiling or clipping), in order to minimize expansion of the subarachnoid hemorrhage. Their total body balance is recorded, and initially input and output are matched, to prevent both hypovolemic cerebral hypoperfusion, while also minimizing volume overload in these critically ill patients (often with cardiopulmonary compromise). These patients undergo daily TCDs of major cerebral arteries and EEG (if their Hunt & Hess classification is greater than 3 and/or their modified Fisher scale is greater than 2), and are started on standard dosing of nimodipine. If comatose on initial presentation, these patients also undergo placement of an external ventricular drain to manage their ICPs and optimize their cerebral perfusion pressures. Once the aneurysm is secured, their systolic blood pressures are allowed autoregulation, while avoiding relative hypotension. Arterial flow velocities as measured by TCD are trended for increases in mean flow velocities >50 cm/sec per day, which are concerning for vasospasm. Likewise, EEG is continuously recorded and analyzed for asymmetric increases in alpha band power, which are thought to correlate with tissue ischemia. This TCD/EEG information is integrated with clinical findings from the neurological examination of these patients (which is limited on comatose patients). If symptomatic vasospasm is suspected (after ruling out other potential causes of exam changes, as discussed in the Management section), hypervolemic and/or pharmacological hypertension are attempted, which can often resolve the neurological symptoms and/or findings. If refractory, patients undergo further evaluation for vasospasm with CTA head, MRI brain, and/or catheter cerebral angiography, which can corroborate vasospasm in expected

hemodilution is advocated by Triple H therapy, the optimal hemoglobin concentration is unknown, and current guidelines actually recommend blood transfusions when hemoglobin levels are <7 g/dl in patients without DCI, or <10 g/dl in patients with DCI, in order to optimize the oxygen carrier capability of blood [78].

The efficacy of Triple H therapy in improving cerebral perfusion was investigated in SAH patients undergoing different aspects of the therapy. Using PET scans, this study found that fluid augmentation, induced hypertension, or transfusion of erythrocytes independently improved oxygen delivery. However, induced hypertension was the most effective intervention among the three, and blood transfusions were effective only when hemoglobin levels were <9 g/dl [79].

While hypervolemic hypertension represents a state in which neurologic deficits that are attributable to vasospasm can be reversed, it can also have potential systemic adverse consequences. Therefore, it should be employed with an understanding of the patient's systemic disease burden, as well as the viability of the brain tissue that it is intended to rescue (i.e., strokes have not been completed). Among the potential consequences that this medical approach can have in the brain of these patients are exacerbations of cerebral edema and intracranial hypertension, as well as systemically leading to pulmonary edema, acute respiratory distress syndrome, cardiac arrhythmias, and myocardial infarction [80].

Systemic Prophylactic Therapies

Several pharmacological agents to prevent vasospasm and DCI in SAH patients have been tested in randomized controlled trials. A meta-analysis of these studies showed that while often the drugs tested can reduce the incidence of angiographic vasospasm, clinical outcomes are unfortunately not benefited by the intervention [81]. A notable exception is the drug nimodipine, which perplexingly improves outcomes, but does not have a significant effect on radiographic vasospasm [9].

Nimodipine is an L-type voltage-gated calcium channels blocker, which produces preferential arterial dilation, and has been shown to increase cerebral blood flow in healthy individuals after a single oral dose [82]. Based on the notion that cerebral arterial smooth muscle depends more heavily on calcium signaling for their

brain territories that correspond to the observed neurological deficits and/or abnormal TCD/EEG signals. The endovascular approach affords access for intra-arterial delivery of vasodilators. If successful, this rescue therapy can lead to resolution of neurological deficit(s) and normalization of TCDs/EEG findings. Symptomatic vasospasm can unfortunately recur, and the patient could even cycle through medical and rescue endovascular interventions on a daily basis during the vasospasm window. As the vasospasm window closes, successfully treated patients autoregulate their systolic blood pressure, maintain an even total body fluid balance, continue nimodipine until day 21 or discharge (whichever happens first), and might need rehabilitation for any deficits due to the initial ictus. However, if their vasospasm-related neurological deficits persist, with corresponding strokes on MRI brain, their care shifts predominantly to stroke management and rehabilitation

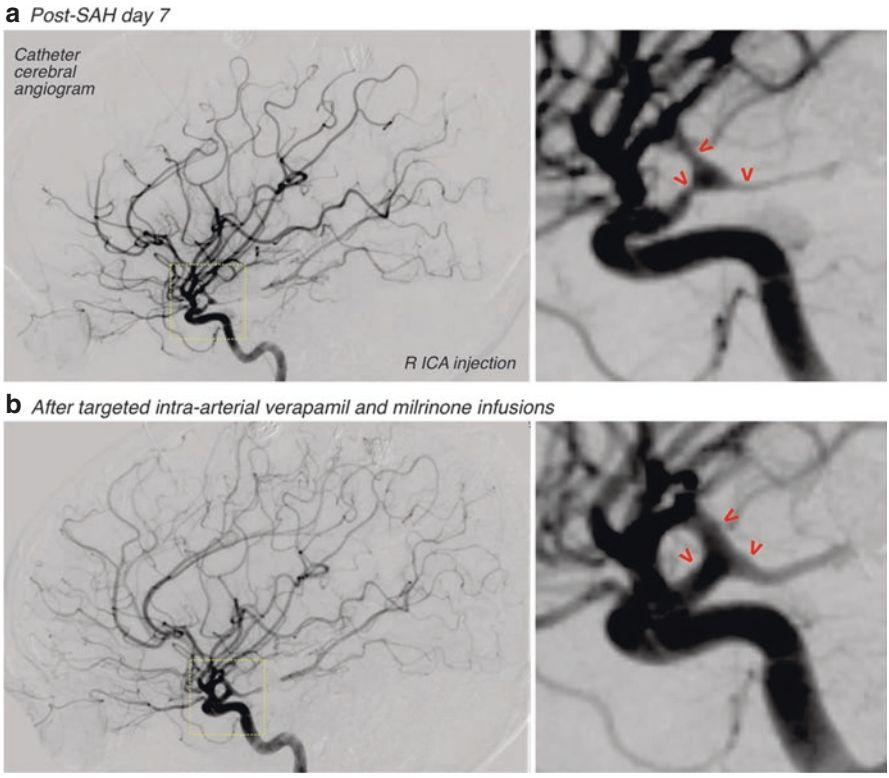

Fig. 9.3 Rescue endovascular therapy for patients with refractory symptomatic cerebral vasospasm. These catheter cerebral angiograms are from the same patient for whom a series of head CTs are depicted in Fig. 9.1. On post-SAH day 7, this patient developed refractory neurological deficits, which did not resolve in spite of hypervolemic and pharmacologically induced hypertension. (**a**) The patient underwent a catheter cerebral angiogram, which showed diffuse cerebral vasospasm, most prominent on the right side anterior circulation (red arrows, on right internal carotid artery, or R ICA injection), matching the patient's left-sided symptoms. The right panel is a magnified window (yellow dashed lines on the left panel). (**b**) The patient's right internal carotid artery was infused with 30 mg of verapamil and 2.5 mg of milrinone, leading to significant vasodilation of major arteries on the imaged field (red arrows), as well as earlier perfusion of distal cortical territories on the arterial phase

contractility than in peripheral arteries, it was suggested that a calcium channel antagonist, such as nimodipine, could selectively dilate cerebral arteries and help prevent vasospasm after SAH [83]. This hypothesis was tested in several randomized clinical trials in the United States and internationally between 1983 and 1988 [84]. It was found in these studies that indeed nimodipine reduces the risk of poor outcomes in SAH patients by one third. Current guidelines recommend administering oral nimodipine at doses that do not cause hypotension (between 60 and 90 mg) every 4 hours from the time of presentation until 21 days after the initial ictus. As mentioned above, surprisingly, in these clinical trials, nimodipine did not alter the

incidence or severity of vasospasm. Although the precise mechanism through which nimodipine improves outcomes in SAH remains unknown, leading theories suggest that it might slightly attenuate vasospasm (although not radiographically apparent) without significant hemodynamic effects, therefore causing a net improvement of cerebral perfusion. Other hypotheses suggest that nimodipine might inhibit cortical spreading ischemia and/or has fibrinolytic activity that reduces thrombus formation [62, 85].

Other agents acting on the mechanisms of cerebral vasospasm delineated in Fig. 9.1 have also been tested. In particular, clazosentran, an endothelin receptor antagonist, was shown to reduce radiographic vasospasm in SAH patients, although it did not significantly affect their outcomes [86–89]. Administration of clazosentran was complicated by hypotension and pulmonary effects, which are thought to counteract its cerebral vasodilatory effects. Similarly, nitric oxide donors under investigation seem to have limited efficacy due to dose-limiting hypotension, development of tolerance, and cyanide toxicity [53].

Another anti-inflammatory agent that has been studied is fasudil, a rho kinase inhibitor that blocks tumor necrosis factor-induced interleukin-6 release, decreases intracellular calcium mediated signaling, and thus can reduce endothelial smooth muscle contraction [90]. In randomized clinical trials, fasudil reduced the incidence of angiographic vasospasm and strokes, and improved chances for functional recovery [91]. Other anti-inflammatory agents, such as steroids and NSAIDs, have been clinically unsuccessful so far [92, 93].

Although these and multiple other clinical trials have been carried out with limited success, emerging concepts from these studies point to vasospasm as a dynamic pathological process that should be treated with targeted strategies for cerebral vasodilation that do not negatively impact cerebral perfusion. This is particularly the case with calcium channel, endothelin receptor antagonists, and nitric oxide donors that do not have high cerebrovascular selectivity, and therefore their systemic administration causes systemic hypotension. The systemic effect of these drugs not only reduces cerebral perfusion, but also can lead to complications of volume overload and pulmonary adverse effects. The optimal timing and the duration of these pharmacological interventions also remain to be investigated (e.g., if there are completed strokes, these therapies can increase swelling and further propagate the ischemic injury).

Rescue Interventions

In patients with refractory symptomatic vasospasm, endovascular interventions including balloon angioplasty and/or targeted focal delivery of vasodilatory agents are therapeutic options that can help more immediately resolve cerebral vasospasm.

Balloon angioplasty was introduced for the treatment of SAH-induced vasospasm in 1984 [94]. In the 1990s, there was a 16% overall reduction in mortality across multiple academic centers in the United States in SAH patients treated with

balloon angioplasty for vasospasm [8]. In a subsequent study, SAH patients with radiographic vasospasm that underwent prophylactic angioplasty had improved outcomes, although this was counterbalanced by the risk of arterial injury [95]. Of note, prophylactic angioplasty is currently not the standard of care, but when employed in the context of symptomatic vasospasm, it has a durable effect (possibly due to stretching muscle fibers preventing recurrence of vasospasm). The duration of therapeutic effect is distinction between balloon angioplasty and endovascular infusion of vasodilatory agents (see below).

The endovascular approach also affords the possibility for delivery of pharmacological agents via the same catheter used for angiography, which can be further directed to the point of arterial narrowing. Vasodilators that have been infused focally by this approach include papaverine, nicardipine, nimodipine, verapamil, and milrinone. Among these agents, verapamil has a more negative inotropic effect [96]. In a recent study, in SAH patients with DCI that underwent endovascular delivery of verapamil for treatment of vasospasm had more favorable outcomes if treatment was applied at onset of symptoms, rather than as a second line after induced hypertension [97]. The main limitation of this approach is the short-lived vasodilatory actions of these drugs and the possibility of systemic hypotension at higher infusion doses. In current protocol, SAH patients with refractory vasospasm can undergo intra-arterial focal vasodilation in consecutive days, theoretically for as many treatments as needed to bypass the window of active vasospasm. Ongoing clinical trials will help define the benefit of this intervention, as well as a more definite protocol and the most efficacious agent for targeted vasodilation of vasospastic arteries.

Outlook

Cerebral vasospasm is a complex pathological state that develops following a variety of known insults, such as trauma or SAH. It has also been implicated in a number of other neurological diseases, including epilepsy, migraine, and reversible cerebral vasoconstriction syndrome, in which its trigger is not well defined. As discussed in the Pathophysiology section, vasospasm happens as a result of interactions between physical, molecular and cellular processes that ultimately alter signaling in vascular smooth muscle, which contracts persistently thus narrowing the arterial wall and compromising the perfusion of its target brain territory. Future studies can aim to define the mechanisms of vasospasm under these other disease states, and their overlap with the picture presented here, with the aim of expanding the clinical utility of the therapies that have been successful for SAH-induced vasospasm. Furthermore, as the field continues its quest for new therapeutic avenues for cerebral vasospasm, prospective clinical trials should be structured with an understanding of vasospasm as a dynamic pathological process, in which targeted strategies for cerebral vasodilation should be instituted immediately after the onset of DCI, while minimizing their negative impact on systemic physiology and cerebral perfusion.

References

1. Gull W, others. Cases of aneurism of the cerebral vessels. Guys Hosp Rep. 1859;5:281–304.
2. Beadles CF. Aneurisms of the larger cerebral arteries. Brain. 1907;30(3):285–336.
3. Robertson EG. Cerebral lesions due to intracranial aneurysms. Brain. 1949;72(2):150–85.
4. Fisher CM. Clinical syndromes in cerebral thrombosis, hypertensive hemorrhage, and ruptured saccular aneurysm. Neurosurgery. 1975;22(CN_suppl_1):117–47.
5. Fisher C, Kistler J, Davis J. Relation of cerebral vasospasm to subarachnoid hemorrhage visualized by computerized tomographic scanning. Neurosurgery. 1980;6(1):1–9.
6. Saito I, et al. Vasospasm assessed by angiography and computerized tomography. J Neurosurg. 1979;51(4):466–75.
7. Ecker A, Riemenschneider PA. Arteriographic demonstration of spasm of the intracranial arteries with special reference to saccular arterial aneurisms. J Neurosurg. 1951;8(6):660–7.
8. Macdonald RL, Weir B. Cerebral vasospasm. Elsevier; San Diego, California. 2001.
9. Macdonald RLJNRN. Delayed neurological deterioration after subarachnoid haemorrhage. Nat Rev Neurol. 2014;10(1):44.
10. Takemae T, et al. Computed tomography of ruptured intracranial aneurysms in acute stage–relationship between vasospasm and high density on CT scan (author's transl). No to shinkei= Brain and nerve. 1978;30(8):861–6.
11. Reilly C, et al. Clot volume and clearance rate as independent predictors of vasospasm after aneurysmal subarachnoid hemorrhage. J Neurosurg. 2004;101(2):255–61.
12. KOIKE T, et al. Clinical analysis of cerebral vasospasm following subarachnoid hemorrhage—part 1 sequential changes of incidence and degree and its clinical significance—. Neurol Med Chir. 1979;19(8):793–800.
13. Crowley RW, et al. Angiographic vasospasm is strongly correlated with cerebral infarction after subarachnoid hemorrhage. Stroke. 2011;42(4):919–23.
14. Ito H. A clinical study on vasospasm following subarachnoid hemorrhage using the ratio of inner diameters of cerebral arteries to the ganglionic portion of internal carotid artery (author's transl). No to shinkei= Brain and nerve. 1978;30(7):795–804.
15. Ochi RP, Vieco PT, Gross CE. CT angiography of cerebral vasospasm with conventional angiographic comparison. AJNR Am J Neuroradiol. 1997;18(2):265–9.
16. Takagi R, et al. Evaluation of three-dimensional CT angiography (3D-CTA) for the diagnosis of cerebral vasospasm. Nihon Igaku Hoshasen Gakkai Zasshi. 1997;57(1):64–6.
17. Chaudhary SR, et al. Prospective evaluation of multidetector-row CT angiography for the diagnosis of vasospasm following subarachnoid hemorrhage: a comparison with digital subtraction angiography. Cerebrovasc Dis. 2008;25(1–2):144–50.
18. Aaslid R, Markwalder T-M, Nornes H. Noninvasive transcranial Doppler ultrasound recording of flow velocity in basal cerebral arteries. J Neurosurg. 1982;57(6):769–74.
19. Lindegaard K-F, et al. Cerebral vasospasm after subarachnoid haemorrhage investigated by means of transcranial Doppler ultrasound. Springer; Vienna, Austria. 1988.
20. Fahmy M, Smith R. Identification of presymptomatic cerebral vasospasm by transcranial Doppler sonography. 1992. Amer Heart Assoc 7272 Greenville Avenue, Dallas, TX 75231-4596.
21. Grosset D, et al. Prediction of symptomatic vasospasm after subarachnoid hemorrhage by rapidly increasing transcranial Doppler velocity and cerebral blood flow changes. Stroke. 1992;23(5):674–9.
22. Fontanella M, et al. Vasospasm after SAH due to aneurysm rupture of the anterior circle of Willis: value of TCD monitoring. Neurol Res. 2008;30(3):256–61.
23. Wintermark M, et al. Vasospasm after subarachnoid hemorrhage: utility of perfusion CT and CT angiography on diagnosis and management. Am J Neuroradiol. 2006;27(1):26–34.
24. Sozen T, et al. A clinical review of cerebral vasospasm and delayed ischaemia following aneurysm rupture. Acta Neurochir Suppl. 2011;110:5–6.

25. Fletcher TM, Taveras JM, Pool JL. Cerebral vasospasm in angiography for intracranial aneurysms: incidence and significance in one hundred consecutive angiograms. AMA Arch Neurol. 1959;1(1):38–47.
26. Dorsch N. Incidence, effects and treatment of ischemia following aneurysm rupture. In: Sano K, et al., editors. Cerebral vasospasm. Tokyo: University of Tokyo Press; 1990. p. 495–8.
27. Taneda M, et al. Angiographic demonstration of acute phase of intracranial arterial spasm following aneurysm rupture: case report. J Neurosurg. 1990;73(6):958–61.
28. Lovelock C, Rinkel G, Rothwell P. Time trends in outcome of subarachnoid hemorrhage: population-based study and systematic review. Neurology. 2010;74(19):1494–501.
29. Lanzino G, et al. Age and outcome after aneurysmal subarachnoid hemorrhage: why do older patients fare worse? J Neurosurg. 1996;85(3):410–8.
30. Rosenørn J, Eskesen V, Schmidt K. Clinical features and outcome in females and males with ruptured intracranial saccular aneurysms. Br J Neurosurg. 1993;7(3):287–90.
31. Lasner TM, et al. Cigarette smoking—induced increase in the risk of symptomatic vasospasm after aneurysmal subarachnoid hemorrhage. J Neurosurg. 1997;87(3):381–4.
32. Weir BK, et al. Cigarette smoking as a cause of aneurysmal subarachnoid hemorrhage and risk for vasospasm: a report of the Cooperative Aneurysm Study. J Neurosurg. 1998;89(3):405–11.
33. de Rooij NK, et al. Delayed cerebral ischemia after subarachnoid hemorrhage: a systematic review of clinical, laboratory, and radiological predictors. Stroke. 2013;44(1):43–54.
34. Pool JL, Jacobson S, Fletcher TA. Cerebral vasospasm-clinical and experimental evidence. J Am Med Assoc. 1958;167(13):1599–601.
35. Rothenberg SF, Corday E. Etiology of the transient cerebral stroke. J Am Med Assoc. 1957;164(18):2005–8.
36. Hakim S, Fisher CM. A new technique for the microscopic examination of cerebral vessels in vivo. J Neurosurg. 1957;14(4):405–12.
37. Gurdjian ES, et al. Cinephotomicrography of the pial circulation; a study of factors influencing vascular caliber; preliminary report. AMA Arch Neurol Psychiatry. 1958;80(4):418–35.
38. Echlin FA. Vasospasm and focal cerebral ischemia: an experimental study. Arch Neurol Psychiatr. 1942;47(1):77–96.
39. Hara H, Nosko M, Weir B. Cerebral perivascular nerves in subarachnoid hemorrhage: a histochemical and immunohistochemical study. J Neurosurg. 1986;65(4):531–9.
40. Uemura Y, et al. Changes of vasoactive intestinal polypeptide-like immunoreactivity in cerebrovascular nerve fibers after subarachnoid hemorrhage: an experimental study in the dog. Neurosci Lett. 1986;71(2):137–41.
41. Bevan JA, Bevan RD, Frazee JG. Functional arterial changes in chronic cerebrovasospasm in monkeys: an in vitro assessment of the contribution to arterial narrowing. Stroke. 1987;18(2):472–81.
42. MIYAOKA M, et al. Etiology and treatment of prolonged vasospasm—experimental and clinical studies—. Neurol Med Chir. 1976;16(2):103–14.
43. Alpers BJ, Forster FM. The reparative processes in subarachnoid hemorrhage. J Neuropathol Exp Neurol. 1945;4(3):262–8.
44. Hammes EM. Reaction of the meninges to blood. Arch Neurol Psychiatr. 1944;52(6):505–14.
45. Kajikawa H, et al. Cerebral vasospasm and hemoglobins—clinical and experimental studies. Neurol Med Chir. 1979;19(1):61–71.
46. German JW, et al. Systemic complement depletion inhibits experimental cerebral vasospasm. Neurosurgery. 1996;39(1):141–6.
47. Chaichana KL, et al. Haptoglobin 2-2 genotype determines chronic vasospasm after experimental subarachnoid hemorrhage. Stroke. 2007;38(12):3266–71.
48. Borsody M, et al. Haptoglobin and the development of cerebral artery vasospasm after subarachnoid hemorrhage. Neurology. 2006;66(5):634–40.
49. Jackson IJ. Aseptic hemogenic meningitis: an experimental study of aseptic meningeal reactions due to blood and its breakdown products. Arch Neurol Psychiatr. 1949;62(5):572–89.

50. Tourtellotte WW, et al. Spontaneous subarachnoid hemorrhage: factors affecting the rate of clearing of the cerebrospinal fluid. Neurology. 1964;14(4):301.
51. Pradilla G, et al. Inflammation and cerebral vasospasm after subarachnoid hemorrhage. Neurosurg Clin N Am. 2010;21(2):365–79.
52. Vorkapic P, Bevan JA, Bevan RD. Longitudinal in vivo and in vitro time-course study of chronic cerebrovasospasm in the rabbit basilar artery. Neurosurg Rev. 1991;14(3):215–9.
53. Pluta RM, et al. Cerebral vasospasm following subarachnoid hemorrhage: time for a new world of thought. Neurol Res. 2009;31(2):151–8.
54. Suzuki H, et al. Endothelin immunoreactivity in cerebrospinal fluid of patients with subarachnoid haemorrhage. Ann Med. 1990;22(4):233–6.
55. Ehrenreich H, et al. Long term monitoring of immunoreactive endothelin-1 and endothelin-3 in ventricular cerebrospinal fluid, plasma, and 24-h urine of patients with subarachnoid hemorrhage. Res Exp Med. 1992;192(1):257–68.
56. Suzuki M, et al. Increased levels of nitrite/nitrate in the cerebrospinal fluid of patients with subarachnoid hemorrhage. Neurosurg Rev. 1999;22(2):96–8.
57. Kaura V, Bonner S. Subarachnoid haemorrhage: early clinical indicators and biomarkers. Trends Anaesth Crit Care. 2012;2(1):42–7.
58. Lad SP, et al. Proteomic biomarker discovery in cerebrospinal fluid for cerebral vasospasm following subarachnoid hemorrhage. J Stroke Cerebrovasc Dis. 2012;21(1):30–41.
59. Fishman J, Ryan G, Karnovsky M. Endothelial regeneration in the rat carotid artery and the significance of endothelial denudation in the pathogenesis of myointimal thickening. Lab Invest. 1975;32(3):339–51.
60. Burns ER, Spaet TH, Stemerman MB. Response of the arterial wall to endothelial removal: an autoradiographic study. Proc Soc Exp Biol Med. 1978;159(3):473–7.
61. Kin H, et al. The pathological study of so-called vasospasm. Neurol Med Chir. 1976;16(2):115–25.
62. Dreier JP. The role of spreading depression, spreading depolarization and spreading ischemia in neurological disease. Nat Med. 2011;17(4):439–47.
63. Sabri M, et al. Mechanisms of microthrombi formation after experimental subarachnoid hemorrhage. Neuroscience. 2012;224:26–37.
64. Stoltenburg-Didinger G, Schwarz K. Brain lesions secondary to subarachnoid hemorrhage due to ruptured aneurysms. In: Cervós-Navarro J, Ferszt R, editors. Stroke and microcirculation. New York: Raven Press; 1987. pp. 471–80.
65. Stein SC, et al. Thromboembolism and delayed cerebral ischemia after subarachnoid hemorrhage: an autopsy study. Neurosurgery. 2006;59(4):781–8.
66. Mayberg MR. Cerebral vasospasm. Neurosurg Clin N Am. 1998;9(3):615–27.
67. Hinson HE, Sheth KN. Manifestations of the hyperadrenergic state after acute brain injury. Curr Opin Crit Care. 2012;18(2):139–45.
68. Tam AK, et al. Impact of systemic inflammatory response syndrome on vasospasm, cerebral infarction, and outcome after subarachnoid hemorrhage: exploratory analysis of CONSCIOUS-1 database. Neurocrit Care. 2010;13(2):182–9.
69. Diringer MN, et al. Critical care management of patients following aneurysmal subarachnoid hemorrhage: recommendations from the Neurocritical Care Society's Multidisciplinary Consensus Conference. Neurocrit Care. 2011;15(2):211–40.
70. Heros RC, Zervas NT, Varsos V. Cerebral vasospasm after subarachnoid hemorrhage: an update. Ann Neurol. 1983;14(6):599–608.
71. Kosnik EJ, Hunt WE. Postoperative hypertension in the management of patients with intracranial arterial aneurysms. J Neurosurg. 1976;45(2):148–54.
72. Connolly ES Jr, et al. Guidelines for the management of aneurysmal subarachnoid hemorrhage: a guideline for healthcare professionals from the American Heart Association/American Stroke Association. Stroke. 2012;43(6):1711–37.
73. Hasan D, et al. Effect of fluid intake and antihypertensive treatment on cerebral ischemia after subarachnoid hemorrhage. Stroke. 1989;20(11):1511–5.

74. Treggiari MM, others. Hemodynamic management of subarachnoid hemorrhage. Neurocrit Care. 2011;15(2):329.
75. Kassell NF, et al. Treatment of ischemic deficits from vasospasm with intravascular volume expansion and induced arterial hypertension. Neurosurgery. 1982;11(3):337–43.
76. Pritz MB, et al. Treatment of patients with neurological deficits associated with cerebral vasospasm by intravascular volume expansion. Neurosurgery. 1978;3(3):364–8.
77. Giannotta S, McGillicuddy J, Kindt G. Diagnosis and treatment of postoperative cerebral vasospasm. Surg Neurol. 1977;8(4):286–90.
78. Le Roux PD, others. Anemia and transfusion after subarachnoid hemorrhage. Neurocrit Care. 2011;15(2):342.
79. Dhar R, et al. Comparison of induced hypertension, fluid bolus, and blood transfusion to augment cerebral oxygen delivery after subarachnoid hemorrhage. J Neurosurg. 2012;116(3):648–56.
80. McKhann GM II, Le Roux PD. Perioperative and intensive care unit care of patients with aneurysmal subarachnoid hemorrhage. Neurosurg Clin N Am. 1998;9(3):595–613.
81. Etminan N, et al. Effect of pharmaceutical treatment on vasospasm, delayed cerebral ischemia, and clinical outcome in patients with aneurysmal subarachnoid hemorrhage: a systematic review and meta-analysis. J Cereb Blood Flow Metab. 2011;31(6):1443–51.
82. Langley MS, Sorkin EM. Nimodipine. Drugs. 1989;37(5):669–99.
83. Allen GS, et al. Cerebral arterial spasm–a controlled trial of nimodipine in patients with subarachnoid hemorrhage. N Engl J Med. 1983;308(11):619–24.
84. Mees SD, et al. Calcium antagonists for aneurysmal subarachnoid haemorrhage. Cochrane Database Syst Rev. 2007;(3):CD000277.
85. Vergouwen MD, et al. Microthrombosis after aneurysmal subarachnoid hemorrhage: an additional explanation for delayed cerebral ischemia. J Cereb Blood Flow Metab. 2008;28(11):1761–70.
86. Macdonald RL, et al. Clazosentan to overcome neurological ischemia and infarction occurring after subarachnoid hemorrhage (CONSCIOUS-1) randomized, double-blind, placebo-controlled phase 2 dose-finding trial. Stroke. 2008;39(11):3015–21.
87. Macdonald RL, et al. Clazosentan, an endothelin receptor antagonist, in patients with aneurysmal subarachnoid haemorrhage undergoing surgical clipping: a randomised, double-blind, placebo-controlled phase 3 trial (CONSCIOUS-2). Lancet Neurol. 2011;10(7):618–25.
88. Macdonald RL, et al. Randomized trial of clazosentan in patients with aneurysmal subarachnoid hemorrhage undergoing endovascular coiling. Stroke. 2012;43(6):1463–9.
89. Vergouwen MD, Algra A, Rinkel GJ. Endothelin receptor antagonists for aneurysmal subarachnoid hemorrhage: a systematic review and meta-analysis update. Stroke. 2012;43(10):2671–6.
90. Satoh S-I, et al. Amelioration of endothelial damage/dysfunction is a possible mechanism for the neuroprotective effects of Rho-kinase inhibitors against ischemic brain damage. Brain Res Bull. 2010;81(1):191–5.
91. Liu GJ, et al. Systematic assessment and meta-analysis of the efficacy and safety of fasudil in the treatment of cerebral vasospasm in patients with subarachnoid hemorrhage. Eur J Clin Pharmacol. 2012;68(2):131–9.
92. Tiebosch IA, et al. Effect of interferon-β on neuroinflammation, brain injury and neurological outcome after experimental subarachnoid hemorrhage. Neurocrit Care. 2013;18(1):96–105.
93. Feigin VL, et al. Corticosteroids for aneurysmal subarachnoid haemorrhage and primary intracerebral haemorrhage. Cochrane Database Syst Rev. 2005;(3):CD004583.
94. Zubkov YN, Nikiforov B, Shustin V. Balloon catheter technique for dilatation of constricted cerebral arteries after aneurysmal SAH. Acta Neurochir. 1984;70(1):65–79.
95. Zwienenberg-Lee M, et al. Effect of prophylactic transluminal balloon angioplasty on cerebral vasospasm and outcome in patients with Fisher grade III subarachnoid hemorrhage: results of a phase II multicenter, randomized, clinical trial. Stroke. 2008;39(6):1759–65.
96. DeWitt CR, Waksman JC. Pharmacology, pathophysiology and management of calcium channel blocker and β-blocker toxicity. Toxicol Rev. 2004;23(4):223–38.
97. Jabbarli R, et al. Endovascular treatment of cerebral vasospasm after subarachnoid hemorrhage: more is more. Neurology. 2019;93(5):e458–66.

Part III
Stroke

Chapter 10
Acute Ischemic Stroke Presentation, Natural History, and Treatment

Sujani Bandela, Aaisha S. Mozumder, and Lee A. Birnbaum

Background

Ischemic stroke constitutes about 75% of all stroke, is one of the leading causes of death, and is the number one cause of long-term disability. Thus, significant effort and research have focused on stroke therapies that include acute interventions with intravenous thrombolysis (IVT) and mechanical thrombectomy (MT), subacute therapy with neuro-protection, and chronic treatment with stem cells. Thus far, only IVT and MT have demonstrated improved clinical outcomes in multi-center randomized clinical studies. The National Institute of Neurological Disorders and Stroke (NINDS) alteplase (tPA) trial was a 1995 landmark acute stroke management study and demonstrated that intravenous (IV) tPA, when administered up to 3 hours from last known well (LKW), resulted in improved 90-day clinical outcomes compared to placebo [1]. Additionally, tPA treated patients showed a greater than four-point reduction in their National Institutional Health Stroke Scale (NIHSS) or resolution of the neurological deficits at 24 hours post treatment. Despite these positive results, widespread tPA utilization for acute stroke was initially hampered by emergency medicine skepticism, inadequate inpatient neurology coverage, and underdeveloped stroke systems of care. Lack of community outreach and stroke awareness also contributed to tPA under-utilization as many patients had delayed presentations that were beyond the 3-hour time window. Even today, IVT is administered in less than 5% of all ischemic strokes and less frequently among women as well as Black and Hispanic populations [2].

To increase IVT rates, community outreach and stroke education have been pivotal for public awareness of stroke signs and symptoms. Prehospital assessments

S. Bandela · A. S. Mozumder · L. A. Birnbaum (✉)
Department of Neurology, Division of Vascular Neurology, University of Texas Health San Antonio, San Antonio, TX, USA
e-mail: Bandela@uthscsa.edu; mozumder@uthscsa.edu; birnbaum@uthscsa.edu

J. R. Mascitelli, M. J. Binning (eds.), *Introduction to Vascular Neurosurgery*,
https://doi.org/10.1007/978-3-030-88196-2_10

such as Face Arm Speech Time (FAST) and more recently Balance Eyes FAST (BEFAST) emphasize the need to call 911 immediately. In addition to early patient arrival, IVT rates have increased as a result of the expanded time window up to 4.5 hours. In 2008, the ECASS III trial demonstrated safety and efficacy of tPA in the 3–4.5-hour window from LKW [3]. Although IV tPA is only approved by the Food and Drug Administration for up to 3 hours, standard of care for IVT in clinical practice is up to 4.5 hours.

An additional acute intervention for ischemic stroke is MT or intra-arterial clot removal. MT is performed for large vessel occlusion (LVO) stroke which is often the most devastating with long-term disability and death. Meta-analysis of the MT trials shows that the number needed to treat for independent outcome at 90 days is three [4]. Because IVT and MT are likely synergistic, eligible LVO patients presenting within 4.5 hours should receive IVT in addition to MT. For drip and ship stroke models, IVT can be started early in the LVO triage and may recanalize the LVO prior to MT. For patients presenting directly to a MT center, the utility of IVT first versus direct to MT is being evaluated. The triage of acute stroke continues to evolve with more efficient IVT using Tenecteplase (TNK), enhanced thrombectomy devices, and further extension of treatment time windows with advanced neuroimaging.

Clinical Presentation

The clinical presentation of acute ischemic stroke is determined by the affected vascular territory of the brain.

Middle Cerebral Artery (MCA)

Middle cerebral artery strokes are the most common strokes among LVO. Proximal MCA (M1) occlusion is frequently characterized by contralateral hemiparesis (arm and face greater than leg), contralateral hemisensory loss, contralateral hemianopia, and ipsilateral gaze deviation, as well as aphasia (dominant hemisphere) or hemineglect (nondominant hemisphere). The MCA has two major divisions including the superior that supplies the Rolandic and pre-Rolandic areas and the inferior that supplies the lateral temporal and inferior parietal lobes. Left MCA stroke often presents with aphasia because it is overwhelmingly the dominant hemisphere. Left hemisphere language dominance is noted in 96% of strong right handers and 73% of strong left handers. In addition to having disabling weakness, left MCA strokes carry worse disability due to aphasia. Right MCA strokes often present with disabling weakness as well as sensory and visual neglect.

Anterior Cerebral Artery (ACA)

Occlusion of the ACA often results in contralateral motor weakness with minimal sensory deficit (two-point discrimination) of the leg, transcortical aphasia (dominant hemisphere), contralateral neglect (nondominant hemisphere), and frontal lobe behavioral abnormalities that include grasp reflex, impaired judgment, urinary incontinence, and, if bilateral, abulia. Furthermore, infarction of supplementary motor area and other frontal lobe regions can lead to "alien limb syndrome," in which the hand or leg acts independently of the mind.

Posterior Cerebral Artery (PCA)

Occlusion of the PCA typically manifests as contralateral homonymous hemianopia or contralateral quadrantanopsia. However, larger PCA infarction also results in contralateral hemiparesis (posterior limb of internal capsule), contralateral sensory loss, cognitive dysfunction, and rarely thalamic aphasia (thalamus). Syndromes of the paramedian arteries, including the proximal PCA, involve the midbrain and present mainly with ipsilateral third-nerve palsy in addition to contralateral hemiplegia (Weber's syndrome), contralateral ataxic tremor (Claude's syndrome), or contralateral ataxic tremor and hemiplegia (Benedikt's syndrome). If the artery of Percheron is present, then a PCA infarction may cause bilateral paramedian thalamic infarct and result in altered level of consciousness, vertical gaze palsy, and memory disturbances. The cognitive dysfunction that may occur in PCA strokes includes alexia without agraphia or inability to read with retention of writing and spelling. This clinical presentation results from dominant left PCA strokes that affect the splenium of the corpus callosum. Additionally, dominant left PCA strokes may cause color agnosia or the ability to detect color.

Vertebrobasilar Stroke Syndrome

Vertebrobasilar artery occlusion can be fatal due to potential widespread brainstem infarction leading to multiple cranial nerve abnormalities, long tract signs, and coma. Posterior inferior cerebellar artery occlusion may give rise to lateral medullary syndrome, or Wallenberg's syndrome. This is a relatively common brainstem infarct usually caused by vertebral artery V4 segment thrombosis or vertebral artery dissection. It is characterized by ipsilateral Horner's syndrome, ataxia, vertigo, palatal weakness, loss of taste, nystagmus, and decreased facial pain and temperature, as well as contralateral hemi-body pain and temperature impairment. Medial medullary syndrome is caused by occlusion of paramedian branches that originate from

the vertebral artery V4 segment and anterior spinal artery origin. It results in ipsilateral tongue weakness and contralateral hemiplegia with decreased proprioception and vibration sense.

In the pons, the medial pontine syndromes are relatively common and clinically significant, usually caused by lacunar disease as mentioned below. If tegmentum is also involved in addition to medial pontine basis, it presents mainly with contralateral hemiplegia, dysarthria combined with ipsilateral face weakness (Millard-Gubler syndrome), ipsilateral horizontal gaze palsy (Pontine wrong way eyes), or ipsilateral face weakness and horizontal gaze palsy (Foville's syndrome). Lateral pons can be affected by anterior inferior cerebellar artery (AICA) infarction and superior cerebellar artery (SCA) infarction. The lateral tegmental syndrome of AICA syndrome can resemble lateral medullary syndrome (ipsilateral Horner's syndrome, ataxia, vertigo, nystagmus, pain, and temperature sensory loss in the ipsilateral face and contralateral body); however, the presence of ipsilateral deafness and the absence of hoarseness or loss of taste differentiate it from lateral medullary syndrome. SCA syndrome is characterized by ipsilateral ataxia and contralateral decreased pain and temperature sensation with variable features of lateral tegmental involvement.

The distal end of the basilar artery, or basilar tip, is often occluded by an embolus and results in oculomotor disturbances, hemianopia, somnolence, delirium or vivid visual hallucinations (peduncular hallucinosis), coma, transient loss of consciousness, and ataxia. The mid-basilar artery occlusion causes ventral pontine infarction and leads to "locked-in" syndrome. A patient will be quadriplegic and mute but retain consciousness, cognition, and minimal voluntary movements such as vertical eye movement or eyelid elevation.

Lacunar Infarcts

Lacunar infarcts are small (<1.5 centimeters) subcortical infarcts resulting from occlusion of small penetrating end arteries that include lenticulostriates, thalamoperforators, pontine/basilar-perforators, and recurrent artery of Huebner. The most common risk factors are hypertension, hyperlipidemia, smoking, and diabetes mellitus. Most lacunar infarcts are clinically silent; however, an accumulation of chronic microvascular ischemic changes is associated with vascular dementia, vascular parkinsonism with more gait predominant parkinsonian manifestations, ataxia, and bladder incontinence. Depending on the location of lacunar infarction, symptomatic patients may present with a clinical lacunar syndrome. The five most distinctive syndromes with typical localizations include pure motor hemiparesis (internal capsule and corona radiata), pure sensory stroke (thalamus), sensorimotor stroke (thalamocapsular), ataxic hemiparesis (basis pontis, thalamocapsular, and corona radiata), and clumsy hand-dysarthria (basis pontis).

Natural History

The stroke severity and overall clinical outcome can be affected by the occlusion location and number of occluded vessels in AIS patients. In a meta-analysis of mostly pre-endovascular era AIS data, dependence or death rates within 3–6 months (defined by a modified Rankin Scale [mRS] score of ≥ 3) were more than double for patients after LVO versus without LVO (64% vs. 24%, $P < 0.0001$), and mortality alone was also significantly higher (26.2% vs. 1.3%, $P < 0.0001$) [5]. When evaluating occlusion location, intracranial ICA and BA LVOs are linked with higher NIHSS scores and worse clinical outcomes than more distal vessels occlusions including second segments of MCA, ACA, and PCA [6]. Additionally, mean NIHSS scores increase proportionally with the number of vessels occluded [6]. Like LVO, lacunar strokes may be disabling; however, they are associated with greater potential for long-term recovery and less mortality. Without acute treatment, patients with lacunar strokes demonstrate greatest improvement within the first few days or weeks of stroke onset and maximal recovery within 3–6 months.

Embolic strokes to the MCA, ACA, PCA, and vertebrobasilar region are often greater than 1.5 centimeters, associated with more lasting and disabling deficits, and frequently benefit from acute ischemic treatment including IVT and MT. Embolic strokes involving the MCA or cerebellum may have malignant edema that is life threatening. Stroke patients that have malignant cerebral edema should be closely watched in a neuroscience intensive care unit with frequent neuro checks as many will require hypernatremia, external ventricular drain, or decompressive craniectomy.

The spectrum of stroke care encompasses a multidisciplinary approach that includes acute care, subacute and long-term rehabilitation, and secondary stroke prevention. Outpatient stroke care should focus on risk factors such as dyslipidemia, hypertension, diabetes, obstructive sleep apnea, and occult irregular heart rate including atrial fibrillation. An aggressive plan of antiplatelet therapy, statin, antihypertensive medications, and diabetic medications with good exercise therapy is not only pivotal to prevent recurrent strokes but also help in stroke recovery. Post stroke depression is a common sequela and should be addressed to optimize rehabilitation and recovery.

Advanced Neuroimaging

Computerized tomography (CT) head scan is widely used for LVO triage as it is readily available in emergency rooms and, unlike MRI, does not require prescreening. A non-contrast CT (NCCT) head not only rules out hemorrhage but also triages LVO for MT by identifying a hyperdense sign or calculating ischemia using the Alberta Stroke Program Early CT Score (ASPECTS) [7]. The ASPECTS score is a quantitative measurement of early ischemia detection that divides the middle

cerebral artery (MCA) distribution into 10 regions. To calculate ASPECTS, the regions are scrutinized on NCCT for hypoattenuation which indicates early cytotoxic edema and irreversible brain injury. For each region involved, a point is subtracted from the total number of 10. An LVO with high ASPECTS (7–10) corresponds inversely with degree of infarction and is associated with less intracerebral hemorrhages (ICH), fatal outcomes, and long-term disability. On the contrary, those with low ASPECTS (0–3) are often excluded from MT due to large ischemic core and malignant profile. A NCCT also facilitates LVO triage if a hyperdense sign is noted. Hyperdense signs indicate an acute thrombus and are frequently seen with proximal LVO of the internal carotid artery terminus and MCA first segment. A proximal thrombus often carries a large clot burden and infrequently recanalizes with IVT alone. Thus, MT, in combination with IVT when appropriate, is often required.

Advanced neuroimaging for acute ischemic stroke has extended treatment time windows for both IVT and MT. The triage of LVO stroke with CT perfusion (CTP) has expanded MT treatment up to 24 hours from LKW. CTP calculates the estimated core, or infarcted tissue, and compares it to the penumbra, or area with reduced blood flow at risk of infarction (Fig. 10.1). The DWI or CTP Assessment with Clinical Mismatch in the Triage of Wake-Up and Late Presenting Strokes Undergoing Neuro-intervention with Trevo (DAWN) [8] and the Endovascular Therapy Following Imaging Evaluation for Ischemic Stroke (DEFUSE-3) [9] trials evaluated acute anterior circulation LVO with a core infarct of less than 51 cc of tissue with LKW up to 24 hours and less than 70 cc of tissue with LKW up to 16 hours, respectively. When compared to medical management alone, MT in these trials was associated with improved recanalization rates and better clinical outcomes at 90 days. In clinical practice, however, CTP is not always available at spoke hospitals and therefore, frequently completed upon arrival to MT centers. To increase triage efficiency, NCCT ASPECTS from the transferring hospital may be used as a surrogate for CTP (Table 10.1).

The utilization of CTP is variable for LKW within 6 hours as NCCT and CTA may be sufficient to determine MT eligibility within the early time window. CTP also has limited application for posterior circulation strokes as it poorly details brainstem ischemia. Although clinical examination, NCCT, and CTA are utilized to triage posterior circulation LVO, an emergent MRI is often helpful for basilar occlusions. MT has been mostly studied with anterior circulation stroke but is frequently performed up to 24 hours for basilar occlusions, which are associated with significant morbidity and mortality. Despite its limited accessibility in the acute setting, MRI can be helpful for not only basilar occlusions, but also to differentiate ischemic stroke from mimics and to extend the time window for IVT.

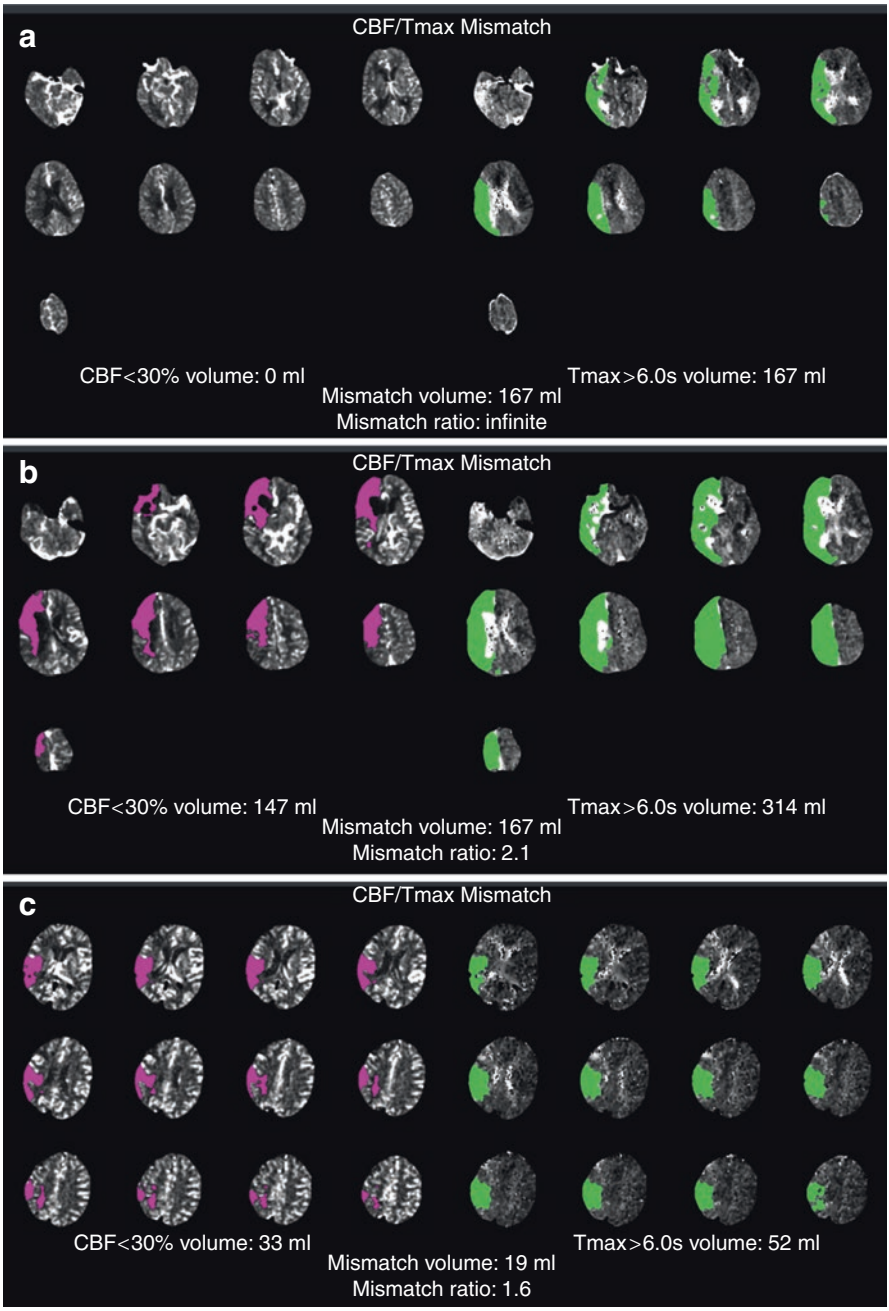

Fig. 10.1 RAPID output mismatch profiles of CT Perfusion for LVO stroke: (**a**) favorable mismatch no core and large penumbra; (**b**) unfavorable mismatch large core with malignant profile; (**c**) intermediate mismatch with medium core and medium penumbra

Table 10.1 Comparison of Alberta Stroke Program Early CT Score (ASPECTS) versus CT perfusion

ASPECTS score	CT perfusion
Unenhanced CT head	Contrast enhanced CT head
No post-processing or automated software	Post-processing or automated software
Readily available at any hospital with CT scanner	Mostly available at Thrombectomy-Capable Centers; some Primary Stroke Centers
Manual or automated scoring system	Automated core: penumbra mismatch ratio
Limited to middle cerebral artery stroke	Not limited to vascular territory

Intravenous Thrombolytics

IVT has been shown to be safe and effective for the treatment of acute ischemic stroke up to LKW 4.5 hours [3]. MRI protocols have been designed and studied to further extend the IVT treatment window. For example, the WAKE-UP trial enrolled unknown LKW subjects, obtained MR diffusion weighted (DWI) and fluid attenuated inverted recovery (FLAIR) imaging, and randomized to IVT or placebo [10]. Overall, patients who received IVT had better functional outcomes despite increased ICH rates. The MR WITNESS trial also found IVT to be safe in stroke patients with unwitnessed onset and DWI-FLAIR mismatch [11]. The evidence supports the use of MRI to expand the LKW time window for IVT in clinical practice.

A common reason for IVT exclusion is presentation delay as some patients are unaware of stroke signs and symptoms while others live in remote areas with limited access to stroke hospitals. Tele-stroke, however, has greatly expanded patient access to IVT and LVO triage. The American Heart Association Stroke guidelines note benefit from tele-stroke in remote areas with improved IVT times and greater access to MT centers [12]. Tele-stroke has enabled IVT times in remote locations to be comparable with those of large academic centers. Despite the overall shortage of stroke providers, the field has greatly expanded in clinical care and research as a result of tele-stroke practices.

Alteplase has been the IVT of choice since the NINDS Stroke Study was published in 1995. Although it demonstrates favorable fibrinolytic characteristics, tPA has a short half-life and therefore requires a bolus followed by a 1-hour infusion. The infusion is an additional source of potential mis-dosing and adds complexity to drip and ship models. Therefore, IV TNK has been explored as an alternative due to its longer half-life, greater fibrin specificity, and single bolus delivery (Table 10.2). TNK is a genetically modified variant of tPA that has more fibrin specific molecules and lasts longer in the system. Alteplase has a half-life of 7 minutes compared with 24 minutes for TNK.

Several trials have shown TNK to be safe and at least as effective as tPA for the treatment of acute ischemic stroke. The EXTEND-IA TNK study included LVO subjects that underwent MT after IVT randomization to TNK (0.25 mg/kg) or tPA (0.9 mg/kg) within 4.5 hours after symptom onset [13]. The study showed that TNK

Table 10.2 Comparison of alteplase to tenecteplase

Alteplase	Tenecteplase
Less fibrin specific	More fibrin specific
Short half-life 7 minutes	Half-life 24 minutes
10% bolus, 90% infusion over 1 hour	Single bolus over 5 seconds
More expensive	Less expensive
Dosage is 0.9 mg/kg; max 90 mg	Dosage is 0.25 mg/kg; max 25 mg

Table 10.3 Comparison of prehospital stroke severity assessments: Vision Aphasia Neglect (VAN), Cincinnati Stroke Triage Assessment Tool (C-STAT), Los Angeles Motor Scale (LAMS), and Rapid Arterial Occlusion Evaluation (RACE)

Prehospital stroke severity assessment	Prehospital sensitivity; specificity	Description	Items
VAN[5]	81%; 38%	4-items, dichotomized scale, positive or negative	Weakness of arms; visual field; aphasia; neglect
C-STAT[3]	71%; 67%	3-items, 0- to 5-point scale, positive score ≥2	Gaze; arm weakness; level of consciousness
LAMS[4]	76%; 65%	3-items, 0- to 5-point scale, positive score ≥4	Facial droop; arm drift; grip strength
RACE[2]	84%; 60%	5 of 6-items, 0- to 9-point scale, positive score ≥5	Facial palsy; arm motor function; leg motor function; head and gaze deviation; based on side, do only one: R side: aphasia or L side: agnosia

was associated with a higher incidence of reperfusion and better functional outcome at 90 days. In the NOR-Test study, TNK was studied in non-LVO, low NIHSS stroke at a higher dose of 0.4 mg/kg and was shown to be safe [14]. Although different doses have been studied, the EXTEND-IA TNK Part 2 showed that 0.25 mg/kg, rather than 0.4 mg/kg, is the optimal TNK dose for safety and efficacy with LVO stroke [15].

Large Vessel Occlusion Triage

Prehospital EMS triage is pivotal to identify not only acute stroke but also LVO that may benefit from bypass protocols to expedite MT. To facilitate LVO triage, numerous prehospital stroke severity tools have been published. However, only Rapid Arterial Occlusion Evaluation (RACE), Cincinnati Stroke Triage Assessment Tool (C-STAT), Los Angeles Motor Scale (LAMS), and Vision Aphasia Neglect (VAN) have been validated in both prehospital settings and external datasets (Table 10.3).

The optimal prehospital stroke severity scale remains unclear because none predict LVO with both high sensitivity and specificity [16]. Recent prehospital stroke severity publications demonstrated good sensitivity and specificity for RACE [17] (84% and 60%), C-STAT [18] (71% and 67%), LAMS [19] (76% and 65%), and VAN [20] (81% and 38%).

Stroke severity tools generally test a combination of motor and cortical deficits. For example, the VAN assessment starts with arm weakness and then examines vision, aphasia, and neglect. Similarly, C-STAT evaluates for arm weakness as well as conjugate gaze deviation, orientation, and simple commands. LAMS does not incorporate cortical signs but rather relies solely on motor weakness including face, arm, and grip. Finally, RACE includes multiple assessments of motor with face, arm, and leg as well as cortical signs with gaze deviation, aphasia, and agnosia. Although VAN has the advantage of being a dichotomized tool, C-STAT and LAMS are relatively simple 3-item assessments with either one single cortical assessment or none, respectively. RACE performs best in published studies but is a categorical 6-item test that requires severity testing for weakness and cortical signs.

Prior to implementation of a prehospital LVO triage, additional bypass travel times to a MT center as well as LKW cutoff times require consideration. Bypass protocols often utilize LKW cutoffs of less than 6 or 24 hours. Although LVO subjects in both time windows show benefit, MT is time-dependent, and its efficacy decreases in a linear fashion. Thus, prehospital bypass protocols of LKW less than 24 hours, compared to those less than 6 hours, will bypass a greater proportion of LVO that is not eligible for MT due to infarction or unfavorable perfusion studies. Prehospital bypass protocols strive to balance a reduction of MT delays without overburdening MT centers with unnecessary transfers. Although the current American Stroke Association guidelines do not recommend a specific time window for prehospital bypass [12], the Mission: Lifeline Severity-based Stroke Triage Algorithm for EMS recommends transfer of prehospital patients with suspected LVO LKW less than 24 hours directly to a MT center if the additional bypass travel time is less than 30 minutes and will not disqualify for IVT [21]. In urban areas, Thrombectomy-capable Stroke Centers (TSCs) are enabling more widespread access to MT, reducing additional bypass travel times, and minimizing disqualification for IVT.

DIDO is a key metric for non-endovascular stroke centers, which is now tracked in The Joint Commission measures STK-OP-1a and ASR-OP-2a for Primary Stroke Centers and Acute Stroke Ready Hospitals, respectively. DIDO time refers to the duration from initial patient arrival at the non-endovascular facility to discharge to the endovascular stroke center. The Brain Attack Coalition recommends a DIDO time of 2 hours or less to expedite MT [22]. Longer DIDO times may have an inferior outcome in patients with incomplete reperfusion. However, this finding has not been observed in patients with complete reperfusion – suggesting probable mitigation of prolonged DIDO time by successful MT [23]. Widespread quality improvement efforts to reduce DIDO times are underway and are being greatly enhanced by cloud-based imaging applications.

Future Considerations

Compared to other stroke subtypes, LVO is associated with greater disability and death as a result of malignant cerebral edema in the young and aspiration pneumonia in the elderly. The MT trials demonstrated independent outcomes for LVO with minimal infarction or favorable mismatch profiles up to LKW less than 24 hours. The benefit of MT for LVO with greater infarction or less favorable mismatch pattern is unknown. The Thrombectomy for Emergent Salvage of Large Anterior Circulation Ischemic Stroke (TESLA) trial is evaluating MT for LVO with low ASPECTS on NCCT head up to 24 hours. Although the number needed to benefit will likely be greater, MT in patients with less favorable mismatch profiles may trend for more independent outcomes, fewer hemi-craniectomies, and shorter hospital stays.

When LVO presents to a non-endovascular center, IVT is important to enhance early recanalization as DIDO times may be 2 hours or more. TNK is being studied for LVO up to LKW 24 hours to facilitate early recanalization. The Thrombolysis in Imaging-eligible, Late-window Patients to Assess the Efficacy and Safety of Tenecteplase (TIMELESS) trial is evaluating TNK (0.25 mg/kg) versus placebo followed by MT for LVO in the extended time window of 4.5–24 hours. If TNK proves effective beyond 4.5 hours, then LVO bypass protocols will need reconsideration to optimize "bolus" and ship models. However, the benefit of IVT for LVO presenting directly to MT centers is less clear. The DIRECT-MT study investigated MT with or without IVT in LVO stroke presenting to MT centers and concluded that MT alone was noninferior with regard to functional outcome [24]. The SKIP study shared a similar randomized design but did not show noninferiority of direct MT compared to combined IVT and MT with respect to favorable outcomes [25]. Because both studies had short interval times from alteplase initiation to groin puncture, the results are less applicable to non-endovascular or drip-and-ship hospitals.

Conclusion

The treatment of acute stroke has evolved far beyond the initial tPA trials. Current and future studies will continue to expand acute stroke therapies by optimizing drug, device, and delivery. Because each healthcare region is unique, individual stroke systems will be tasked to implement care with careful considerations of their infrastructures, geographies, and resources.

References

1. National Institute of Neurological Disorders and Stroke rt-PA Stroke Study Group. Tissue plasminogen activator for acute ischemic stroke. N Engl J Med. 1995;333(24):1581–7. https://doi.org/10.1056/NEJM199512143332401. PMID: 7477192.

2. Reed SD, Cramer SC, Blough DK, et al. Treatment with tissue plasminogen activator and inpatient mortality rates for patients with ischemic stroke treated in community hospitals. Stroke. 2001;32(8):1832–40. https://doi.org/10.1161/01.str.32.8.1832. PMID: 11486113.
3. Hacke W, Kaste M, Bluhmki E, et al. ECASS Investigators. Thrombolysis with alteplase 3 to 4.5 hours after acute ischemic stroke. N Engl J Med. 2008;359(13):1317–29. https://doi.org/10.1056/NEJMoa0804656. PMID: 18815396.
4. Goyal M, Menon BK, van Zwam WH, et al. HERMES collaborators. Endovascular thrombectomy after large-vessel ischaemic stroke: a meta-analysis of individual patient data from five randomised trials. Lancet. 2016;387(10029):1723–31. https://doi.org/10.1016/S0140-6736(16)00163-X. Epub 2016 Feb 18. PMID: 26898852.
5. Malhotra K, Gornbein J, Saver JL. Ischemic strokes due to large-vessel occlusions contribute disproportionately to stroke-related dependence and death: a review. Front Neurol. 2017;8:651. https://doi.org/10.3389/fneur.2017.00651. PMID: 29250029; PMCID: PMC5715197.
6. Smith WS, Lev MH, English JD, Camargo EC, Chou M, Johnston SC, Gonzalez G, Schaefer PW, Dillon WP, Koroshetz WJ, Furie KL. Significance of large vessel intracranial occlusion causing acute ischemic stroke and TIA. Stroke. 2009;40(12):3834–40. https://doi.org/10.1161/STROKEAHA.109.561787. Epub 2009 Oct 15. PMID: 19834014; PMCID: PMC2796543.
7. Barber PA, Demchuk AM, Zhang J, Buchan AM. Validity and reliability of a quantitative computed tomography score in predicting outcome of hyperacute stroke before thrombolytic therapy. ASPECTS Study Group. Alberta Stroke Programme Early CT Score. Lancet. 2000;355(9216):1670–4. https://doi.org/10.1016/s0140-6736(00)02237-6. Erratum in: Lancet 2000 Jun 17;355(9221):2170. PMID: 10905241.
8. Nogueira RG, Jadhav AP, Haussen DC, et al. DAWN Trial Investigators. Thrombectomy 6 to 24 hours after stroke with a mismatch between deficit and infarct. N Engl J Med. 2018;378(1):11–21. https://doi.org/10.1056/NEJMoa1706442. Epub 2017 Nov 11. PubMed PMID: 29129157.
9. Albers GW, Marks MP, Kemp S, et al. DEFUSE 3 Investigators. Thrombectomy for stroke at 6 to 16 hours with selection by perfusion imaging. N Engl J Med. 2018;378(8):708–18. https://doi.org/10.1056/NEJMoa1713973. Epub 2018 Jan 24. PubMed PMID: 29364767; PubMed Central PMCID: PMC6590673.
10. Thomalla G, Simonsen CZ, Boutitie F, et al. WAKE-UP Investigators. MRI-guided thrombolysis for stroke with unknown time of onset. N Engl J Med. 2018;379(7):611–22. https://doi.org/10.1056/NEJMoa1804355. Epub 2018 May 16. PMID: 29766770.
11. Schwamm LH, Wu O, Song SS, et al. MR WITNESS Investigators. Intravenous thrombolysis in unwitnessed stroke onset: MR WITNESS trial results. Ann Neurol. 2018;83(5):980–93. https://doi.org/10.1002/ana.25235. Epub 2018 Apr 27. PMID: 29689135; PMCID: PMC6095471.
12. Powers WJ, Rabinstein AA, Ackerson T, et al. Guidelines for the early management of patients with acute ischemic stroke: 2019 update to the 2018 guidelines for the early management of acute ischemic stroke: a guideline for healthcare professionals from the American Heart Association/American Stroke Association. Stroke. 2019;50(12):e344–418. https://doi.org/10.1161/STR.0000000000000211. Epub 2019 Oct 30. Erratum in: Stroke. 2019 Dec;50(12):e440–1. PMID: 31662037.
13. Campbell BC, Mitchell PJ, Churilov L, et al. EXTEND-IA TNK Investigators. Tenecteplase versus alteplase before endovascular thrombectomy (EXTEND-IA TNK): a multicenter, randomized, controlled study. Int J Stroke. 2018;13(3):328–34. https://doi.org/10.1177/1747493017733935. Epub 2017 Sep 27. PMID: 28952914.
14. Logallo N, Novotny V, Assmus J, et al. Tenecteplase versus alteplase for management of acute ischaemic stroke (NOR-TEST): a phase 3, randomised, open-label, blinded endpoint trial. Lancet Neurol. 2017;16(10):781–8. https://doi.org/10.1016/S1474-4422(17)30253-3. Epub 2017 Aug 2. PMID: 28780236.
15. Campbell BCV, Mitchell PJ, Churilov L, et al. EXTEND-IA TNK part 2 investigators. Effect of intravenous tenecteplase dose on cerebral reperfusion before Thrombectomy in patients with large vessel occlusion ischemic stroke: the EXTEND-IA TNK part 2 randomized clini-

cal trial. JAMA. 2020;323(13):1257–65. https://doi.org/10.1001/jama.2020.1511. PMID: 32078683; PMCID: PMC7139271.
16. Smith EE, Kent DM, Bulsara KR, et al. On behalf of the American Heart Association Stroke Council. Accuracy of prediction instruments for diagnosing large vessel occlusion in individuals with suspected stroke: a systematic review for the 2018 guidelines for the early management of patients with acute ischemic stroke. [published correction appears in Stroke. 2018;49:e139]. Stroke. 2018;49:e111–22.
17. Carrera D, Gorchs M, Querol M, et al. Revalidation of the RACE scale after its regional implementation in Catalonia: a triage tool for large vessel occlusion. J Neurointerv Surg. 2019;11(8):751–6. https://doi.org/10.1136/neurintsurg-2018-014519.
18. Li JL, McMullan JT, Sucharew H, et al. Potential impact of C-STAT for prehospital stroke triage up to 24 hours on a regional stroke system. Prehosp Emerg Care. 2019; https://doi.org/10.1080/10903127.2019.1676343.
19. Noorian AR, Sanossian N, Shkirkova K, et al. Los Angeles motor scale to identify large vessel occlusion: prehospital validation and comparison with other screens. Stroke. 2018;49(3):565–72. https://doi.org/10.1161/STROKEAHA.117.019228.
20. Birnbaum L, Wampler D, Shadman A, et al. Paramedic utilization of Vision, Aphasia, Neglect (VAN) stroke severity scale in the prehospital setting predicts emergent large vessel occlusion stroke. J NeuroInterv Surg. Published Online First. 2020; https://doi.org/10.1136/neurintsurg-2020-016054.
21. American Heart Association. Severity-based stroke triage algorithm for EMS. https://www.heart.org/missionlifelinestroke. 2020.
22. The Joint Commission. Specifications Manual for Joint Commission National Quality Measures (v2021A1). https://manual.jointcommission.org/releases/TJC2021A1/index.html.
23. McTaggart RA, Moldovan K, Oliver LA, et al. Door-in-door-out time at primary stroke centers may predict outcome for emergent large vessel occlusion patients. Stroke. 2018;49(12):2969–74. https://doi.org/10.1161/STROKEAHA.118.021936. PMID: 30571428.
24. Yang P, Zhang Y, Zhang L, et al. DIRECT-MT Investigators. Endovascular thrombectomy with or without intravenous alteplase in acute stroke. N Engl J Med. 2020;382(21):1981–93. https://doi.org/10.1056/NEJMoa2001123. Epub 2020 May 6. PMID: 32374959.
25. Suzuki K, Kimura K, Takeuchi M, et al. The randomized study of endovascular therapy with versus without intravenous tissue plasminogen activator in acute stroke with ICA and M1 occlusion (SKIP study). Int J Stroke. 2019;14(7):752–5. https://doi.org/10.1177/1747493019840932. Epub 2019 Mar 29. PMID: 30924762.

Chapter 11
Endovascular Management of Stroke

Matías Negrotto, Mithun G. Sattur, and Alejandro M. Spiotta

Philosophy of Mechanical Thrombectomy

The use of intravenous recombinant tissue plasminogen activator (IV rTPA) became standard of care following demonstration of its unequivocal benefit in several randomized trials in the USA and internationally (NINDS1, 2, ECAS 1 to 3) [1, 2]. Guidelines advocate administration within 4.5 hours after onset of stroke (last known normal or LKN status) that translates to a statistically significant chance of a favorable outcome, as defined by both improvements in NIHSS at 24 hours and mRS or Barthel index scores at 90 days. However, it became apparent that the efficacy of thrombolysis with TPA is limited in patients with large artery occlusion. This provided the impetus to intensively explore mechanical thrombectomy for recanalization.

Endovascular Treatment: Initial Negative Trials

In March 2013, in a single issue *New England Journal of Medicine* published the first three multicenter, prospective, randomized, controlled trials (IMS 3, SYNTHESIS, MR RESCUE) [3–5] using first-generation devices (MERCI system – Concentric Medical Inc., CA, USA) to evaluate the efficacy of endovascular

M. Negrotto (✉)
Hospital Maciel, Montevideo, Uruguay

Hospital Universitario de Clínicas, Montevideo, Uruguay

M. G. Sattur · A. M. Spiotta
Medical University of South Carolina, Mt Pleasant, SC, USA
e-mail: sattur@musc.edu; spiotta@musc.edu

J. R. Mascitelli, M. J. Binning (eds.), *Introduction to Vascular Neurosurgery*,
https://doi.org/10.1007/978-3-030-88196-2_11

treatment for ischemic stroke. The trial failed to show benefit of intra-arterial revascularization and was stopped early because of futility, according to the prespecified criteria – there was no significant difference between the endovascular-therapy and intravenous t-PA groups in the overall proportion of participants in achieving a modified Rankin score of 2 or less. The overall consensus was that procedural technique and patient selection were still unrefined. Despite the negative results, these studies paved the way for new trials that justified endovascular stroke therapy.

Endovascular Treatment: Positive Trials

In 2015 five successful trials using new generation devices (MR CLEAN, ESCAPE, EXTEND-IA, SWIFT PRIME, REVASCAT) [6–10] were published, conclusively demonstrating safety and efficacy of mechanical thrombectomy in patients with anterior circulation large vessel occlusion. These trials included patients within 6 hours of symptom onset (up to 8 hours in REVASCAT). Since then, techniques for mechanical thrombectomy have evolved further, and many other studies have confirmed that the superiority of endovascular stroke treatment and interventionalists around the world can now choose between a variety of methods which are both safe and effective.

MR CLEAN included patients with a NIHSS more than 2, with less than 6 hours of evolution since the onset of symptoms to treatment, confirming proximal vascular occlusion by CT angiography, with ASPECTS score of 7–10. No significant changes were observed in terms of mortality; however, there was a statistically significant decrease in morbidity with a mRS of 0–2: 33% with endovascular treatment vs 19% control group. One main disadvantage was the wait between the initiation of iv thrombolytic and endovascular therapy with a delay in reperfusion.

ESCAPE included patients with a NIHSS more than 12, ASPECTS more than 5, a therapeutic window of 12 hours, with diagnosis of proximal occlusion by CT angiography and perfusion for evaluation of circulation. This study was stopped early because of the clear benefit and efficacy of endovascular treatment with a decrease in morbidity and mortality.

EXTEND-IA also used a selection criteria based on perfusion images in patients with LVO, no age limits, no NIHSS limits, and time to treatment less than 4.5 hrs. It showed a favorable outcome mRS of 0–2 of 71% with intervention vs. 40% control group and a decrease in mortality of 9% vs. 20% in the control group.

SWIFT PRIME included patients with an NIHSS between 8 and 29, ASPECTS more than 6. Large vessel occlusion was diagnosed by CT angiography or MR angiography.

The modified Rankin Scale (mRS) score of 0–2 in the intervention group was 60% which was higher than that in MR CLEAN (33%) and similar to that observed in the ESCAPE trial (53%) and the EXTEND-IA trial (71%). There was no significant decrease in mortality.

REVASCAT assessed contributed evidence to support the efficacy of neurovascular thrombectomy in patients with anterior circulation stroke who could be treated within 8 hours after the onset of symptoms. It included patients with NIHSS more than 6, diagnosis of proximal occlusion by CT angiography, and ASPECTS greater than 7. It showed clear favorable results mRS of 0–2 of 44% with intervention vs. 28% control group, with no significant change in mortality.

Extending the Time Window for Thrombectomy

In 2018, automated image processing from CT perfusion or MR imaging data enabled investigation into extending the benefits of thrombectomy into late time windows. The physiologic basis is identifying patients with good collateral circulation that allows their infarcts to evolve relatively slowly. DAWN and DEFUSE 3 were the positive trials which showed benefit extending the time window for thrombectomy from 6 to 24 hours. Both trials used the Rapid Processing of Perfusion and Diffusion (RAPID) automated software platform (iSchemaView, Menlo Park, CA) to determine imaging eligibility for all patients. The RAPID imaging maps show tissue that is likely to be irreversibly damaged and estimate the size of the stroke if reperfusion does not occur.

The **DAWN** trial [11] used computed tomographic (CT) perfusion or magnetic resonance diffusion weighted imaging to select patients with large vessel occlusion stroke who had last been known to be well 6–24 hours earlier and who had a mismatch between clinical deficit and infarct. Patients had to have a mismatch between the severity of the clinical deficit and the infarct volume, which was defined according to the following criteria: Patients aged over 80 had to have an NIHSS score over 10 and a core volume less than 21 mL. For patients younger than 80 years, requirements were an NIHSS score of over 10 and a core less than 31 mL or an NIHSS score over 20 and a core less than 51 mL. Results showed that thrombectomy in DAWN-eligible patients was associated with improvement in clinical outcomes and functional independence (mRS 0–2) compared to standard medical therapy.

DEFUSE 3 [12] demonstrated that endovascular therapy, plus medical treatment, results in better functional outcome and decrease in mortality at 90 days than standard medical therapy alone for ischemic stroke patients with salvageable tissue on brain imaging, who are treated between 6 and 16 hours after the patient was last known to be well.

This trial also used computed tomographic (CT) perfusion or magnetic resonance diffusion weighted imaging to select patients with large vessel occlusion. Eligible patients had an initial infarct size of less than 70 ml, a ratio of the volume of ischemic tissue on perfusion imaging to infarct volume of 1.8 or more, and a mismatch volume of more than 15 ml.

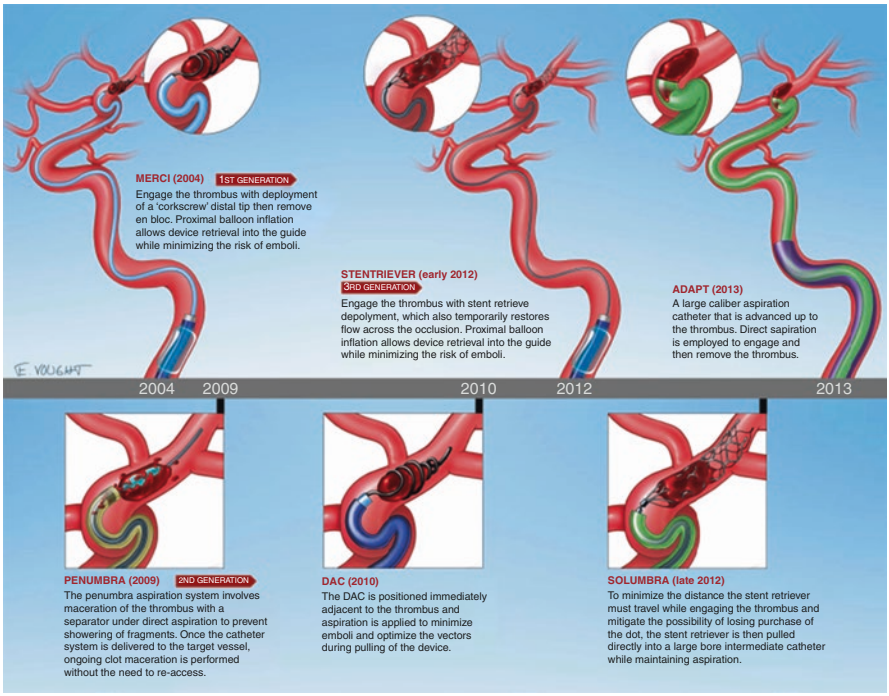

Fig. 11.1 Illustration depicting the major steps in evolution of thrombectomy devices, beginning from the first-generation concept to state-of-the-art approaches. (Adapted from: Spiotta et al. [15])

Techniques of Mechanical Thrombectomy (Fig. 11.1)

Current stroke guidelines by the American Heart Association/American Stroke Association recommend that large vessel strokes can safely be treated with mechanical thrombectomy up to 24 hours after a stroke in selected patients (reference 2018 guidelines). The evidence from the above randomized trials in favor of mechanical thrombectomy comes from studies in which patients in the endovascular groups were treated using stent retrievers. However, the parallel technical strategy of contact aspiration or ADAPT has been demonstrated as a valid standalone technique. **ASTER** [13] and **COMPASS** [14] trials confirmed that there was no statistically significant difference between ADAPT (a direct aspiration first pass technique) and stent retriever as frontline mechanical thrombectomy strategies in the treatment of large vessel occlusion stroke. In COMPASS there was no difference in mRS scores at 90 days or TICI 2b-3 recanalization. Furthermore, there were no differences in distal embolization or symptomatic hemorrhage. Recent large patient series have buttressed the role of ADAPT technique in achieving high percentage of successful recanalization in short procedural times.

Stent Retriever Technique

The initial retrievable stents were Solitaire (Medtronic, Dublin, Ireland) (approved by FDA in 2012) and Trevo (Stryker); newer stent retrievers with changes in design have been introduced since 2015 [15]. These devices are self-expandable stents delivered via a microcatheter, which continues to permit intracranial blood flow when fully deployed. The stent traps the clot and permits retrieval. With more than 80% of patients enrolled in MR CLEAN, EXTEND-IA, ESCAPE, and SWIFT PRIME undergoing thrombectomy with retrievable stents, these studies demonstrated the efficacy of this technique [16]. Revascularization defined as TICI 2b/3 reperfusion was overwhelmingly in favor of endovascular therapy across all of these trials.

Brief Technical Steps

A guide catheter 6–8 F is introduced over a 0.035 inch guidewire and the relevant artery is catheterized. Another option could be to use a proximal balloon guide catheter (BGC) 8–9 F [17]. However, BGC placement may not always be easy if the stroke patient is elderly or a tortuous segment is encountered during the passage of aortic arch and/or common carotid artery [17]. In some difficult cases of extreme tortuosity, a triple coaxial technique using an intermediate catheter 5–6 F (Sofia; Microvention or Navien; Medtronic Neurovascular) is required.

After an angiography to confirm the place of the clot, the microcatheter (usually between 0.021 and 0.027 inch as inner diameter) is navigated beyond the occlusion using a 0.014 inch microguidewire. Once correct microcatheter location is confirmed within the occluded parent artery, the self-expandable stent is advanced past the occlusion site and deployed to cover the entire thrombus. As the retrievable stent is unsheathed from the microcatheter, it deploys integrating into the clot and providing immediate reperfusion [16]. Another angiogram may be performed to confirm proper stent position and revascularization. The stent is left in situ typically for 3–5 minutes to allow it to integrate the thrombus by radial force. Then, the stent and the microcatheter are retrieved by pulling them back into the guide catheter under proximal aspiration through the guide catheter, pulling out the clot.

Another technique is that when we have the stent-retriever positioned we can start pulling back only the microcatheter, maintaining the stent stable in order to maximize the lumen to aspirate. Finally, the stent retriever is pulled directly into the guide catheter, or to the intermediate catheter while maintaining aspiration and both are removed together. The stent retriever can be withdrawn back into the catheter under direct aspiration applied locally or may choose to withdraw the stent retriever entirely or partially into the aspiration catheter and then pull both the stent retriever and the aspiration catheter. Application of suction with either a pump or manual syringe aspiration during retrieval may promote clot purchase and reduce

embolisms [15]. If a BGC was used, it could aid aspiration and help clot retrieval when the stent retriever is being dragged back into the guide catheter [17]. Using a balloon guide catheter with the balloon inflated during the stent retriever maneuver, the antegrade bloodstream is suppressed.

Direct Aspiration First Pass Technique (Adapt) (Case 1)

The introduction of the Penumbra aspiration catheter and pump system (Penumbra) allowed ADAPT to evolve [13, 14] (Figs. 11.2 and 11.3). Before the existence of this new system the use of direct aspiration for arterial occlusion was restricted to non-tortuous vessels, limited by the lack of catheters large enough to provide enough aspiration, yet flexible and atraumatic enough to navigate the tortuous intracranial vasculature [16]. The Penumbra (Alemeda, CA) reperfusion catheter, on the other hand, had a large internal diameter but was not very stiff; therefore, it was very effective at advancement into intracranial vessels providing an efficient and effective means of recanalization in patients with large vessel occlusions. TICI 2b or 3 recanalization can be achieved in over 70% and up to 81% especially with larger catheters [18–20]. Rescue therapy may include the use of a retrievable stent.

Brief Technical Steps (Case 1)

The first step is to use guiding catheter 6–8 F or a balloon guide catheter 8–9 F. After confirmation of the position of the thrombus, the aspiration catheter is introduced. The main concept is to use a large bore aspiration catheter with the largest size (usually a 0.068, 0.070 or increasingly a 0.072 in catheter) that the vessel can accommodate. In smaller caliber vessels either a 3 Max or a 4 Max (Penumbra, Inc.) can be used. This aspiration catheter is advanced over a microcatheter and a microguidewire to the proximal surface of the thrombus. After removing the microcatheter and guidewire, aspiration is applied constantly by manual suction using a syringe or using the Penumbra (Alemeda, CA) aspiration pump. The catheter is slightly advanced to ensure firm engagement with the clot. Absence of backflow mostly indicates the thrombus is trapped in the catheter. If free blood flow starts going into the catheter, this suggests the wedged clot is disrupted and sucked. The key technical nuance is clot ingestion by the catheter. The aspiration catheter is slowly and carefully removed under continuous aspiration [17]. At the same time, aspiration is also applied to the sideport of the guide catheter to prevent dislodging the thrombus from the catheter aperture as it is withdrawn into the sheath. Avoiding the use of a stent retriever leads to lower device cost [21].

Case 1
A 51-year-old man presented with right-sided facial palsy, left gaze deviation, and right-sided weakness; he had a National Institutes of Health Stroke Scale (NIHSS)

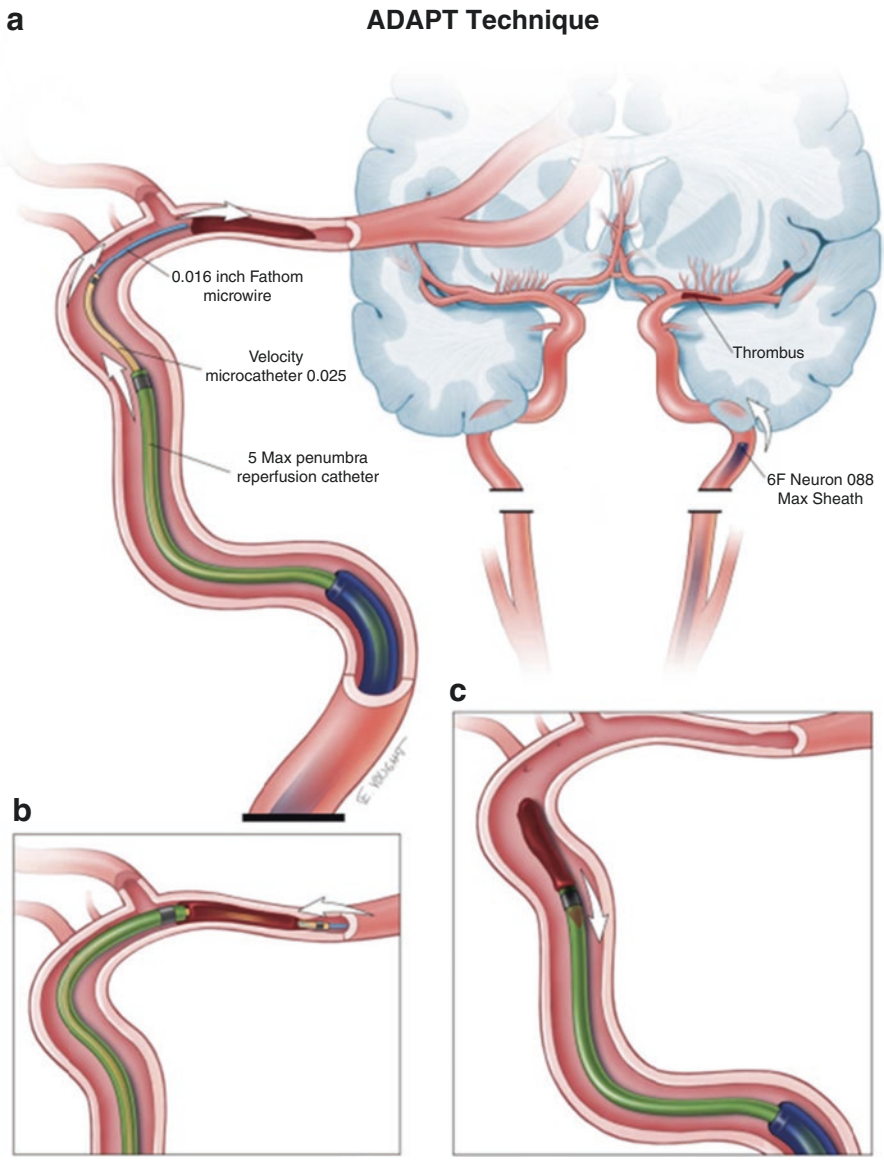

Fig. 11.2 Illustration of the ADAPT technique in a middle cerebral artery clot. (**a**) The Neuron Max guide catheter is positioned as far distally as possible in the supplying internal carotid artery. Through this a 5 Max reperfusion catheter is advanced over a Velocity microcatheter with a 0.016 inch Fathom wire. (**b**) The Fathom wire and Velocity microcatheter are advanced through and distal to the thrombus to provide stable support for the 5 Max to be advanced to the face of the thrombus. (**c**) Aspiration is applied to the 5 Max until aspiration becomes occlusive and the 5 Max is then removed while maintaining aspiration to ensure the clot remains engaged in the catheter tip. (Adapted from: Turk AS, Spiotta A, et al. Initial clinical experience with the ADAPT technique: a direct aspiration first pass technique for stroke thrombectomy. J NeuroIntervent Surg. 2013;6(3):231–7. https://doi.org/10.1136/neurintsurg-2013-010713)

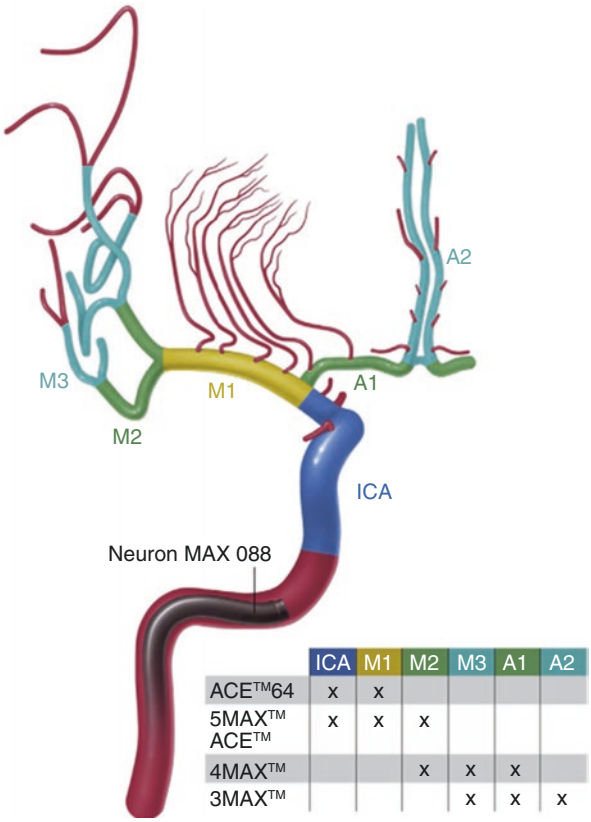

Fig. 11.3 Illustration demonstrating aspiration catheter size recommendations for anterior circulation thrombectomy. The guide catheter is positioned in the internal carotid artery (ICA), providing a platform for thrombectomy with aspiration catheters. (Adapted from: Jan Vargas, Spiotta Alex, et al. Experience with A Direct Aspiration First Pass Technique (ADAPT) for Thrombectomy in Distal Cerebral Artery Occlusions Causing Acute Ischemic Stroke. World Neurosurg. 2017;99:31–36. https://doi.org/10.1016/j.wneu.2016.11.035. Epub 2016 Nov 29)

score of 10. The patient underwent non-contrast CT and CT angiography of the brain demonstrating an Alberta Stroke Program Early CT score (ASPECTS) of 8; the CT angiogram showed a left M1 occlusion with little collateral circulation. The patient had exclusion criteria for intravenous thrombolysis, so given his favorable imaging it was decided to perform a thrombectomy. Time to recanalization was 20 minutes with a TICI 3 (Fig. 11.4). The treatment was performed using a right femoral 9 Fr sheath, Guide sheath, 0.071 in aspiration catheter, and 0.035 in microcatheter)

Solumbra (Case 2)

This term is sometimes applied to the combined use of aspiration and stent-retriever thrombectomy where the large-bore aspiration catheters can function as a direct distal conduit for stent retrievers [15] (derived from "Solitaire" FR (Medtronic Neurovascular) and "Penumbra" reperfusion catheter (Penumbra). We use a large bore distal aspiration catheter which is advanced as closely as possible to the thrombus before performing the stent retriever maneuver. This strategy may promote

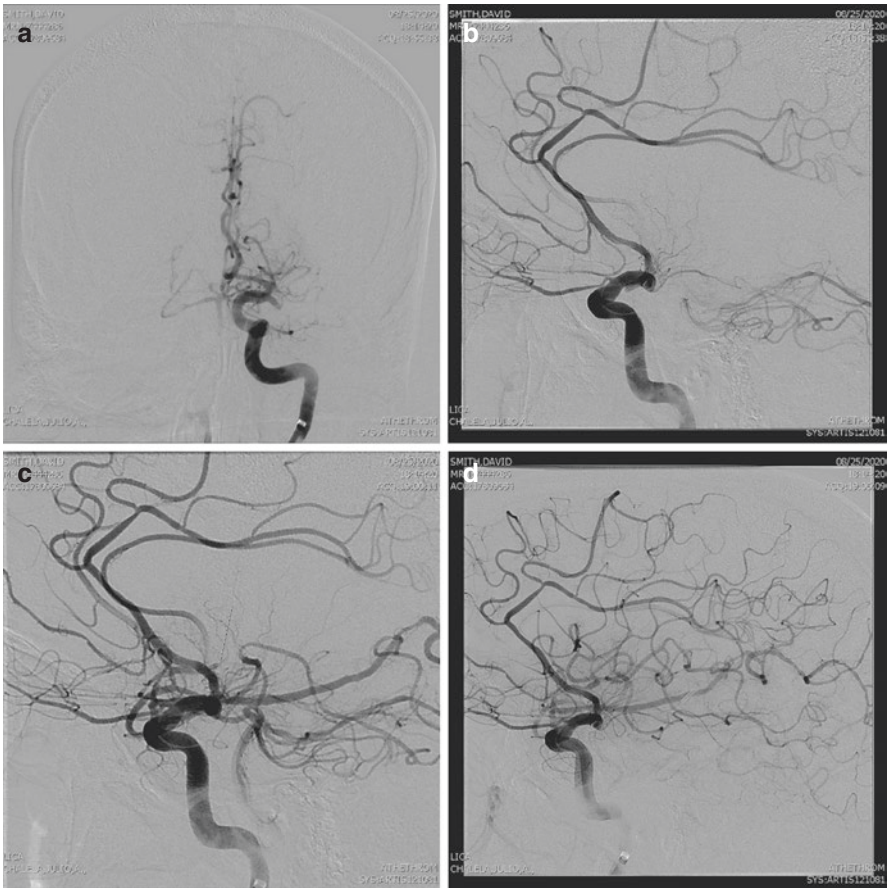

Fig. 11.4 (**a**) Front view showing occlusion of left M1 shortly after ICA bifurcation. (**b**) Lateral view of occlusion. (**c**) Lateral view following first pass aspiration. (**d**) Lateral view following second pass aspiration and final recanalization

entrapment of the clot within the stent reducing the incidence of thrombus fragmentation and distal embolization or embolizations to new, previously uninvolved vascular territories [17]. For example, first a guiding catheter 6–8 F or a balloon guide catheter 8–9 F is navigated into the internal carotid artery. Then, a 5 Max (Penumbra, Inc.) catheter can be advanced over a 0.25 microcatheter and microwire to the site of the occlusion. We have to pass the thrombus with the microcatheter, verify its position, and the stent retriever is deployed. When we have the stent-retriever positioned the microcatheter can be removed in order to maximize the lumen to aspirate with the 5 Max afterward. Finally, the stent retriever is pulled directly into the 5 Max while maintaining aspiration (for embolic protection) and both are removed together.

In conjunction with distal aspiration at the large bore aspiration catheter the risk of distal embolization can be reduced effectively.

Case 2

A 75-year-old man with a history of hypertension and diabetes mellitus presented with a left middle cerebral artery (MCA) stroke syndrome; he had a National Institutes of Health Stroke Scale (NIHSS) score of 23. He was last known normal to consultation 85 minutes before. The patient underwent non-contrast CT and CT angiography of the brain demonstrating an Alberta Stroke Program Early CT score (ASPECTS) of 9; the CT angiogram showed a left M1 occlusion (Fig. 11.5). Time to recanalization was 31 minutes with a TICI 3. The treatment was performed using a right femoral 9 Fr sheath, guide catheter, 0.071 in aspiration catheter, 0.035 in microcatheter, and 0.016 in wire. Two attempts were made with aspiration and then a final pass with stent retriever for distal M2 clot using a 4 × 20 mm stent retriever (Fig. 11.6). His NIHSS score at 1 hour was 4 and mRS (modified ranking scale) at 3 months was 1

Difficult and Challenging Situations

Large Vessel Occlusions with Carotid Artery Occlusion (Tandem Lesions)

Cervical carotid artery atherosclerotic disease is responsible for approximately 15–30% of acute ischemic strokes, which are mostly due to an artery-to-artery embolism with or without a cervical carotid artery occlusion (tandem occlusion) [17, 21]. The ESCAPE and REVASCAT trials showed the relatively common

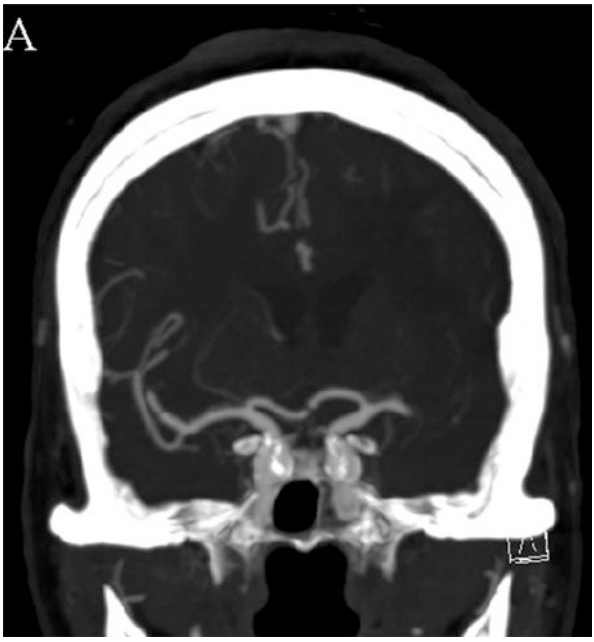

Fig. 11.5 (**a**) Angio CT showing left M1 occlusion

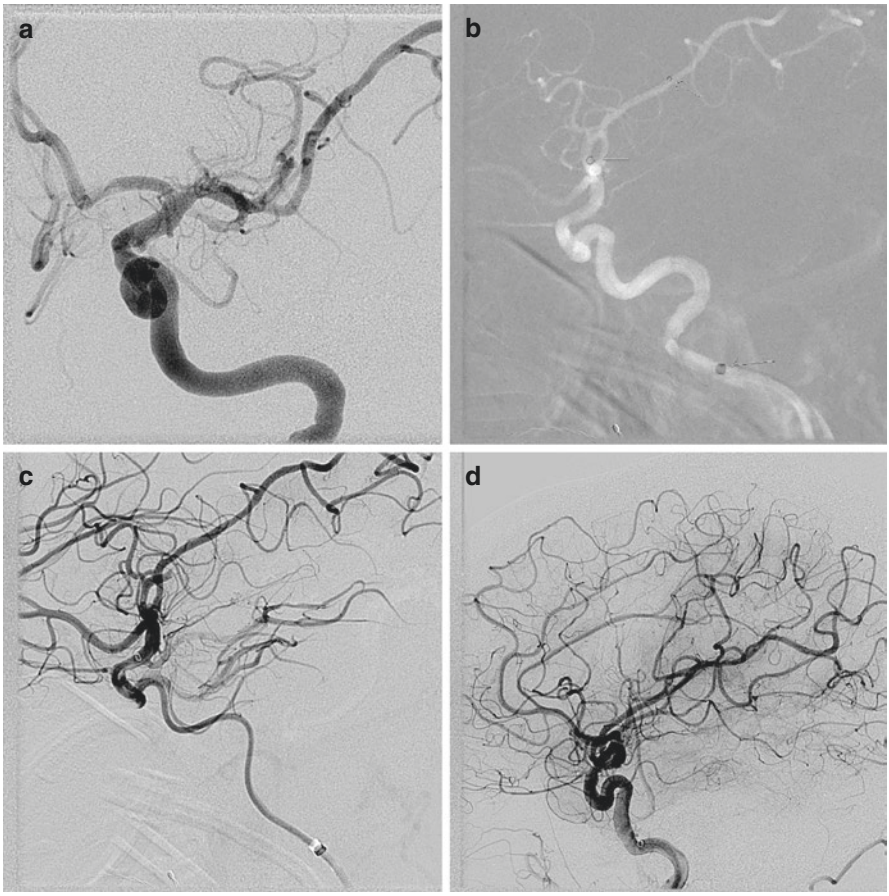

Fig. 11.6 (**a**): Oblique projection showing left M2 superior division occlusion. (**b**) Tri-axial set up guide catheter (Neuron Max), aspiration catheter (Vecta), and microcatheter (3 Max) from proximal to distal. (**c**) Clot in mid M2 after aspiration attempts. (**d**) Final recanalization

frequency of tandem strokes, which represented 12.7% and 15.8%, respectively, of all AIS undergoing thrombectomy over the study period. Acute ischemic strokes due to tandem occlusions are associated with very poor prognosis if treated only medically; however, there is evidence supporting that thrombectomy using stent-retrievers with emergency stenting of cervical ICA is associated with acceptable safety and efficacy in acute anterior stroke patients with tandem occlusion [22, 23].

Endovascular treatment of tandem occlusions is more complex and takes more time since this requires emergency ICA stenting in an acute setting as well as treatment of intracranial thrombus. Despite its complexity, successful reperfusion can be achieved in 60–80% of cases using current techniques [24].

Controversies in treating tandem occlusions include the following: (a) use of carotid stenting (with antiplatelet therapy) or balloon angioplasty alone and (b)

sequence of treatment, i.e., proximal to distal or vice versa. Growing evidence supports stenting with antiplatelet therapy for extracranial internal carotid artery lesions, even in patients who receive prior intravenous thrombolysis [24, 25]. Sequence of recanalization has not been shown to influence outcome and is largely a matter of operator preference [25, 26]. Treating the cervical (proximal) lesion first (antegrade technique) provides accessibility to the distal occlusion, addressing the proximal lesion in a controlled manner and allowing taking a large bore catheter distally to manage the intracranial occlusion. Also, potential embolic clot is blocked by distal emboli and is addressed during the later phase of the procedure. On the other hand, treating the intracranial occlusion first (retrograde technique) has the advantage of faster reperfusion, but theoretically increases the risk of distal emboli.

Initial step in treating a tandem occlusion is to catheterize the common carotid artery with an 8 F guide catheter and interpret the cause of the internal carotid occlusion (high grade atherosclerotic stenosis, dissection, or thromboembolic). A microcatheter with a 0.014 microwire is used to confirm presence in true lumen and to localize the intracranial occlusion. With a proximal-to-distal anterograde technique, a stent is deployed across the stenosis. Pre- or post-stenting angioplasty is performed. Then a 6 F guide catheter is taken across the stent and intracranial thrombectomy is performed.

Posterior Circulation Occlusion (Case 3)

There are currently only observational data available on endovascular thrombectomy for posterior circulation stroke (Class III evidence), with no published randomized trial to date that has evaluated endovascular intervention versus standard medical treatment or different methods of endovascular intervention against each other [27]. There has traditionally been a hesitant attitude regarding outcomes for posterior circulation LVO (PC-LVO) due to several reasons: late presentation, higher NIHSS due to frequent brainstem involvement, delay in treatment, and prior studies showing poor results of intra-arterial thrombolysis [28]. The problem is also magnified because of the difficulty in interpreting ischemic changes on CT and CT perfusion studies at the level of the brainstem [29].

However, evidence from retrospective studies has demonstrated similar rates of successful recanalization with mechanical thrombectomy achieved in posterior circulation stroke (PCS) and anterior circulation stroke [30]. Both stent retriever and aspiration thrombectomy as primary treatment approaches are effective in achieving successful recanalization. A review and meta-analysis including observational series data of outcomes with stent retriever thrombectomy in basilar artery occlusion showed an overall recanalization rate of 81%, and the pooled estimate of favorable clinical outcome of 42% [31]. A systematic review and

meta-analysis comparing aspiration thrombectomy and stent retriever thrombectomy [27] showed superior rates of successful recanalization, complete recanalization, faster procedural time, and improved safety profile seen for primary aspiration thrombectomy compared with primary stent retriever thrombectomy (although there was no statistically significant difference for the primary clinical outcomes of mortality and favorable outcome (mRS score 0–2) at 3 months). A multicenter retrospective study with 345 patients with posterior circulation strokes [30] showed that the use of ADAPT was more likely to result in better functional recovery after posterior circulation thrombectomy compared to stent retriever or combined approach.

Therefore, despite the lack of randomized clinical trials to prove efficacy as with anterior circulation stroke, mechanical thrombectomy should be offered to patients with PC-LVO especially with acute basilar artery occlusion. This is more important in cases where there is a fluctuating exam and limited brainstem changes on MRI, regardless of the time elapsed [32] (it is reasonable to exclude patients with a terminal neurological exam correlating with irreversible brainstem damage on MR imaging).

Case 3

An 87-year-old man with a history of hypertension and coronary artery disease treated with aspirin and plavix presented with a pontine syndrome. He was last known normal 14 hours ago. The patient underwent non-contrast CT, CT angiography, and CT perfusion of the brain demonstrating mid basilar occlusion with pontine ischemia (Fig. 11.7). The patient had exclusion criteria for intravenous thrombolysis. Time to consultation was 8 minutes and time to recanalization was 18 minutes. The treatment was performed using radial approach (Fig. 11.8) with a 5/6 sheath, 0.071 in aspiration catheter, and 0.035 in microcatheter with a 0.016 in wire. MRI 24 hours after intervention showed small unilateral pontine infarct (Fig. 11.9)

Distal Occlusions

In this chapter we consider distal occlusion as MCA occlusion distal to M1 (M2-M3-M4 segments), any segments of ACA, and any segments of PCA. If patients present with vessel occlusions distal to the M2 segments, the current guidelines recommend treatment with IVT. The benefit of MT performed in distal vessels remains controversial. The AHA 2019 Guidelines for the Early Management of Patients with Acute Ischemic Stroke provide a weak recommendation (2b) for M2 or M3 thrombectomy suggesting that it may be reasonable in certain cases but no strong evidence is available [33].

There is growing evidence on safety and efficacy of EVT over standard care practice for M2 segment occlusions using new-generation thrombectomy devices

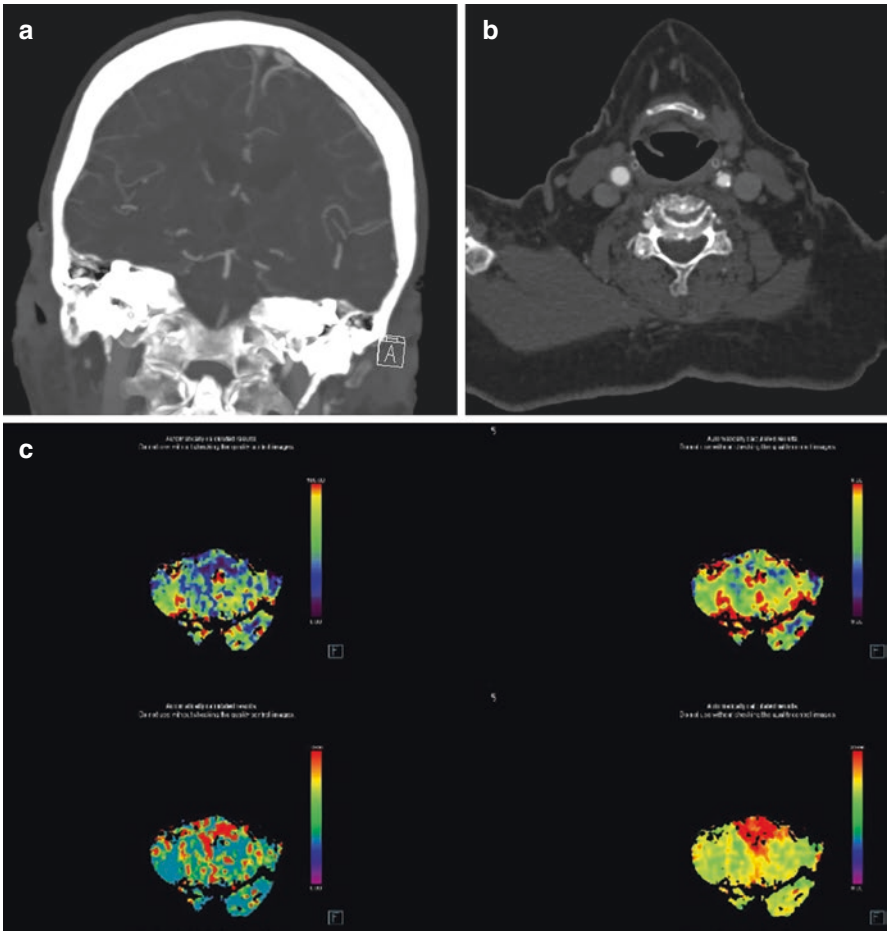

Fig. 11.7 (**a**) Angio CT showing mid-basilar occlusion, and (**b**) right vertebral dominant. (**c**) Perfusion imaging showing pontine ischemia

[34–36]. Recently, some studies have proved that MT for distal occlusions can be safely performed with high functional independence and recanalization rates, but it may be associated with an increased risk of complications [35, 37]. Despite the higher rate of hemorrhage occurring in M2 patients, results are favorable for intervention [35].

Comparing different techniques, MT using the new generation of SR in distal anterior circulation is associated with a similar successful revascularization rate compared to MT using ADAPT. However, functional independence at 3 months is higher in the ADAPT group and mortality is higher in the SR group [37].

Fig. 11.8 Angiography. (**a**) Right radial approach. (**b**) Mid basilar occlusion. (**c**) TICI 3 recanalization

The indication for thrombectomy in this kind of patients must be precise to minimize putting in risk patients that would not benefit from the procedure [35]. We recommend careful risk-benefit assessment. We must know that distal arteries are smaller in caliber, have thinner walls, are typically more tortuous, and the occlusion is more difficult to detect. We think that a proper selection for endovascular revascularization is a patient with an occluded dominant M2-segment which supplies eloquent territory, with significant penumbra at risk and with moderate to severe deficit.

Large randomized trials are still necessary to investigate factors associated with a favorable outcome of endovascular treatment in acute ischemic stroke from distal intracranial vessel occlusions.

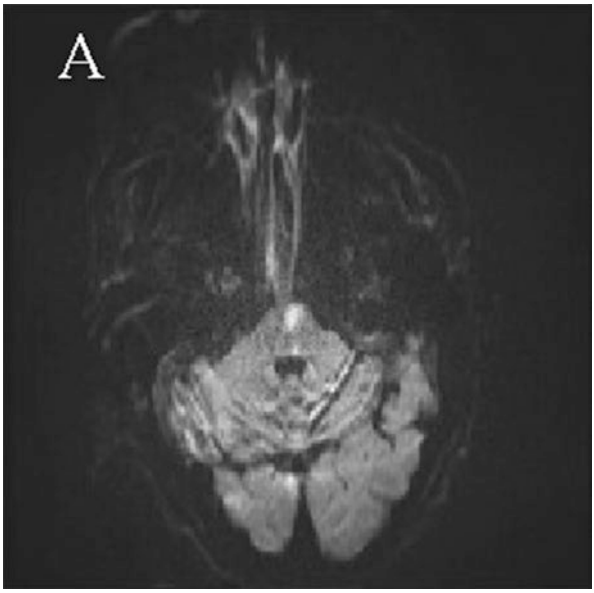

Fig. 11.9 (**a**) MRI 24 hours after intervention showing small unilateral pontine infarct

References

1. The National Institute of Neurological Disorders and Stroke rt-PA Stroke Study Group. Tissue plasminogen activator for acute ischemic stroke. N Engl J Med. 1995;333(24):1581–7.
2. Hacke W, Kaste M, Bluhmki E, Brozman M, Dávalos A, Guidetti D. Et al; ECASS Investigators. Thrombolysis with alteplase 3 to 4.5 hours after acute ischemic stroke. N Engl J Med. 2008;359(13):1317–29.
3. Kidwell CS, Jahan R, Gornbein J, Alger JR, Nenov V, Ajani Z, et al. A trial of imaging selection and endovascular treatment for ischemic stroke. N Engl J Med. 2013;368:914–23. (MR RESCUE).
4. Ciccone A, Valvassori L, Nichelatti M, Sgoifo A, Ponzio M, Sterzi R, et al. Endovascular treatment for acute ischemic stroke. N Engl J Med. 2013;368:904–13. (SYNTHESIS).
5. Broderick JP, Palesch YY, Demchuk AM, Yeatts SD, Khatri P, Hill MD, et al. Endovascular therapy after intravenous t-pa versus t-pa alone for stroke. N Engl J Med. 2013;368:893–903. (IMS 3).
6. Bekhemer O, Beumer F, Berg V, Lingsma H, Schonewile Y, Nederkoom V. The Randomized Trial of Intraarterial Treatment for Acute Ischemic Stroke (Mr. CLEAN). N Engl J Med. 2015;372
7. Goyal M, Demchuk A, Menon B, Eesa M, Rempel J, Thornton J, Roy D. Randomized assay of rapid endovascular treatment of ischemic stroke (ESCAPE). N Engl J Med. 2015;
8. Campbell B, Mitchell P, Kleinig T, Dewey H, Churilov L, Yassi N. Endovascular therapy for ischemic stroke with perfusion-imaging selection (EXTEND -IA). N Engl J Med. 2015;
9. Saver J, Mayank M, Bonafe A, Diener M, Elad P, Levy I. Thrombectomy Stent-Retriever alter Intravenous t-PA vs. t-PA Alone in Stroke (SWIFT PRIME). N Engl J Med. 2015.
10. Jovin T, Chamorro A, Cobo E, Miquel M, Molina C, Rovira A. Thrombectomy within 8 hours after symptom onset in ischemic stroke (REVASCAT). N Engl J Med. 2015.
11. Nogueira RG, Jadhav AP, Haussen DC, Bonafe A, Budzik RF, Bhuva P, et al. Thrombectomy 6 to 24 hours after stroke with a mismatch between deficit and infarct. N Engl J Med. 2018.

12. Albers GW, Marks MP, Kemp S, Christensen S, Tsai JP, Ortega-Gutierrez S, et al. Thrombectomy for stroke at 6 to 16 hours with selection by perfusion imaging. N Engl J Med. 2018;
13. Lapergue B, RaphaelBlanc BG, Labreuche J, Duhamel A, GautierMarnat, et al. Effect of endovascular contact aspiration vs stent retriever on revascularization in patients with acute ischemic stroke and large vessel occlusion. The ASTER Randomized Clinical Trial JAMA. 2017;318(5):443–52. https://doi.org/10.1001/jama.2017.9644.
14. Turk AS, Siddiqui A, Fifi JT, De Leacy RA, Fiorella DJ, Spiotta AM, et al. Aspiration Thrombectomy Versus Stent Retriever Thrombectomy as First-Line Approach for Large Vessel Occlusion (COMPASS): A Multicentre, Randomised, Open Label, Blinded Outcome, Non-Inferiority Trial. Lancet. 2019;393(10175):998–1008. https://doi.org/10.1016/S0140-6736(19)30297-1.
15. Spiotta AM, Chaudry MI, Hui FK, Turner RD, Kellogg RT, Turk AS. Evolution of thrombectomy approaches and devices for acute stroke: a technical review. J NeuroIntervent Surg. 2015;7:2–7. https://doi.org/10.1136/neurintsurg-2013-011022.
16. Munich SA, Vakharia K, Levy EI. Overview of mechanical thrombectomy techniques. Neurosurgery. 2019;85(suppl_1):S60–7. https://doi.org/10.1093/neuros/nyz071.
17. Kang D-H, Park J. Endovascular stroke therapy focused on stent retriever thrombectomy and direct clot aspiration: historical review and modern application. J Korean Neurosurg Soc. 2017;60(3):335–47. https://doi.org/10.3340/jkns.2016.0809.005.
18. Mocco J, Zaidat OO, von Kummer R, et al. Aspiration thrombectomy after intravenous alteplase versus intravenous alteplase alone. Stroke. 2016;47(9):2331–8.
19. Turk AS, Frei D, Fiorella D, Mocco J, Baxter B, Spiotta A. ADAPT FAST study: a direct aspiration first pass technique for acute stroke thrombectomy. J NeuroIntervent Surg. 2014;6:252–3.
20. Spiotta A, Alawieh A, Chatterjee AR, Vargas J, Chaudry MI, Lena J. Lessons learned over more than 500 stroke thrombectomies using ADAPT with increasing aspiration catheter size. Neurosurgery. 2020;86(1):61–70. https://doi.org/10.1093/neuros/nyy444.
21. Holmstedt CA, Turan TN, Chimowitz MI. Atherosclerotic intracranial arterial stenosis: risk factors, diagnosis, and treatment. Lancet Neurol. 2013;12:1106–14.
22. Sivan-Hoffmann R, Gory B, Armoiry X, Goyal M, Riva R, Labeyrie PE. Stent-retriever thrombectomy for acute anterior ischemic stroke with tandem occlusion: a systematic review and meta-analysis. Eur Soc Radiol. 2016; https://doi.org/10.1007/s00330-016-4338-y.
23. Grigoryan M, Haussen DC, Hassan AE, Lima A, Grossberg J, Rebello LC. Endovascular treatment of acute ischemic stroke due to tandem occlusions: large Multicenter series and systematic review. Cerebrovasc Diseases. 2016;41:306–12.
24. Anadani M, Spiotta A, Alawieh A, Turjman F, Piotin M, Steglich-Arnholm H. Effect of extracranial lesion severity on outcome of endovascular thrombectomy in patients with anterior circulation tandem occlusion: analysis of the TITAN registry. J NeuroIntervent Surg. 2019;0:1–5. https://doi.org/10.1136/neurintsurg-2018-014629.
25. Zhu F, Bracard S, Anxionnat R, Derelle A-L, Tonnelet R, Liang L. Impact of emergent cervical carotid stenting in tandem occlusion strokes treated by thrombectomy: a review of the TITAN collaboration. Front Neurol. 2019;10:206. https://doi.org/10.3389/fneur.2019.00206.
26. Wilson MP, Murad MH, Krings T, Pereira VM, O'Kelly C, Rempel J. Management of tandem occlusions in acute ischemic stroke – intracranial versus extracranial first and extracranial stenting versus angioplasty alone: a systematic review and meta-analysis. J NeuroIntervent Surg. 2018;0:1–9. https://doi.org/10.1136/neurintsurg-2017-013707.
27. Sheng K, Tong M. Aspiration thrombectomy for posterior circulation stroke: A systematic review and meta-analysis. Asian J Neurosurg. [serial online] 2020 [cited 2020 Aug 25];15:251–61.
28. Schonewille WJ, Wijman CAC, Michel P, Rueckert CM, Weimar C, Mattle HP, Engelter ST, Tanne D, Muir KW, Molina CA, Thijs V, Audebert H, Pfefferkorn T, Szabo K, Lindsberg PJ, de Freitas G, Kappelle LJ, Algra A, BASICS study group. On behalf of the BASICS study group. Treatment and outcomes of acute basilar artery occlusion in the basilar artery international cooperation study (BASICS): a prospective registry study. Lancet Neurol. 2009;8:724–30.

29. Van der Hoeven EJ, Dankbaar JW, Algra A, Vos JA, Niesten JM, van Seeters T, van der Schaaf I, Schonewille WJ, Kappelle LJ, Velthuis BK, Investigators DUST. Additional diagnostic value of computed tomography perfusion for detection of acute ischemic stroke in the posterior circulation. Stroke. 2015;46:1113–5.
30. Alawieh AM, Eid M, Anadani M, Sattur M, Maier IL, Spiotta AM, et al. Thrombectomy technique predicts outcome in posterior circulation stroke—insights from the STAR collaboration. Neurosurgery. 2020:nyaa179. https://doi.org/10.1093/neuros/nyaa179.
31. Gory B, Eldesouky I, Sivan-Hoffmann R, et al. Outcomes of stent retriever thrombectomy in basilar artery occlusion: an observational study and systematic review. J Neurol Neurosurg Psychiatry. 2016;87(5):520–5.
32. Chaudry I, Feng W, Holmstedt C, Turner R, Adams R, Turk AS. Delayed basilar artery recanalization 100 hours after symptom onset. J Neurointervent Surg. 2010;2(4):345–7.
33. Powers WJ, Rabinstein AA, Ackerson T, Adeoye OM, Bambakidis NC, Becker K, et al. Guidelines for the early Management of Patients with Acute Ischemic Stroke: 2019 update to the 2018 guidelines for the early Management of Acute Ischemic Stroke: a guideline for healthcare professionals from the American Heart Association/American Stroke Association. Stroke. 2019;50:e344–418.
34. Sarraj A, Sangha N, Hussain MS, Wisco D, Vora N, Elijovich L, et al. Endovascular therapy for acute ischemic stroke with occlusion of the middle cerebral artery M2 segment. JAMA Neurol. 2016;73:1291–6. https://doi.org/10.1001/jamaneurol.2016.2773.
35. Saber H, Narayanan S, Palla M, Saver JL, Nogueira RG, Yoo AJ, et al. Mechanical thrombectomy for acute ischemic stroke with occlusion of the M2 segment of the middle cerebral artery: a meta-analysis [published online ahead of print November 10, 2017]. J Neurointerv Surg. https://doi.org/10.1136/neurintsurg-2017-013515.
36. Anadani M, Alawieh A, Arthur AS, Kim J-T, Leacy RD, Spiotta A. Abstract 148: Mechanical Thrombectomy for Distal Occlusions: Efficacy, Functional and Safety Outcomes. Insights From the STAR Collaboration. Stroke. 51:A148.
37. Barchetti G, Cagnazzo F, Raz E, Barbagallo G, Toccaceli G, Peschillo S. Mechanical thrombectomy of distal occlusions using ADAPT compared to new generation of mini – 017 microcatheter compatible – stent retrievers: a meta-analysis. World Neurosurg. 2019; https://doi.org/10.1016/j.wneu.2019.10.030.

Chapter 12
Surgical Management of Extracranial Carotid Disease

Mohanad Sulaiman and Zakaria Hakma

Introduction

Stroke is the second most common cause of death among people over 60 and the second leading cause of disability among all ages. Carotid artery stenosis causes 15% of all ischemic strokes, and this risk of stroke correlates with the degree of stenosis and with presence of vulnerable plaques.

Atherosclerotic plaques begin to form in the carotid artery at 20 years of age and build-up of plaque can progress rapidly and lead to atherosclerosis and stenosis of the artery, which may or may not be symptomatic clinically by causing thromboembolic or stenotic/hypoperfusion complications. Carotid endarterectomy (CEA) is the most frequently performed operation to prevent stroke in patients who have either symptomatic or asymptomatic internal carotid artery stenosis. Carotid angioplasty and stenting is another option that was brought to the forefront. Yet, major trials have not proven these new technologies superior to endarterectomy in the treatment of carotid stenosis. CEA and stenting are among the most studied surgical procedures in history. Both forms of revascularization are proven to be safe when performed by experienced practitioners in properly selected patients.

This chapter describes the indications for CEA, including patient assessment and planning, and surgical considerations. Finally, operative technique is described in detail.

M. Sulaiman · Z. Hakma (✉)
Global Neuroscience Institute (GNI), Chester, PA, USA
e-mail: msulaiman@gnineuro.org; zhakma@gnineuro.org

J. R. Mascitelli, M. J. Binning (eds.), *Introduction to Vascular Neurosurgery*,
https://doi.org/10.1007/978-3-030-88196-2_12

Indications

The indication for treatment of symptomatic carotid stenosis was established through the North American symptomatic Carotid Endarterectomy Trial (NASCET) [1], and the European Carotid Surgery Trial (ECST) [2] in which patients suffering an episode of amaurosis fugax, hemispheric transient ischemic attach (TIA) or mild (nondisabling) stroke and ipsilateral high-grade stenosis (>70%) received a significant benefit from carotid endarterectomy (CEA) compared to medical management. CEA in this patient population reduced the absolute risk of subsequent stroke by 17% and death from any cause by 7% at 18 months compared to optimal medical management. This improvement in morbidity and mortality was twice as good for patients with 90–99% stenosis.

In addition, the latter study [3] found that there was benefit from CEA in patients with moderate (50–69%) carotid stenosis, and that patients with less than 50% stenosis gained no significant benefit from CEA.

These studies form the basis of current practice guidelines: patients with 50% or higher stenosis of the carotid artery and history of ipsilateral stroke or TIA are recommended to have CEA. The benefit of surgery is greatest in men who are nondiabetic and in patients who have hemispheric symptoms instead of amaurosis fugax. Additionally, Patients with plaque ulceration are at higher risk than those with smooth plaques.

Frequently carotid artery stenosis is asymptomatic and usually discovered as a carotid bruit with a non-specific visual complaints, dizziness, or syncope not associated with TIA or stroke [4]**.** The effect of prophylactic CEA in asymptomatic patients has been demonstrated in two large studies: The Asymptomatic Carotid Surgery Trial (ACST) [5] and The Asymptomatic Carotid Atherosclerosis Study (ACAS) [6]**.** These studies demonstrated a significant 5-year reduction (by 7.2% in ACST and by 5.9% in ACAS) in ipsilateral stroke or perioperative stroke or death risk in asymptomatic patients with >60% stenosis, with no benefit in patients over 75 years of age due to their increased probability of dying from causes other than stroke. On the other hand, the longer a patient survives after CEA, the greater the potential benefit since the adverse consequences of surgery are limited to the perioperative period. Unlike ACST, the benefit could not be demonstrated in women as sub-group in ACAS trial (There was also a higher perioperative complication rate for women in ACAS).

We offer a prophylactic CEA for asymptomatic patients below age 75 with a five- year life expectancy and 60% to 99% stenosis particularly in the presence of intraplaque hemorrhage, lipid-rich necrotic core, or thinning/rupture of the fibrous cap on MRI of carotid plaque which likely progress rapidly and associated with increased risk of future stroke or TIA in patients with carotid atherosclerotic disease [7]. The benefit is not as great for women, and the benefit depends on the ability to perform surgery with a combined morbidity/ mortality of less than 3%.

The presence of contralateral carotid artery stenosis or occlusion is not uncommon. However, it is not a contraindication to CEA and should not discourage a

surgeon from performing an endarterectomy for patients with appropriate lesions [8]**.** It is our practice to operate in the setting of bilateral disease. We start with the symptomatic side first, or the side with a greater degree of stenosis or concerning plaque characteristics in the case of asymptomatic disease. In the cases of chronic contralateral occlusion, we approach these cases with EEG monitoring and selective shunting.

Imaging and Diagnosis

Symptomatic carotid artery stenosis will usually be assessed as part of a stroke/TIA protocol. Although multiple imaging modalities are available to evaluate the extracranial vascular disease, there is no agreement regarding the appropriate imaging required prior to CEA.

Carotid duplex ultrasonography (CDU) provides a safe, quick, and relatively cost-effective initial diagnostic study. It is useful in detecting a significant stenosis but has a relatively low specificity for those patients with 50% to 60% carotid stenosis and can be of limited use in the sitting of significant calcification and string sign. It may overestimate the degree of stenosis and cannot scan above the angle of the mandible. Given these limitations, patients with an abnormal screening test should obtain a second confirmatory noninvasive test, such as computed tomography angiography (CTA) or magnetic resonance angiography (MRA), to evaluate the carotid stenosis and bifurcation. CTA provides detailed information regarding plaque morphology, calcifications of the aortic arch, and the relationship of the ICA bifurcation to the angle of the mandible. On the other hand, MRA can provide value in detecting more detailed characteristics of the atherosclerotic plaque, including lipid content and intraplaque hemorrhage. If the two noninvasive tests are discordant, then cerebral catheter angiography should be considered, which remains the gold standard for preoperative evaluation of carotid stenosis with a nearly 100% sensitivity and specificity [9, 10]. We studied the importance of using angiography as a confirmatory test for degree of stenosis and to examine patient's intracranial vasculature before definitive surgical treatment. Overall, we found that medical or surgical decision management was changed in 43% of cases investigated with digital subtraction angiography owing to a discrepancy between the measured percentage stenosis. In patients with potentially treatable carotid stenosis, angiography revealed nonsignificant stenosis 25.7% of the time [11].

Pre-Operative Medical Management

A patient undergoing CEA should be on antiplatelet therapy (unless contraindicated) prior to surgery. Antiplatelet reduce the risk of MI and stroke of any cause in patients undergoing CEA [15]**.** Patient taking aspirin preoperatively are instructed

to continue their therapy without interruption. Patients taking clopidogrel (Plavix) or ticlopidine (Ticlid) are switched to a daily aspirin one week before surgery (this strategy markedly reduces intraoperative oozing associated with these medications). Patients on warfarin or other anticoagulation therapy should be preoperatively admitted to the hospital and have their iatrogenic coagulopathy converted to IV heparin therapy. The heparin should be continued to the operating room and is stopped when the arterial closure is complete. Statins (HMG-CoA reductase inhibitors) decrease perioperative morbidity and mortality and may reduce carotid plaque progression and the incidence of transition from asymptomatic to symptomatic carotid stenosis [16]**.**

Surgical Considerations

1. *High risk patients for CEA:*

Patients may be classified as high risk for CEA based on numerous anatomic features and comorbidities [13]. High risk anatomic features include: contralateral carotid occlusion or significant bilateral carotid stenosis, contralateral laryngeal nerve palsy, prior neck or head radiation therapy or radical neck surgery, tandem lesions larger than target lesion, surgically inaccessible (very high carotid bifurcation "lesions above the C2 vertebra" or common carotid artery lesions below the clavicle), restenosis following a prior CEA, laryngectomy or tracheostomy, or inability to extend head as a result of arthritis or other condition.

Comorbidities that may preclude CEA include clinically significant cardiac disease (unstable angina, recent myocardial infarction (>24 hours and <30 days), class III or IV congestive heart failure, left ventricular ejection fraction <30%, severe pulmonary disease.

2. *Carotid artery stenting:*

Patients at high risk for CEA may be candidates for carotid angioplasty and stenting (CAS). A broad overview of CAS is presented in-depth in another chapter in this book. However, it is important to discuss some crucial points here.

The Carotid Revascularization Endarterectomy versus Stenting Trials (CREST) demonstrated that CAS and CEA had similar outcomes for symptomatic and asymptomatic men and women in terms of postoperative complications such as restenosis, myocardial infarction (MI), long-term stroke, and/or death. However, the risk of periprocedural stroke was significantly higher in patients undergoing CAS vs. CEA (4.1% vs. 2.3%), whereas CEA is associated with a higher risk of periprocedural myocardial infarction (1.1% vs. 2.3%) and cranial nerve injuries (0.3 vs. 4.7%). Additionally, older age (>70 years) was associated with worse outcome after stenting, potentially secondary to tortuous or calcified arch anatomies in these patients [14].

The decision to treat high risk carotid stenosis by CEA or CAS is controversial. However, the most widely accepted indications for CAS are patients with clinically significant cardiac risk of anesthesia or those with high- risk neck anatomic features, including very high carotid bifurcation, restenosis following a prior CEA, or prior neck radiation or radical neck surgery. We do recommend endovascular treatment with angioplasty and stenting for acute carotid occlusion especially in the presence of symptomatic acute occlusion with a large ischemic penumbra.

3. *Timing for surgery*

A pooled analysis of randomized controlled trials concluded that surgical revascularization for patients with symptomatic carotid stenosis is most beneficial when it occurs within 14 days of the TIA or minor stroke. The number of patients needed to undergo surgery (number needed to treat) to prevent one ipsilateral stroke was 5 for those patients randomized within 2 weeks after their last ischemic event versus 125 for patients randomized after 2 weeks from the onset of symptoms [12]. The current literature points to change the paradigm towards early carotid surgery, specifically targeted within 48 hours if the index event is TIA, and within 7 days if the index event is stroke. It is generally our practice to perform the CEA during the same hospital stay after a stroke especially if the volume of the stroke is small and in absence of any hemorrhagic conversion.

4. *Anesthesia and monitoring*

Intraoperative monitoring through Somato-Sensory Evoked Potentials (SSEP) and Electro Encephalogram (EEG) is used to assess intraoperative hypoperfusion. Assessment of the patient's neck mobility is also important for this procedure.

Anesthesia may be general, regional, or local. The multicenter, randomized controlled General Anesthesia versus Local Anesthesia (GALA) Trial [17] found no significant differences in the prevention of stroke, MI, or death for either anesthetic technique. However, general anesthesia allows for a more controlled surgical environment and cerebral protection from anesthetic and adjunctive agents by reducing the cerebral metabolic rate for oxygen.

Operative Anatomy

CEA takes place in the anterior triangle of the neck. The borders of this triangle include the inferior border of the mandible superiorly, the anterior border of the sternocleidomastoid muscle laterally, and the sagittal line down the midline of the neck medially. Both the left and right common carotids bifurcate into an internal and external carotid artery, classically at the level of the third or fourth cervical vertebra, near the superior border of the thyroid cartilage (Fig. 12.1). The deep cervical fascia forms the carotid sheath, surrounding the carotid arteries, internal jugular vein (IJV), and vagus nerve.

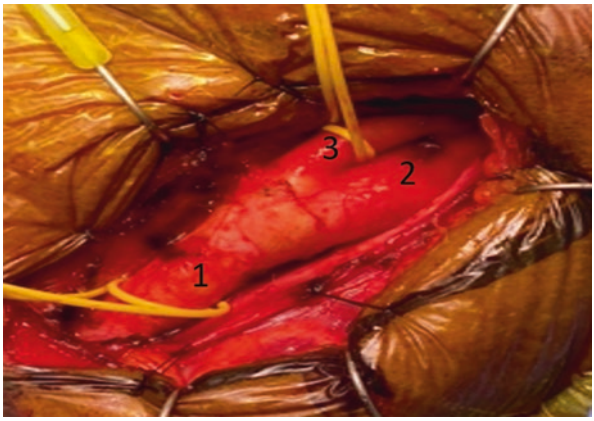

Fig. 12.1 The common carotid artery (1) is dissected circumferentially free of its sheath. It bifurcates into an internal (2) and external (3) carotid artery

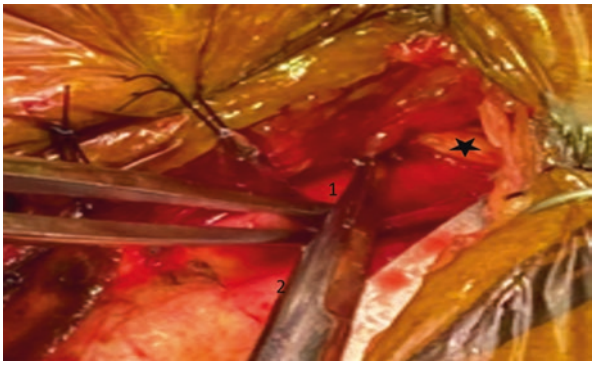

Fig. 12.2 The hypoglossal nerve (*) runs superficial to the ECA (1) and ICA (2)

The jugular vein lies lateral to the carotid artery and its anteriorly oriented branch, the common facial vein, often lies directly superficial to the carotid bifurcation and should be suture ligated and divided to facilitate exposure. The anatomy of the external carotid artery (ECA) and its branches are the key landmarks for reaching an appropriate exposure. The ECA is located medial to the internal carotid artery (ICA) and has eight branches: the first branch is the superior thyroid artery, lingual and facial arteries arise from its anterior surface whereas the occipital and posterior auricular arteries arise from its posterior surface, and the ascending pharyngeal artery arises from its medial surface. The ECA gives its terminal branches: maxillary and superficial temporal arteries within the parotid gland. The ICA is found medial to the ECA in around 10% of patients; this anatomical variant should be recognized on preoperative imaging and surgical dissection should be directed medial to the ECA.

Nerves that are particularly important during this procedure are the hypoglossal and vagal nerves. Hypoglossal nerve injury is the most common nerve injury during CEA. The hypoglossal nerve runs superficial to the ECA and ICA and crosses the ICA at the distal end of the dissection (Fig. 12.2). It must be identified and preserved throughout the duration of the case. The location of the hypoglossal nerve

can be discerned by pursuing the ansa cervicalis superiorly where it joins the hypoglossal nerve Finally, the vagus nerve and its superior laryngeal branch runs within the posterolateral aspect of carotid sheath, behind the carotid artery and jugular vein. Care must be taken to avoid disruption of these structures when dissection below the carotid is needed. Damage to the superior laryngeal branch of the vagus nerve will result in significant postoperative dysphagia.

The omohyoid muscle typically marks the inferior extent of the dissection and usually can be left intact.

Surgical Procedure

1. *Position*:

The patient is positioned supine with a shoulder roll laid transversely under the shoulders to assist with a slight degree of neck extension to open the operative space between the chin and clavicle. A piece of tape may be used to provide gentle traction on the mandible, allowing for increased exposure, especially in cases involving high bifurcations or plaques. The patient's head is rotated 20 degrees away from the operative side to expose the anterior triangle of the neck. Turning the head further will move the sternocleidomastoid muscle over the carotid sheath and interfere with the exposure.

Two anatomical landmarks are identified with preoperative radiographic studies to estimate the rostral extent of the required exposure. The first is the angle of the mandible, which is palpated and marked before skin incision. The second is the position of the carotid bifurcation, particularly its relationship with the distal extent of the cervical plaque (Fig. 12.3).

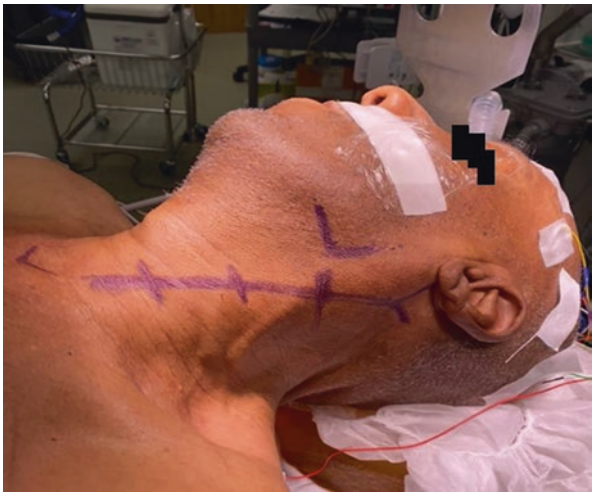

Fig. 12.3 The patient's head is rotated 20 degrees away from the operative side. The angle of the mandible and the sternal notch are marked. A longitudinal incision is made along the anterior border of the sternocleidomastoid muscle (the incision is made between top 2 hashmarks)

2. *Exposure*:

The level of the bifurcation as well as the location and length of the plaque can be estimated via surface landmarks. The thyroid cartilage estimates the level of C4–5. The angle of the mandible and the hyoid bone estimate the location of C3, while the inferior teeth estimate the level of C2. The mastoid tip should be palpated and marked as it represents the direction in which the incision may be extended if higher exposure is needed. A longitudinal incision is fashioned along the anterior border of the sternocleidomastoid muscle. This is carried down through the platysma, and a plane just medial to the anterior border of the sternocleidomastoid is identified and opened further via blunt dissection. Deep dissection in this region without following the medial surface of the muscle can lead to swallowing dysfunction caused by injury to the recurrent laryngeal nerve which runs in the tracheaesophageal groove. The transverse sensory cervical nerve may be encountered and can be sacrificed to facilitate the exposure. This maneuver leads to numbness over the anterior neck area that resolves in 3–6 months. The common facial vein (CFV) often lies directly superficial to the carotid bifurcation and should be suture ligated or clipped and divided to facilitate exposure. The omohyoid muscle typically marks the inferior extent of the dissection and can usually be left intact.

The neurovascular bundle containing the carotid artery can then be easily identified and palpated. Sharp dissection can be used to open the cervical fascia, followed by blunt dissection. Continued blunt dissection further isolates the carotid sheath; a sharp vertical incision exposes the underlying carotid artery.

Two nerves, the vagus and the ansa cervicalis, should be identified during this dissection process. The vagus nerve and its superior laryngeal branch lie deep and lateral to the carotid artery and internal jugular vein (in the groove between the carotid artery and jugular vein. The ansa cervicalis runs superficial to the ICA and serves as a roadmap to the hypoglossal nerve (XII) which should be identified to avoid damage to it. XII can arise anywhere from the carotid bifurcation to the angle of the mandible.

The dissection of the carotid sheath begins with the exposure of the common carotid artery (CCA), ECA, and the ICA. The distal exposure of the ICA must extend well beyond the plaque which can be estimated by gentle palpation, intraoperative doppler and by visualization as the area where the artery turns from yellowish to its normal pinker color.

The carotid bulb may be anesthetized with ≈ 2–3 ml of 1% plain lidocaine using a 27 Ga needle. This may be done routinely, or, as we prefer, only if hypotension and/or bradycardia occur during dissection (indicating IX nerve stimulation). Enough dissection has been established when there is adequate room for the arteriotomy, vessel loop, and a small low closing force bulldog clamp around the ICA just above the border of the plaque, as well as a vessel clamp (large soft-shoe Fogarty vascular clamp) around the CCA. The length of the plaque also determines what the extent of appropriate exposure is.

The dissection continues along the anterior aspect of the ICA. The length and location of the plaque may require more rostral exposure. If rostral mobilization of

the hypoglossal nerve is necessary, the ansa cervicalis can be transected where it joins the hypoglossal nerve to untether the latter nerve. The hypoglossal nerve is then retracted using a vessel loop. A small arterial branch of the ECA to the sternocleidomastoid muscle rarely requires coagulation and transection to facilitate adequate mobilization of the hypoglossal nerve. If a high exposure is mandatory, the posterior belly of the digastric muscle may be transected without any untoward consequences.

Lastly, the ECA is exposed circumferentially around its proximal end, just distal to the bifurcation. The identification of the superior thyroid artery (the first branch of the ECA) helps differentiate the ECA from the ICA (the ICA is located posterior to the ECA). It is important to circumferentially dissect and isolate the CCA, ICA and ECA. Such circumferential dissection allows for proper manipulation of the artery during clamping and arteriotomy. Following circumferential isolation of the arteries, vessel loops are wrapped twice around each major arterial branch. A Rummel tourniquet may be used around the CCA and pulled through a rubber sleeve. This maneuver allows constriction of the vessel around an intraluminal shunt. 5000 IU of intravenous heparin is typically given when we start dissecting around the plaque and the ICA. Prior to further cross-clamping, a mild increase in systolic blood pressure of approximately 20% (systolic blood pressure 160–180 mmHg) is induced by the anesthesiologist to prevent any alterations in EEG recordings during ICA occlusion. Then, attention can be turned to the arteriotomy.

3. *Arteriotomy & Endarterectomy*:

After adequate proximal and distal vascular control is obtained, a sterile marking pen defines the intended arteriotomy. Clamping of the carotid system commences as follows (mnemonic: ICE), first with the ICA, followed by the CCA and then the ECA. Clamping in this order ensures that potential thromboembolic debris preferentially enters the ECA circulation. A small bulldog clamp is placed on the distal ICA, distal to the corresponding vascular loop. Next, the large soft-shoe Fogarty vascular clamp is used to occlude the CCA. Finally, a second bulldog clamp is applied across the lumen of the ECA. The superior thyroid artery is also occluded by using a temporary aneurysm clip.

We do not use a shunt in every case, but rather determine whether a shunt is needed or not for each patient. This is predominantly based on whether there is adequate collateral perfusion of the ipsilateral cerebral hemisphere seen on preoperative vascular imaging as well as whether carotid cross-clamping has any effect on the EEG or SSEP monitoring. Changes in the EEG or SSEP mandate a trial of induced hypertension facilitated by anesthesia as mentioned above; however, if there is no immediate improvement in the EEG or SSEP recording, then an intraluminal shunt is placed. The shunt is first inserted into the CCA and the Rummel tourniquet is tightened around it, then the remaining shunt is passed more proximally into the CCA after the Fogarty vascular clamp has been opened. This method eliminates bleeding after opening the clamp because the tourniquet has already been secured. The distal end is opened to confirm blood flow and to clear any debris from

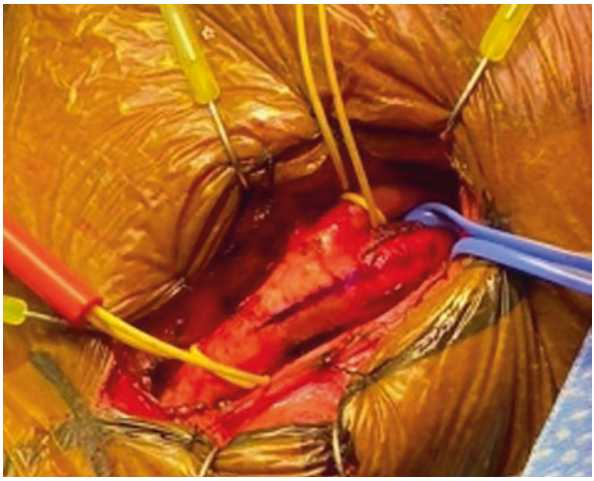

Fig. 12.4 The intended arteriotomy is defined by using a sterile marking pen

the tubing. The shunt is then inserted in the ICA and secured. A handheld Doppler is used to auscultate flow in the tubing. The intended arteriotomy is defined by using a sterile marking pen then the arteriotomy is begun in the CCA with a #11 scalpel Fig. 12.4.

Once the lumen is entered, Potts' scissors carry the incision rostrally taking care to stay in the middle of the lateral exposure of the carotid artery, away from the apex of the bifurcation—until normal vessel intima is encountered. It is imperative for the arteriotomy to reach above the plaque in the distal ICA. Dissection of the plaque begins at the proximal end of the arteriotomy within the CCA. It is important to start the dissection below the bulk of the plaque and truncate the plaque sharply at the proximal extent of the arteriotomy. The plaque is then circumferentially dissected with a Penfield No. 4 up to the origin of the ECA and gently pulled out of the ECA with a hemostat. Finally, the dissection is carried distally into the ICA. Careful inspection of the intima is required to identify any residual debris or plaque material for removal. If the plaque extends proximally into the CCA and no smooth edges are identified, then the plaque is transected sharply with either a number 15-blade knife or tenotomy scissors. If the dissection is taken superiorly enough, then the plaque usually feathers distally into the ICA and can be easily removed (Fig. 12.5). In some cases, however, at the distal endpoint, the plaque may leave a "shelf" with tattered edges that must be cleaned. These edges must be tacked down with a double-armed unbraided suture 6–0 Prolene. If tacked down sutures are necessary, both needles must be directed inside to outside so that the knot is tied on the external surface of the vessel. After plaque removal, the arteriotomy site is irrigated with heparinized saline to detect and remove any residual atheromatous fragments.

4. *Closure*:

Primary arteriotomy closure is performed with 6–0 Prolene suture in a running water-tight vascular closure fashion. Front-wall intimal flaps must be included

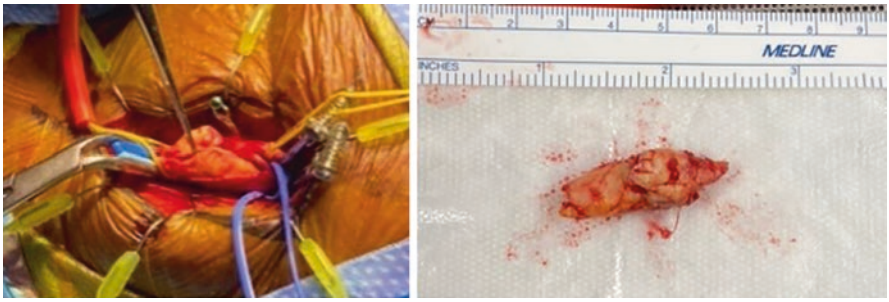

Fig. 12.5 The plaque is circumferentially dissected and gently pulled out of the ECA with a hemostat. (Note, adequate proximal and distal vascular control is achieved before Arteriotomy & Endarterectomy as described above)

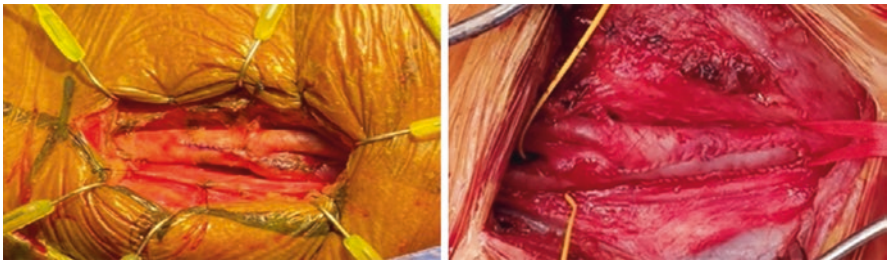

Fig. 12.6 The arterial wall closure using a 6–0 prolene running suture (left). patch angioplasty is indicated in case of small caliber of the ICA (right)

within the stitch to avoid arterial dissection. Starting at the distal ICA and running proximally until one- half or one- third of arteriotomy remains. A second suture is then started at the proximal CCA and run distally. This double-suture technique from both sides of the arteriotomy allows correction of wall-length discrepancies from either side, a feature especially helpful in cases where the arteriotomy is inadvertently not straight. A healthy bite of the arterial wall should be taken on both sides to ensure that the stitch will hold and the irregular edge of the arteriotomy is not exposed to the lumen. Periodic irrigation of the lumen with heparin solution should be continued during the entire process. Alternatively, when the ICA is of small caliber and the edges of the arteriotomy are uneven, a patch may be sewn into the arteriotomy site using a prosthetic material, preferably the Hemashield collagen-impregnated Dacron patch graft (Hemashield: Maquet Getinge Group, Rastatt, Germany) or bovine pericardium patch. The patch material is placed over the surgical field and cut according to the length of the arteriotomy. The principles of suturing the patch are similar to those described above Fig. 12.6.

Prior to complete closure, the ICA clamp should be temporarily removed to allow back-bleeding. The clamp is then replaced, and the CCA clamp is temporarily removed and then replaced. This maneuver facilitates removal of any air or surgical debris remaining within the lumen. As the last stitch is thrown we typically irrigate

the lumen before tying the suture to flush air out of the lumen, and the vascular clamps are removed in the reverse sequence in which they were initially placed—ECA, CCA, and finally, 10 seconds later, from the ICA. This sequence of clamp removal ensures that any atheromatous debris or air emboli are flushed into the extracranial circulation rather than into the intracerebral circulation. Once all the clamps are removed, the suture lines are inspected for any leakage, the majority of which may be addressed simply with the application of surgical gauze and light pressure. If needed, single throw 6–0 Prolene sutures are used to buttress the arterial closure at arterial leak points. The repair is then lined with Surgicel and the hand-held Doppler is used to confirm vessel patency. Wound is closed in anatomic layers. A Hemovac drain is placed within the subplatysmal space. The only layer closed underneath the skin and subcutaneous tissue is the platysma, which is completed with 3–0 vicryl sutures. The deep subcutaneous tissues are also closed using 3–0 vicryl sutures. The skin edges are then approximated using a 4–0 monocryl subcuticular sutures.

Postoperative Care

Postoperative monitoring (including telemetry and blood pressure monitoring) should be performed in the intensive care unit (ICU) and patients' neurological function should be evaluated hourly immediately after surgery. During the first 12 to 24 hours postoperatively, blood pressures are frequently labile, and the goal is to maintain the systolic blood pressure (SBP) above 100 mmHg and below 160 mm Hg. It is critical to maintain an arterial line overnight to identify and treat hypertension promptly as many CEA patients demonstrate cerebral autonomic dysregulation that predisposes them to cerebral hyperperfusion injuries and hematoma formation. All patients are maintained on 325 mg of aspirin daily for the rest of their lives. Postoperative antibiotics are only utilized for 24 hours. Patients are started on soft diet the night of surgery. Early mobility and ambulation are encouraged the evening of surgery. The drain is typically removed on postoperative day 1, and nearly all patients can be discharged on the first postoperative day**.**

Our long-term follow- up of carotid patients involves a visit at six weeks and another at three months. We routinely perform a postoperative CDU examination at three months and then at six months intervals thereafter to follow both the operated and the silent side.

Complications and Management

Most complications from CEA occur within 24 hours of surgery [18]. The overall in-hospital mortality after CEA is 0.57–1.4%, and the major nonneurological perioperative complication is MI [19]. Common complications associated with CEA

include ischemic complications, hemorrhagic complications, postoperative hematoma formation, and cranial nerve injury.

Stroke is the second most common cause of death following CEA. The postoperative stroke rate in CREST trial is 5.4% for symptomatic patients and 3.6% for asymptomatic patients [14]. It is generally accepted that this risk can be reduced by attention to technical details during surgery. It is attributable to multiple factors, including plaque emboli, platelet aggregates, intracerebral hemorrhagic (ICH), postoperative ICA occlusion, improper flushing, and relative hypotension. Any new postoperative decline or deficit in neurologic status, including TIA, should be addressed aggressively with immediate noncontrast head CT. If the CT is negative for hemorrhage, CTA of the head and neck are performed to evaluate the cerebral vasculature and endarterectomy site.

If an acute occlusion of the carotid artery is identified, the patient should be taken for cerebral angiography to attempt direct thrombectomy or clot lysis or stenting. If this is unsuccessful or unavailable, the patient should be returned immediately to the operating room for exploration and to reestablish patency.

A lack of radiographic ischemic complication with deterioration in neurologic status can imply cerebral hyperperfusion syndrome (CHS) that result from return of cerebral blood flow to an area that has lost autoregulation. CHS has been identified in 0.3–2.2% of patients post CEA with peaked onset on the sixth postoperative day. CHS typically presents with neurological deficits, altered mental status, seizures, or headache [20]. Strict control of blood pressure in the postoperative setting can prevent cerebral hyperperfusion and its consequences. Therefore, blood pressure should be managed aggressively with intravenous antihypertensive medications such B- blockers (labetalol) or vasodilators (hydralazine) [21].

A postoperative neck hematoma is another significant, although rare, postoperative complication following CEA. It could be detected in the early stage through visual inspection and palpation of the trachea along with clinical evidence of dysphagia, hoarseness, or difficulty swallowing. The drain output may also provide a clue. A rapidly enlarging hematoma threatens the patient's airway and constitutes a surgical and anesthetic emergency. When possible, immediate return to the operating room and intubation in a controlled setting are preferred. If imminent airway compromise and/or stridor are present, immediate opening of the surgical site may be necessary to allow for decompression of the trachea, even at the bedside, and before intubating the patient. Once the airway has been secured, surgical exploration of the hematoma and arteriotomy can commence. Re-exploratory surgery often discloses nonspecific venous source, but occasionally could be from an inadequate arteriotomy closure.

Cranial nerve injuries are the most common complications associated with CEA with an incidence rate of 5.6%. This includes injury to the ipsilateral hypoglossal nerve, which causes tongue deviation to the side of the injury; vagus or recurrent laryngeal nerve injury, which causes unilateral vocal cord paralysis; and a branch of facial nerve known as the marginal mandibular nerve, which causes loss of unilateral depressor motion of the lips. These injuries are related to dissection, excessive traction, compression, or stretching during surgery and are typically transient with complete resolution within 3 to 6 months [22].

Late carotid artery restenosis is not an uncommon complication following CEA with variable incidence based on different definitions of restenosis. Although many surgeons use patch angioplasty for closure in an attempt to prevent restenosis, studies have found no significant difference in the rate of restenosis regardless of whether patch angioplasty or primary closure was performed [23]. Patients with carotid restenosis after CEA can safely undergo both redo CEA or CAS. However, CAS patients have better follow-up results in terms of secondary restenosis, periprocedural cranial nerve injury, and re-interventions [24].

Conclusion

CEA is an effective procedure for stroke prevention in select patients with symptomatic and asymptomatic carotid artery stenosis. It has relatively low morbidity and mortality and reduces the risk of subsequent stroke or death. This fact is supported by numerous large randomized controlled trials. However, the benefit is greater in patients with symptomatic disease. Stroke is also a potential complication of CEA; therefore, physicians must educate patients regarding potential complications of the procedure and about controlling risk factors for stroke through smoking cessation, maintaining a healthy weight, and lowering cholesterol. Regular exercise is highly recommended as well. Optimal medical therapy with antiplatelet agents, anticholesterol medications, and blood pressure control should be recommended for all patients with carotid stenosis.

Despite continued evolution of endovascular technology, CEA remains a first-line intervention for the properly selected patients while carotid angioplasty and stenting is reserved for high-risk patients who cannot safely undergo CEA.

References

1. Barnett WH. Beneficial effect of carotid endarterectomy in symptomatic patients with high-grade carotid stenosis. North American symptomatic carotid endarterectomy trial collaborators [see comments]. N Engl J Med. 1991.
2. C. W, B. F, A. F, P. S, J. S. Randomised trial of endarterectomy for recently symptomatic carotid stenosis: final results of the MRC European carotid surgery trial (ECST). Lancet. 1998.
3. Barnett H, Barnes RW, Clagett GP, Ferguson GG, Robertson JT, Walker PM. Symptomatic carotid artery stenosis: a solvable problem north american symptomatic carotid endarterectomy trial. Stroke. 1992; https://doi.org/10.1161/01.STR.23.8.1048.
4. Moneta GL, Taylor DC, Nicholls SC, Bergelin RO, Zierler RE, Kazmers A, Clowes AW, Strandness DE. Operative versus nonoperative management of asymptomatic high-grade internal carotid artery stenosis: improved results with endarterectomy. Stroke. 1987; https://doi.org/10.1161/01.STR.18.6.1005.
5. Halliday A, Mansfield A, Marro J, et al. Prevention of disabling and fatal strokes by successful carotid endarterectomy in patients without recent neurological symptoms: randomised controlled trial. Lancet. 2004;363:1491–502.

6. Endarterectomy for asymptomatic carotid artery stenosis. Executive Committee for the Asymptomatic Carotid Atherosclerosis Study. JAMA J Am Med Assoc. 1995. https://doi.org/10.1001/jama.273.18.1421.
7. Gupta A, Baradaran H, Schweitzer AD, Kamel H, Pandya A, Delgado D, Dunning A, Mushlin AI, Sanelli PC. Carotid plaque MRI and stroke risk: a systematic review and meta-analysis. Stroke. 2013;44(11):3071–7. https://doi.org/10.1161/STROKEAHA.113.002551. Epub 2013 Aug 29. PMID: 23988640.
8. Gasecki AP, Eliasziw M, Ferguson GG, Hachinski V, Barnett HJM. Long-term prognosis and effect of endarterectomy in patients with symptomatic severe carotid stenosis and contralateral carotid stenosis or occlusion: results from NASCET. J Neurosurg. 1995; https://doi.org/10.3171/jns.1995.83.5.0778.
9. Buskens E, Nederkoorn PJ, Buijs-Van Der Woude T, Mali WPTM, Kappelle LJ, Eikelboom BC, Van Der Graaf Y, Hunink MGM. Imaging of carotid arteries in symptomatic patients: cost-effectiveness of diagnostic strategies. Radiology. 2004;233:101–12.
10. Koelemay MJW, Nederkoorn PJ, Reitsma JB, Majoie CB. Systematic review of computed tomographic angiography for assessment of carotid artery disease. Stroke. 2004;35:2306–12.
11. Felbaum DR, Maxwell C, Naydin S, et al. Carotid stenosis: utility of diagnostic angiography. World Neurosurg. 2019;121:e962–6.
12. Rothwell PM, Eliasziw M, Gutnikov SA, Warlow CP, Barnett HJM. Endarterectomy for symptomatic carotid stenosis in relation to clinical subgroups and timing of surgery. Lancet. 2004; https://doi.org/10.1016/S0140-6736(04)15785-1.
13. Yadav JS, Wholey MH, Kuntz RE, et al. Protected carotid-artery stenting versus endarterectomy in high-risk patients. N Engl J Med. 2004;351:1493–501.
14. Mantese VA, Timaran CH, Chiu D, Begg RJ, Brott TG. The carotid revascularization endarterectomy versus stenting trial (CREST): stenting versus carotid endarterectomy for carotid disease. Stroke. 2010; https://doi.org/10.1161/STROKEAHA.110.595330.
15. Engelter S, Lyrer P. Antiplatelet therapy for preventing stroke and other vascular events after carotid endarterectomy. Cochrane Database Syst Rev. 2003; https://doi.org/10.1002/14651858.cd001458.
16. Brooke BS, McGirt MJ, Woodworth GF, Chang DC, Roseborough GS, Freischlag JA, Perler BA. Preoperative statin and diuretic use influence the presentation of patients undergoing carotid endarterectomy: results of a large single-institution case-control study. J Vasc Surg. 2007;45:298–303.
17. Lewis SC, Warlow CP, Bodenham AR, et al. General anaesthesia versus local anaesthesia for carotid surgery (GALA): a multicentre, randomised controlled trial. Lancet. 2008; https://doi.org/10.1016/S0140-6736(08)61699-2.
18. Roddy SP, Estes JM, Kwoun MO, O'donnell TF Jr, Mackey WC. Factors predicting prolonged length of stay after carotid endarterectomy. J Vasc Surg. 2000;32(3):550–4. https://doi.org/10.1067/mva.2000.107759.
19. McPhee JT, Schanzer A, Messina LM, Eslami MH. Carotid artery stenting has increased rates of postprocedure stroke, death, and resource utilization than does carotid endarterectomy in the United States, 2005. J Vasc Surg. 2008; https://doi.org/10.1016/j.jvs.2008.07.017.
20. Ogasawara K, Sakai N, Kuroiwa T, et al. Intracranial hemorrhage associated with cerebral hyperperfusion syndrome following carotid endarterectomy and carotid artery stenting: retrospective review of 4494 patients. J Neurosurg. 2007;107(6):1130–6. https://doi.org/10.3171/JNS-07/12/1130.
21. Bouri S, Thapar A, Shalhoub J, Jayasooriya G, Fernando A, Franklin I, Davies A. Hypertension and the post-carotid endarterectomy cerebral hyperperfusion syndrome. Int J Surg. 2011; https://doi.org/10.1016/j.ijsu.2011.07.046.
22. Fokkema M, de Borst GJ, Nolan BW, Indes J, Buck DB, Lo RC, Moll FL, Schermerhorn ML. Clinical relevance of cranial nerve injury following carotid endarterectomy. J Vasc Surg. 2014; https://doi.org/10.1016/j.jvs.2013.11.078.

23. Rerkasem K, Rothwell PM. Patches of different types for carotid patch angioplasty. Cochrane Database Syst Rev. 2010; https://doi.org/10.1002/14651858.cd000071.pub3.
24. Texakalidis P, Giannopoulos S, Kokkinidis DG, Karasavvidis T, Rangel-Castilla L, Reavey-Cantwell J. Carotid artery endarterectomy versus carotid artery stenting for patients with contralateral carotid occlusion: a systematic review and meta-analysis. World Neurosurg. 2018; https://doi.org/10.1016/j.wneu.2018.08.183.

Chapter 13
Endovascular Management of Extracranial Carotid Disease

Vincent N. Nguyen and Daniel A. Hoit

Introduction

Epidemiology

Extracranial atherosclerotic carotid disease remains the third most common cause of ischemic stroke among all patients, and the second most common cause in adults under 45 years old. Stroke is the third most common cause of death in developed countries and a leading cause of long-term disability [1]. In total, 87% of strokes are ischemic, 10% hemorrhagic, and 3% from aneurysmal and non-aneurysmal subarachnoid hemorrhage [2]. Carotid stenosis greater than 50% carries a 9% prevalence in men and 6–7% in women [3, 4]. It is estimated that 7–18% of first strokes are associated with carotid stenosis [5, 6]. Recurrent stroke risk is 4–15% during the first year and 25% by 5 years [7]. There have not been any consistent gender or racial differences seen in the incidence of carotid atherosclerosis [8].

Pathophysiology

Extracranial carotid atherosclerosis may cause stroke by several mechanisms [9]:

- Artery-to-artery embolism of cholesterol crystals or other debris
- Atheroembolism of acute thrombus

V. N. Nguyen · D. A. Hoit (✉)
University of Tennessee/Semmes-Murphey Clinic Department of Neurosurgery, Knoxville, TN, USA
e-mail: dhoit@semmes-murphey.com

J. R. Mascitelli, M. J. Binning (eds.), *Introduction to Vascular Neurosurgery*,
https://doi.org/10.1007/978-3-030-88196-2_13

- Dissection and structural occlusion of the artery wall
- Acute occlusion
- Reduced cerebral perfusion with progressive plaque growth and stenosis

The North American Symptomatic Carotid Endarterectomy Trial (NASCET) showed a clear correlation between degree of stenosis and risk of stroke in symptomatic patients [10].

Atherosclerosis is a chronic inflammatory response in the subendothelium caused by lipid deposition. Uncomplicated plaques are uniform and covered by a fibrous cap. Complicated plaques can have hemorrhage, necrosis, ulceration, and calcification with exposure of these particles to the bloodstream. The posterior wall of the internal carotid artery immediately beyond the bifurcation is the most susceptible to atherosclerosis [11].

Carotid disease is diagnosed via a combination of a detailed neurologic exam, auscultation, noninvasive testing such as carotid duplex ultrasonography, computed tomographic angiography, or magnetic resonance angiography. Digital subtraction angiography (DSA) is considered the gold standard for the measurement of degree of stenosis as noninvasive modalities may suffer from limitations due to calcification of the vessel or flow velocity within the artery.

Clinical Presentation

Patients suffering neurologic symptoms from carotid stenosis can present in a multitude of ways depending on the time of onset and permanence of deficits. Transient ischemic attacks (TIA) are temporary deficits experienced for less than 24 hours. Reversible ischemic deficits are temporary reversible deficits that can afflict a patient for up to 7 days. Finally, strokes are permanent deficits which impact a patient's ensuing quality of life [11].

Endovascular Interventions for Carotid Stenosis

The 18-month stroke rate is 19–33% with medical therapy alone in symptomatic patients. This can be reduced by CEA or stenting [10]. Ideally, intervention should take place within 2 weeks if not contraindicated but is acceptable within 6 months of the patient's index presentation [7, 10, 12]. Contraindications for intervention include the following:

- Severe stroke mRS greater than or equal to 3
- Chronic total carotid occlusion
- Carotid stenosis <50%
- Extremely high risk for perioperative complications

Patient Selection

Certain patient factors may favor endovascular treatment over open surgical endarterectomy (CEA). These include:

- Unfavorable for surgical access (i.e., high carotid bifurcation and spinal immobility)
- Stenosis occurring as a result of radiation
- Previous endarterectomy with recurrent stenosis
- Clinically significant medical comorbidities (pulmonary and cardiac), or other diseases that significantly increase the risk of anesthesia and surgery
- Unfavorable neck anatomy, including contralateral vocal cord paralysis, open tracheostomy, previous neck radiation, or other previous radical neck dissection surgery
- Contralateral complete carotid occlusion

CEA remains the standard treatment for symptomatic internal carotid artery stenosis in low-risk surgical patients. Periprocedural complication rates (stroke and death) for endovascular treatment should be <6% for the interventionalist or center. Carotid stenting is an option for symptomatic (≥50%) or asymptomatic high-grade (≥80%) internal carotid artery stenosis when CEA is considered a higher risk due to the factors as above [13, 14].

Contraindications to carotid stenting are either absolute or relative. Absolute contraindications include inability to gain vascular access, visible intralesional thrombus, or active infection. Relative contraindications include severe carotid tortuosity, calcification, or near occlusion [15].

Clinical Trials

Randomized clinical trials for symptomatic patients with occlusive carotid disease undergoing CEA or carotid artery stenting have shown equivalence of benefit. Two meta-analyses have shown similar findings comparing outcomes and complications from carotid endarterectomy versus stenting [16, 17]. The rates of periprocedural stroke are slightly higher with carotid artery stenting, but the rates of cranial neuropathy, perioperative myocardial infarction, and access site hematoma are lower with carotid stenting.

The details of the most important randomized trials are as follows:

- *ICSS:* In the International Carotid Stenting Study (ICSS) trial, over 1700 adults over age 40 with symptomatic carotid artery stenosis ≥50% were randomized to treatment by CEA or CAS [18, 19]. Exclusions were major debilitating stroke without useful recovery of function or a previous open or endovascular procedure in the target artery. The 30-day all-cause stroke risk was significantly higher

for the stenting group (7.0 versus 3.3%) with more diffusion (DWI) brain lesions on MRI. At 4.2 years of median follow-up, the cumulative risk of any stroke was significantly higher for the stenting group (15.2 versus 9.4%). However, the 5-year all-cause risk of death was similar for the stenting and endarterectomy groups (17.4 versus 17.2%).

- *SPACE:* The multicenter European Stent-Protected Angioplasty versus Carotid Endarterectomy (SPACE) trial randomized 1183 symptomatic carotid stenosis patients (≥70%) to either stenting or CEA [20]. High-risk and debilitated patients were excluded as well as patients who underwent prior revascularization procedures. Early termination of the trial occurred due to issues with funding and recruitment. Similar outcomes for both the CEA and CAS with respect to death and ipsilateral stroke up to 2 years after the procedure were observed. Recurrent stenosis over 70% was more common in the stenting group.
- *EVA-3S:* The French Endarterectomy Versus Angioplasty in Patients with Symptomatic Severe Carotid Stenosis (EVA-3S) trial randomized 527 patients to stenting or CEA [21]. Excess mortality in the stenting group led to premature trial termination. Stroke and death rates in the early and long term were higher with stenting than CEA, mainly due to periprocedural stroke. Training of operators was felt to be inadequate and the use of distal protection devices was irregular, highlighting the need for more rigorous standardization in future trials.
- *CREST:* The Carotid Revascularization Endarterectomy versus Stenting Trial (CREST) randomized 2502 patients to CEA or CAS [22–24]. Both asymptomatic and symptomatic patients were included. The overall efficacy and safety of the two procedures were similar. Additionally, benefits were equal among men and women and in patients with asymptomatic and symptomatic diseases. Younger patients derived a greater benefit from stenting, while older patients did better with endarterectomy. A subset analysis found that stroke occurring at a higher rate in the CAS group had a larger effect on quality-of-life metrics, whereas myocardial infarction or cranial neuropathy had a relatively less negative impact on quality of life.
- *SAPPHIRE:* The Stenting and Angioplasty with Protection in Patients at High Risk for Endarterectomy (SAPPHIRE) trial found that stenting was not inferior to CEA, examining the treatment of asymptomatic disease in patients who met high-risk CEA criteria [25, 26]. The study suffered from selection bias in the determination of patients who were deemed too high risk for CEA.

ACST-2 and CREST-2 are two ongoing randomized trials further comparing long-term outcomes of CEA versus stenting [27, 28]. ACST-2 has a target enrollment of 3600 asymptomatic patients with equivalent eligibility for either CEA or stenting by the end of 2019 and will publish its results in 2021. CREST-2 is two-arm multicenter trial randomizing patients to either endarterectomy versus medical management or stenting versus medical management, with plans to complete enrollment of 2480 patients by December 2022. These trials will continue to refine the best individualized treatment approach for asymptomatic patients with carotid stenosis given modern interventional and medical management strategies.

Anatomic Considerations in Patient Selection

Unfavorable features, often more common in the elderly that increase stroke risk for transfemoral carotid stenting, include [29]:

- Type 2 or 3 aortic arch
- CCA/ICA tortuosity >30 degrees
- Plaque calcification
- Long-segment stenosis
- Arch vessel origin stenosis >50%
- Seven age-related white matter lesions

Technical Considerations

Although stroke risk has been shown to be higher for CAS versus CEA, continued improvements in access, carotid stent technology, distal embolic protection devices, and overall technique may shift the balance toward stenting.

The procedural steps for CAS are summarized in Table 13.1.

Percutaneous Vascular Access

Vascular access is most common through the common femoral artery (CFA). Placement of a short 8F sheath in the CFA allows for the exchange of diagnostic catheters for guide catheters with minimal patient discomfort. Most carotid stent

Table 13.1 Summary of procedural steps for carotid artery stenting

Number	Step
1	Access: Transfemoral or transradial
2	Heparinization
3	Guide catheter delivery to target common carotid artery
4	Device selection: distal protection device, pre-stent angioplasty balloon, stent, post-stent angioplasty balloon, recapture device
5	Confirmation of goal ACT
6	DPD deployment
7	Pre-stent angioplasty if necessary
8	Stent delivery
9	Post-stent angioplasty
10	DPD recovery
11	Repeat cervical and cerebral angiography to assess for branch occlusion
12	Access closure

systems require a 6F or greater lumen for device delivery. A number of guide catheters are available for this purpose ranging in length from 80 to 105 cm. Stable placement in the common carotid artery is necessary for embolic protection device, balloon, and stent delivery. We perform ipsilateral cerebral angiography prior to stent placement as a baseline to compare to post-intervention runs for identification of branch occlusions and improvements in flow hemodynamics.

Transradial access for neurointerventional procedures is a new alternative to transfemoral access. Long used in cardiac and peripheral applications, transradial access offers advantages in patient comfort, safety, and access for certain arch and great-vessel configurations. Delivery of a suitably sized guide catheter for interventional procedures is possible in many patients. The technical details of approach selection and catheter selection are covered elsewhere in this book.

Embolic Protection Devices

The two main embolic protection devices (EPD) are distal filters and proximal occluders, which include flow arrest and flow reversal. Transcarotid artery revascularization (TCAR) falls under this latter category of proximal occlusion and will be discussed later in this chapter. Although the available evidence is conflicting regarding the specific benefit of use of EPDs in carotid stenting, reimbursement is dependent on its use in the United States.

Distal Filters

Distal filters or distal protection devices (DPD) are the most common embolic protection devices used in carotid stenting [30, 31, 32]. They are designed to catch any debris traveling antegrade during stent placement while allowing continuous forward flow. Their deployment carries the risk of embolization particularly with tight stenoses, as they must be deployed after crossing the lesion. As wires, they have limitations in shapability and steerability. Unprotected predilation of the stenosis with a balloon over a bare wire in order to gain distal access for filter deployment may in itself cause atheroembolization from the lesion [33]. Figure 13.1 demonstrates a commonly used distal protection device in our practice. Vasospasm is a common occurrence with distal protection devices even with proper sizing. Care must be taken in the exchange maneuvers with the stent and balloons to minimize the backward and forward motion of the basket in the distal ICA. When retrieving the filter, complete capture in the retrieval catheter is necessary to avoid entanglement of the basket in the deployed stent.

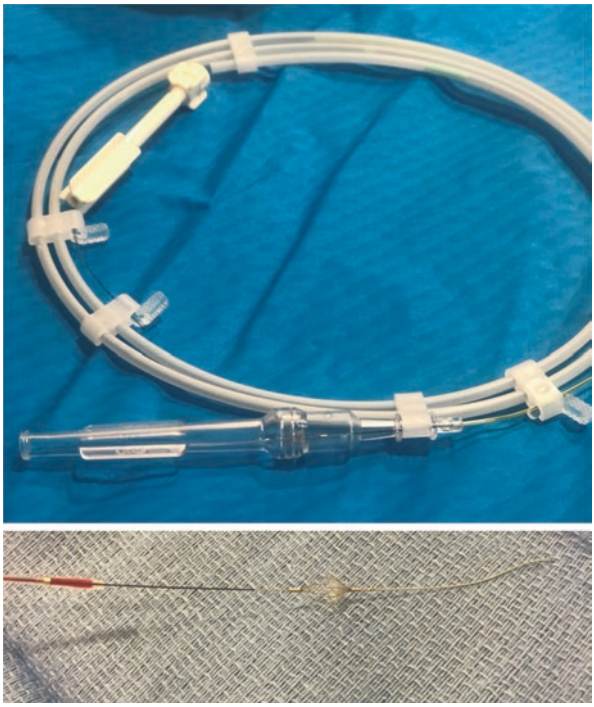

Fig. 13.1 Distal protection devices like the AngioGuard (Cordis) protect against distal embolization during carotid stenting but require first crossing the lesion without protection

Flow Arrest

Proximal balloons are deployed in the common and external carotid arteries which arrest forward flow in the internal carotid artery prior to the lesion being crossed, preventing distal embolization and stroke.

The proximal internal carotid is suctioned prior to deflating the balloons to clear any debris. These balloons carry certain disadvantages, including the requirement for larger sheaths with concomitant associated risk of access-related complications, as well as the risk of cerebral ischemia [34]. This complication may be mitigated by the pre-evaluation of collateral flow. Vessel injury can also occur with balloon inflation [35].

Carotid Stents

The two main architectural groups of carotid stents are open cell and closed cell. Open-cell stents are more flexible and may be preferable when dealing with tortuous anatomy or distorted lesions to ease delivery [30, 36]. A lower percentage of

patients in the ICSS trial had restenosis with the use of an open-cell architecture stent [37].

Closed-cell stents have completely interconnected stent struts with more radial force and thus leave less uncovered areas, which may better prevent embolization of small particles that can more easily penetrate through an open-cell system [38].

Dual-layered stents are a newer advancement that combine a stent frame with a micromesh lattice to provide better coverage of a plaque with high vessel adaptability.

In our experience, the most commonly used stent is the open-cell type. The stent diameter is chosen 1–2 mm oversized to the largest vessel segment it will be placed in. Oversizing the stent to the lesion and ICA has the added benefit of keeping the cell structure partially closed and increasing metal coverage of the atherosclerotic lesion. Placement of the stent should cover the entirety of the internal carotid artery lesion with care taken not to land the ends of the stent at the apex of vessel curvature as this may result in kinking of the vessel.

Angioplasty

Balloon angioplasty can be performed before stenting or after stenting. For tight lesions that will not permit passage of the stent, a pre-angioplasty step is necessary. Rarely, it may be impossible to cross the lesion with a filterwire and so a small balloon over a microwire can be used to create a more passable channel. After stent deployment, angioplasty with a balloon sized to the ICA or slightly smaller can be performed if there is residual stenosis. Oversizing the balloon may result in pushing the stent through the plaque, thus "mashing the potato" and increasing the possibility of embolic debris. The angioplasty should be performed entirely within the confines of the stent to avoid distal or proximal dissection. Our practice is to have atropine immediately available during balloon inflation to counteract bradycardia due to carotid bulb baroreceptor stimulation.

Periprocedural Management

We recommend dual antiplatelet therapy initiation at least 48 hours prior to the procedure and for at least 4–6 weeks post-procedure. At least one antiplatelet agent is then recommended for long term. Ticlopidine can be used for those intolerant to clopidogrel. Statin administration and control of hypertension are also strongly recommended when indicated.

Stenting can be performed with local anesthesia and sedation with close cardiopulmonary monitoring, or under general anesthesia.

We heparinize to an activated clotting time (ACT) of 250–300 seconds prior to any manipulation of guidewires and catheters in the arch and carotid artery.

Bivalirudin is an alternative for patients with contraindications to heparin administration.

Continuous blood pressure monitoring, adequate hydration, and adjustment of antihypertensive medication perioperatively are critical to avoid unnecessary intraprocedural hypotension. Hypotension and vasovagal responses particularly during post-stenting angioplasty stimulation of the carotid baroreceptor are managed with atropine or glycopyrrolate or a transcutaneous pacer in patients under general anesthesia. Persistent bradycardia warrants consideration for pacemaker. Phenylephrine or dopamine can be used for persistent hypotension, particularly in the postoperative phase. Blood pressure is strictly managed to a systolic of less than 140 postoperatively to prevent intracerebral hemorrhage and reperfusion syndrome.

Post-procedural duplex ultrasounds are performed within 3 months for a new baseline. Repeat surveillance studies are performed as clinically indicated, typically every 6–12 months, and may be discontinued if findings are stable over a prolonged period.

A summary of the stenting procedure is shown in Fig. 13.2.

Complications

A majority of post-stent complications occur within 6 hours of the procedure, with later events occurring over 24 hours following the procedure being mostly related to access or stroke. Stroke remains the most significant complication in carotid stenting. A variety of mechanisms may contribute [39] to the following:

- Thromboembolism
- Hypoperfusion due to bradycardia and/or baroreceptor stimulation
- Cerebral hyperperfusion
- Intracerebral hemorrhage
- Stent thrombosis
- Noncompliance with antiplatelet therapy

Cerebral hyperperfusion after carotid stenting is rare but most commonly encountered when significant stenosis is corrected resulting in >100% cerebral perfusion postoperatively [40]. Complaints of headaches may herald the onset of seizures and intracerebral hemorrhage. Perioperative control of hypertension is thus critical particularly in those with preexisting uncontrolled hypertension or significant carotid stenosis [41].

Other organs are at risk during stenting, including the cardiac and renal systems. The rates of cardiac ischemia are lower with endovascular treatment than with open endarterectomy at 1–2.4%; however, one must remain vigilant especially in patients who experience profound bradycardia or hypotension during and after the procedure [19, 22]. The volume of contrast administered should be closely monitored and limited in patients with chronic kidney dysfunction to avoid contrast-induced nephropathy.

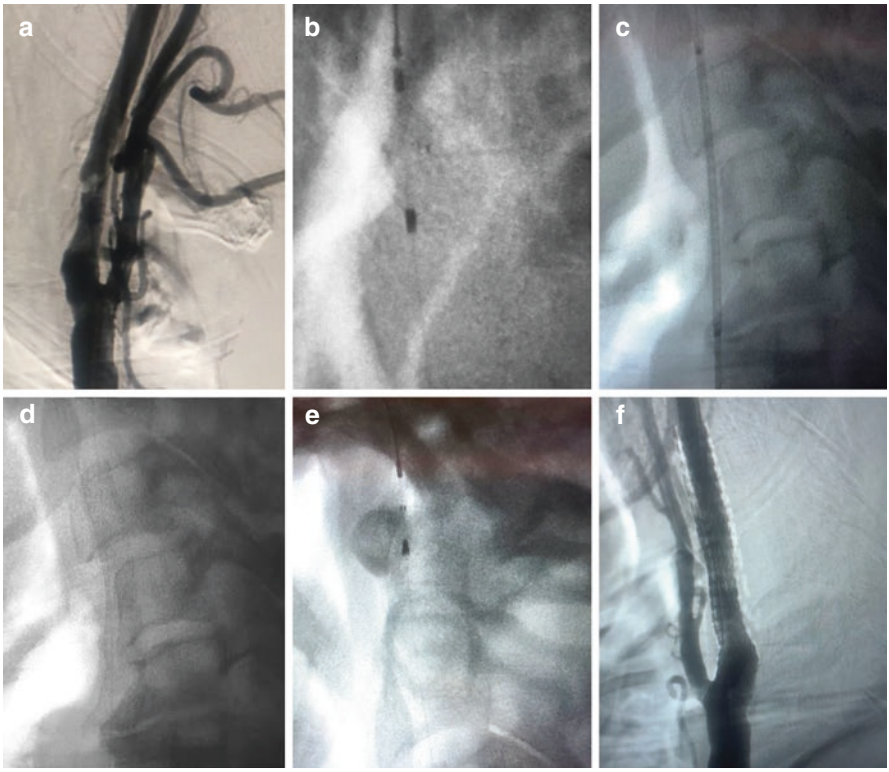

Fig. 13.2 A symptomatic carotid stenosis measuring 70% is seen in the distal internal carotid artery in an 80-year-old patient (**a**). A distal protection device has been deployed across the lesion. It is shown to be in the open configuration by the distance between the markers on the basket (**b**). In simple lesions, it is possible to advance the stent through without a predilation step (**c**). After angioplasty within the stent, the stenosis has resolved (**d**). The retrieval device closes the basket markers when the distal protection device is fully captured (**e**). Final pictures show satisfactory coverage of the lesion (**f**)

Other complications are as follows [1]:

- Vascular: target vessel perforation, vasospasm, and restenosis
- Neurologic: TIA, stroke, ICH, and seizure
- Technical: device failure, stent fracture, and access site injury

Evaluation for Recurrence and Subsequent Management

In general, post-procedure stenosis after stenting compares favorably with rates seen with CEA. Some cases of carotid restenosis following stenting may be related to mismanagement of antiplatelet therapies. Beyond 30 days, early restenosis after CAS is mainly due to neointimal hyperplasia, which may be due to vascular injury

caused by the stent. Neointimal hyperplasia related to CAS may be due to stent overdilation or imperfect positioning of the carotid stent in the vessel leading to ongoing vascular injury. This has been found more often in poorly controlled diabetics, women, and those with hyperlipidemia [11].

Repeat stenting for symptomatic restenosis or rapidly progressive stenosis that may indicate risk of complete occlusion is recommended. Stenting can also be used for recurrent stenosis after CEA [1].

Transcarotid Artery Revascularization (TCAR)

Transcarotid artery revascularization (TCAR) is a distinct hybrid approach to carotid stenting that combines open surgical exposure of the common carotid artery with endovascular stenting, combining the benefits of direct surgical control with minimally invasive treatment while reducing embolic stroke risk from navigating the aortic arch. Dynamic flow reversal is used for cerebral embolic protection. TCAR uses a specific arterial sheath in the common carotid artery for stent deployment, a venous sheath in the common femoral vein, and a flow controller with a built-in filter for flow reversal. Occlusion of the common carotid artery proximal to the arterial sheath causes a "reversal of flow" pressure gradient that sends cerebral arterial blood flow into the neuroprotection device system that captures and isolates embolic material and then shunts clean blood into the venous system for return to the patient's own circulation [42, 43].

Patient Selection

The National Coverage Decision by the Centers for Medicare and Medicaid Services created in March 2005 provides coverage for stent placement in patients with carotid stenosis. The TCAR Surveillance Project (TSP) extends this coverage to patients with >80% asymptomatic stenosis or > 50% symptomatic stenosis. The TSP is designed to track long-term clinical outcomes with TCAR for comparison with other accepted procedures [44].

Patients with tortuous internal carotid or aortic arch anatomy or peripheral vascular disease with calcification may be better candidates for TCAR than transfemoral stenting. However, other less hospitable factors including prior neck radiation or radical neck surgery may preclude access.

Technical Considerations

The learning curve for TCAR appears to be short in terms of complication rates with increasing efficiency with more case exposure [45]. A new specially designed stent for use with the TCAR system is the ENROUTE stent, which is an open, small cell

design with a shorter 57 cm delivery system [46]. Other stents can be used if they fit in the arterial sheath safely.

Anatomic requirements typically determined by ultrasound or CT angiography include [47] the following:

- Distance >5 cm between access site and lesion
- Common carotid artery diameter > 6 cm
- Common carotid access and clamp sites must be free of significant disease

Dual antiplatelet therapy and statin administration are recommended, similar to transfemoral carotid stenting pre-procedure preparation.

Procedural Steps

A small cutdown over the proximal common carotid artery is made through a short transverse or longitudinal incision just above the clavicle centered between the two heads of the sternocleidomastoid muscle. Dissection proceeds to protect the vagus nerve and jugular vein in the carotid sheath while isolating the carotid artery with a vascular loop. A "buddy" U suture is placed in the common carotid artery with a 5-0 suture at the planned puncture site.

Micropuncture access is then performed with appropriate baseline angiography. A stiff 0.035" Amplatz Super Stiff wire with a 1-cm floppy tip is advanced for arterial sheath insertion without disturbing the carotid plaque.

A venous sheath is inserted into the common femoral vein under ultrasound guidance, and then an arterial sheath is connected to the flow controller which is then connected to venous sheath for shunting.

Flow reversal is performed by occluding the proximal common carotid which establishes a pressure differential between the high arterial pressure from the cerebral circulation and low venous pressure in the common femoral vein. Injecting saline into the venous sheath and watching it clear away with blood confirm proper directional flow.

The ICA stenosis is crossed with a 0.014-inch wire, predilated, and then stent is deployed. At least 2 minutes of clearance time post-stent deployment is recommended. Repeat angiography was performed to confirm adequate stent apposition and flow across the lesion.

Antegrade flow is restored and hemostasis of the carotid puncture site is achieved with the previously placed buddy stitch. Protamine for heparin reversal is recommended during closure. Manual pressure over venous puncture site and neck closure is performed in a layered fashion.

Table 13.2 outlines these procedural steps for the successful performance of TCAR.

A summary of the TCAR procedure is shown in Fig. 13.3.

Table 13.2 Summary of procedural steps for transcarotid artery revascularization (TCAR)

Number	Step
1	Common carotid cutdown and isolation with 5-0 “buddy” U suture
2	Micropuncture access and control angiography
3	Arterial sheath insertion using 0.035” Amplatz Super Stiff wire
4	Venous sheath insertion into common femoral vein
5	Flow controller connected between arterial and venous sheaths with flow reversal
6	Cross ICA stenosis with 0.014 in wire with predilation
7	Stent deployment
8	Repeat angiography
9	Restoration of antegrade flow
10	Hemostasis and closure

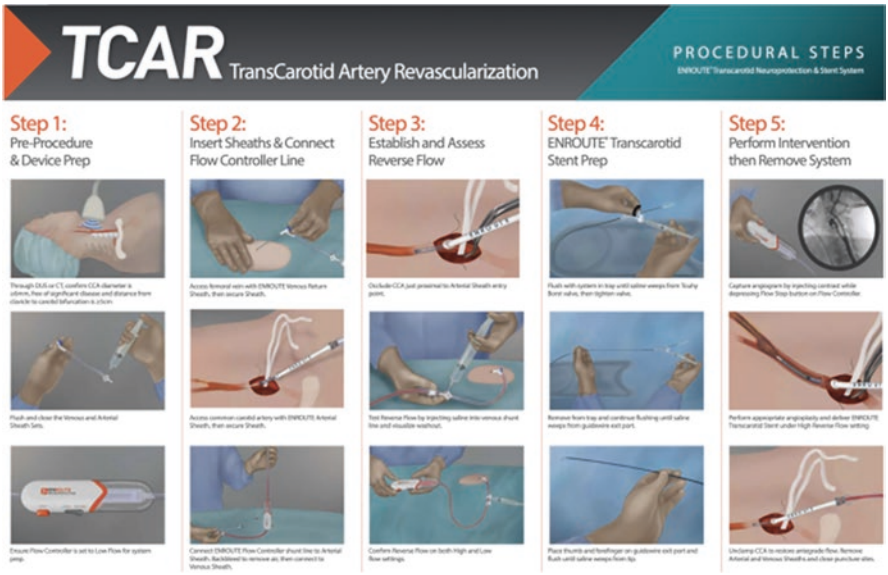

Fig. 13.3 Procedural steps for TCAR are outlined in this quick reference guide. (Images courtesy of Silk Road Medical, Inc.)

TCAR Trials

Results from preclinical studies, prospective single-arm studies, and registry data analyses indicate that TCAR results in low amounts of periprocedural microembolization, MRI-detectable cerebral lesions, neurologic events, cardiac ischemia, and death compared to traditional transfemoral carotid stenting [48–50].

The Safety and Efficacy Study for Reverse Flow Used During Carotid Artery Stenting Procedure (ROADSTER) study was a prospective, single-arm, multicenter clinical trial that enrolled 208 high-risk patients with either symptomatic 50% or

greater stenosis or asymptomatic 70% or greater stenosis to evaluate TCAR and the ENROUTE Transcarotid Neuroprotection System (NPS) [42]. In total, 141 patients were evaluated for outcome analysis. The stroke rate was 1.4%, all minor in nature, while the combined stroke/death/MI rate was 3.5%. Over 40% of patients were over 75 years old and a large majority (80%) were asymptomatic. The study had an overall low mean flow reversal time of 13 minutes. Further follow-up studies have similarly shown low stroke incidence of 0.6% and no neurologic-related deaths [50].

ROADSTER 2 is a more recent post-approval registry that evaluated the efficacy of the procedure in TCAR-naive and beginner operators. The study showed excellent early outcomes with high technical success with continued low rates of stroke and death [49]. Further long-term follow-up data, particularly pitting TCAR against traditional transfemoral stenting and open endarterectomy, are needed to validate these findings.

Other observational and registry analyses (TSP) have shown TCAR to carry at least equivalent outcomes to CEA. Propensity matched stroke and death rates at 30 days and 1 year are similar, although TCAR was associated with lower rates of cranial nerve injury. TCAR versus traditional transfemoral stenting has also shown similar findings with lower rates of in-hospital TIA, stroke, and death [48, 51]. TCAR is more commonly performed under general anesthesia compared to transfemoral stenting.

Conclusions

Endovascular treatment of carotid stenosis is a vital option for the treatment of high-risk surgical patients in need of carotid revascularization. Transfemoral carotid stenting has been shown to have similar long-term outcomes to carotid endarterectomy with lower rates of myocardial infarction and cranial neuropathy, but higher periprocedural stroke risk.

Transcarotid artery revascularization (TCAR) is a novel approach combining an open surgical approach with endovascular stenting to reduce the thromboembolic risk associated with crossing the aortic arch during transfemoral approaches. Perioperative medication optimization (antiplatelet and antihypertensives) and aggressive risk factor modification remain cornerstones of successful endovascular treatment plans.

References

1. Ooi YC, Gonzalez NR. Management of extracranial carotid artery disease. Cardiol Clin. 2015;33(1):1–35.
2. Rosamond W, Flegal K, Furie K, Go A, Greenlund K, Haase N, et al. Heart disease and stroke statistics--2008 update: a report from the American Heart Association Statistics Committee and Stroke Statistics Subcommittee. Circulation. 2008;117(4):e25–146.

3. Fine-Edelstein JS, Wolf PA, O'Leary DH, Poehlman H, Belanger AJ, Kase CS, et al. Precursors of extracranial carotid atherosclerosis in the Framingham Study. Neurology. 1994;44(6):1046–50.
4. O'Leary DH, Polak JF, Kronmal RA, Kittner SJ, Bond MG, Wolfson SK Jr, et al. Distribution and correlates of sonographically detected carotid artery disease in the Cardiovascular Health Study. The CHS Collaborative Research Group. Stroke. 1992;23(12):1752–60.
5. White H, Boden-Albala B, Wang C, Elkind MS, Rundek T, Wright CB, et al. Ischemic stroke subtype incidence among whites, blacks, and Hispanics: the Northern Manhattan Study. Circulation. 2005;111(10):1327–31.
6. Petty GW, Brown RD Jr, Whisnant JP, Sicks JD, O'Fallon WM, Wiebers DO. Ischemic stroke subtypes: a population-based study of incidence and risk factors. Stroke. 1999;30(12):2513–6.
7. Barnett HJ, Taylor DW, Eliasziw M, Fox AJ, Ferguson GG, Haynes RB, et al. Benefit of carotid endarterectomy in patients with symptomatic moderate or severe stenosis. North American Symptomatic Carotid Endarterectomy Trial Collaborators. N Engl J Med. 1998;339(20):1415–25.
8. Wityk RJ, Lehman D, Klag M, Coresh J, Ahn H, Litt B. Race and sex differences in the distribution of cerebral atherosclerosis. Stroke. 1996;27(11):1974–80.
9. Gonzalez NR, Liebeskind DS, Dusick JR, Mayor F, Saver J. Intracranial arterial stenoses: current viewpoints, novel approaches, and surgical perspectives. Neurosurg Rev. 2013;36(2):175–84. discussion 84-5
10. Clinical alert: benefit of carotid endarterectomy for patients with high-grade stenosis of the internal carotid artery. National Institute of Neurological Disorders and Stroke Stroke and Trauma Division. North American Symptomatic Carotid Endarterectomy Trial (NASCET) investigators. Stroke 1991;22(6):816–817.
11. Tummala RP. In: Deshaies EM, editor. Extracranial arterial occlusive disease. New York: Thieme; 2012.
12. Rothwell PM, Eliasziw M, Gutnikov SA, Warlow CP, Barnett HJ, Carotid Endarterectomy Trialists C. Endarterectomy for symptomatic carotid stenosis in relation to clinical subgroups and timing of surgery. Lancet. 2004;363(9413):915–24.
13. Kernan WN, Ovbiagele B, Black HR, Bravata DM, Chimowitz MI, Ezekowitz MD, et al. Guidelines for the prevention of stroke in patients with stroke and transient ischemic attack: a guideline for healthcare professionals from the American Heart Association/American Stroke Association. Stroke. 2014;45(7):2160–236.
14. Brott TG, Halperin JL, Abbara S, Bacharach JM, Barr JD, Bush RL, et al. 2011 ASA/ACCF/AHA/AANN/AANS/ACR/ASNR/CNS/SAIP/SCAI/SIR/SNIS/SVM/SVS guideline on the management of patients with extracranial carotid and vertebral artery disease. Stroke. 2011;42(8):e464–540.
15. White CJ, Ramee SR, Collins TJ, Jenkins JS, Silva JA, Chan AW, et al. Carotid stents to prevent stroke: a nonsurgical option. Ochsner J. 2003;5(1):18–23.
16. Bonati LH, Lyrer P, Ederle J, Featherstone R, Brown MM. Percutaneous transluminal balloon angioplasty and stenting for carotid artery stenosis. Cochrane Database Syst Rev. 2012;9:CD000515.
17. Brott TG, Calvet D, Howard G, Gregson J, Algra A, Becquemin JP, et al. Long-term outcomes of stenting and endarterectomy for symptomatic carotid stenosis: a preplanned pooled analysis of individual patient data. Lancet Neurol. 2019;18(4):348–56.
18. Bonati LH, Dobson J, Featherstone RL, Ederle J, van der Worp HB, de Borst GJ, et al. Long-term outcomes after stenting versus endarterectomy for treatment of symptomatic carotid stenosis: the International Carotid Stenting Study (ICSS) randomised trial. Lancet. 2015;385(9967):529–38.
19. International Carotid Stenting Study i, Ederle J, Dobson J, Featherstone RL, Bonati LH, van der Worp HB, et al. Carotid artery stenting compared with endarterectomy in patients with symptomatic carotid stenosis (International Carotid Stenting Study): an interim analysis of a randomised controlled trial. Lancet. 2010;375(9719):985–97.

20. Group SC, Ringleb PA, Allenberg J, Bruckmann H, Eckstein HH, Fraedrich G, et al. 30 day results from the SPACE trial of stent-protected angioplasty versus carotid endarterectomy in symptomatic patients: a randomised non-inferiority trial. Lancet. 2006;368(9543):1239–47.
21. Mas JL, Trinquart L, Leys D, Albucher JF, Rousseau H, Viguier A, et al. Endarterectomy Versus Angioplasty in Patients with Symptomatic Severe Carotid Stenosis (EVA-3S) trial: results up to 4 years from a randomised, multicentre trial. Lancet Neurol. 2008;7(10):885–92.
22. Brott TG, Hobson RW 2nd, Howard G, Roubin GS, Clark WM, Brooks W, et al. Stenting versus endarterectomy for treatment of carotid-artery stenosis. N Engl J Med. 2010;363(1):11–23.
23. Brott TG, Howard G, Roubin GS, Meschia JF, Mackey A, Brooks W, et al. Long-term results of stenting versus endarterectomy for carotid-artery stenosis. N Engl J Med. 2016;374(11):1021–31.
24. Silver FL, Mackey A, Clark WM, Brooks W, Timaran CH, Chiu D, et al. Safety of stenting and endarterectomy by symptomatic status in the carotid revascularization endarterectomy versus stenting trial (CREST). Stroke. 2011;42(3):675–80.
25. Yadav JS. Carotid stenting in high-risk patients: design and rationale of the SAPPHIRE trial. Cleve Clin J Med. 2004;71(Suppl 1):S45–6.
26. Yadav JS, Wholey MH, Kuntz RE, Fayad P, Katzen BT, Mishkel GJ, et al. Protected carotid-artery stenting versus endarterectomy in high-risk patients. N Engl J Med. 2004;351(15):1493–501.
27. Mott M, Koroshetz W, Wright CB. CREST-2: identifying the best method of stroke prevention for carotid artery stenosis: National Institute of Neurological Disorders and Stroke organizational update. Stroke. 2017;48(5):e130–e1.
28. Bulbulia R, Halliday A. The Asymptomatic Carotid Surgery Trial-2 (ACST-2): an ongoing randomised controlled trial comparing carotid endarterectomy with carotid artery stenting to prevent stroke. Health Technol Assess. 2017;21(57):1–40.
29. Lam RC, Lin SC, DeRubertis B, Hynecek R, Kent KC, Faries PL. The impact of increasing age on anatomic factors affecting carotid angioplasty and stenting. J Vasc Surg. 2007;45(5):875–80.
30. Giri J, Kennedy KF, Weinberg I, Hawkins BM, Press MC, Drachman D, et al. Comparative effectiveness of commonly used devices for carotid artery stenting: an NCDR Analysis (National Cardiovascular Data Registry). JACC Cardiovasc Interv. 2014;7(2):171–7.
31. Stabile E, Sannino A, Schiattarella GG, Gargiulo G, Toscano E, Brevetti L, et al. Cerebral embolic lesions detected with diffusion-weighted magnetic resonance imaging following carotid artery stenting: a meta-analysis of 8 studies comparing filter cerebral protection and proximal balloon occlusion. JACC Cardiovasc Interv. 2014;7(10):1177–83.
32. Scheinert D, Reimers B, Cremonesi A, Schmidt A, Sievert H, Rohde S, et al. Independent modular filter for embolic protection in carotid stenting. Circ Cardiovasc Interv. 2017;10(3):e004244.
33. Siewiorek GM, Eskandari MK, Finol EA. The Angioguard embolic protection device. Expert Rev Med Devices. 2008;5(3):287–96.
34. Giugliano G, Stabile E, Biamino G, Petroni G, Sannino A, Brevetti L, et al. Predictors of carotid occlusion intolerance during proximal protected carotid artery stenting. JACC Cardiovasc Interv. 2014;7(11):1237–44.
35. Brown MM. Carotid artery stenting–evolution of a technique to rival carotid endarterectomy. Am J Med. 2004;116(4):273–5.
36. Nikas DN, Kompara G, Reimers B. Carotid stents: which is the best option? J Cardiovasc Surg. 2011;52(6):779–93.
37. Muller MD, Gregson J, McCabe DJH, Nederkoorn PJ, van der Worp HB, de Borst GJ, et al. Stent design, restenosis and recurrent stroke after carotid artery stenting in the international carotid stenting study. Stroke. 2019;50(11):3013–20.
38. White CJ. Carotid artery stenting. J Am Coll Cardiol. 2014;64(7):722–31.
39. Moulakakis KG, Mylonas SN, Lazaris A, Tsivgoulis G, Kakisis J, Sfyroeras GS, et al. Acute carotid stent thrombosis: a comprehensive review. Vasc Endovasc Surg. 2016;50(7):511–21.

40. Timaran CH, Veith FJ, Rosero EB, Modrall JG, Valentine RJ, Clagett GP. Intracranial hemorrhage after carotid endarterectomy and carotid stenting in the United States in 2005. J Vasc Surg. 2009;49(3):623–8; discussion 8-9
41. Abou-Chebl A, Yadav JS, Reginelli JP, Bajzer C, Bhatt D, Krieger DW. Intracranial hemorrhage and hyperperfusion syndrome following carotid artery stenting: risk factors, prevention, and treatment. J Am Coll Cardiol. 2004;43(9):1596–601.
42. Kwolek CJ, Jaff MR, Leal JI, Hopkins LN, Shah RM, Hanover TM, et al. Results of the ROADSTER multicenter trial of transcarotid stenting with dynamic flow reversal. J Vasc Surg. 2015;62(5):1227–34.
43. Malas MB, Leal J, Kashyap V, Cambria RP, Kwolek CJ, Criado E. Technical aspects of transcarotid artery revascularization using the ENROUTE transcarotid neuroprotection and stent system. J Vasc Surg. 2017;65(3):916–20.
44. Kashyap VS, King AH, Liang P, Eldrup-Jorgensen J, Wang GJ, Malas MB, et al. Learning curve for surgeons adopting transcarotid artery revascularization based on the vascular quality initiative-transcarotid artery revascularization surveillance project. J Am Coll Surg. 2020;230(1):113–20.
45. King AH, Kumins NH, Foteh MI, Jim J, Apple JM, Kashyap VS. The learning curve of transcarotid artery revascularization. J Vasc Surg. 2019;70(2):516–21.
46. Alvarez B, Matas M, Ribo M, Maeso J, Yugueros X, Alvarez-Sabin J. Transcervical carotid stenting with flow reversal is a safe technique for high-risk patients older than 70 years. J Vasc Surg. 2012;55(4):978–84.
47. Kumins NH, King AH, Ambani RN, Thomas JP, Kim AH, Augustin G, et al. Anatomic criteria in the selection of treatment modality for atherosclerotic carotid artery disease. J Vasc Surg. 2020;72(4):1395–404.
48. Kashyap VS, King AH, Foteh MI, Janko M, Jim J, Motaganahalli RL, et al. A multi-institutional analysis of transcarotid artery revascularization compared to carotid endarterectomy. J Vasc Surg. 2019;70(1):123–9.
49. Kashyap VS, Schneider PA, Foteh M, Motaganahalli R, Shah R, Eckstein HH, et al. Early outcomes in the ROADSTER 2 study of transcarotid artery revascularization in patients with significant carotid artery disease. Stroke. 2020;51(9):2620–9.
50. Malas MB, Leal Lorenzo JI, Nejim B, Hanover TM, Mehta M, Kashyap V, et al. Analysis of the ROADSTER pivotal and extended-access cohorts shows excellent 1-year durability of transcarotid stenting with dynamic flow reversal. J Vasc Surg. 2019;69(6):1786–96.
51. Schermerhorn ML, Liang P, Eldrup-Jorgensen J, Cronenwett JL, Nolan BW, Kashyap VS, et al. Association of transcarotid artery revascularization vs transfemoral carotid artery stenting with stroke or death among patients with carotid artery stenosis. JAMA. 2019;322(23):2313–22.

Chapter 14
Intracranial Atherosclerotic Disease

Rudy J. Rahme and Erol Veznedaroglu

Introduction

Despite our best efforts, stroke continues to be the fifth leading cause of mortality in the United States and a leading cause of morbidity [1]. The prevalence of stroke is estimated to be at 3% of the US adult population with an incidence of 795,000 strokes per year, 87% of which is ischemic in nature. Over the past three decades, the global lifetime risk of stroke has increased to 24.9%, a relative increase of 8.9% compared to 1990 [1]. This is due to an aging population with an accumulation of risk factors despite an overall improvement in the incidence of stroke. By the year 2030, the prevalence of stroke is projected to be at 3.9%, with an additional 3.4 million adults in the United States suffering a stroke. In addition, the estimated prevalence of transient ischemic attacks (TIA) in the United States is 2.3%, or approximately five million adults. This number is likely an underrepresentation since it is based on self-reported symptoms.

Intracranial atherosclerotic disease (ICAD) constitutes 8–10% of ischemic strokes, with significant variation based on race and ethnicity [2, 3]. Despite numerous trials and significant advances in medical and interventional/surgical options, ICAD remains challenging to treat with recurrence rates as high as 20% [4]. The treatment paradigms for ICAD continue to evolve as our understanding of the

R. J. Rahme
Department of Neurosurgery, Global Neuroscience Institute, Philadelphia, PA, USA
e-mail: rrahme@gnineuro.org

E. Veznedaroglu (✉)
Department of Neurosurgery, Drexel University College of Medicine, Drexel Neurosciences Institute, Global Neurosciences Institute, Philadelphia, PA, USA
e-mail: evez@gnineuro.org

J. R. Mascitelli, M. J. Binning (eds.), *Introduction to Vascular Neurosurgery*,
https://doi.org/10.1007/978-3-030-88196-2_14

mechanisms underlying the pathophysiology improves. In this chapter, we review the epidemiology, natural history, diagnosis, and various treatment options of ICAD.

Epidemiology and Risk Factors

The role of ICAD in ischemic stroke was first reported in the 1960s. The Joint Study of Extracranial Arterial Occlusion, published in 1968, evaluated 4748 patients who presented with ischemic stroke [5]. Eighty percent of these patients (3788) underwent a 4-vessel diagnostic angiogram. The most common location of ICAD was noted to be the basilar artery (BA), followed by the intracranial carotid arteries (ICA), then the intracranial vertebral arteries (VA), middle cerebral arteries (MCA), anterior cerebral arteries (ACA), and finally the posterior cerebral arteries (PCA). It should be noted though that based on more recent data, the MCA location seems to be the most common location of ICAD accounting for about one-third of all cases, followed by ICA, BA, VA, and finally a combination of territories [6]. In the initial report from 1968, 6.1% of patients had isolated intracranial disease with no evidence of extracranial atherosclerosis [5]. The findings of this study were limited by the quality of angiography at that time and by the racial makeup of the study population. In fact, 84% of patients were white with a 2:1 male to female ratio. However, more recent epidemiological studies revealed that ICAD is particularly prevalent in African American, Hispanic, and Asian populations [3, 7, 8]. Adjusted incidence of ICAD-related stroke was reported to be 15, 13, and 3 per 100,000 in African American, Hispanic, and white populations respectively [9]. In addition, ICAD is the etiology of stroke in up to 50% of cases in Asian populations [8]. The reasons for the discrepancy between various races and ethnicities could be related to multiple factors including genetic predilection as well as difference in lifestyle and risk factor profiles. In terms of sex predilection, the male to female ratio varies from 1.25 to 0.76 depending on age [10]. Men tend to develop ICAD earlier than women. However, progression of disease is faster in females which explains the inversion of the ratio in older populations [11].

Risk factors of ICAD are similar to those of stroke in general and include age, hypertension, dyslipidemia, smoking, diabetes, metabolic syndrome, and sedentary lifestyle [12]. In a post hoc analysis of the Warfarin-Aspirin Symptomatic Intracranial Disease (WASID) trial, the most important factors associated with recurrent stroke were hypertension (systolic blood pressure >140 mm Hg) and elevated cholesterol levels [13]. In fact, presence of lipid disorder was an independent predictor of severe stenosis [14]. Progression of stenosis and risk of recurrent stroke have also been linked to proinflammatory biomarkers such as C-reactive protein and E-selectin, as well as impaired fibrinolysis [15]. On the other hand, high HDL concentrations have been linked to stenosis stability [16]. In addition, risk factors seem to vary by location of ICAD: basilar stenoses are more often associated with older age and dyslipidemia whereas intracranial carotid artery

stenoses are linked to diabetes, and middle cerebral artery stenoses are more often found in women and African Americans. Most importantly intracranial atherosclerosis appears to be a modifiable process with possible regression in up to 20% of patients [17].

Mechanism of Stroke

ICAD can cause TIA and strokes through multiple mechanisms: artery-to-artery embolism, hemodynamic insufficiency, occlusion of small perforators, or various combinations of these mechanisms. The distinction could be made based on imaging findings with excellent interrater reliability [18]. Watershed infarcts most likely correlate with hemodynamic insufficiency. These patients typically have poor collateral circulation and often have hypertension as a modifiable risk factor [19]. If the stroke territory is distal, wedge-shaped, and corresponds to an arterial territory or in the presence of multiple small distal infarcts, the mechanism is likely artery-to-artery embolism. Patients with dyslipidemia often have vulnerable plaques which can rupture and lead to distal emboli. In addition, high wall shear stress from hypertension can cause endothelial cell dysfunction and render the plaque more vulnerable as well. Therefore, hypertension is often found in patients with mixed mechanism of strokes combining hypoperfusion and artery-to-artery emboli [18]. Finally, lacunar subcortical infarcts are most likely due to occlusion of small perforators which are thought to occur more frequently in the posterior circulation [20]. The relative frequency of each mechanism is variable among different studies, likely due to differences in inclusion criteria, specifically the degree of stenosis [20–22]. Other imaging modalities can also be used to distinguish the various mechanism of stroke. Transcranial Doppler (TCD) for example can be used to detect microemboli which would argue for an embolic etiology.

The mechanism of stroke has treatment implications. In patients with documented hypoperfusion on imaging, either CT or MR, lowering blood pressure, while beneficial to reduce recurrence of stroke in most other cases, can be detrimental. In addition, risk of recurrence was found to be higher when multiple mechanisms are involved [18]. Therefore, when multiple mechanisms are suspected to be involved in the stroke, intense therapeutic interventions, including dual antiplatelet therapy and high dose statins, should be initiated.

Imaging and Differential Diagnosis

The diagnostic gold standard for ICAD is conventional cerebral angiography. However, noninvasive imaging is preferred as first line since it is less invasive, lower risk profile, less expensive, and more widely available. The Stroke Outcomes and Neuroimaging of Intracranial Atherosclerosis (SONIA) trial was a prospective

multicenter study that aimed to evaluate TCD and MRA as diagnostic tools for ICAD [23]. Both modalities had high negative predictive values (86 and 91% respectively) and poor positive predictive values (36 and 59% respectively). CTA had a similar profile with a negative predictive value of 73% and a positive predictive value of 47% [24]. In addition, noninvasive imaging tends to overestimate the degree of stenosis and might not be accurate enough to differentiate between critical stenosis and occlusion.

Diagnostic cerebral angiogram is often not necessary in ICAD, specifically since it might not alter the management in the majority of cases. However, the benefits of diagnostic angiogram are manifold. First, it allows for an accurate assessment of the degree of stenosis and therefore subclassify the lesion on the Mori classification: type A refers to short (≤5 mm) and concentric lesion; type B are 5–10 mm in length, tubular or eccentric, with minor angulation, or with complete occlusion less than 3 months old; type C are long (>10 mm) complex eccentric lesions, with severe angulation, or occluded for longer than 3 months. This classification has clinical implications with the highest risk of restenosis and stroke with type C, followed by B and then A lesions. Second, it permits a comprehensive study of the intracranial and extracranial vasculature, including an analysis of the collateral circulation. Finally, in complex and uncertain cases, it helps establish the diagnosis of ICAD and differentiate it from other similar appearing vascular diseases.

The differential diagnosis includes arterial dissection, moyamoya disease, vasculitis, fibromuscular dysplasia, and other vasculopathies such as vasospasm and reversible cerebral vasoconstriction syndrome. Moyamoya disease is arguably the diagnosis that most closely resembles ICAD. However, the localized stenosis at the distal internal carotid artery and the proximal circle of Willis in addition to the dilated lenticulostriates can help distinguish moyamoya disease from ICAD. In cases of arterial dissection, the presence of a false lumen, an intimal flap, or a dissecting aneurysm are typical signs. In some instances, clinical presentation can be the differentiating factor. For example, in RCVS, patients present with thunderclap headaches. Vasculitis, on the other hand, has a subacute presentation and is characterized on imaging by "string of beads" sign predominantly in the smaller distal intracranial vessels. Finally, fibromuscular dysplasia affects the extracranial internal carotid arteries, the vertebral arteries, and the renal arteries. In rare instances, it can affect the large intracranial arteries such as the middle and anterior cerebral arteries.

Vessel wall MR imaging is a novel imaging modality that allows direct visualization of the vessel wall as opposed to the traditional imaging techniques which focus on the vessel lumen [25]. ICAD lesions were often found to be eccentric and heterogeneously enhancing. In contrast, RCVS lesions were concentric and non-enhancing; inflammatory vasculopathies were concentric and diffusely enhancing. The addition of vessel imaging significantly improved the diagnostic accuracy of ICAD as well as the interrater reliability [25]. However, vessel wall imaging is still not widely available in clinical practice.

Treatment

Treatment of ICAD has gone through multiple phases through the past few decades. The initial enthusiasm for bypass was quickly tempered after the publication of the extracranial-intracranial bypass trial in 1985 [26]. Despite many flaws of this trial, including poor patient selection, medical management became the mainstay of ICAD treatment. With the development of endovascular techniques, stenting and angioplasty promised to offer an alternative to medical management specifically since the rate of stroke recurrence with medical management remained relatively high. The initial feasibility, non-randomized trials with both balloon-mounted and self-expanding stents showed promise and lead to FDA approval and designation of humanitarian device exemption in patients with recurrent TIA/Strokes despite medical management [27–30]. However, the SAMMPRIS and VISSIT trials failed to replicate these results and revealed significantly higher rate of strokes with endovascular management compared to medical therapy [31, 32]. Medical management therefore remained first line therapy. However, since the publication of these two trials, multiple subgroup analyses were performed and improved our understanding of the pathophysiology of ICAD leading to renewed interest in open surgical and endovascular interventions for select cases.

Medical Management

Antiplatelet Therapy Versus Anticoagulation

The initial treatment of ICAD was anticoagulation and was first reported in 1955 [33]. Subsequent retrospective studies seemed to confirm the superiority of warfarin over aspirin in that population [34–36]. In fact, the initial WASID retrospective multicenter study published in 1995 enrolled 151 patients, 88 treated with warfarin and 63 with aspirin [35]. The median follow-up was 14.9 and 19.3 months for the warfarin and the aspirin groups, respectively. The warfarin group was significantly less likely to have a major vascular event compared to the aspirin group (8.4 per 100 patient-years of follow up vs. 18.1 per 100 patient-years, $p = 0.01$). However, the prospective, randomized, double-blinded, multicenter trial by the WASID group published in 2005, revealed no benefit of warfarin over aspirin in ICAD treatment [6]. The trial enrolled 569 patients with 50–99% stenosis and was stopped early due to safety concerns for patients randomized in the warfarin group. The overall rate of adverse events in the warfarin group, including death, was significantly higher than in the aspirin group (4.3 vs. 9.7; hazard ratio: 0.46; 95% confidence interval: 0.23–0.90; $P = 0.02$). This statistically significant difference persisted when subcategorizing the adverse events into major hemorrhage (3.2% vs. 8.3%, HR: 0.39; 95% CI: 0.18–0.84, $P = 0.01$) and myocardial infarction or sudden death (2.9% vs. 7.3%, HR: 0.40, 95% CI: 0.18–0.91; $P = 0.02$). Further

analysis of subgroups thought to be at a high risk of stroke, including patients with 70–99% stenosis, posterior circulation stenosis, and those who failed medical therapy (stroke while on medical treatment), confirmed the findings of the main trial with no benefit of warfarin over aspirin [37, 38]. The role of novel anticoagulants in ICAD has yet to be studied, and there are currently no data to support their use in this population.

The benefit of dual antiplatelet therapy has been well documented in ICAD patients, specifically in the acute post stroke/TIA setting in patients with high-grade stenoses (70–99%). In the CLAIR (clopidogrel plus aspirin for infarction reduction in acute stroke or transient ischemic attack patients with large artery stenosis and microembolic signals) trial patients on aspirin and clopidogrel with recent (≤7 days) symptomatic intracranial or extracranial atherosclerosis had less microemboli detected on TCD [39]. These findings were replicated in the Clopidogrel and Aspirin for Reduction of Emboli in Symptomatic Carotid Stenosis (CARESS) study [40]. Both trials were prospective and randomized and did not show any increased risk with dual antiplatelet therapy compared to monotherapy. In a weighed meta-analysis of the CLAIR and the CARESS trials, there was significantly lower rate of stroke recurrence in patients on aspirin and clopidogrel compared to those on aspirin alone [39]. The benefit of short-term dual antiplatelet therapy initiated shortly after the onset of TIA or stroke was further corroborated with the Clopidogrel in high-risk patients with Acute Nondisabling Cerebrovascular Events (CHANCE) trial [41].

In summary, patients with severe ICAD (70–99% stenosis) benefit from short-term dual antiplatelet therapy followed by monotherapy. The duration of dual antiplatelet therapy is not well established but is typically around 90 days. Other antiplatelet agents such as cilostazol, ticagrelor, and extended-release dipyridamole were briefly studied, but there are no current data to support their use in ICAD. Cilostazol is a phosphodiesterase inhibitor with some vasodilator and possible antiatherogenic properties. While initial data comparing cilostazol added to aspirin compared to placebo and aspirin were promising, further studies comparing aspirin and clopidogrel to aspirin and cilostazol failed to show any difference between both groups [42, 43]. An important factor to consider is clopidogrel resistance in carriers of the cytochrome P 2C19 mutation. In these patients, alternative antiplatelet medications such as ticagrelor might need to be considered despite the lack of evidence.

Risk Factor Modification

Risk factor modifications including blood pressure control, smoking cessation, lipid lowering drugs, and diabetes control have been studied extensively for secondary stroke prevention. However, no trials were done to address risk factors specifically in ICAD. The data that we have are based on post hoc analyses from the WASID, COSS, SAMMPRIS, and VERiTAS trials [13, 44–47]. Based on these analyses,

blood pressure lowering to <140 mmHg is not only safe but also beneficial in decreasing the risk of recurrent stroke even in cases of severe stenosis. However, there is a theoretical concern that patients with hypoperfusion might have an increased risk of stroke with lower blood pressure. It should be noted though that follow-up of the WASID trial revealed that patients that were maintained at a higher blood pressure to avoid hypoperfusion did not have a lower risk of stroke in the involved territory and had a higher overall rate of stroke [44]. Therefore, unless perfusion imaging clearly demonstrates hypoperfusion, blood pressure control with a systolic goal of <140 mmHg should be initiated.

Physical activity was an independent factor for lower risk of stroke in a post hoc analysis of the SAMMPRIS trial [45]. Statin therapy is recommended to decrease overall risk of stroke and cardiovascular events. This is also true for ICAD. A post hoc analysis of the SAMMPRIS trial revealed that lowering the LDL level decreases the risk of stroke. However, when using LDL level of 70 mg/dl as cutoff – as dictated in the ACC/AHA guidelines for cardiovascular risk – no statistical difference was noted despite a trend toward lower risk of stroke with LDL <70 mg/dl. Further evidence of the importance of risk factor control comes from a comparison of the WASID and the SAMMPRIS trials. The medical management in the SAMMPRIS arm had intensive interventions with a lifestyle coach. The rate of stroke at 30 days and at 1 year was significantly lower than expected based on the WASID trial (5.8% vs. 10.7% at 30 days; 12.2% vs. 25% at 1 year).

Surgery

Direct Bypass

Prior to the publication of the extracranial-intracranial (EC-IC) bypass trial in 1985, bypass was one of the main treatments for stroke prevention in stenosis or occlusion of the internal carotid artery or middle cerebral artery [48]. The EC-IC bypass trial enrolled 1377 patient randomized to either medical management or surgical bypass. The study failed to show any benefit of surgery over medical management despite at 96% bypass patency rate. Subgroup analyses did not reveal any particular groups that would benefit from surgery. However, patient selection was flawed as highlighted by the fact that patients with severe middle cerebral artery stenosis fared significantly worse. With this in mind, in order to improve patient selection, the Carotid Occlusion Surgery Study (COSS) enrolled patient with recently symptomatic carotid occlusion and with evidence of cerebral ischemia based on increased oxygen extraction fraction [26]. Patients were randomized into bypass surgery or medical management. The study was stopped early due to futility. The primary endpoint of stroke or death was reached in 21% of patients in the surgery group and in 22.7% of the medical group. The 30-day rate of ipsilateral stroke was 14.3% in the surgery group and 2% in the medical group.

Indirect Bypass

Despite the failures of direct bypass trials, and due to the persistently high rates of stroke with best medical management as evidenced by the SAMMPRIS and the WASID trials, there was renewed interest in surgical interventions. Encephaloduroarteriosynangiosis (EDAS) is less technically challenging than direct bypass and does not require temporary occlusion of an already at-risk ischemic brain. The Encephaloduroarteriosynangiosis revascularization for symptomatic intracranial atherosclerotic stenoocclusive (ERSIAS) trial is a phase II study developed to evaluate the feasibility, safety, and preliminary efficacy of EDAS in patients with ICAD [49]. The trial prospectively enrolled 52 patients with a follow-up of 24.5 months. The primary endpoint was stroke or death within 30 days of surgery and stroke in the territory of interest beyond 30 days. The primary endpoint occurred in five (9.6%) patients at 1 year, which reached the threshold for non-futility. The trial is now advancing to phase III. At 2-year follow up, the rate of stroke was lower than that of matched medically treated patients in the SAMMPRIS and COSS trials (9.6% vs. 21.2%; $P = 0.07$). These results are encouraging but further studies are needed prior to making any conclusions.

Endovascular Therapy

Stenting

Endovascular management of ICAD showed initial promise in the Stenting of Symptomatic Atherosclerotic Lesions in the Vertebral or Intracranial Arteries (SSYLVIA) trial [28]. This prospective, non-randomized feasibility study used the balloon-expanded Neurolink system (Guidant Corporation, Santa Clara, CA) and enrolled a total of 61 symptomatic patients with ≥50% stenosis, 43 of whom had intracranial atherosclerosis. Four patients (6.6%) had strokes at 30 days. The rate of >50% stenosis at 6 months was 32.4% for intracranial stents, 39% of whom were symptomatic. The balloon-expanded Neurolink system was granted Humanitarian Device Exemption by the FDA for patients with symptomatic intracranial atherosclerosis despite medical therapy. A few other prospective non-randomized studies followed with similar results using the Wingspan (Stryker, Kalamazoo, MI) self-expanding stent [27, 29, 30]. The Wingspan was developed specifically for intracranial use and was designed to be more flexible to navigate around the tortuosity of intracranial vessels. In addition, the self-expanding design allows it to better conform to the vessel wall. This is used in conjunction with the Gateway balloon (Boston Scientific Corporation, Fremont, CA) for the angioplasty (Figs. 14.1 and 14.2).

The Stenting and Aggressive Medical Management for Preventing Recurrent Stroke in Intracranial Stenosis (SAMMPRIS) trial was a prospective randomized trial designed to compare the emerging angioplasty and stenting technology for

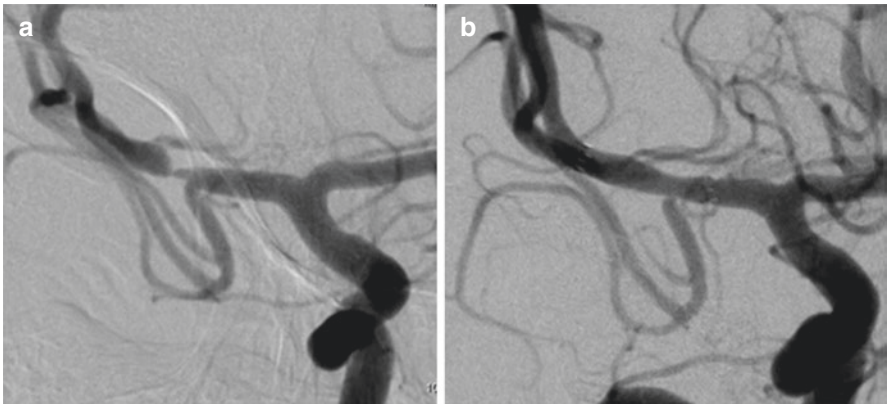

Fig. 14.1 (**a**) Right internal carotid AP view from a diagnostic cerebral angiogram revealing severe non-calcified focal stenosis at the M1 segment. (**b**) Post-angioplasty and stenting with excellent revascularization and restoration of flow distal to the stenosis

ICAD to best medical management. The trial enrolled patients with 70–99% stenosis within 30 days after a TIA or stroke [31]. The trial was stopped early by the Data and Safety Monitoring Board due to the significantly higher rate of stroke or death at 30 days in the interventional group compared to the medical group (14.7% vs. 5.8%, respectively). The very high rate of periprocedural stroke or death in the stenting group, much higher than anticipated based on previous data, raised many questions. ICAD is not a homogeneous disease. A short segment concentric stenosis in the anterior circulation is not equivalent to a longer lesion with significant angulation in the posterior circulation. However, SAMMPRIS did not categorize patients based on Mori classification nor on location. In addition, composition of the plaque can have significant implication. Unstable ruptured plaques with hemorrhage or a large lipid core are more friable and therefore higher risk for embolization during any manipulation. Perhaps these unstable plaques are better treated with maximal medical management and endovascular approaches reserved for stable fibrous plaques with hemodynamic compromise. Another potential explanation for the high rate of periprocedural complication in SAMMPRIS is the fact that only 8% of enrolled patients would have actually met the initial HDE criteria set by the FDA for ICAD stenting. One main conclusion from the SAMMPRIS trial is that intensive medical intervention for risk factor control is effective in reducing the risk of stroke or TIA. However, despite assigning a lifestyle coach to patients with personalized plans, which obviously is not reproducible in settings outside a trial, the rate of stroke or death remained at 12% with medical management at 1 year. This clearly emphasized the need for better treatment options for ICAD. After the SAMMPRIS trial, the FDA restricted the approval for the Wingspan stent to patients between 22 and 80 years of age who have 70–99% stenosis, with two or more strokes despite best medical management and with good recovery (modified ranking scale of 3 or less). The treatment should not occur within 7 days of onset of symptoms. The

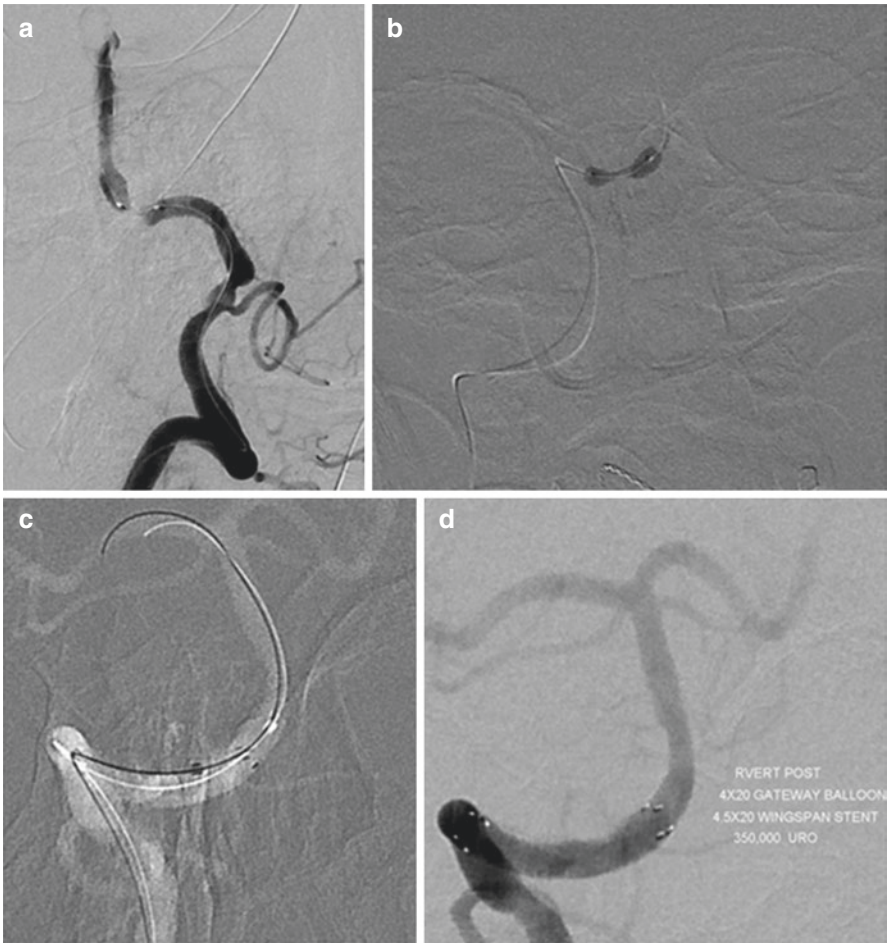

Fig. 14.2 (**a**) Right vertebral artery lateral view from a diagnostic cerebral angiogram revealing severe focal stenosis at the vertebrobasilar junction. Poor flow is noted in the basilar artery. (**b**) 4 × 20 mm Gateway balloon inflated at the level of the stenosis. Note balloon waist at the area of calcification. (**c**) 4.5 × 20 mm wingspan stent deployed across the stenotic segment. (**d**) Right vertebral artery AP view post-angioplasty and stenting with excellent revascularization and restoration of robust flow in the basilar artery

difference between the two SAMMPRIS trial groups persisted at the 1- and 3-year follow-ups and was largely driven by the periprocedural rates.

The Vitesse Intracranial Stent Study for Ischemic Stroke Therapy (VISSIT) trial was an international randomized trial comparing stenting with a balloon-expandable stent, the Pharos Vitesse stent (Codman & Shurtleff, Raynham, Massachusetts, USA), to medical management [32]. The periprocedural rates in the stenting group

were significantly higher than the medical group (24% vs. 9%) and the trial was stopped early after an interim analysis suggested futility.

The results of a post market surveillance trial of the Wingspan stent mandated by the FDA and based on the updated inclusion criteria were recently published [50, 51]. The trial was designed to enroll 389 patients. However, it was stopped early at the interim analysis, with only 152 consecutive patients enrolled, due to lower-than-expected 2.6% periprocedural event rate. This was lower than the 4% safety benchmark set for the interim analysis. At 72 hours, two patients (1.3%) had non-fatal strokes and two patients (1.3%) had died. The 1-year follow-up (WOVEN trial) of 129/152 patients revealed seven additional strokes, only one major, and no deaths beyond the periprocedural phase [51]. At 1 year, the rate of stroke or death from on-label stenting of ICAD was 8.5%. There was a 17.6% restenosis rate defined as ≥70% narrowing. Of the seven strokes, six had evidence of restenosis on delayed imaging. The low rate of periprocedural and 1-year events is even more remarkable when considering that the study population is composed of patients who failed maximal medical therapy with history of multiple strokes. Based on these results, stenting remains an option for patients with severe ICAD who meet the FDA set criteria.

Submaximal Angioplasty

Submaximal angioplasty can be a treatment option for ICAD patients who fail medical management. The interest in this technique increased after the SAMMPRIS results were published. Angioplasty offers many advantages. While medical therapy can stabilize the plaque, in some instances, symptoms are driven by hypoperfusion. Based on the law of Poiseuille, the flow of blood is directly proportional to the radius of the vessel to the fourth power. Therefore, even a minor increase in vessel diameter (decrease in stenosis) could lead to a significant improvement in blood flow to the target territory (Fig. 14.3). In addition, a submaximal angioplasty could reduce the risk of hemorrhage related to sudden hyperperfusion in a territory with impaired autoregulation. Angioplasty is technically less challenging than stenting and is thought to have a higher safety profile with less vessel manipulation, specifically with submaximal inflation of the balloon. A meta-analysis of nine studies with a total of 395 patients with symptomatic ICAD revealed a periprocedural risk of stroke or death of 4.9% [52]. This rate compares favorably to both the medical and interventional arms of the SAMMPRIS and the VISSIT trials. The long-term rate of stroke or death beyond the 30 periprocedural days was also low at 3.7%. The success rate of angioplasty was at 96.4%. Submaximal angioplasty is therefore a valid alternative in select patients with hemodynamic insufficiency with low procedure risk and sustained clinical benefit. The main concern remains the risk of restenosis and the need for repeat intervention.

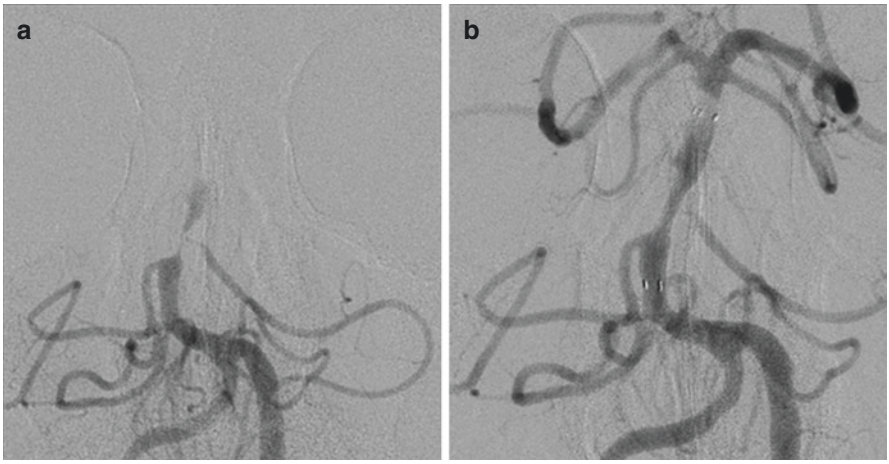

Fig. 14.3 (**a**) Severe midbasilar noncompliant stenosis with poor flow distal to the stenosis. (**b**) Post multiple inflations of balloon and stent placement with significant restoration of flow despite submaximal angioplasty

Future Directive

In the decade since SAMMPRIS was published, various treatment paradigms have been proposed for ICAD. However, all treatment options remain flawed with high rates of failure. ICAD is a highly heterogeneous disease based on patient and plaque characteristics. Advanced imaging modalities, such as vessel wall MRI, might hold the key to individualized treatments based on plaque composition. In addition, analyzing the failures of medical therapy might yield clues as to the reasons behind them, such as possible resistance to certain medications, with the potential to implement specific treatments for specific patients. Restenosis is another possible target for future trials. Whether with angioplasty alone or angioplasty and stenting, the rate of restenosis remains high with suggested correlation between restenosis and recurrence of stroke. A staged approach with angioplasty followed by delayed stenting has been proposed as a potential strategy to decrease risk of restenosis and at the same time decrease periprocedural risk. Finally, cerebral hypoperfusion has been correlated with cognitive decline in atherosclerotic disease [53, 54]. However, the effect or ICAD treatment, if any, on cognition has not been well studied and is not yet established. Whether revascularization, either through angioplasty and stenting or through indirect bypass, will yield better cognitive outcomes compared to medical management is yet to be seen.

Conclusion

Intracranial atherosclerotic disease remains one of the more challenging diseases to treat despite significant advances in our understanding of its pathophysiology and the hemodynamic mechanisms behind stroke in this population. Maximal medical therapy remains the mainstay of treatment. This includes dual anti-platelet therapy for a short period of time followed by single anti-platelet therapy and risk factor control. Endovascular therapy is reserved for patients who fail maximal medical therapy. The best approach for endovascular treatment of ICAD has not yet been determined. When done on-label with the new FDA guidelines, stenting seems to have low periprocedural risk and a sustained benefit even when compared to best medical management. Submaximal angioplasty is a potential alternative to stenting. Encephaloduroarteriosynangiosis is yet another flow augmentation strategy that is currently showing promise for this patient population. Further trials are needed to fully understand the nuanced, perhaps even individualized, approach to this disease.

References

1. Virani SS, Alonso A, Benjamin EJ, Bittencourt MS, Callaway CW, Carson AP, et al. Heart disease and stroke Statistics-2020 update: a report from the American Heart Association. Circulation. 2020;141(9):e139–596.
2. Bogousslavsky J, Van Melle G, Regli F. The Lausanne stroke registry: analysis of 1,000 consecutive patients with first stroke. Stroke. 1988;19(9):1083–92.
3. Sacco RL, Kargman DE, Gu Q, Zamanillo MC. Race-ethnicity and determinants of intracranial atherosclerotic cerebral infarction. The Northern Manhattan Stroke Study Stroke. 1995;26(1):14–20.
4. Sangha RS, Naidech AM, Corado C, Ansari SA, Prabhakaran S. Challenges in the medical Management of Symptomatic Intracranial Stenosis in an urban setting. Stroke. 2017;48(8):2158–63.
5. Hass WK, Fields WS, North RR, Kircheff CNE II, Bauer RB. Joint study of extracranial arterial occlusion. II. Arteriography, techniques, sites, and complications. JAMA. 1968;203(11):961–8.
6. Chimowitz MI, Lynn MJ, Howlett-Smith H, Stern BJ, Hertzberg VS, Frankel MR, et al. Comparison of warfarin and aspirin for symptomatic intracranial arterial stenosis. N Engl J Med. 2005;352(13):1305–16.
7. Qureshi AI, Safdar K, Patel M, Janssen RS, Frankel MR. Stroke in young black patients. Risk factors, subtypes, and prognosis. Stroke. 1995;26(11):1995–8.
8. Wityk RJ, Lehman D, Klag M, Coresh J, Ahn H, Litt B. Race and sex differences in the distribution of cerebral atherosclerosis. Stroke. 1996;27(11):1974–80.
9. White H, Boden-Albala B, Wang C, Elkind MS, Rundek T, Wright CB, et al. Ischemic stroke subtype incidence among whites, blacks, and Hispanics: the northern Manhattan study. Circulation. 2005;111(10):1327–31.
10. Go AS, Mozaffarian D, Roger VL, Benjamin EJ, Berry JD, Borden WB, et al. Heart disease and stroke statistics--2013 update: a report from the American Heart Association. Circulation. 2013;127(1):e6–e245.
11. Bae HJ, Lee J, Park JM, Kwon O, Koo JS, Kim BK, et al. Risk factors of intracranial cerebral atherosclerosis among asymptomatics. Cerebrovasc Dis. 2007;24(4):355–60.

12. Holmstedt CA, Turan TN, Chimowitz MI. Atherosclerotic intracranial arterial stenosis: risk factors, diagnosis, and treatment. Lancet Neurol. 2013;12(11):1106–14.
13. Chaturvedi S, Turan TN, Lynn MJ, Kasner SE, Romano J, Cotsonis G, et al. Risk factor status and vascular events in patients with symptomatic intracranial stenosis. Neurology. 2007;69(22):2063–8.
14. Turan TN, Makki AA, Tsappidi S, Cotsonis G, Lynn MJ, Cloft HJ, et al. Risk factors associated with severity and location of intracranial arterial stenosis. Stroke. 2010;41(8):1636–40.
15. Arenillas JF, Alvarez-Sabin J, Molina CA, Chacon P, Fernandez-Cadenas I, Ribo M, et al. Progression of symptomatic intracranial large artery atherosclerosis is associated with a proinflammatory state and impaired fibrinolysis. Stroke. 2008;39(5):1456–63.
16. Kim DE, Kim JY, Jeong SW, Cho YJ, Park JM, Lee JH, et al. Association between changes in lipid profiles and progression of symptomatic intracranial atherosclerotic stenosis: a prospective multicenter study. Stroke. 2012;43(7):1824–30.
17. Akins PT, Pilgram TK, Cross DT 3rd, Moran CJ. Natural history of stenosis from intracranial atherosclerosis by serial angiography. Stroke. 1998;29(2):433–8.
18. Feng X, Chan KL, Lan L, Abrigo J, Liu J, Fang H, et al. Stroke mechanisms in symptomatic intracranial atherosclerotic disease: classification and clinical implications. Stroke. 2019;50(10):2692–9.
19. Menon BK, Smith EE, Coutts SB, Welsh DG, Faber JE, Goyal M, et al. Leptomeningeal collaterals are associated with modifiable metabolic risk factors. Ann Neurol. 2013;74(2):241–8.
20. Lopez-Cancio E, Matheus MG, Romano JG, Liebeskind DS, Prabhakaran S, Turan TN, et al. Infarct patterns, collaterals and likely causative mechanisms of stroke in symptomatic intracranial atherosclerosis. Cerebrovasc Dis. 2014;37(6):417–22.
21. Kim JS, Nah HW, Park SM, Kim SK, Cho KH, Lee J, et al. Risk factors and stroke mechanisms in atherosclerotic stroke: intracranial compared with extracranial and anterior compared with posterior circulation disease. Stroke. 2012;43(12):3313–8.
22. Banerjee C, Chimowitz MI. Stroke caused by atherosclerosis of the major intracranial arteries. Circ Res. 2017;120(3):502–13.
23. Feldmann E, Wilterdink JL, Kosinski A, Lynn M, Chimowitz MI, Sarafin J, et al. The stroke outcomes and neuroimaging of intracranial atherosclerosis (SONIA) trial. Neurology. 2007;68(24):2099–106.
24. Liebeskind DS, Kosinski AS, Saver JL, Feldmann E, Investigators S. Computed tomography angiography in the stroke outcomes and neuroimaging of intracranial atherosclerosis (SONIA) study. Interv Neurol. 2014;2(4):153–9.
25. Mossa-Basha M, Alexander M, Gaddikeri S, Yuan C, Gandhi D. Vessel wall imaging for intracranial vascular disease evaluation. J Neurointerv Surg. 2016;8(11):1154–9.
26. Powers WJ, Clarke WR, Grubb RL Jr, Videen TO, Adams HP Jr, Derdeyn CP, et al. Extracranial-intracranial bypass surgery for stroke prevention in hemodynamic cerebral ischemia: the carotid occlusion surgery study randomized trial. JAMA. 2011;306(18):1983–92.
27. Fiorella D, Levy EI, Turk AS, Albuquerque FC, Niemann DB, Aagaard-Kienitz B, et al. US multicenter experience with the wingspan stent system for the treatment of intracranial atheromatous disease: periprocedural results. Stroke. 2007;38(3):881–7.
28. Investigators SS. Stenting of symptomatic atherosclerotic lesions in the vertebral or intracranial arteries (SSYLVIA): study results. Stroke. 2004;35(6):1388–92.
29. Bose A, Hartmann M, Henkes H, Liu HM, Teng MM, Szikora I, et al. A novel, self-expanding, nitinol stent in medically refractory intracranial atherosclerotic stenoses: the wingspan study. Stroke. 2007;38(5):1531–7.
30. Costalat V, Maldonado IL, Zerlauth JB, Menjot N, Riquelme C, Machi P, et al. Endovascular treatment of symptomatic intracranial arterial stenosis: six-year experience in a single-center series of 42 consecutive patients with acute and mid-term results. Neurosurgery. 2010;67(6):1505–13; discussion 13-4.

31. Derdeyn CP, Chimowitz MI, Lynn MJ, Fiorella D, Turan TN, Janis LS, et al. Aggressive medical treatment with or without stenting in high-risk patients with intracranial artery stenosis (SAMMPRIS): the final results of a randomised trial. Lancet. 2014;383(9914):333–41.
32. Zaidat OO, Fitzsimmons BF, Woodward BK, Wang Z, Killer-Oberpfalzer M, Wakhloo A, et al. Effect of a balloon-expandable intracranial stent vs medical therapy on risk of stroke in patients with symptomatic intracranial stenosis: the VISSIT randomized clinical trial. JAMA. 2015;313(12):1240–8.
33. Millikan CH, Siekert RG, Shick RM. Studies in cerebrovascular disease. III. The use of anticoagulant drugs in the treatment of insufficiency or thrombosis within the basilar arterial system. Proc Staff Meet Mayo Clin. 1955;30(6):116–26.
34. Prognosis of patients with symptomatic vertebral or basilar artery stenosis. The Warfarin-Aspirin Symptomatic Intracranial Disease (WASID) Study Group. Stroke. 1998;29(7):1389–92.
35. Chimowitz MI, Kokkinos J, Strong J, Brown MB, Levine SR, Silliman S, et al. The warfarin-aspirin symptomatic intracranial disease study. Neurology. 1995;45(8):1488–93.
36. Thijs VN, Albers GW. Symptomatic intracranial atherosclerosis: outcome of patients who fail antithrombotic therapy. Neurology. 2000;55(4):490–7.
37. Kasner SE, Lynn MJ, Chimowitz MI, Frankel MR, Howlett-Smith H, Hertzberg VS, et al. Warfarin vs aspirin for symptomatic intracranial stenosis: subgroup analyses from WASID. Neurology. 2006;67(7):1275–8.
38. Turan TN, Maidan L, Cotsonis G, Lynn MJ, Romano JG, Levine SR, et al. Failure of antithrombotic therapy and risk of stroke in patients with symptomatic intracranial stenosis. Stroke. 2009;40(2):505–9.
39. Wong KS, Chen C, Fu J, Chang HM, Suwanwela NC, Huang YN, et al. Clopidogrel plus aspirin versus aspirin alone for reducing embolisation in patients with acute symptomatic cerebral or carotid artery stenosis (CLAIR study): a randomised, open-label, blinded-endpoint trial. Lancet Neurol. 2010;9(5):489–97.
40. Markus HS, Droste DW, Kaps M, Larrue V, Lees KR, Siebler M, et al. Dual antiplatelet therapy with clopidogrel and aspirin in symptomatic carotid stenosis evaluated using Doppler embolic signal detection: the Clopidogrel and aspirin for reduction of emboli in symptomatic carotid stenosis (CARESS) trial. Circulation. 2005;111(17):2233–40.
41. Wang Y, Wang Y, Zhao X, Liu L, Wang D, Wang C, et al. Clopidogrel with aspirin in acute minor stroke or transient ischemic attack. N Engl J Med. 2013;369(1):11–9.
42. Kwon SU, Cho YJ, Koo JS, Bae HJ, Lee YS, Hong KS, et al. Cilostazol prevents the progression of the symptomatic intracranial arterial stenosis: the multicenter double-blind placebo-controlled trial of cilostazol in symptomatic intracranial arterial stenosis. Stroke. 2005;36(4):782–6.
43. Kwon SU, Hong KS, Kang DW, Park JM, Lee JH, Cho YJ, et al. Efficacy and safety of combination antiplatelet therapies in patients with symptomatic intracranial atherosclerotic stenosis. Stroke. 2011;42(10):2883–90.
44. Turan TN, Cotsonis G, Lynn MJ, Chaturvedi S, Chimowitz M. Warfarin-aspirin symptomatic intracranial disease trial I. relationship between blood pressure and stroke recurrence in patients with intracranial arterial stenosis. Circulation. 2007;115(23):2969–75.
45. Turan TN, Nizam A, Lynn MJ, Egan BM, Le NA, Lopes-Virella MF, et al. Relationship between risk factor control and vascular events in the SAMMPRIS trial. Neurology. 2017;88(4):379–85.
46. Powers WJ, Clarke WR, Grubb RL Jr, Videen TO, Adams HP Jr, Derdeyn CP, et al. Lower stroke risk with lower blood pressure in hemodynamic cerebral ischemia. Neurology. 2014;82(12):1027–32.
47. Amin-Hanjani S, Turan TN, Du X, Pandey DK, Rose-Finnell L, Richardson D, et al. Higher stroke risk with lower blood pressure in hemodynamic Vertebrobasilar disease: analysis from the VERiTAS study. J Stroke Cerebrovasc Dis. 2017;26(2):403–10.
48. Group EIBS. Failure of extracranial-intracranial arterial bypass to reduce the risk of ischemic stroke. Results of an international randomized trial. N Engl J Med. 1985;313(19):1191–200.

49. Gonzalez NR, Jiang H, Lyden P, Song S, Schlick K, Dumitrascu O, et al. Encephaloduroarteriosynangiosis (EDAS) revascularization for symptomatic intracranial atherosclerotic steno-occlusive (ERSIAS) phase-II objective performance criterion trial. Int J Stroke. 2020;1747493020967256.
50. Alexander MJ, Zauner A, Chaloupka JC, Baxter B, Callison RC, Gupta R, et al. WEAVE trial: final results in 152 on-label patients. Stroke. 2019;50(4):889–94.
51. Alexander MJ, Zauner A, Gupta R, Alshekhlee A, Fraser JF, Toth G, et al. The WOVEN trial: wingspan one-year vascular events and neurologic outcomes. J Neurointerv Surg. 2020.
52. Stapleton CJ, Chen YF, Shallwani H, Vakharia K, Turan TN, Woo HH, et al. Submaximal angioplasty for symptomatic intracranial atherosclerotic disease: a meta-analysis of Peri-procedural and long-term risk. Neurosurgery. 2020;86(6):755–62.
53. Silvestrini M, Paolino I, Vernieri F, Pedone C, Baruffaldi R, Gobbi B, et al. Cerebral hemodynamics and cognitive performance in patients with asymptomatic carotid stenosis. Neurology. 2009;72(12):1062–8.
54. Marshall RS, Festa JR, Cheung YK, Chen R, Pavol MA, Derdeyn CP, et al. Cerebral hemodynamics and cognitive impairment: baseline data from the RECON trial. Neurology. 2012;78(4):250–5.

Chapter 15
Moyamoya Disease

Svetlana Kvint and Jan-Karl Burkhardt

Introduction

A rare and, to date, enigmatic disorder of the cerebral vasculature, moyamoya disease, is characterized by the progressive stenosis of the supraclinoid portion of the internal carotid artery (ICA), its proximal branches, and, in singular cases, the posterior circulation. Reactive neovascularization – a compensatory response to the cerebral ischemia that is consequent to the primary pathologic process – results in a collateral network supplied by small vessels arising at the carotid apex, cortical surface, leptomeninges, and external carotid artery branches. The characteristic angiographic appearance of this collateral circulation – likened to "something hazy just like a puff of smoke drifting in the air" – prompted the eponym *moyamoya* by Suzuki and Takaku in 1969 [1].

When concurrent with associated disorders, *moyamoya* angiography is a hallmark of moyamoya syndrome. In isolation, it is a key criterion for the diagnosis of moyamoya disease. Regardless of the context, clinical management is complicated by the dual demands of a progressive ischemic burden and the hemorrhagic potential of friable and anomaly prone collateral vessels. Through its review of pathogenesis, clinical presentation, diagnostic criteria, and therapeutic modalities, this chapter aims to highlight advances and key considerations necessary for the successful management of moyamoya disease.

S. Kvint · J.-K. Burkhardt (✉)
Department of Neurosurgery, Hospital of the University of Pennsylvania, Philadelphia, PA, USA
e-mail: Svetlana.Kvint@pennmedicine.upenn.edu; Jan.Burkhardt@pennmedicine.upenn.edu

J. R. Mascitelli, M. J. Binning (eds.), *Introduction to Vascular Neurosurgery*,
https://doi.org/10.1007/978-3-030-88196-2_15

Epidemiology

Originally reported in the East Asian population and demonstrating a unique bias to the region, moyamoya disease has since been observed – albeit less frequently – in a multitude of ethnic backgrounds, including American and European populations. While the specifics vary across regions, moyamoya disease has as well-established female predilection (ratio of 1:2.5) and a bimodal incidence – peaking among the young and middle-aged [2]. Serial epidemiological studies have demonstrated an increasing incidence and prevalence of moyamoya disease over time (Table 15.1). While a pathophysiologic cause cannot be excluded, it is likely that this trend reflects the following: (1) the increased accessibility of non-invasive diagnostic techniques; (2) increased disease awareness; and (3) recognition of the familial clustering of moyamoya disease. When compared to the general population, the risk of moyamoya disease is roughly 30–40 times higher among the family members of affected individuals [3, 4]. Screening of these high-risk individuals has expectedly augmented disease prevalence. In fact, in a contemporary Japanese survey, regional rates of asymptomatic registered moyamoya patients approached 17% [3]. Prevalence rates have been further supplemented by improved management techniques and an increasing number of survivors.

Pathogenesis

Pathology

Histopathologic examination of affected feeding arteries reveals vascular occlusion consequent to fibrocellular thickening of the intima, irregular undulation of the internal elastic lamina, and hyperplasia of smooth muscle cells. Requisite collateral flow is achieved through the following: (1) moyamoya vessels – fragile, microaneurysm prone vessels localized to the base of the brain and characterized by a thin media and fragmented elastic lamina; (2) cortical microvascularization – defined by increased vascular density and microvascular diameter; and (3) external carotid artery collateral networks – arising from the middle meningeal, ethmoidal, and occipital arteries. While it has long been postulated that these basal and cortical vessels represent a compensatory mechanism for central vascular occlusion, recent angiographic data revealed that neovascularization occurs prior to the onset of significant hemodynamic impairment [5]. This suggests that neovascularization is an active disease process rather than a passive compensation for decreased cerebral blood flow – a hypothesis that adds to the complexity inherent to the pathophysiology of moyamoya disease.

Table 15.1 Recent epidemiologic studies on moyamoya disease

Authors	Year of survey	Country	Number of patients	Sex ratio (F/M)	Age distribution	Prevalence per 100,000	Incidence per 100,000
Wakai et al. [3]	1995	Japan	1176	1.8	*Two peaks* First: 20–14 both sexes Second: 45–49 in men, 40–45 in women	3.16	0.35
Kuriyama et al. [62]	2004	Japan	1240	1.8	*Three peaks* First: 10–14 in men, 20–24 in women Second: 35–39 in men, 50–54 in women Third: 55–59 in men	6.03	0.54
Im et al. [63]	2004–2008	Korea	2987 (2005) 3329 (2006) 4051 (2007) 4517 (2008)	1.94	*Two peaks* First: 10–19 Second: 40–49	6.3 7.0 8.6 9.1	
Ahn et al. [2]	2007–2011	Korea	4047 (2007) 4975 (2008) 6038 (2009) 7031 (2010) 8154 (2011)	1.9	*Two peaks* First: 5–19 Second: 45–59	8.2 10.0 12.113.9 16.1	1.7 1.9 2.2 2.1 2.3
Chen et al. [64]	2000–2011	Taiwan	422	1.4	*Two peaks* First: 5–9 in men, 10–14 in women Second: 40–44 in both	1.61	
Uchino et al. [65]	1987–1998	United States	298	2.2	*Two peaks* First: 5–9 Second: 55–59		0.086 (overall) 0.28 (Asian Americans) 0.13 (African Americans) 0.06 (White) 0.03 (Hispanic)

Genetics

Although it is clear that genetic factors play a role in moyamoya disease, they have yet to be fully elucidated. Most familial cases of the disease appear to be polygenic or demonstrate autosomal dominant inheritance with incomplete penetrance. Loci at 3p24, 6q25, 8q23, 12p1, and 17q25 have been shown to have a role in disease development [6]. In fact, although its role in disease pathogenesis remains undefined, a single haplotype of the *RNF213* locus on chromosome 17q25 is the first identified susceptibility gene for moyamoya disease. Mutation analysis of *RNF213* identified a founder mutation present in 95% familial moyamoya disease patients, 73% of non-familial moyamoya disease patients, and only 1.4% of controls is a Japanese cohort [7]. Furthermore, the c.14576G > A variant of *RNF213* is associated with significantly earlier disease onset and a more severe form of moyamoya disease in Japanese and Korean patients [8]. Finally, it has been observed that the clinical presentation of patients may be related to their mutation at the *RNF213* locus: the R4810K mutation in ischemic, and A4399T mutation in hemorrhagic moyamoya disease [9].

Pathophysiology

Although the etiology of moyamoya disease has yet to be elucidated, increasing evidence suggests that it is a primarily proliferative disease – one in which endothelial and smooth muscle cell proliferation results in the development of vessel occlusion, as well as enhanced, but aberrant angiogenesis.

Endothelial Progenitor Cells

Endothelial progenitor cells have been shown to function in the maintenance of vasculature and blood flow in infarcted areas among acute myocardial infarction and ischemic stroke patients. Notably, moyamoya disease patients demonstrate both defective function and decreased circulating levels of these cells [6].

Endothelial Cells

Caveolin-1 is a cell surface plasma membrane protein that plays a major role in the regulation of endothelial signal transduction. Negatively regulating endothelial proliferation and positively regulating tube formation, it is a key regulator of

angiogenesis [10, 11]. Importantly, caveolin-1 serum levels are decreased in adult patients with moyamoya disease – markedly so among those with the RNF213 variant [6]. The resulting increased proliferation and decreased/impaired tube formation suggest that the nature of neovascularization in moyamoya disease is an aberrant rather than compensatory process.

Smooth Muscle Cells

Linkage analysis and association studies indicate that mutations in smooth muscle cells – ACTA2 mutation – may trigger an increased proliferation of smooth muscle cells contributing to the occlusive vasculopathy seen in moyamoya disease [12]. Furthermore, gene expression varies between smooth muscle progenitor cells isolated from moyamoya disease patients and healthy controls. These findings suggest that dysregulated proliferation and impaired maturation of smooth muscle cells both play a role in the pathogenesis of moyamoya disease [13].

Cytokines

Various categories of cytokines are associated with moyamoya disease. These include the following: (1) growth factors – vascular endothelial growth factor, fibroblast growth factor, platelet-derived growth factor, and hepatocyte growth factor; (2) cytokines related to vascular remodeling and angiogenesis – matrix metalloproteinases and their inhibitors, hypoxia-inducible factor-1α, and cellular retinoic binding protein-1 (CRABP-1); and (3) cytokines related to inflammation [6]. To date, studies investigating the pathogenic role of these factors have proven inconclusive.

Environmental Factors

The presence of the *RNF213* polymorphism in unaffected individuals underscores the fact that a genetic abnormality is not the singular determinant for disease development. Twin studies and experiments with genetically engineered mice suggest that environmental factors and/or secondary insults play an important role in genetically susceptible individuals. To date, autoimmunity, infection, chronic inflammatory conditions, and cranial irradiation have all been described in association with moyamoya disease. Still, as *RNF213* is predominantly expressed in leukocytes and the spleen, autoimmunity may be key among these.

Moyamoya Diagnosis

A diagnosis of moyamoya disease or moyamoya syndrome should be considered in all patients – particularly children and young adults – who present to care with acute neurological deficits or clinical history suggestive of cerebral ischemia. Although the differential diagnosis for these symptoms is broad, a diagnosis of moyamoya can be readily and reliably confirmed or excluded by standard radiographic techniques [14] (Table 15.2). Patient presentation determines the modality and order of diagnostic imaging.

Computed Tomography (CT)

CT is the modality of choice in the acute setting. Readily demonstrating intraventricular, intraparenchymal, and subarachnoid hemorrhage, it guides emergent intervention. Further, in the absence of acute findings, CT can demonstrate chronic ischemic changes – small areas of hypodensity in the cortical watershed zones, basal ganglia, deep white matter, or periventricular regions – suggestive of prior flow-related versus embolic ischemic insults. Normal CT findings should be interpreted with care as patients presenting solely with TIAs will not demonstrate imaging sequelae.

Computed Tomographic Angiography (CTA)

CTA is used to examine the steno-occlusion of the distal ICA, MCA, and ACA, as well as identify leptomeningeal collaterals in moyamoya patients. Furthermore, it can reveal the presence of aneurysms and pseudoaneurysms. Unfortunately, CTA imaging is limited in that the extent of moyamoya may be over- or underestimated based on the scan acquisition time relative to the mean transit time of contrast through the affected area. As such, CTA is often reserved for situations in which magnetic resonance imaging is contraindicated or not readily available.

Digital Subtraction Angiography (DSA)

DSA serves as the gold standard for the diagnosis of moyamoya disease. Allowing for the selective imaging of the internal carotid, vertebral and external carotid artery distributions, it defines the extent of carotid occlusion and characterizes the origins

Table 15.2 Diagnostic criteria for moyamoya disease

Diagnostic criteria for moyamoya disease
A. Cerebral angiography should show at least the following findings: 1. Stenosis or occlusion at the terminal portion of the ICA and/or at proximal portion of ACA and/or MCA. 2. Abnormal vascular networks in the vicinity of the occlusive or stenotic lesions in the arterial phase. 3. (1) and (2) observed bilaterally.
B. When MRI and MRA imaging demonstrate all of the findings listed below, conventional cerebral angiography is not mandatory: 1. Stenosis or occlusion at terminal portion of ICA and at the proximal portion of ACA and MCA on MRA. 2. An abnormal vascular network in the basal ganglia on MRA. An abnormal vascular network can be diagnosed when more than two apparent flow voids are observed in one side of the basal ganglia on MRI. 3. (1) and (2) observed bilaterally.
C. Cerebrovascular disease with the following basic diseases or conditions should be eliminated: 1. Arteriosclerosis 2. Autoimmune disease 3. Meningitis 4. Brain neoplasm 5. Down syndrome 6. Recklinghausen's disease 7. Head trauma 8. Irradiation to the head 9. Others (e.g., sickle cell disease and tuberous sclerosis)
D. Instructive pathological findings: 1. Intimal thickening and the resulting stenosis or occlusion of the lumen are observed in and around the terminal portion of the ICA usually on both sides. Lipid deposits are occasionally seen in the proliferating intima. 2. Arteries constituting the circle of Willis such as the ACAs, MCAs, and posterior communicating arteries often show stenosis of various degrees or occlusion associated with fibrocellular thickening of the intima, a waving of the internal elastic lamina and an attenuation of the media. 3. Numerous small vascular channels (perforators and anastomotic branches) are observed around the circle of Willis. 4. Reticular conglomerates of small vessels are often seen in the pia matter.
Diagnosis: In reference to A and D, the criteria are classified as follows: 1. Definite case: Fulfills criteria A or B and C. in children, a case that fulfills A-1 and A-2 (or B-1 and B-2) on one side and have remarkable stenosis at the terminal portion of the ICA on the opposite side is also included. 2. Probable case: One which fulfills A-1 and A-2 or B-1 and B-2 and C (unilateral involvement).

of collateral supply. Furthermore, it reliably facilitates the detection of concurrent aneurysms and arteriovenous malformations. Despite these advantages, as an invasive technique, DSA is associated with procedure-related complications. As such, some clinicians now reserve DSA for bypass surgery planning and rely on a combination of noninvasive tests for moyamoya diagnosis.

Magnetic Resonance Imaging (MRI)

MRI is the method of choice for detecting symptomatic or asymptomatic brain lesions in the acute condition. Diffusion weighted imaging allows for the detection of acute infarcts, while T1- and T2-weighted imaging facilitates the detection of chronic infarcts and microbleeds. These strengths account for its increasing use in the screening and primary imaging of patients with symptoms suggestive of moyamoya. Reduced flow voids in the internal, middle, and anterior cerebral arteries coupled with prominent flow voids through the basal ganglia and thalamus from collateral vessels are virtually diagnostic of moyamoya. The "ivy sign," a linear pattern of increased signal in the leptomeninges and perivascular spaces on fluid-attenuated inversion recovery sequences, is similarly characteristic [15].

Magnetic Resonance Angiography (MRA)

MRA imaging allows for the reliable, noninvasive detection of steno-occlusion of the distal ICA, MCA, and ACA. Unfortunately, the technique is limited in the diagnosis of moyamoya vessels: sensitivity and specificity of 73% and 100%, respectively [16]. Further, MRA imaging has limited value in the evaluation of the ECA system.

Moyamoya Syndrome

The classification of moyamoya vasculopathy requires careful consideration of angiographic anatomy and clinical history (Fig. 15.1). A diagnosis of moyamoya disease relies on the observation of an idiopathic, bilateral, steno-oclusive disease in the supraclinoid carotid. In contrast, moyamoya syndrome encompasses the following: (1) idiopathic, unilateral, carotid steno-oclusive disease; and (2) unilateral or bilateral moyamoya vasculopathy occurring in the context of associated underlying disease conditions (Table 15.3). While the relationship between these disease states and moyamoya vasculopathy remains unclear, it has been suggested that they serve as triggers in genetically susceptible individuals.

Clinical Presentation

The clinical manifestations of moyamoya disease include transient ischemic attacks (TIAs), ischemic strokes, hemorrhagic strokes, seizures, headache, cognitive impairment, and movement disorders. While ischemic stroke is the most common

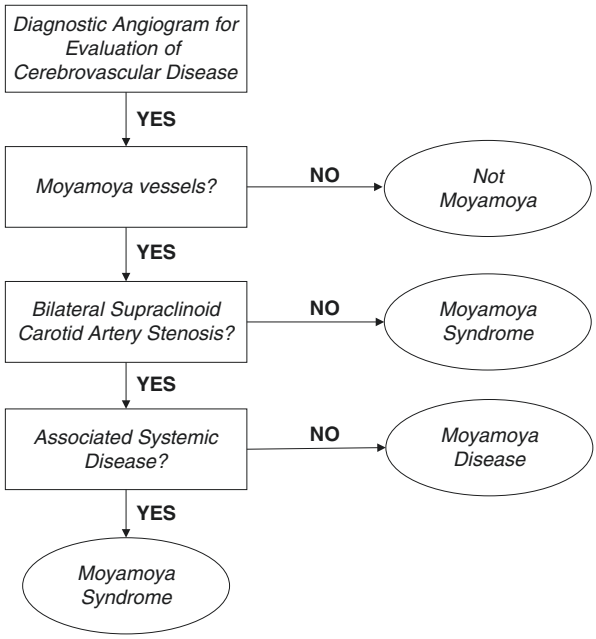

Fig 15.1 Algorithmic approach for the classification of moyamoya vasculopathy

clinical manifestation overall, presenting symptoms vary with age at diagnosis [17]. Ischemic symptoms predominate in the pediatric population: 90% of children present with stroke and 7.5% present with TIAs [18]. Intellectual decline, seizures, and involuntary movements are also commonly reported in this age group. In contrast, a hemorrhagic presentation is approximately seven times more common in adults than their pediatric counterparts (14.6% vs. 2.1%) [19].

Ischemic moyamoya disease patients most frequently present with symptoms of hemiparesis, speech disturbances, and hemisensory abnormalities – localizing pathology to the anterior circulation [20, 21]. In a review of 410 consecutive pediatric cases, Kim et al. attributed ischemic symptoms to the middle cerebral artery, anterior cerebral artery, and posterior cerebral artery territories in 92, 52, and 10 of the cases, respectively [21]. Although relatively uncommon – developing in the late stages of disease – posterior cerebral artery involvement is present in 29% of patients, with comparable incidence between children and adults [22, 23]. Importantly, as a consequence of long-standing major vessel occlusion, altered vascular territories develop; as such, infarct topography is non-classical in the majority of moyamoya patients [24]. Regardless of the vascular territory in question, TIAs may be precipitated by hyperventilation – presumably via a hypocarbia induced vasoconstriction – as well as stress, infection, and dehydration.

More than half of adult moyamoya disease patients are diagnosed with intracranial – intraventricular, intracerebral, or subarachnoid – hemorrhage. There are three main recognized causes of intracranial bleeding in moyamoya disease: (1) rupture of dilated, stressed, and microaneurysm prone moyamoya vessels; (2) fibrinoid

Table 15.3 Conditions associated with moyamoya syndrome

Conditions associated with moyamoya syndrome	
Vascular disorders	Atherosclerosis Traumatic dissection Craniocervical radiotherapy Hypertension Fibromuscular dysplasia Renal artery stenosis Giant cervicofacial hemangioma Coarctation of the aorta
Infectious disorders	Tuberculous meningitis Pneumococcal meningitis Leptospirosis HIV
Neoplastic	Tuberous sclerosis Parasellar tumor
Genetic/hereditary disorders	Neurofibromatosis Down syndrome Noonan syndrome Trisomy 12p syndrome Apert syndrome Marfan syndrome Turner syndrome Von Recklinghausen disease Hirschsprung disease Congenital cardiac anomaly
Hematological	Sickle cell disease Essential thrombocytopenia Hereditary spherocytosis Protein C deficiency Protein S deficiency Aplastic anemia Fanconi anemia Hyperhomocysteinemia
Connective tissue disorders	Systemic lupus erythematous Antiphospholipid antibody syndrome Livedo reticularis Sarcoidosis Behçet disease
Endocrine disorders	Hyperthyroidism Diabetes mellitus

necrosis in arterial perforators; and (3) rupture of saccular aneurysms – consequent to shifting circulatory patterns at the base of the brain and detected in up to 14% of moyamoya patients. Presenting symptoms reflect the site and size of hemorrhage and can include an alteration of level of consciousness, headache, meningismus, focal neurological deficits, and speech disturbance. Hemorrhagic localization in moyamoya disease is distinct from that of primary intracerebral hemorrhage. A case-control study by Nah et al. showed that the prevalence of isolated intraventricular hemorrhage was higher among moyamoya disease patients (37.6% versus

2.2%, $P < 0.001$). The prevalence of intraventricular extension from primary intraparenchymal foci was also higher in moyamoya disease patients (69.8% versus 1.9%, $P < 0.001$) [25]. Intracerebral hemorrhage occurs in up to 30% of moyamoya patients [20]. When present, the order of frequency is as follows: lobar (37.9%), putaminal (36.2%), thalamic (8.6%), callosal (6.9%), and caudate (3.4%) [25].

Seizures, cognitive impairment, headaches, and movement disorders are relatively infrequent but debilitating sequelae of moyamoya disease. Significant and prolonged brain hypoperfusion results in cortical atrophy, manifesting as progressive cognitive decline in both adult and pediatric patients [26, 27]. Headache is highly prevalent in moyamoya disease. Thought to be due to cortical spreading depression resulting from cerebral hypoperfusion or the triggering of nociceptors by dural collateral vessels, they are often migrainous in nature, and can serve as the first presenting symptom of disease [28]. As such, early neurovascular imaging should be considered in patients with new onset, refractory migraine-like headaches – especially in the setting of other neurological symptoms – to exclude underlying moyamoya disease. Seen in less than 5% of patients and presumed to be consequent to ischemic dysfunction of the basal ganglia and/or cortical-subcortical circuitry, seizures and movement disorders (chorea, dystonia, and dyskinesia) are infrequent presentations of moyamoya disease [29].

Natural History

The natural history of moyamoya disease is quite variable. Patient progression can follow an indolent, sporadic, or rapid course. Regardless of the rate of clinical progression, however, more than 50% of untreated moyamoya patients exhibit progressive neurological dysfunction and a poor clinical outcome [30].

Adult Disease

Data regarding the course of untreated moyamoya disease are limited. In 2015, Cho et al. studied the clinical outcomes of 241 adult moyamoya patients classified into three groups based on clinical presentation: hemorrhagic ($n = 62$); ischemic ($n = 144$); and asymptomatic ($n = 35$) [31]. The group reported an annual stroke risk of 4.5% as well as annual risk of rebleeding in the hemorrhagic group and recurrent ischemic events in the ischemic group of 4.3% and 3.0%, respectively. There was no significant difference in the cumulative stroke risk among the three groups, suggesting that asymptomatic patients warrant close clinical attention and consideration of therapeutic intervention. Patients with an initial hemorrhagic presentation tended to develop hemorrhagic strokes while an ischemic presentation was usually followed by recurrent ischemic strokes. In 2019, Kang et al. reported results of a survey of 128 patients with conservatively managed hemorrhagic moyamoya

disease. The cohort exhibited a rebleeding rate of 4.5% per year, with a cumulative risk of rebleeding of 7.8% at 5 years, 22.6% at 10 years, and 35.9% at 15 years. Familiarity with these rates is crucial in that rebleeding is the most important factor associated with poor prognosis in patients with hemorrhagic moyamoya disease: 11.04-fold risk of death in comparison with patients without rebleeding ($P = 0.02$) [32]. This phenomenon may, at least in part, be related to the increased rates of ischemic infarction seen in moyamoya patients following hemorrhagic events [25, 33].

Pediatric Disease

In a series of 27 pediatric moyamoya patients followed for a period of up to 15 years, outcomes were reported as follows: no sequelae in five (19%), occasional TIA or headache alone in nine (33%), mild intellectual and/or motor impairment in seven (26%), requirement for special school or care by parents or institutions after reaching the teen years in three (11%), continuous 24-hour care in two (7%), and death in one (3%) [34]. While further observational data are limited, it is generally accepted that poorer prognosis is associated with earlier age at onset. The majority of children develop more severe angiographic grades of disease within 5–10 years of diagnosis. In some, this worsening progresses after adolescence [35].

Unilateral Disease

At times, moyamoya phenomena may manifest as unilateral disease. While it remains unclear whether this represents a unique disease entity or an earlier stage of diagnosis, Kelly et al. reported a 38.9% progression rate to bilateral disease [36]. Young age at onset of disease and the presence of minor changes in the contralateral ACA, intracranial ICA, and MCA were important predictors of increased risk of progression. As such, patients with these characteristics should be followed for both contralateral and overall disease progression.

Staging

In 1969, Suzuki et al. described six progressive stages of the angiographic evolution of moyamoya disease [1] (Table 15.4) (Fig. 15.2). While accurately depicting the degree of vascular stenosis and collateral vessel development, this staging system provides no information on the degree of cerebral infarction of vascular reserve. As such, the Suzuki staging system neither correlates with disease

Table 15.4 Suzuki staging of moyamoya

Suzuki staging of moyamoya	
Suzuki stage	Angiographic description
I	Isolated narrowing of supraclinoid carotid (C1-C2 segment)
II	Progressive narrowing of carotid. Dilation of native cerebral arteries. Early formation of moyamoya vessels in basal carotid circulation.
III	Severe carotid stenosis with decreased flow in middle and anterior cerebral arteries. Intensification of moyamoya vasculature in basal regions. Exuberant moyamoya vessel formation.
IV	Severe carotid stenosis with impaired filling of middle, anterior, and posterior cerebral arteries. Minimization of moyamoya vessels.
V	Complete cessation of flow in ipsilateral middle, anterior, and posterior cerebral arteries. Further minimization of moyamoya vessels.
VI	Disappearance of moyamoya vessels. Filling of cerebral vasculature by external carotid supply via leptomeningeal anastomoses.

severity nor risk of clinical symptoms [37]. Specifically, a history of prior infarct and/or impaired hemodynamics are predictive of stroke risk in both symptomatic and asymptomatic moyamoya patients [31, 32, 37]. In a historical prospective cohort study of 40 asymptomatic moyamoya patients, Kuroda et al. detected silent infarction and impaired vascular hemodynamics in 20% and 40% of patients, respectively. During a mean follow-up of 43.7 months, 20.6% of patients suffered a TIA, stroke, or intracranial hemorrhage. The authors quoted a 3.2% annual risk for any stroke. As such, asymptomatic moyamoya is not a silent disorder and requires consideration and incorporation into disease staging systems [38].

Currently available functional vascular imaging modalities service this need by generating direct and indirect measures of cerebral blood flow (CBF), cerebral metabolic function, and cerebrovascular reactivity. Cerebral blood flow is typically measured via the introduction of a tracer that can be tracked through the cerebral circulation serially over time. The mean transit time (MTT) and an estimation of cerebral blood volume (CBV) can be derived from tracer concentration levels in a region of interest over time. CBF, in turn, is derived from these values: CVB/MTT. Diminished CBF is thought to correlate with vessel stenosis and may be apparent in ischemic regions [39]. Cerebral metabolic function is inferred from the oxygen extraction fraction. Specifically, in ischemic tissue, the oxygen extraction fraction increases as a greater percentage of oxygen is extracted from red blood cells to meet equivalent metabolic demands in the setting of decreased CBF. The assessment of cerebrovascular reactivity relies on the measurement of CBF before and after a hypercapnic challenge. While CBF increases in response to a hypercarbic challenge in controls, the response is stalled in moyamoya patients as a consequence of the persistent maximal dilation of moyamoya vessels. Patients exhibiting this so-called exhaustion of cerebrovascular reserve are at higher risk for ischemic symptoms and stroke [40].

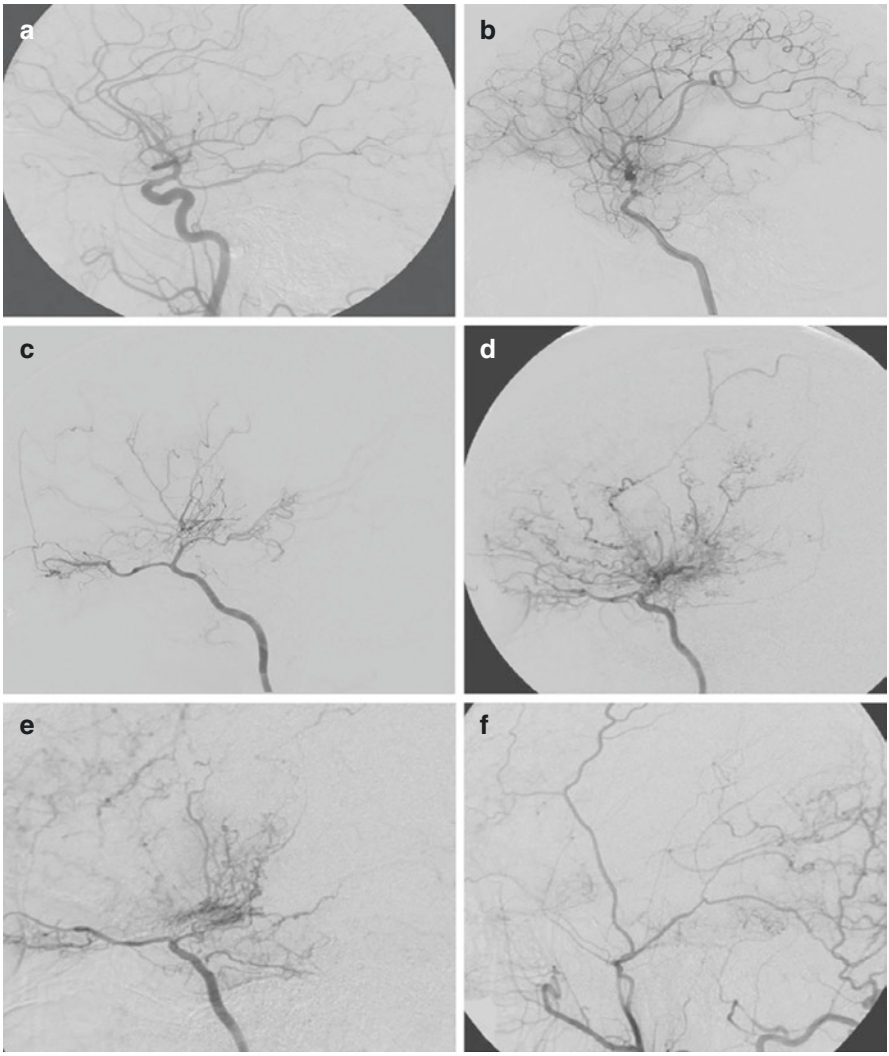

Fig. 15.2 Representative internal carotid (**a**-**e**) and external carotid (**f**) artery angiograms demonstrating the Suzuki staging of moyamoya. (**a**). *Stage I* disease with narrowing of supraclinoid ICA. (**b**) *Stage II* disease with dilatation of MCA and early formation of basal moyamoya vessels. (**c**) *Stage III* disease with occlusion of the MCA and ACA but patent posterior communicating artery and further formation of moyamoya vessels. (**d**) *Stage IV* disease with intensification of moyamoya vessels and loss of posterior communicating artery. (**e**) *Stage V* disease with diminishing moyamoya vessels as prominence of external collateral increases. (**f**) *Stage VI* disease with loss of moyamoya vessels and collateral supply via the external carotid artery. (Source: Wanebo et al. [66])

Computed Tomography Perfusion and Magnetic Resonance Imaging Perfusion

CT perfusion utilizes an iodinated contrast agent to track the transit of blood through the cerebral vasculature. MR perfusion achieves the same with the use of gadolinium contrast or endogenous contrast generated by arterial spin labeling. These methods are limited by variability related to changes in blood pressure, hematocrit, as well as motion and susceptibility artifacts. An acetazolamide challenge is used as an adjunct to estimate cerebrovascular reactivity and to detect steal phenomenon. As a carbonic anhydrase inhibitor, acetazolamide induces carbonic acidosis, triggering a considerable increase in CBF in regions with preserved cerebrovascular reactivity.

Xenon Computed Tomography

Xenon CT relies on xenon – a radiopaque, diffusible gas – accumulation in brain tissue following delivery via inhalation of a gas mixture with oxygen. Xenon accumulation correlates with blood flow and is used to derive estimates of CBF. Cerebrovascular reactivity is calculated via the addition of a hypercarbic challenge to the study protocol.

Positron Emission Tomography

PET scanning uses $^{15}O_2$ to measure the oxygen extraction fraction. PET imaging is limited by its availability and by the short half-life of ^{15}O. In fact, a cyclotron or high-energy linear accelerator is needed on site to generate the necessary radiopharmaceuticals.

Single-Photon Emission Computed Tomography

A radioactive tracer – either [123I] *N*-isopropyl-*p*-iodoamphetamine autoradiography (^{123}I-IMP-ARG) or technetium hexamethylpropylene amine oxide (^{99m}Tc-HMPAO) – is injected intravenously. The tracer crosses the blood–brain barrier and is temporarily accumulates in brain tissue. As above, the amount of accumulated tracer correlates with blood flow. A hypercarbic challenge allows for the measurement of cerebrovascular reactivity, provided there is an appropriate washout period.

Blood Oxygen Level–Dependent (BOLD) Magnetic Resonance Imaging

BOLD MRI is a functional technique based on detecting the difference between the field inhomogeneity created by deoxyhemoglobin (dHb) contained within red blood cells in the microvasculature and the relatively homogenous field of adjacent parenchyma [41]. As the BOLD sequence detects susceptibility caused by dHb, signal intensity decreases when dHb concentrations increase. The BOLD technique has been adapted for evaluation of cerebrovascular reactivity. Following a hypercapnic challenge, regions with normal cerebrovascular reactivity demonstrate an increase in regional blood flow and consequent increase in BOLD signal. Those with exhausted cerebrovascular reserve demonstrate a relative increase in dHb and consequent decrease in BOLD signal.

Incorporating the gains of functional vascular imaging, Czababka et al. have proposed a novel grading system – the Berlin moyamoya grading system – to estimate the likelihood of clinical symptoms in moyamoya patients (Table 15.5). The grading system utilizes DSA characteristics, MRI features, and cerebrovascular reserve capacity to stratify patients into three grades: mild, moderate, and severe [42].

Medical Treatment

In the acute stage, management of moyamoya patients is largely supportive and borrows heavily from ischemic and hemorrhagic stroke treatment guidelines. Focus is placed on the management of elevated intracranial pressure, hematoma evacuation, drainage of intraventricular hemorrhage via an external ventricular drain, and seizure control. Critical care physicians target normothermia and normoglycemia

Table 15.5 Berlin moyamoya grading protocol

Berlin moyamoya grading protocol		
Variable	Characteristics	Points
Digital subtraction angiography	Steno-occlusive lesion + moyamoya vessels	1
	Steno-occlusive lesion + moyamoya vessels + intracranial compensation routes	2
	Steno-occlusive lesion + extracranial compensation routes	3
MRI	No signs of ischemia, hemorrhage, or atrophy	0
	Signs of ischemia, hemorrhage, or atrophy	1
Cerebrovascular reserve capacity	No steal phenomenon (≥5%)	0
	Steal phenomenon (<5%)	2

Score:
Grade I – mild – (1–2 points)
Grade II – moderate – (3–4 points)
Grade III – severe – (5–6 points)

while working to minimize periods of hypotension, hypovolemia, hypoxia, and hypocarbia.

No currently available medical therapy can halt or reverse the arteriopathic process in moyamoya disease. As such, medical management in moyamoya disease is primarily focused on secondary stroke prevention. While the role of hemodynamic compromise as the primary cause of ischemic symptoms has been long established, recent evidence has highlighted the role of emboli in ischemic episodes. High-intensity transient signals (HITS) – transcranial Doppler recordings believed to reflect microemboli – are detected in about 12–20% of moyamoya disease patients [43, 44]. Their presence was predicted by recent clinical ischemic events and carried a corrected odds ratio of 10.6 for stroke in the next year [44]. While there are no randomized, controlled trials that examine the efficacy of antiplatelets in the prevention of stroke in moyamoya patients, many clinicians prescribe daily antiplatelet therapy, referencing its utility in non-moyamoya stroke patients. Utilization is not ubiquitous and reflects hemorrhagic presentation rates across regions and ethnicities [45].

While the treatment of moyamoya syndrome is largely analogous to that of moyamoya disease, it is important to recognize that the nature of the underlying condition influences patients' clinical course and effects prognosis. Specifically, for moyamoya syndrome associated with hormonal abnormalities, such as hyperthyroidism, correction of the hormonal abnormality has been reported to be effective [46]. A similar effect has been described following immunosuppressive therapy in moyamoya syndrome associated with autoimmune disease [47].

Surgical Treatment

Although antiplatelet agents are commonly used in moyamoya patients, there are little data to support their beneficial effect on the natural history of the disease. Hallemeier et al. reported 5-year stroke-free survival rates of only 35% and 18% for patients receiving medical management for unilateral and bilateral moyamoya disease, respectively [48]. Relatedly, Kraemer et al. found that, in medically treated patients, the Kaplan–Meier risk for recurrent stroke after the first ischemic event was approximately 80% in the first year [49]. These data underscore the fact that medical therapy alone is insufficient. Surgical revascularization therapy attempts to address this void by improving cerebral blood flow and stabilizing the cerebrovascular dynamics of moyamoya patients. As the arteriopathy of moyamoya disease affects the ICA while sparing the ECA, surgical revascularization techniques utilize the ECA as source of augmented blood flow to the ischemic hemisphere. Revascularization surgery is the most effective treatment for hemorrhagic and ischemic moyamoya disease. Generally accepted indications for revascularization include recurrent clinical symptoms due to (1) cerebral ischemia or (2) decreased regional cerebral blood flow, vascular response, and reserve in perfusion studies

[14]. Current revascularization strategies are classified into two categories: direct and indirect bypass surgery.

Direct Revascularization

Direct surgical intervention for moyamoya disease is typically performed in adults and using a superficial temporal artery (STA)-to-MCA end-to-side anastomosis (Fig. 15.3); however, use of STA-to-ACA, STA-to-PCA, and occipital artery-to-MCA (Fig. 15.4) or PCA anastomoses and interposition vein grafts has also been reported. If not already initiated, daily antiplatelet therapy should be started prior to surgical intervention.

STA-to-MCA Anastomosis Technique

The patient is positioned supine on the operating table and the head is secured in place using a Mayfield clamp. The course of the STA and its frontal and parietal branches are marked on the patient's scalp from the root of the zygoma as far distally as possible above the superficial temporal line (usually 9–10 cm) with the help of a handheld Doppler probe. A skin incision is made over the STA along its course with the aid of the operating microscope. Microdissection of the STA should continue until a length of approximately 7 cm of STA is mobilized. The STA is then kept moist, in a papaverine-soaked sponge, and under minimal tension until the time of anastomosis. Next, the temporalis muscle is sharply divided and mobilized via subperiosteal dissection. A craniotomy centered over the Sylvian fissure is then turned to expose the underlying frontal and temporal lobes. The dura is subsequently opened in a cruciate fashion – with care to avoid interruption of large middle meningeal dural arteries – under microscopic guidance to expose the underlying brain. Next, a suitable recipient artery – typically a frontal M4 MCA branch that approximates the caliber of the donor STA branch and follows a straight course – is identified. The arachnoid overlying this cortical branch is dissected to allow for the mobilization of approximately 10 mm of MCA. In anticipation of the anastomosis, 10 mm of adventitia is removed from the STA while it is still intact. The vessel is then temporarily occluded proximally and sectioned distally. Temporary aneurysm clips are subsequently applied to occlude the M4 branch prior to arteriotomy. An anastomosis between distal end of the STA and side of the MCA segment is then completed in a running or interrupted fashion using 10–0 sutures. Once the anastomosis is completed, the distal MCA clip is removed and the degree and location of any bleeding from the anastomosis are assessed and reinforced. Subsequent clip removal follows a characteristic sequence to minimize embolic sequelae. Once the proximal STA clip is removed, flow through the anastomosis is assessed with an

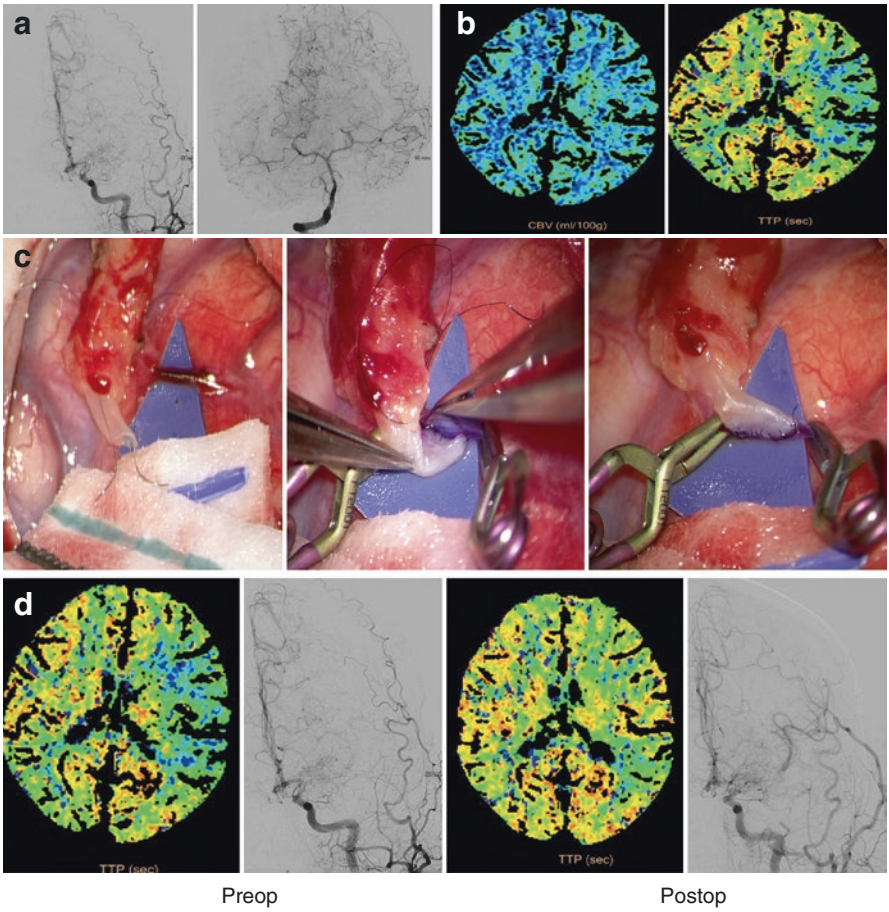

Fig. 15.3 A 28-year-old female presenting with progressing TIAs manifesting with aphasia and right-sided weakness. (**a**). Anteroposterior left common carotid and vertebral angiograms demonstrating carotid occlusion with collateralization reconstituting suboptimal blood flow in the middle cerebral artery territory. (**b**) Baseline computed tomography perfusion images demonstrating decreased perfusion in the left MCA territory with increased time to peak (TTP) and normal cerebral blood volume (CBV) (**c**) Intraoperative view demonstrating stages of the direct STA-to-MCA end-to-side anastomosis to a frontal M4 artery. (**d**) Juxtaposition of pre- and post-op operative perfusion and angiogram imaging demonstrating a patent anastomosis and improved perfusion with decrease in TTP

indocyanine green angiogram and/or Doppler ultrasonogram and/or intraoperative catheter angiogram. Assuming patent flow and adequate hemostasis, the bone flap is replaced and the temporalis muscle loosely reapproximated to prevent constriction of the bypass. Incisional closure is completed with standard techniques. Importantly, patients are maintained on antiplatelet agents indefinitely to prevent thrombosis of the bypass.

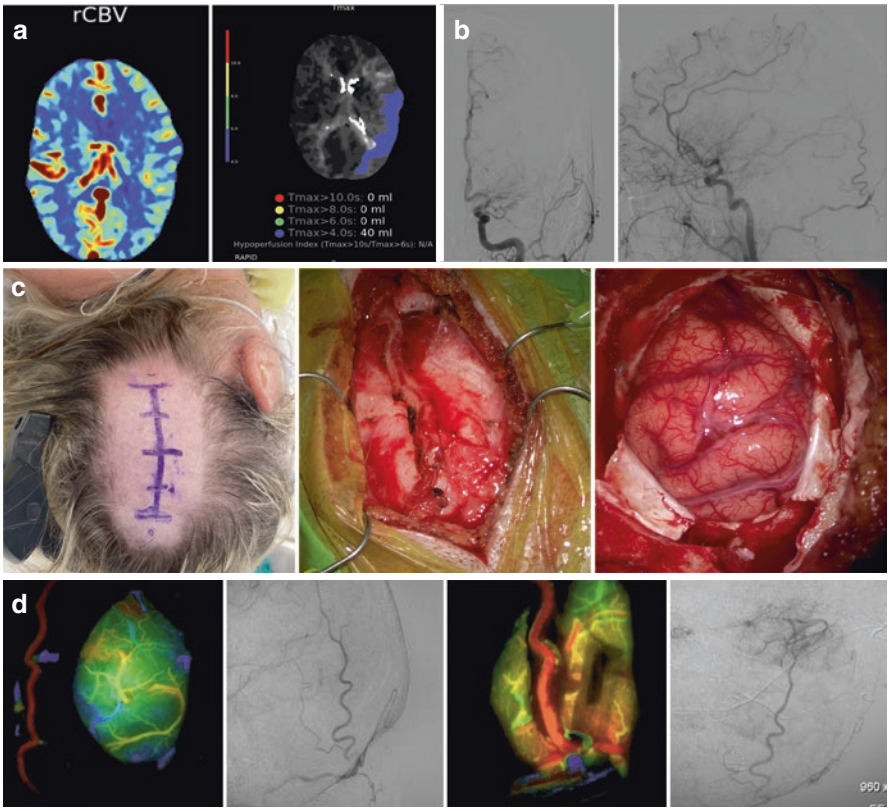

Fig. 15.4 A 60-year-old female with history of two failed STA-MCA bypasses in an outside hospital, presenting to care with progressive aphasia and intermittent right-sided weakness. (**a**). CT perfusion imaging demonstrating significant hypoperfusion involving the posterior aspect of the left hemisphere. (**b**). Anteroposterior and lateral angiograms demonstrating classic moyamoya appearance in the supraclinoid internal carotid artery with occlusion of the middle cerebral artery (M1 segment). There is delayed filling of posterior aspect of the frontal, parietal, and temporal lobes. One branch of the previous STA-MCA anastomosis is occluded the other one fills just a small anterior frontal area. (**c**) Intraoperative sequential stages of a left OA-MCA bypass: positioning, occipital artery harvest, and craniotomy with dura opening to expose the angular artery (recipient artery). (**d**) Juxtaposition of pre- and post-anastomosis indocyanine green video and catheter angiograms with patent flow

Indirect Revascularization

In adults, indirect revascularization is mainly used in addition to direct revascularization techniques; in contrast, it is the principal approach in pediatric patients. The selection of a bypass technique is determined by patients' individual anatomy. The small diameter of potential donor and cortical recipient vessels often precludes direct bypass in pediatric patients. Similarly, advanced stages of moyamoya disease

often prove to be a technical challenge. In the early stages of the disease, the caliber of affected vessels is relatively normal – ideal for direct anastomosis – and cortical collateralization is not yet extensive. Chronic disease, in turn, is characterized by the following: (1) distal small cortical vessels with significant dilatation; (2) larger vessels with reduced vessel diameter; and (3) extensive collateralization. These qualities are associated with increased perioperative risk for infarction or hyperperfusion syndrome; as such, they are considered to be less attractive for direct revascularization. In such cases, an indirect bypass using vascularized donor tissue – STA, galea, dura, muscle, and omentum – can be used to promote leptomeningeal collateral formation. Indirect bypass procedures recommend themselves in that they avoid: (1) ischemia from temporary arterial occlusion; (2) extended anesthesia time; and (3) the hyperperfusion syndrome associated with the sudden increase in blood flow provided by a direct anastomosis. Unfortunately, the latter strength is the technique's greatest limitation: indirect anastomosis patients are dependent on the uncertain and gradual ingrowth of vessels to achieved augmented cerebral blood flow.

Encephaloduroarteriosynangiosis (EDAS)

As described above, the STA is carefully dissected through a skin incision approximating the course of the most robust STA branch. Once the branch is dissected free of the surrounding temporalis fascia, adherent adventitia is removed around the entire length of the arterial branch so as to not impede angiogenesis. A craniotomy is turned over the Sylvian fissure and the dura opened in a cruciate fashion. The arachnoid overlying the cortex is opened to allow direct contact between the STA donor branch and the cortical arteries. The STA branch is then placed in direct opposition to the underlying cortex and pial synangiosis is achieved as the STA branch is sutured to the dissected arachnoid using several interrupted. The dural leaflets are then inverted and folded underneath the skull, allowing for an additional source of blood flow for cortical neovascularization. After meticulous hemostasis, the craniotomy flap is carefully beveled and secured in place. The scalp is then closed in the usual fashion taking care not to harm the intact STA.

Encephalomyosynangiosis (EMS)

A linear or curvilinear incision allows access to the temporalis muscle and facilitates subperiosteal dissection of the muscle from the underlying cranium, taking care to preserve its blood supply. Following a large craniotomy, the dura is opened widely and inverted. The muscle is then placed directly on top of the underlying brain and secured in place via sutures to the dural edges. The bone flap – shaved on

the inferior aspect to avoid compression of the temporalis muscle – is then replaced and secured. Use of a split-thickness temporalis muscle graft has been proposed in an effort to reduce the poor cosmetic effect and bulk of muscle mass in the epidural space associated with traditional EMS technique [50].

Encephaloduroarteriomyosynangiosis (EDAMS)

EDAMS incorporates aspects of all the major indirect revascularization techniques. The dural leaflets are opened in a cruciate fashion and inverted onto the underlying cortex as previously described. Pial synangiosis is then performed and the temporalis muscle is placed over the remaining exposed cortex. Bone flap placement and closure are performed using the techniques described above.

Omental Transplantation

Advocates of omental transplantation reference the relative plasticity of the graft material and its ability to cover a large surface area of ischemic cortex. The greater omentum is harvested via a midline abdominal incision, with care taken to preserve the gastroepiploic vessels. A large craniotomy is fashioned following the identification and dissection of the STA and the superficial temporal vein. Direct end-to-end or end-to-side anastomoses is then performed – first between the STA and gastroepiploic artery and then between the superficial temporal vein and gastroepiploic vein. This sequence allows for a confirmation of adequate flow through the graft on the venous end. Following a wide dural opening, the vascularized graft is placed directly in contact with the cerebral cortex.

Multiple Burr Holes

Either a bicoronal or midline sagittal incision is made with care taken to avoid the interruption of major scalp arteries supplied by the external carotid and/or occipital arteries. The distribution of burr holes should be tailored to the cortical territories at risk for infarction. The pericranium can be dissected in a triangular shape over projected sites prior to bur hole creation. Following a cruciate dural opening, the underlying arachnoid is incised sharply and the dural leaflets inverted underneath the native skull. The preserved pericranium can then be inserted onto the cortex to further augment blood flow.

Outcomes Following Revascularization

The superiority of surgical revascularization over conservative medical management in ischemic moyamoya patients has been demonstrated in multiple surgical series. Most recently, Kim et al. reported the results of a retrospective, case-control study involving 441 ischemic moyamoya patients – of which 301 underwent revascularization surgery and 140 were treated conservatively [51]. They found that the actuarial 10-year cumulative incidence rate for any kind of stroke was significantly lower in the revascularization group than in the control group (9.4% vs. 19.6%, $p = 0.04$). The relative risk reduction was also superior (52.0%) in the revascularization group, with a number needed to treat of 10. Specific consideration of ischemic stroke yielded a 10-year rate of 13.3% and 3.9% in the control and revascularization groups, respectively ($p = 0.019$). The relative risk reduction for ischemic stroke in the revascularization group was 70.7%, and the number needed to treat was 11.

In 2009, Guzman et al. reported the Stanford experience with 264 patients undergoing 450 revascularization procedures [19]. Direct revascularization was the selected approach in the majority of cases (95% of adults and 76% of children). The group reported a significant reduction in TIAs after treatment. Specifically, of the 171 patients presenting with TIAs, 82.5% were TIA free at 1 month and 91.8% at 1 year or later. A similar effect was observed in patients presenting with headaches. Of the 48% of patients presenting with headaches, greater than 80% were headache free at the last follow-up. Overall, patients experienced a significant clinical improvement: mean preoperative mRS score of 1.62 and a mean mRS score of 0.83 at a mean follow-up of 4.9 years ($p < 0.0001$). Frequency analysis releveled that quality of life improved, remained unchanged, or worsened in 71.2%, 23.6%, and 5.2% of patients, respectively. Importantly, in the multivariate analysis, the strongest predictor of a good outcome after surgery was an mRS score ≤ 2 prior to surgery (OR 26.2, $p < 0.0001$). These benefits were achieved in the setting of a low risk profile. The overall incidence of stroke in the postoperative period and up to the last follow-up was as follows: 3.8% and 3.4% for ischemic and hemorrhagic events, respectively. The overall mortality rate after surgical revascularization was 2.3% during a mean follow-up period of 4.9 years. The cumulative 5-year Kaplan–Meier risk of perioperative or subsequent stroke or death was 5.5%.

While the efficacy of revascularization for ischemic moyamoya disease has been generally accepted, evidence in support revascularization in patients with a hemorrhagic presentation is less robust. Fujii et al. retrospectively reviewed clinical outcomes in 290 hemorrhagic moyamoya patients treated with revascularization versus conservative management [52]. While the group reported a trend toward reduced rates of recurrent hemorrhage in the surgical group (19.1% vs. 28.3%), it failed to reach statistical significance. In a retrospective review of 22 hemorrhagic moyamoya patients treated with direct bypass, EDAS or conservative management, Kawaguchi et al. found that the incidence of future stroke events in patients who had undergone a direct bypass was significantly lower than that in patients who had been treated conservatively or with EDAS ($p < 0.05$) [53].

To date, studies comparing the clinical outcomes achieved by indirect and direct revascularization techniques have favored the superiority of the latter. In a review of 124 adult moyamoya disease patients treated via direct, indirect, or combined bypass, Lee et al. found that direct and combined bypasses were more effective in preventing recurrent ischemic stroke than indirect bypass surgery ($P < 0.05$). Similarly, the extent of revascularization and reduction of moyamoya vessels were greater in the direct or combined bypass cohort ($P < 0.05$) [54]. Further, a meta-analysis of 16 studies by Qian et al. indicated that compared to direct bypass surgery, indirect bypass surgery had a lower efficacy with regard to secondary stroke risk reduction (OR of 1.79, 95% CI, 1.14–2.82, $P = 0.01$), while no significant difference was detected in perioperative complication rates [55].

Perioperative Care

Patients with moyamoya vasculature present unique challenges for perioperative management. Appropriate preoperative optimization, anesthetic management, and intraoperative monitoring are crucial for successful patient outcomes. Although there are no randomized clinical trials to support a specific anesthetic or monitoring regimen, a consideration of disease specific pathology allows for the informed application of fundamental principles. As previously stated, moyamoya patients are characterized by impaired regional cerebral blood flow and functionally abnormal vasculature. Cerebrovascular autoregulation is severely attenuated and cerebral blood flow in affected regions is wholly pressure dependent. Further, while moyamoya vessels appear to be incapable of dilation in response to hypercapnia, they are exceptionally sensitive to and constrict in the setting of hypocapnia.

With these caveats in mind, interventions are selected in accordance with three cornerstones of perioperative moyamoya patient management: (1) maintain a favorable supply (cerebral blood flow) to demand (cerebral metabolic rate) ration through the perioperative period; (2) reduce ischemic potential during vessel cross-clamping; and (3) facilitate early detection and prompt correction of a suboptimal supply-to-demand ratio. As such, we recommend the following:

1. Surgery should be scheduled during periods of relative clinical stability – intervals between ischemic or hemorrhagic symptoms.
2. Ensure sufficient hydration and an accurate assessment of patients' fluid status. The goal of fluid management is to maintain normovolemia and a hematocrit between 30% and 36%.
3. Maintain normocapnia at all times.
4. Ensure preoperative placement of an arterial catheter for continuous pressure monitoring during induction, surgery, and postoperative recovery.
5. Target a core temperature of 33 °C using either surface cooling or invasive techniques.
6. Maintain patients' mean arterial blood pressure at preinduction levels throughout induction, surgery, and postoperative recovery using titrated doses of both

ephedrine and phenylephrine. As moyamoya vessels do not constrict in response to phenylephrine or ephedrine, these agents can be used to maintain an appropriate perfusion pressure.
7. Ensure continuous monitoring of cortical function by means of electroencephalography, somatosensory evoked potentials, and motor evoked potentials.
8. Ensure burst-suppression and MAP at 10% higher than the preoperative level, prior to arterial cross-clamping.

Endovascular Therapy

There is limited experience with angioplasty and/or stenting in the moyamoya population. In 2014, a review of 28 endovascular (11 stent and 17 angioplasty) procedures reported a therapeutic success – defined as a lack of both angiographic and clinical recurrence at follow-up – rate of 25% [56]. The cumulative monthly angiographic and clinical recurrence rates were 9.3% and 8.0%, respectively. Two procedures (7%) were complicated by devastating intracerebral hemorrhage. Ineffective vessel dilation was observed in another three (11%). At this time, there is no evidence that angioplasty or stenting improves the natural history of moyamoya. When considered in the context of the procedural risk profile, currently available data argue against the routine endovascular treatment of ischemic moyamoya patients. Interestingly, the successful use of angioplasty as a bridge to surgical revascularization has been reported [57]. Additionally, endovascular rescue therapy has been described in the setting of donor vessel injury and as a means to boost flow in donor vessels before or after revascularization surgery [58–60].

The endovascular embolization of pseudoaneurysm like-lesions using N-butyl-cyanoacrylate glue has been reported in the literature [61]. Although this procedure may be theoretically effective in preventing rebleeding among hemorrhagic moyamoya patients, the technique is very demanding due to the deep location of the vascular lesions and nature of the conduit vessels.

Conclusion

Moyamoya is an increasingly recognized cause of stroke among both children and adults. A high index of suspicion is crucial for optimizing outcomes as it facilitates prompt diagnosis and initiation of therapy in the early stages of the disease. Surgical revascularization is the only effective treatment for reducing the risk of stroke in moyamoya disease patients. When technically feasible, a direct STA-MCA bypass is the procedure of choice. Indirect bypass is an effective option in patients in whom direct bypass cannot be performed. Regardless of the surgical approach, strict attention to and optimization of perioperative management techniques are essential to minimize the risk of adverse events.

References

1. Suzuki J, Takaku A. Cerebrovascular "moyamoya" disease. Disease showing abnormal net-like vessels in base of brain. Arch Neurol. 1969;20(3):288–99.
2. Ahn IM, et al. Incidence, prevalence, and survival of moyamoya disease in Korea: a nationwide, population-based study. Stroke. 2014;45(4):1090–5.
3. Wakai K, et al. Epidemiological features of moyamoya disease in Japan: findings from a nationwide survey. Clin Neurol Neurosurg. 1997;99(Suppl 2):S1–5.
4. Baba T, Houkin K, Kuroda S. Novel epidemiological features of moyamoya disease. J Neurol Neurosurg Psychiatry. 2008;79(8):900–4.
5. Kim SJ, et al. Neovascularization precedes occlusion in moyamoya disease: angiographic findings in 172 pediatric patients. Eur Neurol. 2014;72(5–6):299–305.
6. Bang OY, Fujimura M, Kim SK. The pathophysiology of Moyamoya disease: an update. J Stroke. 2016;18(1):12–20.
7. Kamada F, et al. A genome-wide association study identifies RNF213 as the first Moyamoya disease gene. J Hum Genet. 2011;56(1):34–40.
8. Miyatake S, et al. Homozygous c.14576G>A variant of RNF213 predicts early-onset and severe form of moyamoya disease. Neurology. 2012;78(11):803–10.
9. Wu Z, et al. Molecular analysis of RNF213 gene for moyamoya disease in the Chinese Han population. PLoS One. 2012;7(10):e48179.
10. Liu J, et al. Caveolin-1 expression enhances endothelial capillary tubule formation. J Biol Chem. 2002;277(12):10661–8.
11. Chang SH, et al. Vascular permeability and pathological angiogenesis in caveolin-1-null mice. Am J Pathol. 2009;175(4):1768–76.
12. Guo DC, et al. Mutations in smooth muscle alpha-actin (ACTA2) cause coronary artery disease, stroke, and Moyamoya disease, along with thoracic aortic disease. Am J Hum Genet. 2009;84(5):617–27.
13. Kang HS, et al. Smooth-muscle progenitor cells isolated from patients with moyamoya disease: novel experimental cell model. J Neurosurg. 2014;120(2):415–25.
14. Fukui M. Guidelines for the diagnosis and treatment of spontaneous occlusion of the circle of Willis ('moyamoya' disease). Research Committee on Spontaneous Occlusion of the Circle of Willis (Moyamoya Disease) of the Ministry of Health and Welfare, Japan. Clin Neurol Neurosurg. 1997;99(Suppl 2):S238–40.
15. Maeda M, Tsuchida C. "Ivy sign" on fluid-attenuated inversion-recovery images in childhood moyamoya disease. AJNR Am J Neuroradiol. 1999;20(10):1836–8.
16. Yamada I, Suzuki S, Matsushima Y. Moyamoya disease: comparison of assessment with MR angiography and MR imaging versus conventional angiography. Radiology. 1995;196(1):211–8.
17. Kim JS. Moyamoya disease: epidemiology, clinical features, and diagnosis. J Stroke. 2016;18(1):2–11.
18. Lee S, et al. Moyamoya disease in children: results from the international pediatric stroke study. J Child Neurol. 2017;32(11):924–9.
19. Guzman R, et al. Clinical outcome after 450 revascularization procedures for moyamoya disease. Clinical article. J Neurosurg. 2009;111(5):927–35.
20. Suzuki J, Kodama N. Moyamoya disease--a review. Stroke. 1983;14(1):104–9.
21. Kim SK, et al. Pediatric moyamoya disease: an analysis of 410 consecutive cases. Ann Neurol. 2010;68(1):92–101.
22. Kim JM, Lee SH, Roh JK. Changing ischaemic lesion patterns in adult moyamoya disease. J Neurol Neurosurg Psychiatry. 2009;80(1):36–40.
23. Hishikawa T, et al. Assessment of the difference in posterior circulation involvement between pediatric and adult patients with moyamoya disease. J Neurosurg. 2013;119(4):961–5.
24. Cho HJ, et al. The different infarct patterns between adulthood-onset and childhood-onset moyamoya disease. J Neurol Neurosurg Psychiatry. 2011;82(1):38–40.

25. Nah HW, et al. Moyamoya disease-related versus primary intracerebral hemorrhage: [corrected] location and outcomes are different. Stroke. 2012;43(7):1947–50.
26. Hogan AM, et al. Intellectual decline in children with moyamoya and sickle cell anaemia. Dev Med Child Neurol. 2005;47(12):824–9.
27. Imaizumi C, et al. Serial intelligence test scores in pediatric moyamoya disease. Neuropediatrics. 1999;30(6):294–9.
28. Seol HJ, et al. Headache in pediatric moyamoya disease: review of 204 consecutive cases. J Neurosurg. 2005;103(5 Suppl):439–42.
29. Kuroda S, Houkin K. Moyamoya disease: current concepts and future perspectives. Lancet Neurol. 2008;7(11):1056–66.
30. Choi JU, et al. Natural history of moyamoya disease: comparison of activity of daily living in surgery and non surgery groups. Clin Neurol Neurosurg. 1997;99(Suppl 2):S11–8.
31. Cho WS, et al. The natural clinical course of hemodynamically stable adult moyamoya disease. J Neurosurg. 2015;122(1):82–9.
32. Kang S, et al. Natural course of moyamoya disease in patients with prior hemorrhagic stroke. Stroke. 2019;50(5):1060–6.
33. Su IC, et al. Acute cerebral ischemia following intraventricular hemorrhage in moyamoya disease: early perfusion computed tomography findings. J Neurosurg. 2008;109(6):1049–51.
34. Kurokawa T, et al. Prognosis of occlusive disease of the circle of Willis (moyamoya disease) in children. Pediatr Neurol. 1985;1(5):274–7.
35. Ishii K, et al. Temporal profile of angiographical stages of moyamoya disease: when does moyamoya disease progress? Neurol Res. 2003;25(4):405–10.
36. Kelly ME, et al. Progression of unilateral moyamoya disease: a clinical series. Cerebrovasc Dis. 2006;22(2–3):109–15.
37. Lee M, et al. Quantitative hemodynamic studies in moyamoya disease: a review. Neurosurg Focus. 2009;26(4):E5.
38. Kuroda S, et al. Radiological findings, clinical course, and outcome in asymptomatic moyamoya disease: results of multicenter survey in Japan. Stroke. 2007;38(5):1430–5.
39. Neff KW, et al. 2D cine phase-contrast MRI for volume flow evaluation of the brain-supplying circulation in moyamoya disease. AJR Am J Roentgenol. 2006;187(1):W107–15.
40. Ogasawara K, Ogawa A, Yoshimoto T. Cerebrovascular reactivity to acetazolamide and outcome in patients with symptomatic internal carotid or middle cerebral artery occlusion: a xenon-133 single-photon emission computed tomography study. Stroke. 2002;33(7):1857–62.
41. Logothetis NK, Pfeuffer J. On the nature of the BOLD fMRI contrast mechanism. Magn Reson Imaging. 2004;22(10):1517–31.
42. Czabanka M, et al. Proposal for a new grading of Moyamoya disease in adult patients. Cerebrovasc Dis. 2011;32(1):41–50.
43. Horn P, et al. Hemodynamic reserve and high-intensity transient signals in moyamoya disease. Cerebrovasc Dis. 2005;19(3):141–6.
44. Chen J, et al. Microembolic signals predict cerebral ischaemic events in patients with moyamoya disease. Eur J Neurol. 2014;21(5):785–90.
45. Kraemer M, et al. What is the expert's option on antiplatelet therapy in moyamoya disease? Results of a worldwide Survey. Eur J Neurol. 2012;19(1):163–7.
46. Im SH, et al. Moyamoya disease associated with Graves disease: special considerations regarding clinical significance and management. J Neurosurg. 2005;102(6):1013–7.
47. Czartoski T, et al. Postinfectious vasculopathy with evolution to moyamoya syndrome. J Neurol Neurosurg Psychiatry. 2005;76(2):256–9.
48. Hallemeier CL, et al. Clinical features and outcome in North American adults with moyamoya phenomenon. Stroke. 2006;37(6):1490–6.
49. Kraemer M, Heienbrok W, Berlit P. Moyamoya disease in Europeans. Stroke. 2008;39(12):3193–200.
50. Tu YK, et al. Combined encephalo-arterio-synangiosis and encephalo-myo-synangiosis in the treatment of moyamoya disease. Clin Neurol Neurosurg. 1997;99(Suppl 2):S118–22.

51. Kim T, et al. Stroke prevention by direct revascularization for patients with adult-onset moyamoya disease presenting with ischemia. J Neurosurg. 2016;124(6):1788–93.
52. Fujii K, et al. The efficacy of bypass surgery for the patients with hemorrhagic moyamoya disease. Clin Neurol Neurosurg. 1997;99(Suppl 2):S194–5.
53. Kawaguchi S, Okuno S, Sakaki T. Effect of direct arterial bypass on the prevention of future stroke in patients with the hemorrhagic variety of moyamoya disease. J Neurosurg. 2000;93(3):397–401.
54. Lee SB, et al. Long-term follow-up results in 142 adult patients with moyamoya disease according to management modality. Acta Neurochir. 2012;154(7):1179–87.
55. Qian C, et al. The efficacy of surgical treatment for the secondary prevention of stroke in symptomatic moyamoya disease: a meta-analysis. Medicine (Baltimore). 2015;94(49):e2218.
56. Gross BA, Thomas AJ, Frerichs KU. Endovascular treatment of symptomatic moyamoya. Neurosurg Rev. 2014;37(4):579–83.
57. El-Hakam LM, et al. Angioplasty for acute stroke with pediatric moyamoya syndrome. J Child Neurol. 2010;25(10):1278–83.
58. LoPresti MA, et al. Endovascular stenting for rescue of a failed donor graft during superficial temporal artery to middle cerebral artery bypass surgery: case report. J Neurosurg Pediatr. 2019:1–5.
59. Goethe EA, et al. Endovascular "boost": external carotid angioplasty to augment flow before superficial temporal-middle cerebral artery bypass. World Neurosurg. 2019;130:474–8.
60. Kubota Y, et al. T-configuration stent placement for carotid bifurcation stenosis co-existing with ipsilateral intracranial stenosis: a case report and literature review. J Stroke Cerebrovasc Dis. 2020;30(2):105472.
61. Kim SH, et al. Endovascular treatment of ruptured aneurysms or pseudoaneurysms on the collateral vessels in patients with moyamoya disease. Neurosurgery. 2009;65(5):1000–4; discussion 1004
62. Kuriyama S, et al. Prevalence and clinicoepidemiological features of moyamoya disease in Japan: findings from a nationwide epidemiological survey. Stroke. 2008;39(1):42–7.
63. Im SH, et al. Prevalence and epidemiological features of moyamoya disease in Korea. J Cerebrovasc Endovasc Neurosurg. 2012;14(2):75–8.
64. Chen PC, et al. Epidemiology of moyamoya disease in Taiwan: a nationwide population-based study. Stroke. 2014;45(5):1258–63.
65. Uchino K, et al. Moyamoya disease in Washington State and California. Neurology. 2005;65(6):956–8.
66. Wanebo JE, Khan N, Zabramski JM, Spetzler RF. Moyamoya disease: diagnosis and treatment [Internet]. Stuttgart: Thieme; 2014. Available from: https://doi.org/10.1055/b-002-91663

Chapter 16
Posterior Circulation Stroke and Vertebrobasilar Insufficiency

Rimal H. Dossani, Justin M. Cappuzzo, Muhammad Waqas, Neil Almeida, and Elad I. Levy

Abbreviations or Acronyms

AICA	Anterior inferior cerebellar artery
AP	Anteroposterior
AVM	Arteriovenous malformation
BA	Basilar artery
CT	Computed tomography
CTA	CT angiography
CTP	CT perfusion

R. H. Dossani · J. M. Cappuzzo · M. Waqas
Department of Neurosurgery, Jacobs School of Medicine and Biomedical Sciences, University at Buffalo, Buffalo, NY, USA

Department of Neurosurgery, Gates Vascular Institute at Kaleida Health, Buffalo, NY, USA
e-mail: rdossani@ubns.com; jcappuzzo@ubns.com; mwaqas@ubns.com

N. Almeida
School of Medicine and Health Sciences, The George Washington University, Washington, DC, USA

E. I. Levy (✉)
Department of Neurosurgery, Jacobs School of Medicine and Biomedical Sciences, University at Buffalo, Buffalo, NY, USA

Department of Neurosurgery, Gates Vascular Institute at Kaleida Health, Buffalo, NY, USA

Department of Radiology, Jacobs School of Medicine and Biomedical Sciences, University at Buffalo, Buffalo, NY, USA

Canon Stroke and Vascular Research Center, University at Buffalo, Buffalo, NY, USA

Jacobs Institute, Buffalo, NY, USA
e-mail: elevy@ubns.com

J. R. Mascitelli, M. J. Binning (eds.), *Introduction to Vascular Neurosurgery*,
https://doi.org/10.1007/978-3-030-88196-2_16

HINTS	Head-Impulse–Nystagmus–Test-of-Skew
IST-3	Third International Stroke Trial
ISUIA	International Study of Unruptured Intracranial Aneurysms
IV	Intravenous
MRA	Magnetic resonance angiography
MRI	Magnetic resonance imaging
NIHSS	National Institutes of Health Stroke Scale
PC-ASPECTS	Posterior Circulation Acute Stroke Prognosis Early CT Score
PCA	Posterior cerebral artery
PCoA	Posterior communicating artery
PICA	Posterior inferior cerebellar artery
rtPA	Recombinant tissue plasminogen activator
SCA	Superior cerebellar artery
TCD	Transcranial Doppler
VBI	Vertebrobasilar insufficiency
TIA	Transient ischemic attack
VBJ	Vertebrobasilar junction
VERiTAS	Vertebrobasilar Flow Evaluation and Risk of Transient Ischemic Attack and Stroke
WASID	Warfarin–Aspirin Symptomatic Intracranial Disease

Introduction

Stroke is a primary cause of death and disability worldwide. Approximately 800,000 individuals within the United States suffer from stroke annually [1]. These individuals predominantly suffer from stroke affecting the anterior circulation, but the posterior circulation is associated with nearly 20% of ischemic stroke cases [2]. In contrast to the anterior circulation, posterior circulation stroke may present with a much wider variety of clinical manifestations [3]. In this chapter, we discuss posterior circulation anatomical variants, disease mechanisms within the posterior circulation, clinical presentations, imaging, and management of different types of posterior circulation stroke variants with a specific focus on vertebrobasilar insufficiency (VBI). We review the subsets of etiologies of VBI, including subclavian steal, vertebral artery (VA) stenosis, basilar artery (BA) stenosis, posterior circulation arteriovenous malformations (AVMs), and the current literature and our experience in treating and managing these disease processes.

Anatomical Variants of the Posterior Circulation

The posterior circulation consists of major arteries, including the bilateral VAs, posterior inferior cerebellar artery (PICA), basilar artery (BA), and bilateral posterior cerebral arteries (PCAs). This complex circulation system provides vascular supply

to a multitude of areas with physiological and functional diversity, including the brainstem, cerebellum, thalami, medial temporal lobe, and occipital visual cortex. Insight of the vascular region involved in stroke is critical in diagnosing the causative vascular lesion and mechanism of stroke.

Recognition of the various anatomical variants of the posterior circulation is imperative to distinguish benign findings from pathological conditions. The circle of Willis is an anastomotic arterial ring with variants; studies have shown that it is complete in only 20% of individuals [4]. A fetal-type PCA is defined as a dominant posterior communicating artery (PCoA) with a hypoplastic or aplastic P1 segment that results in predominant supply to the posterior territories from the anterior circulation. de Monyé et al. reported that there is no increased risk of ischemic stroke in the territory of the PCA in patients with a fetal origin of the PCA [5].

In addition, the BA supplies the brainstem and arises from the union of the two VAs. Investigators have postulated that asymmetric vertebral flow contributes to BA curvature and is a potential determinant for the occurrence of infarcts around the vertebrobasilar junction (VBJ) [6].

Furthermore, the artery of Percheron is a vascular variant in which there is a thalamic perforating artery arising from the proximal PCA (P1 segment) and provides bilateral supply to the paramedian thalami. This normal, but rare, finding is a common cause of stroke within this territory [7, 8].

Disease Mechanisms of Posterior Circulation Stroke

A multitude of etiologies contribute to posterior circulation stroke, including atherosclerosis, VA dissection, cardioembolism, and compromise of small penetrating arteries. It is critical for clinicians to have an understanding of the pathophysiology when investigating the etiology of a posterior circulation stroke.

The intracranial arteries can often be compromised by atherosclerosis. Independent risk factors contributing to atherosclerosis include age, hypertension, and diabetes mellitus [9]. Intracranial atherosclerosis could potentially lead to thromboembolism within the vasculature, contributing to the formation of an infarct. In an analysis of the largest published registry of patients with posterior circulation disease (including demographics/risk factors, types of lesions, and follow-up data), the New England Medical Center Posterior Circulation Registry (n = 207 patients), Caplan et al. revealed that the most common sites of atherosclerosis are the basilar artery followed by the internal carotid artery, middle cerebral artery, VA, PCA, and anterior cerebral artery [10]. Specifically, atherosclerosis can often present in the distal vertebral and basilar arteries. The most common locations of atherosclerosis within the VA are the V1 and V4 segments [11]. The carotid arteries are more likely than the VAs to have fibrous plaques and fatty streaks within the arterial walls [12].

Dissection of the VA is an additional etiology of posterior circulation stroke and can arise spontaneously or from trauma and accounts for 15% of stroke [13]. The extracranial segments of the carotid and vertebral arteries are postulated to have greater mobility than their intracranial compartments and are thus much more likely

to undergo dissection. Specifically, VA dissections are most likely to arise in the V2 (35%) and V3 segments (34%), where there is a differential between motility of two segments of the VA as it travels out of the foramen transversarium [14, 15]. Intracranial extension of the VA dissection has a higher risk of leading to the formation of aneurysm and overall mortality [14]. Particularly, if the dissection involves the V4 segment, involvement of the PICA may pose a greater risk of stroke, as there is less collateralization from the opposing VA. It is imperative for clinicians to be aware of common presenting symptoms of VA dissection, including neck pain, headache (typically occipital), and history of trauma.

Cardiac embolism is an additional risk factor that is responsible for a large proportion of ischemic stroke of the posterior circulation. Kamel et al. describe a multitude of factors that contribute to cardioembolic stroke, including atrial fibrillation, systolic heart failure, recent myocardial infarction, prosthetic heart valves, patent foramen ovale, and infective endocarditis [16]. Caplan et al. note that embolism is one of the most common mechanisms of stroke of the posterior circulation [10]. Recent studies have demonstrated that about half of strokes involving cardioembolic origin involve multiple cerebral arterial territories [17].

Furthermore, the small penetrating arteries could potentially be compromised, thus contributing to posterior circulation lacunar infarcts. A multitude of pathological mechanisms contribute to small vessel disease, specifically lipohyalinosis of the arterial wall [18]. Hypertension is a risk factor that increases the risk of the formation of lipohyalinosis of these small penetrating arteries. Which is a direct contributor to small vessel infarcts [11].

Vertebrobasilar Insufficiency

VBI is characterized by insufficient blood flow to those parts of the brain fed by the posterior circulation, which includes the bilateral VAs, the BA, and the bilateral PCAs. The posterior circulation supplies the cerebellum, brainstem, and occipital cortex. The most common cause of VBI is progressive atherosclerosis of the blood vessels comprising the posterior circulation. Other causes include spontaneous or traumatic dissection of the cervical VAs as well as embolism from a cardiac or peripheral source. Symptoms of VBI include dizziness, lightheadedness, vertigo, syncope, ataxia, hemibody numbness or weakness, difficulty swallowing, and homonymous hemianopsia, among others. Vertebrobasilar syndrome may occur as a result of the following clinical entities: subclavian steal, VA ostial stenosis, or BA stenosis and intracranial VA stenosis:

(a) *Subclavian Steal* (Fig. 16.1): When the subclavian artery is occluded or highly stenotic proximal to the origin of the VA, circulation to the arm is sustained by reversal of flow in the VA. Upon exertional activity of the arm, such as lifting the arm over the head for a prolonged period of time, the VA reverses flow and directs blood to supply the demand for circulation to the ipsilateral arm. As a result, blood supply is shunted from the vertebrobasilar posterior circulation

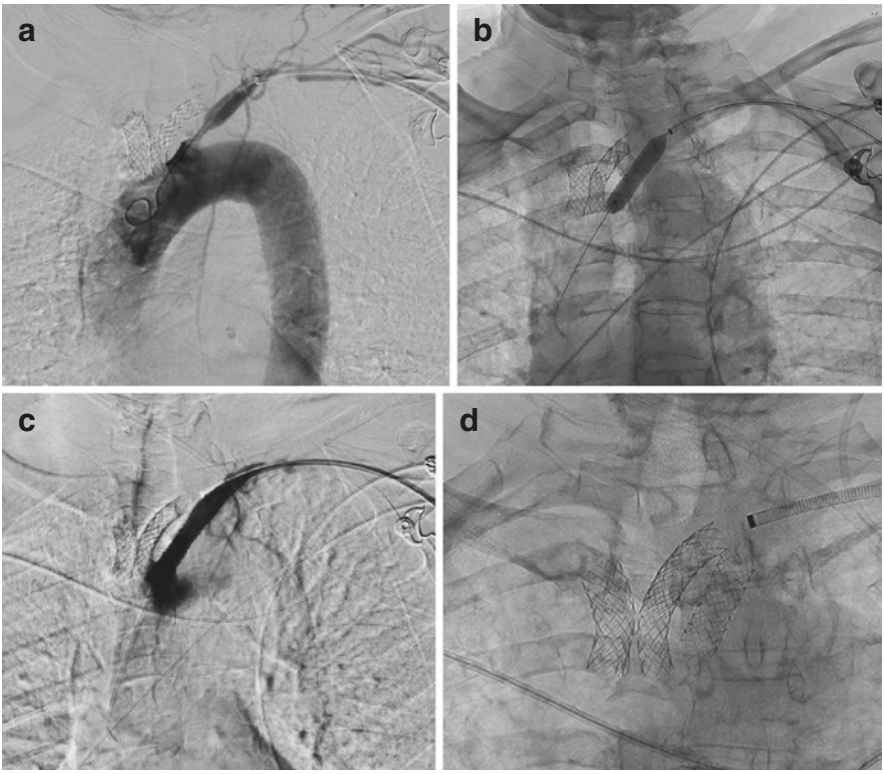

Fig. 16.1 Left subclavian ostial stenosis. A 65-year-old woman presented with dizziness and vertigo while painting the ceiling in her home. She was diagnosed with left subclavian artery ostial stenosis and was electively scheduled for left subclavian artery stent placement. A pigtail catheter injection of the aortic arch (**a**) showed previous ostial stents at the innominate and left common carotid artery origins as well as >80% stenosis of the left subclavian artery origin. A balloon-mounted, covered stent was deployed across the stenosis (**b**). Subsequent injections demonstrated near resolution of the subclavian artery ostial stenosis (**c**). Fluoroscopic anteroposterior (AP) imaging demonstrates successful balloon-mounted stent deployment (**d**)

toward the arm, which leads to symptoms of VBI. A key sign of subclavian steal syndrome is a systolic blood pressure of 20 mm Hg or less on the affected side compared to the pressure on the opposite arm. Doppler ultrasound imaging evaluation demonstrates reversal of flow in the ipsilateral VA. Furthermore, diagnostic angiography demonstrates no anterograde flow in the VA ipsilateral to the subclavian stenosis; however, selective injection of the contralateral subclavian artery demonstrates anterograde flow in the contralateral VA up to the VBJ, with reversal of flow in the ipsilateral VA to supply the subclavian artery distal to the stenosis. Subclavian steal syndrome is treated using balloon-mounted, covered stents through an endovascular approach. When endovascular approaches are not successful (for example, in the setting of chronic total occlusion of the subclavian artery), a carotid-to-subclavian artery bypass is a viable option for revascularizing the left subclavian artery.

(b) *Vertebral Artery Ostial Stenosis* (Fig. 16.2): A common cause of VBI is VA stenosis at its origin from the subclavian artery, also known as VA ostial stenosis. VA ostial stenosis may cause artery-to-artery embolus and transient ischemic attack (TIA) or stroke in the posterior circulation. Occasionally, the emboli are large enough to cause large vessel occlusion at the VBJ or BA. In such circumstances, a procedure involving stenting of the VA ostium followed by mechanical thrombectomy of the large vessel occlusion can be lifesaving. The threshold for treatment of symptomatic VA ostial stenosis is controversial. Data from the North American Symptomatic Carotid Endarterectomy Trial, which demonstrated benefit for carotid revascularization in symptomatic patients with >70% stenosis, are extrapolated to extracranial VA ostial stenosis, as no prospective clinical trials exist for treatment for this disease process [19]. Our protocol is to treat symptomatic ostial stenosis >70% in the dominant VA with balloon-mounted stents. When endovascular stenting is not feasible, as in the

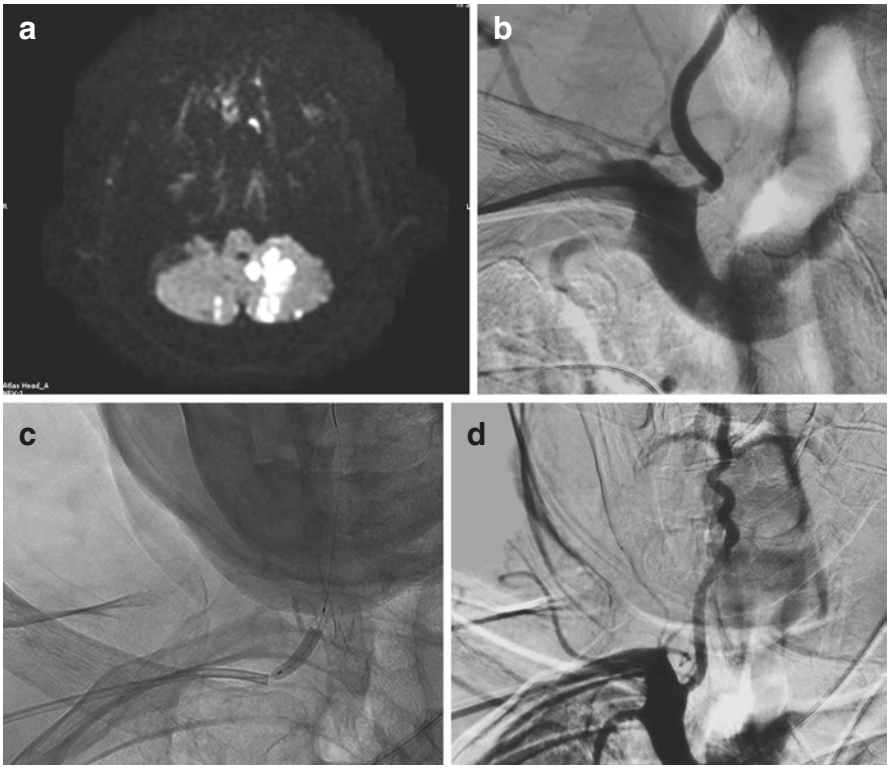

Fig. 16.2 Right vertebral artery (VA) ostial stenosis. A 72-year-old man presented with ataxia of his left upper and lower extremities. Magnetic resonance imaging (MRI) demonstrated left cerebellar infarcts (**a**). Diagnostic catheter angiography revealed >80% ostial stenosis of the right VA (**b**). The left VA was chronically occluded at its origin from the subclavian artery. A balloon-mounted stent was deployed across the right VA stenosis (**c**). Subsequent injections demonstrated near-complete resolution of the stenosis with improved flow across the right vertebral artery ostium (**d**)

case of severe vessel tortuosity, a VA (V1 segment)-to-carotid transposition is an effective surgical strategy to manage VA ostial stenosis.

(c) *Basilar Stenosis and Intracranial Vertebral Stenosis* (Fig. 16.3): Vertebrobasilar stenosis is associated with a stroke recurrence risk between 5 and 15% annually [20] and up to 33% in the first month when treated with medical therapy alone [21]. The Warfarin–Aspirin Symptomatic Intracranial Disease (WASID) study group reported a risk of stroke recurrence in the posterior circulation of 23% in the aspirin group versus 10% in the warfarin group among a cohort of 569

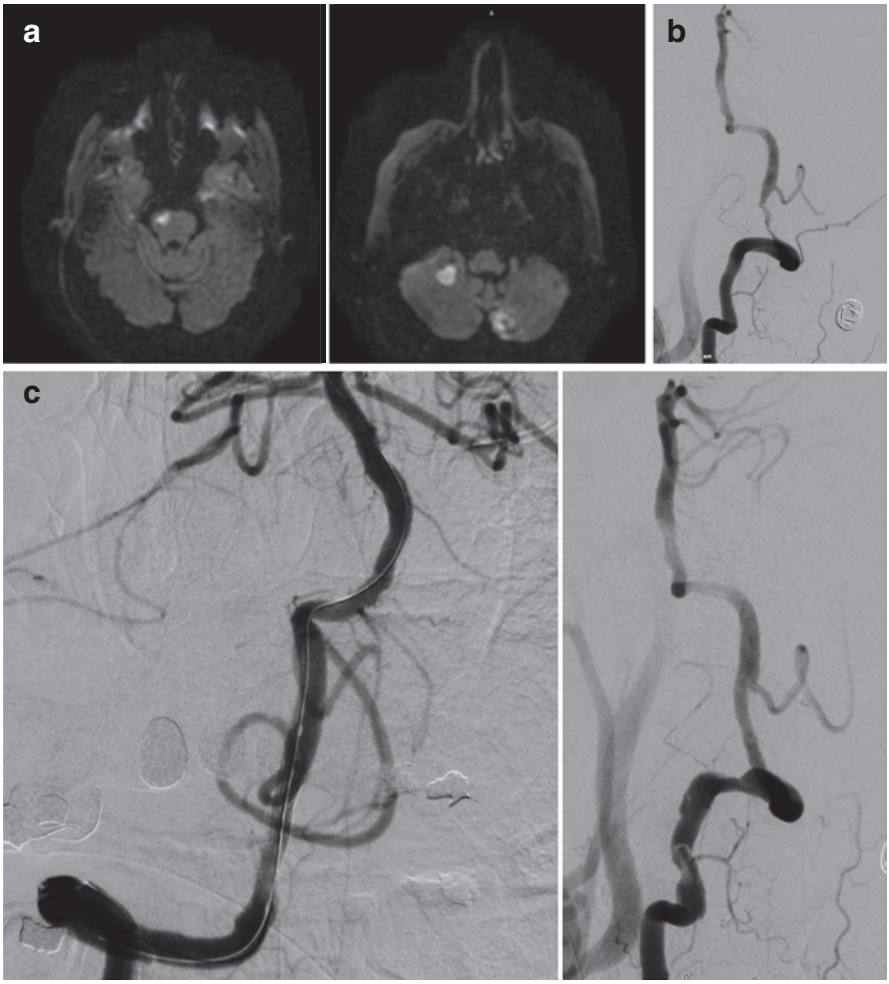

Fig. 16.3 Intracranial VA stenosis. A 57-year-old woman presented with ataxia and vertigo. MRI demonstrated an infarct in the right midbrain as well as bilateral cerebellar infarcts (**a**, left, right). Catheter angiography demonstrated severe right V4 VA stenosis proximal to the origin of the posterior inferior cerebellar artery (**b**). The left VA was occluded at its origin from the subclavian artery. A balloon-mounted stent was placed to treat the VA stenosis. Subsequent injections demonstrated resolution of the right V4 VA stenosis in the AP (**c**-left) and lateral (**c**-right) planes

patients who presented with TIA or stroke [22]. Post hoc analysis demonstrated that patients with BA stenosis benefited from warfarin therapy [23]. The risk of stroke recurrence correlates with stenosis severity. The WASID study investigators found that the risk of stroke recurrence was 19% with ≥70% stenosis versus 10% for <70% stenosis [22]. For patients with ≥70% symptomatic posterior circulation stenosis who suffer from recurrent stroke despite medical management with dual antiplatelet therapy or anticoagulation, we offer submaximal angioplasty of up to 80% of the nominal parent vessel diameter. Stenting is reserved for patients with recurrent stroke despite maximal medical therapy and submaximal angioplasty. A systematic review and meta-analysis of patients with symptomatic intracranial vertebrobasilar stenosis showed that stroke recurrence was 9.6 per 100-person years in the medical group versus 7.2 per 100-person years in the endovascular group, demonstrating that the risk of stroke recurrence was comparable between the medical and endovascular groups [24]. Additionally, the Vertebrobasilar Flow Evaluation and Risk of Transient Ischemic Attack and Stroke (VERiTAS) Study group included 72 patients for their study, with 18 (25%) meeting low-flow criteria (defined as more than 20% reduction in normal parameters for blood flow to the posterior circulation), and found that compared to patients with the normal flow on quantitative magnetic resonance angiography, the risk of stroke was found to be as high as 20% in 1 year, compared to 4% per year in the normal flow group, with a hazard ratio of 11.55 [25] (Fig. 16.4). Specifically, low flow was defined as <40 ml/min in both PCAs or in one PCA if additional criteria were present [25].

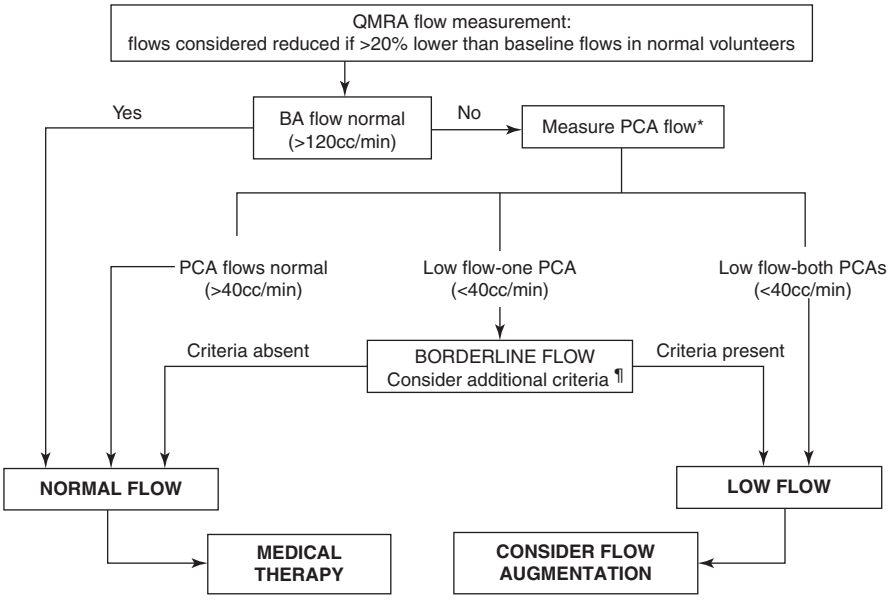

Fig. 16.4 The Vertebrobasilar Flow Evaluation and Risk of Transient Ischemic Attack and Stroke (VERiTAS) Study group used this treatment algorithm to demonstrate measurements of cerebral blood flow and subsequent management. (Amin-Hanjani et al. [25])

Hemorrhagic Posterior Circulation Stroke

A thorough discussion of hemorrhagic posterior circulation stroke is beyond the scope of this chapter. Hemorrhagic strokes in the posterior circulation occur due to the presence of an underlying vascular lesion, such as AVM, dural arteriovenous fistula, or aneurysm, or due to medical causes, such as hypertension. Ruptured AVMs in the posterior circulation present with headache, nausea, and vomiting. Depending on the severity of the hemorrhage, patients may also present with obtundation, inability to protect the airway, or coma.

Cerebellar AVMs comprise approximately 70% of infratentorial AVMs and approximately 10–15% of all AVMs. The Spetzler–Martin grading score ranges from 0 to 5 and accounts for AVM size (<3 cm = 1 point, 3-6 cm = 2 points, and >6 cm = 3 points), eloquence (eloquent = 1 point and noneloquent = 0 points), and venous drainage (deep = 1 point and superficial = 0 points) [26]. A more recent AVM grading system known as the Lawton–Young AVM Supplementary Grading Scale accounts for patient age (<20 years = 1 point, 20–40 years = 2 points, and >40 years = 3 points), hemorrhagic presentation (unruptured = 1 point and ruptured = 0 points), and nidal diffuseness (compact nidus = 0 points and diffuse nidus = 1 point) in addition to AVM size, eloquence, and venous drainage [27]. A prospective registry of brain AVMs at the University of California, San Francisco demonstrated that ruptured posterior fossa AVMs had worse outcomes than those in supratentorial locations and recommended a more "aggressive surgical posture" toward posterior fossa AVMs as compared to supratentorial AVMs [28].

Posterior circulation aneurysms are commonly located in the following locations: PCoA origin, PICA origin, and basilar apex. Less common locations for posterior circulation aneurysms include the origin of the left superior cerebellar artery at its origin from the basilar quadrifurcation, dolichoectatic holobasilar aneurysms, and PCA aneurysms. The International Study of Unruptured Intracranial Aneurysms (ISUIA) investigators assessed the natural history of 1937 unruptured intracranial aneurysms and divided the patients into two groups: those with a history of subarachnoid hemorrhage and those without. The ISUIA investigators predicted that the relative risk of rupture was 13.8 for aneurysms at the basilar tip, 13.6 for those in the vertebrobasilar or posterior cerebral distribution, and 8.0 for those in the PCoA, as compared to other locations [29]. Both endovascular and open neurosurgical treatment options are available for posterior circulation aneurysms. However, posterior circulation aneurysms are more likely to be treated using endovascular means due to the advancement and widespread availability of endovascular therapies. A Swiss registry of patients with ruptured posterior circulation aneurysms from 2009 to 2014 demonstrated that endovascular treatment options were performed in 88.7% of patients [30].

Hypertensive hemorrhage in the posterior fossa typically occurs in the cerebellum or pons. The treatment is medical management using vasoactive intravenous drips, such as nicardipine, to maintain systolic blood pressure <140 mm Hg. Emergent placement of an external ventricular drain may be necessary for posterior

fossa hypertensive bleeds, resulting in intraventricular hemorrhage or fourth ventricular compression. Surgical hematoma evacuation is recommended for mass-occupying cerebellar hypertensive hematomas (usually >3 cm in diameter) [31].

Different Locations of Posterior Circulation Stroke

Posterior circulation stroke is a broad term that encompasses several different types of pathologies. The management, as we will see later, is directly affected by the location of posterior circulation stroke. These specific etiologies include top of the basilar, midbasilar, VBJ, tandem occlusion/stenosis, and vertebrobasilar intracranial atherosclerosis disease. Each of these pathologies affords different management strategies that will be touched upon later in the chapter.

Clinical Presentation

As previously discussed, the posterior circulation supplies the brainstem, thalamus, cerebellum, inferior temporal lobe, and occipital lobe; thus, posterior circulation stroke can result in a wide range of symptoms [32]. This anatomical diversity of the posterior circulation sheds insight into the myriad of clinical presentations of posterior circulation stroke.

An analysis of the New England Medical Center Posterior Circulation Registry highlights associated presenting symptoms [10]. This analysis reported that the most common presenting symptoms were dizziness (47%), unilateral limb weakness (41%), dysarthria (31%), headache (28%), and nausea or vomiting (27%). The most frequent signs were unilateral limb weakness (38%), gait ataxia (31%), unilateral limb ataxia (30%), dysarthria (28%), and nystagmus (24%) [33]. However, a patient will present differently depending on the location of the lesion. For example, a patient with a complete BA occlusion will typically present with comatose-like symptoms including posturing and lower cranial nerve deficits.

In the New England Medical Center Registry, Caplan et al. described a topographic classification that delineates the intracranial vertebrobasilar system into proximal, middle, and distal territories [10]. This study defined the region that is supplied by the intracranial VAs and the posterior inferior cerebellar arteries (PICAs) up to the VBJ as constituting the proximal territory. The middle territory is comprised of the BA and the anterior inferior cerebellar arteries (AICAs) up to the superior cerebellar arteries (SCAs). The distal territory is comprised of the rostral BA, SCAs, and PCAs. Infarcts involving the proximal, middle, and distal territory have characteristic presentations. Proximal territory circulation infarcts are noted to cause Horner's syndrome, dysphagia, nausea, and vomiting. Middle territory circulation infarcts are characteristically associated with weakness of the limbs and nuclear facial palsy. Distal territory circulation infarcts can lead to visual

impairment and lethargy [3]. The presentation of a young patient with trauma, neck pain, and headache is highly suggestive of VA dissection.

Furthermore, Thömke et al. reported that a significant number of individuals present with cranial nerve palsies caused by brainstem ischemia as the sole symptom [34]. These most frequently include isolated palsies of the third and sixth cranial nerves and less frequently involve the fourth, fifth, and seventh cranial nerves [34]. Therefore, it is important to keep in mind that cerebrovascular brainstem disease may often present as isolated cranial nerve palsy.

There are several classic syndromes involving the posterior circulation that are particularly noteworthy. Lateral medullary syndrome, also known as Wallenberg syndrome, is due to a vascular event, particularly an event involving the PICA or VA. Multiple structures are potentially impacted in this syndrome leading to varied symptoms; these structures include the spinothalamic tract, trigeminal nerve, glossopharyngeal nerve, vagus nerve, vestibular nucleus, nucleus ambiguus, descending sympathetic tract, and cerebellum [35–37]. Common symptoms of the lateral medullary syndrome include vertigo, nystagmus, and vomiting due to impairment of the vestibular nuclei, contralateral impairment of pain and temperature in the trunk and limbs due to impairment of the spinothalamic tract, ipsilateral loss of pain and temperature of the face due to involvement of the trigeminal nerve, ipsilateral dysphagia and dysarthria due to the involvement of the nucleus ambiguus, ipsilateral gait ataxia due to cerebellar involvement, ipsilateral Horner syndrome due to impairment of descending sympathetic fibers, and ipsilateral absent gag reflex and hoarseness due to impairment of the glossopharyngeal nerve.

Locked-in syndrome is a consequence of BA occlusion and is characterized by quadriplegia, anarthria, and limited communication via eye movements. Due to midbasilar occlusion, there is infarction of the basilar region of the pons [38].

In addition, vertebrobasilar artery syndrome is due to the involvement of the proximal territory of the posterior circulation, as described previously. This syndrome commonly manifests with nausea, vomiting, nystagmus, unilateral limb weakness, gait, ataxia, and fifth cranial nerve findings [2]. Furthermore, Caplan et al. report that in 25% of the cases in the New England Medical Center Registry, a vertebrobasilar TIA may precede posterior circulation stroke [10].

Kattah et al. reported on Head-Impulse–Nystagmus–Test-of-Skew (HINTS) methodology, which is utilized to diagnose stroke in acute vestibular syndrome [39]. This technique uses bedside evaluation of oculomotor findings to reliably identify stroke associated with this syndrome and avoid misdiagnosis of a potential posterior fossa infarct [39].

Imaging Modalities

Noncontrast head computed tomography (CT) is the initial diagnostic neuroimaging modality to primarily exclude intracranial hemorrhage. However, CT provides suboptimal visualization of posterior circulation infarcts [40]. Thus, early ischemic changes

may not be evident on CT, and magnetic resonance imaging (MRI) with diffusion-weighted images is the superior modality to investigate infarction [41]. MRI has the advantage of visualizing the posterior fossa and detection of hyperacute infarct lesions [42]. In the acute setting, it is critical to consider that MRI may not always be safely performed due to various factors including limitations on time, presence of a pacemaker, or other contraindications [3]. Imaging of the posterior circulation is warranted if posterior circulation stroke is suspected. To accomplish this aim, CT angiography (CTA) of the head and neck [or magnetic resonance angiography (MRA)] is performed [2]. This neuroimaging modality remains the gold standard for vascular imaging with excellent sensitivity and specificity for vascular abnormalities.

At our institution, we rely on CT perfusion (CTP) imaging in conjunction with CTA of the head and neck (named a CT stroke study for the combination of these two modalities) for initial management for all strokes (including suspected posterior circulation strokes). The benefits of this are numerous over MRI and MRA. CTA and CTP imaging can be completed much more quickly than MRI, making this combination modality pivotal in the diagnosis and/or treatment of stroke. Additionally, current blood flow/volume relationships can be demonstrated on CTP imaging, which is not able possible with MRI alone. MRI will reveal whether a stroke has occurred; however, information regarding the ischemic penumbra is not revealed unless MR perfusion imaging is obtained. Ischemic penumbra is defined as the region of the brain with decreased blood flow and subsequent increased risk of infarction [43]. Additionally, CTA may be more accurate than MRA with respect to showing stenosis, because MRA has been known to overestimate stenosis severity. Additionally, CTA and CTP are much more readily available in centers that do not have MRI and MRA capabilities. Unfortunately, CTP is not as reliable in the brainstem and posterior fossa, and noncontrast head CT is also sometimes difficult to assess for hypodensity; therefore, MRI does sometimes play a larger role in guiding treatment for posterior circulation stroke compared to anterior circulation stroke—particularly for patients with lower National Institutes of Health Stroke Scale (NIHSS) scores. We typically perform mechanical thrombectomy for patients with symptoms of BA occlusion, regardless of CTP findings and time of stroke symptom onset, because untreated BA occlusion is fatal. Finally, no one imaging modality (of those listed above) showed superiority in our case series investigating predictors of outcomes from endovascular treatment of posterior circulation strokes [44].

Markers for signs of ischemic damage of the parenchyma include sulcal effacement and loss of gray–white junction differentiation [45–47]. Ischemic signs on CT in the early period of stroke have not been corroborated for the posterior circulation. Goldmakher et al. reported that the presence of a hyperdense BA sign-on noncontrast head CT in individuals with a high pretest probability of posterior circulation stroke based on their clinical symptoms is a strong predictor of BA thrombosis [48]. Khan et al. investigated noninvasive detection of VA stenosis and determined that contrast-enhanced MRA is the most sensitive imaging modality to detect VA stenosis compared to CTA. Ultrasound has been demonstrated to have low sensitivity and could often miss VA stenosis [49]. Bedside transcranial Doppler (TCD) imaging is a widely utilized diagnostic imaging modality for the assessment of intracranial obstruction in

patients who have experienced ischemic stroke [50]. However, difficulty in assessing pertinent anatomy due to variation and tortuosity of the vasculature in the posterior circulation poses a unique challenge to using ultrasonographic assessment for posterior circulation stroke. Tsivoulis et al. compared a novel imaging modality, transcranial power motion-mode Doppler, with the diagnostic accuracy of angiography and found satisfactory agreement between the two imaging modalities [50].

The NIHSS has been widely applied in patients suffering from acute ischemic stroke. Studies have shown that for anterior circulation stroke, the volume of lesions on diffusion-weighted imaging correlates with NIHSS score [51]. Linfante et al. reported that DWI lesion volume did not significantly correlate with NIHSS score in the acute phase of posterior circulation stroke, postulating that this measure favors symptoms of anterior circulation stroke [40]. The Posterior Circulation Acute Stroke Prognosis Early CT Score (PC-ASPECTS) has been proposed as a tool for the detection of early ischemic damage. This score has been proposed to help in identifying individuals with BA occlusions who are not likely to benefit from treatment with endovascular recanalization [52]. Lin et al. performed receiver-operating characteristic curve analysis comparing PC-ASPECTS to baseline NIHSS score and reported that PC-ASPECTS has more reliability than NIHSS for predicting functional outcomes of posterior circulation stroke. Following posterior circulation acute ischemic stroke, a PC-ASPECTS score of >7 is a useful standard for the prediction of a positive functional outcome [42].

Management of Posterior Circulation Stroke

Stroke treatment is rapidly evolving, and it is critical to understand diagnostic strategies and decision-making in order to appropriately determine the treatment regimen.

Acute management options for posterior circulation stroke include intravenous (IV) recombinant tissue plasminogen activator (rtPA), intra-arterial thrombolysis, and endovascular thrombectomy [3]. Treatment of acute stroke is based on the last known normal time, which is a critical factor for IV rtPA eligibility. As previously discussed, NIHSS is a determinant of stroke severity but is superior for predicting functional outcome for anterior circulation stroke compared to ischemic stroke of the posterior circulation.

Intraarterial Thrombolysis

Several authors have investigated the utility of intraarterial thrombolytics as an option for the treatment of posterior circulation stroke [53–57]. Hacke et al. investigated patients who angiographically demonstrated thrombotic vertebrobasilar artery occlusions and received either local intraarterial thrombolytic therapy

(urokinase or streptokinase) or conventional therapy consisting of antiplatelet agents. They reported an association between the technical success of thrombolysis of vertebrobasilar artery occlusions and favorable clinical outcomes [54]. Rha et al. further investigated the relationship between recanalization and clinical outcome in acute ischemic stroke. They reported a 63.2% recanalization rate for occlusions in the vertebrobasilar system with intraarterial thrombolytics [57]. It is well understood that patients with ischemic stroke due to occlusion of the basilar or vertebral arteries can undergo neurological deterioration. There is currently a paucity of investigations studying the use of intraarterial thrombolysis. Macleod et al. performed a randomized controlled trial with a small cohort of 16 patients involving the utility of intraarterial thrombolysis in patients with BA occlusion and established the need for larger-scale studies investigating this treatment modality [56].

Intravenous Fibrinolysis

Intravenous thrombolysis with alteplase is the first-line treatment modality for patients with an acute ischemic stroke last known well within 4.5 hours [53]. The Third International Stroke Trial (IST-3) collaborative group demonstrated that treatment with IV-tPA within 6 hours of initial symptom onset was associated with improved patient outcome and health-related quality of life [58]. Future studies aim to investigate the efficacy of other agents with longer treatment windows [58]. Strbian et al. investigated the effect of extensive baseline ischemia on patient outcome following thrombolysis of BA occlusion. Extensive baseline ischemia was defined by the investigators as PC-ASPECTS less than 8. The results indicated that in the absence of extensive baseline ischemia, recanalization of BA occlusion produced good outcomes in approximately 50% of patients [59].

Mechanical Thrombectomy

There are no level I data to support the use of mechanical thrombectomy for posterior circulation stroke. However, several observational studies have described the safety and efficacy of mechanical thrombectomy for acute BA, VBJ, and PCA occlusions (Fig. 16.5). A multicenter prospective registry compared the safety and efficacy of mechanical thrombectomy between anterior and posterior circulation strokes. Of 139 patients included in the study, 84.9% had BA occlusion, followed by VA occlusion (in 16.5%) and PCA occlusion (in 4.3%) [60]. Patients with posterior circulation stroke tended to have lower median NIHSS score at baseline (12 vs. 15, $P = 0.024$). No symptomatic intracranial hemorrhage occurred in posterior circulation stroke compared to 3% in anterior circulation stroke ($P = 0.010$). The median NIHSS score at discharge was 3 in posterior circulation stroke and 4 in anterior

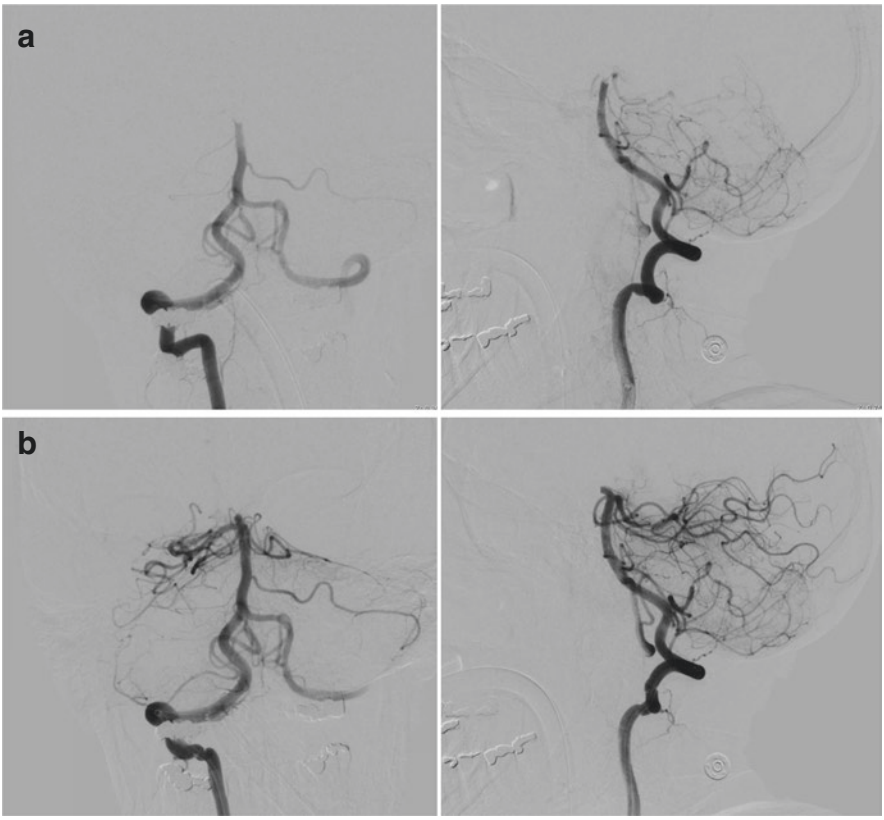

Fig. 16.5 Basilar apex occlusion**.** An 80-year-old woman presented with acute left-sided hemiparesis and obtundation. Her National Institutes of Health Stroke Scale score was 22. Intubation was performed. Computed tomography angiography showed occlusion at the basilar apex. Catheter angiography revealed occlusion at the level of the basilar apex in the AP (**a**-left) and lateral (**a**-right) planes. Mechanical thrombectomy was performed with a combination of a stent retriever and an aspiration catheter, and the basilar apex was recanalized (**b**, AP-left, lateral-right) with similar views. The left posterior cerebral artery was chronically occluded and was not visualized

circulation stroke. Favorable functional outcome at 3 months (modified Rankin Scale score 0–2: 38.0% vs. 42.6%, $P = 0.392$) and mortality did not differ significantly between posterior circulation stroke and anterior circulation stroke (33.7% vs. 30.8%, $P = 0.539$) [60].

The essence of recanalization therapies in the management of acute stroke is to save the ischemic penumbra. The "recanalization hypothesis" states that opening the occluded vessels restores cerebral blood flow to these threatened regions [57]. Weber et al. established the safety and effectiveness of mechanical thrombectomy for posterior circulation stroke [60]. Specifically, the investigators reported that mechanical thrombectomy in posterior circulation stroke has a lower risk of symptomatic intracranial hemorrhage and comparable efficacy to ACS [60].

In addition, Rha et al. performed a meta-analysis investigating recanalization and reported that mechanical thrombectomy is strongly associated with improved functional outcomes and reduced mortality [57]. Their findings indicated that recanalization is a marker of therapeutic activity as evident in their analysis of early phase trials of thrombolytic treatment in acute ischemic stroke. Kidwell et al. investigated whether penumbral imaging would identify patients who would differentially benefit from endovascular therapy for acute ischemic stroke within 8 hours after symptom onset compared to standard of care [61]. Their results indicated ultimately that there was no treatment benefit in patients with a favorable penumbral pattern. In addition, there was no added benefit due to mechanical embolectomy compared to standard medical care.

Researchers have directly compared the endovascular treatment to the aforementioned intravenous rtPA. Ciccone et al. investigated this aim and randomly assigned patients in their study to receive either endovascular treatment (intraarterial thrombolysis with rtPA, mechanical clot disruption or retrieval, or a combination of these treatments) or intravenous rtPA [62]. Ultimately, the results of their trial indicated that in patients with acute ischemic stroke, endovascular therapy is not superior to treatment with intravenous rtPA [62].

At our institution, we tend to perform mechanical thrombectomy on all patients with an NIHSS score >6 with BA occlusion (top of basilar, midbasilar, and VBJ), regardless of the time of symptom onset and CTP findings. From our perspective, the risk benefit of thrombectomy in these patients almost always is in favor of thrombectomy as untreated BA occlusion is a death sentence in almost every case. We demonstrated good clinical outcomes using a Solitaire stent retriever (Medtronic) in a case series of 12 patients with posterior circulation stroke [63]. Additionally, we found that both stent retriever and aspiration thrombectomy were effective methods of achieving recanalization in patients with posterior circulation stroke [44].

Treatment of acute ischemic stroke pertaining to anterior circulation involves utilizing mechanical endovascular thrombectomy up to 24 hours [64]. Research efforts aim to establish similar protocols for the treatment of posterior circulation stroke. Due to differences in pathophysiology and brain function compared to the anterior circulation, the selection of devices and management strategies of posterior circulation stroke need to be optimized. Lee et al. reported that the presence of PCoA, technical success of recanalization, and the patient's initial neurological status are critical factors impacting patient outcomes in posterior circulation stroke [65].

Conclusion

It is critical for healthcare professionals to be cognizant of vascular neuroimaging modalities that are key to the diagnosis of posterior circulation stroke and also to have an understanding of the limitations of quantitative assessment measures, such as the NIHSS. In addition, an understanding of treatment modalities can optimize short- and long-term patient outcomes. In patients who meet the eligibility criteria,

IV rtPA remains the recommended first-line treatment. Mechanical thrombectomy is useful in select cases of acute vertebrobasilar occlusion with a favorable clinical and imaging profile.

The management of VBI depends on the underlying etiology. Because atherosclerosis is the underlying etiology for most cases of VBI, medical management with dual antiplatelets is the first-line treatment for symptomatic disease. Endovascular or surgical management is reserved for symptomatic disease not responsive to medical management.

References

1. Virani SS, Alonso A, Benjamin EJ, Bittencourt MS, Callaway CW, Carson AP, et al. Heart disease and stroke Statistics-2020 update: a report from the American Heart Association. Circulation. 2020;141(9):e139–596.
2. Go S. Posterior circulation ischemic stroke. Mo Med. 2015;112(3):192–6.
3. Nouh A, Remke J, Ruland S. Ischemic posterior circulation stroke: a review of anatomy, clinical presentations, diagnosis, and current management. Front Neurol. 2014;5(30).
4. Bugnicourt JM, Garcia PY, Peltier J, Bonnaire B, Picard C, Godefroy O. Incomplete posterior circle of Willis: a risk factor for migraine? Headache. 2009;49(6):879–86.
5. de Monyé C, Dippel DW, Siepman TA, Dijkshoorn ML, Tanghe HL, van der Lugt A. Is a fetal origin of the posterior cerebral artery a risk factor for TIA or ischemic stroke? A study with 16-multidetector-row CT angiography. J Neurol. 2008;255(2):239–45.
6. Hong JM, Chung CS, Bang OY, Yong SW, Joo IS, Huh K. Vertebral artery dominance contributes to basilar artery curvature and peri-vertebrobasilar junctional infarcts. J Neurol Neurosurg Psychiatry. 2009;80(10):1087–92.
7. Griessenauer CJ, Loukas M, Tubbs RS, Cohen-Gadol AA. The artery of Percheron: an anatomic study with potential neurosurgical and neuroendovascular importance. Br J Neurosurg. 2014;28(1):81–5.
8. Lazzaro NA, Wright B, Castillo M, Fischbein NJ, Glastonbury CM, Hildenbrand PG, et al. Rtery of percheron infarction: imaging patterns and clinical spectrum. AJNR Am J Neuroradiol. 2010;31(7):1283–9.
9. Qureshi AI, Caplan LR. Intracranial atherosclerosis. Lancet. 2014;383:984–98.
10. Caplan LR, Wityk RJ, Glass TA, Tapia J, Pazdera L, Chang HM, et al. New England Medical Center posterior circulation registry. Ann Neurol. 2004;56(3):389–98.
11. Savitz SI, Caplan LR. Vertebrobasilar disease. N Engl J Med. 2005;352(25):2618–26.
12. Solberg LA, Eggen DA. Localization and sequence of development of atherosclerotic lesions in the carotid and vertebral arteries. Circulation. 1971;43(5):711–24.
13. Yesilot Barlas N, Putaala J, Waje-Andreassen U, Vassilopoulou S, Nardi K, Bahar SZ. Etiology of first-ever ischaemic stroke in European young adults: the 15 cities young stroke study
. Eur J Neurol. 2013;20(11):1431–9.
14. Arnold M, Bousser MG, Fahrni G, Fischer U, Georgiadis D, Gandjour J. Vertebral artery dissection presenting findings and predictors of outcome. Stroke. 2006;37(10).
15. Rodallec MH, Marteau V, Gerber S, Desmottes L, Zins M. Craniocervical arterial dissection: spectrum of imaging findings and differential diagnosis. Radiographics: a review publication of the Radiological Society of North America, Inc. 2008;28(6):1711–28.
16. Kamel H, Healey JS. Cardioembolic stroke. Circ Res. 2017;120(3):514–26.
17. Nah HW, Lee JW, Chung CH, Choo SJ, Kwon SU, Kim JS, et al. New brain infarcts on magnetic resonance imaging after coronary artery bypass graft surgery: lesion patterns, mechanism, and predictors. Ann Neurol. 2014;76:347–55.

18. Caplan LR. Lacunar infarction and small vessel disease: pathology and pathophysiology. J Stroke. 2015;17(1):2–6.
19. Ferguson GG, Eliasziw M, Barr HW, Clagett GP, Barnes RW, Wallace MC, et al. The north American symptomatic carotid endarterectomy trial: surgical results in 1415 patients. Stroke. 1999;30(9):1751–8.
20. Qureshi AI, Ziai WC, Yahia AM, Mohammad Y, Sen S, Agarwal P, et al. Stroke-free survival and its determinants in patients with symptomatic vertebrobasilar stenosis: a multicenter study. Neurosurgery. 2003;52(5):1033–9. discussion 9-40
21. Gulli G, Khan S, Markus HS. Vertebrobasilar stenosis predicts high early recurrent stroke risk in posterior circulation stroke and TIA. Stroke. 2009;40(8):2732–7.
22. Chimowitz MI, Kokkinos J, Strong J, Brown MB, Levine SR, Silliman S, et al. The warfarin–aspirin symptomatic intracranial disease study. Neurology. 1995;45(8):1488–93.
23. Kasner SE, Lynn MJ, Chimowitz MI, Frankel MR, Howlett-Smith H, Hertzberg VS, et al. Warfarin vs aspirin for symptomatic intracranial stenosis: subgroup analyses from WASID. Neurology. 2006;67(7):1275–8.
24. Abuzinadah AR, Alanazy MH, Almekhlafi MA, Duan Y, Zhu H, Mazighi M, et al. Stroke recurrence rates among patients with symptomatic intracranial vertebrobasilar stenoses: systematic review and meta-analysis. J Neurointerv Surg. 2016;8(2):112–6.
25. Amin-Hanjani S, Stapleton CJ, Du X, Rose-Finnell L, Pandey DK, Elkind MSV, et al. Hypoperfusion symptoms poorly predict hemodynamic compromise and stroke risk in Vertebrobasilar disease. Stroke. 2019;50(2):495–7.
26. Spetzler RF, Martin NA. A proposed grading system for arteriovenous malformations. J Neurosurg. 1986;65(4):476–83.
27. Lawton MT, Kim H, McCulloch CE, Mikhak B, Young WL. A supplementary grading scale for selecting patients with brain arteriovenous malformations for surgery. Neurosurgery. 2010;66(4):702–13; discussion 13.
28. Abla AA, Nelson J, Rutledge WC, Young WL, Kim H, Lawton MT. The natural history of AVM hemorrhage in the posterior fossa: comparison of hematoma volumes and neurological outcomes in patients with ruptured infra- and supratentorial AVMs. Neurosurg Focus. 2014;37(3):E6.
29. International Study of Unruptured Intracranial Aneurysms I. Unruptured intracranial aneurysms--risk of rupture and risks of surgical intervention. N Engl J Med. 1998;339(24):1725–33.
30. Maduri R, Starnoni D, Rocca A, Bervini D, Zumofen DW, Stienen MN, et al. Ruptured posterior circulation aneurysms: epidemiology, patterns of care, and outcomes from the Swiss SOS national registry. Acta Neurochir. 2019;161(4):769–79.
31. Broderick J, Connolly S, Feldmann E, Hanley D, Kase C, Krieger D, et al. Guidelines for the management of spontaneous intracerebral hemorrhage in adults: 2007 update: a guideline from the American Heart Association/American Stroke Association stroke council, high blood pressure research council, and the quality of care and outcomes in research interdisciplinary working group. Stroke. 2007;38(6):2001–23.
32. Markus HS, van der Worp HB, Rothwell PM. Posterior circulation ischemic stroke and transient ischemic attack: diagnosis, investigation, and secondary prevention. Lancet Neurology. 2013;12(10):989–98.
33. Searls DE, Pazdera L, Korbel E, Vysata O, Caplan LR. Symptoms and signs of posterior circulation ischemia in the new England medical center posterior circulation registry. Arch Neurol. 2011;69(3):346–51.
34. Thömke F, Gutmann L, Stoeter P, Hopf HC. Cerebrovascular brainstem diseases with isolated cranial nerve palsies. Cerebrovasc Dis. 2002;13(3):147–55.
35. Battel I, Koch I, Biddau F, Carollo C, Piccione F, Meneghello F, et al. Efficacy of botulinum toxin type-a and swallowing treatment for oropharyngeal dysphagia recovery in a patient with lateral medullary syndrome. Eur J Phys Rehabil Med. 2017;53(5):798–801.
36. Kim H, Lee HJ, Park JW. Clinical course and outcome in patients with severe dysphagia after lateral medullary syndrome. Ther Adv Neurol Disord. 2018.

37. Sampath V, Gowda MR, Vinay HR, Preethi S. Persistent hiccups (singultus) as the presenting symptom of lateral medullary syndrome. Indian J Psychol Med. 2014;36(3):341–3.
38. Raibagkar P, Chavali RV, Kaplan TB. Reverse locked-in syndrome. Neurocrit Care. 2017;27(1):108–14.
39. Kattah JC, Talkad AV, Wang DZ, Hsieh YH, Newman-Toker DE. HINTS to diagnose stroke in the acute vestibular syndrome: three-step bedside oculomotor examination more sensitive than early MRI diffusion-weighted imaging. Stroke. 2009;40(11):3504–10.
40. Linfante I, Llinas RH, Schlaug G, Chaves C, Warach S, Caplan LR. Diffusion-weighted imaging and National Institutes of Health stroke scale in the acute phase of posterior-circulation stroke. Arch Neurol. 2001;58(4):621–8.
41. Benjamin P, Khan F, MacKinnon AD. The use of diffusion weighted imaging to evaluate pathology outside the brain parenchyma in neuroimaging studies Br J Radiol. 2017;90(1072).
42. Lin S, Chen C, Hu H, Bai C. Predicting functional outcomes of posterior circulation acute ischemic stroke in first 36 h of stroke onset. J Neurol. 2018;265:926–32.
43. Fisher M. Characterizing the target of acute stroke therapy. Stroke. 1997;28(4):866–72.
44. Mokin M, Sonig A, Sivakanthan S, Ren Z, Elijovich L, Arthur A, et al. Clinical and procedural predictors of outcomes from the endovascular treatment of posterior circulation strokes. Stroke. 2016;47(3):782–8.
45. Haussen DC, Lima A, Frankel M, Anderson A, Belagaje S, Nahab F. Sulcal effacement with preserved gray-white junction: a sign of reversible ischemia. Stroke. 2015;46(6):1704–6.
46. Mainali S, Wahba M, Elijovich L. Detection of early ischemic changes in noncontrast CT head improved with "stroke windows". ISRN Neurosci. 2014;
47. Moulin T, Cattin F, Crépin L, Tatu L, Chavot D, Piotin M. Early CT signs in acute middle cerebral artery infarction: predictive value for subsequent infarct locations and outcome. Neurology 1996;47:366–375.
48. Goldmakher GV, Camargo EC, Furie KL, Singhal AB, Roccatagliata L, Halpern EF, et al. Hyperdense basilar artery sign on unenhanced CT predicts thrombus and outcome in acute posterior circulation stroke. Stroke. 2009;134(9).
49. Khan S, Rich P, Clifton A, Markus HS. Noninvasive detection of vertebral artery stenosis a comparison of contrast-enhanced MR angiography, CT angiography, and ultrasound. Stroke. 2009;40:3499–503.
50. Tsivgoulis G, Sharma VK, Lao AY, Malkoff MD, Alexandrov AV. Validation of transcranial Doppler with computed tomography angiography in acute cerebral ischemia. Stroke. 2007;38:1245–9.
51. Lövblad KO, Baird AE, Schlaug G, Benfield A, Siewert B, Voetsch B, et al. Ischemic lesion volumes in acute stroke by diffusion-weighted magnetic resonance imaging correlate with clinical outcome. Ann Neurol. 1997;42(2):164–70.
52. Mundiyanapurath S, Möhlenbruch M, Ringleb PA, Bösel J, Wick W, Bendszus M, et al. Posterior Circulation Acute Stroke Prognosis Early Computed Tomography Score Using Hypointense Vessels on Susceptibility Weighted Imaging Independently Predicts Outcome in Patients with Basilar Artery Occlusion. PLoS One. 2015;10(7).
53. Hacke W, Kaste M, Bluhmki E, Brozman M, Dávalos A, Guidetti D, et al. Thrombolysis with alteplase 3 to 4.5 hours after acute ischemic stroke. N Engl J Med. 2008;359(13):1317–29.
54. Hacke W, Zeumer H, Ferbert A, Brückmann H, del Zoppo GJ. Intra-arterial thrombolytic therapy improves outcome in patients with acute vertebrobasilar occlusive disease. Stroke. 1988;19(10):1216–2210.
55. Lindsberg PJ, Mattle HP. Therapy of basilar artery occlusion a systematic analysis comparing intra-arterial and intravenous thrombolysis. Stroke. 2006;37(3).
56. Macleod MR, Davis SM, Mitchell PJ, Gerraty RP, Donnan GA. Results of a multicentre, randomised controlled trial of intra-arterial urokinase in the treatment of acute posterior circulation ischaemic stroke. Cerebrovasc Dis. 2005;20(1):12–7.
57. Rha JH, Saver JL. The impact of recanalization on ischemic stroke outcome: a meta-analysis. Stroke. 2007;38(3):967–73.

58. Sandercock P, Lindley R, Wardlaw J, Dennis M, Group ISTC. Third international stroke trial (IST-3) of thrombolysis for acute ischaemic stroke. . Trials. 2008;9(37).
59. Strbian D, Sairanen T, Silvennoinen H, Salonen O, Kaste M, Lindsberg PJ. Thrombolysis of basilar artery occlusion: impact of baseline ischemia and time. Ann Neurol. 2013;73(6):688–94.
60. Weber R, Minnerup J, Nordmeyer H, Eyding J, Krogias C, Hadisurya J, et al. Thrombectomy in posterior circulation stroke: differences in procedures and outcome compared to anterior circulation stroke in the prospective multicentre REVASK registry. Eur J Neurol. 2019;26(2):299–305.
61. Kidwell CS, Jahan R, Gornbein J. A trial of imaging selection and endovascular treatment for ischemic stroke. N Engl J Med. 2013;368(10):914–23.
62. Ciccone A, Valvassori L, Nichelatti M, Sgoifo A, Ponzio M, Sterzi R, et al. Endovascular treatment for acute ischemic stroke. N Engl J Med. 2013;368(10):904–13.
63. Sonig A, Krishna C, Natarajan SK, Liu J, Hopkins LN, Snyder KV, et al. Stent retriever-assisted mechanical Thrombectomy for acute basilar artery occlusion: single US institution experience. Oper Neurosurg (Hagerstown). 2016;12(3):250–9.
64. Nogueira RG, Jadhav AP, Haussen DC, Bonafe A, Budzik RF, Bhuva P, et al. Thrombectomy 6 to 24 hours after stroke with a mismatch between deficit and infarct. N Engl J Med. 2018;378(1):11–21.
65. Lee HN, Kim BT, Im SB. Implications of mechanical endovascular Thrombectomy for acute basilar and posterior cerebral artery occlusion. J Cerebrovasc Endovasc Neurosurg. 2018;20(3):168–75.

Chapter 17
Intracerebral Hemorrhage

Christina P. Rossitto, J Mocco, and Christopher P. Kellner

Introduction

Intracerebral hemorrhage (ICH) is a common and deadly disease with few treatment options. It is the most devastating type of stroke, with 40% of patients dead at 1 month and 75% of patients dead or severely disabled 6 months after the hemorrhage. Intracerebral hemorrhage comprises 15% of all strokes tallying two million hemorrhages globally each year [1, 2]. Hypertension is the most common cause of spontaneous ICH followed by amyloid angiopathy; anticoagulation-associated hemorrhages; neoplasm; underlying coagulopathy; and underlying macroscopic cerebrovascular disease, such as aneurysms, arteriovenous malformations, dural arteriovenous fistulae, cavernous malformations, hemangioblastomas, as well as others [3]. ICH risk factors include being male, older age, being from a low- or middle-income country, hypertension, hypocholesterolemia, smoking, excessive alcohol intake, drug use, Asian race, and genetic predispositions (Table 17.1) [4, 5].

Advancements in early recognition, imaging capabilities, effective and rapid interhospital and care-team communication, neurointensive care, and neurorehabilitation have all increased the likelihood of improved functional outcome in this challenging disease [6]. The evaluation and management of patients with ICH focus on stabilization, diagnostic workup, and prevention of complications. Medical management includes blood pressure and intracranial pressure management as well as reversal of any anticoagulation medications and treatment of any complications that occur as a result of the ICH and subsequent neurologic debilitation. Complications resulting from the hemorrhage may include hydrocephalus, ischemic stroke, and seizure, while complications associated with neurologic debilitation include deep

C. P. Rossitto · J Mocco · C. P. Kellner (✉)
Department of Neurosurgery, Icahn School of Medicine at Mount Sinai, New York, NY, USA
e-mail: christina.rossitto@icahn.mssm.edu; j.mocco@mountsinai.org; christopher.kellner@mountsinai.org

J. R. Mascitelli, M. J. Binning (eds.), *Introduction to Vascular Neurosurgery*,
https://doi.org/10.1007/978-3-030-88196-2_17

Table 17.1 Key facts in intracerebral hemorrhage

Morbidity and mortality	Common etiologies	Interventions	Predictors of poor outcome
40% 1-month mortality 75% dead or disabled at 6 months	Hypertension Cerebral amyloid angiopathy (CAA) Oral anticoagulation Underlying lesion Drug use	BP control OAC reversal ICP management Decompression Hematoma evacuation	Advanced age Larger hematoma Subcortical location Poor initial exam Presence of IVH

venous thrombosis, pulmonary embolism, pneumonia, urinary tract infection, and decubitus ulcer, as well as others.

Surgery for ICH is currently indicated for subgroups of patients and is supported by pathophysiologic reasoning, preclinical experimental support, and evidence from randomized clinical trials. Current American Heart Association guidelines from 2015 on the treatment of spontaneous ICH conclude that "for most patients with supratentorial ICH, the usefulness of surgery is not well established" [7]. Surgery for supratentorial ICH should be considered as a life-saving measure in a deteriorating patient. In patients with cerebellar ICH, early surgery may be appropriate for patients with brainstem compression and/or hydrocephalus from ventricular obstruction. As medical understanding and technical management improve, the role of surgery for ICH is poised to expand. In this chapter, we discuss the pathophysiology, diagnostic evaluation, medical management, surgical management, prognosis, and future of ICH.

Pathophysiology

The management of ICH is driven by its complex pathophysiology. Intracerebral hemorrhage develops from a bleeding point within the parenchyma that results in extravasation and accumulation of a hematoma within the brain tissue. The bleeding is most commonly caused by the rupture of an artery weakened over time by chronic hypertension or by the accumulation of amyloid protein in the vessel wall. When a subcortical hemorrhage occurs secondary to hypertension, the pathologic rupture site on the perforating artery is often caused by a Charcot–Bouchard microaneurysm. Lobar ICHs are more likely to be caused by cerebral amyloid angiopathy, a disease whose incidence increases directly with age.

The outward force of the expanding hemorrhage is balanced by the counterforce of perihematomal brain matter eventually leading to coagulation of the bleeding source. The formation of the hematoma triggers two injurious processes. Immediately, primary mechanical injury occurs due to the mass effect of the clot. In minutes to hours, the mechanical stress causes increased intracranial pressure, direct traumatic injury, compression of adjacent microcirculation, ischemia, and edema [8]. Large hemorrhages can significantly increase intracranial pressure potentially

leading to brainstem compression and herniation. Clinically significant hematoma expansion occurs in at least 33% of patients within the first 24 hours, further worsening the outcome for those patients [9, 10]. Preclinical studies in which agarose was injected stereotactically into the caudate of rats with and without hemoglobin support the understanding that the initial injury occurs from the mass effect of the hematoma and subsequent mechanical disruption rather than interaction with blood specifically [11].

Secondary injury is then caused by the inflammatory response incurred by the presence of blood as well as the degradation and removal of blood products. Injury occurs over days to weeks as a function of the initial hematoma volume. Toxicity related to the presence of blood is both time- and dose-dependent. Hemoglobin digestion and direct contact of blood products with the brain parenchyma lead to neuroinflammation described radiographically as perihematomal edema. The degree of perihematomal edema correlates with poor outcome after ICH [12, 13]. Hematotoxicity, hypermetabolism, excitotoxicity, spreading depression, and oxidative stress leading to blood–brain-barrier breakdown, edema, dysfunction, and cell death contribute to injury [14].

Preclinical and clinical studies strongly suggest a link between hematoma removal and improved outcomes. Early hematoma evacuation has been associated with improved neurologic recovery, improved motor evoked potentials, and decreased perihematomal injury in four different animal models of spontaneous ICH: rat, rabbit, dog, and pig [15–19]. Data from both MISTIE II and MISTIE III demonstrated a correlation between the proportional volume of hematoma removal and reduction in perihematomal edema [20, 21]. However, the clinical benefit of surgical hematoma removal remains controversial and will be discussed in detail later in this chapter.

Initial Evaluation

ICH is a medical emergency and rapid treatment is required. The clinical presentation of ICH includes sudden headache, nausea, vomiting, depressed consciousness or confusion, delirium, and hemiparesis, aphasia, or other focal symptoms. Focal or generalized seizures may also occur. If the hemorrhage is located in the posterior fossa, it may cause cerebellar or brainstem deficits such as conjugate eye deviation, pinpoint pupils, and coma. The priorities of early management include airway management, cardiovascular support, and prompt transport to a stroke center. It is also important to investigate the patient's medical history and medication use to determine if anticoagulation reversal is required [7].

The initial neurologic examination is critical to both early management and long-term prognosis. The use of the Glasgow Coma Scale (GCS) is the most common and a component of the ICH Score and other prognostic tools. Use of the National Institutes of Health Stroke Scale (NIHSS) score is increasingly common as well as patients presenting with acute neurologic findings are included in acute stroke code

protocols developed for the rapid triage of patients potentially eligible for thrombolysis or thrombectomy. The ICH Score tallies points gained for lower GCS, age ≥ 80, ICH volume ≥ 30 mL, IVH, and infratentorial location (Table 17.2) to predict mortality at 30 days and is the most universally used prognostic score in ICH [22, 23]. However, since many of the presenting symptoms are not unique to ICH and present similarly to ischemic stroke, neuroimaging is mandatory in the initial evaluation.

CT and MRI can both be utilized in the initial evaluation of the ICH patient. MRI offers more detailed characterization, but CT is often more easily accessible and can be performed rapidly within the stroke workup [24]. Noncontrast CT is the practical method of confirming the clinical presentation of ICH as a high-density mass. Noncontrast CT quickly reveals volume, location, and extension into other intracranial compartments such as the intraventricular, subarachnoid, or subdural spaces. The ABC/2 method is a quick and easily validated method for estimating hematoma volume calculation from standard radiographic imaging software in clinical use (Fig. 17.1). The original ABC/2 formula included a complex method for calculating C in which if the hemorrhage area for a particular slice was greater than 75% of the

Table 17.2 Anticoagulation medications and reversal strategies

Anticoagulants	Mechanism	Reversal agents	Monitoring
Warfarin	Vitamin K antagonist	Vitamin K, 4F-PCC, FFP	PT/INR
Heparin	Unfractionated heparin	Protamine	aPTT
Enoxaparin	LMWH	Protamine	AntiXa activity
Fondaparinux	Factor Xa inhibitor	aPCC, rFVII	AntiXa activity
Dabigatran	Direct thrombin inhibitor	Idarucizumab, aPCC, Dialysis	aPTT, dTT
Rivaroxaban	Direct Xa inhibitor	Andexanat, aPCC, 3/4F-PCC	PT, AntiXa activity
Apixaban	Direct Xa inhibitor	Andexanat, aPCC, 3/4F-PCC	AntiXa activity

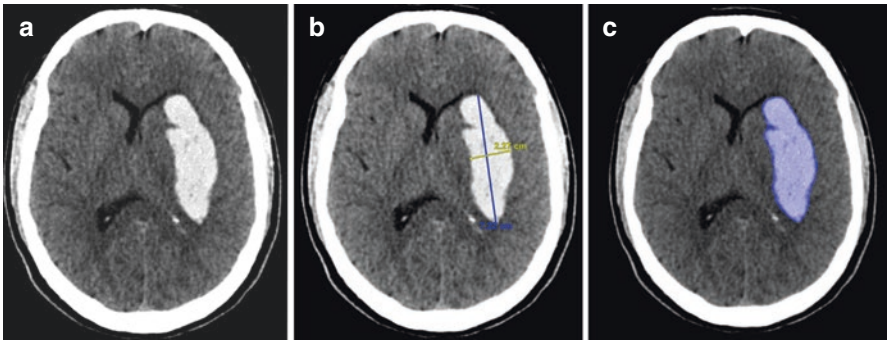

Fig. 17.1 (**a**) demonstrates a noncontrast CT with a large left subcortical intracerebral hemorrhage; (**b**) demonstrates the A and B measurements performed in the ABC/2 assessment of hematoma volume. To obtain the value of C, the number of slices with hematoma visible is counted and divided by 1/slice thickness in centimeters; (**c**) demonstrates output from an automatic calculation performed by an AI-derived algorithm developed by Viz.AI

area seen on the slice where the hemorrhage was largest, the slice was considered one hemorrhage slice for determining C. If the area was approximately 25–75% of the area, the slice was considered half a hemorrhage slice; and if the area was less than 25% of the area on the slice with the largest amount of hemorrhage, the slice was not considered a hemorrhage slice [25]. A modified ABC/2 formula (mABC/2) has been proposed and validated in which C is calculated as any slice in which blood is seen is counted as a full slice, although this shorter method may result in slightly less accurate measurements than the Kothari method [26]. When available, hematoma volume can be calculated automatically by artificial intelligence-powered mobile image assessment software [27]. Several additional markers of the shape and density of ICH can predict the likelihood of hematoma expansion and prognosis [28]. Effective quantification of hematoma volume is important in estimating prognosis, determining eligibility for minimally invasive surgical evacuation particularly in the posterior fossa where surgical evacuation is recommended for clots measuring greater than 3 cm in a single dimension.

Vascular imaging should also be included in the initial imaging set to evaluate for an underlying vascular lesion such as a vascular malformation or aneurysm. Hemorrhages due to a an arteriovenous malformation may be supported with CT findings of abnormal calcification in or around the hemorrhage or serpentine structures seen in the parenchyma. CTA may demonstrate hypervascularity or abnormal vessels in or around the hemorrhage. Intracerebral hemorrhage caused by aneurysmal rupture is more likely to present in the interhemispheric or Sylvian fissures with subarachnoid hemorrhage. Hypertensive ICH is likely to present in the basal ganglia or thalamus, while ICH associated with amyloid angiopathy is more likely to occur in the cortical region. The "spot sign" on CT angiography suggests active extravasation of contrast and correlates closely with hematoma expansion and in-hospital mortality [1]. Neuroimaging will be discussed further in the upcoming section *Imaging Considerations*.

BP and ICP Management

Given that hypertension is the most common cause of ICH, high blood pressure is common in ICH and exacerbated by stress, pain, and elevated ICP. 70% of patients found to have ICH, present to the hospital with systolic blood pressure > 140 mmHg [29]. High systolic blood pressure in ICH is correlated with hematoma expansion, poor neurological outcomes, and death [30]. The AHA/ASA 2015 guidelines state the following regarding blood pressure management:

- For ICH patients presenting with SBP between 150 and 220 mm Hg and without contraindication to acute BP treatment, acute lowering of SBP to 140 mm Hg is safe *(Class I; Level of Evidence A)* and can be effective for improving functional outcome *(Class IIa; Level of Evidence B).*

- For ICH patients presenting with SBP >220 mm Hg, it may be reasonable to consider aggressive reduction of BP with a continuous intravenous infusion and frequent BP monitoring *(Class IIb; Level of Evidence C)*.

There have been two major trials addressing the question of intensive, early blood pressure control in the ICH: the Intensive Blood Pressure Reduction in Acute Cerebral Hemorrhage Trial 2 (INTERACT2) and the Intensive Blood-Pressure Lowering in Patients with Acute Cerebral Hemorrhage (ATACH2) trials [31, 32]. The INTERACT2 trial assessed intensive blood pressure lowering treatment (target systolic BP <140 mm Hg within 1 hour) or guideline-recommended treatment (target systolic BP <180 mm Hg) for patients with ICH presenting with SBP ≥ 180. This trial was negative for its primary outcome of death or disability at 90 days [52.0% vs. 55.6% (OR 0.87; 95% CI 0.75–1.01; $P = 0.06$)], but a secondary analysis examining ordinal mRS shift suggested a benefit to intensive blood pressure control (OR for greater disability 0.87; 95% CI 0.77–1.00; $P = 0.04$). ATACH2 was designed to compare intensive blood pressure management (target SBP 110-139 mmHg) versus standard BP management (target SBP 140–179 mmHg) within 4.5 hours of ictus with IV nicardipine for patients with ICH with hematoma volume < 60 mL and GCS > 4 with SBP ≥ 180. This study was also negative for the primary outcome of death or major disability (LR 1.04, 95% CI 0.85 to 1.27, $P = 0.72$). In summary, acute BP control to <140 mm Hg is reasonable and safe and can be effective in improving functional outcome with class IIa evidence.

According to the Monro–Kellie doctrine, the sum of volumes of the brain, cerebrospinal fluid (CSF), and intracerebral blood is constant, indicating that an increase in one should cause a reciprocal decrease in either one or both of the remaining two. In the case of ICH, the mass of the hematoma has been added to the previously fixed intracranial volume inevitably leading to an increase in ICP [33]. By modulating CBF and CSF, the brain can accommodate small hematomas with only a transient increase in ICP. These compensation mechanisms, however, cannot accommodate moderate to large hematomas and ICP will therefore inevitably rise. Hydrocephalus and edema in these patients increase ICP further.

ICP monitoring is performed with a ventriculostomy catheter (VC) or an intracranial ICP probe. Complications associated with ventriculostomy including ICH, IVH, malfunction, and infection. There is a 35–45% rate of hemorrhage associated with ventriculostomy placement, although only 2% of these hemorrhages are symptomatic [34]. ICP management guidelines are similar to traumatic ICH management guidelines and include a recommendation for ICP monitoring when the GCS score is between 3 and 8 [35]. In ICH patients with GCS ≤8, ICP monitoring is indicated due to potential mass effect from hematoma, transtentorial herniation, IVH, or hydrocephalus.

Additional management of elevated ICP includes 30° elevation of the head of the bed, intubation and ventilation, sedation, removal of any constrictions to the cervical veins, mannitol, and hypertonic saline [36]. Hematoma evacuation and decompressive craniotomy may also be indicated and are discussed in other sections of this chapter.

Anticoagulation and Antiplatelet Reversal

Up to 20% of patients with ICH take oral anticoagulants (OACs)—a proportion that has quintupled from 5% in the late 80s and is likely to continue to increase with the aging population and the increasingly prevalent use of OACs [37]. Warfarin is a Vitamin K antagonist (VKA) and the most common ICH-associated anticoagulant [38]. Direct oral anticoagulants (DOACs) represent a newer class of anticoagulants that directly inhibit either thrombin or factor Xa. The available medications in the United States, their mechanisms of action, and standard reversal strategies are listed in Table 17.2.

Antiplatelet agents are also commonly associated with ICH, taken by approximately 23% of patients presenting with ICH prior to the hemorrhage [39]. Antiplatelet reversal with platelets is not recommended given the recent findings in the PATCH trial. In this trial, 190 patients from 41 centers were randomized to receive or not receive platelets to reverse dual antiplatelet use. The odds of death or dependence at 3 months was higher in the platelet transfusion group than in the standard care group (adjusted common odds ratio 2·05, 95% CI 1·18–3·56; $p = 0·01$) [40]. Desmopressin is recommended to be given at 0.4 μg/kg IV to reverse antiplatelet activity. This medication, DDAVP, leads to the release of von Willebrand Factor and has been shown to normalize platelet function after aspirin use at least for a few hours [41]. When patients are undergoing surgical intervention, antiplatelet reversal is at the discretion of the surgeon considering those patients are specifically at high risk for bleeding during surgery that may outweigh the negative impact of receiving a platelet transfusion seen in the PATCH trial.

Imaging Considerations

Computed tomography (CT) is routinely used for the emergent imaging obtained for an ICH patient. Often, these patients present with newly discovered symptoms and it is impossible to effectively differentiate ischemic and hemorrhagic stroke at that early time point, so the patient will often present as a stroke code. CT is also the standard imaging modality for ICH due to its ease of acquisition and accuracy of diagnosis for hemorrhage and hydrocephalus.

In many cases, a CTA will be performed with the initial CT as part of a stroke code to assess for the presence of an LVO, considering that the cause of sudden acute focal symptoms may be a large ischemic stroke that would necessitate rapid triage to thrombectomy. CTA is also valuable as an initial assessment for ICH to assess for the presence of spot sign, vascular malformation, or aneurysm. If an LVO is seen in the setting of a downstream hemorrhage, hemorrhagic transformation of a stroke would be chief in the differential diagnosis. If a cerebral venous sinus occlusion is suspected, a CT venogram can be performed with the CTA. Practically, the venous sinuses can often be seen on the CTA itself. Clinical or radiographic features

that would be suggestive of a CVST include the history of prior venous occlusions, a history of coagulopathy, and multifocal cortical hemorrhages.

Numerous features on CT and CTA have been shown to correlate with hematoma expansion. Overall, clinically significant expansion occurs in 38% of patients in the first 24 hours [9]. Spot sign is a hyperintensity within the hematoma seen on the CT angiogram that may indicate active extravasation (Fig. 17.2). It is seen in 33% of patients and correlates to hematoma expansion with a positive predictive value of 77% for hematoma expansion [42]. Numerous hematoma characteristics on CT have also been shown to correlate to expansion. These include heterogeneity, irregular contour, black hole sign, swirl sign, and others [43]. Often, a repeat CT is performed 3–6 hours after the first CT to evaluate for hematoma expansion and hydrocephalus.

MRI is obtained as part of the initial evaluation in some institutions, but this is less common. MRI should be performed when the patient is stable to obtain one to aid in the diagnosis of the etiology of the ICH. Gradient echo can provide information about the location and burden of unrelated microhemorrhages, generally hinting at a hypertensive etiology for subcortical microhemorrhages and CAA for cortical microhemorrhages and siderosis. The Boston criteria are helpful for diagnosing CAA and were recently modified to including MRI findings of siderosis with improved sensitivity (Table 17.3) [44]. Diffusion-weighted imaging (DWI) is helpful for diagnosing the concurrent embolic or watershed ischemic injury, which occurs in 20–25% of patients with ICH. DWI may also help diagnose hemorrhagic transformation if the hemorrhage occurs within a larger region of DWI positivity [45]. The T2 series is the best to demonstrate T2 white matter disease burden, or leukoaraiosis, which correlates with hematoma occurrence and expansion. The T1 and T1 with contrast series can help to identify an underlying lesion such as a hemorrhagic tumor.

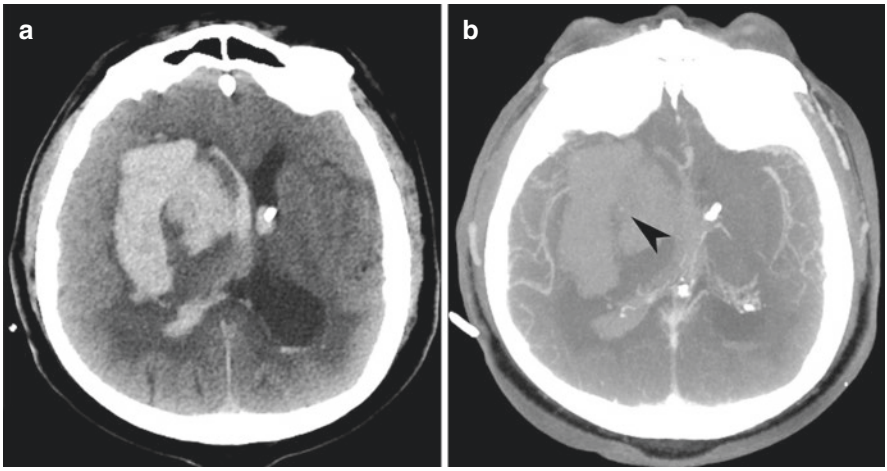

Fig. 17.2 (**a**) is a noncontrast head CT demonstrating a large right basal ganglia hemorrhage with intraventricular extension; (**b**) is a CT angiogram with a spot sign in the center of the hematoma (black arrowhead)

Table 17.3 Classic and modified Boston criteria for the diagnosis of cerebral amyloid angiopathy

	Classic Boston criteria	Terms added by the modified Boston criteria
Definitive CAA	Full postmortem exam demonstrating:	No modification
	Lobar, cortical, or corticosubcortical hemorrhage	
	Severe CAA with vasculopathy	
	Absence of other diagnostic lesions	
Probably CAA with supporting pathology	Clinical data and pathologic tissue demonstrating:	No modification
	Lobar, cortical, or corticosubcortical hemorrhage	
	Some degree of CAA in specimen	
	Absence of other diagnostic lesion	
Probable CAA	Clinical data and MRI or CT demonstrating:	
	Multiple hemorrhages restricted to lobar, cortical, or corticosubcortical regions	Single lobar, cortical, or corticosubcortical hemorrhage and focal or disseminated superficial siderosis
	Age ≥ 55	
	Absence of other causes of hemorrhage	
Possible CAA	Clinical data and MRI or CT demonstrating:	
	Single lobar, cortical, or corticosubcortical hemorrhage	Focal or disseminated superficial Siderosis
	Age ≥ 55	
	Absence of other causes of hemorrhage	

Discussing Prognosis

ICH has a poor prognosis overall with 40% of patients dead at 1 month and 75% of patients dead or severely disabled 6 months after the hemorrhage [1, 2]. A population-based cohort study of patients hospitalized after ICH in the Greater Cincinnati/Northern Kentucky area found the 10-year survival to be 18% [46]. However, there is some evidence to suggest that the mortality rate has improved since the early 2000s, particularly in patients who are less than 75 years old. These outcome improvements are most likely due to strides in neurocritical care and rehabilitation strategies [47]. Survivors of ICH regain consciousness and improve neurologic abilities gradually and to varying degrees. In the vast majority of cases, recovery occurs slowly over a period of years.

The most significant predictor of prognosis is hematoma volume. One study found that hematoma volume in combination with Glasgow Coma Scale score was predictive of 30-day mortality with a sensitivity of 96% and a specificity of 98%. The study found that patients with a parenchymal hemorrhage volume of at least

60 mL and a Glasgow Coma Scale score of 8 or less predicted a 30-day mortality of 91%. Patients with a volume of less than 30 mL and a Glasgow Coma Scale score of at least 9 predicted a 30-day mortality of 19% [48].

Another predictor of ICH prognosis is hematoma growth in the first 24 hours. A meta-analysis of 218 patients with spontaneous ICH who underwent head CT scan within 3 hours of onset and follow-up head CT within 24 hours found that for every 10% increase in ICH growth, mortality increased by 5% (hazard ratio 1.05, 95% CI 1.03–1.08) [10]. These predictions are most relevant for absolute increases in hemorrhage rather than relative volume growth. Hematoma growth can be predicted through contrast extravasation and "spot sign" on CTA, anticoagulants, and baseline volumes.

Additional predictors of functional outcome after ICH include advanced age, initial neurologic exam (often reported as the GCS), the presence of IVH, and hematoma location. Location portends poor outcome generally with the thalamic location being worse than basal ganglia location, which is worse than a cortical location. The ICH Score, described earlier in this chapter, is a prognostic score that predicts mortality at 30 days. Numerous other scores have been developed to predict mortality and functional outcome [49].

In patients who undergo surgical intervention, other factors may come into play that predict outcome. A preponderance of preclinical and clinical data suggest that time to evacuation is an important predictor of outcome after surgical intervention [50], although intervention at an early time point may carry an elevated risk of intraoperative or immediate postoperative hemorrhage [51]. Newer techniques, such as endoscopic evacuation with the SCUBA technique, may mitigate the increased risk of bleeding previously associated with surgery in the early time period [52]. Clinical trials, such as the Dutch Intracerebral Hemorrhage Trial (DIST, NCT03608423) in the Netherlands, the Ultra-Early, Minimally inVAsive intraCerebral Haemorrhage evacUATion Versus Standard trEatment trial (EVACUATE, NCT04434807) in Australia, the Minimally Invasive IntRaceRebral HemORrhage Evacuation Registry (MIRROR, NCT04494295), and the planned Minimally Invasive Neuro-endoscopic Ultra-Early Targeted ICH Evacuation (MINUTE) trial in the United States, will evaluate the value of early minimally invasive ICH evacuation.

A Brief History of Surgery for ICH

The argument for surgical hematoma removal is to mitigate damage caused by the hematoma by removing the mechanical pressure that the hematoma exerts on the surrounding tissue and halting the secondary inflammatory injury pathways that appear to be dose- (clot volume) and time-dependent. Major trials evaluating the role of surgery for ICH have failed to demonstrate a benefit to surgery [53, 54]. However, single-center clinical trials, some multicenter trials, and a patient-level meta-analysis have suggested a benefit for minimally invasive ICH evacuation under certain conditions [55]. The 2015 AHA Guidelines for the management of

ICH state that surgical intervention should be recommended in the case of large cerebellar hemorrhages causing brain stem compression or hydrocephalus [7]. The remaining sections of this chapter will discuss the history of surgery for ICH, indications for decompressive surgery, and current options for minimally invasive surgical evacuation, and provide a case example.

Studies evaluating the benefits of surgery for ICH began in the 1960s. The first controlled study of craniotomy for supratentorial hematoma removal was published by McKissock in 1961 [56]. In this study, 180 patients presenting with spontaneous ICH were randomized to craniotomy with evacuation or medical management. The study showed no benefit to surgery regarding mortality or functional outcome. In 1989, Auer et al. randomized 100 patients at a single center to minimally invasive endoscopic evacuation versus medical management and showed improved favorable functional outcome (40 vs. 25%, $p < 0.01$) and mortality (40 vs. 25%, $p < 0.01$) 6 months after ictus in the surgical group [57]. By 1997, Prasad et al. analyzed 373 articles on surgery for ICH and concluded that endoscopic evacuation offered potential improvements for primary supratentorial intracerebral hematoma but necessitated a multicenter randomized trial [58].

In 2005, The Surgical Trial in Intracerebral Haemorrhage (STICH) found that patients with spontaneous supratentorial ICH who underwent early surgery did not have better outcomes compared to patients who underwent initial conservative therapy in regards to the primary outcome of all-cause mortality (36% vs. 41% (HR 0.86; 95% CI 0.72–1.04; $P = 0.12$) [53]. Post hoc subgroup analyses of patients in the STICH trial suggested that patients with GCS ≥ 9 and hemorrhages within 1 cm of the cortical surface may benefit from surgery. STICH II was therefore performed, selecting specifically for conscious patients with superficial hemorrhages [54]. Although STICH demonstrated a strong trend in favor of surgery, the result did not reach significance and, therefore, the take-home message from both STICH trials is that open surgery in general did not appear to result in improved outcome.

The Minimally Invasive Surgery Plus Rt-PA for ICH Evacuation (MISTIE) trial first published preliminary results demonstrating feasibility and safety in 2008 [59]. In 2016, MISTIE phase II found MIS + rt-PA to be safe and feasible while suggesting that the procedure may improve functional outcome at 6 months [60]. The Intraoperative Stereotactic Computed Tomography-Guided Endoscopic Surgery (ICES) study, a small 14 patient pilot endoscopic arm of MISTIE II, further suggested that endoscopic evacuation appeared reliable and safe in reducing hematoma volume (68 ± 21.6% reduction) in a short procedure (mean operative time 1.9 hours, IQR 1.5–2.2) with good functional outcome (43% mRS 0–3 at 6 months) [61].

MISTIE III was an open-label blinded endpoint trial at 78 hospitals across the world with 506 patients randomized to minimally invasive surgery or medical management. MISTIE phase III demonstrated that, overall, the MISTIE technique did not improve functional outcome in select patients with ICH. The study did, however, suggest a relationship between surgical evacuation percentage and functional outcome, such that in patients with ≤15 mL residual hematoma after surgery compared to medical management, functional outcome at one year appeared to be superior [62]. In this procedure, the prespecified surgical goal of ≤15 mL residual clot

volume was achieved in only 58% of patients. These barriers show that procedure standardization and rigorous training are critical in performing minimally invasive ICH evacuation. Beyond the goal of 15 mL residual volume, the MISTIE team demonstrated that each 1 mL of hematoma volume reduction below 15 mL leads to a 10% increase in the chance of the patient achieving a good functional outcome ($p = 0.002$) [63].

There are ongoing studies evaluating endoscopic hematoma evacuation techniques in addition to the DIST, EVACUATE, and MIRROR studies mentioned above. A Single-Arm, Feasibility Study of Minimally Invasive Endoscopic Surgical Treatment With Apollo for Supratentorial ICH (INVEST, NCT02654015) is a multicenter, single-arm feasibility study of endoscopic evacuation with an adjunctive aspiration device [64]. A Prospective, Multicenter Study of endoscopic evacuation with Artemis titled, Minimally Invasive Neuro Evacuation Device (MIND, NCT03342664) is an RCT comparing medical management versus endoscopic evacuation [65]. The Early MiNimally invasive Removal of IntraCerebral Hemorrhage (ENRICH, NCT02880878) trial is an RCT near completion at the time of writing of this chapter that compares early evacuation with the NICO system (Indianapolis, IA) to medical management.

Indications for Decompression

Decompressive hemicraniectomy is a surgical procedure used to relieve severely elevated intracranial pressure. The surgeon removes the skull bone flap to allow the edematous brain to swell outwards and to prevent herniation. In addition to reducing ICP, decompression can improve cerebral compliance, oxygen supply, and perfusion [66].

In one meta-analysis of decompressive hemicraniectomy, the procedure was mainly performed on patients with GCS scores of 8 or less and hematomas greater than 60 mL in volume [66]. The study found that hydrocephalus was the most frequent complication and occurred in approximately 20% of patients. In a preclinical study of decompressive craniectomy, rats underwent blood injection in the basal ganglia to induce ICH. They were then imaged and randomly allocated to undergo craniectomy at 1, 6, or 24 hours. The craniectomy groups had significantly lower mortality ($P < 0.01$), better neurological outcome ($P < 0.001$), and improved behavioral outcome. Additionally, the ICH + no craniectomy group trended toward more robust apoptosis [67]. However, decompression in humans with or without clot evacuation has not been shown to improve functional outcomes and is reserved to be used as a life-saving measure in select patients.

In cerebellar hemorrhage with a diameter greater than 3 cm or for clots causing brainstem compression or hydrocephalus through compression of the fourth ventricle, decompression should be performed as soon as possible [7]. Cerebellar decompression should also be performed in patients who are deteriorating neurologically, experiencing hydrocephalus due to ventricular obstruction, or

experiencing brainstem compression. If external drainage is placed without posterior fossa decompression, an upward herniation may occur [7].

Indications for Minimally Invasive Evacuation

Minimally invasive surgery for intracerebral hemorrhage evacuation remains a controversial treatment strategy. Numerous single-center studies and a large RCT in China have demonstrated a benefit for this strategy, and taken together, all RCTs up to 2018 demonstrated a functional benefit at the study endpoint with an OR of 0.46 (CI 0.36–0.57) that minimally invasive surgery led to a poor outcome at the study endpoint. Results from MISTIE 3 demonstrated that stereotactic thrombolysis with catheter drainage did not improve functional outcome at 1 year but reaching the surgical goal of leaving no more than 15 mL at the end of treatment may result in improved functional outcome, as discussed above. Additional studies linked the amount of hematoma removed to reduction in perihematomal edema, suggesting an antiinflammatory neuroprotective mechanism associated with clot removal.

Stereotactic Thrombolysis with Catheter Drainage

Stereotactic thrombolysis with catheter drainage ("the MISTIE Techniques") is the most rigorously studied minimally invasive strategy given the MISTIE 2 and MISTIE 3 studied. Patients are eligible to undergo this procedure if the CT angiogram does not show a spot sign and if the hematoma does not expand after a repeat stability CT. The procedure is often performed under general anesthesia and consists of stereotactic placement of an EVD catheter into the hematoma along the long axis. A 14F sheath is guided into the hematoma, the obturator is removed, and a 10 mL syringe is used for direct aspiration. After aspiration, an external ventricular drainage catheter is inserted into the cannula and tunneled out of the skin within a drainage system. The goal is to allow maximum exposure of the clot to instilled rt-PA [68]. The catheter is then left in place until 4 days or the surgical goal is met.

Craniopuncture

Craniopuncture is similar to the MISTIE technique. During craniopuncture, a disposable YL-1 craniopuncture needle is drilled into the skull and passed into the hematoma. Multiple needles may be placed into the same hematoma. After the needles are placed, a CT head is used to confirm their location within the bleed.

Urokinase is then injected into the hematoma and permitted to stay for 2 hours before being permitted to passively drain out. Before the future injections, any lysed hematoma is aspirated through the needles. In a 2008 randomized clinical trial, 377 patients were treated with craniopuncture versus medical management. The patient cohort presented with hematomas between 25 and 40 mL and a GCS of at least 9 [69]. The study found a significant benefit from craniopuncture: 40.9% of surgical patients were mRS 3–6, while 63% of the medical management arm were mRS 3–6 3 months after the hemorrhage.

Endoscopic Evacuation

Endoscopic evacuation is performed using a 19F or 6.3 mm stereotactically guided sheath and endoscopy, possibly with an adjunctive aspiration device. The sheath is placed into the hematoma and the endoscope is passed through the sheath. Evacuation can be performed in either the angio-suite or operating room. The surgeon can evaluate the percentage of blood removed using intraoperative CT or burr hole ultrasound [70]. If endoscopic evacuation is being done in the angio-suite, intraoperative cone-beam CT can be obtained to evaluate performance. Endoscopic evacuation can be performed in a dry or fluid-filled surgical field. Neuroendoscopy is well established in pediatric and tumor neurosurgery for ventricular, endonasal, and skull base surgery. Any bleeding vessels can be cauterized using a bipolar cautery device through the working channel of the endoscope. One day after the operation, a CT is performed. If rebleeding has not occurred, it should be used to validate the final hematoma evacuation percentage. Variations of endoscopic evacuation have been assessed in multiple studies including Auer et al. [57] and Intraoperative Stereotactic Computed Tomography-Guided Endoscopic Surgery (ICES) [61].

The Stereotactic ICH Underwater Blood Aspiration (SCUBA) technique is one way in which minimally invasive endoscopic evacuation can be performed, focusing on operating in a fluid-filled field with continuous irrigation use of an adjunctive aspiration instrument to achieve high evacuation rates while directly visualizing and cauterizing active bleeding vessels [71]. The SCUBA technique has demonstrated consistent hematoma evacuation percentages and good safety, averaging 87% evacuation over 100 patients with no patients suffering a symptomatic rebleed within 72 hours and only one patient suffering a symptomatic rebleed within 30 days [72]. Factors predicting functional outcome in patients undergoing SCUBA within 72 hours of ictus include advanced age, subcortical clot location, presence of IVH, and increased time to evacuation [52]. Unlike the MISTIE technique, the SCUBA technique can be performed emergently without demonstrated hematoma stability and in the presence of a spot sign, therefore making this surgical strategy applicable

to a wide range of patients presenting with ICH. The Minimally Invasive Endoscopic Surgical Treatment With Apollo/Artemis for Supratentorial ICH (INVEST) is a multicenter, single-arm feasibility study on the Apollo/Artemis system and Artemis Device for 20–80 mL hematomas in patients presenting with NIHSS≥6 [64]. A Prospective, Multicenter Study of Artemis a Minimally Invasive Neuro Evacuation Device (MIND) is a multicenter randomized clinical trial evaluating the Artemis Neuro Evacuation Device with medical management versus medical management alone [65]. The DIST trial is also underway to assess early endoscopic ICH evacuation performed within 8 hours.

Endoscope-Assisted Evacuation

Another variation of minimally invasive evacuation is endoscope-assisted evacuation of ICH is performed through a small craniotomy 2–3 cm in diameter, with a 1 cm stereotactic sheath or port through which to pass a thin endoscope and a multifunctional cannula to perform irrigation, cautery, and aspiration. Nagasaka et al. have shown the efficacy of this technique. In 15 cases, they achieved nearly complete hematoma evacuation. They were able to effectively manage Intraoperative arterial bleeding and did not observe any surgical complications or rebleeding [73]. Kuo et al. have demonstrated the safety and efficacy of this procedure in an ultraearly and early cohort of patients with subcortical ICH [74]. This group performed 68 evacuations within 12 hours with 84% of the procedures that were performed within 4 hours. In this largely ultraearly evacuation series, the hematoma evacuation rate was 93%, mean operative time was 85 minutes, and the rebleeding rate was 1.5%.

Surgiscopic Evacuation

Surgiscopic evacuation is similar to endoscopic evacuation while utilizing a novel scope with an enlarged working channel. The surgiscope is a device in which the port is disposable, and visualization is achieved with a small camera mounted on the mouth of the port permitting visualization down the channel [75]. A single multifunctional instrument, the Aurora Evacuator, is used down the enlarged working channel. The first edition of the Evacuator performed aspiration and morcellation, while the second iteration performs aspiration, morcellation, irrigation, and cauterization. The MIRROR and EVACUATE studies are underway monitoring patients who undergo evacuation with this technique in the early (< 12 hours) time window.

Endoport-Mediated Evacuation

In endoport-mediated evacuation, an endoport is stereotactically guided into the hematoma, and visualization is achieved through direct visualization with loupes, an exoscope, or microscope. In this technique, a craniotomy is performed, and often, a transsulcal parafascicular trajectory is chosen to minimally interrupt white matter fibers. This technique facilitates the use of bimanual surgery with suction and bipolar cautery making the technique accessible to a wide range of neurosurgeons. Labib et al. demonstrated the success of this technique in a multicenter series on 39 patients. The group reported hematoma evacuation over 90% in the majority of the patients and statistically significant improvements in GCS score [76]. The ENRICH RCT is underway evaluating early evacuation (within 24 hours of ictus) for hematomas in the 20–80 mL range who undergo minimally invasive endoport-mediated evacuation with the NICO BrainPath and Myriad evacuator.

Surgical Considerations with Case Example

With preclinical and clinical data in support of early evacuation, some trials and centers are performing early minimally invasive ICH evacuation. Minimally invasive surgiscopic evacuation is one form of evacuation that utilizes the Aurora System (Integra Lifesciences, New Jersey) which consists of a disposable port with a camera mounted on the proximal end called a Surgiscope and an aspiration/morcellation instrument called an Evacuator. A small 1.50-2c craniectomy is made at a point on the skull along the long axis of the hematoma. The Surgiscope is guided stereotactically into the center of the hematoma. The Evacuator is then used to gently evacuate the hematoma while avoiding causing bleeding from the friable cavity walls. If bleeding is encountered, monopolar cautery is transmitted through the Aurora Evacuator to cauterize the offending vessel. Irrigation is directed down the Surgiscope to wash the channel, facilitate the detection of bleeding or oozing vessels, and complete the evacuation.

The case example shown here is that of a 55-year-old male with hypertension and atrial fibrillation on aspirin who was brought in after being found down with left hemiplegia and confusion. The patient was able to communicate that the symptoms had just occurred prior to being found. CT head demonstrated a 35 mL right basal ganglia ICH and CT angiogram showed no spot sign, aneurysm, or vascular malformation (Fig. 17.3b). A repeat volumetric CT was performed shortly after for operative planning and demonstrated slight hematoma expansion, now measuring 40 mL (Fig. 17.3a). An access trajectory was planned into the center of the hematoma along the long axis of the hematoma (Fig. 17.3c).

After the evacuation was complete, an intraoperative cone-beam CT was performed, demonstrating good evacuation of the hematoma (Fig. 17.3d). A CT head

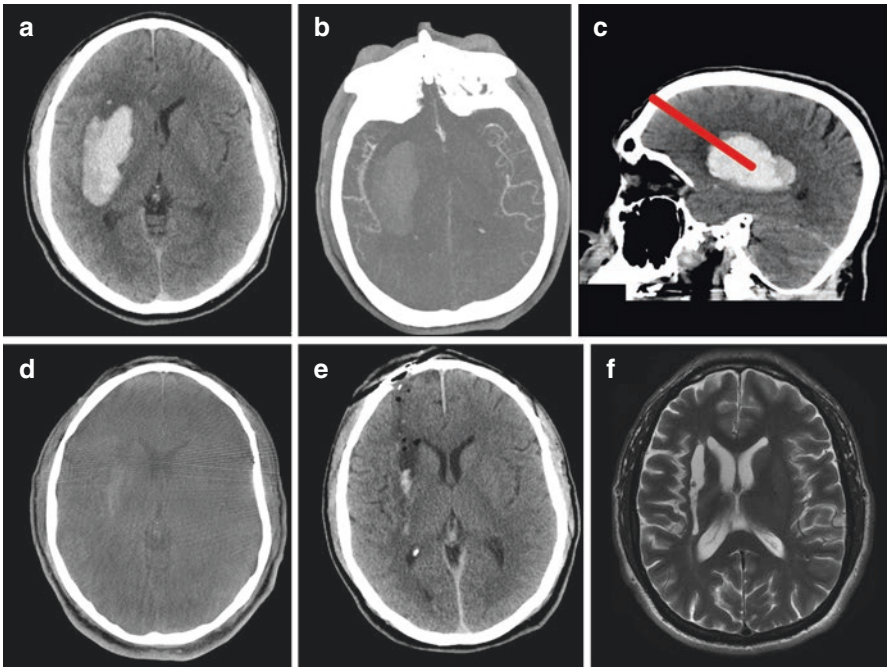

Fig. 17.3 (**a**) demonstrates a 40 mL right basal ganglia ICH; (**b**) is a CT angiogram demonstrating no spot sign, vascular malformation, or aneurysm; (**c**) demonstrates the planned trajectory along the long axis of the hematoma from a frontal starting point; (**d**) is an intraoperative cone-beam CT demonstrating good evacuation with minimal residual hematoma; (**e**) is a noncontrast head CT performed 24 hours after the procedure demonstrating a good evacuation with minimal residual blood; (**f**) is a T2 sequence of an MRI brain performed 6 months after the hemorrhage and evacuation demonstrating a small cavity in the prior location of the hemorrhage

was performed on postoperative day 1, approximately 24 hours after the procedure, which demonstrated good evacuation with a small amount of residual hematoma (Fig. 17.3e). The patient left the NSICU on post bleed day 3; at 30 days, he was walking 240 feet with a quad cane and climbing four stairs in acute rehab; and at 6 months, he was living at home independently with subtle left hand weakness and numbness for an mRS 3 and NIHSS 3. MRI at 6 months showed a small cavity at the location of the hematoma (Fig. 17.3f).

Conclusion

Despite significant effort in the form of randomized clinical trials, ICH remains the deadliest and most debilitating form of stroke. The mainstays of treatment remain stabilization through blood pressure and intracranial pressure control, anticoagulation reversal, and surgery for select patients. While major surgical evacuation trials

have been negative, evidence suggests that an active evacuation strategy performed at an early time point with strong training and quality metrics is likely to help patients with this disease. Past trials have taught the field a significant amount and shaped ongoing and near-future trials that are likely to advance the field.

References

1. Qureshi AI, Tuhrim S, Broderick JP, Batjer HH, Hondo H, Hanley DF. Spontaneous intracerebral hemorrhage. N Engl J Med. 2001;344:1450–60.
2. Krishnamurthi RV, Feigin VL, Forouzanfar MH, et al. Global and regional burden of first-ever ischaemic and haemorrhagic stroke during 1990–2010: findings from the global burden of disease study 2010. Lancet Glob Health. 2013;1:e259–81.
3. Arakawa S, Saku Y, Ibayashi S, Nagao T, Fujishima M. Blood pressure control and recurrence of hypertensive brain hemorrhage. Stroke. 1998;29:1806–9.
4. Naff NJ, Wemmer J, Hoenig-Rigamonti K, Rigamonti DR. A longitudinal study of patients with venous malformations documentation of a negligible hemorrhage risk and benign natural history. Neurology. 1998;50:1709–14.
5. An SJ, Kim TJ, Yoon B-W. Epidemiology, risk factors, and clinical features of intracerebral hemorrhage: an update. J Stroke Cerebrovasc Dis. 2017;19:3–10.
6. Tuhrim S. Intracerebral hemorrhage–improving outcome by reducing volume? N Engl J Med. 2008;358:2174–6.
7. Hemphill JC, Claude Hemphill J, Greenberg SM, et al. Guidelines for the management of spontaneous intracerebral hemorrhage. Stroke. 2015;46:2032–60.
8. Sinar EJ, Mendelow AD, Graham DI, Teasdale GM. Experimental intracerebral hemorrhage: effects of a temporary mass lesion. J Neurosurg. 1987;66:568–76.
9. Brott T, Broderick J, Kothari R, Barsan W, Tomsick T, Sauerbeck L, Spilker J, Duldner J, Khoury J. Early hemorrhage growth in patients with intracerebral hemorrhage. Stroke. 1997;28:1–5.
10. Davis SM, Broderick J, Hennerici M, Brun NC, Diringer MN, Mayer SA, Begtrup K, Steiner T, Recombinant Activated Factor VII Intracerebral Hemorrhage Trial Investigators. Hematoma growth is a determinant of mortality and poor outcome after intracerebral hemorrhage. Neurology. 2006;66:1175–81.
11. Guo T, Ren P, Li X, Luo T, Gong Y, Hao S, Wang B. Neural injuries induced by hydrostatic pressure associated with mass effect after intracerebral hemorrhage. Sci Rep. 2018;8:9195.
12. Wu TY, Sharma G, Strbian D, Putaala J, Desmond PM, Tatlisumak T, Davis SM, Meretoja A. Natural history of perihematomal edema and impact on outcome after intracerebral hemorrhage. Stroke. 2017;48:873–9.
13. Murthy SB, Moradiya Y, Dawson J, Lees KR, Hanley DF, Ziai WC, Collaborators VISTA-ICH. Perihematomal edema and functional outcomes in intracerebral hemorrhage: influence of hematoma volume and location. Stroke. 2015;46:3088–92.
14. Aronowski J, Zhao X. Molecular pathophysiology of cerebral hemorrhage: secondary brain injury. Stroke. 2011;42:1781–6.
15. Wagner KR, Xi G, Hua Y, Kleinholz M, de Courten-Myers GM, Myers RE, Broderick JP, Brott TG. Lobar intracerebral hemorrhage model in pigs: rapid edema development in perihematomal white matter. Stroke. 1996;27:490–7.
16. Wu G, Wang L, Wang F, Feng A, Sheng F. Minimally invasive procedures for intracerebral hematoma evacuation in early stages decrease perihematomal glutamate level and improve neurological function in a rabbit model of ICH. Brain Res. 2013;1492:140–7.

17. Wang L, Wu G, Sheng F, Wang F, Feng A. Minimally invasive procedures reduce perihematomal endothelin-1 levels and the permeability of the BBB in a rabbit model of intracerebral hematoma. Neurol Sci. 2013;34:41–9.
18. Lopez Valdes E, Hernandez Lain A, Calandre L, Grau M, Cabello A, Gomez-Escalonilla C. Time window for clinical effectiveness of mass evacuation in a rat balloon model mimicking an intraparenchymatous hematoma. J Neurol Sci. 2000;174:40–6.
19. Wu G, Zhong W. Effect of minimally invasive surgery for cerebral hematoma evacuation in different stages on motor evoked potential and thrombin in dog model of intracranial hemorrhage. Neurol Res. 2010;32:127–33.
20. Mould WA, Carhuapoma JR, Muschelli J, et al. Minimally invasive surgery plus recombinant tissue-type plasminogen activator for intracerebral hemorrhage evacuation decreases perihematomal edema. Stroke. 2013;44:627–34.
21. Mould WA, Muschelli J, Avadhani R, McBee N, Lane K, Thompson R, Ziai W, Zuccarello M, Awad I, Hanley DF. Reduction in perihematomal edema leads to improved clinical outcomes: results from the MISTIE III trial. Stroke. 2019;50:A15.
22. Claude Hemphill J, Bonovich DC, Besmertis L, Manley GT, Claiborne Johnston S. The ICH score. Stroke. 2001;32:891–7.
23. Clarke JL, Johnston SC, Farrant M, Bernstein R, Tong D, Hemphill JC 3rd. External validation of the ICH score. Neurocrit Care. 2004;1:53–60.
24. Fiebach JB, Schellinger PD, Gass A, et al. Stroke magnetic resonance imaging is accurate in hyperacute intracerebral hemorrhage: a multicenter study on the validity of stroke imaging. Stroke. 2004;35:502–6.
25. Kothari RU, Brott T, Broderick JP, Barsan WG, Sauerbeck LR, Zuccarello M, Khoury J. The ABCs of measuring intracerebral hemorrhage volumes. Stroke. 1996;27:1304–5.
26. Delcourt C, Carcel C, Zheng D, et al. Comparison of ABC methods with computerized estimates of intracerebral hemorrhage volume: the INTERACT2 study. Cerebrovasc Dis Extra. 2019;9:148–54.
27. Soun JE, Chow DS, Nagamine M, Takhtawala RS, Filippi CG, Yu W, Chang PD. Artificial intelligence and acute stroke imaging. Am J Neuroradiol. 2021;42:2–11.
28. Wei Y, Zhu G, Gao Y, Chang J, Zhang H, Liu N, Tian C, Jiang P, Gao Y. Island sign predicts hematoma expansion and poor outcome after intracerebral hemorrhage: a systematic review and meta-analysis. Front Neurol. 2020 https://doi.org/10.3389/fneur.2020.00429.
29. Qureshi AI, Ezzeddine MA, Nasar A, Suri MFK, Kirmani JF, Hussein HM, Divani AA, Reddi AS. Prevalence of elevated blood pressure in 563,704 adult patients with stroke presenting to the ED in the United States. Am J Emerg Med. 2007;25:32–8.
30. Sakamoto Y, Koga M, Yamagami H, et al. Systolic blood pressure after intravenous antihypertensive treatment and clinical outcomes in hyperacute intracerebral hemorrhage: the stroke acute management with urgent risk-factor assessment and improvement-intracerebral hemorrhage study. Stroke. 2013;44:1846–51.
31. Anderson CS, Heeley E, Huang Y, et al. Rapid blood-pressure lowering in patients with acute intracerebral hemorrhage. N Engl J Med. 2013;368:2355–65.
32. Qureshi AI, Palesch YY, Barsan WG, et al. Intensive blood-pressure lowering in patients with acute cerebral hemorrhage. N Engl J Med. 2016;375:1033–43.
33. Kalisvaart ACJ, Wilkinson CM, Gu S, Kung TFC, Yager J, Winship IR, van Landeghem FKH, Colbourne F. An update to the Monro–Kellie doctrine to reflect tissue compliance after severe ischemic and hemorrhagic stroke. Sci Rep. 2020. https://doi.org/10.1038/s41598-020-78880-4.
34. Gardner PA, Engh J, Atteberry D, Moossy JJ. Hemorrhage rates after external ventricular drain placement. J Neurosurg. 2009;110:1021–5.
35. Brain Trauma Foundation, American Association of Neurological Surgeons, Congress of Neurological Surgeons, et al. Guidelines for the management of severe traumatic brain injury. IX. Cerebral perfusion thresholds. J Neurotrauma. 2007;24(Suppl 1):S59–64.
36. Kamel H, Navi BB, Nakagawa K, Hemphill JC 3rd, Ko NU. Hypertonic saline versus mannitol for the treatment of elevated intracranial pressure: a meta-analysis of randomized clinical trials. Crit Care Med. 2011;39:554–9.

37. Flaherty ML, Kissela B, Woo D, Kleindorfer D, Alwell K, Sekar P, Moomaw CJ, Haverbusch M, Broderick JP. The increasing incidence of anticoagulant-associated intracerebral hemorrhage. Neurology. 2007;68:116–21.
38. Huhtakangas J, Tetri S, Juvela S, Saloheimo P, Bode MK, Hillbom M. Effect of increased warfarin use on warfarin-related cerebral hemorrhage. Stroke. 2011;42:2431–5.
39. Naidech AM, Batjer HH, Bernstein RA. Prior antiplatelet therapy and outcome following intracerebral hemorrhage: a systematic review. Neurology. 2011;76:1607.
40. Baharoglu MI, Cordonnier C, Al-Shahi Salman R, et al. Platelet transfusion versus standard care after acute stroke due to spontaneous cerebral haemorrhage associated with antiplatelet therapy (PATCH): a randomised, open-label, phase 3 trial. Lancet. 2016;387:2605–13.
41. Naidech AM, Maas MB, Levasseur-Franklin KE, et al. Desmopressin improves platelet activity in acute intracerebral hemorrhage. Stroke. 2014;45:2451–3.
42. Wada R, Aviv RI, Fox AJ, Sahlas DJ, Gladstone DJ, Tomlinson G, Symons SP. CT angiography "spot sign" predicts hematoma expansion in acute intracerebral hemorrhage. Stroke. 2007;38:1257–62.
43. Law ZK, Ali A, Krishnan K, et al. Noncontrast computed tomography signs as predictors of hematoma expansion, clinical outcome, and response to tranexamic acid in acute intracerebral hemorrhage. Stroke. 2020;51:121–8.
44. Zhang H-L, Linn J, Bruckmann H, Greenberg SM. Prevalence of superficial siderosis in patients with cerebral amyloid angiopathy. Neurology. 2010;75:1571; author reply 1571
45. Prabhakaran S, Naidech AM. Ischemic brain injury after intracerebral hemorrhage: a critical review. Stroke. 2012;43:2258–63.
46. Flaherty ML, Haverbusch M, Sekar P, Kissela B, Kleindorfer D, Moomaw CJ, Sauerbeck L, Schneider A, Broderick JP, Woo D. Long-term mortality after intracerebral hemorrhage. Neurology. 2006;66:1182–6.
47. Jolink WMT, Klijn CJM, Paul JA, Jaap Kappelle L, Vaartjes I. Time trends in incidence, case fatality, and mortality of intracerebral hemorrhage. Neurology. 2015;85:1318–24.
48. Broderick JP, Brott TG, Duldner JE, Tomsick T, Huster G. Volume of intracerebral hemorrhage. A powerful and easy-to-use predictor of 30-day mortality. Stroke. 1993;24:987–93.
49. Citerio G, Giulia Abate M. Faculty opinions recommendation of clinical grading scales in intracerebral hemorrhage. Faculty Opinions – Post-Publication Peer Review of the Biomedical Literature. 2010. https://doi.org/10.3410/f.4786957.4691055.
50. Kellner CP, Schupper AJ, Mocco J. Surgical evacuation of intracerebral hemorrhage: the potential importance of timing. Stroke. 2021;52:3391–8. https://doi.org/10.1161/AHA121032238.
51. Morgenstern LB, Demchuk AM, Kim DH. Rebleeding leads to poor outcome in ultra-early craniotomy for intracerebral hemorrhage. Neurology. 2001.
52. Kellner CP, Song R, Ali M, et al. Time to evacuation and functional outcome after minimally invasive endoscopic intracerebral hemorrhage evacuation. Stroke. https://doi.org/10.1161/STROKEAHA.121.034392.
53. Mendelow AD, Gregson BA, Fernandes HM, Murray GD, Teasdale GM, Hope DT, Karimi A, Shaw MDM, Barer DH, STICH investigators. Early surgery versus initial conservative treatment in patients with spontaneous supratentorial intracerebral haematomas in the International Surgical Trial in Intracerebral Haemorrhage (STICH): a randomised trial. Lancet. 2005;365:387–97.
54. Mendelow AD, David Mendelow A, Gregson BA, Rowan EN, Murray GD, Gholkar A, Mitchell PM. Early surgery versus initial conservative treatment in patients with spontaneous supratentorial lobar intracerebral haematomas (STICH II): a randomised trial. Lancet. 2013;382:397–408.
55. Gregson BA, Mitchell P, Mendelow AD. Surgical decision making in brain hemorrhage. Stroke. 2019;50:1108–15.
56. Mckissock W, Richardson A, Taylor J. Primary intracerebral hæmorrhage. Lancet. 1961;278:221–6. https://doi.org/10.1016/s0140-6736(61)90353-1. Accessed 19 Aug 2020
57. Auer LM, Deinsberger W, Niederkorn K, Gell G, Kleinert R, Schneider G, Holzer P, Bone G, Mokry M, Körner E. Endoscopic surgery versus medical treatment for spontaneous intracerebral hematoma: a randomized study. J Neurosurg. 1989;70:530–5.

58. Prasad K, Browman G, Srivastava A, Menon G. Surgery in primary supratentorial intracerebral hematoma: a meta-analysis of randomized trials. Acta Neurol Scand. 1997;95:103–10.
59. Morgan T, Zuccarello M, Narayan R, Keyl P, Lane K, Hanley D. Preliminary findings of the minimally-invasive surgery plus rtPA for intracerebral hemorrhage evacuation (MISTIE) clinical trial. Acta Neurochir Suppl. 2008;105:147–51.
60. Hanley DF, Thompson RE, Muschelli J, et al. Safety and efficacy of minimally invasive surgery plus alteplase in intracerebral haemorrhage evacuation (MISTIE): a randomised, controlled, open-label, phase 2 trial. Lancet Neurol. 2016;15:1228–37.
61. Vespa P, Hanley D, Betz J, et al. ICES (intraoperative stereotactic computed tomography-guided endoscopic surgery) for brain hemorrhage: a multicenter randomized controlled trial. Stroke. 2016;47:2749–55.
62. Hanley DF, Thompson RE, Rosenblum M, et al. Efficacy and safety of minimally invasive surgery with thrombolysis in intracerebral haemorrhage evacuation (MISTIE III): a randomised, controlled, open-label, blinded endpoint phase 3 trial. Lancet. 2019;393:1021–32.
63. Kellner CP, Arthur AS, Bain M, Fiorella D, Mocco J. MISTIE III: a big step in the right direction. J Neurointerv Surg. 2019;11:326–7.
64. INVEST feasibility – minimally invasive endoscopic surgery with Apollo in patients with brain hemorrhage. https://clinicaltrials.gov/ct2/show/NCT02654015. Accessed 18 Aug 2020.
65. MIND: Artemis in the removal of intracerebral hemorrhage. https://clinicaltrials.gov/ct2/show/NCT03342664. Accessed 18 Aug 2020.
66. Takeuchi S, Wada K, Nagatani K, Otani N, Mori K. Decompressive hemicraniectomy for spontaneous intracerebral hemorrhage. Neurosurg Focus. 2013;34:E5.
67. Marinkovic I, Strbian D, Pedrono E, Vekovischeva OY, Shekhar S, Durukan A, Korpi ER, Abo-Ramadan U, Tatlisumak T. Decompressive craniectomy for intracerebral hemorrhage. Neurosurgery. 2009;65:780–6, 1 p following 786; discussion 786
68. Carhuapoma JR, Barrett RJ, Keyl PM, Hanley DF, Johnson RR. Stereotactic aspiration-thrombolysis of intracerebral hemorrhage and its impact on perihematoma brain edema. Neurocrit Care. 2008;8:322–9.
69. Wang W-Z, Jiang B, Liu H-M, Li D, Lu C-Z, Zhao Y-D, Sander JW. Minimally invasive craniopuncture therapy vs. conservative treatment for spontaneous intracerebral hemorrhage: results from a randomized clinical trial in China. Int J Stroke. 2009;4:11–6.
70. Rothrock RJ, Chartrain AG, Scaggiante J, Pan J, Song R, Hom D, Lieber AC, Bederson JB, Mocco J, Kellner CP. Advanced techniques for endoscopic intracerebral hemorrhage evacuation: a technical report with case examples. Oper Neurosurg (Hagerstown). 2020. https://doi.org/10.1093/ons/opaa089.
71. Kellner CP, Chartrain AG, Nistal DA, Scaggiante J, Hom D, Ghatan S, Bederson JB, Mocco J. The stereotactic intracerebral hemorrhage underwater blood aspiration (SCUBA) technique for minimally invasive endoscopic intracerebral hemorrhage evacuation. J Neurointerv Surg. 2018;10:771–6.
72. Kellner CP, Song R, Pan J, et al. Long-term functional outcome following minimally invasive endoscopic intracerebral hemorrhage evacuation. J Neurointerv Surg. 2020;12:489–94.
73. Nagasaka T, Tsugeno M, Ikeda H, Okamoto T, Takagawa Y, Inao S, Wakabayashi T. Balanced irrigation-suction technique with a multifunctional suction cannula and its application for intraoperative hemorrhage in endoscopic evacuation of intracerebral hematomas: technical note. Neurosurgery. 2009;65:E826–7; discussion E827
74. Kuo L-T, Chen C-M, Li C-H, Tsai J-C, Chiu H-C, Liu L-C, Tu Y-K, Huang AP-H. Early endoscope-assisted hematoma evacuation in patients with supratentorial intracerebral hemorrhage: case selection, surgical technique, and long-term results. Neurosurg Focus. 2011;30:E9.
75. Troiani Z, Ascanio LC, Yaeger KA, Ali M, Kellner CP. Minimally invasive surgiscopic evacuation of intracerebral hemorrhage. J Neurointerv Surg. 2021;13:400.
76. Labib MA, Shah M, Kassam AB, et al. The safety and feasibility of image-guided BrainPath-mediated transsulcul hematoma evacuation: a multicenter study. Neurosurgery. 2017;80:515–24.

Chapter 18
Sinus Thrombosis

Eric Quach, Anand Kaul, and Rami O. Almefty

Background

Cerebral venous thrombosis (CVT) is a rare condition affecting the dural venous sinuses and cortical veins with potentially devastating neurological sequela. CVT may account for 0.5–1% of all cerebrovascular incidents [1]. The true incidence of CVT is likely higher than what is reported in the literature secondary to the difficulty of diagnosing CVT in a timely manner while the patient is asymptomatic. Delay in diagnosis leads to a dramatically high incidence of poor outcomes secondary to this disease process. The dural venous sinuses most affected are the superior sagittal sinus (70–80%), transverse sinuses, and sigmoid sinuses (70%), and less frequently the cavernous and straight sinuses. In one-third of cases, multiple sinuses are involved and cerebellar/cortical vein thrombosis has been demonstrated as high as 30–40% of the time [2].

Epidemiology

The first report of CVT was described in the nineteenth century by the French physician Ribes in a 45-year-old male with headaches and seizures [3, 4]. Shortly after, Abercrombie reported a case of CVT in a postpartum woman with headaches and seizures [5]. Both cases of CVT were discovered at the time of autopsy, as would often be the case until the advent and proliferation of catheter-based angiography,

E. Quach · A. Kaul · R. O. Almefty (✉)
Department of Neurosurgery, Temple University Hospital, Philadelphia, PA, USA
e-mail: eric.quach2@tuhs.temple.edu; anand.kaul@tuhs.temple.edu; rami.almefty@tuhs.temple.edu

J. R. Mascitelli, M. J. Binning (eds.), *Introduction to Vascular Neurosurgery*,
https://doi.org/10.1007/978-3-030-88196-2_18

CT, and MRI venography which helped to facilitate earlier diagnosis. These imaging modalities helped facilitate earlier diagnosis of CVT and development of studies and patient registries to further understand CVT, its true incidence, natural history, diagnosis, and management [3, 6–8]. Early angiographic studies demonstrated mortality rates in the 30–50% range [9]. The largest study to date, the International Study on Cerebral Venous and Dural Sinuses Thrombosis (ISCVT), was a multinational, prospective, observational study evaluating patients with CVT from 1998 through 2001. Ultimately, 624 patients were enrolled and followed with an overall mortality rate of 4.3% in the acute phase, and 3.4% mortality 30 days from symptom onset [6].

Risk Factors

The pathogenesis of thrombus formation within the dural venous sinuses is manifold (Table 18.1). Systemic illnesses, malignancy, infections, and intracranial abnormalities associated with the release of pro-inflammatory cytokines and

Table 18.1 Causes and risk factors associated with cerebral venous sinus thrombosis

Acquired prothrombotic states	**Mechanical**
Pregnancy	Neurosurgical procedures
Antiphospholipid antibody	Trauma
Nephrotic syndrome	Intravenous drug abuse
	Jugular vein catheterization
Genetic prothrombotic conditions	**Infections**
Protein C and S deficiency	Sinusitis
Protein C resistance	Mastoiditis
Prothrombin mutation	Meningitis
Antithrombin deficiency	Systemic infections
Methylenetetrahydrofolate reductase (MTHFR) mutations	
Hematological and oncological diseases	**Drugs**
Central nervous system tumors	Oral contraceptives
Systemic malignancies	Hormone replacement therapy
Hematological malignancies	Androgen therapy
Polycythemia	Lithium
Heparin-induced thrombocytopenia	Intravenous immunoglobulin therapy
Paroxysmal nocturnal hemoglobinuria	Illicit drugs
Thrombocythemia	Steroids
	Asparaginase
Inflammatory and autoimmune diseases	**Miscellaneous causes**
Systemic lupus erythematosus	Dehydration
Behcet's syndrome	Arteriovenous malformations
Sarcoidosis	Dural AV fistulas
Inflammatory bowel disease	Postradiation effect
Wegener granulomatosis	

alteration in cerebral blood flow can portend to increased risk of thrombus formation and propagation. CVT has a reported female sex predominance specifically among women of ages 24–35. Studies have shown that approximately 70–80% of CVT occurs in females of reproductive age [10] likely secondary to the elevated risk of thromboembolism and secondary to oral contraceptive medications, pregnancy, and puerperium. Hypercoagulable states such as blood coagulation cascade abnormalities such as protein C/S deficiency, antithrombin III dysfunction, prothrombin gene mutation G21210A, and Factor V Leiden. Underlying malignancy, inflammatory conditions, cranial trauma, and intracranial infections can cause space-occupying lesions which can either directly cause vascular compression and alteration in venous outflow or create a pro-inflammatory prothrombotic state increasing the risk of CVT and cortical vein thrombosis propagation. Iatrogenic causes of venous thrombosis have been reported as well, secondary to various skull base neurosurgical approaches and direct sinus injury [11] or intracranial hypotension secondary to CSF leak after lumbar puncture or spinal anesthesia [12].

Prognostic Factors

Based on data from the ISCVT trial, GCS less than nine on presentation, cerebral hemorrhage, malignancy, male sex, age >37 years, mental status disorders defined as frontal lobe syndromes, delirium, personality changes, thrombosis involving the deep cerebral venous system, and CNS infection were found to be related to increased risk of death or dependence [6]. Additional studies have included parenchymal lesions greater than 6 cm and the presence of bilateral Babinski signs upon presentation as predictors of poor outcome [13]. Prognostic scoring systems such as the CVT Grading Scale have been developed using these variables in order to help predict patient outcomes (Tables 18.2 and 18.3) [13, 14].

Table 18.2 Proposed CVT grading scale variables and risk points

Prognostic variables	Risk points assigned
Parenchymal lesion >6 cm	3
Bilateral Babinski signs	3
Coma	3
Male gender	2
Stupor	2
Parenchymal hemorrhage	2
Somnolence	1
Awake and alert	0

Adapted from Barboza et al. [13]

Table 18.3 CVT grading scale, classification, and associated mortality

CVT grading scale	Grading classification	30-Day mortality
0–2	Mild	0.4%
3–7	Moderate	9.9%
8–13	Severe	61.4%
Total score range: 0–13		

Adapted from Barboza et al. [13]

Presentation

The presentation for patients with CVT is dependent on the underlying etiology as well as the chronicity of thrombus. Acute CVT presentations are commonly noted with infectious or obstetric etiologies (28%), while subacute (41%) and chronic (31%) are most commonly noted with inflammatory disorders [2]. The presenting symptoms are also dependent on which sinus is involved, rate of thrombus propagation, and thrombus burden [2].

Headache is commonly the primary presenting symptom reportedly occurring in 74–90% of patients. It is possible to miss this in the diagnostic workup of usually, unexpected or severe headaches. In rare cases, acute onset thunderclap headaches may be a harbinger of acute CVT [15]. The common signs and symptoms of elevated intracranial pressure such as headaches, nausea, vomiting, vertigo, dizziness, and visual disturbances with or without papilledema are possible. Pseudotumor cerebri (PTC) can insidiously present in similar fashion and also commonly in young women of child bearing age. However, PTC should be considered a diagnosis of exclusion and venous imaging should be obtained to distinguish the two entities [16, 17]. Adults may present with seizures at the time of diagnosis of CVT in 32–39% of cases [18, 19]. CVT generally does not present with focal neurological deficits such as cranial nerve palsies; however, in the setting of venous infarction and hemorrhagic conversion, these deficits are more likely.

Cerebral venous thrombosis results in a state of venous hypertension and cerebral ischemia leading to neuronal cell death, and cerebral edema with hemorrhagic conversion of the infarction often leading to elevated intracranial pressure [20]. Venous hypertension leads to dilated venous vasculature and cerebral capillary beds which causes an increase in interstitial brain edema. Decreased venous outflow leads to a decrease in capillary bed perfusion pressures and overall increased cerebral blood volume with a concurrent decrease in cerebral blood flow. A decrease in blood flow can lead to local cerebral ischemia which decreases oxygen delivery necessary for Na/K ATPases leading to a large influx of water and subsequent cell death characteristic of cytotoxic edema in greater proportion to the extracellular fluid shifts seen in vasogenic edema. Venous hypertension results in eventual tearing of veins, resulting in both subarachnoid and intraparenchymal hemorrhage [21].

Diagnosis

The natural history of CVT is one that is inherently a chronic process with a highly variable clinical presentation. The high degree of redundancy within the cerebral venous system allows for the differential collateralization of venous outflow in the setting of veno-occlusive disease. This is also why venous infarction is a more insidious process which may go clinically unnoticed for some time. Cerebral veins are valveless, unlike peripheral veins, and thus, the directionality of flow is dependent entirely on pressure gradients [22]. These alterations in flow allow for a mild degree of compensation secondary to venous dilatation. The flow through these neighboring territories is generally sluggish and can even completely halt flow which will eventually lead to propagation of thrombus along cortical venous channels overall worsening venous hypertension and its sequala. The average delay in diagnosis from the onset of symptoms is approximately 7 days [3, 23].

Noncontrast computed tomography head is a useful modality for the initial evaluation of patients in whom there is a concern for active neurological dysfunction. Acute thrombus in a cerebral vein may appear as a hyperdensity in a venous tubular shape known as a "cord" sign in 20–25% of cases and disappears generally within 1–2 weeks [2, 10, 24] (Fig. 18.1). Venous hyperdensity is a rather nonspecific sign, however, and can represent physiological derangements such as an elevated hematocrit in patients with polycythemia or dehydration [24]. In these latter scenarios, it is more likely that the entirety of the vascular network appears hyperdense rather than a single or few venous channels.

Prolonged occlusion may show early venous infarction in the form of hypodensity and cerebral edema in a nonarterial vascular distribution with or without the presence of hemorrhage. Contrast-enhanced CT may demonstrate an "empty delta" sign within the dural venous sinuses which can be further elucidated with a CT

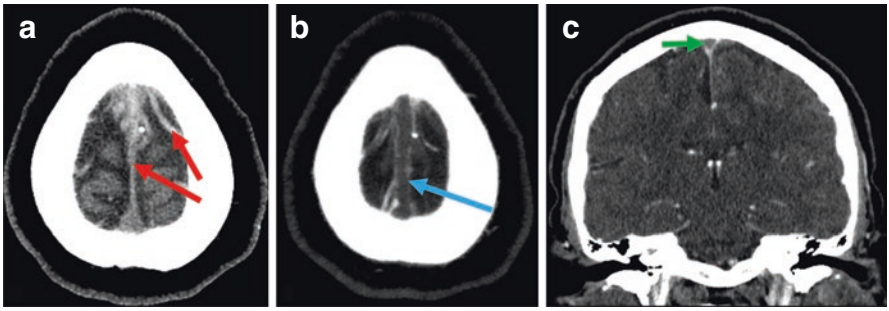

Fig. 18.1 Diagnostic computed tomography (CT) of venous sinus thrombosis. (**a**) Axial noncontrast CT head showing hyperdensity within the superior sagittal sinus and within thrombosed cortical veins known as "cord sign." (red arrows) (**b**) CT venography axial image showing lack of contrast filling within the superior sagittal sinus (blue arrow) and (**c**) coronal image displaying "empty-delta" sign signifying lack of venous contrast enhancement in the occluded superior sagittal sinus (green arrow)

venogram [2, 24] (Fig. 18.2). MRI is the most sensitive diagnostic modality for identifying thrombus secondary to CVT secondary to its ability to identify blood degeneration products with high sensitivity, specifically on T2-weighted images and gradient recalled echo (GRE) (Fig. 18.3) [24]. An acute clot appears isointense on T1 sequence and hypointense on T2 sequence and has FLAIR signal similar to the appearance of a normal dural venous sinus, potentially obscuring appropriate diagnosis [24] (Table 18.4). Magnetic resonance venography (MRV) and GRE sequences improve diagnostic accuracy as thrombus would appear hypointense amid the normal venous flow-related hyperintensity [24]. Subacute (7–14 days old) methemoglobin demonstrates hyperintensity in all T1, T2, GRE, and diffusion sequences [24]. Chronic thrombus will appear less uniform in regard to clot signal, but signal characteristics include isointense T1, iso-hyperintense T2, and hypointense GRE [24].

In cases where CT and MR imaging cannot definitively confirm the diagnosis of cortical vein or CVST, digital subtraction angiography may be indicated (Fig. 18.4). The angiogram can be especially helpful in identifying cortical venous thrombosis even in the absence of sinus thrombosis [25].

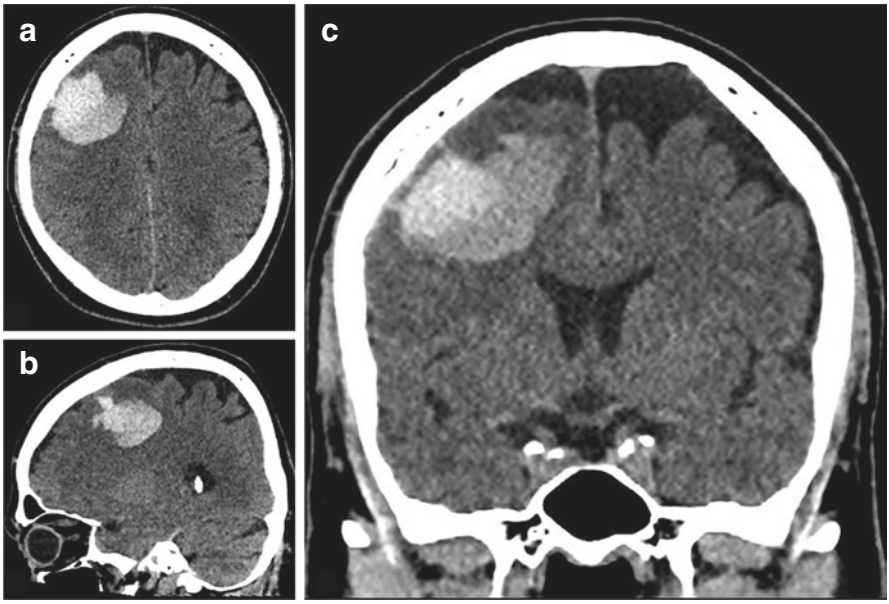

Fig. 18.2 Noncontrast computed tomography (CT) showing venous infarct in axial (**a**) sagittal (**b**) and coronal (**c**) planes. There is mixed density within the intraparenchymal hematoma cavity indicating both acute and subacute blood products within the infarct. A regional mass effect is noted secondary to surrounding vasogenic edema around the clot. Note that there is no definitive vascular territory for this infarction as with arterial stroke and the clot appears to come to the cortical surface indicating the likelihood of an occluded cortical vein

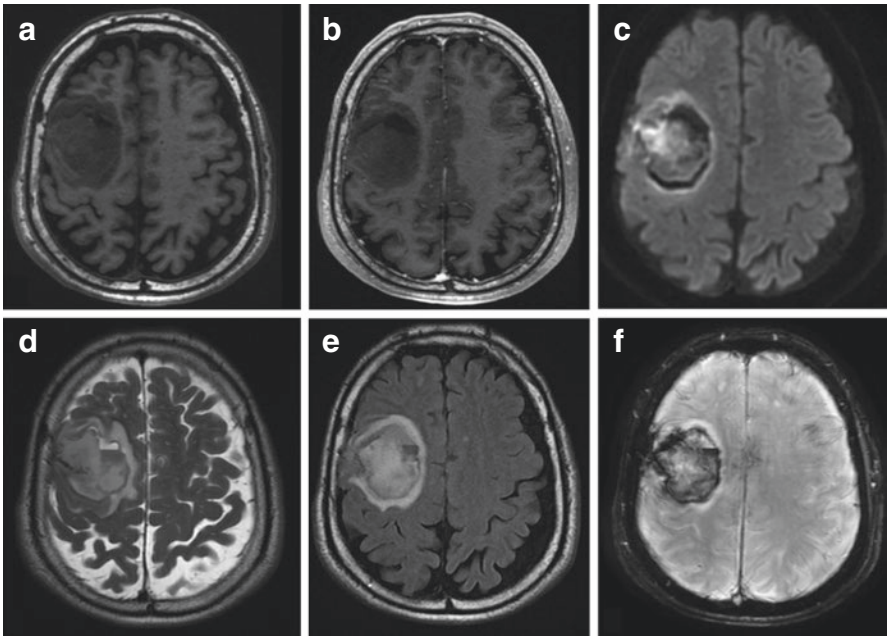

Fig. 18.3 Axial magnetic resonance imaging (MRI) sequences showing venous infarction with surrounding vasogenic edema. Pre- and post-gadolinium-enhanced T1 sequences show in **a** and **b**, respectively. Diffusion-weighted imaging (**c**), T2 (**d**), and FLAIR (**e**) demonstrate the extent of not only venous infarct but surrounding cytotoxic and vasogenic edema. Gradient recalled echo (GRE) shown in (**f**) pertinent for showing mineralized deposits which indicates blood products

Table 18.4 Appearance of venous sinus thrombosis on MRI based on age of clot

Age	T1	T2/FLAIR	GRE	DWI
Acute (0–5 days)	Isointense	Hypointense	Hypointense	–
Subacute (5–14 days)	Hyperintense	Hyperintense	Hyperintense	Hyperintense
Chronic (>14 days)	Isointense	Iso-hyperintense	Hypointense	–

Adapted from Bonneville [24]
(−) indicates high variability

Management of CVT Associated Complications

Seizures

Seizures occur in 32–39% of patients at the time of diagnosis of CVT with death from status epilepticus occurring in nearly 12.8% of patients [18, 19, 26]. Early seizures, as defined as 2 weeks within diagnosis, occurred in 6.9% of patients and were associated with supratentorial lesions. Antiepileptic drugs were associated with a 70% lower risk of early seizures developing in patients with a supratentorial

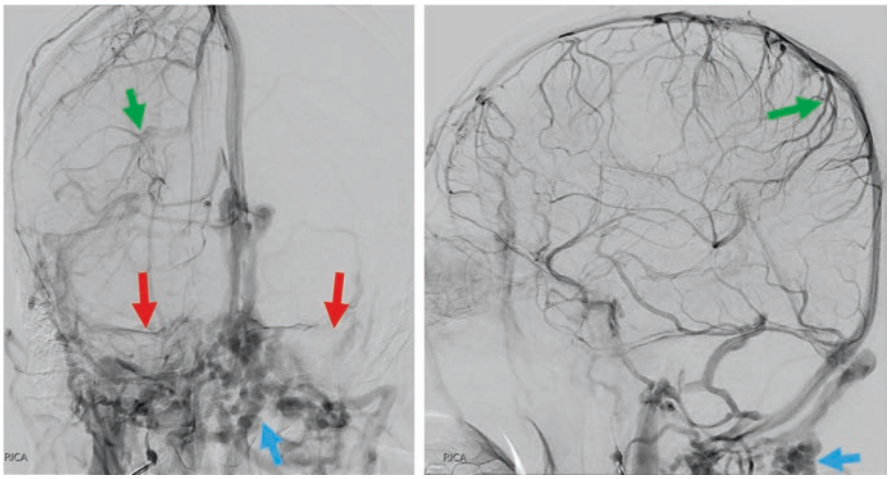

Fig. 18.4 Anterior–posterior (AP) and lateral radiographs of the venous phase of a diagnostic digital subtraction angiogram from a right internal carotid artery injection indicating bilateral transverse sinus occlusions (red arrows). The lack of venous outflow through transverse sinuses causes significant venous congestion (green arrows) within the cortical venous system late into the venous phase and the development of suboccipital neck muscle venous collaterals for aid in venous outflow (blue arrows)

lesion that did not present with a seizure, but this was a nonsignificant relationship [27]. Parenchymal lesions on CT/MRI at diagnosis were associated with an increased risk of seizures, particularly if the patient also presented with sensory deficits [19]. Other studies have also demonstrated that the presence of a motor deficit, intracranial hemorrhage, and cortical vein thrombosis may be independent predictors of early epileptic seizures [26]. Furthermore, based on ISCVT data, seizures were the most frequent complication encountered at follow-up, with 10% of patients reporting late seizures [6]. As a result, patients with CVT and high-risk factors for the development of seizures may be considered for antiepileptic prophylaxis in these patients, but due to the lack of evidence, both the AHA and ESO do not make guidelines regarding the routine use of antiepileptic prophylaxis in patients that did not present with seizures [1, 26–28]. Data are lacking regarding the relationship between antiepileptics and functional outcome data as well as the particular antiepileptic choice and duration [1].

Hydrocephalus and Intracranial Hypertension

CVT may impair the ability of arachnoid granulations to absorb CSF, resulting in communicating hydrocephalus in up to 4% of patients with CVT [29]. Obstructive hydrocephalus may occur due to intraventricular hemorrhage from venous

infarction that results in parenchymal hemorrhage, although this is typically seen in neonates due to internal cerebral vein thrombosis [30, 31].

Nearly 40% of patients with CVT will demonstrate isolated intracranial hypertension and present with papilledema and third and/or sixth nerve palsies. This is secondary to CSF malabsorption due to impaired arachnoid granulation absorption, as well as venous outflow obstruction due to sinus thrombosis [18]. Prolonged untreated papilledema can result in permanent blindness unless the underlying cause of elevated ICP is addressed with CSF diversion. Optic nerve sheath fenestration has been performed in order to treat papilledema and visual loss secondary to cerebral venous sinus thrombosis, but does not directly address the underlying etiology of intracranial hypertension and is not common practice [32]. Directed treatment of the thrombosis including anticoagulation to aid in recanalization of venous outflow may result in the reduction of intracranial pressure, but for refractory situations, methods for CSF diversion with ventricular drains, lumbar punctures, and ventriculo- or lumboperitoneal shunts in persistent situations may be necessary. Despite this, there are data to suggest that shunting in the acute setting of CVT may not be effective in preventing death, but this study included patients in which shunting rather than a decompressive craniectomy was the primary treatment even in the presence of a space-occupying lesion [33]. Such procedures may interrupt anticoagulation or have an elevated procedural risk due to periprocedural anticoagulation. Ultimately, if intracranial hypertension remains refractory despite maximal medical therapies such as osmotic diuresis and hypertonic therapy, a decompressive craniectomy may be performed as a life-saving procedure.

Development of Dural Arteriovenous Fistulas

Thrombosis of the sagittal sinus, transverse sinus, and cavernous sinuses have been demonstrated to induce dural arteriovenous fistulas (dAVF) and pial fistulas after cortical vein thrombosis [34]. The occurrence of a dAVF after CVT is not well known due to lack of available studies with cerebral angiographic follow-up data. dAVFs may also result in CVT due to prolonged venous hypertension, and given the increased risk of hemorrhage with dAVFs, systemic anticoagulation as would be typically done for CVT without treatment of the fistula may result in poor outcomes [35]. A dAVF should remain in the differential in any patient with a prior history of CVT presenting with new neurological symptoms.

Treatment

Guidelines from the AHA and ESO support the rapid initiation of anticoagulation upon diagnosis of cerebral venous thrombosis to prevent thrombus propagation and aid with recanalization of the venous sinus. Functional recovery has been tied to

venous sinus recanalization, with a 3.3-fold increase in odds of complete functional recovery [36]. The rate of recanalization after anticoagulation has been reported to be from 47 to100%, with most instances occurring in the first few months after treatment for CVT but may occur up to 1 year [36].

The use of heparin and anticoagulation for treatment of CVT had remained controversial for decades due to concern regarding the risk of promoting or aggravating intracerebral hemorrhage. In the 1990s, two published randomized controlled trials examining the treatment of cerebral venous thrombosis with intravenous heparin or low-molecular-weight heparin (LMWH) comprising a total of 79 patients demonstrated decreased mortality and improved functional outcomes in those receiving anticoagulation, even with the presence of pretreatment intracranial hemorrhage [37, 38].

The first randomized, blinded, placebo-controlled trial of intravenous heparin for CVT was carried out in a single center in Berlin. The study was halted after enrolling 20 patients due to interim analysis demonstrating increased mortality in the placebo arm [37]. The study enrolled patients with venous sinus thrombosis as demonstrated on catheter-based angiography. The primary outcome of the study was measured by clinical status at 3 months, with the secondary outcome being intracranial hemorrhage. A total of 20 patients were enrolled, with ten patients receiving intravenous unfractionated heparin (UFH) administered as a 3000 unit bolus followed by an adjusted-dose continuous infusion titrating activated partial thromboplastin time to 2–2.5 control values and ten patients receiving placebo. Of the heparin group, by 3 months, eight recovered completely and two were classified as having mild deficits. In the placebo group, one recovered completely, six had minor deficits, and three died by 3 months. Notably, no patient in the heparin group developed ICH, while two in the placebo group did [37]. The authors also retrospectively evaluated the relationship between heparinization and development of intracranial hemorrhage. The study authors felt that the data demonstrated the effectiveness of heparin as a treatment for CVT and that it did not promote intracranial hemorrhage.

A second randomized controlled trial was carried out at multiple centers in The Netherlands and the UK where patients were randomized to LMWH nadroparin or placebo. Patients were diagnosed with CVST via catheter-based angiography or by MRI. Primary outcomes were scores for activities of daily living, the Oxford Stroke Handicap scale, and death. Secondary endpoints included symptomatic ICH and other bleeding. At 3 months, 21% of the placebo group had a poor outcome compared to 13% in the LWMH group. This demonstrated a nonsignificant improvement in the proportion of participants achieving a good functional outcome for LMWH [38]. There was no symptomatic hemorrhage in either group, with one patient suffering a nonfatal hemorrhage in the LWMH group.

A Cochrane meta-analysis of the 79 patients in the two trials demonstrated a nonsignificant difference in favor of therapeutic treatment of CSVT with heparin. In these trials, no patients on heparin developed new ICH formation and only one patient receiving nadroparin developed a nonfatal hemorrhage [39].

There have been additional retrospective and observational studies evaluating the efficacy of anticoagulation for CVT in various circumstances such as patients with

preceding intraparenchymal hemorrhage and the presence of posterior fossa lesions consisting of hemorrhage, infarct, or edema [6, 37, 40]. In a retrospective series of CVT patients, 42% presented with concurrent ICH. Those treated with IV heparin demonstrated 52% complete recovery and a 15% mortality rate. In patients that were not anticoagulated, 23% demonstrated complete recovery with a mortality rate of 69% [37].

The ISCVT study demonstrated that 39% of patients with CVT presented with ICH, of which 73% were treated with UFH within 24 hours of presentation. Delayed ICH, defined as the development of hemorrhage after presentation occurred in 5.8% of all patients in the study, with 63.9% occurring in those that had already presented with parenchymal hemorrhage. While the development of delayed ICH was associated with the presence of intraparenchymal hemorrhage on admission, delayed hemorrhage in these patients was not influenced by heparin after a multivariate analysis was performed [41]. While posterior fossa lesion in the setting of CVT was a poor prognostic factor with a nonsignificant increase in the rates of new hemorrhage with anticoagulation in these patients, the decrease in poor outcomes favored anticoagulation despite the presence of posterior fossa lesions [40]. Overall, data from the aforementioned studies illustrate improved functional recovery and decreased morbidity with anticoagulation for CVT even in the setting of parenchymal hemorrhage compared to those that did not receive treatment. As a result, anticoagulation remains the recommended initial treatment of CVT even in the setting of intracranial hemorrhage [1, 28]. This must be tailored with the specific patient situation and the risks and benefits of anticoagulation weighed.

Choice of Anticoagulant

Most data regarding anticoagulation of CVT in the acute phase support the utilization of UFH or LWMH. Data from venous thromboembolism treatment for DVT, PE, and CVT management have demonstrated a decreased risk of major hemorrhage including development of fewer intracerebral hemorrhages, thrombotic complications, and death with LWMH when compared to heparin [42, 43]. An additional randomized trial specifically examined patients with CVT and directly compared LMWH with UFH in adult patients with cerebral venous thrombosis. Patients were randomized to LMWH and UFH groups for 14 days followed by oral anticoagulation. In total, 19% of those allocated to heparin died during hospitalization compared with 0% in the LMWH group. Major hemorrhagic complications occurred only in the heparin group, although they were all extracranial complications [44]. As a result, EAN and AHA guidelines suggest that LWMH may be preferred to unfractionated intravenous heparin given data suggesting improved efficacy and safety of LMWH over heparin [1, 28]. Heparin remains an option in patients that are unable to receive LMWH due to renal insufficiency or in patients that may require emergent neurosurgical procedures and require rapid reversal of heparin with protamine sulfate. An additional disadvantage of heparin is that it requires titration of

the infusion to achieve therapeutic levels, and there may be delays and difficulties maintaining a therapeutic window due to reliance on serial lab draws to titrate dosing.

The recommended duration of anticoagulation remains controversial, with data consisting of observational studies supporting the initiation of anticoagulation with LMWH or UFH as a bridge to oral anticoagulation with a vitamin K antagonist in order to help promote recanalization and prevent recurrence of CVT or other venous thromboembolic events [45]. There is an overall 6.5% annual risk of recurrent systemic venous thrombosis in patients with CVT [6]. Of the patients with recurrent CVT and/or VTE at remote sites, 64.3% of patients with recurrent CVT and 58.3% of patients with VTE were on anticoagulation at the time of recurrence [6, 46]. 63% of the recurrent CVT and/or VTE occurred within the first year [6, 46]. The AHA guidelines recommend bridging to a vitamin K antagonist with a goal INR of 2–3 for 3–6 months in patients with a provoked CVT, 6–12 months with unprovoked CVT, and indefinite anticoagulation in those with recurrent CVT, VTE after CVT, or any patient with severe thrombophilia with a first CVT event [1].

With the emergence of direct oral anticoagulants (DOACs), there remain little data regarding the benefits of DOACs over vitamin K antagonists. There has been one randomized trial comparing patients with CVT to either treatment with Warfarin or Dabigatran after being stabilized on 5–15 days of systemic anticoagulation with IV heparin. Both Warfarin and Dabigatran were found to have similar risks of bleeding and recanalization rates with no recurrent VTE in either group (Ferro 2019). Two small observational case series have evaluated the utilization of rivaroxaban ($n = 7$) and dabigatran ($n = 15$) as long-term oral anticoagulation for patients with CVT and did not find any major hemorrhagic complications or recurrent thrombotic events, suggesting that DOACs may be a safe and effective oral anticoagulation option in patients with CVT [47, 48].

Endovascular Management

While most patients with CVT recover with anticoagulation therapy alone, approximately 20% of patients with CVT may continue to deteriorate despite anticoagulation [1, 6, 28]. It is proposed that patients with larger and more extensive thrombus burden are at higher risk for deterioration and that endovascular treatment may help rapidly decrease thrombus burden, promote swift recanalization of the venous sinus, and quickly decrease venous congestion. However, there have been insufficient data to define specific indications and patient populations that would benefit from endovascular CVT management. Furthermore, there are no well-defined criteria for what constitutes failure of anticoagulation and timeline to define treatment failure. The majority of data regarding endovascular treatments for CVT are based predominantly on case reports and case series.

There has been one randomized control trial, Thrombolysis or Anticoagulation for Cerebral Venous Thrombosis (TO-ACT), randomizing patients with severe

CVT to standard medical care with systemic anticoagulation or to mechanical and/or catheter-directed thrombolysis along with standard medical care with systemic anticoagulation [49]. The study involved eight centers and included patients with CVT and a high probability of poor outcome defined as the presence of mental status disorder (delirium, personality or behavioral changes, and frontal lobe syndromes), Glasgow Coma Scale score less than 9, ICH, or thrombosis involving the deep cerebral venous system. The study was terminated after preliminary analysis demonstrated that the mortality rate was higher in patients randomized to endovascular treatment at 6 and 12 months (12% vs 3%) [49]. There was a nonsignificant decreased rate of new symptomatic ICH in the endovascular group (3% vs 9%) [49].

Citing the strength of current data comprised predominantly case reports and case series, the ESO does not make guidelines regarding endovascular treatment of CVT, while the AHA feels that endovascular management is an option if clinical deterioration occurs [1, 28].

Endovascular strategies for the treatment of CVT include catheter-directed thrombolysis, direct aspiration thrombectomy, stent-retriever thrombectomy, balloon thrombectomy, and balloon angioplasty and stenting. There are little data to suggest that one strategy should be utilized over the other [50]. Utilization of these techniques requires both arterial access to perform diagnostic cerebral angiography with the utilization of the venous phase to visualize the sinus occlusion, and venous access to provide the working channel through which the intervention would be performed. Additionally, long-term anticoagulation remains necessary even with these endovascular management options for CVT in order to prevent recurrent thrombosis [51].

Catheter-Directed Thrombolysis

There have been many reports utilizing various thrombolytic agents, such as urokinase, streptokinase, and tissue plasminogen activator for the treatment of cerebral venous sinus thrombosis, even in the presence of hemorrhagic venous infarcts. Treated patients typically presented with poor neurological exams or had failed heparin anticoagulation, and the decision to proceed with endovascular management was made when the patient's neurological exam is declined. Patients with extensive CVT have been treated with a microcatheter infusion at 1–2 mg/hour with repeat angiography performed at 12–24 hours to measure response to thrombolysis and guide the conclusion of therapy. Catheter-directed thrombolysis has been successfully used as an adjunct for multimodality endovascular treatment for CVT [52]. The risk of intracranial hemorrhage remains a risk though, with a systematic review and analysis demonstrating new ICH formation in 17% of patients after thrombolysis, with 5% suffering a clinical decline as a result [53].

Direct Aspiration Thrombectomy

The use of large-bore distal aspiration catheters, originally designed for intracranial arterial thrombectomies, has been applied to perform thrombus aspiration in CVT, often in conjunction with catheter-directed thrombolysis and stent-retriever thrombectomy [54, 55]. Primary treatment of CVT with just direct aspiration may also decrease the time needed to recanalize the venous sinus by foregoing administration of thrombolytics, with similar recanalization rates and favorable outcomes compared to administration of thrombolytics with direct aspiration [54]. The AngioJet device (MEDRAD Inc., Warrendale, Pennsylvania, USA) was initially designed for peripheral vascular and coronary thrombectomies via rheolysis with a high-velocity saline jet to perform thrombolysis with aspiration [56]. The device is rigid, does not track as well as large-bore aspiration catheters designed for intracranial use, and, as a result, has a risk of perforating the venous sinus [54]. Despite this, it has been successfully utilized for direct aspiration treatment of CVT with persistent recanalization of the treated venous sinuses but has been found to have lower rates of complete recanalization and a lower likelihood of a good outcome than other thrombectomy devices [52, 56].

Stent Retrieval Thrombectomy

Application of stent retrieval thrombectomy devices initially designed for ischemic strokes such as the Solitaire (Medtronic, Minneapolis, Minnesota, USA) and Trevo (Stryker, Kalamazoo, Michigan, USA) devices has been effectively utilized for the treatment of CVT, with and without catheter-directed thrombolysis and aspiration [57–60]. The stent retrieval device is deployed across the thrombus and removed into the aspiration catheter but also has been used to function as an anchor to assist with direct aspiration in the venous sinus with an aspiration catheter [58].

Balloon Thrombectomy

An additional mechanical thrombectomy technique includes balloon thrombectomy with a TransForm balloon catheter (Stryker, Kalamazoo, Michigan, USA) with an aspiration catheter [61]. The balloon is advanced past the site of thrombus, inflated, and then retracted toward the aspiration catheter in order to dislodge thrombus. In this case series, most patients demonstrated improved functional outcomes, and all patients received systemic heparin before and after the procedure, with one patient developing fatal hemorrhagic infarcts despite venous sinus recanalization [61]. Large balloon catheters such as 3F and 4F catheters are also utilized to match the larger size of the dural venous sinuses in order to perform effective thrombectomy [51].

Balloon Venoplasty and Stenting

As a rescue therapy, balloon venoplasty with the placement of a stent has been described in cases that failed systemic anticoagulation, catheter-directed thrombolysis, and mechanical thrombectomy strategies [62]. In this case series, patients were anticoagulated and initiated on antiplatelet therapies after stent placement with an Enterprise stent (Johnson and Johnson, New Brunswick, New Jersey, USA) in the superior sagittal sinus with persistent recanalization achieved in the two reported patients at 2 years [62]. There are otherwise limited data regarding the role of acute stent placement as an initial endovascular treatment of CVT.

Overall, there is a growing body of literature regarding the role of endovascular therapy in patients with CVT, although the majority of these data are limited to case series and case reports in patients that demonstrated neurological decline despite systemic anticoagulation or presented with severe neurological deficits. Recanalization rates with endovascular treatments have been reported to be as high as 83.5%, with 62.6% of patients achieving a good functional outcome [63]. Even with endovascular treatments, mortality in patients that require endovascular treatment remains high (18.6–27%) as these patients represent a more severely affected group [52, 63]. Given the relative efficacy and safety of systemic anticoagulation, endovascular treatment harbors risks but remains a treatment option in patients with failed anticoagulation or poor neurological exams due to the degree of venous hypertension and thrombus burden. It is not clear if there is a particular endovascular technique that is optimal for patients with CVT, and a retrospective study highlighted that multimodality endovascular treatment was performed in 62% of cases [52, 63]. Until additional data or techniques emerge, endovascular therapies should be guided by the individual patient's clinical situation in order to select the optimal thrombectomy strategies.

Surgical Management

Open Surgical Venous Sinus Thrombectomy

Open sinus thrombectomy has been performed in cases of severe, CVT refractory to anticoagulation [64–66]. In one case, sinus thrombectomy was performed with a balloon and in situ thrombolysis with t-PA in conjunction with bilateral decompressive craniectomies [66]. Three other cases involved open sinus thrombectomy with a catheter left in place for local infusion of t-PA into the sagittal sinus [65]. Many of the cases required repeated treatments, with some developing surgery-related complications such as an epidural hematoma but ultimately led to significant improvement in functional outcomes [64, 65]. Given the growth of endovascular approaches, the role of open surgical sinus thrombectomy will likely diminish further and be reserved for the most severe and refractory CVT cases.

Decompressive Craniectomy

Transtentorial herniation is the most common cause of death in the acute setting of CVT patients [67]. Nearly 40% of patients with CVT also present with intracranial hypertension which may become refractory with extension of sinus thrombosis or addition of mass lesions such as hemorrhagic venous infarct (Ameri 1992). Decompressive craniectomy does not directly treat the sinus thrombosis, but provides patients with a life-saving procedure with the possibility of providing good functional outcomes (modified Rankin scale 0–2) in 60% of patients particularly when performed within 12 hours of admission or in patients younger than 40 [68–70]. In one of the studies, one of the patients underwent endovascular treatment of sinus thrombus due to lack of clinical improvement despite a decompressive craniectomy, and 9 out of the 10 patients had an associated hemorrhagic venous infarct [70]. Craniectomy may also facilitate hematoma evacuation, given that patients with CVT may present with hemorrhagic venous infarcts with mass effect. The timing of when to resume systemic anticoagulation for the treatment of the sinus thrombosis after a craniectomy remains poorly understood with some suggesting initiation of heparin 6–24 hours after surgery as safe [66, 71]. Overall, there are limited data to guide which patients should undergo craniectomy or the optimal temporal relationship of combined open and endovascular approaches to treat patients with CVT.

Conclusion

Based on current literature and guidelines, we propose a treatment algorithm for the diagnosis and management of CVT (Fig. 18.5). In summary, CVT results in a variable clinical presentation that may be difficult to diagnose with potentially fatal outcomes. Headache is the most common presenting symptom, and a high index of clinical suspicion is required to ensure timely diagnosis via CTV/MRV as well as catheter-based cerebral angiography if other imaging modalities are not adequate. Patients presenting with coma, cerebral hemorrhage, malignancy, male sex, mental status disorders, thrombosis involving deep cerebral venous system, and infection are at greater risk of death or dependence. Anticoagulation with LMWH or unfractionated heparin is recommended in the acute phase of the presentation even in the presence of ICH in order to prevent thrombus progression, promote recanalization, and decrease venous congestion. Transition to oral anticoagulation for 3–12 months depending on risk factors, and clinical history is recommended in order to prevent recurrent CVT and remote VTE events. Sequela associated with CVT such as seizures and intracranial hypertension needs to be treated. For patients with persistent neurological decline or failure of systemic anticoagulation therapy, endovascular techniques such as catheter-directed thrombolysis and mechanical thrombectomy have emerged as successful treatment options to help promote venous sinus

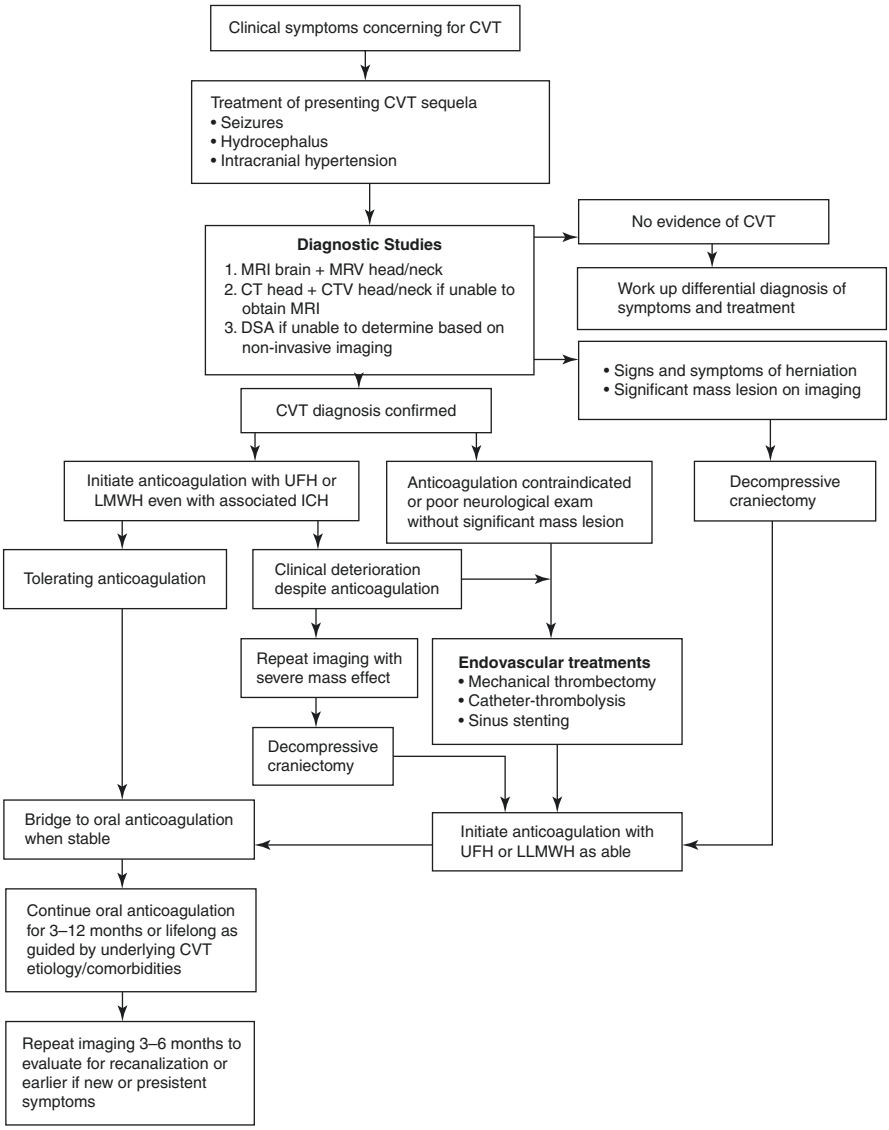

Fig. 18.5 Proposed treatment algorithm for CVT diagnosis and management

recanalization and decrease venous congestion. Patients with significant associated mass effect may require life-saving decompressive craniectomy. Despite these treatment options, CVT may result in significant morbidity and mortality. There remains significant room for continued studies to further define optimal management strategies for CVT.

References

1. Saposnik G, Barinagarrementeria F, Brown RD, Bushnell CD, Cucchiara B, Cushman M, et al. Diagnosis and management of cerebral venous thrombosis: a statement for healthcare professionals from the American Heart Association/American Stroke Association. Stroke. 2011;42(4):1158–92.
2. Renowden S. Cerebral venous sinus thrombosis. Eur Radiol. 2004;14(2):215–26.
3. Silvis SM, de Sousa DA, Ferro JM, Coutinho JM. Cerebral venous thrombosis. Nat Rev. 2017;13(9):555–65.
4. Ribes F. Exposé succinct des recherches faites sur la phlébite. Gueffier; 1825.
5. Abercrombie J. ART. XV. Pathological and practical researches on the diseases of the brain and the spinal cord. Am J Med Sci. 1828;4:384–9.
6. Ferro JM, Canhão P, Stam J, Bousser MG, Barinagarrementeria F. Prognosis of cerebral vein and dural sinus thrombosis: results of the international study on cerebral vein and dural sinus thrombosis (ISCVT). Stroke. 2004;35(3):664–70.
7. Goldberg AL, Rosenbaum AE, Wang H, Kim WS, Lewis VL, Hanley DF. Computed tomography of dural sinus thrombosis. J Comput Assist Tomogr. 1986;10(1):16–20.
8. Mattle HP, Wentz KU, Edelman RR, Wallner B, Finn JP, Barnes P, et al. Cerebral venography with MR. Radiology. 1991;178(2):453–8.
9. Krayenbuhl HA. Cerebral venous and sinus thrombosis. Neurol Med Chir (Tokyo). 1968;10:1–24.
10. Stam J. Thrombosis of the cerebral veins and sinuses. N Engl J Med. 2005;352(17):1791–8.
11. Li L-F, Pu JK-S, Tsang C-P, Tsang AC-O, Lui W-M, Leung GK-K. Iatrogenic sigmoid sinus occlusion rescued by graft repair and endovascular thrombolysis. World Neurosurg. 2017;104:1047.e13–7.
12. Honig A, Eliahou R, Pikkel YY, Leker RR. Iatrogenic intracranial hypotension and cerebral venous thrombosis. J Neurol Sci. 2016;366:191–4.
13. Barboza MA, Chiquete E, Arauz A, Merlos-Benitez M, Quiroz-Compeán A, Barinagarrementería F, et al. A practical score for prediction of outcome after cerebral venous thrombosis. Front Neurol. 2018;9(Oct):882.
14. Ferro JM, Bacelar-Nicolau H, Rodrigues T, Bacelar-Nicolau L, Canhão P, Crassard I, et al. Risk score to predict the outcome of patients with cerebral vein and dural sinus thrombosis. Cerebrovasc Dis. 2009;28(1):39–44.
15. De Bruijn SFTM, Stam J, Kappelle LJ. Thunderclap headache as first symptom of cerebral venous sinus thrombosis. Lancet. 1996;348(9042):1623–5.
16. Leker RR, Steiner I. Features of dural sinus thrombosis simulating pseudotumor cerebri. Eur J Neurol. 1999;6(5):601–4.
17. Tehindrazanarivelo A, Evrard S, Schaison M, Mas J-L, Dormont D, Bousser M-G. Prospective study of cerebral sinus venous thrombosis in patients presenting with benign intracranial hypertension. Cerebrovasc Dis. 1992;2(1):22–7.
18. Ameri A, Bousser M-G. Cerebral venous thrombosis. Neurol Clin. 1992;10(1):87–111.
19. Ferro JM, Correia M, Rosas MJ, Pinto AN, Neves G. Seizures in cerebral vein and dural sinus thrombosis. Cerebrovasc Dis. 2003;15(1–2):78–83.
20. Schaller B, Graf R. Cerebral venous infarction: the pathophysiological concept. Cerebrovasc Dis. Karger Publishers. 2004;18:179–88.
21. Fujita K, Kojima N, Tamaki N, Matsumoto S. Brain edema in intracranial venous hypertension. In: Brain edema. Berlin Heidelberg: Springer; 1985. p. 228–34.
22. Bering EA, Salibi B. Production of hydrocephalus by increased cephalic-venous pressure. Arch Neurol Psychiatr. 1959;81(6):693–8.
23. Ferro JM, Canhão P, Stam J, Bousser M-G, Barinagarrementeria F, Massaro A, et al. Delay in the diagnosis of cerebral vein and dural sinus thrombosis: influence on outcome. Stroke. 2009;40(9):3133–8.

24. Bonneville F. Imaging of cerebral venous thrombosis. Diagn Interv Imaging. Elsevier Masson SAS. 2014;95:1145–50.
25. Dormont D, Anxionnat R, Evrard S, Louaille C, Chiras J, Marsault C. MRI in cerebral venous thrombosis. J Neuroradiol. 1994;21(2):81–99.
26. Masuhr F, Busch M, Amberger N, Ortwein H, Weih M, Neumann K, et al. Risk and predictors of early epileptic seizures in acute cerebral venous and sinus thrombosis. Eur J Neurol. 2006;13(8):852–6.
27. José MF, Patrícia C, Marie-Germaine B, Jan S, Fernando B. Early seizures in cerebral vein and dural sinus thrombosis. Stroke. 2008;39(4):1152–8.
28. Ferro JM, Bousser MG, Canhão P, Coutinho JM, Crassard I, Dentali F, et al. European Stroke Organization guideline for the diagnosis and treatment of cerebral venous thrombosis – endorsed by the European Academy of Neurology. Eur J Neurol. 2017;24(10):1203–13.
29. Wasay M, Bakshi R, Bobustuc G, Kojan S, Sheikh Z, Dai A, et al. Cerebral venous thrombosis: analysis of a multicenter cohort from the United States. J Stroke Cerebrovasc Dis. 2008;17(2):49–54.
30. Wu YW, Hamrick SEG, Miller SP, Haward MF, Lai MC, Callen PW, et al. Intraventricular hemorrhage in term neonates caused by sinovenous thrombosis. Ann Neurol. 2003;54(1): 123–6.
31. Karina JK, de Vries Linda S, van Straaten H, (Irma) LM, Benders Manon JNL, Rutger AJN, Floris G. Anticoagulation Therapy and Imaging in Neonates With a Unilateral Thalamic Hemorrhage Due to Cerebral Sinovenous Thrombosis. Stroke 2009;40(8):2754–60.
32. Murdock J, Tzu JH, Schatz NJ, Lee WW. Optic nerve sheath fenestration for the treatment of papilledema secondary to cerebral venous thrombosis. J Neuroophthalmol. 2014;34(1):67–9.
33. Lobo S, Ferro JM, Barinagarrementeria F, Bousser MG, Canhão P, Stam J. Shunting in acute cerebral venous thrombosis: a systematic review. Cerebrovasc Dis. 2014;37(1):38–42.
34. Constantine CP, Van VH, Christopher FD, Todd EL, Adel MM, Philip MM, et al. Acquired pial arteriovenous fistula following cerebral vein thrombosis. Stroke. 1999;30(11):2487–90.
35. Sun L-L, Tang W-X, Liu L, Wang W, Zhang S-X, Liu Z-J. Dural arteriovenous fistula disguised as cerebral venous sinus thrombosis. J Zhejiang Univ. 2017;18(8):733–6.
36. de Sousa DA, Lucas NL, Patrícia C, José MF. Recanalization in cerebral venous thrombosis. Stroke. 2018;49(8):1828–35.
37. Einhäupl KM, Villringer A, Mehraein S, Garner C, Pellkofer M, Haberl RL, et al. Heparin treatment in sinus venous thrombosis. Lancet. 1991;338(8767):597–600.
38. De Bruijn SFTM, Stam J. Randomized, placebo-controlled trial of anticoagulant treatment with low-molecular-weight heparin for cerebral sinus thrombosis. Stroke. 1999;30(3):484–8.
39. Coutinho J, de Bruijn S, de Veber G, Stam J. Anticoagulation for cerebral venous sinus thrombosis. Cochrane Database Syst Rev. 2011;(8):CD002005.
40. de Sousa DA, Ferro JM, Canhão P, Barinagarrementeria F, Bousser M-G, Stam J, et al. Cerebral venous thrombosis causing posterior fossa lesions: description of a case series and assessment of safety of anticoagulation. Cerebrovasc Dis. 2014;38(5):384–8.
41. Marie G, José MF, Patrícia C, Jan S, Marie-Germaine B, Fernando B, et al. Predictors of outcome in patients with cerebral venous thrombosis and intracerebral hemorrhage. Stroke. 2007;38(2):337–42.
42. Jonathan MC, José MF, Patrícia C, Fernando B, Marie-Germaine B, Jan S. Unfractionated or low–molecular weight heparin for the treatment of cerebral venous thrombosis. Stroke. 2010;41(11):2575–80.
43. van Dongen CJ, van den Belt AG, Prins MH, Lensing A. Fixed dose subcutaneous low molecular weight heparins versus adjusted dose unfractionated heparin for venous thromboembolism. Cochrane Database Syst Rev. John Wiley & Sons, Ltd. 2004;(9):CD001100.
44. Misra UK, Kalita J, Chandra S, Kumar B, Bansal V. Low molecular weight heparin versus unfractionated heparin in cerebral venous sinus thrombosis: a randomized controlled trial. Eur J Neurol. 2012;19(7):1030–6.

45. Idiculla PS, Gurala D, Palanisamy M, Vijayakumar R, Dhandapani S, Nagarajan E. Cerebral venous thrombosis: a comprehensive review. Eur Neurol. 2020;83:1–11.
46. Miranda B, Ferro JM, Canhão P, Stam J, Bousser MG, Barinagarrementeria F, et al. Venous thromboembolic events after cerebral vein thrombosis. Stroke. 2010;41(9):1901–6.
47. Christina G, Daniel R, Christian H, Peter AR, Simon N. Novel factor xa inhibitor for the treatment of cerebral venous and sinus thrombosis. Stroke. 2014;45(8):2469–71.
48. Mendonça MD, Barbosa R, Cruz-e-Silva V, Calado S, Viana-Baptista M. Oral direct thrombin inhibitor as an alternative in the management of cerebral venous thrombosis: a series of 15 patients. Int J Stroke. 2015;10(7):1115–8.
49. Coutinho JM, Zuurbier SM, Bousser MG, Ji X, Canhao P, Roos YB, et al. Effect of endovascular treatment with medical management vs standard care on severe cerebral venous thrombosis: the TO-ACT randomized clinical trial. JAMA Neurol. 2020;77(8):966–73.
50. Siddiqui FM, Banerjee C, Zuurbier SM, Hao Q, Ahn C, Pride GL, et al. Mechanical thrombectomy versus intrasinus thrombolysis for cerebral venous sinus thrombosis: a non-randomized comparison. Interv Neuroradiol. 2014;20(3):336–44.
51. Lee S-K, Mokin M, Hetts SW, Fifi JT, Bousser M-G, Fraser JF. Current endovascular strategies for cerebral venous thrombosis: report of the SNIS Standards and Guidelines Committee. J NeuroIntervent Surg. 2018;10(8):803.
52. Mokin M, Lopes DK, Binning MJ, Veznedaroglu E, Liebman KM, Arthur AS, et al. Endovascular treatment of cerebral venous thrombosis: contemporary multicenter experience. Interv Neuroradiol. 2015;21(4):520–6.
53. Canhão P, Falcão F, Ferro JM. Thrombolytics for cerebral sinus thrombosis. Cerebrovasc Dis. 2003;15(3):159–66.
54. Jankowitz BT, Bodily LM, Jumaa M, Syed ZF, Jovin TG. Manual aspiration thrombectomy for cerebral venous sinus thrombosis. J NeuroIntervent Surg. 2013;5(6):534.
55. Gariel F, Berge J, Dousset V. Neurological recovery after coma related to diffuse cerebral venous sinus thrombosis. Interest in thrombi-aspiration with Penumbra system. Interv Neuroradiol. 2015;21(2):218–21.
56. Dashti SR, Hu YC, Yao T, Fiorella D, Mitha AP, Albuquerque FC, et al. Mechanical thrombectomy as first-line treatment for venous sinus thrombosis: technical considerations and preliminary results using the AngioJet device. J NeuroIntervent Surg. 2013;5(1):49.
57. Taniguchi S, Harada K, Kajihara M, Fukuyama K. Combined use of stent-retriever and aspiration thrombectomy for cerebral venous sinus thrombosis involving the straight sinus: a case report. Interv Neuroradiol. 2017;23(6):605–8.
58. Mascitelli JR, Pain M, Zarzour HK, Baxter P, Ghatan S, Mocco J. Republished: sinus thrombectomy for purulent cerebral venous sinus thrombosis utilizing a novel combination of the Trevo stent retriever and the Penumbra ACE aspiration catheter: the stent anchor with mobile aspiration technique. J NeuroIntervent Surg. 2016;8(6):e24.
59. Froehler MT. Successful treatment of cerebral venous sinus thrombosis with the Solitaire FR thrombectomy device. J NeuroIntervent Surg. 2013;5(6):e45.
60. Chen C, Wang Q, Li X, Lu Z, He J, Fang Q, et al. Stent retriever thrombectomy combined with local thrombolytic therapy for cerebral venous sinus thrombosis: a case report Corrigendum in /10.3892/etm.2017.5676. Exp Ther Med. 2017;14(5):3961–70.
61. Matsuda Y, Okada H, Chung J, Crowley RW, Lopes DK. Novel balloon-and-aspiration method for cerebral venous sinus thrombosis: dental-floss technique. Neurosurg Focus FOC. 2017;42(4):E19.
62. Adachi H, Mineharu Y, Ishikawa T, Imamura H, Yamamoto S, Todo K, et al. Stenting for acute cerebral venous sinus thrombosis in the superior sagittal sinus. Interv Neuroradiol. 2015;21(6):719–23.
63. Yeo LLL, Lye PPS, Yee KW, Cunli Y, Ming TT, Ho AFW, et al. Deep cerebral venous thrombosis treatment. Clin Neuroradiol. 2020;30(4):661–70.
64. Persson L, Lilja A. Extensive dural sinus thrombosis treated by surgical removal and local streptokinase infusion. Neurosurgery. 1990;26(1):117–21.

65. Ekseth K, Boström S, Vegfors M. Reversibility of severe sagittal sinus thrombosis with open surgical thrombectomy combined with local infusion of tissue plasminogen activator: technical case report. Neurosurgery. 1998;43(4):960–4.
66. Lechanoine F, Janot K, Herbreteau D, Maldonado IL, Velut S. Surgical thrombectomy combined with bilateral decompressive craniectomy in a life-threatening case of coma from cerebral venous sinus thrombosis: case report and literature review. World Neurosurg. 2018;120:485–9.
67. Patrícia C, José MF, Arne GL, Marie-Germaine B, Jan S, Fernando B. Causes and predictors of death in cerebral venous thrombosis. Stroke. 2005;36(8):1720–5.
68. José MF, Isabelle C, Jonathan MC, Patrícia C, Fernando B, Brett C, et al. Decompressive surgery in cerebrovenous thrombosis. Stroke. 2011;42(10):2825–31.
69. Aaron S, Alexander M, Moorthy RK, Mani S, Mathew V, Patil AKB, et al. Decompressive craniectomy in cerebral venous thrombosis: a single centre experience. J Neurol Neurosurg Psychiatry. 2013;84(9):995.
70. Zuurbier SM, Coutinho JM, Majoie CBLM, Coert BA, van den Munckhof P, Stam J. Decompressive hemicraniectomy in severe cerebral venous thrombosis: a prospective case series. J Neurol. 2012;259(6):1099–105.
71. Keller E, Pangalu A, Fandino J, Könü D, Yonekawa Y. Decompressive craniectomy in severe cerebral venous and dural sinus thrombosis. In: Yonekawa Y, Keller E, Sakurai Y, Tsukahara T, editors. New trends of surgery for stroke and its perioperative. Vienna: Springer Vienna; 2005. p. 177–83.

Part IV
Vascular Malformations

Chapter 19
Arteriovenous Malformations: Presentation and Natural History

Andrew J. Ringer and Ryan Tackla

Introduction

Brain arteriovenous malformations (AVMs) consist of a network of abnormal arteries and veins with no intervening capillary bed or functional neural tissue [1]. This nidus is characterized by direct fistulous connections from artery to vein that contribute to their unique anatomy and complex vascular physiology. Shunting of high-flow, arterial blood into the normally low-flow, venous system creates higher-than-normal pressures through the feeding arteries, nidus, and draining veins [2]. Besides the high flow rates, various other factors that include shear stress, venous obstruction, arterial steal, and compartmentalization contribute to vascular complexities of AVMs. Size and location of the lesion create a range of clinical symptoms. In considering natural history, the anticipated risks of hemorrhage or seizure and resulting morbidity and mortality must be weighed with the risks of the patient's treatment and the psychological burden of living with a potentially life-threatening AVM.

Epidemiology

Although AVMs of the brain can present at any age, they are a leading cause of hemorrhage in children and young adults [3]. A 2013 meta-analysis identified that a mean age at the time of rupture was mid-30s, confirming the findings of previous natural history studies with at least 200 patients [1].

A. J. Ringer (✉) · R. Tackla
Mayfield Clinic, Cincinnati, OH, USA
e-mail: aringer@mayfieldclinic.com; mkemper@mayfieldclinic.com; rtackla@mayfieldclinic.com

J. R. Mascitelli, M. J. Binning (eds.), *Introduction to Vascular Neurosurgery*,
https://doi.org/10.1007/978-3-030-88196-2_19

Their true incidence and prevalence are difficult to estimate because of the rarity of disease, lack of epidemiological studies, and varied presentation. However, two efforts using defined populations included the Scottish Intracranial Vascular Malformations Study [3, 4] and the New York Islands AVM Study [5] that estimated the population prevalence ranges between 10 and 18 per 100,000 in the adults. Findings from these studies, which relied on some retrospective data, were later corroborated in three large prospective, population-based studies that estimated the incidence at 1 new case per 100,000 person-years [4, 6, 7]. By some estimates, this leads to an excess risk of death between 0.7 and 2.9% annually in patients who harbor brain AVMs [8].

Presentation

The array of AVM symptoms ranges from headaches or seizures to major disabling or fatal hemorrhage (Table 19.1). Brain AVMs were previously felt to be quite uncommon. However, the proportion presenting prior to hemorrhage significantly increased when noninvasive imaging became widely available [4, 5]. Since that time, approximately 50% of brain AVMs are discovered in the absence of hemorrhage, 15–30% with seizure, and the remainder with headache or focal neurological deficits. In the ARUBA trial, a prospective comparison of outcomes was based on treatment selection in 223 patients without a history of hemorrhage, and 93 (41.7%) patients who were asymptomatic from their brain AVM [9].

Risk Factors for Hemorrhage

Predicting the natural history of brain AVMs is difficult given the uniqueness of the angioarchitecture, varied clinical presentations, and therapeutic modalities. With no medical therapies to slow disease progression, clinical studies have attempted to determine risks of hemorrhage and other factors, including weighing risks of treatment versus spontaneous hemorrhage in the natural course of the disease. As the most common presentation with resulting morbidity and mortality, hemorrhage has been most often studied as the primary risk factor.

Table 19.1 Mode of presentation summarized from the three of the largest studies [4, 5, 9]. Shaded areas show rows of symptoms that were combined for incidence rate

Symptom at presentation, *n* (%)	Scottish Al-Shahi et al. [4] *N* = 79	New York Islands Stapf et al. [5] *N* = 284	ARUBA Mohr et al. [9] *N* = 223
Bleeding from AVM	42 (53.2%)	108 (38.0%)	NA
Seizure	25 (31.6%)		95 (42.6%)
Headache	6 (7.6%)*		115 (51.6%)
Focal deficit/other		176 (62%)**	42 (18.8%)
Incidental	6 (7.6%)		93 (41.7%)

*combined headache + focal deficit/other [4]

**combined seizure headache + focal deficit/other headache + incidental [5]

Prior Hemorrhage

Few factors have proven as influential on the risk of future hemorrhage as a history of prior hemorrhage. This has been a consistent finding in a number of studies [10–16]. In a consecutive series of 305 patients with AVMs who underwent treatment at a single hospital, Yamada et al. reported an annual 6.84% risk of hemorrhage, noting that this risk was heavily influenced by the hemorrhage rate in the first 5 years [11]. In their experience, risk of recurrent hemorrhage was 15.42% in the first year, 5.32% in the subsequent 4 years, and 1.72% after more than 5 years. Interestingly, the same authors noted a similar 6.48% annual rate of hemorrhage in patients who presented with headache but no confirmed hemorrhage. Their findings raised the question about whether some patients with headache had actually suffered occult hemorrhage.

Demographics

Hemorrhage rates between men and women did not significantly differ in most reports [9, 17, 18]. However, there are exceptions, and some studies have reported higher rates in women. Yamada et al. [11] estimated that the risk of hemorrhage was significantly higher in women (HR = 2.93), whereas Karlsson et al. [19] found that the risk of hemorrhage was only higher in women during their fertile years compared with men in the same age group. Despite this, in a series of 623 patients treated in Helsinki, men with AVMs had higher mortality rates than women [18].

Age may play a role in predicting the risk of hemorrhage. Among studies suggesting that age is a risk factor for hemorrhage, several studies identified higher rates of hemorrhage in children. Yamada et al. [11] cited a significantly higher rate of hemorrhage among children in their series (HR = 2.69). This finding was corroborated by Fullerton et al. who compared long-term hemorrhage risk between children and adults [20]. However, others have proposed a higher risk with advancing age [10]. Race or ethnicity is an inconsistent risk factor for hemorrhage with most studies reporting no difference in age or not reporting differences by ethnicity. One review cited an increased risk of hemorrhage among Hispanics with a hazard ratio of 1.9 compared with whites [15].

Angioarchitecture

Many authors have suggested that AVM location, size, and venous anatomy can influence natural history. Angiographic features of AVMs sometimes used to stratify the risk of hemorrhage are more often used to predict the outcome of surgical treatment [21]. Variability in terminology and reporting of imaging findings among authors also makes it difficult to directly correlate outcomes with imaging features.

Deep location is often cited as a predictor of presentation with hemorrhage or with future hemorrhage after initial diagnosis [10–12, 22]. For example, AVMs of the posterior fossa are considered higher risk for hemorrhage [23]. This risk may be at least partially due to the deep location of the posterior fossa and an increased incidence of associated aneurysms (see below).

The association of AVM nidus size with hemorrhage at presentation is more complex. Many reports find no association between maximum diameter of the nidus and risk of hemorrhage [1]. Others, however, have suggested that smaller size might increase the risk of hemorrhage [11, 24, 25]. Aiming to identify clinical and angiographic factors associated with hemorrhage in 100 patients with AVMs, Langer et al. identified nidal diameter < 3 cm along with the history of hypertension and deep venous drainage as independent risk factors; they looked at both sharp and diffuse nidal margins [24], whereas larger AVM size (>5 cm) has been associated with increased risk of subsequent hemorrhage [26].

Deep venous drainage is often cited as a risk both for hemorrhage and poor outcomes with surgical treatment [21]. What remains unclear, however, is if this feature is a risk factor independent of deep location for the AVM nidus as these features are frequently associated. Regardless, deep venous drainage has been associated with an increased risk of initial hemorrhagic presentation and with subsequent hemorrhage [10, 27].

Venous strictures and venous aneurysms have been reported and may have some predictive value of hemorrhage. However, there is no consensus on this influence. Some cite venous aneurysms as a potential site for hemorrhage, whereas others have suggested that they represent a protective adaptation that reduces this risk [28]. This conclusion was drawn from the higher incidence of venous aneurysms found in older patients with no history of bleeding. Venous strictures, which may represent an obstruction of outflow, have been suggested as a risk factor for hemorrhage [29, 30].

Associated Aneurysms

The incidence of intracranial aneurysms associated with brain AVMs exceeds that found in the general population. Some studies have reported aneurysm incidence at rates of 18% or higher in individuals harboring brain AVMs [31–34]. However, a precise estimate may be difficult given that the complex angiographic appearance of many AVMs obscures the detection of some intranidal aneurysms unless superselective catheterization is used.

Various classification schemes and standard nomenclature have been proposed for the aneurysms associated with AVM-based hemodynamic and histopathologic features [35, 36]. In their proposed classification, Redekop et al. used anatomical and angiographic relationships to determine incidence and bleeding rates in 632 patients with AVMs (Table 19.2) [36]. They classified three groups of aneurysms as intranidal (filling prior to the substantial venous filling, within the borders of the

Table 19.2 Clinical presentation of 97 patients with aneurysms and AVMs adapted from Redekop et al. [36]. Reprinted with permission from Journal of Neurosurgery Publishing Group (JNSPG)

Presentation	Status of intranidal aneurysm No. of patients (%)	
Type	With aneurysm	Without aneurysm
Bleeding from AVM	22 (63%)	13 (21%)
Bleeding from aneurysm	3 (9%)	10 (16%)
Bleeding, unknown source		2 (3%)
Seizure	7 (20%)	20 (32%)
Other	3 (9%)	17 (27%)
Total	35 patients	62 patients

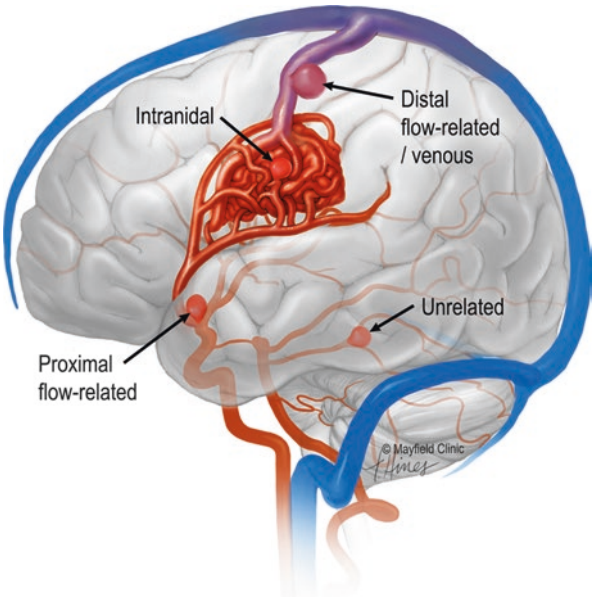

Fig. 19.1 Arterial aneurysms found in conjunction with brain AVMs. Redekop et al. defined aneurysm features (rates %) as intranidal (5.5%) (within the AVM nidus, fills early during angiography); flow-related (11.2%) including proximal (on major artery with eventual supply to AVM) or distal [on AVM feeding artery; or unrelated (0.8%) (i.e., on an artery unrelated to AVM supply)] [36]. Venous aneurysms can also occur. (Reprinted with permission from Mayfield Clinic)

nidus); flow-related (arising from an artery feeding the AVM, subclassified as proximal or distal); or unrelated (arising from arteries with no supply to the AVM) (Fig. 19.1). Of their 632 patients, 97 patients harbored aneurysms that included 35 (5.5%) patients with intranidal aneurysms and 71 (11.2%) patients with flow-related aneurysms. Flow-related aneurysms were considered proximal if they arose from the internal carotid artery, the vertebral or basilar artery, the circle of Willis, or the A1 and M1 segments of the anterior and middle cerebral arteries, respectively. Aneurysms were considered distal flow-related aneurysms if arising beyond these segments of a feeding artery.

It is generally believed that aneurysms lead to a higher risk of hemorrhage as the initial presentation. In several studies, a higher incidence of both initial presentation with hemorrhage and recurrent hemorrhage occurred in patients with both brain

AVMs and aneurysms than in patients with brain AVMs without aneurysms [37–42]. In one meta-analysis, the presence of an intracranial aneurysm was estimated to increase the risk of presentation with hemorrhage by 80% in individuals with brain AVMs [32], but opinions on this issue are not uniform. For instance, some authors have suggested that prenidal or flow-related aneurysms are at higher risk of hemorrhage than intranidal aneurysms, whereas others proposed that the high flow and shear stress of the fistula within the nidus make intranidal aneurysms more prone to rupture [36, 43] and that the high flow of the nearby shunt puts intranidal aneurysms at higher risk of hemorrhage [44]. In their series, Redekop et al. reported that 72% of patients with intranidal aneurysms presented with hemorrhage compared with 40% of patients with flow-related aneurysms and 36% of patients without associated aneurysms; for most of this latter group, hemorrhage was attributed to the AVM nidus.

Formation of an aneurysm in the presence of an AVM is suspected to be largely related to the flow dynamics of the AVM itself. There are data to suggest that flow-related aneurysms are in fact influenced by the flow of the AVM nidus. Redekop et al. noted that distal flow-related aneurysms that arose on a feeding artery close to the AVM, rather than near the circle of Willis, were much more likely to regress after AVM treatment than proximal flow-related aneurysms [36]. However, given that aneurysms only form on feeding arteries in a minority of individuals who harbor an AVM, their formation is likely multifactorial. Some reports cite an increased incidence of aneurysms in AVMs fed by the posterior circulation, including those with a supratentorial nidus [39, 40]. This may be related to higher peak systolic pressures in the posterior circulation [45]. Others note that feeding arteries of smaller caliber rather than large caliber are more likely to develop aneurysms, suggesting that the ability of the artery to compensate for the increased hemodynamics of the AVM may influence the rate of aneurysm formation [46].

Risk Factors for Seizure

Following hemorrhage, seizure is the second most common presentation of an AVM that affects 20–45% of patients [47, 48]. The precise pathogenesis of seizure caused by an AVM may be multifactorial, including those related to hemorrhage or post-hemorrhagic hemosiderin staining or other factors, such as vascular steal, perinidal edema, and nidus size and location [47–50]. Additionally, Hoh et al. reported that seizures occur more often in men and individuals less than 65 years of age with brain AVM [51].

Anatomic factors that may influence seizure risk include AVM location, angiographic supply, and venous anatomy. In their multicenter review of 2333 patients with brain AVMs, Chen et al. identified a cortical location as the greatest predictor of seizure with rates of 27% versus 0.3% for non-cortical locations [52]. This finding was supported by Zhen et al. who cited a frontal or temporal location as the

highest risk [53]. Although Chen et al. [52] also noted that a smaller nidus size was more likely to present with seizures, this finding has been inconsistent in other studies [54]. Angiographic features associated with an increased seizure risk include superficial venous drainage, superficial location with external carotid artery or middle cerebral artery feeding, and presence of venous ectasia [55–57]. One study suggested that venous congestion and findings of high-flow shunting, such as significant arterial dilation and aneurysm formation, may be associated with seizures [49]. In support of the theory that AVM-related flow influences seizure risk, Shankar et al. reviewed 78 unruptured AVMs and established an angiographic scoring system to predict seizure risk [58]. Based on their scoring that included cortical location, venous outflow stenosis, and presence of long pial draining vein (i.e., 1 point per feature), they noted a high 98% specificity for seizures with a score of 3. Others have used MRI findings to correlate with a presentation with seizures. In their review of 165 patients with unruptured AVMs, Benson et al. identified perinidal edema, perinidal T2, venous aneurysms or varices, and presence of a long draining vein being present more often in the 57 patients who presented with seizures [59].

Summary

With their complex angioarchitecture and vascular physiology, brain AVMs create diagnostic and treatment challenges. Natural history includes annual rates of 3% for hemorrhage, although not always associated with disability, and 1% for seizure that can change over time, affected by other risk factors such as deep venous drainage, AVM size, and treatment modality. In our practice, we focus on three key determinants for a new patient with an AVM, outside of an emergency. *First, is there evidence of a previous hemorrhage?* A thorough history will assess for evidence of prior hemorrhage followed by imaging studies to confirm such evidence or not. With evidence of hemorrhage, a more aggressive treatment is pursued. *Second, are there seizures?* Seizures easily controlled by a single antiepileptic medication may not require treatment, especially for complex or high-grade AVMs. Treatment is considered for patients to eliminate the need for medications or for seizures refractory to medication. *Third, are there any high-risk features?* Headache as a presenting symptom is challenging in terms of identifying its source, such as AVM related or region. These patients are offered diagnostic angiography to better reveal angioarchitecture, identify any associated aneurysm, and form a more detailed analysis of angiographic features not readily available with noninvasive imaging. A detailed understanding of each patient's relevant history, medical risk factors, and life expectancy, coupled with the specific angiographic architecture of the AVM, permits a more precise estimation of the natural history risk for that patient. Management recommendations must include this estimate and a candid discussion of treatment risks to select the course best suited to an individual.

References

1. Can A, Gross BA, Du R. The natural history of cerebral arteriovenous malformations. In: Spetzler R, Moon K, Almefty RO, editors. Handbook of clinical neurology, Vol. 143 (3rd series). New York: Elsevier; 2017.
2. Derdeyn CP, Zipfel GJ, Albuquerque FC, Cooke DL, Feldmann E, Sheehan JP, Torner JC, American Heart Association Stroke Council. Management of brain arteriovenous malformations: a scientific statement for healthcare professionals from the American Heart Association/American Stroke Association. Stroke. 2017;48(8):e200–24. https://doi.org/10.1161/STR.0000000000000134. Epub 2017 Jun 22
3. Al-Shahi R, Fang JS, Lewis SC, Warlow CP. Prevalence of adults with brain arteriovenous malformations: a community based study in Scotland using capture-recapture analysis. J Neurol Neurosurg Psychiatry. 2002;73(5):547–51.
4. Al-Shahi R, Bhattacharya JJ, Currie DG, the Scottish Intracranial Vascular Malformation Study Collaborators, et al. Prospective, population-based detection of intracranial vascular malformations in adults: the Scottish Intracranial Vascular Malformation Study (SIVMS). Stroke. 2003;34:1163–9.
5. Stapf C, Mast H, Sciacca RR, Berenstein A, Nelson PK, Gobin YP, Pile-Spellman J, Mohr JP, New York Islands AVM Study Collaborators. The New York Islands AVM Study: design, study progress, and initial results. Stroke. 2003;34(5):e29–33. https://doi.org/10.1161/01.STR.0000068784.36838.19. Epub 2003 Apr 10. PMID:12690217.
6. Berman MF, Sciacca RR, Pile-Spellman J, Stapf C, Connolly ES Jr, Mohr JP, et al. The epidemiology of brain arteriovenous malformations. Neurosurgery. 2000;47(2):389–96.
7. Gabriel RA, Kim H, Sidney S, McCulloch CE, Singh V, Johnston SC, et al. Ten-year detection rate of brain arteriovenous malformations in a large, multiethnic, defined population. Stroke. 2010;41(1):21–7.
8. Laakso A, Dashti R, Seppanen J, Juvela S, Vaart K, Niemela M, et al. Long-term excess mortality in 623 patients with brain arteriovenous malformations. Neurosurgery. 2008;63(2):244–53.
9. Mohr JP, Parides MK, Stapf C, Moquete E, Moy CS, Overbey JR, et al. Medical management with or without interventional therapy for unruptured brain arteriovenous malformations (ARUBA): a multicentre, non-blinded, randomised trial. Lancet. 2014;383(9917):614–21. [PubMed:24268105].
10. Stapf C, Mast H, Sciacca RR, Choi JH, Khaw AV, Connolly ES, et al. Predictors of hemorrhage in patients with untreated brain arteriovenous malformation. Neurology. 2006;66(9):1350–5. [PubMed: 16682666].
11. Yamada S, Takagi Y, Nozaki K, Kikuta K, Hashimoto N. Risk factors for subsequent hemorrhage in patients with cerebral arteriovenous malformations. J Neurosurg. 2007;107(5):965–72. [PubMed: 17977268].
12. Hernesniemi JA, Dashti R, Juvela S, Vaart K, Niemela M, Laakso A. Natural history of brain arteriovenous malformations: a long-term follow-up study of risk of hemorrhage in 238 patients. Neurosurgery. 2008;63(5):823–31. [PubMed: 19005371].
13. da Costa L, Wallace MC, Ter Brugge KG, O'Kelly C, Willinsky RA, Tymianski M. The natural history and predictive features of hemorrhage from brain arteriovenous malformations. Stroke. 2009;40(1):100–5. [PubMed: 19008469].
14. Halim AX, Johnston SC, Singh V, McCulloch CE, Bennett JP, Achrol AS, et al. Longitudinal risk of intracranial hemorrhage in patients with arteriovenous malformation of the brain within a defined population. Stroke. 2004;35(7):1697–702. [PubMed: 15166396].
15. Kim H, Sidney S, McCulloch CE, Poon KY, Singh V, Johnston SC, et al. Racial/ethnic differences in longitudinal risk of intracranial hemorrhage in brain arteriovenous malformation patients. Stroke. 2007;38(9):2430–7. [PubMed: 17673729].
16. Brown RD Jr, Wiebers DO, Forbes G, O'Fallon WM, Piepgras DG, Marsh WR, et al. The natural history of unruptured intracranial arteriovenous malformations. J Neurosurg. 1988;68(3):352–7. [PubMed: 3343606].

17. Wedderburn CJ, van Beijnum J, Bhattacharya JJ, Counsell CE, Papanastassiou V, Ritchie V, Roberts RC, Sellar RJ, Warlow CP, Al-Shahi Salman R, SIVMS Collaborators. Outcome after interventional or conservative management of unruptured brain arteriovenous malformations: a prospective, population-based cohort study. Lancet Neurol. 2008;7:223–30.
18. Laakso A, Dashti R, Seppänen J, Juvela S, Väärt K, Niemelä M, Sankila R, Hernesniemi JA. Long-term excess mortality in 623 patients with brain arteriovenous malformations. Neurosurgery. 2008;63:244–53.
19. Karlsson B, Lindquist C, Johansson A, Steiner L. Annual risk for the first hemorrhage from untreated cerebral arteriovenous malformations. Minim Invasive Neurosurg. 1997;40(2):40–6. [PubMed: 9228335].
20. Fullerton HJ, Achrol AS, Johnston SC, McCulloch CE, Higashida RT, Lawton MT, Sidney S. Young WL; UCSF BAVM study project. Long-term hemorrhage risk in children versus adults with brain arteriovenous malformations. Stroke. 2005;36(10):2099–104. https://doi.org/10.1161/01.STR.0000181746.77149.2b. Epub 2005 Sep 1. PMID: 16141419.
21. Spetzler RF, Martin NA. A proposed grading system for arteriovenous malformations. J Neurosurg. 1986;65(4):476–83. https://doi.org/10.3171/jns.1986.65.4.0476. PMID: 3760956.
22. Stefani MA, Porter PJ, terBrugge KG, Montanera W, Willinsky RA, Wallace MC. Large and deep brain arteriovenous malformations are associated with risk of future hemorrhage. Stroke. 2002;33(5):1220–4. [PubMed: 11988594].
23. Khaw AV, Mohr JP, Sciacca RR, Schumacher HC, Hartmann A, Pile-Spellman J, et al. Association of infratentorial brain arteriovenous malformations with hemorrhage at initial presentation. Stroke. 2004;35:660–3.
24. Langer DJ, Lasner TM, Hurst RW, Flamm ES, Zager EL, King JT Jr. Hypertension, small size, and deep venous drainage are associated with risk of hemorrhagic presentation of cerebral arteriovenous malformations. Neurosurgery. 1998;42(3):481–6. [PubMed: 9526981].
25. Spetzler RF, Hargraves RW, McCormick PW, Zabramski JM, Flom RA, Zimmerman RS. Relationship of perfusion pressure and size to risk of hemorrhage from arteriovenous malformations. J Neurosurg. 1992;76(6):918–23. [PubMed: 1588424]
26. Rutledge WC, Ko NU, Lawton MT, Kim H. Hemorrhage rates and risk factors in the natural history course of brain arteriovenous malformations. Transl Stroke Res. 2014;5(5):538–42. https://doi.org/10.1007/s12975-014-0351-0. Epub 2014 Jun 15. PMID: 24930128.
27. Mast H, Young WL, Koennecke HC, Sciacca RR, Osipov A, Pile-Spellman J, et al. Risk of spontaneous haemorrhage after diagnosis of cerebral arteriovenous malformation. Lancet. 1997;350:1065–8.
28. Hetts SW, Cooke DL, Nelson J, Gupta N, Fullerton H, Amans MR, Narvid JA, Moftakhar P, McSwain H, Dowd CF, Higashida RT, Halbach VV, Lawton MT, Kim H. Influence of patient age on angioarchitecture of brain arteriovenous malformations. AJNR Am J Neuroradiol. 2014;35(7):1376–80. https://doi.org/10.3174/ajnr.A3886. PMID: 24627452; PMCID: PMC4102659.
29. Marks MP, Lane B, Steinberg GK, Chang PJ. Hemorrhage in intracerebral arteriovenous malformations: angiographic determinants. Radiology. 1990;176(3):807–13. https://doi.org/10.1148/radiology.176.3.2389040. PMID: 2389040.
30. Miyasaka Y, Yada K, Ohwada T, Kitahara T, Kurata A, Irikura K. An analysis of the venous drainage system as a factor in hemorrhage from arteriovenous malformations. J Neurosurg. 1992;76(2):239–43. https://doi.org/10.3171/jns.1992.76.2.0239. PMID: 1730953.1992.
31. Flores BC, Klinger DR, Rickert KL, Barnett SL, Welch BG, White JA, Batjer HH, Samson DS. Management of intracranial aneurysms associated with arteriovenous malformations. Neurosurg Focus. 2014;37(3):E11. https://doi.org/10.3171/2014.6.FOCUS14165. PMID: 25175430.
32. Gross BA, Du R. Natural history of cerebral arteriovenous malformations: a meta-analysis. J Neurosurg. 2013;118(2):437–43. https://doi.org/10.3171/2012.10.JNS121280. Epub 2012 Nov 30. PMID: 23198804.

33. Westphal M, Grzyska U. Clinical significance of pedicle aneurysms on feeding vessels, especially those located in infratentorial arteriovenous malformations. J Neurosurg. 2000;92(6):995–1001. https://doi.org/10.3171/jns.2000.92.6.0995. PMID: 10839261.
34. Lv X, Li Y, Yang X, Jiang C, Wu Z. Characteristics of arteriovenous malformations associated with cerebral aneurysms. World Neurosurg. 2011;76(3–4):288–91. https://doi.org/10.1016/j.wneu.2011.03.022. PMID: 21986426.
35. Rammos SK, Gardenghi B, Bortolotti C, Cloft HJ, Lanzino G. Aneurysms associated with brain arteriovenous malformations. AJNR Am J Neuroradiol. 2016;37(11):1966–71. https://doi.org/10.3174/ajnr.A4869. Epub 2016 Jun 23. PMID: 27339951.
36. Redekop G, TerBrugge K, Montanera W, Willinsky R. Arterial aneurysms associated with cerebral arteriovenous malformations: classification, incidence, and risk of hemorrhage. J Neurosurg. 1998;89(4):539–46. https://doi.org/10.3171/jns.1998.89.4.0539. PMID: 9761046.
37. Stapf C, Mohr JP, Pile-Spellman J, et al. Concurrent arterial aneurysms in brain arteriovenous malformations with haemorrhagic presentation. J Neurol Neurosurg Psychiatry. 2002;73:294–8.
38. Brown RD Jr, Wiebers DO, Forbes GS. Unruptured intracranial aneurysms and arteriovenous malformations: frequency of intracranial hemorrhage and relationship of lesions. J Neurosurg. 1990;73:859–63.
39. Abla AA, Nelson J, Rutledge WC, Young WL, Kim H, Lawton MT. The natural history of AVM hemorrhage in the posterior fossa: comparison of hematoma volumes and neurological outcomes in patients with ruptured infra- and supratentorial AVMs. Neurosurg Focus. 2014;37(3):E6. https://doi.org/10.3171/2014.7.FOCUS14211. PMID: 25175444; PMCID: PMC4425310.
40. da Costa L, Thines L, Dehdashti AR, Wallace MC, Willinsky RA, Tymianski M, Schwartz ML, ter Brugge KG. Management and clinical outcome of posterior fossa arteriovenous malformations: report on a single-centre 15-year experience. J Neurol Neurosurg Psychiatry. 2009;80(4):376–9. https://doi.org/10.1136/jnnp.2008.152710. Epub 2008 Nov 21. PMID: 19028763.
41. Gross BA, Ropper AE, Du R. Vascular complications of stereotactic radiosurgery for arteriovenous malformations. Clin Neurol Neurosurg. 2013;115(6):713–7. https://doi.org/10.1016/j.clineuro.2012.08.008. Epub 2012 Aug 19. PMID: 22910397.
42. Platz J, Berkefeld J, Singer OC, Wolff R, Seifert V, Konczalla J, Güresir E. Frequency, risk of hemorrhage and treatment considerations for cerebral arteriovenous malformations with associated aneurysms. Acta Neurochir. 2014;156(11):2025–34. https://doi.org/10.1007/s00701-014-2225-3. Epub 2014 Sep 23. PMID: 25246143.
43. Elhammady MS, Aziz-Sultan MA, Heros RC. The management of cerebral arteriovenous malformations associated with aneurysms. World Neurosurg. 2013;80(5):e123–9. https://doi.org/10.1016/j.wneu.2013.06.004. Epub 2013 Jun 18. PMID: 23791958.
44. D'Aliberti G, Talamonti G, Cenzato M, La Camera A, Debernardi A, Valvassori L, Mariangela P, Nichelatti M. Arterial and venous aneurysms associated with arteriovenous malformations. World Neurosurg. 2015;83(2):188–96. https://doi.org/10.1016/j.wneu.2014.05.037. Epub 2014 Jun 7. PMID: 24915068.
45. Morgan MK, Alsahli K, Wiedmann M, Assaad NN, Heller GZ. Factors associated with proximal intracranial aneurysms to brain arteriovenous malformations: a prospective cohort study. Neurosurgery. 2016;78(6):787–92. https://doi.org/10.1227/NEU.0000000000001114. PMID: 26565987.
46. Shakur SF, Amin-Hanjani S, Mostafa H, et al. Hemodynamic characteristics of cerebral arteriovenous malformation feeder vessels with and without aneurysms. Stroke. 2015;46:1997–9.
47. Fennell VS, Martirosyan NL, Atwal GS, Kalani MYS, Ponce FA, Lemole GM Jr. Hemodynamics associated with intracerebral arteriovenous malformations: the effects of treatment modalities. Neurosurgery. 2018;83:611–21.
48. Lawton MT, Rutledge WC, Kim H, Stapf C, Whitehead KJ, Li DY. Brain arteriovenous malformations. Nat Rev Dis Primers. 2015;1:15008.

49. Fierstra J, Conklin J, Krings T, Slessarev M, Han JS, Fisher JA. Impaired peri-nidal cerebrovascular reserve in seizure patients with brain arteriovenous malformations. Brain. 2011;134:100–9.
50. Zhang Y, Yan P, Liang F, Ma C, Liang S, Jiang C. Predictors of epilepsy presentation in unruptured brain arteriovenous malformations: a quantitative evaluation of location and radiomics features on T2-weighted imaging. World Neurosurg. 2019;125:e1008–15.
51. Hoh BL, Chapman PH, Loeffler JS, Carter BS, Ogilvy CS. Results of multimodality treatment for 141 patients with brain arteriovenous malformations and seizures: factors associated with seizure incidence and seizure outcomes. Neurosurgery. 2002;51:303–11.
52. Chen CJ, Shabo LM, Ding D, Ironside N, Kano H, Mathieu D. Seizure presentation in patients with brain arteriovenous malformations treated with stereotactic radiosurgery: a multicenter study. World Neurosurg. 2019;126:e634–40.
53. Zhang B, Feng X, Peng F, Wang L, Guo EK, Zhang Y. Seizure predictors and outcome after Onyx embolization in patients with brain arteriovenous malformations. Interv Neuroradiol. 2019;25:124–31.
54. Stapf C, Khaw AV, Sciacca RR, Hofmeister C, Schumacher HC, Pile-Spellman J. Effect of age on clinical and morphological characteristics in patients with brain arteriovenous malformation. Stroke. 2003;34:2664–9.
55. Cordero-Tous N, Jorques-Infante AM, Santos-Martin L, Alcazar-Romero PP, Fandiño-Benito E, Martin-Linares JM. Angiographic characteristics of epileptogenic arteriovenous malformations and effectiveness in the seizure control after treatment with radiosurgery. J Radiosurg SBRT. 2014;3:103–10.
56. Garcin B, Houdart E, Porcher R, Manchon E, Saint-Maurice JP, Bresson D. Epileptic seizures at initial presentation in patients with brain arteriovenous malformation. Neurology. 2012;78:626–31.
57. Turjman F, Massoud TF, Sayre JW, Viñuela F, Guglielmi G, Duckwiler G. Epilepsy associated with cerebral arteriovenous malformations: a multivariate analysis of angioarchitectural characteristics. AJNR Am J Neuroradiol. 1995;16:345–50.
58. Shankar JJS, Menezes RJ, Pohlmann-Eden B, Wallace C, terBrugge K, Krings T. Angioarchitecture of brain AVM determines the presentation with seizures: proposed scoring system. AJNR Am J Neuroradiol. 2013;34:1028–34.
59. Benson JC, Chiu S, Flemming K, Nasr DM, Lanzino G, Brinjikji W. MR characteristics of unruptured intracranial arteriovenous malformations associated with seizure as initial clinical presentation. J Neurointerv Surg. 2020;12:186–91.

Chapter 20
Arteriovenous Malformations: Treatment and Management

Rudy J. Rahme, Rohin Singh, Nicole De La Pena, Evelyn L. Turcotte, and Bernard R. Bendok

Abbreviations

AVMs	Arteriovenous malformations
ARUBA	A randomized trial of unruptured brain AVMs
ARE	Adverse radiation effects
DTI	Diffusion tensor imaging
fMRI	Functional MRI
NBCA	*n-butyl cyanoacrylate*
QMRA	Quantitative magnetic resonance angiography

R. J. Rahme · E. L. Turcotte
Department of Neurological Surgery, Mayo Clinic, Phoenix, AZ, USA

Precision Neuro-therapeutics Innovation Lab, Mayo Clinic, Phoenix, AZ, USA

Neurosurgery Simulation and Innovation Lab, Mayo Clinic, Phoenix, AZ, USA

R. Singh · N. De La Pena
Mayo Clinic Alix School of Medicine, Mayo Clinic, Scottsdale, AZ, USA

B. R. Bendok (✉)
Department of Neurological Surgery, Mayo Clinic, Phoenix, AZ, USA

Precision Neuro-therapeutics Innovation Lab, Mayo Clinic, Phoenix, AZ, USA

Neurosurgery Simulation and Innovation Lab, Mayo Clinic, Phoenix, AZ, USA

Department of Otolaryngology, Mayo Clinic, Phoenix, AZ, USA

Department of Radiology, Mayo Clinic, Phoenix, AZ, USA
e-mail: Bendok.Bernard@mayo.edu

J. R. Mascitelli, M. J. Binning (eds.), *Introduction to Vascular Neurosurgery*,
https://doi.org/10.1007/978-3-030-88196-2_20

Introduction

Arteriovenous malformations are complex vascular lesions characterized by abnormal connections between arteries and veins forming a tangle of vessels, without an intervening capillary bed (see Fig. 20.1). First described by Luschka and Virchow in the mid-nineteenth century as "vascular hamartomas," these lesions proved to be highly challenging to the early pioneering neurosurgeons, who cautioned against resecting them [1]. In 1932, the Swedish neurosurgeon Herbert Olivecrona introduced the surgical technique of circumferential AVM disconnection and successfully resected a cerebellar AVM in a 37-year-old man. By 1954, he had performed 125 AVM resections with a mortality rate of 9%. The next major innovation happened in 1957 with the introduction of the operative microscope to neurosurgery by Theodor Kurz (during the resection of cranial nerve VII schwannoma) which was later popularized by Gazi Yasargil in 1967. This development ushered in the era of vascular microneurosurgery.

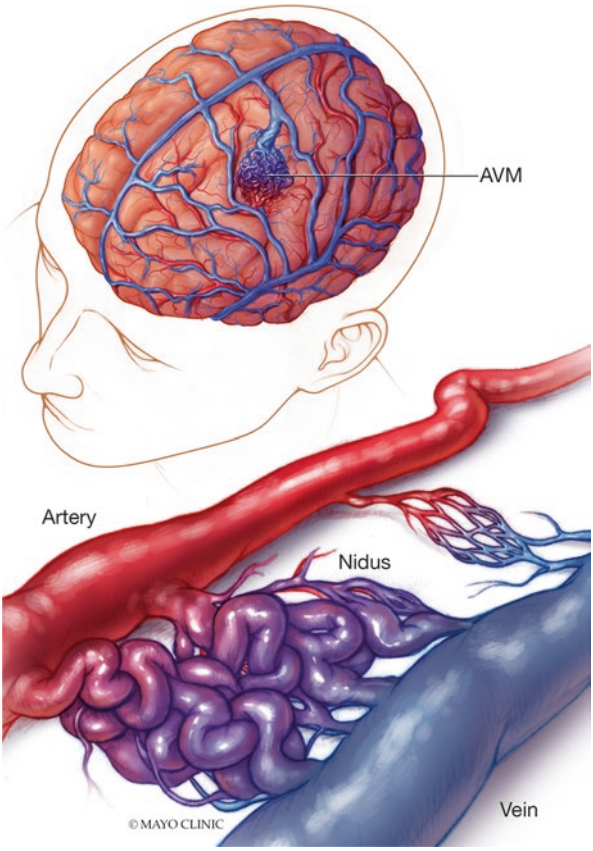

Fig. 20.1 Illustration of an arteriovenous malformation. Arteriovenous malformations are complex vascular lesions characterized by abnormal connections between arteries and veins forming a tangle of vessels without an intervening capillary bed, called a nidus. From Mayo Clinic Patient Education [89]; used with permission of Mayo Foundation for Medical Education and Research, all rights reserved

Since the introduction of microsurgery, several other treatment modalities have been developed such as endovascular embolization and radiosurgery. However, due to the highly variable and complex nature of AVMs, a single approach is often insufficient and a combination of modalities is necessary to appropriately treat these lesions.

Grading Tools and Prognostication

Several models have been developed to evaluate the risk of intervention in AVMs. The Spetzler-Martin grading system, developed in 1986, is among the most commonly used microsurgical risk assessment tool (see Table 20.1). This grading system evaluates AVMs based on their size, location, and pattern of venous drainage [2]. In 2010, the Lawton-Young supplementary grading scale was developed to further stratify pre-interventional risk and prognosticate neurological outcomes following AVM surgery (see Table 20.2) [3]. This scale took into account various other factors such as the patient's age, hemorrhage history, and architecture of the feeding arteries. In 2011, Spetzler and Ponce proposed a new simplified classification based

Table 20.1 Spetzler-Martin grading system

Spetzler-Martin grading system		
Size of the AVM "largest diameter of the nidus" (cm)	Small (<3 cm)	1
	Medium (3–6 cm)	2
	Large (>6 cm)	3
Pattern of venous drainage	Superficial	0
	Deep	1
Neurological eloquence of the brain regions adjacent to the AVM	Non-eloquent	0
	Eloquent	1
Total	1–5	

Table 20.2 Lawton-Young supplementary grading scale

Lawton-Young supplementary grading scale		
Age	<20 years	1
	20–40 years	2
	>40 years	3
Unruptured presentation	No	0
	Yes	1
Diffuse	No	0
	Yes	1
Total	1–5	

on the Spetzler-Martin grading (Table 20.3) [4]. They combined grades I and II into one class and grades IV and V into one group. This was based on the fact that treatment approaches and outcomes are similar between these grades.

The utility of the Spetzler-Martin Scale for AVM evaluation is limited to surgical intervention and does not include variables specific to other treatment modalities. In 2013, Starke et al. introduced the Virginia Radiosurgery AVM scale that took into account the volume of the AVM, location of the AVM in relation to eloquent brain regions, and the patient's history of hemorrhage (see Table 20.4) [5]. Scores ranged from 1 to 4 with lower scores correlating with more favorable outcomes. Positive outcomes were seen in 80% of patients with a score of 0–1 compared to 45% of patients with a score of 3–4. Even after correcting for Gamma Knife treatment parameters such as peripheral dose and number of isocenters, their grading scale was found to have a strong predictive value for outcomes with radiosurgery for AVMs.

In 2015, the Buffalo Grading System was proposed to classify the risk of endovascular treatment of AVMs (see Table 20.5). This scale ranges from a score of 1 to 5, and

Table 20.3 Spetzler-Ponce grading system

Spetzler-Ponce grading system		
Class A	Spetzler-Martin grades I & II	Surgical resection
Class B	Spetzler-Martin grade III	Multimodality treatment
Class C	Spetzler-Martin grades IV & V	No treatment with exceptions

Table 20.4 Virginia radiosurgery AVM scale

Virginia radiosurgery AVM scale		
AVM volume (cm^3)	<2 cm^3	1
	2–4 cm^3	2
	>4 cm^3	3
Unruptured presentation	Superficial	0
	Deep	1
Neurological eloquence of the brain regions adjacent to the AVM	Non-eloquent	0
	Eloquent	1
Total	1–4	

Table 20.5 Buffalo grading system

Buffalo grading system		
Number of arterial pedicles	1 or 2	1
	3 or 4	2
	5 or more	3
Diameter of arterial pedicles	>1 mm	0
	≤1 mm	1
Nidus location	Non-eloquent	0
	Eloquent	1
Total	1–5	

assigns risk based on three parameters: number of arterial pedicles, diameter of the arterial pedicles, and location of the nidus (eloquent vs non-eloquent) [6]. In 2019, the predictive validity of this scale was confirmed in a study of 104 consecutive patients. The Buffalo Score outperformed similar endovascular grading scales in predicting [7].

Conservative Management: ARUBA Trial

The ARUBA (A Randomized Trial of Unruptured Brain AVMs) trial was a randomized controlled trial comparing conservative medical management to intervention in AVM treatment [8]. A total of 114 patients were randomized to interventional therapy (IT) and 109 to medical management before the trial was stopped prematurely. Of the 114 patients in the intervention group, 76 had a grade I or II AVM. The data and safety monitoring board recommended halting enrollment due to significantly worse outcomes in the IT group. The risk of stroke or death was found to be significantly lower in the medical management group compared to the IT group with a hazard ratio of 0.27 (95% CI 0.14–0.54). The intervention group had a higher number of strokes (45 vs 12), and neurological deficits unrelated to stroke (14 vs 1) as well. However, the trial design had severe flaws limiting its internal and external validity.

Much has been written about the limitation of ARUBA. The key concern with the trial relates to the treatment arm. The treatment decisions were left to the treating physician with no specific protocols. Surprisingly and notably, there was a very low rate of microsurgical resection (5/76 patients) even for low Spetzler-Martin grade AVMs which are curable with surgery with relative low morbidity. Thirty patients were treated with standalone embolization with up to six embolization sessions per patient. While endovascular approaches can be effective as a standalone treatment for select small AVMs, the rate of cure remains very low for most lesions. In addition, embolization with intent to cure appears to have a higher rate of complication than presurgical embolization [9]. It should also be noted that partial embolization of AVMs likely increases the risk of hemorrhage [10]. Radiosurgery was the selected treatment in 31 patients. However, there is a long latency period with radiosurgery during which the AVM is still at risk of hemorrhage. These treatment paradigms do not reflect the real-life practice, at least in North America, where microsurgical resection remains the treatment of choice for surgically accessible AVMs, significantly limiting the external validity of the trial. In fact, multiple case series of ARUBA-eligible patients treated with microsurgical resection were reported, revealing lower stroke and death rates compared to the ARUBA trial [11, 12]. Finally, one of the main overlooked findings of this trial is the high rate of stroke or death with conservative management of AVMs (10.1%) over a period of less than 3 years. Therefore, ARUBA represents a failure of the specific strategies used in the trial on a heterogenous group pod AVMs. One lesson from the trial is that serial embolization alone is not an ideal starter for most AVMS. Rather, what ARUBA demonstrates is that multimodal therapy, including microsurgical resection, remains the treatment of choice for many AVMs.

Treatment Strategies

Due to their complexity, AVMs often require a multimodal treatment approach with various combinations of endovascular, microsurgical, and radiosurgical techniques in order to safely achieve a cure. Treatment often starts with control of high-risk features whenever safely feasible. Therefore, a thorough diagnostic angiogram with possible superselective catheterization of arterial feeders is necessary to formulate a treatment strategy. Superselective angiograms are safe and improve our understanding of AVM flow dynamics. They also have a higher sensitivity of detecting associated aneurysms [13].

Endovascular Approaches

Endovascular approaches have multiple indications in the diagnosis and treatment of AVMs. They can be used as a standalone treatment or as an adjunct to microsurgery or radiosurgery (see Fig. 20.2).

Embolization for intracranial AVMs was first introduced in 1960 by Luessenhop and Spence at Georgetown University Medical School [14]. The authors reported the case of a 47-year-old female who underwent embolization of a large left frontal AVM using pellets of methyl methacrylate injected directly into the cervical internal carotid artery after surgical exposure of the carotid. Endovascular techniques and technology have come a long way since that time.

Preoperative Embolization

Targeted preoperative embolization has multiple indications. These include control of deep feeders, progressive decrease of AVM flow to reduce intraoperative and postoperative risk of hemorrhage and facilitate AVM resection, normalization of peri-AVM hemodynamics, occlusion of associated proximal aneurysms, and control of rupture site in hemorrhagic presentations. In addition, the embolic cast can sometimes provide a clear plane of dissection during surgery. Preoperative embolization has been shown to reduce operative time and intraoperative blood loss. In 1993, Jafar et al. reported a series of patients treated with and without preoperative embolization with NBCA [15]. In the embolization group, the AVMs were significantly larger and of a higher Spetzler-Martin grade compared to the non-embolization group. However, the operative time and intraoperative blood loss were not significantly different between the two groups. The authors concluded that embolization converts lesions of a larger size and higher grade into the equivalent of a smaller size and grade lesions. Additionally, there were no significant differences in surgical complications or long-term neurological outcomes between the two groups. In fact, further studies revealed an improved postsurgical outcome following preoperative

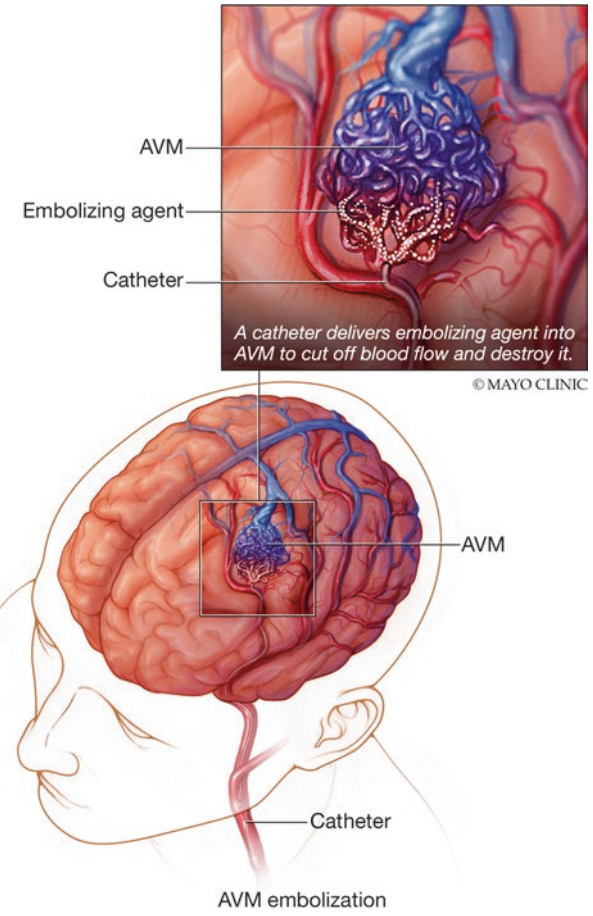

Fig. 20.2 Endovascular approaches to AVMs. Endovascular embolization of AVMs. Figure 20.2 illustrates the delivery of an embolic agent into an AVM. Embolization may be used as a standalone treatment or as an adjunct to microsurgery or radiosurgery. From Mayo Clinic Patient Education [89]; used with permission of Mayo Foundation for Medical Education and Research, all rights reserved

embolization as opposed to surgery alone [16, 17]. However, preoperative embolization should be used judiciously due to the potential added risk of complications associated with the procedure. In fact, for many Spetzler-Martin grade I or II AVMs, the benefits may not outweigh the risks of preoperative embolization due to the low morbidity associated with standalone surgical resection of these lesions [18].

One mechanism through which embolization mitigates surgical and postoperative risk is by altering the hemodynamics within the AVM nidus and in the peri-AVM normal brain. Staged embolization leads to progressive decrease in flow velocities as well as peak velocities in the arterial feeders and the draining veins [19]. These changes are not limited to the AVM nidus though, with normalization of flow in the arterial supply to both hemispheres, as revealed by the 4D flow study by Markl et al. [19]. This effectively slows the arteriovenous shunting through the nidus with slower filling of the veins and decrease in the peri-AVM vascular steal phenomenon. Alaraj et al. retrospectively reviewed AVM flow rates pre- and post-embolization using quantitative magnetic resonance angiography (QMRA) and

found a 29% drop in AVM flow after each embolization session, leading to a total drop of 75% after the final embolization [20]. They additionally observed that the total number of pedicles and intranidal fistulas embolized during any session was significantly associated with the total decrease of AVM flow. However, it is important to avoid aggressive embolization with abrupt decreases in AVM flow which significantly increase the risk of post-embolization hemorrhage [21]. In fact, staging of embolization sessions also appears to be beneficial in preventing postoperative vascular overload of surrounding brain tissue by reducing blood flow through the nidus in a stepwise fashion [20, 22, 23]. Finally, deep feeder control is one of the major benefits of preoperative embolization. These tiny vessels can be difficult to control intraoperatively and can rupture and retract into the surrounding white matter leading to intracerebral hemorrhage [24].

Pre- and Post-radiosurgery Embolization

The role of endovascular embolization as an adjunct to radiosurgery in AVMs is controversial. While the initial thought was that embolization can increase the efficacy of radiosurgery by reducing the nidus size, recent data seems to suggest that pre-radiosurgery embolization reduces the rate of AVM obliteration [25–27]. The reasons for this are manifold. It has been hypothesized that during the latency period following radiosurgery, the embolized portions of the nidus, which are often left outside of the field of radiation, can recanalize [28–30]. In fact, embolization has been found to induce angiogenesis, which can also contribute to the recanalization of the previously embolized part of the AVM [30–32]. In addition, embolization can increase the difficulty of adequately defining the nidus during radiosurgery planning by obscuring its boundaries and by fragmenting it into noncontiguous compartments. Therefore, embolization may be best used post-radiosurgery to treat associated aneurysms. Whether post-radiosurgery embolization can help us to improve occlusion rates remains an open question.

Pre-radiosurgery embolization can still play a limited role though. In particular, due to the long latency period after radiosurgery, embolization can be used to address high-risk features of an AVM, such as associated aneurysms. Kano et al. analyzed a cohort of 996 patients treated with stereotactic radiosurgery and found that the presence of an aneurysm was significantly associated with an increased risk of hemorrhage after radiosurgery, with an annual hemorrhage rate of 6.4% in these patients compared to 0.8% in patients with clipped or embolized aneurysms [33]. In addition, in a retrospective study of 86 AVM patients treated with “targeted embolization” with Onyx (eV3 neurovascular, Irvine, CA) to eliminate AVM-associated aneurysms, Xiaochuan et al. revealed that hemorrhagic complications were significantly lower in patients who received targeted embolization than in those who did not [34]. However, the effect of embolization on hemorrhage risk remains unclear in the literature, as several other studies have reported no decrease in the risk of hemorrhage between patients who undergo embolization prior to radiosurgery compared to radiosurgery alone [25, 27, 35].

Standalone Therapy

Standalone therapy includes palliative measures as well as embolization with intent to cure. The main goal of palliative treatment is to alleviate neurological symptoms related to ischemia from vascular steal and/or venous hypertension in patients with high-grade untreatable AVMs. Palliative treatment can also address high-risk features associated with hemorrhage. In a retrospective study of 14 patients with Spetzler-Martin grade IV or V AVMs presenting with progressive neurological deficits, Al-Yamany et al. reported an improvement in neurological deficits in 42% of patients after palliative embolization, with stabilization of deficits in an additional 50% [36]. However, it is important to note that palliative embolization does not improve overall outcomes [37]. In fact, while palliative embolization can temporarily alleviate symptoms, it can also lead to ischemia-induced angiogenesis with the recruitment of collateral flow [24]. The end result could be a higher complexity AVM with increased flow and worsened symptoms. Therefore, palliative embolization should be used as a last resort.

In select cases, endovascular embolization can be used as standalone treatment with intent to cure. This is typically reserved for small AVMs with a single or low number of arterial feeders. Reports of angiographic cure rates with embolization alone vary from 5% to 94% [13, 38–42]. This wide variability is explained by the heterogeneity of AVMs included in these studies in terms of size, Spetzler-Martin grade, number of arterial feeders, and location. In a systematic review of AVMs treated with standalone embolization with intent to cure, Wu et al. found that complete obliteration was reported in 58% of AVMs with completed treatment, and in 46% of AVMs in the entire cohort of 597 patients [43]. However, the morbidity rate was high at 24% with a mortality rate of 1.5%. The most common complication was hemorrhage which occurred in 10% of patients.

Factors associated with a high rate of complete occlusion with embolization alone include small size (≤3 cm), single easily accessible arterial feeder, and noneloquent location [9, 44, 45]. In addition, Valavanis and Yasargil hypothesized that AVM morphology, as opposed to size and number of feeders, was the key factor that predicted successful occlusion of these lesions, where fistulous-predominant AVMs were easier to embolize than the pure plexiform type [44]. From a technical perspective, an arterial pedicle that allows for safe reflux of Onyx in order to form a plug around the microcatheter has also been associated with a higher rate of complete obliteration. Finally, an unobstructed view of the draining vein, specifically its proximal portion, is also a key factor which allows for more aggressive and safe embolization.

Risks and Complications of Embolization

Large clinical series of AVM embolization have reported highly variable mortality rates of 0–4.3% and morbidity rates ranging from 0% to 24.5% [13, 46]. Again, the variability of these rates is related to the heterogeneity of the AVM population as

well as the different indications and techniques of embolization. The most common complications include ischemic or hemorrhagic strokes. Ischemic events can occur due to migration or reflux of the embolic material into the normal vasculature or the draining veins. A clear understanding of the arterial supply to the AVM including "en passage" vessels can decrease that risk. Hemorrhage can result from intraprocedural rupture due to microwire perforation or from a traumatic withdrawal of a microcatheter entrapped in the Onyx cast. Recent development of microcatheters with detachable tips has decreased the risk of this complication [47]. Finally, early occlusion of the draining vein can lead to a substantial retrograde increase in pressure in the nidus, resulting in hemorrhage.

Post-embolization hemorrhage can lead to severe morbidity and mortality. Subat et al. performed a meta-analysis of AVM patients embolized with cyanoacrylate or ethylene vinyl alcohol copolymer between 1990 and 2019 [45]. They found that out of 8009 patients, the total periprocedural hemorrhage rate was 4.8%, with a high mortality and morbidity rate associated with hemorrhage at 14.6% and 45%, respectively. Several studies have analyzed predictive risk factors for periprocedural hemorrhage after embolization. Heidenreich et al. revealed that in a retrospective study of 125 AVM embolizations using NBCA, AVM reduction >60% in a single session was a significant risk factor of hemorrhage, with an odds ratio of 18.8. In addition, small AVMs were also associated with a greater hemorrhage risk [21]. Jordan et al. also found that smaller AVMs and large flow reductions per session were associated with higher hemorrhage rates [48]. The authors postulated that the aggressive flow reduction during embolization of small AVMs could lead to flow redistribution in the remaining arterial feeders. The sudden rise in perfusion pressure could lead to rupture of these nidal vessels. These studies highlight the importance of avoiding overly aggressive embolization.

Two theories have been advanced to explain the post-procedure hemorrhage phenomenon. The first theory is Normal Perfusion Pressure Breakthrough introduced by Spetzler et al. in 1978. The authors reported several cases where reestablishment of perfusion following resection of an AVM resulted in capillary breakthrough leading to malignant edema and hemorrhage. The surrounding brain parenchyma in relation to the AVM is chronically ischemic due to the vascular "steal" of blood flow through the low-resistance AVM, as well as the elevated venous pressures [22, 49]. Spetzler et al. postulated that normal vessels supplying brain parenchyma surrounding the AVM become chronically dilated in response to the relative ischemia due to the steal phenomenon. This results in an impairment of the normal autoregulation of these vessels. When normal perfusion pressure is suddenly reestablished, the surrounding tissue might not be able to increase the resistance of the vessels in response to increased pressure. Stepwise reperfusion through a staged approach may help reestablish autoregulation in these vessels.

The second theory is the occlusive hyperemia theory described by Al-Rodhan et al. in 1993 [50]. These authors proposed two separate but interrelated mechanisms that could lead to the edema and hemorrhage seen after AVM resection: stagnation of flow in prior arterial feeders and obstruction of draining veins. The stagnant

arterial flow in former AVM feeders leads to further hypoperfusion and ischemia in surrounding brain parenchyma. The obstruction of venous outflow leads to passive hyperemia and further arterial stagnation [50].

Microsurgical Treatment

The first surgical exposure of an AVM was performed by Italian surgeon Davide Giordano in 1889. However, this was limited to exposure and palliative ligation of a left parietal feeding artery. The French surgeon Jules-Émile Péan is credited with the first complete resection of an AVM in 1889. However, early experiences of surgical treatment of AVMs consisted of ligation of cortical veins which led to "calamitous results" as Harvey Cushing put it himself [1]. Attempts of surgical resection also had poor outcomes consisting of incomplete resection and significant morbidities and mortalities. It was not until Olivecrona's groundbreaking technique of circumferential dissection that outcomes with surgical resection became acceptable. Surgical resection quickly became the mainstay of AVM treatment. To this day, microsurgical resection remains a key pillar in the treatment of most AVMs.

Principles of AVM Microsurgery

When planning the craniotomy for microsurgical AVM resection, a wide exposure via a large craniotomy is preferred. A larger craniotomy allows for greater visualization and control of nearby vasculature, and improved cortical mapping when needed. Understanding the three-dimensional structure of AVMs through two-dimensional scans can be difficult. Recently, a variety of image guidance systems, including 3D augmented and virtual reality systems, became available, allowing for greater precision in surgical planning which is essential to avoid critical structures during exposure. Reports have been published supporting the usefulness of virtual reality both pre- and intraoperatively [51]. Diffusion tensor imaging (DTI) and functional MRI (fMRI) have also successfully been implemented in the preoperative assessment of AVMs, allowing for a greater understanding of the relationship between AVMs and white matter tracts and eloquent brain regions, therefore improving the safety of microsurgical resection [52, 53].

Once adequate exposure has been obtained, a complete understanding of the surgical anatomy is fundamental prior to the resection. The draining veins should be identified early on and preserved until all the arterial supply is disconnected. Indocyanine green angiography can help identify the arterialized, early filling, veins. Starting superficially, a circumferential dissection of the arterial feeders is performed (see Fig. 20.3). A few key principles should be observed while dissecting the nidus. First, "en passage" vessels should be preserved. These are arteries that supply normal brain parenchyma while also giving off branches to the AVM. These arteries can be identified preoperatively with a thorough analysis of the diagnostic

angiogram (superselective angiography can be helpful). Second, as the dissection gets deeper, small fragile arterial feeders are encountered. These vessels are often subjected to chronic high flow and do not respond well to cautery. AVM clips should be used as needed to control these thin-walled feeders. Using controlled suction, these feeders can be gently "lifted up" allowing for controlled and easy clipping. It is important to avoid tearing these feeders which can result in them being pulled back into white matter. This has the dual risk of deep hemorrhage and an increased risk of white matter injury from this hemorrhage and/or the dissection needed to find and control them. Use of cottonoids and cotton balls to achieve hemostasis by holding pressure on these bleeders is discouraged, since it does little to stop these arteries from bleeding and therefore risks intracerebral hemorrhage. Third, after all arterial supply has been disconnected, draining veins can be dissected and cut. However, sometimes, it can be difficult to differentiate veins from arteries. In these situations, a temporary clip can be placed on the vessel in question and the nidus is observed for any signs of outflow obstruction. In the absence of these signs, the vessel is coagulated and cut. Finally, after delivery of the nidus, meticulous hemostasis should be achieved by carefully inspecting the resection cavity.

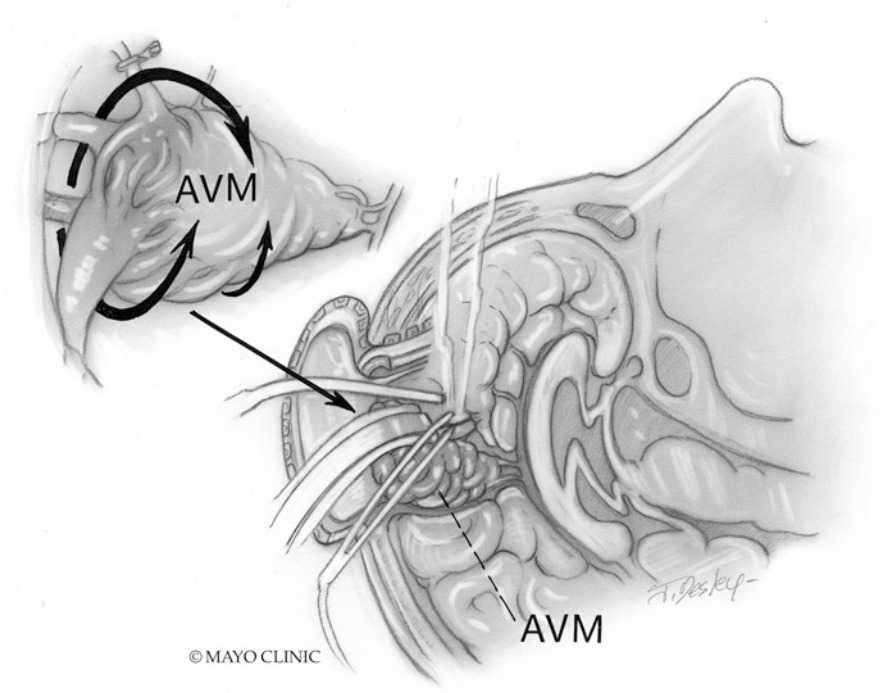

Fig. 20.3 Circumferential dissection of an AVM. Figure 20.3 illustrates the circumferential dissection technique. Used with permission of Mayo Foundation for Medical Education and Research, all rights reserved

Surgery Post-embolization or Radiosurgery

Preoperative embolization may allow for quicker and safer resection of certain lesions as discussed earlier in the chapter. While the majority of grade 1 and 2 lesions can be safely resected without embolization, larger and more deeply located lesions may benefit from multimodal approaches. Embolization of deep arterial feeders and proximal aneurysms can drastically simplify the approach and reduce the risk of hemorrhage intraoperatively [54].

Radiosurgery can also help facilitate surgical resection of AVMs and has been shown to decrease morbidity in some scenarios. In a series of 344 patients who underwent microsurgical resection of their AVMs, preoperative radiosurgical treatment was shown to significantly reduce the size of the AVM by a mean of 78%, and the Spetzler-Martin grade in 52% of cases [55]. The mean operative time, blood loss, and length of hospital stay were also significantly decreased compared to those who did not receive preoperative radiosurgery. This combination approach is best recommended for unruptured AVMs and can help facilitate resection of previously inoperable lesions. Additionally, if radiosurgery is chosen as a standalone treatment, but fails to completely obliterate the AVM within 3–5 years, microsurgical resection can be used to remove the residual nidus [55].

Acute Ruptured Emergency

In patients with hemorrhagic presentation, the first step after settling medical issues, hydrocephalus and ICP, is determining and addressing the site of rupture, whether it is the actual AVM nidus or an associated aneurysm. Endovascular management can often adequately treat the rupture site if it can be clearly identified angiographically. Microsurgical resection of the AVM should be postponed beyond the acute phase to allow the brain to relax and the cytotoxic edema to subside. However, the resection may be best performed before complete resolution of the hematoma since its presence creates a dissection plane eliminating the need for further white matter dissection. A study by Beecher et al. analyzed the safety of delayed treatment in 102 patients with hemorrhagic presentations of AVMs. Patients were treated at least 4 weeks after the initial presentation. Delayed intervention posed a low (<1%) risk of rehemorrhage in most patients, though the timeline to treatment should be modified if high-risk features such as aneurysms are discovered [56]. In cases with large hematomas and elevated intracranial pressure, decompressive hemicraniectomy without AVM resection could be attempted, even with the partial evacuation of the hematoma without disturbing the nidus. Other temporizing measures include medical management and external ventricular drain placement. Continuous monitoring for seizures, especially in patients who are comatose, could also be considered as an extra safety measure [54].

Surgical Outcomes

The outcomes of microsurgical resection of AVMs are highly variable and depend on patient and AVM characteristics. For Spetzler-Martin grade I and II, the rate of complete resection is close to 100% with only 5% risk of minor deficits. On the opposite end of the spectrum, grade IV and V AVMs are high-risk lesions that often require a multimodal approach with endovascular and radiosurgical modalities. However, despite all the advances in techniques and technology, treatment of these lesions remains challenging. In fact, conservative or palliative management is often recommended in these patients when they are asymptomatic [57]. Grade III AVMs are a heterogeneous group making it difficult to assess surgical risk and outcome. Nevertheless, microsurgical resection seems to achieve a favorable outcome in 70–89% of cases [58]. AVM location can also affect outcome. In particular, posterior fossa AVMs are high-risk lesions due to their proximity to sensitive structures. Rates of complete resection, morbidity, and mortality for the posterior fossa location are highly variable, as expected, and range from 43% to 100%, 9% to 25%, and 0% to 15%, respectively, emphasizing the need for careful case selection [59, 60]. Recurrence of AVMs after documented complete obliteration after microsurgical resection is an extremely rare but documented and poorly understood phenomenon [61]. Rates of recurrence are thought to be higher in the pediatric population and should be taken into account for postoperative follow-up [61, 62]. Similarly, patients with underlying genetic anomalies such as hereditary hemorrhagic telangiectasia are at increased risk of recurrence and should be followed up more closely [63, 64].

Radiosurgical Treatment

Stereotactic radiosurgery can be used as a standalone therapy or in association with endovascular embolization and/or microsurgery, as discussed previously. Typically, radiosurgery is used for small AVMs (<3 cm in diameter or 10 cm^3 in volume) in deep or eloquent brain areas. Irradiation of the vascular endothelium generates an inflammatory response, stimulating smooth muscle proliferation and collagen deposition and resulting in progressive luminal obstruction and nidal obliteration [65, 66]. Radiosurgical treatment is beneficial as it is noninvasive, has a minimal risk of procedural complications, and is performed in an outpatient setting. In general, obliteration is achieved in 70–80% of cases [24, 67]. However, occlusion of the nidus takes up to 5 years to achieve, with a persistent risk of hemorrhage during the latency period. In general, AVMs are monitored post-radiosurgery via MRI every 6–12 months. Angiography is typically performed to confirm obliteration of the nidus.

Radiosurgery Outcomes

Initial reports of successful treatment of AVMs with stereotactic radiosurgery were published in the 1970s by Steiner and colleagues at the Karolinska Institute in Stockholm using Gamma Knife radiosurgery [68]. From their studies ranging from the years 1977 to 1991, their cumulative rate of complete obliteration of AVMs was between 79 and 95% [69]. Lunsford et al. also reported their experience at the University of Pittsburgh treating 227 AVMs with Gamma Knife radiosurgery. They found that 2-year obliteration rates were highest for lesions less than 1 cm^3, at 100%, and lowest for lesions greater than 4 cm^3, at 58%, while their overall 2-year obliteration rate was 80% [70]. Stereotactic radiosurgery can also be useful in addressing AVM-related seizure, headache, and neurological deficits [69, 70]. While initial stereotactic radiosurgeries were performed on Gamma Knife technology, there are currently other devices and modalities of stereotactic radiosurgery that can be used to treat AVMs, including particle beam and linear accelerator. These different technologies appear to have similar patient outcomes. Betti and Rosler pioneered the use of linear accelerator radiosurgery and reported a 66% obliteration rate [71]. For Bragg-peak proton beam therapy, although the initial obliteration rate reported by Kjellberg et al. was only 20%, Steinberg et al. reported a 3-year obliteration rate of 92% in their series using this type of stereotactic radiosurgery [72, 73]. However, independent of radiation modality, the rate of obliteration remains heavily dependent on radiated volume. Therefore, AVM size should be taken into account when interpreting occlusion rates.

Multiple factors can affect the efficacy of radiosurgery. AVM volume, appropriate targeting, and radiosurgical margin dose appear to have the highest impact [74–78]. Margin doses must be formulated to balance the effective dose for the size of the lesion against the risks of radiation effects on normal surrounding tissue. Flickinger et al. reviewed their series of 197 AVM patients treated with Gamma Knife radiosurgery and revealed a complete occlusion rate of 72% at 3-year angiographic follow-up [74]. The median target volume was 4.1 cc (range: 0.06–18 cc) and the median minimum target dose was 20 Gy (range: 12–25.6 Gy). A multivariate logistic regression analysis revealed that minimum target dose was independently and significantly correlated with obliteration rate [74]. In addition to AVM-related factors, targeting errors can lead to failed initial radiosurgical obliteration [28, 76]. In a report of 45 patients who initially had incomplete obliteration with radiosurgery, Pollock et al. reported that the most common reasons for needing a second treatment were incomplete angiographic definition of the nidus, recanalization of the AVM nidus after embolization, and incomplete nidus recognition due to obstruction from a hematoma [28]. These challenges in target planning highlight the importance of utilizing comprehensive imaging modalities to create the dosimetry plan, such as CT or MR angiography, as opposed to relying on conventional diagnostic angiography alone [79].

More recently, data compiled from the International Radiosurgery Research Foundation on 2248 AVM treated with Gamma Knife from 1988 to 2013 was published [80]. Data was collected retrospectively from eight different centers with a median follow-up of 7 years (range: 1–20 years). The median treated volume was 4.3 cm^3. The delivered mean margin dose was 20.5 Gy. The results revealed an overall obliteration rate of 64.7%. After eliminating the postradiation hemorrhages (1.1% annual risk) and the radiation-induced changes (29.2% total, 9.7% symptomatic, 2.7% with permanent deficit), the rate of favorable outcome with Gamma Knife was calculated at 60.3%. Factors that were associated with poor outcome in a multivariate analysis were prior embolization, larger volume, prior AVM hemorrhage, multiple isocenters, eloquent location, and lower margin dose.

For large AVMs (>10cm^3), a staged radiosurgery approach could be used to divide the nidus into multiple smaller foci of radiation to increase the delivered dose and therefore the efficacy of treatment [67]. Eloquent location is often one of the indications of radiosurgery, including brainstem and basal ganglia. Retrospective data from six centers including 205 patients with brainstem AVMs treated with radiosurgery revealed an obliteration rate of 65.4% with a mean follow-up of 69 months [81]. Radiographic radiation effect was noted in 35.6% of patients with 14.6% symptomatic, all of whom had permanent deficits including cranial nerve deficits and long tract signs. The post-radiosurgery annual hemorrhage rate (latency period) was 1.5%. Improved rates of complete obliteration correlated with a margin dose of >20 Gy. Patients with higher margin and maximum doses also had earlier obliteration of their AVMs. The study also revealed that occlusion rates continued to improve even 10 years out from the procedure.

Risks of Radiosurgery

Adverse events related to radiosurgery are typically delayed with very low risk of immediate complication. Adverse radiation effects (ARE) are post-radiosurgical imaging changes appearing as perinidal T2-weighted hyperintensities that develop 6–18 months after treatment [67]. These can be symptomatic, with the onset of neurologic deficits, or asymptomatic radiographic findings. Flickinger et al. reviewed the follow-up imaging of 307 AVM patients treated with Gamma Knife radiosurgery and found that ARE developed in 30.5% of patients and were symptomatic in 10.7% of all patients, with a median time of onset of 12 and 14 months for radiologic and symptomatic ARE, respectively. Multivariate logistic regression modeling identified volume receiving ≥12 Gy as the only significant predictor of the development of ARE [82]. In their retrospective review of 85 patients treated with Gamma Knife, Hayhurst et al. additionally identified a target volume threshold of 4 cm^3 above which there is a substantial increased incidence of ARE [83]. These changes can regress in 95% of asymptomatic cases and in approximately half of the

symptomatic patients 3 years after the treatment. A course of high-dose corticosteroids is often prescribed for patients with ARE, and in select cases of refractory edema, Bevacizumab can be used [84]. Another potential complication of radiation is cyst formation which occurs less commonly and in a more delayed fashion than ARE and develops in 2–5% of patients [67, 85].

The major limitation of radiosurgery remains the delayed obliteration of the AVM nidus, resulting in a persistent risk of hemorrhage during the latency period. While most studies revealed that this risk is comparable to the natural history of untreated AVMs [66, 86], there are some reports of decreased risk even prior to complete thrombosis of the nidus [87]. In a multicenter, retrospective cohort study within the International Radiosurgery Research Foundation, Ding and colleagues analyzed the hemorrhage risks associated with AVMs both before and after stereotactic radiosurgery in 2320 patients [88]. They found that significant predictors of post-radiosurgical hemorrhage were deep AVM location, the presence of AVM-associated aneurysms, and lower margin dose. While the AVM hemorrhage rate decreased significantly from pre-radiosurgery to after treatment (15.4 hemorrhages/1000 person-years to 11.9), this reduction appeared to be driven by obliteration of the AVM nidus. Therefore, the authors concluded that there is insufficient evidence to indicate that stereotactic radiosurgery protects from AVM hemorrhage in patients who do not achieve nidal obliteration [88]. The natural history of AVMs appears to remain unchanged until the nidus is completely occluded.

Conclusions

Arteriovenous malformations are complex and heterogeneous lesions, and often require multimodal treatment strategies. They are typically diagnosed in the third and fourth decades of life and carry a significant lifetime risk of hemorrhage. Diagnostic angiograms with superselective catheterization allow for a better understanding of the angioarchitecture of these lesions. Advanced imaging can also elucidate the relationship of the AVM to the surrounding brain parenchyma. Based on AVM size, location, angioarchitecture, and associated high-risk features, as well as patient characteristics, a treatment strategy which can incorporate all three treatment modalities is then devised. Recurrences after angiographically confirmed complete occlusion are extremely rare but can occur.

Permissions Please see attached document labeled “Permissions” and return to Evelyn Turcotte at turcotte.evelyn@mayo.edu. Phone: 480–522-8520.

Contributor Agreement Please see attached document labeled “Contributor Agreement.”

References

1. Cohen-Gadol AA, Spencer DD, Harvey W. Cushing and cerebrovascular surgery: part II, Vascular malformations. J Neurosurg. 2004;101(3):553–9.
2. Spetzler RF, Martin NA. A proposed grading system for arteriovenous malformations. J Neurosurg. 1986;65(4):476–83.
3. Lawton MT, Kim H, McCulloch CE, Mikhak B, Young WL. A supplementary grading scale for selecting patients with brain arteriovenous malformations for surgery. Neurosurgery. 2010;66(4):702–13; discussion 13.
4. Spetzler RF, Ponce FA. A 3-tier classification of cerebral arteriovenous malformations. Clinical article J Neurosurg. 2011;114(3):842–9.
5. Starke RM, Yen C-P, Ding D, Sheehan JP. A practical grading scale for predicting outcome after radiosurgery for arteriovenous malformations: analysis of 1012 treated patients. J Neurosurg JNS. 2013;119(4):981.
6. Dumont TM, Kan P, Snyder KV, Hopkins LN, Siddiqui AH, Levy EI. A proposed grading system for endovascular treatment of cerebral arteriovenous malformations: Buffalo score. Surg Neurol Int. 2015;6:3.
7. Pulli B, Stapleton CJ, Walcott BP, Koch MJ, Raymond SB, Leslie-Mazwi TM, et al. Comparison of predictive grading systems for procedural risk in endovascular treatment of brain arteriovenous malformations: analysis of 104 consecutive patients. J Neurosurg. 2019:1–9.
8. Mohr JP, Parides MK, Stapf C, Moquete E, Moy CS, Overbey JR, et al. Medical management with or without interventional therapy for unruptured brain arteriovenous malformations (ARUBA): a multicentre, non-blinded, randomised trial. Lancet. 2014;383(9917):614–21.
9. Wu EM, El Ahmadieh TY, McDougall CM, Aoun SG, Mehta N, Neeley OJ, et al. Embolization of brain arteriovenous malformations with intent to cure: a systematic review. J Neurosurg. 2019;132(2):388–99.
10. Kalani MY, Albuquerque FC, Fiorella D, McDougall CG. Endovascular treatment of cerebral arteriovenous malformations. Neuroimaging Clin N Am. 2013;23(4):605–24.
11. Rutledge WC, Abla AA, Nelson J, Halbach VV, Kim H, Lawton MT. Treatment and outcomes of ARUBA-eligible patients with unruptured brain arteriovenous malformations at a single institution. Neurosurg Focus. 2014;37(3):E8.
12. Lang M, Moore NZ, Rasmussen PA, Bain MD. Treatment outcomes of a randomized trial of Unruptured brain arteriovenous malformation-eligible unruptured brain arteriovenous malformation patients. Neurosurgery. 2018;83(3):548–55.
13. Potts MB, Zumofen DW, Raz E, Nelson PK, Riina HA. Curing arteriovenous malformations using embolization. Neurosurg Focus FOC. 2014;37(3):E19.
14. Luessenhop AJ, Spence WT. Artificial embolization of cerebral arteries. Report of use in a case of arteriovenous malformation. J Am Med Assoc. 1960;172:1153–5.
15. Jafar JJ, Davis AJ, Berenstein A, Choi IS, Kupersmith MJ. The effect of embolization with N-butyl cyanoacrylate prior to surgical resection of cerebral arteriovenous malformations. J Neurosurg. 1993;78(1):60.
16. DeMeritt JS, Pile-Spellman J, Mast H, Moohan N, Lu DC, Young WL, et al. Outcome analysis of preoperative embolization with N-butyl cyanoacrylate in cerebral arteriovenous malformations. Am J Neuroradiol. 1995;16(9):1801–7.
17. Pasqualin A, Scienza R, Cioffi F, Barone G, Benati A, Beltramello A, et al. Treatment of cerebral arteriovenous malformations with a combination of preoperative embolization and surgery. Neurosurgery. 1991;29(3):358–68.
18. Morgan MK, Zurin AA, Harrington T, Little N. Changing role for preoperative embolisation in the management of arteriovenous malformations of the brain. J Clin Neurosci. 2000;7(6):527–30.
19. Markl M, Wu C, Hurley MC, Ansari SA, Carroll TJ, Rahme RJ, et al. Cerebral arteriovenous malformation: complex 3D hemodynamics and 3D blood flow alterations during staged embolization. J Magn Reson Imaging. 2013;38(4):946–50.

20. Alaraj A, Amin-Hanjani S, Shakur SF, Aletich VA, Ivanov A, Carlson AP, et al. Quantitative assessment of changes in cerebral arteriovenous malformation hemodynamics after embolization. Stroke. 2015;46(4):942–7.
21. Heidenreich JO, Hartlieb S, Stendel R, Pietilä TA, Schlattmann P, Wolf KJ, et al. Bleeding complications after endovascular therapy of cerebral arteriovenous malformations. AJNR Am J Neuroradiol. 2006;27(2):313–6.
22. Spetzler RF, Martin NA, Carter LP, Flom RA, Raudzens PA, Wilkinson E. Surgical management of large AVM's by staged embolization and operative excision. J Neurosurg. 1987;67(1):17.
23. Hongo K, Kobayashi S, Takemae T, Nakagawa H, Mabuchi S. Staged surgery for a large cerebral arteriovenous malformation to prevent the overload phenomenon. J Clin Neurosci. 1998;5(Suppl):84–6.
24. Ogilvy CS, Stieg PE, Awad I, Brown RD Jr, Kondziolka D, Rosenwasser R, et al. Recommendations for the management of intracranial arteriovenous malformations: a statement for healthcare professionals from a special writing group of the Stroke Council, American Stroke Association. Circulation. 2001;103(21):2644–57.
25. Russell D, Peck T, Ding D, Chen C-J, Taylor DG, Starke RM, et al. Stereotactic radiosurgery alone or combined with embolization for brain arteriovenous malformations: a systematic review and meta-analysis. J Neurosurg JNS. 2018;128(5):1338.
26. Andrade-Souza YM, Ramani M, Scora D, Tsao MN, terBrugge K, Schwartz ML. Embolization before radiosurgery reduces the obliteration rate of arteriovenous malformations. Neurosurgery. 2007;60(3):443–51; discussion 51-2.
27. Xu F, Zhong J, Ray A, Manjila S, Bambakidis NC. Stereotactic radiosurgery with and without embolization for intracranial arteriovenous malformations: a systematic review and meta-analysis. Neurosurg Focus. 2014;37(3):E16.
28. Pollock BE, Kondziolka D, Lunsford LD, Bissonette D, Flickinger JC. Repeat stereotactic radiosurgery of arteriovenous malformations: factors associated with incomplete obliteration. Neurosurgery. 1996;38(2):318–24.
29. Chen C-J, Ding D, Lee C-C, Kearns KN, Pomeraniec IJ, Cifarelli CP, et al. Embolization of brain arteriovenous malformations with versus without onyx before stereotactic radiosurgery. Neurosurgery. 2020;88(2):366–74.
30. Kwon Y, Jeon SR, Kim JH, Lee JK, Ra DS, Lee DJ, et al. Analysis of the causes of treatment failure in gamma knife radiosurgery for intracranial arteriovenous malformations. J Neurosurg. 2000;93(supplement_3):104.
31. Akakin A, Ozkan A, Akgun E, Koc DY, Konya D, Pamir MN, et al. Endovascular treatment increases but gamma knife radiosurgery decreases angiogenic activity of arteriovenous malformations: an in vivo experimental study using a rat cornea model. Neurosurgery. 2010;66(1):121–9; discussion 9-30.
32. Buell TJ, Ding D, Starke RM, Webster Crowley R, Liu KC. Embolization-induced angiogenesis in cerebral arteriovenous malformations. J Clin Neurosci. 2014;21(11):1866–71.
33. Kano H, Kondziolka D, Flickinger JC, Yang HC, Park KJ, Flannery TJ, et al. Aneurysms increase the risk of rebleeding after stereotactic radiosurgery for hemorrhagic arteriovenous malformations. Stroke. 2012;43(10):2586–91.
34. Xiaochuan H, Yuhua J, Xianli L, Hongchao Y, Yang Z, Youxiang L. Targeted embolization reduces hemorrhage complications in partially embolized cerebral AVM combined with gamma knife surgery. Interv Neuroradiol. 2015;21(1):80–7.
35. Ding D, Xu Z, Starke RM, Yen CP, Shih HH, Buell TJ, et al. Radiosurgery for cerebral arteriovenous malformations with associated arterial aneurysms. World Neurosurg. 2016;87:77–90.
36. Al-Yamany M, Terbrugge KG, Willinsky R, Montanera W, Tymianski M, Wallace MC. Palliative embolisation of brain arteriovenous malformations presenting with progressive neurological deficit. Interv Neuroradiol. 2000;6(3):177–83.
37. Kwon OK, Han DH, Han MH, Chung YS. Palliatively treated cerebral arteriovenous malformations: follow-up results. J Clin Neurosci. 2000;7(Suppl 1):69–72.

38. Reig AS, Rajaram R, Simon S, Mericle RA. Complete angiographic obliteration of intracranial AVMs with endovascular embolization: incomplete embolic nidal opacification is associated with AVM recurrence. J Neurointerv Surg. 2010;2(3):202–7.
39. Katsaridis V, Papagiannaki C, Aimar E. Curative embolization of cerebral arteriovenous malformations (AVMs) with Onyx in 101 patients. Neuroradiology. 2008;50(7):589–97.
40. Mounayer C, Hammami N, Piotin M, Spelle L, Benndorf G, Kessler I, et al. Nidal embolization of brain arteriovenous malformations using Onyx in 94 patients. Am J Neuroradiol. 2007;28(3):518–23.
41. Lundqvist C, Wikholm G, Svendsen P. Embolization of cerebral arteriovenous malformations: part II–aspects of complications and late outcome. Neurosurgery. 1996;39(3):460–7; discussion 7-9.
42. Xu F, Ni W, Liao Y, Gu Y, Xu B, Leng B, et al. Onyx embolization for the treatment of brain arteriovenous malformations. Acta Neurochir. 2011;153(4):869–78.
43. Wu EM, Ahmadieh TYE, McDougall CM, Aoun SG, Mehta N, Neeley OJ, et al. Embolization of brain arteriovenous malformations with intent to cure: a systematic review. J Neurosurg JNS. 2020;132(2):388.
44. Valavanis A, Yaşargil MG. The endovascular treatment of brain arteriovenous malformations. Adv Tech Stand Neurosurg. 1998;24:131–214.
45. Subat YW, Dasenbrock HH, Gross BA, Patel NJ, Frerichs KU, Du R, et al. Periprocedural intracranial hemorrhage after embolization of cerebral arteriovenous malformations: a meta-analysis. J Neurosurg. 2019:1–11.
46. Bruno CA Jr, Meyers PM. Endovascular management of arteriovenous malformations of the brain. Interv Neurol. 2013;1(3–4):109–23.
47. Peschillo S, Caporlingua A, Colonnese C, Guidetti G. Brain AVMs: an endovascular, surgical, and radiosurgical update. Scientific World J. 2014;2014:834931.
48. Jordan JA, Llibre JC, Vázquez F, Rodríguez R, Prince JA, Ugarte JC. Predictors of hemorrhagic complications from endovascular treatment of cerebral arteriovenous malformations. Interv Neuroradiol. 2014;20(1):74–82.
49. Lindegaard K-F, Grolimund P, Aaslid R, Nornes H. Evaluation of cerebral AVM's using transcranial Doppler ultrasound. J Neurosurg. 1986;65(3):335.
50. al-Rodhan NR, Sundt TM Jr, Piepgras DG, Nichols DA, Rüfenacht D, Stevens LN. Occlusive hyperemia: a theory for the hemodynamic complications following resection of intracerebral arteriovenous malformations. J Neurosurg. 1993;78(2):167–75.
51. Steinberger J, Nistal D, Schlachter L, Costa A, Oemke H, Bederson JB. A virtual-reality, 360-degree fly-through of an arteriovenous malformation resection: 2-dimensional operative video. Oper Neurosurg (Hagerstown). 2020;18(1):E11.
52. Lin F, Wu J, Zhao B, Tong X, Jin Z, Cao Y, et al. Preoperative functional findings and surgical outcomes in patients with motor cortical arteriovenous malformation. World Neurosurg. 2016;85:273–81.
53. Ellis MJ, Rutka JT, Kulkarni AV, Dirks PB, Widjaja E. Corticospinal tract mapping in children with ruptured arteriovenous malformations using functionally guided diffusion-tensor imaging. J Neurosurg Pediatr. 2012;9(5):505.
54. Bendok BR, El Tecle NE, El Ahmadieh TY, Koht A, Gallagher TA, Carroll TJ, et al. Advances and innovations in brain arteriovenous malformation surgery. Neurosurgery. 2014;74(Suppl 1):S60–73.
55. Sanchez-Mejia RO, McDermott MW, Tan J, Kim H, Young WL, Lawton MT. Radiosurgery facilitates resection of brain arteriovenous malformations and reduces surgical morbidity. Neurosurgery. 2009;64(2):231–8; discussion 8-40.
56. Beecher JS, Lyon K, Ban VS, Vance A, McDougall CM, Whitworth LA, et al. Delayed treatment of ruptured brain AVMs: is it ok to wait? J Neurosurg JNS. 2018;128(4):999.
57. Ding D, Ilyas A, Sheehan JP. Contemporary management of high-grade brain arteriovenous malformations. Neurosurgery. 2018;65(CN_suppl_1):24–33.
58. Pradilla G, Coon AL, Huang J, Tamargo RJ. Surgical treatment of cranial arteriovenous malformations and dural arteriovenous fistulas. Neurosurg Clin N Am. 2012;23(1):105–22.

59. Arnaout OM, Gross BA, Eddleman CS, Bendok BR, Getch CC, Batjer HH. Posterior fossa arteriovenous malformations. Neurosurg Focus. 2009;26(5):E12.
60. O'Shaughnessy BA, Getch CC, Bendok BR, Batjer HH. Microsurgical resection of infratentorial arteriovenous malformations. Neurosurg Focus. 2005;19(2):E5.
61. Ali MJ, Bendok BR, Rosenblatt S, Rose JE, Getch CC, Batjer HH. Recurrence of pediatric cerebral arteriovenous malformations after angiographically documented resection. Pediatr Neurosurg. 2003;39(1):32–8.
62. Jimenez JE, Gersey ZC, Wagner J, Snelling B, Ambekar S, Peterson EC. Role of follow-up imaging after resection of brain arteriovenous malformations in pediatric patients: a systematic review of the literature. J Neurosurg Pediatr. 2017;19(2):149.
63. Dupuis O, Delagrange L, Dupuis-Girod S. Hereditary haemorrhagic telangiectasia and pregnancy: a review of the literature. Orphanet J Rare Dis. 2020;15(1):5.
64. Kim H, Marchuk DA, Pawlikowska L, Chen Y, Su H, Yang GY, et al. Genetic considerations relevant to intracranial hemorrhage and brain arteriovenous malformations. Acta Neurochir Suppl. 2008;105:199–206.
65. Schneider BF, Eberhard DA, Steiner LE. Histopathology of arteriovenous malformations after gamma knife radiosurgery. J Neurosurg. 1997;87(3):352–7.
66. Ogilvy CS. Radiation therapy for arteriovenous malformations: a review. Neurosurgery. 1990;26(5):725–35.
67. Ding D, Starke RM, Sheehan JP. Radiosurgery for the management of cerebral arteriovenous malformations. Handb Clin Neurol. 2017;143:69–83.
68. Steiner L, Leksell L, Greitz T, Forster DM, Backlund EO. Stereotaxic radiosurgery for cerebral arteriovenous malformations. Report of a case. Acta Chir Scand. 1972;138(5):459–64.
69. Steiner L, Lindquist C, Adler JR, Torner JC, Alves W, Steiner M. Clinical outcome of radiosurgery for cerebral arteriovenous malformations. J Neurosurg. 1992;77(1):1.
70. Lunsford LD, Kondziolka D, Flickinger JC, Bissonette DJ, Jungreis CA, Maitz AH, et al. Stereotactic radiosurgery for arteriovenous malformations of the brain. J Neurosurg. 1991;75(4):512–24.
71. Betti OO, Munari C, Rosler R. Stereotactic radiosurgery with the linear accelerator: treatment of arteriovenous malformations. Neurosurgery. 1989;24(3):311–21.
72. Kjellberg RN, Hanamura T, Davis KR, Lyons SL, Adams RD. Bragg-peak proton-beam therapy for arteriovenous malformations of the brain. N Engl J Med. 1983;309(5):269–74.
73. Steinberg GK, Fabrikant JI, Marks MP, Levy RP, Frankel KA, Phillips MH, et al. Stereotactic heavy-charged-particle Bragg-peak radiation for intracranial arteriovenous malformations. N Engl J Med. 1990;323(2):96–101.
74. Flickinger JC, Pollock BE, Kondziolka D, Lunsford LD. A dose-response analysis of arteriovenous malformation obliteration after radiosurgery. Int J Radiat Oncol Biol Phys. 1996;36(4):873–9.
75. Karlsson B, Lindquist C, Steiner L. Prediction of obliteration after gamma knife surgery for cerebral arteriovenous malformations. Neurosurgery. 1997;40(3):425–30; discussion 30-1.
76. Ellis TL, Friedman WA, Bova FJ, Kubilis PS, Buatti JM. Analysis of treatment failure after radiosurgery for arteriovenous malformations. J Neurosurg. 1998;89(1):104–10.
77. Liscák R, Vladyka V, Simonová G, Urgosík D, Novotný J Jr, Janousková L, et al. Arteriovenous malformations after Leksell gamma knife radiosurgery: rate of obliteration and complications. Neurosurgery. 2007;60(6):1005–14; discussion 15-6.
78. Cohen-Inbar O, Starke RM, Paisan G, Kano H, Huang PP, Rodriguez-Mercado R, et al. Early versus late arteriovenous malformation responders after stereotactic radiosurgery: an international multicenter study. J Neurosurg. 2017;127(3):503–11.
79. Friedman WA. Stereotactic radiosurgery of intracranial arteriovenous malformations. Neurosurg Clin N Am. 2013;24(4):561–74.
80. Starke RM, Kano H, Ding D, Lee JY, Mathieu D, Whitesell J, et al. Stereotactic radiosurgery for cerebral arteriovenous malformations: evaluation of long-term outcomes in a multicenter cohort. J Neurosurg. 2017;126(1):36–44.

81. Cohen-Inbar O, Starke RM, Lee CC, Kano H, Huang P, Kondziolka D, et al. Stereotactic radiosurgery for brainstem arteriovenous malformations: a multicenter study. Neurosurgery. 2017;81(6):910–20.
82. Flickinger JC, Kondziolka D, Pollock BE, Maitz AH, Lunsford LD. Complications from arteriovenous malformation radiosurgery: multivariate analysis and risk modeling. Int J Radiat Oncol Biol Phys. 1997;38(3):485–90.
83. Hayhurst C, Monsalves E, van Prooijen M, Cusimano M, Tsao M, Menard C, et al. Pretreatment predictors of adverse radiation effects after radiosurgery for arteriovenous malformation. Int J Radiat Oncol Biol Phys. 2012;82(2):803–8.
84. Williams BJ, Park DM, Sheehan JP. Bevacizumab used for the treatment of severe, refractory perilesional edema due to an arteriovenous malformation treated with stereotactic radiosurgery. J Neurosurg. 2012;116(5):972–7.
85. Matsuo T, Kamada K, Izumo T, Hayashi N, Nagata I. Cyst formation after linac-based radiosurgery for arteriovenous malformation: examination of predictive factors using magnetic resonance imaging. Clin Neurol Neurosurg. 2014;121:10–6.
86. Yen CP, Sheehan JP, Schwyzer L, Schlesinger D. Hemorrhage risk of cerebral arteriovenous malformations before and during the latency period after GAMMA knife radiosurgery. Stroke. 2011;42(6):1691–6.
87. Karlsson B, Lindquist C, Steiner L. Effect of Gamma Knife surgery on the risk of rupture prior to AVM obliteration. Minim Invasive Neurosurg. 1996;39(1):21–7.
88. Ding D, Chen CJ, Starke RM, Kano H, Lee JYK, Mathieu D, et al. Risk of brain arteriovenous malformation hemorrhage before and after stereotactic radiosurgery. Stroke. 2019;50(6):1384–91.
89. Mayo Clinic Patient Education. Arteriovenous Malformation (AVM) [MC6732]. Rochester: Mayo Clinic; 2010. p. 3–12.

Chapter 21
Dural Arteriovenous Fistulas

Joshua D. Burks, Vaidya Govindarajan, Vasu A. Sinai, Aria M. Jamshidi, Evan M. Luther, and Robert M. Starke

Introduction

Arteriovenous fistulae (AVFs) occur due to a direct connection between an artery and a vein, resulting in a shunt. They may occur anywhere in the body, although those occurring intracranially are frequently referred to neurosurgeons and neurointerventionalists for evaluation. In this chapter, we specifically focus on the treatment of intracranial vascular malformations supplied by dural arteries, specifically dural arteriovenous fistula (dAVF). Pathophysiology, presentation, and treatment strategies vary widely based on the type and grade of pathology.

Recent advances in neurointerventional techniques have dramatically improved outcomes in patients afflicted with these lesions. For instance, prior to endovascular intervention, mortality for VOGM was 100% without treatment and 90% with treatment [1]. Similarly, CCF was historically treated with open surgical ligation [2, 3] and as with any surgery within the cavernous sinus carrying high rates of morbidity. These lesions will be discussed in detail in a separate chapter. Clinicians now have an extensive arsenal at their disposal, which may include a combination of microsurgery, endovascular therapy, or radiation therapy depending on the type, location, and symptomatology.

In addition to understanding appropriate therapeutic options for each type of lesion, treatment paradigms for each of these lesions must be guided by a thorough understanding of the natural history for each lesion type. For some lesions, observation and conservative management alone are appropriate, whereas in other cases

J. D. Burks (✉) · V. Govindarajan · V. A. Sinai · A. M. Jamshidi · E. M. Luther · R. M. Starke
University of Miami Miller School of Medicine, Department of Neurosurgery, Miami, FL, USA
e-mail: joshua.burks@jhsmiami.org; vxg270@med.miami.edu; vasu.sinai@jhsmiami.org; aria.jamshidi@jhsmiami.org; evan.luther@jhsmiami.org; rstarke@med.miami.edu

J. R. Mascitelli, M. J. Binning (eds.), *Introduction to Vascular Neurosurgery*,
https://doi.org/10.1007/978-3-030-88196-2_21

microsurgery is the treatment of choice. To this end, we outline the principal classification scales used to characterize dural-based vascular malformations, as well as clinical features, and describe accepted approaches for management.

Dural Arteriovenous Fistulae (dAVFs)

Description

A dural arteriovenous fistula (dAVF) is a pathological arteriovenous shunt between the meningeal arteries and dural venous sinuses or dural veins. The Scottish Intracranial Vascular Malformation Study (SIVMS) reported a dAVF incidence of 0.16 per 100,000, the lowest among intracranial vascular malformations [4]. The etiology of dAVF remains unclear though it has been suggested that most cases of dAVF are idiopathic, with a small subset forming secondarily to venous sinus thrombosis caused by trauma, inflammation, hypercoagulable states, etc. [5]. Despite variations in etiology and mechanism, there is a common progression of dural arteriovenous fistulae; as the sinus outflow worsens, venous flow through the sinuses reverses, resulting in retrograde flow through the cortical veins. This phenomenon, known as cortical venous drainage (CVD), results in venous hypertension spreading throughout the brain and spinal cord [6].

Pathophysiology

Early animal studies demonstrated that while venous sinus thrombosis may be a precipitating factor for dAVF as stated earlier, venous hypertension alone is sufficient to induce dAVF formation [7]. Nevertheless, the clinical presentation of dAVF typically results from venous hypertension directly caused by venous thrombosis. This may occur particularly in patients in a hypercoagulable state who otherwise have normal venous drainage [8, 9]. A landmark study performed by Lawton and colleagues in 1997 demonstrated that the degree of angiogenesis was significantly correlated with the formation of dAVF [10]. However, while these researchers were able to demonstrate that hypertension and angiogenesis were significantly correlated with dAVF formation independently, they were unable to demonstrate a significant correlation between hypertension and angiogenesis, nor were they able to identify specific angiogenic factors that may play a role in dAVF formation.

Vascular endothelial growth factor (VEGF) was the first angiogenic factor implicated in the formation of dAVF by Shin and colleagues [11], with a later study by the same group demonstrating that dural VEGF expression increases up to 1 week post-induction of venous hypertension and that VEGF expression is restricted to the connective tissue and endothelial layer of the dura [12].

One possible mechanism for VEGF-mediated dAVF formation posits that increased dural venous pressure and decreased cerebral perfusion pressure are associated with increased VEGF expression and fibroblast proliferation, findings that corroborate the well-established role of fibroblast-derived VEGF in pathological angiogenesis of other diseases, such as cancer [13]. The above mechanism is particularly salient in the context of trauma-induced dAVF, where maintenance of cerebral perfusion pressure is critical in the management of traumatic brain injury [14]. It may be possible that low cerebral perfusion pressure in the context of traumatic brain injury can predispose individuals to the formation of dAVF, possibly through the increased expression of hypoxia-inducible factor 1-α and VEGF [15].

Clinical Presentation

The clinical presentation of dAVF is highly variable, depending on the location of the fistula. However, all dAVF symptoms can be separated based on whether they are produced by hemorrhage or not and typically present in the fifth and sixth decades of life [11].

The two most common nonhemorrhagic symptoms include pulsatile tinnitus and ocular findings. Fistulae present at the level of the sigmoid or transverse sinuses commonly present with pulsatile tinnitus, caused by turbulent flow in the region whose vibrations radiate toward the inner ear. The pulsatile tinnitus can be auscultated in the mastoid region and is typically present in patients who have normal otoscopic examinations [16]. A third, common presentation of aggressive dAVF can be seizures secondary to cerebral edema caused by venous congestion [17].

As with any arteriovenous anomaly, hemorrhage is a concern and may be a presenting symptom of dAVF, and approximately 20% of dAVF patients will present with hemorrhage. Typically, the hemorrhages are intraparenchymal or subarachnoid, though there are rare cases of subdural hemorrhages [18]. A commonality of hemorrhagic symptoms is the presence of headache, particularly in the case of subarachnoid hemorrhage. However, subdural hemorrhage has been known to present with a similar type of intense headache seen in subarachnoid hemorrhage [18].

Cranial nerve findings may also be present, particularly for lesions occurring within the tentorium [19]. Rarely, there may be severe progressive myelopathy as a result of dAVF with spinal venous drainage [20] (more later). Another rare presentation is dementia, which has an increased frequency in patients who developed dAVF of the superior sagittal sinus [21]. Hydrocephalus has been frequently reported in the literature and described with dAVF-induced dementia [22, 23].

Just as there are varied symptoms associated with dAVF (with such exceptions as pulsatile tinnitus and ocular findings), there is also variation in imaging findings, and diagnosis may not be readily apparent with conventional neuroimaging. However, dAVF is principally characterized by early drainage into a venous sinus of a dural artery, with or without retrograde blood flow into the sinus or nearby cortical cerebral veins [16].

Classification of Dural Arteriovenous Fistulae

There are many classification schemes for characterizing dAVF. The two most common are the Borden and Cognard classification schemes. The Borden classification classifies fistulae based on their location and the presence or absence of CVD. The Cognard classification classifies fistulae based on the direction of venous flow (anterograde versus retrograde), presence or absence of CVD, and if the fistula involves venous ectasia (dilations of veins or venules) or spinal venous drainage [24]. The two classification schemes are further described here.

Borden Classification Scheme

In the Borden classification scheme, there are three major types (I-III) of dAVF, with two subtypes (a and b). Borden Type I fistulae drain directly into the dural venous sinus or meningeal vein in an anterograde fashion. Type I fistulae can have single or multiple connections and are typically benign. Type I fistulae tend to present with the pathognomonic sign of pulsatile tinnitus when draining into the transverse/sigmoid sinus and may also produce cranial nerve findings.

Borden Type II fistulae have anterograde drainage into a dural sinus, but there is retrograde flow from the dural sinus into the subarachnoid veins, with neurological deficits arising from the resulting venous hypertension or hemorrhage.

Borden Type III fistulae also drain retrogradely into the subarachnoid veins from a vein that normally drains into a dural sinus. However, they are distinguished from Type II fistulae in that Type III fistulae drain directly into subarachnoid veins while Type II fistulae first drain anterogradely into a dural sinus and then flow retrogradely from the dural sinus into the subarachnoid veins. Typically, these fistulae are found near the wall of the dural venous sinus and tend to have more diffuse effects on central nervous system than type I or type II dAVF. Type III fistulae often present with hemorrhage or symptoms consistent with venous hypertension of the cortical veins. There may also be symptoms of myelopathy associated with hypertension in the deep venous system and perimedullary spinal venous plexuses [25].

Subtype “a” fistulae are also known as simple fistulae that are defined as a direct connection between a single meningeal artery and a draining vein or sinus. Subtype “a” fistulae can be found under any of the three general dAVF types. Subtype “b” fistulae are defined as multiple fistulae that are fed by multiple arteries and can be found with any of the three general dAVF types. An important feature to distinguish within subtype “b” fistulae is drainage type. When multiple fistulae drain into a single location, this is considered a single fistula. However, when the individual arterial sources drain into multiple locations (typically subarachnoid veins according to Borden), each arterial source is considered a separate fistula [20].

Cognard Classification Scheme

There are five types of dAVFs under the Cognard classification scheme, with Type II fistulae having subtype "a," subtype "b," or combined (a + b) subtype. Type I fistulae are present in the main dural sinuses with anterograde flow. Typically, Type I fistulae are benign.

As stated previously, Type II fistulae are divided into separate subtypes dependent on which structures they reflux into. Type IIa fistulae reflux into the main dural sinuses, type IIb fistulae reflux into cortical veins, and type IIa + b fistulae reflux into both the main dural sinuses and the cortical veins. The main complication of type II fistulae is the increased risk of hemorrhage and intracranial hypertension. Type IIa fistulae have an increased likelihood of presenting with intracranial hypertension, while type IIb fistulae have an increased likelihood of hemorrhage (10% of such patients according to Cognard).

Type III fistulae are characterized by direct cortical venous drainage in the absence of venous ectasia. There is an increased risk of hemorrhage in type III fistulae (40% of type III patients in Cognard's study) as compared to type IIb fistulae. Type IV fistulae are characterized by direct cortical venous drainage in the presence of venous ectasia, and there is an even higher risk of hemorrhage (65% of type IV patients in Cognard's study). Type V fistulae involve spinal venous drainage, and as a result, present with progressive myelopathy (50% of type V patients in Cognard's study) [26]. A summary of the Borden and Cognard classification systems is displayed in Table 21.1.

Table 21.1 Summary of Borden and Cognard classification systems for dural arteriovenous fistulae (dAVF)

	Borden	Cognard
Description	Three types Type I: Direct anterograde drainage into dural venous sinus or meningeal vein Type II: Anterograde drainage into dural venous sinus and retrograde flow from dural sinus to subarachnoid veins Type III: Direct retrograde flow to subarachnoid vein, bypassing dural venous sinus	Five types Type I: Anterograde flow into dural sinuses Type II: Three subtypes based on draining structure. Type III: Direct cortical venous drainage with no ectasia Type IV: Direct cortical venous drainage with ectasia Type V: Spinal venous drainage
Subtypes	Subtype a: Direct connection between meningeal artery and vein or sinus (single fistula) Subtype b: Multiple fistulae fed by multiple arteries	Three subtypes in Type II IIa: Reflux into main dural sinuses IIb: Reflux into cortical veins IIa + b: Reflux into main dural sinuses and cortical veins

Treatment

Treatment of dAVF is generally considered for types involving cortical venous drainage. Other circumstances in which treatment may be considered include the presence of neurological symptoms, history of hemorrhage, increased intraocular pressure, edema, seizures, and refractory symptoms. Therapies are focused on disrupting the flow of blood through the fistula by occluding or excising the fistula, or by occluding the dural venous drainage [27]. A number of treatment strategies have been suggested including manual carotid occlusion and radiosurgery [28], but we will discuss methods employed most frequently below.

Patients have historically been treated with microsurgery with favorable outcomes [29]. The goals of surgery involve a combination of coagulating arterial feeders, fistula excision, ligation of venous outflow, and disconnection of cortical venous drainage. In these cases, particular attention is necessary during exposure and bone removal to avoid tearing dura near the fistula which can lead to massive, sudden blood loss [29]. As a standard practice, surgeons often have blood products available at the time of surgery. Open microsurgery remains an important adjunct in the treatment of some types of dAVFs.

At present, patients are more often treated through endovascular surgery or in some cases a combination of embolization and open surgery [30]. Several different techniques may be employed depending on the arterial pattern supplying the fistula. Coils may be deployed to eliminate venous drainage through a transvenous route as it is more difficult to deploy coils across the fistula from the arterial side. With this approach, it is important to avoid occluding venous drainage if the target vein provides significant drainage for normal veins. In these cases, partial occlusion may be the best option, which reduces the lesion to a lower-risk type (as described earlier). Liquid embolic materials like Onyx may be pushed from the arterial side or used in combination with venous coiling to achieve cure. Onyx is typically pushed as close to the fistulous point as possible and then allowed to flow into the venous side to create occlusion [31]. NBCA can be used similar to Onyx but is employed less frequency as it has a side effect profile similar to other iodinated contrast materials.

Ultimately, the best treatment strategy is in many cases complex and requires a multidisciplinary approach involving a neurosurgeon and neuro-interventionalist [32]. Lesions involving the anterior cranial fossa and tentorium are still generally more favorably treated with surgery. The current body of literature suggests that high rates of cure with low morbidity may be achieved with proper management. A sample case is presented in Fig. 21.1.

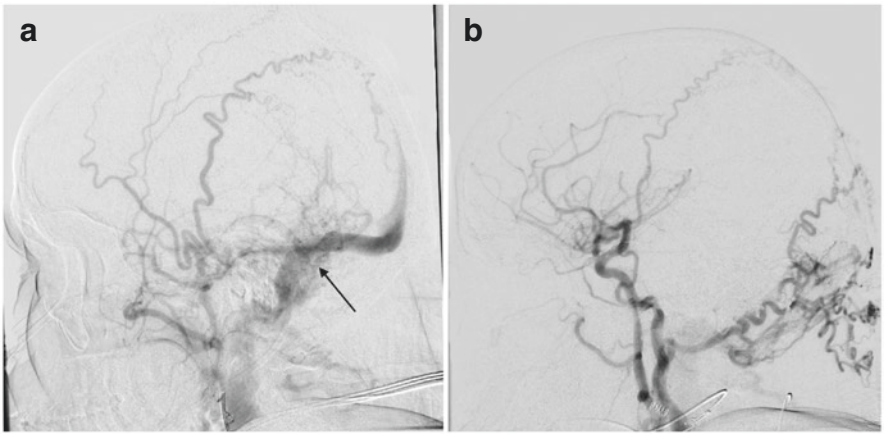

Fig. 21.1 In this case, a 52-year-old who presented with pulsatile tinnitus of the right ear was diagnosed by cerebral angiogram to have a Borden grade 2 (Cognard type IIb) dural arteriovenous fistula. Right external carotid angiogram is shown in lateral view (**a**). The fistula is located at the junction of the transverse, and sigmoid sinuses (arrow) are supplied by branches of the middle meningeal, superficial temporal, and occipital (not shown) arteries. Contrast is shown in the late arterial phase, filling the superior sagittal, transverse, and sigmoid sinus, as well as cortical veins. The lesion was treated endovascularly by injecting Onyx™ (Medtronic, USA) embolic liquid into carefully selected segments of feeding arteries to halt blood flow to the nidus of the fistula, resulting in cure (**b**)

Conclusion

dAVF represents a complex group of lesions that require a deep understanding of the anatomy of the fistula and grade to determine the most appropriate treatment or no treatment at all. This chapter is an overview of the pathophysiology, presentation, and treatment of these varied lesions.

References

1. Jones BV, Ball WS, Tomsick TA, Millard J, Crone KR. Vein of Galen aneurysmal malformation: diagnosis and treatment of 13 children with extended clinical follow-up. AJNR Am J Neuroradiol. 2002;23(10):1717–24.
2. Dolenc V. Direct microsurgical repair of intracavernous vascular lesions. J Neurosurg. 1983;58(6):824–31.
3. Parkinson D, Downs AR, Whytehead LL, Syslak WB. Carotid cavernous fistula: direct repair with preservation of carotid. Surgery. 1974;76(6):882–9.
4. Al-Shahi R, Bhattacharya JJ, Currie DG, Papanastassiou V, Ritchie V, Roberts RC, et al. Prospective, population-based detection of intracranial vascular malformations in adults: The Scottish Intracranial Vascular Malformation Study (SIVMS). Stroke. 2003;34(5):1163–9.

5. Wanke I, Rüfenacht DA. The Dural AV-Fistula (DAVF), the most frequent acquired vascular malformation of the central nervous system (CNS). Clin Neuroradiol. 2015;25(2):325–32.
6. Reynolds MR, Lanzino G, Zipfel GJ. Intracranial dural arteriovenous fistulae. Stroke. 2017;48(5):1424–31.
7. Terada T, Higashida RT, Halbach VV, Dowd CF, Tsuura M, Komai N, et al. Development of acquired arteriovenous fistulas in rats due to venous hypertension. J Neurosurg. 1994;80(5):884–9.
8. Safavi-Abbasi S, Di Rocco F, Nakaji P, Feigl GC, Gharabaghi A, Samii M, et al. Thrombophilia due to factor V and factor II mutations and formation of a dural arteriovenous fistula: case report and review of a rare entity. Skull Base. 2008;18(2):135–43.
9. Polster SP, Zeineddine HA, Baron J, Lee S-K, Awad IA. Patients with cranial dural arteriovenous fistulas may benefit from expanded hypercoagulability and cancer screening. J Neurosurg JNS. 2018;129(4):954.
10. Lawton MT, Jacobowitz R, Spetzler RF. Redefined role of angiogenesis in the pathogenesis of dural arteriovenous malformations. J Neurosurg. 1997;87(2):267–74.
11. Uranishi R, Nakase H, Sakaki T. Expression of angiogenic growth factors in dural arteriovenous fistula. J Neurosurg. 1999;91(5):781–6.
12. Shin Y, Nakase H, Nakamura M, Shimada K, Konishi N, Sakaki T. Expression of angiogenic growth factor in the rat DAVF model. Neurol Res. 2007;29(7):727–33.
13. Kojima T, Miyachi S, Sahara Y, Nakai K, Okamoto T, Hattori K, et al. The relationship between venous hypertension and expression of vascular endothelial growth factor: hemodynamic and immunohistochemical examinations in a rat venous hypertension model. Surg Neurol. 2007;68(3):277–84; discussion 84
14. Vella MA, Crandall ML, Patel MB. Acute management of traumatic brain injury. Surg Clin North Am. 2017;97(5):1015–30.
15. Wang SS, Li CH, Zhang XJ, Wang RM. Investigation of the mechanism of dural arteriovenous fistula formation induced by high intracranial venous pressure in a rabbit model. BMC Neurosci. 2014;15:101.
16. Serulle Y, Miller TR, Gandhi D. Dural arteriovenous fistulae: imaging and management. Neuroimaging Clin N Am. 2016;26(2):247–58.
17. Kanemaru K, Kinouchi H, Yoshioka H, Yagi T, Wakai T, Hashimoto K, et al. Cerebral hemodynamic disturbance in dural arteriovenous fistula with retrograde leptomeningeal venous drainage: a prospective study using 123I-iodoamphetamine single photon emission computed tomography. J Neurosurg JNS. 2015;123(1):110.
18. Bhogal P, Yeo LL, Söderman M. Dural arteriovenous fistula presenting as tentorial subdural hemorrhage. Clin Neuroradiol. 2019;29(3):555–61.
19. Sato H, Wada H, Noro S, Saga T, Kamada K. Subarachnoid hemorrhage with concurrent dural and perimedullary arteriovenous fistulas at craniocervical junction: case report and literature review. World Neurosurg. 2019;127:331–4.
20. Khan S, Polston DW, Shields RW, Rasmussen P, Gupta R. Tentorial Dural arteriovenous fistula presenting with Quadriparesis: case report and review of the literature. J Stroke Cerebrovasc Dis. 2009;18(6):428–34.
21. Brito A, Tsang ACO, Hilditch C, Nicholson P, Krings T, Brinjikji W. Intracranial Dural arteriovenous fistula as a reversible cause of dementia: case series and literature review. World Neurosurg. 2019;121:e543–e53.
22. Nakahara Y, Ogata A, Takase Y, Maeda K, Okamoto H, Matsushima T, et al. Treatment of dural arteriovenous fistula presenting as typical symptoms of hydrocephalus caused by venous congestion: case report. Neurol Med Chir. 2011;51(3):229–32.
23. Ernst GL, Carlson AP. Transverse sinus dural arteriovenous fistula presenting with acute hydrocephalus from cerebellar venous engorgement resolving with endovascular treatment. J Neurol Surg A Cent Eur Neurosurg. 2016;77(6):538–42.
24. Gandhi D, Chen J, Pearl M, Huang J, Gemmete JJ, Kathuria S. Intracranial dural arteriovenous fistulas: classification, imaging findings, and treatment. AJNR Am J Neuroradiol. 2012;33(6):1007–13.

25. Borden JA, Wu JK, Shucart WA. A proposed classification for spinal and cranial dural arteriovenous fistulous malformations and implications for treatment. J Neurosurg. 1995;82(2):166–79.
26. Cognard C, Gobin YP, Pierot L, Bailly AL, Houdart E, Casasco A, et al. Cerebral dural arteriovenous fistulas: clinical and angiographic correlation with a revised classification of venous drainage. Radiology. 1995;194(3):671–80.
27. Thompson BG, Doppman JL, Oldfield EH. Treatment of cranial dural arteriovenous fistulae by interruption of leptomeningeal venous drainage. J Neurosurg. 1994;80(4):617–23.
28. Pan DH-c, Chung W-y, Guo W-y, Wu H-m, Liu K-d, Shiau C-y, et al. Stereotactic radiosurgery for the treatment of dural arteriovenous fistulas involving the transverse—sigmoid sinus. J Neurosurg. 2002;96(5):823.
29. Sundt TM, Piepgras DG. The surgical approach to arteriovenous malformations of the lateral and sigmoid dural sinuses. J Neurosurg. 1983;59(1):32.
30. Barnwell SL, Halbach VV, Higashida RT, Hieshima G, Wilson CB. Complex dural arteriovenous fistulas. J Neurosurg. 1989;71(3):352.
31. Maimon S, Nossek E, Strauss I, Blumenthal D, Frolov V, Ram Z. Transarterial treatment with onyx of intracranial dural arteriovenous fistula with cortical drainage in 17 patients. Am J Neuroradiol. 2011;32(11):2180–4.
32. Cohen SD, Goins JL, Butler SG, Morris PP, Browne JD. Dural arteriovenous fistula: diagnosis, treatment, and outcomes. Laryngoscope. 2009;119(2):293–7.

Chapter 22
Carotid Cavernous Fistulas And Vein of Galen Malformations

Anja I. Srienc, Anna L. Huguenard, Vivek P. Gupta, and Joshua W. Osbun

Technical Terms, Abbreviations

AVM	Arteriovenous malformation
CCF	Carotid-cavernous fistulae
CT	Computed tomography
CTA	Computed tomography angiogram
ECA	External carotid artery
EVD	External ventricular drain
ICA	Internal carotid artery
MRI	Magnetic resonance imaging
MRA	Magnetic resonance angiogram
nBCA	n-butyl-cyanoacrylate
VOGM	Vein of Galen malformations

Introduction

Arteriovenous fistulae are broadly defined by abnormal communication between arterial and venous vessels and can manifest with symptoms related to hemorrhage, venous congestion, or downstream effects due to high-volume arterial-venous shunting. Here, two common forms of intracranial arteriovenous fistulae are discussed: carotid-cavernous fistulae and vein of Galen malformations.

A. I. Srienc · A. L. Huguenard · V. P. Gupta · J. W. Osbun (✉)
Washington University in St. Louis, Department of Neurosurgery, St. Louis, MO, USA
e-mail: asrienc@wustl.edu; ahuguenard@wustl.edu; vivek.gupta@wustl.edu; josbun@wustl.edu

J. R. Mascitelli, M. J. Binning (eds.), *Introduction to Vascular Neurosurgery*,
https://doi.org/10.1007/978-3-030-88196-2_22

Carotid-Cavernous Fistulae

Carotid-cavernous fistulae (CCF) are abnormal vascular shunts between the carotid artery and its branches, and the venous channels of the cavernous sinus. While some CCF may remain asymptomatic, venous hypertension due to these lesions often causes symptoms; the specific constellation of symptoms is defined by the pattern of venous drainage from the fistula since venous engorgement results in a mass effect on local anatomic structures. Classically, CCF cause ocular symptoms including conjunctival injection due to dilation of conjunctival and episcleral veins, proptosis, elevated intraocular pressure, which can result in vision loss, eyelid swelling, and can be associated with cranial nerve palsies particularly of the oculomotor, trochlear, and/or abducens nerves. On exam, patients present with unilateral eye redness and exophthalmos; occasionally, a bruit can be auscultated over the affected globe. Bilateral symptoms can also occur, but this is less common [1].

Classification

CCF can be classified based on blood flow (high-flow vs low-flow), etiology (traumatic vs spontaneous), or anatomic vascular supply. Barrow et al. created an anatomically based classification scheme in 1985 that is now widely used. In the Barrow classification system (summarized in Table 22.1), CCF are divided into four categories [2]. Type A fistulae involve a direct connection between the internal carotid artery (ICA) and the cavernous sinus. Types B, C, and D fistulae are considered indirect dural arteriovenous fistulae: type B fistulae are fed by dural branches of the ICA; type C fistulae are shunts between meningeal branches of the external carotid artery (ECA) and the cavernous sinus; and type D fistulae are supplied by branches of both the ICA and ECA. Of all CCF, type A fistulae are the most common, accounting for up to 80% of all CCF [2–4]. Of the indirect types, type D fistulae are the most common [2, 5].

The Thomas classification system was proposed in 2015 as an alternative to the Barrow classification of CCF [6]. This new system is based on venous drainage patterns, with the argument that venous drainage better predicts clinical presentation and ease of endovascular access to the fistula. In this nomenclature, type 1 CCF drain posteriorly with venous outflow via the inferior petrosal sinus, superior

Table 22.1 Summary of carotid-cavernous fistulae types according to the Barrow classification [2]

	Arterial supply
Type A	Direct connection between ICA and cavernous sinus
Type B	Connection between meningeal branches of ICA and cavernous sinus
Type C	Connection between meningeal branches of ECA and cavernous sinus
Type D	Connection between branches of both ICA and ECA and cavernous sinus

ICA Internal carotid artery, *ECA* external carotid artery

petrosal sinus, pterygoid plexus, or parapharyngeal plexus. Type 2 CCF drain posteriorly *and* anteriorly through the superior and inferior ophthalmic veins. Type 3 CCF exhibit anterior drainage only. Type 4 CCF have evidence of retrograde drainage into cortical veins. Type 5 CCF are akin to Barrow type A CCF and are direct connections between the ICA and the cavernous sinus. Type 3 fistulae were found to be the most common, followed by type 5 CCF. The Thomas classification system was recently validated in an independent study that retrospectively analyzed the symptoms and treatment of 94 patients with CCF. There was a good predictive correlation between the Thomas classification and presenting symptoms and treatment strategy [7]. Nevertheless, this classification system has not been widely adopted.

Epidemiology and Etiology

Trauma is the primary etiology of direct CCF. The incidence of CCF is 0.2% and one series reported that up to 4% of patients with basilar skull fractures develop CCF [1, 3]. Post-traumatic fistulae are more common in young males, reflecting the demographic distribution of head injuries [1, 4, 8]. Traumatic CCF are often high-flow type A fistulae that present acutely with more severe symptoms such as a sudden increase in intraocular pressure and require urgent intervention [8]. Acute high-flow fistulae have decreased in incidence over the past 50 years with shoulder belts and car safety standards. Less commonly, type A direct fistulae can also form after rupture of a cavernous carotid aneurysm or may occur spontaneously [2, 3, 9, 10]. CCF that form spontaneously are more likely to be low-flow, type B, C, or D lesions. Risk factors for spontaneous CCF include venous thrombosis, atherosclerosis [4, 5], hypertension [2, 5, 11], connective tissue disease [12, 13], and minor trauma [1–3, 5]. The pathophysiology of spontaneous CCF is not fully understood, though some have posited that these fistulae form as the result of spontaneous thrombosis of the cavernous sinus outflow tracts [14]. Spontaneous CCF occur most commonly in older women, typically in the sixth or seventh decades of life [2, 4, 5, 11].

Clinical Considerations

Treatment decisions for CCF depend on initial presenting symptoms, flow rate, and pattern of drainage. High-flow direct fistulae frequently require intervention since they rarely resolve spontaneously and tend to associate with more significant symptoms [2, 15, 16]. Indirect, low-flow fistulae can resolve spontaneously but may take a relapsing-remitting course that can impede accurate diagnosis or can progress to more severe symptoms requiring intervention [16, 17]. Posteriorly draining CCF can be associated with cranial nerve palsies, including trigeminal neuropathies or facial paresis [5–7]. Anteriorly draining CCF typically drain via the ophthalmic veins and

present with ocular or visual symptoms [6, 7]. Asymptomatic or mildly symptomatic CCF can be managed conservatively. However, invasive treatment becomes indicated if cortical venous reflux is identified on angiography, since such a finding is associated with increased risk for intracranial hemorrhage. Ocular symptoms such as proptosis, decrease in ocular motility, pain, elevated intraocular pressure, or loss of visual acuity also prompt more urgent intervention. Rarely, CCF can present as massive epistaxis that can be life-threatening unless it is rapidly controlled [18].

Management

Obliteration of the fistulous arteriovenous connection while maintaining normal vascular anatomy is the primary goal of CCF treatment. The timing and treatment approach depends on clinical and anatomic factors.

Conservative, Noninvasive Management

Given that a significant proportion of CCF resolve spontaneously, observation and management of mild symptoms can be an appropriate strategy for a subset of patients [17, 19]. A noninvasive treatment approach involves compression therapy in which the carotid artery and jugular vein are manually compressed for 5–10 minutes up to ten times daily [20]. This causes hemodynamic changes through the CCF, resulting in thrombosis. Manual compression techniques have also been applied to the angular vein in the superomedial orbit. The highest success with manual compression was seen in patients with indirect CCF who exhibited venous drainage through only the superior ophthalmic vein; in these patients, CCF resolution rates range from 30% to 34% [20–22]. Prior to using the manual compression technique, it is important to establish that compression does not alter CCF blood flow dynamics in a way that results in cortical venous reflux. This can be tested at the time of diagnostic digital subtraction angiography [23]. It is equally important to establish that reduced carotid blood flow can be tolerated by the patient without resultant symptomatic cerebral ischemia. This can be done by a compression trial while monitoring the patient clinically or performing compression with the contralateral hand [18].

Endovascular Treatment

Endovascular methods are the mainstay of CCF treatment when aggressive intervention is indicated. Treatment indications include visual impairment, progressive exophthalmos, intractable pain, elevated intraocular pressures, oculoparesis, or cortical reflux [4, 5, 8, 24]. The endovascular approach to the fistula, whether transarterial, transvenous, or both, depends on the CCF type and its venous drainage [3, 5–7]. Direct CCF can be accessed transarterially since they directly connect the ICA

to the cavernous sinus, while the preferred method of accessing indirect CCF is through a transvenous approach, often via the internal jugular vein and ultimately the inferior petrosal sinus into the cavernous sinus [25].

For direct CCF, transarterial access is through the ICA. These lesions were once treated with detachable balloons [3, 10], but these devices were taken off the market in 2004. Since then, coil embolization has been the preferred method of embolization, with or without balloon or stent assistance [18, 26–28]. Liquid embolic agents have also been used as adjuncts to treat direct CCF. However, the use of these substances must be judicious because the risk of using liquid embolic agents includes reflux through the fistula into collaterals with the ICA and/or cavernous sinus edema resulting in cranial neuropathies [24, 26–28]. Successful transarterial treatment of type A CCF can also be achieved with flow-diverting stents (either alone or in combination with embolization) [29] or with stent-grafts [30]. When the fistula cannot be treated by transarterial access alone, transvenous treatment can be used in combination with transarterial methods, or as an alternative [31]. Rarely, the ICA must be sacrificed when direct targeting of the CCF fails, but this strategy should be reserved for patients who show no deficits on balloon occlusion test [1, 28].

In the case of indirect CCF, most can be treated by a transvenous approach, with success rates ranging from 60% to 95% [23–26]. The most accessed venous conduit to the CCF is the inferior petrosal sinus followed by the facial vein [23, 25–27]. Less commonly, transarterial branches of the ICA or ECA can be accessed to successfully embolize the CCF [26]. When embolizing using a transvenous approach, coils alone are often enough to obliterate the fistula [26, 27], but liquid embolic agents alone or in combination with coil embolization can also be a useful strategy to successfully treat an indirect CCF [28].

Alternative Access Methods

When transvenous or transarterial access cannot be safely accomplished, access to the fistula can be achieved through alternative strategies. These include endovascular routes using puncture of the superior ophthalmic vein, inferior ophthalmic vein, facial vein, pterygoid plexus, or cavernous sinus [19, 24–26, 32]. Alternatively, access can be aided using surgical approaches. In one case report, access to the cavernous sinus was accomplished by an endoscopic transsphenoidal approach [33]. Surgical cutdown of the orbit to access the superior or inferior ophthalmic veins has been described to aid venous puncture of these vessels [24, 34, 35]. Open surgical exposure of the cavernous carotid sinus has also been reported in the literature [24, 34, 35]. In one case report, an orbitozygomatic craniotomy was performed in a hybrid operating room to perform an extradural exposure of the lateral cavernous sinus to obtain venous access; a Barrow type D CCF was then successfully treated through a combination of transarterial and transvenous embolization [36]. Another group describes successful obliteration of a CCF via a pterional craniotomy for intradural pretemporal exposure of the cavernous sinus for direct sinus puncture and Onyx embolization that was confirmed with intraoperative diagnostic angiography [35].

Radiosurgery

For symptomatic CCF that cannot be treated with endovascular or surgical techniques, or for residual CCF that have not responded to treatment, radiosurgery remains an additional treatment option [23, 37–41]. Rates of complete obliteration range from 59% to 90% [37, 39–41]. Data suggest that CCF with restricted venous outflow are more susceptible to radiosurgery that CCF with robust venous drainage [39].

Case Examples

Indirect CCF

The patient is a 70-year-old female who presented to the ophthalmology clinic with complaints of 1 year of left eyelid swelling, conjunctival injection, peripheral diplopia, and eye pain with extreme gaze in all directions. On exam, she was found to have elevated intraocular pressure of 25 in the left eye, proptosis, and episcleral and retinal vascular engorgement. She was referred for digital subtraction angiography due to suspicion of a CCF. She was found to have a left-sided Barrow type D CCF with supply from the right cavernous ICA and branches of the left ECA (Fig. 22.1a, b). She subsequently underwent endovascular transvenous coil embolization of this lesion. Access was obtained through the right basilic vein, and a catheter was introduced into the left cavernous sinus through the left inferior petrosal vein. At the end of the procedure, post-embolization right and left common carotid injections demonstrated total obliteration of the fistula (Fig. 22.1c, d). On clinical follow-up 3 months after embolization, she had total resolution of left eye chemosis and pain, and near resolution of her diplopia.

Direct CCF

The patient is a 65-year-old female who was the restrained driver in a head-on motor vehicle collision and suffered multiple injuries, including visceral injuries requiring exploratory laparotomy, multiple fractures to both lower extremities, and an L4 burst fracture for which she underwent a posterior spinal fusion by neurosurgery. At her neurosurgical follow-up appointment 2 months later, she had developed a right CN VI palsy with complaints of diplopia, pulsatile tinnitus, and a right-sided headache. She reported that these symptoms began after discharge from the hospital while she was still in a rehabilitation facility; at that time, a CTA of the head and neck was done without any abnormalities, and on ophthalmology evaluation, she was given an eye patch and prism glasses. Given her ongoing symptoms, she was referred for digital subtraction angiography to evaluate for

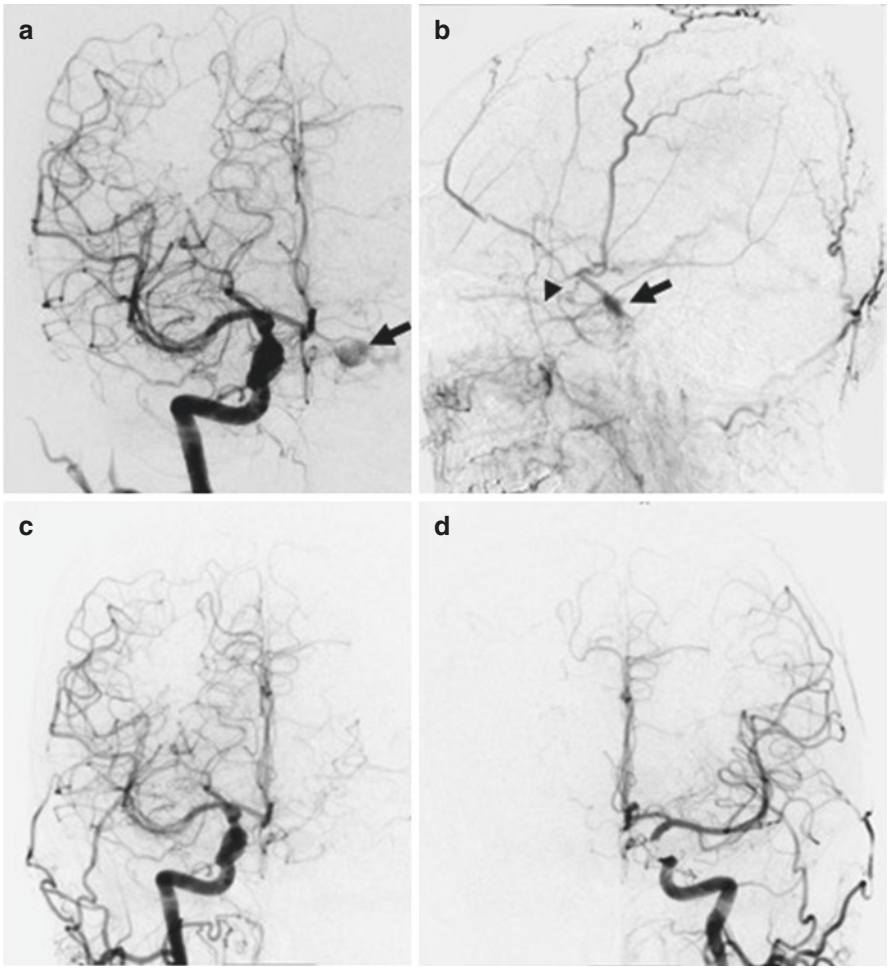

Fig. 22.1 An indirect type D CCF treated with transvenous coil embolization. (**a**) A right ICA injection demonstrates a left carotid cavernous fistula supplied by the right ICA. (**b**) A left ECA injection also demonstrates supply from branches of the left ECA with early filling of the left superior ophthalmic vein (arrowhead). Arrows in (**a**) and (**b**) indicate the CCF. Following coil embolization, common carotid artery injections (right, **c**; left, **d**) demonstrate successful obliteration of the CCF

possible CCF. She was found to have a right Barrow type A CCF (Fig. 22.2a, b). The left cavernous sinus exhibited early filling (Fig. 22.2a, double arrows), and there was reflux into the right superior ophthalmic vein (Fig. 22.2a, b, arrowhead). The CCF was treated with transvenous coil embolization after access was obtained through the inferior petrosal sinus by way of the right brachial vein. Balloon remodeling of the right ICA was performed during coil deployment.

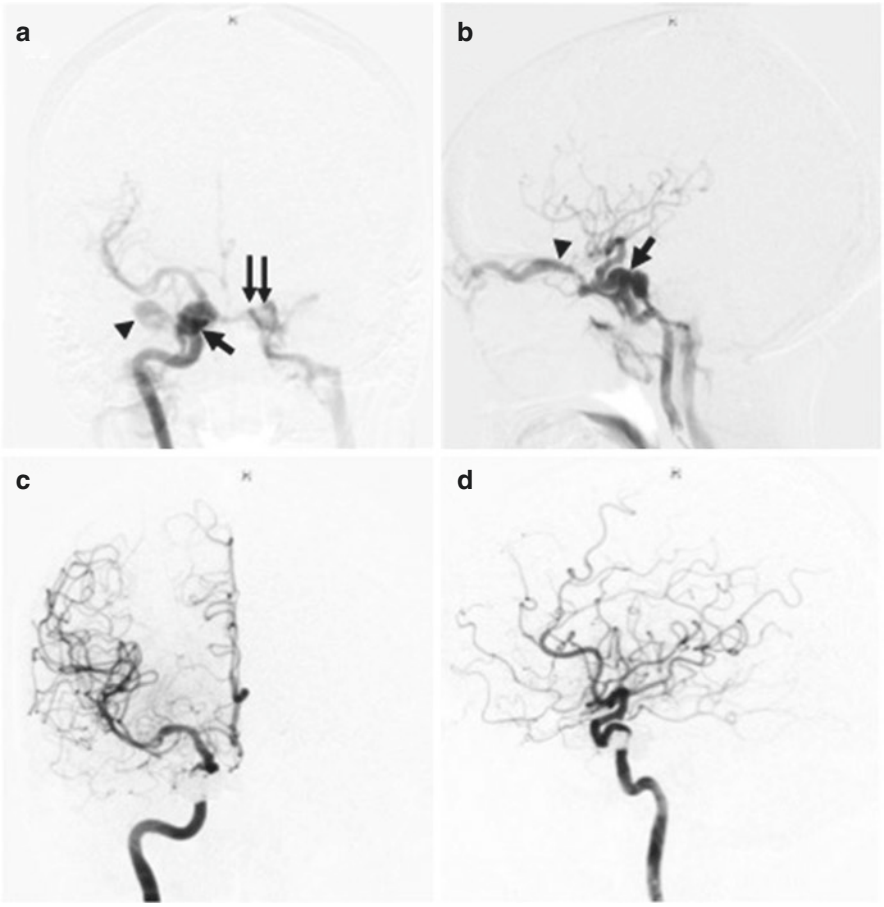

Fig. 22.2 Direct type A CCF treated with transvenous coil embolization and arterial balloon remodeling. (**a**) Coronal and (**b**) sagittal projections of a right ICA injection show a direct fistulous connection between the right ICA and cavernous sinus. The CCF is marked by the arrow. There is an early filling of the right superior ophthalmic vein (arrowhead) and the left cavernous sinus (double arrows). Coil embolization with concurrent balloon remodeling of the right ICA successfully obliterated the CCF, as seen on post-embolization injection of the right ICA (**c**, coronal; **d**, sagittal)

At the end of the procedure, full obliteration of the fistula was demonstrated, without residual early venous opacification (Fig. 22.2c, d). One month after embolization, the patient had significant improvement in proptosis, chemosis, diplopia and tinnitus, and 6 months later she had near-complete resolution of these symptoms.

Vein of Galen Malformations

Epidemiology

Vein of Galen malformations (VOGM) are congenital intracranial high-flow vascular malformations that typically present in neonates or infants [42], and are found three times more often in males than females [43]. While they represent less than 1% of all arteriovenous malformations [42], they account for 30% of pediatric vascular lesions [44, 45].

Formation

A VOGM arises from arteriovenous shunting from the choroidal arteries into the dilated midline persistent median prosencephalic vein of Markowski, which is the precursor of the vein of Galen and internal cerebral veins later in development [46, 47]. The formation of a VOGM is believed to be related to an abnormal morphogenesis of the choroidal vasculature, with the anomalous arteriovenous shunt developing around the 6th to 11th week of gestation [46]. There is a consequent progressive enlargement of the anterior segment of the median prosencephalic vein of Markowski secondary to this abnormal shunting [42, 46, 48]. Other similarly located off-midline arteriovenous malformations can be associated with a dilated vein of Galen due to increased venous flow rather than abnormal embryologic development. These lesions can be distinguished angiographically from VOGMs due to the presence of their intervening nidus [42, 44] and are more appropriately termed as arteriovenous malformations (AVMs).

Most genetic mutations that underlie VOGM are de novo, frequently within chromatin-modifier genes essential for brain and vascular development or ephrin signaling genes [49]. Other mutations including ACVRL1 gene variants [50],

Table 22.2 Yaşargil and Lasjaunias classification schemas for vein of Galen malformations

Yaşargil classification [53]	
Type I	One or more direct fistulae between the pericallosal and posterior cerebral arteries and the vein of Galen
Type II	Thalamoperforator network lies between the arterial feeders and the vein of Galen
Type III	Multiple fistulous connection between different vessels (contains type I and II)
Type IV*	Adjacent arteriovenous malformation that drains into the vein of Galen
Lasjaunias classification [54]	
First type	
Choroidal type	Many choroidal feeders resulting in a nidal network that drain into the median prosencephalic vein of Markowski
Mural type	One or many direct arterial connections into the wall of the median prosencephalic vein of Markowski
Second type*	Secondary dilatation of the vein of Galen due to a deep arteriovenous malformation with venous drainage into the vein of Galen

The * denotes lesions that are not the true vein of Galen malformations

endoglin gene mutations [51], and RASA1 mutations [42] have been implicated, with some overlap found with other AVM syndromes.

Classification

Of the classification schemas proposed for VOGMs [52], the most commonly used clinically are those proposed by Yaşargil et al. [53] and Lasjaunias et al. [54] (Table 22.2). The Yaşargil system includes 4 types of aneurysmal malformations, classified by the arterial feeder patterns [53]. Lesions classified as type I have one or more direct fistulae between the pericallosal and posterior cerebral arteries and the vein of Galen, while type II lesions have a thalamoperforator network lying between the arterial feeders and the vein of Galen. Type III lesions have multiple fistulous connections from different vessels (encompassing types I and II). A type IV lesion has an adjacent arteriovenous malformation that drains into the vein of Galen and therefore is not considered a true VOGM [44, 52, 53].

In the Lasjuanias classification, there are two types of VOGMs delineated by their angiographic appearance [54]. The first type is a primary or true VOGM, which is further partitioned into a mural type and a choroidal type. The mural type of VOGM has one or many direct arterial connections into the wall of the median prosencephalic vein of Markowski, while the choroidal type has many choroidal feeders resulting in a nidal network that drains into the median prosencephalic vein of Markowski. The second type in the Lasjuanias classification is a secondary dilatation of the vein of Galen due to a deep AVM with venous drainage into the vein of Galen [44, 54].

In these classifications, the Yaşargil types I–III and Lasjuanias primary VOGM are considered true VOGM as the pathological vessel is the median prosencephalic vein of Markowski [44, 53, 54]. These true VOGM can be distinguished from the Yaşargil type IV and the Lasjuanias secondary VOGM, as the dilatation of the vein of Galen in these malformations is secondary to increased venous drainage from the AVM rather abnormal embryologic venous development [44, 46].

Clinical Features

Initial diagnosis of a VOGM may occur during childhood, shortly after birth, or in some cases by antenatally via ultrasound after approximately 25 weeks of gestation, when detection of a midline cystic brain mass can be made. In this final group, subsequent Doppler ultrasonography and antenatal MRI can confirm the finding [43]. Pregnant patients are then typically referred to a tertiary care center where additional specialists including high risk obstetrics, interventional neuroradiologists, and pediatric cardiologists, neurologists, and neurosurgeons are available [43].

The clinical presentation of VOGM is highly variable and largely dependent on the size of the malformation and degree of intracranial shunting. A subset of patients with a high volume of shunting can develop hydrops fetalis in utero, or rapid high

output cardiac failure or organ system failure in the early neonatal period [42–44, 55, 56]. While the placenta provides a competing low resistance pathway for blood flow in utero, the flow dynamics change rapidly with delivery [44, 57]. In the neonatal period, the flow through the VOGM rapidly increases with cerebral blood flow accounting for up to 80% of all cardiac output in these patients [44]. Cardiac failure can then result from a combination of increased cardiac demand, pulmonary hypertension due to increased venous return, persistent patent ductus arteriosus or patent foramen ovale, and shunt-related decreased coronary artery blood flow [44, 57].

The neurological manifestations are driven by both the anomalous pattern of cerebral blood flow, as well as the mass effect from the malformation itself. The rapid flow of blood through the VOGM results in a vascular steal and resultant diminished blood flow to the parenchyma and global ischemia [57]. Impaired venous drainage leads to increased venous pressure, and resultant global brain edema [56, 57]. Hydrocephalus can develop both in an obstructive pattern related to compression of CSF outflow via the VOGM directly and in a communicating pattern due to increased venous pressure and poorly developed arachnoid granulations [44, 56, 57]. Other manifestations include facial vein prominence, increased risk for intracranial hemorrhage, seizures, or acute herniation from increased intracranial pressure [42].

Table 22.3 The Bicêtre Neonatal Evaluation Score

Points	Cardiac function	Cerebral function	Respiratory function	Hepatic function	Renal function
5	Normal	Normal	Normal	–	–
4	Overload, not requiring medical intervention	EEG abnormalities, no detectable clinical abnormalities	Tachypnea, finishes bottle	–	–
3	Failure, stable with medical management	Nonconvulsive intermittent neurological signs	Tachypnea, does not finish bottle	Normal	Normal
2	Failure, unstable despite medical management	Isolated convulsion	Assisted ventilation, normal oxygen saturation with $FIO_2 < 25\%$	Hepatomegaly but normal hepatic function	Transient anuria
1	Failure, requiring ventilation	Seizures	Assisted ventilation, normal oxygen saturation with $FIO_2 > 25\%$	Moderate or transient hepatic insufficiency	Unstable diuresis with treatment
0	Resistant to medical therapies	Permanent neurological signs	Assisted ventilation, with persistent desaturation	Abnormal coagulation, elevated enzymes	Anuria

EEG electroencephalogram; table and score adapted from Lasjaunias et al., 2006 [56]

Treatment

The decision on whether to treat a VOGM must account for both the severity of the intracranial and the systemic manifestations of the lesion. The Bicêtre neonatal evaluation score proposed by Lasjuanias et al. (Table 22.3) includes 5 categories of clinical assessment: (1) cardiac function, (2) cerebral function, (3) respiratory function, (4) hepatic function, and (5) renal function [56]. The scale has a maximum score of 21, with a higher score indicating more normal function across these systems. In their experience, patients with a score of less than 8 are not offered treatment given universally poor outcomes. Those scoring 8–12 are offered urgent endovascular intervention, while those with a score of 12 or higher are offered medical management in an attempt to delay intervention until at least 5 months of age [56].

Reliance on spontaneous thrombosis is not considered a viable option, as this occurs only in approximately 1–2.5% of patients [56, 58], and in one large series half of the patients with spontaneous thrombosis had significant neurocognitive delay [56]. Historically, open surgical treatments for VOGM were proposed but they were associated high mortality, and are not considered a practical treatment course in the modern era [42]. These patients may require surgical intervention for sequala of VOGM, however, like ventricular shunting [44, 57].

Contemporary management for these lesions is almost always via endovascular intervention when intervention is indicated based on the patient's clinical presentation. Different centers have reported approaching these lesions via a transvenous [59, 60], transarterial [47, 56, 59], or transtorcular [59] approach. More recent series have favored a transarterial approach, with rare descriptions of combined transvenous and transarterial approaches [61].

Mortality following endovascular intervention is reported in 14–22% of patients [47, 56, 59, 61]. A meta-analysis reviewing endovascular treatment for VOGM found that good neurological outcomes were reported in 62% of patients overall [61]. Factors found to predict poorer outcomes included perinatal presentation or neonatal treatment [61, 62], excessive embolization of the venous outflow [47], treatment of more proximal fistulae before treating distal fistulae [47], use of larger microcatheters in neonates [47], and choroidal angioarchitecture [59, 62]. Improved neurological outcomes were demonstrated when treatment indications followed the Bicêtre neonatal evaluation score [61]. Secondary effects of the shunt such as heart failure and hydrocephalus respond well to embolization. CSF diversion, if necessary, should only be performed after embolization, as it can offset the balance of hydrovenous pressure and worsen the AV shunt.

Patients often require multiple staged endovascular treatments, allowing a progressive rather than abrupt change in the cerebral blood flow. Of the 578 patients included in the meta-analysis, 28% underwent a single treatment, 29% underwent 2 treatments, and the final 43% underwent 3 or more treatments [61].

There is less literature supporting the use of stereotactic radiosurgery (SRS) as either a primary or salvage treatment for VOGM. One small series of 9 patients, 4 of whom had prior embolization treatments, underwent treatment with SRS. Four of these patients had angiographic resolution of their VOGM, and 2 others had diminished flow [63].

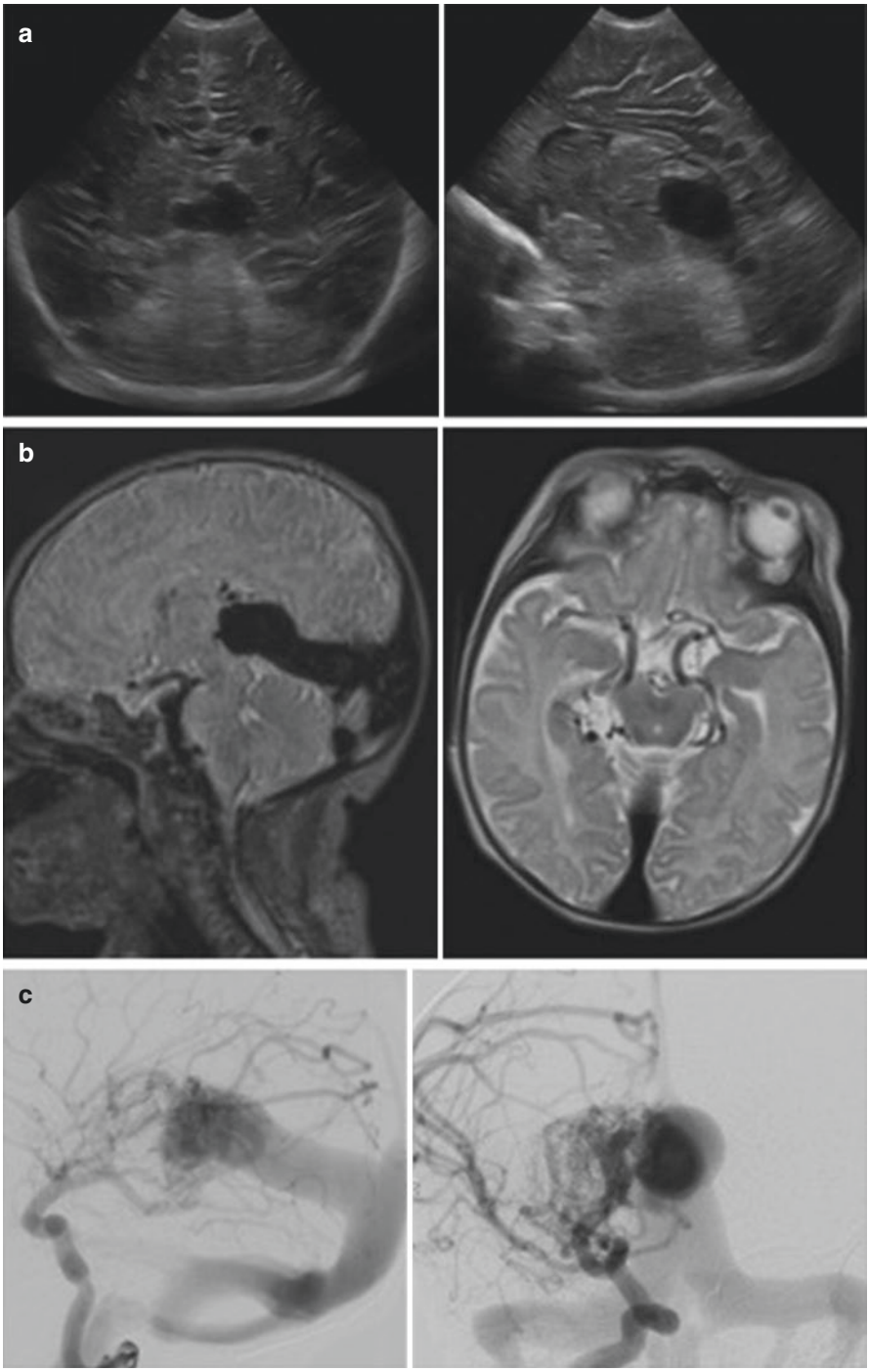

Fig. 22.3 Vein of Galen malformation with clear dilated midline vessel on cranial ultrasound (**a**), and dilated feeding arteries and draining vein on MRI (**b**). Catheter angiogram (**c**) of the Vein of Galen malformation following a right internal carotid artery injection in AP and lateral projections

Case Presentation

This is a case of an infant female who was born via an uncomplicated vaginal delivery at 39 weeks gestation, with an uneventful postnatal course until her second day of life. At that time, she developed significant tachypnea and associated oxygen desaturation to 88% on room air. After transfer to the neonatal intensive care unit, chest x-ray revealed cardiomegaly and subsequent cardiac echocardiogram revealed moderate left ventricular dilation, patent ductus arteriosus, as well as small atrial septal defects.

A cranial ultrasound (Fig. 22.3a) demonstrated a dilated vessel in the midline posteriorly. An MRI/MRA (Fig. 22.3b) revealed enlarged bilateral posterior choroidal arteries and thalamoperforators draining into a dilated median prosencephalic vein of Markowsi, all consistent with a diagnosis of a vein of Galen malformation. Catheter angiogram (Fig. 22.3c) demonstrated an atypical vein of Galen arteriovenous malformation supplied by the right anterior and posterior choroidal arteries with rapid drainage to the vein of Galen and straight sinus, as well as arterial feeders from the posterior division of the right middle cerebral artery branches to a proliferation of vessels to the right of the vein of Galen.

The patient was managed medically for her congestive heart failure until she was 9 months old, at which time she underwent a series of three-staged transarterial Onyx embolization procedures over 4 months. She had stabilization of her cardiac symptoms, with improved weight gain following her embolization procedures.

References

1. Liang W, Xiaofeng Y, Weiguo L, Wusi Q, Gang S, Xuesheng Z. Traumatic carotid cavernous fistula accompanying basilar skull fracture: a study on the incidence of traumatic carotid cavernous fistula in the patients with basilar skull fracture and the prognostic analysis about traumatic carotid cavernous fistula. J Trauma. 2007;63(5):1014–20. – discussion 1020.
2. Barrow DL, Spector RH, Braun IF, Landman JA, Tindall SC, Tindall GT. Classification and treatment of spontaneous carotid-cavernous sinus fistulas. J Neurosurg. 1985;62(2):248–56.
3. Debrun GM, Viñuela F, Fox AJ, Davis KR, Ahn HS. Indications for treatment and classification of 132 carotid-cavernous fistulas. Neurosurgery. 1988;22(2):285–9.
4. Ellis JA, Goldstein H, Connolly ES, Meyers PM. Carotid-cavernous fistulas. Neurosurg Focus. 2012;32(5):E9.
5. Miller NR. Dural carotid-cavernous fistulas: epidemiology, clinical presentation, and management. Neurosurg Clin N Am. 2012;23(1):179–92.
6. Thomas AJ, Chua M, Fusco M, Ogilvy CS, Tubbs RS, Harrigan MR, et al. Proposal of venous drainage-based classification system for carotid cavernous fistulae with validity assessment in a multicenter cohort. Neurosurgery. 2015;77(3):380–5. –discussion385.
7. Leone G, Renieri L, Enriquez-Marulanda A, Dmytriw AA, Nappini S, Laiso A, et al. Carotid cavernous fistulas and dural arteriovenous fistulas of the cavernous sinus: validation of a new classification according to venous drainage. World Neurosurg. 2019;128:e621–31.
8. Gupta AK, Purkayastha S, Krishnamoorthy T, Bodhey NK, Kapilamoorthy TR, Kesavadas C, et al. Endovascular treatment of direct carotid cavernous fistulae: a pictorial review. Neuroradiology. 2006;48(11):831–9.

9. van Rooij WJ, Sluzewski M, Beute GN. Ruptured cavernous sinus aneurysms causing carotid cavernous fistula: incidence, clinical presentation, treatment, and outcome. Am J Neuroradiol. 2006;27(1):185–9.
10. Feiner L, Bennett J, Volpe NJ. Cavernous sinus fistulas: carotid cavernous fistulas and dural arteriovenous malformations. Curr Neurol Neurosci Rep. 2003;3(5):415–20.
11. Oishi A, Miyamoto K, Yoshimura N. Etiology of carotid cavernous fistula in Japanese. Jpn J Ophthalmol. 2009;53(1):40–3.
12. Qi Y, Liu H, Jia J, Li J, Liu A, Jiang C. Endovascular treatment for spontaneous carotid cavernous sinus fistula caused by fibromuscular dysplasia: a rare case report and literature review. Clin Neurol Neurosurg. 2020;195:105882.
13. Adham S, Trystram D, Albuisson J, Domigo V, Legrand A, Jeunemaitre X, et al. Pathophysiology of carotid-cavernous fistulas in vascular Ehlers-Danlos syndrome: a retrospective cohort and comprehensive review. Orphanet J Rare Dis. 2018;13(1):100–10.
14. Robert T, Sylvestre P, Blanc R, Botta D, Ciccio G, Smajda S, et al. Thrombosis of venous outflows of the cavernous sinus: possible aetiology of the cortical venous reflux in case of indirect carotid-cavernous fistulas. Acta Neurochir (Wien). 2017;159(5):835–43.
15. de Keizer R. Carotid-cavernous and orbital arteriovenous fistulas: ocular features, diagnostic and hemodynamic considerations in relation to visual impairment and morbidity. Orbit. 2003;22(2):121–42.
16. Grumann AJ, Boivin-Faure L, Chapot R, Adenis JP, Robert PY. Ophthalmologic outcome of direct and indirect carotid cavernous fistulas. Int Ophthalmol. 2012;32(2):153–9.
17. Sasaki H, Nukui H, Kaneko M, Mitsuka S, Hosaka T, Kakizawa T, et al. Long-term observations in cases with spontaneous carotid-cavernous fistulas. Acta Neurochir (Wien). 1988;90(3–4):117–20.
18. Ko JK, Lee SW, Lee TH, Choi CH. Traumatic carotid cavernous fistula with a connection between the supraclinoid internal carotid artery and cavernous sinus via a pseudoaneurysm presenting with delayed life-threatening epistaxis. NMC Case Rep J. 2017;4(2):43–6.
19. Morton RP, Tariq F, Levitt MR, Nerva JD, Mossa-Basha M, Sekhar LN, et al. Radiographic and clinical outcomes in cavernous carotid fistula with special focus on alternative transvenous access techniques. J Clin Neurosci. 2015;22(5):859–64.
20. Kalsi P, Padmanabhan R, Prasad KSM, Mukerji N. Treatment of low flow, indirect cavernous sinus dural arteriovenous fistulas with external manual carotid compression – the UK experience. Br J Neurosurg. 2020;34(6):701–3.
21. Kai Y, Hamada J-I, Morioka M, Yano S, Kuratsu J-I. Treatment of cavernous sinus dural arteriovenous fistulae by external manual carotid compression. Neurosurgery. 2007;60(2):253–7. –discussion257–8.
22. Higashida RT, Hieshima GB, Halbach VV, Bentson JR, Goto K. Closure of carotid cavernous sinus fistulae by external compression of the carotid artery and jugular vein. Acta Radiol Suppl. 1986;369:580–3.
23. Rodrigues T, Willinsky R, Agid R, terBrugge K, Krings T. Management of dural carotid cavernous fistulas: a single-centre experience. Eur Radiol. 2014;24(12):3051–8.
24. Dye J, Duckwiler G, Gonzalez N, Kaneko N, Goldberg R, Rootman D, et al. Endovascular approaches to the cavernous sinus in the setting of dural arteriovenous fistula. Brain Sci. 2020;10(8):554.
25. de Castro-Afonso LH, Trivelato FP, Rezende MT, Ulhôa AC, Nakiri GS, Monsignore LM, et al. The routes for embolization of dural carotid cavernous fistulas when the endovascular approach is indicated as a first-line strategy. Interv Neuroradiol. 2019;25(1):66–70.
26. Ducruet AF, Albuquerque FC, Crowley RW, McDougall CG. The evolution of endovascular treatment of carotid cavernous fistulas: a single-center experience. World Neurosurg. 2013;80(5):538–48.
27. Meyers PM, Halbach VV, Dowd CF, Lempert TE, Malek AM, Phatouros CC, et al. Dural carotid cavernous fistula: definitive endovascular management and long-term follow-up. Am J Ophthalmol. 2002;134(1):85–92.

28. Hassan T, Rashad S, Aziz W, Sultan A, Ibrahim T. Endovascular modalities for the treatment of cavernous sinus arteriovenous fistulas: a single-center experience. J Stroke Cerebrovasc Dis. 2015;24(12):2824–38.
29. Sumdani H, Aguilar-Salinas P, Avila MJ, El-Ghanem M, Dumont TM. Carotid cavernous fistula treatment via flow diversion: a systematic review of the literature. World Neurosurg. 2021;149:e369.
30. Goelz L, Kreißl L, Gutowski P, Sparenberg P, Kirsch M, Mutze S. Unique indications for covered stent grafts in neuroradiology departments of level 1 trauma centers. J Neurol Surg A Cent Eur Neurosurg. 2020;81(3):243–52.
31. Lin L-M, Colby GP, Jiang B, Pero G, Boccardi E, Coon AL. Transvenous approach for the treatment of direct carotid cavernous fistula following Pipeline embolization of cavernous carotid aneurysm: a report of two cases and review of the literature. BMJ Case Rep. 2014;2014:bcr2014011235.
32. Dashti SR, Fiorella D, Spetzler RF, Albuquerque FC, McDougall CG. Transorbital endovascular embolization of dural carotid-cavernous fistula: access to cavernous sinus through direct puncture: case examples and technical report. Neurosurgery. 2011;68(1 Suppl Operative):75–83. –discussion83.
33. Tang C-L, Liao C-H, Chen W-H, Shen S-C, Lee C-H, Lee H-T, et al. Endoscope-assisted transsphenoidal puncture of the cavernous sinus for embolization of carotid-cavernous fistula in a neurosurgical hybrid operating suite. J Neurosurg. 2017;127(2):327–31.
34. Sur S, Menaker SA, Alvarez C, Chen S, Shah SS, Peterson EC, et al. Multimodal Management of Carotid-Cavernous Fistulas. World Neurosurg. 2020;133:e796–803.
35. Dye JA, Buchanan CC, Gonzalez NR. Integrated open surgical and endovascular embolization treatment of a paracavernous venous plexus fistula: case report. J Neurosurg. 2015;122(4):933–8.
36. Muram S, Khader Eliyas J, Eesa M, Mitha AP. Combined surgical and endovascular approach to treat a carotid cavernous fistula with associated brainstem venous congestion. BMJ Case Rep. 2017;2017:bcr–2017–013248.
37. Starke RM, McCarthy D, Sheinberg D, Connolly ES. Genetic drivers of vein of Galen malformations. Neurosurgery. 2019;85(2):E205–6.
38. Briggs RG, Bonney PA, Algan O, Patel AD, Sughrue ME. Bilateral carotid-cavernous fistulas treated with partial embolization and radiosurgery. Cureus. 2019;11(10):e5886.
39. Wu C-A, Yang H-C, Hu Y-S, Wu H-M, Lin C-J, Luo C-B, et al. Venous outflow restriction as a predictor of cavernous sinus dural arteriovenous fistula obliteration after gamma knife surgery. J Neurosurg. 2019;132(1):1–8.
40. Park S-H, Park K-S, Kang D-H, Hwang J-H, Hwang S-K. Stereotactic radiosurgery for dural carotid cavernous sinus fistulas. World Neurosurg. 2017;106:836–43.
41. Pan H-C, Sun M-H, Sheehan J, Sheu M-L, Chen CC-C, Lee H-T, et al. Radiosurgery for dural carotid-cavernous sinus fistulas: Gamma Knife compared with XKnife radiosurgery. J Neurosurg. 2010;113 Suppl(Special_Supplement):9–20.
42. Morshed RA, Winkler EA, Kim H, Braunstein S, Cooke DL, Hetts SW, et al. High-flow vascular malformations in children. Semin Neurol. 2020;40(3):303–14.
43. Bhattacharya JJ, Thammaroj J. Vein of galen malformations. J Neurol Neurosurg Psychiatr. 2003;74 Suppl 1(90001):i42–4.
44. Recinos PF, Rahmathulla G, Pearl M, Recinos VR, Jallo GI, Gailloud P, et al. Vein of Galen malformations: epidemiology, clinical presentations, management. Neurosurg Clin N Am. 2012;23(1):165–77.
45. Long DM, Seljeskog EL, Chou SN, French LA. Giant arteriovenous malformations of infancy and childhood. J Neurosurg. 1974;40(3):304–12.
46. Raybaud C. Normal and abnormal embryology and development of the intracranial vascular system. Neurosurg Clin N Am. 2010;21(3):399–426.

47. Bhatia K, Mendes-Pereira V, Krings T, Brugge Ter K, Kortman H, Dirks P, et al. Factors contributing to major neurological complications from vein of Galen malformation embolization. JAMA Neurol. 2020;77(8):992–9.
48. Raybaud CA, Strother CM, Hald JK. Aneurysms of the vein of Galen: embryonic considerations and anatomical features relating to the pathogenesis of the malformation. Neuroradiology. 2nd ed. Springer-Verlag. 1989;31(2):109–28.
49. Duran D, Zeng X, Jin SC, Choi J, Nelson-Williams C, Yatsula B, et al. Mutations in chromatin modifier and ephrin signaling genes in vein of Galen malformation. Neuron. 2019;101(3):429–443.e4.
50. Chida A, Shintani M, Wakamatsu H, Tsutsumi Y, Iizuka Y, Kawaguchi N, et al. ACVRL1 gene variant in a patient with vein of Galen aneurysmal malformation. J Pediatr Genet. 2013;2(4):181–9.
51. Tsutsumi Y, Kosaki R, Itoh Y, Tsukamoto K, Matsuoka R, Shintani M, et al. Vein of Galen aneurysmal malformation associated with an endoglin gene mutation. Pediatrics. 2011;128(5):e1307–10.
52. Mortazavi MM, Griessenauer CJ, Foreman P, Bavarsad Shahripour R, Shoja MM, Rozzelle CJ, et al. Vein of Galen aneurysmal malformations: critical analysis of the literature with proposal of a new classification system. J Neurosurg Pediatr. 2nd ed. American Association of Neurological Surgeons. 2013;12(3):293–306.
53. Yaşargil MG, Antic J, Laciga R, Jain KK, Boone SC. Arteriovenous malformations of vein of Galen: microsurgical treatment. Surg Neurol. 1976;3:195–200.
54. Lasjaunias P, Rodesch G, Pruvost P, Laroche FG, Landrieu P. Treatment of vein of Galen aneurysmal malformation. J Neurosurg. 1989;70(5):746–50.
55. Geibprasert S, Krings T, Armstrong D, TerBrugge KG, Raybaud CA. Predicting factors for the follow-up outcome and management decisions in vein of Galen aneurysmal malformations. Childs Nerv Syst. 2010;26(1):35–46.
56. Lasjaunias PL, Chng SM, Sachet M, Alvarez H, Rodesch G, Garcia-Monaco R. The management of vein of Galen aneurysmal malformations. Neurosurgery. 2006;59(5 Suppl 3):S184–94. –discussionS3–13.
57. Hoang S, Choudhri O, Edwards M, Guzman R. Vein of Galen malformation. Neurosurg Focus. 2009;27(5):E8.
58. Yan J, Gopaul R, Wen J, Li X-S, Tang J-F. The natural progression of VGAMs and the need for urgent medical attention: a systematic review and meta-analysis. J Neurointerv Surg. 2017;9(6):564–70.
59. Chow ML, Cooke DL, Fullerton HJ, Amans MR, Narvid J, Dowd CF, et al. Radiological and clinical features of vein of Galen malformations. J Neurointerv Surg. 2015;7(6):443–8.
60. Paúl L, Casasco A, Gil A, Aleu A, Guimaraens L. Arteriovenous fistulas of the vein of Galen region in adults: endovascular treatment. Interv Neuroradiol. 2020;26(6):757–66.
61. Brinjikji W, Krings T, Murad MH, Rouchaud A, Meila D. Endovascular treatment of vein of galen malformations: a systematic review and meta-analysis. AJNR Am J Neuroradiol. 2017;38(12):2308–14.
62. Fullerton HJ, Aminoff AR, Ferriero DM, Gupta N, Dowd CF. Neurodevelopmental outcome after endovascular treatment of vein of Galen malformations. Neurology. Wolters Kluwer Health, Inc. on behalf of the American Academy of Neurology; 2003;61(10):1386–90.
63. Payne BR, Prasad D, Steiner M, Bunge H, Steiner L. Gamma surgery for vein of Galen malformations. J Neurosurg. 2000;93(2):229–36.

Chapter 23
Spinal Vascular Malformations

R. Christopher Spears and Justin F. Fraser

Introduction

Since the first clinical observation in the nineteenth century by Berenbruch, spinal vascular malformations have garnered great clinical and academic interest [1]. Numerous classification schemes have developed over the years, beginning with Virchow's original classification of these entities into two groups: angioma cavernosum, in which blood vessels were not separated by parenchyma, and angioma racemosum, in which parenchyma separated the vessels [2]. Knowledge of these lesions, and therefore their classifications, has evolved over time. These now include arteriovenous lesions, such as dural and pial arteriovenous fistulae and arteriovenous malformations; cavernomas; and spinal aneurysms. Hemangioblastomas are often considered neoplastic vascular lesions; however, the discussion of these tumors is outside the scope of this chapter. We will review epidemiology, pathophysiology, clinical characteristics, imaging features, and treatment strategies for these lesions.

R. Christopher Spears
Department of Neurosurgery, University of Kentucky, Lexington, KY, USA
e-mail: rcsp225@uky.edu

J. F. Fraser (✉)
Departments of Neurosurgery, Neurology, Radiology, and Neuroscience, University of Kentucky, Lexington, KY, USA
e-mail: Jfr235@uky.edu

J. R. Mascitelli, M. J. Binning (eds.), *Introduction to Vascular Neurosurgery*,
https://doi.org/10.1007/978-3-030-88196-2_23

Epidemiology

Spinal vascular malformations are rare lesions, severely limiting the accumulation of substantial epidemiological data. Spinal dural arteriovenous fistulae (SDAVFs) are the most common of the spinal vascular malformations and account for approximately 70% of these lesions [3, 4]. They are believed to be acquired lesions, though the exact etiology remains unknown. This is supported by most patients becoming symptomatic in their middle age [5–7]. Approximately 4% of patients with SDAVF have been found to have a history of trauma [8]. The incidence of SDAVFs has been reported to be 5–10 per million per year, though the disease is probably underdiagnosed [9, 10]. There is a predilection for males, and a meta-analysis has reported men to be affected 5 times more than women with a mean age of 55–60 years at the time of diagnosis [11]. Pediatric spinal arteriovenous fistulae are exceedingly rare, though there are reported cases [12, 13]. The vast majority of SDAVFs are in the thoracolumbar spine, with cervical lesions comprising 2% of cases and sacral lesions comprising 4% [11].

Spinal arteriovenous malformations (AVM) represent approximately 20–30% of spinal vascular shunts [5]. These lesions are thought to be congenital and are often categorized as glomus or juvenile, though, in their modified classification scheme, Spetzler et al. have subdivided these lesions into intradural and extradural–intradural, with intradural lesions being further divided into intramedullary, intramedullary–extramedullary, and conus medullaris [14]. Classification of spinal vascular malformations is further discussed in the "Classification Schemes" section. Glomus AVMs are the most common subtype, and juvenile AVMs (extradural–intradural) are the least common.

Cavernous malformations, also called cavernomas or cavernous hemangiomas, are more common in the brain but still comprise up to 12% of spinal vascular malformations [15–17]. These lesions are being found more frequently with the advent of high-resolution MRI; however, they remain a rare entity in the spinal cord. Estimates have indicated that cavernomas comprise 5% of all intramedullary lesions in adults and 1% of intramedullary lesions in children [18, 19].

Normal Spinal Vascular Anatomy

Blood supply to the spinal cord can be divided into two main sources: the vertebrosubclavian arteries and the thoraco-abdominal aorta. The internal iliac arteries may occasionally provide supply as well [20]. The segmental arteries from these sources give rise to spinal arteries, which provide blood supply to the anterior and posterior nerve roots via radicular arteries [20]. Some of these branches also supply the posterior spinal arteries and pial network (radiculopial arteries) or the spinal cord and anterior spinal artery (radiculomedullary arteries) [21].

The anterior spinal artery (ASA) arises from two branches originating from the medial intracranial vertebral arteries and join at the cervicomedullary junction. This classically runs in the anterior median fissure and supplies the anterior two-thirds of the spinal cord including the anterior horn cells, anterior and lateral corticospinal tracts, and spinothalamic tracts. Numerous anastomoses are present along its length, and it receives radiculomedullary feeders from the vertebral and subclavian arteries, especially from the larger artery of cervical enlargement (artery of Lazorthes) at C5 or C6. The posterior spinal arteries (PSA) may arise from the vertebral or posterior inferior cerebellar arteries (PICA). The PSAs course longitudinally in the posterolateral sulci and supply the dorsal columns [22]. Circumferential branches from the anterior and posterior spinal arteries form the pial plexus.

In addition to the anterior and posterior spinal arteries, the thoracolumbar spinal cord receives blood supply from 6 to 10 radiculomedullary feeders from the aorta and iliac arteries. The most prominent of these is the artery of Adamciewicz (arteria radicularis magna), which most commonly arises on the left at T8-L2 and often makes a classic hairpin turn into the anterior spinal artery, though there is significant variation [23]. The mid-thoracic region is often more vulnerable to compromise than the surrounding regions, especially as the anterior spinal artery may occasionally become discontinuous at these levels, while there are ample anastomoses in the cervical, lower thoracic, and lumbar spine [24, 25].

Venous drainage from the spinal cord, unlike the spinal arterial system, does not have a predominant ventral or dorsal pattern. Venous drainage consists of extensive anastomotic networks including the pial venous plexus and epidural venous plexus, as well as the anterior and posterior spinal veins. The superficial veins on the surface of the spinal cord are drained via radicullomedullary veins, which join the epidural venous plexus [26]. The venous plexi surrounding the spinal cord may become prominently enlarged or arterialized with arteriovenous shunting pathology.

Classification Schemes

Numerous classification schemes for spinal vascular malformations have been proposed [14, 27, 28]. The evolution of these classification systems is influenced by the growing knowledge of the pathophysiology of these lesions though the considerable number of proposals may cause some nomenclature confusion. A widely accepted classification scheme was described by Anson and Spetzler in 1992, which divided spinal vascular malformations into four types (Table 23.1) [28]. Type I described dural arteriovenous fistulae, type II described glomus arteriovenous malformations, type III described juvenile arteriovenous malformations, and type IV described perimedullary arteriovenous fistulae. Later, a modified classification system was described by Spetzler et al. where lesions were divided into three broad categories: neoplasms, spinal aneurysms, and arteriovenous lesions (Table 23.2) [14]. Neoplasms include hemangioblastomas and cavernous malformations. Arteriovenous lesions include arteriovenous fistulae and arteriovenous

Table 23.1 Classification of spinal vascular malformations into types I-IV according to Anson and Spetzler in 1992

Type I	Dural arteriovenous fistula
Type II	Intramedullary glomus arteriovenous malformation
Type III	Extensive arteriovenous malformation extending into the vertebral body and paraspinal tissues
Type IV	Pial arteriovenous fistula Type A – single feeder with moderate venous hypertension Type B – more feeders with increased flow and dilated veins Type C – giant, high-flow lesions with a markedly distended venous network

From Anson and Spetzler [28]

Table 23.2 Modified classification of spinal vascular malformations according to Spetzler et al. in 2002

Neoplasms
Hemangioblastomas
Cavernous malformations
Aneurysms
Arteriovenous lesions
Arteriovenous fistulas
Extradural
Intradural
Ventral
Types A–C
Dorsal
Arteriovenous malformations
Extradural–intradural
Intradural
Intramedullary
Compact
Diffuse
Intramedullary–extramedullary
Conus medullaris

Modified classification of spinal vascular malformations

malformations. Arteriovenous fistulae are further subdivided into intradural (with dorsal and ventral subcategories) and extradural, and arteriovenous malformations are further subdivided into extradural–intradural and intradural. Intradural AVMs are further classified into intramedullary, intramedullary–extramedullary, and conus medullaris.

Arteriovenous Lesions

Arteriovenous lesions refer to direct artery-to-vein connections (shunting) without an intervening capillary bed. This may result in high-flow lesions with elevated venous pressure and venous arterialization. High flow states may lead to steal phenomenon, and elevated venous pressure may lead to decreased arteriovenous gradient, which in turn may lead to decreased venous drainage of the surrounding neural tissue. The complex disturbances of blood flow in these lesions lead to neurologic sequela. Dural arteriovenous fistulae, arteriovenous malformations, and pial arteriovenous fistulae are included in this section.

Dural Arteriovenous Fistulae

Spinal dural arteriovenous fistulae, though rare, are the most common spinal vascular malformations. Their exact etiology is unknown, but they are believed to be acquired lesions, supported by many patients becoming symptomatic in their middle age [5–7]. Similar to cerebral DAVFs, SDAVFs are supplied by arteries that normally supply neural tissue, radiculomeningeal arteries [29]. The arteriovenous lesion is located intradurally with a direct shunt between the radiculomeningeal artery and a radicular vein (Fig. 23.1). This is classically located beneath the pedicle of the vertebral body [29]. The direct arteriovenous connection results in venous

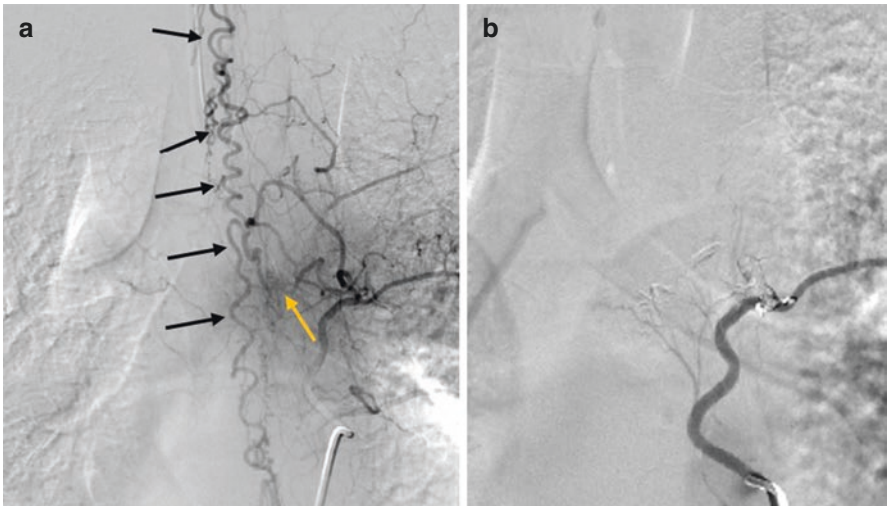

Fig. 23.1 (**a**) Digital subtraction angiogram with injection into the left T5 intercostal artery. A dural arteriovenous fistula (yellow arrow) is present with dilation of the perimedullary veins (black arrows). (**b**) Digital subtraction angiogram with injection into the left T5 intercostal artery after liquid embolization. Repeat injection after embolization reveals no residual fistula

congestion. Since the medullary veins and radicular veins share a common outflow, this leads to intramedullary edema and progressive myelopathy [30, 31]. The first symptoms may sometimes reflect conus medullaris dysfunction despite the remote location of the SDAVF [32]. This may be due to the lower thoracic levels having fewer venous outflow channels, causing the congestive venous edema to first affect the lower regions [26]. The lesion location may therefore not correlate with the level of neurologic symptoms.

Clinical Features

Patients with SDAF may present with a wide range of neurologic symptoms and often have a delayed diagnosis. Jellema et al. performed a retrospective study on 80 patients who were diagnosed with SDAF in six hospitals over a 15-year period [8]. The mean interval between onset of symptoms and diagnosis was 15 months. The delay in diagnosis was greater than 3 years in 19% of patients. The most common early symptoms include gait disturbances, sensory disturbances, and paresthesias. At the time of diagnosis, the most common symptoms were micturition problems and leg weakness. Later stages of the disease may lead to sexual dysfunction and fecal incontinence. Symptoms may additionally include lower motor neuron signs due to the involvement of the anterior horn cells in the lower thoracic spinal cord and conus [32]. Deterioration of the compensatory capacity of the spinal cord to accommodate venous congestion may result in rapidly progressive myelopathy (Foix-Alajouanine syndrome) [33, 34]. In contrast to their cranial counterparts, SDAVFs virtually never present with hemorrhage, likely due to their slow-flow nature [29, 35].

Imaging Features

The classic finding of spinal cord edema with dilated perimedullary vessels is the characteristic appearance of SDAVF on MRI (Fig. 23.2) [32]. Increased T2 signal is present within the central spinal cord with a thin rim of peripheral hypointensity, likely representing deoxygenated blood in capillaries surrounding the edema from venous congestion. The increased T2 signal often spans multiple segments and usually involves the conus [36]. Some contrast enhancement within the cord may be present, signaling chronic venous congestion [37]. In later stages of the disease, spinal cord atrophy may be seen. Shunting often causes arterialized dilation of the perimedullary veins, which may be seen as flow voids on MRI [38]. These may be better seen on constructive interference in steady state (CISS) or fast imaging employing steady-state acquisition (FIESTA) sequences [29]. The location of the dilated vessels and medullary findings do not appear to correlate with the level of the SDAVF.

Spinal digital subtraction angiography (DSA) is the gold standard for diagnosing SDAVF. Given that conventional MRI does not reveal the level of the fistula,

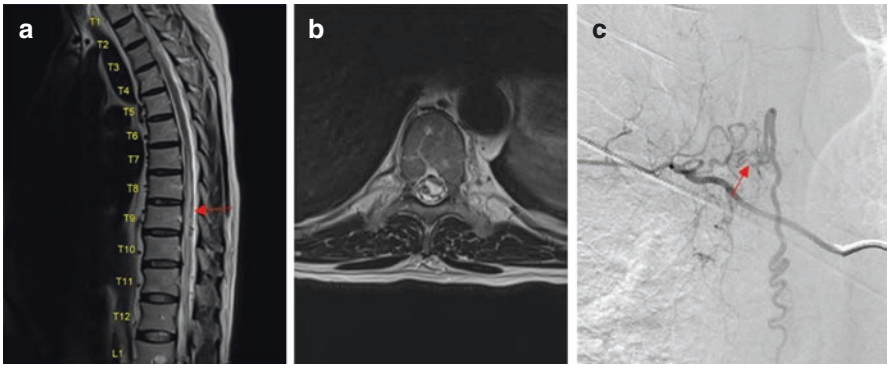

Fig. 23.2 (**a**) T2-weighted sagittal MRI. Increased T2 signal is seen in the lower thoracic spinal cord secondary to venous congestion and intramedullary edema (arrow). (**b**) T2-weighted axial MRI at T9 revealing significant intramedullary edema. (**c**) Digital subtraction angiogram with a right T3 intercostal artery injection revealing a dural arteriovenous fistula (arrow). Note the remote location of the fistula relative to the intramedullary edema of the lower thoracic spinal cord on the MRI

however, complete spinal angiography can be lengthy and cumbersome. Evaluation with MRA to assist with localization of the lesion prior to angiography may be useful to allow a more focused procedure [39, 40]. If this is not revealing, it is important to perform a complete spinal (and sometimes cerebral) angiogram to conduct a thorough search. During spinal DSA, contrast stasis within the radiculomedullary arteries and anterior spinal artery signifies venous congestion and should encourage the operator to look carefully for an SDAVF [38]. Injection of contrast into the segmental artery supplying the fistula leads to early venous filling, and an enlarged network of dilated perimedullary veins may be visible.

Treatment Strategies

Treatment of SDAVFs may involve surgery, endovascular techniques, or a combination of both modalities. The evolution of endovascular techniques has led to this modality becoming the mainstay of treatment of these lesions, with surgery often reserved for refractory cases or those with unfavorable anatomy for embolization [41]. Endovascular therapy typically involves liquid embolic treatment with the goal of occluding the shunting zone, especially the proximal draining vein. Failure to include the draining vein in occlusion of the shunting zone often results in recurrence or persistence of the fistula [42]. Super-selective catheterization of the feeding arteries may sometimes be very difficult or impossible. In these cases, embolization may not be attempted if the operator is unsure that the draining vein can be embolized. A radiopaque coil may be placed to facilitate easy fluoroscopic localization later in the operating room [42, 43]. Neurophysiologic monitoring is often employed during the endovascular treatment of SDAVFs. A sodium amytal challenge test may

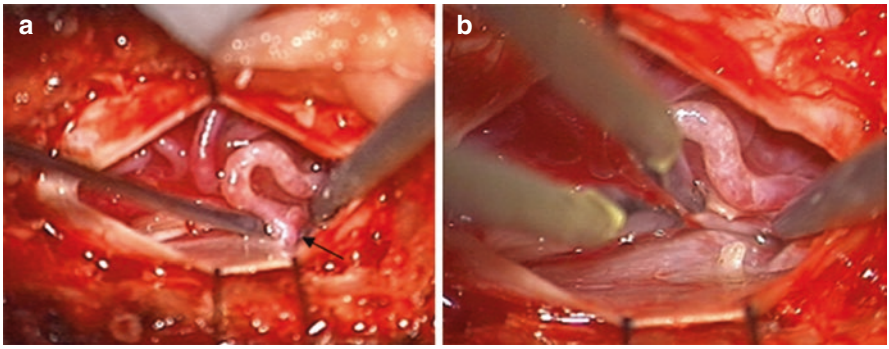

Fig. 23.3 (**a**) Intraoperative photograph revealing a dural arteriovenous fistula from a left T9 feeder. (**b**) Bipolar coagulation of the fistula

be performed once the microcatheter is in its final position immediately prior to embolization. Neuromonitoring changes or the development of symptoms in awake patients may indicate that embolization may not be safe in the microcatheter's current position, and the microcatheter may need to be adjusted or the case aborted.

Open surgical occlusion of SDAVFs is often a relatively straightforward procedure with one meta-analysis reporting occlusion rates of 98% [44]. After the laminectomy and durotomy, the dilated tortuous medullary vein is traced to its point of dural penetration. The preoperative angiogram is a vital resource used as a reference when navigating intraoperative vascular anatomy. Bipolar electrocautery is most often used to occlude the arterialized vein (Fig. 23.3). Normalization of the venous pressures may be visualized over several minutes as they turn from red to blue, suggesting obliteration of the shunting zone, which can be confirmed with a postoperative angiogram. As with other surgical procedures for spinal fistulae and AVMs, indocyanine green angiography with a microscope can be a useful tool to document the change in flow and obliteration.

Arteriovenous Malformations

A spinal arteriovenous malformation (SAVM) is composed of a nidus of aberrant vessels resulting in an arteriovenous shunt. In the spine, these lesions are often subdivided into intramedullary, corresponding with glomus AVMs (type II malformations); extradural–intradural AVMs, corresponding with juvenile or metameric AVMs (type III malformations); and conus medullaris AVMs [14]. Intramedullary AVMs are often subdivided into compact or diffuse. Extradural–intradural AVMs are invested along a somite level and may extensively involve peri-spinous tissue such as bone, muscle, and skin in addition to the spinal cord and dura. Conus medullaris AVM is a relatively newer classification described by Spetzler et al. and represent lesions with a unique location and angioarchitecture in the conus medullaris and rostral cauda equina [14, 45].

Clinical Features

SAVMs are often high-flow, high-pressure lesions, which can result in venous hypertension and hemorrhage. Symptomatology can vary depending on the location of these lesions and their hemodynamics and is caused by hemorrhage, mass effect, or vascular steal. Most patients experience a slow, gradual onset of neurologic dysfunction, but hemorrhage in SAVMs can result in sudden, dramatic symptoms. Hemorrhage may lead to acute back or neck pain, meningismus, loss of consciousness, or acute motor and/or sensory deterioration. A distinct sensory level may be present, correlating with the location of the vascular nidus. Occasionally, a spinal bruit may be noted in patients with high flow lesions [5]. Patients with conus medullaris AVMs can experience symptoms suggestive of cauda equina syndrome as a result of compression of the nerve roots exiting the conus, leading to these patients sometimes having both upper and lower motor neuron symptoms.

Imaging Features

MRI is often the first diagnostic imaging performed when evaluating patients with SAVMs and is highly sensitive, detecting nearly 100% of these lesions [46]. A nidus may be clearly visible with serpentine flow voids. Increased T2 signal may be present around the nidus, suggesting gliosis, edema, or infarction. Evidence of previous hemorrhage may also be present as hematomyelia or cavitation. DSA is important in the assessment of these lesions, providing detailed information on the pathology and the surrounding normal anatomy (Fig. 23.4). Aneurysms may be present within the nidus, a finding associated with an increased risk of hemorrhage [47].

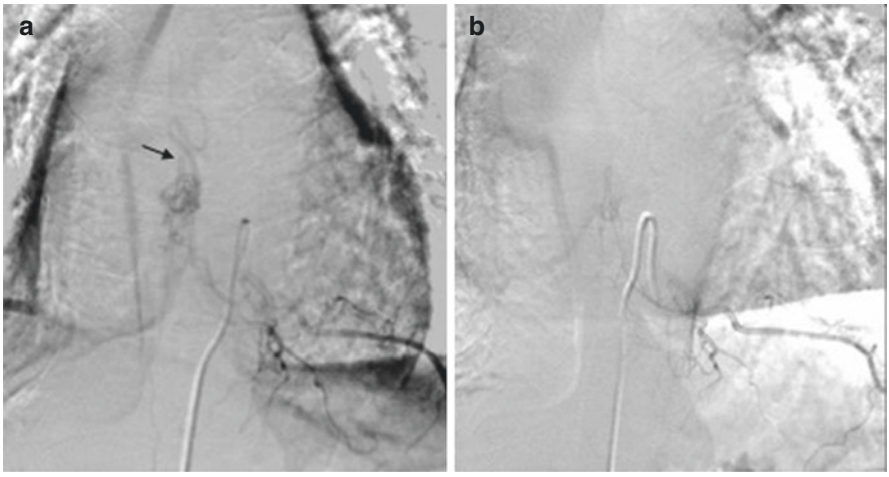

Fig. 23.4 (**a**) Digital subtraction angiogram with left T10 segmental artery injection revealing a spinal arteriovenous malformation in a 55-year-old man with progressive bilateral lower extremity weakness and sensory changes. The artery of Adamkiewicz is seen feeding into the anterior spinal artery (arrow) and arises from one of the main feeding arteries, precluding the patient from safe embolization. He underwent open surgical resection. (**b**) Postoperative angiogram

Treatment Strategies

SAVMs are variable and sometimes formidable lesions, and the treatment paradigm is tailored to individual patients. Open surgical resection has been the mainstay of treatment for intramedullary AVMs, though successful endovascular treatment has been described [48]. The pathophysiology of intramedullary AVMs defines them as a superficial entity, and chasing vascular loops invaginating into the parenchyma should be avoided and instead should be truncated at the pial surface [45]. Extradural–intradural AVMs are often large, extensive lesions that can be very difficult to treat. Given their extensive nature, endovascular therapy is often a mainstay of treatment, though the goal is often palliative to ameliorate the patient's neurologic symptoms. Surgery is reserved for the treatment of a mass effect on the spinal cord and nerve roots [45]. Conus medullaris AVMs are often treated with a combined endovascular and microsurgical approach. Venous structures around these lesions are often significantly dilated, and surgical decompression may significantly relieve neurologic symptoms. Aggressive combined treatment can lead to good outcomes [14]. Intraoperative neurophysiologic monitoring is standard practice at many institutions during surgery for patients with myelopathy or lesions such as intrinsic spinal cord tumors [49, 50]. Intraoperative evaluation of motor evoked potentials (MEPs) and somatosensory evoked potentials (SSEPs) may be a useful tool to predict deleterious maneuvers during resection of some spinal vascular malformations.

Pial Arteriovenous Fistulae

Spinal pial arteriovenous fistulae (SPAVFs), also called perimedullary fistulae (type IV), are arteriovenous malformations deriving their supply from pial arteries, as opposed to dural arteries in SDAVFs [51]. These lesions are often ventral and represent a direct fistulous connection to an enlarged venous network, most commonly supplied by the ASA. They have been classified into three types: type A fistulae are small shunts with slow blood flow from a single feeder and moderate venous hypertension, type B fistulae have more feeders with increased flow and dilated veins, and type C fistulae are giant, high-flow lesions with a markedly distended venous network [28, 52]. These lesions have been associated with Cobb syndrome, hereditary hemorrhagic telangiectasia, and Klippel-Trenaunay-Weber syndrome [53–55].

Clinical Features

Like SDAVFs, these patients often present with venous hypertension resulting in progressive myelopathy. Unlike SDAVFs, however, SPAVFs have more potential for rupture. Patients most commonly present with progressive radiculomyelopathy, though more acute symptoms are possible, and patients may present with

subarachnoid hemorrhage (SAH) [28, 52]. Most common symptoms often include paraparesis, sensory disturbances, and bowel/bladder symptoms. They most commonly affect the lumbar cord and conus medullaris, though they can be present in the thoracic and cervical levels as well [52, 56]. Patients often present in the third to fifth decades of life, though patients with type C lesions present significantly younger, and patients with type A lesions present at older ages [56].

Imaging Features

MRI may reveal findings similar to SDAVFs. These lesions may also be radiographically occult lesions, but serpentine flow voids are the most common finding due to venous enlargement. Congestive edema may also be seen with increased T2 signal, and epidural contrast pooling may also be present on contrasted imaging in addition to enhancement of the enlarged vessels [57, 58]. Angiography provides confirmation of the type of vascular malformation, as well as its definitive location.

Treatment Strategies

Treatment strategies for SPAVFs may involve endovascular embolization, open surgery, or both. The goal of treatment is to occlude the shunting zone while maintaining perfusion of the normal vasculature, especially the ASA and its branches. Given the heterogeneity of these lesions, treatment depends on the angioarchitecture of the individual lesion. Liquid embolic materials are often the agent of choice, though polyvinyl alcohol (PVA) particles may sometimes be used for presurgical embolization. Superselective catheterization of the fistula in small SPAVFs is often very difficult, as the feeding vessel is a distal branch of the ASA [59, 60]. Surgical treatment for most type A and B fistulae is therefore often advocated [51]. Embolization is also difficult with type B lesions due to their multiple feeding arteries [61]. Endovascular embolization is often used for type C lesions, given their increased diameter and high-flow characteristics. Coils may be used to act as a frame for the liquid embolic material to prevent its migration into the venous side of the high-flow shunt [60]. As with DVAF, embolization should include the proximal draining veins to avoid recanalization. A recent systemic pooled analysis of 213 patients from 28 studies was published in 2013 [56]. In total, 23% of type A and type B fistulae were treated with endovascular therapy versus 80% of type C lesions with an obliteration rate of 93% for type A fistulae, 85% for type B, and 71% for type C lesions. During microsurgery, an aneurysm clip may be used to interrupt the fistula to avoid bipolar electrocautery near the spinal cord. A posterior operative approach may be used in fistulae at the conus medullaris or filum terminale, while an anterior approach may be needed in cases occurring at higher levels [51]. Accessing the anterior spinal cord via posterior approach may also be facilitated with larger posterolateral approaches with facetectomy and pedicle removal. The dentate ligaments may be incised to allow the spinal cord to be carefully rotated to access the lesion.

Cavernous Malformations

Spinal cavernous malformations, also called cavernous hemangiomas or cavernomas, are well-circumscribed lesions composed of tightly packed vessels composed of dilated, thin-walled capillaries without intervening parenchymal tissue. They are often classified as neoplastic vascular lesions along with hemangioblastomas [14]. Grossly, they are often described as having a "mulberry" appearance and are hemosiderin stained [62]. These uncommon vascular lesions are most often located intracranially but have been reported to represent approximately 5% of intramedullary lesions in adults [18]. Spinal cavernomas are also more likely to be symptomatic due to the density of the surrounding eloquent neural tissue. Like their cerebral counterparts, their incidence has increased with the advent of MRI [15]. They may occur sporadically or as a familial autosomal dominant disorder with incomplete penetrance and mutations such as in *CCM1, CCM2*, *CCM3, KRIT1,* and *PDCD10* [63, 64].

Clinical Features

Two general patterns of symptoms are associated with spinal cavernous malformations, though presentation may often involve a combination of the two. Acute hemorrhage into the surrounding neural tissues can result in acute neurologic symptoms [65]. Progressive myelopathy is a more common presentation. The mechanism for this may be due to microhemorrhages leading to reactive gliosis. Many patients may have progressive myelopathy accompanied by episodes of acute decline with partial improvement. As with other spinal vascular malformations, specific symptoms vary between patients and the location of the lesion.

Imaging Features

MRI is often diagnostic of cavernous malformations due to their characteristic appearance. They have a heterogenous appearance on T1-weighted images with a surrounding halo on T1- and T2-weighted imaging due to hemosiderin deposits (Fig. 23.5) [66, 67]. This is often described as a "popcorn" appearance on MRI. There may be a nonspecific expansion of the spinal cord at the location of the lesion as well [66]. They are angiographically occult lesions, though approximately 25% of cases are associated with a developmental venous anomaly, which may be seen on DSA [68]. Angiography is therefore not necessary when MRI is diagnostic.

Treatment Strategies

Studies have suggested that minimally symptomatic or incidentally discovered cavernomas can be safely monitored [69, 70]. However, surgery should be considered in patients with severe deterioration or progressive myelopathy. Open surgical

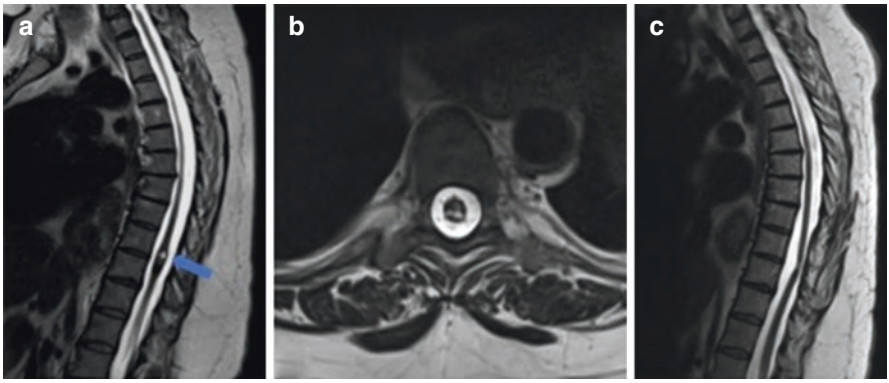

Fig. 23.5 (**a**) Sagittal T2-weighted MRI T-spine of a 54-year-old female with a T9/10 spinal cavernous malformation who presented with progressive relapsing-remitting leg weakness. Loss of T2 signal is present, consistent with hemosiderin deposition (arrow). (**b**) Axial view. (**c**) Sagittal T2-weighted MRI after surgical resection

resection is the mainstay of treatment for symptomatic spinal cavernous malformations. Most cavernomas are amenable to resection via posterior approach using techniques such as hemilaminectomy, laminectomy, laminoplasty, or interlaminar fenestration. Intraoperative neurophysiologic monitoring is often used during resection of these intramedullary lesions. After the dura is opened, cavernous malformations that extend to the cord surface may have hemosiderin staining and a bluish tinge of the pia [71]. The goal of surgery is complete resection, as the residual lesion may result in rehemorrhage [72]. In contrast to cerebral cavernous malformations, resection of the hemosiderin plane is not advised, as this may result in neurologic morbidity without benefit to the patient [73].

Spinal Aneurysms

Isolated spinal aneurysms that are not associated with other vascular malformations are rare lesions. A large series of over 3000 spinal angiograms revealed only one aneurysm [74]. They may present with compressive symptoms but more typically present with rupture (hematorrhachis) with abrupt symptoms [75–77]. In contrast to intracranial aneurysms, spinal aneurysms typically occur along the length of an artery rather than at a branching point. Dissecting dilatations are often fusiform, lacking a clear neck [78, 79]. The ASA is often involved, but other arteries such as the PSA or artery of Adamkiewicz can also be affected [77, 80]. Treatment is tailored to each patient, though cases reported in the literature have typically undergone operative treatment [79, 81].

Table 23.3 Summary of the characteristics and treatments of the spinal vascular malformations

Spinal lesion	Flow type	Frequent hemorrhage on presentation	Tissues involved	Typical treatment
Dural arteriovenous fistula	High	No	Dura	Endovascular (most common) or surgical
Arteriovenous malformation				
Glomus	High	Yes	Spinal cord	Surgical
Juvenile	High	Yes	Mixed	Surgical/endovascular
Pial arteriovenous fistula				
Type A	Low	No	Pia	Surgical
Type B	Moderate	No	Pia	Surgical
Type C	High	Yes	Pia	Endovascular
Cavernous malformation	Low	No (microhemorrhages)	Spinal cord	Surgical if symptomatic, observation if asymptomatic

Conclusion

Spinal vascular malformations are rare lesions affecting the spine. Symptoms associated with these lesions may be nonspecific but often involve myelopathy. Digital subtraction angiography is often the diagnostic test of choice with the exception of cavernous malformations, which are angiographically occult lesions. Treatment is tailored to the individual patient and may be endovascular, surgical, or a combination of these. Table 23.3 summarizes the spinal vascular malformations and their characteristics.

References

1. Berenbruch K. Ein Fall von multiplen Angiolipomen kombiniert mit einem Angiom des Rückenmark. Tübingen, Germany: Medical Faculty Universität Tübingen; 1890.
2. Virchow R. Die krankhaften Geschwülste: Hirschwald. Berlin; 1863.
3. Kendall BE, Logue V. Spinal epidural angiomatous malformations draining into intrathecal veins. Neuroradiology. 1977;13(4):181–9.
4. Merland JJ, Riche MC, Chiras J. Intraspinal extramedullary arteriovenous fistulae draining into the medullary veins. J Neuroradiol. 1980;7(4):271–320.
5. Rosenblum B, Oldfield EH, Doppman JL, Di Chiro G. Spinal arteriovenous malformations: a comparison of dural arteriovenous fistulas and intradural AVM's in 81 patients. J Neurosurg. 1987;67(6):795–802.
6. Jeng Y, Chen DY, Hsu HL, Huang YL, Chen CJ, Tseng YC. Spinal dural arteriovenous fistula: imaging features and its mimics. Korean J Radiol. 2015;16(5):1119–31.

7. Symon L, Kuyama H, Kendall B. Dural arteriovenous malformations of the spine. Clinical features and surgical results in 55 cases. J Neurosurg. 1984;60(2):238–47.
8. Jellema K, Canta LR, Tijssen CC, van Rooij WJ, Koudstaal PJ, van Gijn J. Spinal dural arteriovenous fistulas: clinical features in 80 patients. J Neurol Neurosurg Psychiatry. 2003;74(10):1438–40.
9. Thron A. Spinal dural arteriovenous fistulas. Radiologe. 2001;41(11):955–60.
10. Grandin C, Duprez T, Stroobandt G, Laterre EC, Mathurin P. Spinal dural arterio-venous fistula: an underdiagnosed disease? Acta Neurol Belg. 1997;97(1):17–21.
11. Jellema K, Tijssen CC, van Gijn J. Spinal dural arteriovenous fistulas: a congestive myelopathy that initially mimics a peripheral nerve disorder. Brain. 2006;129(Pt 12):3150–64.
12. Miller BA, Spears RC, Hines TK, Alhajeri A, Fraser JF. A lumbar arteriovenous fistula presenting with intraventricular hemorrhage and hydrocephalus. BMJ Case Rep. 2020;13(3):e015631.
13. Rajadurai J, Kohan S, Wenderoth J. Management of spinal dural arteriovenous fistula in a child with myelopathy. Surg Neurol Int. 2020;11:91.
14. Spetzler RF, Detwiler PW, Riina HA, Porter RW. Modified classification of spinal cord vascular lesions. J Neurosurg. 2002;96(2 Suppl):145–56.
15. Cosgrove GR, Bertrand G, Fontaine S, Robitaille Y, Melanson D. Cavernous angiomas of the spinal cord. J Neurosurg. 1988;68(1):31–6.
16. Gross BA, Du R, Popp AJ, Day AL. Intramedullary spinal cord cavernous malformations. Neurosurg Focus. 2010;29(3):E14.
17. Jellinger K. Pathology of spinal vascular malformations and vascular tumors. Berlin: Springer; 1978.
18. Deutsch H, Jallo GI, Faktorovich A, Epstein F. Spinal intramedullary cavernoma: clinical presentation and surgical outcome. J Neurosurg. 2000;93(1 Suppl):65–70.
19. Spetzger U, Gilsbach JM, Bertalanffy H. Cavernous angiomas of the spinal cord clinical presentation, surgical strategy, and postoperative results. Acta Neurochir. 1995;134(3–4):200–6.
20. Tveten L. Spinal cord vascularity. I. Extraspinal sources of spinal cord arteries in man. Acta Radiol Diagn (Stockh). 1976;17(1):1–16.
21. Steven Garfin FE, Bell G, Bono C, Fischgrund J. Rothman-Simeone and Herkowitz's the spine. Philadelphia: Elsevier; 2017.
22. Crosby E, Gillilian L. Correlative anatomy of the nervous system. New York: The Macmillian Company; 1962.
23. Lazorthes G, Gouaze A, Zadeh JO, Santini JJ, Lazorthes Y, Burdin P. Arterial vascularization of the spinal cord. Recent studies of the anastomotic substitution pathways. J Neurosurg. 1971;35(3):253–62.
24. Yoss R. Vascular supply of the spinal cord: the production of vascular syndromes. Med Bull (Ann Arbor). 1950;16:333–45.
25. Yatsu FM. Neurology in clinical practice: the neurological disorders. Philadelphia: Elsevier; 2004.
26. Tadie M, Hemet J, Freger P, Clavier E, Creissard P. Morphological and functional anatomy of spinal cord veins. J Neuroradiol. 1985;12(1):3–20.
27. Rodesch G, Hurth M, Alvarez H, Tadie M, Lasjaunias P. Classification of spinal cord arteriovenous shunts: proposal for a reappraisal–the Bicetre experience with 155 consecutive patients treated between 1981 and 1999. Neurosurgery. 2002;51(2):374–9; discussion 9–80
28. Anson J, Spetzler R. Classification of spinal arteriovenous malformations and implications for treatment. BNI Quarterly. 1992;8:2–8.
29. Krings T, Geibprasert S. Spinal dural arteriovenous fistulas. AJNR Am J Neuroradiol. 2009;30(4):639–48.
30. Kataoka H, Miyamoto S, Nagata I, Ueba T, Hashimoto N. Venous congestion is a major cause of neurological deterioration in spinal arteriovenous malformations. Neurosurgery. 2001;48(6):1224–9; discussion 9–30
31. Hurst RW, Kenyon LC, Lavi E, Raps EC, Marcotte P. Spinal dural arteriovenous fistula: the pathology of venous hypertensive myelopathy. Neurology. 1995;45(7):1309–13.

32. Koenig E, Thron A, Schrader V, Dichgans J. Spinal arteriovenous malformations and fistulae: clinical, neuroradiological and neurophysiological findings. J Neurol. 1989;236(5):260–6.
33. Criscuolo GR, Oldfield EH, Doppman JL. Reversible acute and subacute myelopathy in patients with dural arteriovenous fistulas. Foix-Alajouanine syndrome reconsidered. J Neurosurg. 1989;70(3):354–9.
34. Foix C, Alajouanine T. La myelite necrotique subaigue. Rev Neurol. 1926;46:1–42.
35. Van Dijk JM, TerBrugge KG, Willinsky RA, Farb RI, Wallace MC. Multidisciplinary management of spinal dural arteriovenous fistulas: clinical presentation and long-term follow-up in 49 patients. Stroke. 2002;33(6):1578–83.
36. Gilbertson JR, Miller GM, Goldman MS, Marsh WR. Spinal dural arteriovenous fistulas: MR and myelographic findings. AJNR Am J Neuroradiol. 1995;16(10):2049–57.
37. De Marco JK, Dillon WP, Halback VV, Tsuruda JS. Dural arteriovenous fistulas: evaluation with MR imaging. Radiology. 1990;175(1):193–9.
38. Krings T, Lasjaunias PL, Hans FJ, Mull M, Nijenhuis RJ, Alvarez H, et al. Imaging in spinal vascular disease. Neuroimaging Clin N Am. 2007;17(1):57–72.
39. Bowen BC, Fraser K, Kochan JP, Pattany PM, Green BA, Quencer RM. Spinal dural arteriovenous fistulas: evaluation with MR angiography. AJNR Am J Neuroradiol. 1995;16(10):2029–43.
40. Farb RI, Kim JK, Willinsky RA, Montanera WJ, ter Brugge K, Derbyshire JA, et al. Spinal dural arteriovenous fistula localization with a technique of first-pass gadolinium-enhanced MR angiography: initial experience. Radiology. 2002;222(3):843–50.
41. Marcus J, Schwarz J, Singh IP, Sigounas D, Knopman J, Gobin YP, et al. Spinal dural arteriovenous fistulas: a review. Curr Atheroscler Rep. 2013;15(7):335.
42. Jellema K, Sluzewski M, van Rooij WJ, Tijssen CC, Beute GN. Embolization of spinal dural arteriovenous fistulas: importance of occlusion of the draining vein. J Neurosurg Spine. 2005;2(5):580–3.
43. Britz GW, Lazar D, Eskridge J, Winn HR. Accurate intraoperative localization of spinal dural arteriovenous fistulae with embolization coil: technical note. Neurosurgery. 2004;55(1):252–4; discussion 4–5
44. Steinmetz MP, Chow MM, Krishnaney AA, Andrews-Hinders D, Benzel EC, Masaryk TJ, et al. Outcome after the treatment of spinal dural arteriovenous fistulae: a contemporary single-institution series and meta-analysis. Neurosurgery. 2004;55(1):77–87; discussion −8.
45. Kim LJ, Spetzler RF. Classification and surgical management of spinal arteriovenous lesions: arteriovenous fistulae and arteriovenous malformations. Neurosurgery. 2006;59(5 Suppl 3):S195–201; discussion S3–13.
46. Doppman JL, Di Chiro G, Dwyer AJ, Frank JL, Oldfield EH. Magnetic resonance imaging of spinal arteriovenous malformations. J Neurosurg. 1987;66(6):830–4.
47. Biondi A, Merland JJ, Hodes JE, Pruvo JP, Reizine D. Aneurysms of spinal arteries associated with intramedullary arteriovenous malformations. I. Angiographic and clinical aspects. AJNR Am J Neuroradiol. 1992;13(3):913–22.
48. Ausman JI, Gold LH, Tadavarthy SM, Amplatz K, Chou SN. Intraparenchymal embolization for obliteration of an intramedullary AVM of the spinal cord. Technical note. J Neurosurg. 1977;47(1):119–25.
49. Clark AJ, Ziewacz JE, Safaee M, Lau D, Lyon R, Chou D, et al. Intraoperative neuromonitoring with MEPs and prediction of postoperative neurological deficits in patients undergoing surgery for cervical and cervicothoracic myelopathy. Neurosurg Focus. 2013;35(1):E7.
50. Sala F, Bricolo A, Faccioli F, Lanteri P, Gerosa M. Surgery for intramedullary spinal cord tumors: the role of intraoperative (neurophysiological) monitoring. Eur Spine J. 2007;16(Suppl 2):S130–9.
51. Barrow DL, Colohan AR, Dawson R. Intradural perimedullary arteriovenous fistulas (type IV spinal cord arteriovenous malformations). J Neurosurg. 1994;81(2):221–9.
52. Gueguen B, Merland JJ, Riche MC, Rey A. Vascular malformations of the spinal cord: intrathecal perimedullary arteriovenous fistulas fed by medullary arteries. Neurology. 1987;37(6):969–79.

53. Antonietti L, Sheth SA, Halbach VV, Higashida RT, Dowd CF, Lawton MT, et al. Long-term outcome in the repair of spinal cord perimedullary arteriovenous fistulas. AJNR Am J Neuroradiol. 2010;31(10):1824–30.
54. Rodesch G, Hurth M, Alvarez H, Tadie M, Lasjaunias P. Spinal cord intradural arteriovenous fistulae: anatomic, clinical, and therapeutic considerations in a series of 32 consecutive patients seen between 1981 and 2000 with emphasis on endovascular therapy. Neurosurgery. 2005;57(5):973–83; discussion −83.
55. Cullen S, Alvarez H, Rodesch G, Lasjaunias P. Spinal arteriovenous shunts presenting before 2 years of age: analysis of 13 cases. Childs Nerv Syst. 2006;22(9):1103–10.
56. Gross BA, Du R. Spinal pial (type IV) arteriovenous fistulae: a systematic pooled analysis of demographics, hemorrhage risk, and treatment results. Neurosurgery. 2013;73(1):141–51; discussion 51
57. Ricolfi F, Gobin PY, Aymard A, Brunelle F, Gaston A, Merland JJ. Giant perimedullary arteriovenous fistulas of the spine: clinical and radiologic features and endovascular treatment. AJNR Am J Neuroradiol. 1997;18(4):677–87.
58. Yang HK, Lee JW, Jo SE, Jung C, Kwon OK, Lee E, et al. MRI findings of spinal arteriovenous fistulas: focusing on localisation of fistulas and differentiation between spinal dural and perimedullary arteriovenous fistulas. Clin Radiol. 2016;71(4):381–8.
59. Riche MC, Melki JP, Merland JJ. Embolization of spinal cord vascular malformations via the anterior spinal artery. AJNR Am J Neuroradiol. 1983;4(3):378–81.
60. Patsalides A, Knopman J, Santillan A, Tsiouris AJ, Riina H, Gobin YP. Endovascular treatment of spinal arteriovenous lesions: beyond the dural fistula. AJNR Am J Neuroradiol. 2011;32(5):798–808.
61. Mourier KL, Gobin YP, George B, Lot G, Merland JJ. Intradural perimedullary arteriovenous fistulae: results of surgical and endovascular treatment in a series of 35 cases. Neurosurgery. 1993;32(6):885–91. discussion 91
62. Russell D, Rubinstein L. Pathology of the nervous system. 5th ed. Baltimore: Williams & Wilkins; 1989.
63. Morrison L, Akers A. Cerebral cavernous malformation, familial. In: Adam MP, Ardinger HH, Pagon RA, Wallace SE, LJH B, Stephens K, et al., editors. . Seattle (WA): GeneReviews((R)); 1993.
64. de Vos IJ, Vreeburg M, Koek GH, van Steensel MA. Review of familial cerebral cavernous malformations and report of seven additional families. Am J Med Genet A. 2017;173(2):338–51.
65. Ogilvy CS, Louis DN, Ojemann RG. Intramedullary cavernous angiomas of the spinal cord: clinical presentation, pathological features, and surgical management. Neurosurgery. 1992;31(2):219–29; discussion 29–30
66. Barnwell SL, Dowd CF, Davis RL, Edwards MS, Gutin PH, Wilson CB. Cryptic vascular malformations of the spinal cord: diagnosis by magnetic resonance imaging and outcome of surgery. J Neurosurg. 1990;72(3):403–7.
67. Abid R, Carlier R, Idir AB, David P, Hurth M, Doyon D. Brain and spinal cord cavernoma. Value of MRI and review of the literature. Apropos of a case. J Radiol. 1993;74(11):563–7.
68. Abdulrauf SI, Kaynar MY, Awad IA. A comparison of the clinical profile of cavernous malformations with and without associated venous malformations. Neurosurgery. 1999;44(1):41–6; discussion 6–7
69. Kim KM, Chung CK, Huh W, Lee WJ, Park SB, Kim CH, et al. Clinical outcomes of conservative management of spinal cord cavernous angiomas. Acta Neurochir. 2013;155(7):1209–14.
70. Kharkar S, Shuck J, Conway J, Rigamonti D. The natural history of conservatively managed symptomatic intramedullary spinal cord cavernomas. Neurosurgery. 2007;60(5):865–72; discussion −72.
71. Endo T, Aizawa-Kohama M, Nagamatsu K, Murakami K, Takahashi A, Tominaga T. Use of microscope-integrated near-infrared indocyanine green videoangiography in the surgical treatment of intramedullary cavernous malformations: report of 8 cases. J Neurosurg Spine. 2013;18(5):443–9.

72. Maslehaty H, Barth H, Petridis AK, Doukas A, Mehdorn HM. Symptomatic spinal cavernous malformations: indication for microsurgical treatment and outcome. Eur Spine J. 2011;20(10):1765–70.
73. Bian LG, Bertalanffy H, Sun QF, Shen JK. Intramedullary cavernous malformations: clinical features and surgical technique via hemilaminectomy. Clin Neurol Neurosurg. 2009;111(6):511–7.
74. Berenstein A, Lasjaunias P. Spine and spinal cord vascular lesions. Berlin, Heidelberg: Springer; 1992.
75. Kinal ME, Sejanovich C. Spinal cord compression by an intramedullary aneurysm; case report and review of the literature. J Neurosurg. 1957;14(5):561–5.
76. Leech PJ, Stokes BA, ApSimon T, Harper C. Unruptured aneurysm of the anterior spinal artery presenting as paraparesis. Case report. J Neurosurg 1976;45(3):331–3.
77. Smith BS, Penka CF, Erickson LS, Matsuo F. Subarachnoid hemorrhage due to anterior spinal artery aneurysm. Neurosurgery. 1986;18(2):217–9.
78. Rengachary SS, Duke DA, Tsai FY, Kragel PJ. Spinal arterial aneurysm: case report. Neurosurgery. 1993;33(1):125–9; discussion 9–30
79. Gonzalez LF, Zabramski JM, Tabrizi P, Wallace RC, Massand MG, Spetzler RF. Spontaneous spinal subarachnoid hemorrhage secondary to spinal aneurysms: diagnosis and treatment paradigm. Neurosurgery. 2005;57(6):1127–31; discussion −31.
80. Garcia CA, Dulcey S, Dulcey J. Ruptured aneurysm of the spinal artery of Adamkiewicz during pregnancy. Neurology. 1979;29(3):394–8.
81. Massand MG, Wallace RC, Gonzalez LF, Zabramski JM, Spetzler RF. Subarachnoid hemorrhage due to isolated spinal artery aneurysm in four patients. AJNR Am J Neuroradiol. 2005;26(9):2415–9.

Chapter 24
Cerebral Cavernous Malformations

Jacob F. Baranoski and Michael T. Lawton

Abbreviations

CCM	Cerebral cavernous malformation
DVA	Developmental venous anomaly
MRI	Magnetic resonance imaging

Introduction

Cerebral cavernous malformations (CCMs), also referred to as cavernous malformations, cavernomas, or cavernous angiomas, are low-flow vascular lesions of the central nervous system [1]. These lesions consist of abnormally dilated capillary endothelial channels with increased permeability that are predisposed to episodic thrombosis and subsequent focal hemorrhage [2]. These hemorrhage events can result in seizures and neurological deficits [3, 4].

J. F. Baranoski
Department of Neurosurgery, Barrow Neurological Institute, St. Joseph's Hospital and Medical Center, Phoenix, AZ, USA
e-mail: Neuropub@barrowneuro.org

M. T. Lawton (✉)
Department of Neurosurgery, Barrow Neurological Institute, St. Joseph's Hospital and Medical Center, Phoenix, AZ, USA

Neuroscience Publications, Phoenix, AZ, USA
e-mail: Neuropub@barrowneuro.org

J. R. Mascitelli, M. J. Binning (eds.), *Introduction to Vascular Neurosurgery*,
https://doi.org/10.1007/978-3-030-88196-2_24

Histopathology

Macroscopic examination of a CCM reveals a characteristic "mulberry" appearance with engorged, aberrantly dilated cavernous vascular channels that form purple clusters (Fig. 24.1a) [5]. Microscopically, CCMs are characterized by densely packed, malformed capillaries embedded in a collagen matrix without intervening neural tissue. These sinusoids are dilated, thin-walled capillaries lined by a thin endothelium lacking smooth muscle and elastic tissue. The abnormal capillaries lack tight junctions, have diminished laminin and collagen IV within their endothelial cells, and are associated with a hypertrophic surrounding basal lamina. Together, these histopathological features predispose the aberrant capillary channels to leakage and recurrent cycles of thrombosis and hemorrhage that result in symptom onset. Due to episodic vascular leakage and microhemorrhage events, the brain parenchyma surrounding a CCM is often gliotic and stained with hemosiderin.

CCMs, particularly the sporadic type (sporadic versus familial subtypes are discussed below), can be associated with developmental venous anomalies (DVAs) [6]. DVAs, also referred to as venous angiomas, are medullary veins arranged in an atypical radial configuration. Although associated with the CCM, these medullary veins also drain normal brain tissue and coalesce into a single, dilated draining vein. Because the DVAs associated with CCMs also drain functioning brain tissue, care must be taken to preserve the DVA during CCM resections [7].

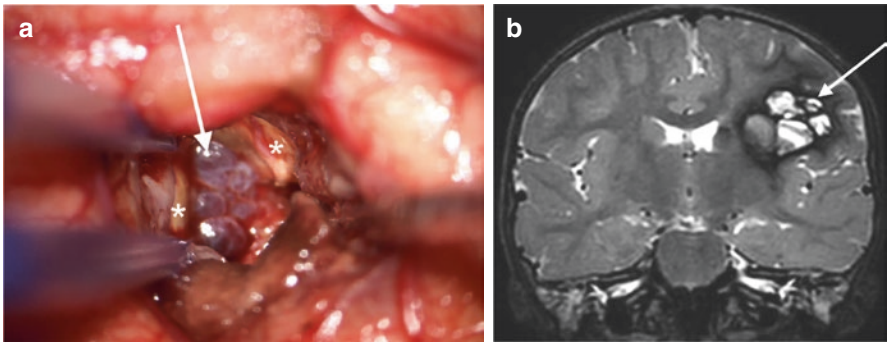

Fig. 24.1 (**a**) Intraoperative surgical microscope photograph demonstrating the dilated sinusoids associated with a cerebral cavernous malformation (*arrow*) and the associated hemosiderin-stained cortical tissue (*asterisks*). (**b**) T2-weighted coronal MRI demonstrating a left supratentorial cavernous malformation with associated hemorrhages of various ages (*arrow*). The arrow also demonstrates the chosen operative approach for resection utilizing a transulcal surgical corridor. (*Used with permission from Barrow Neurological Institute, Phoenix, Arizona*)

Epidemiology

CCMs are more common than is generally suspected and account for 5–15% of all vascular malformations affecting the central nervous system [2]. Estimations based on postmortem and magnetic resonance imaging (MRI) studies suggest that 1 in every 200–250 people, or approximately 35 million individuals worldwide, are affected by cavernous malformations [8–10]. Some patient populations are genetically predisposed to present with CCMs, as discussed below [1, 2]. CCMs occur with equivalent frequency in men and women, with a mean age at diagnosis in the third or fourth decade of life. Some data suggest that symptomatic hemorrhage at presentation is more common among women, but the evidence is not conclusive [11, 12].

Pathogenesis of Sporadic and Familial CCMs

In general, CCMs can occur as either sporadic or familial lesions [1, 13]. Sporadic lesions are isolated events, with patients most commonly having only a single lesion. In contrast, familial CCMs are characterized by multiple lesions due to a germline mutation inherited in an autosomal dominant fashion with variable penetrance. Although CCMs were once considered congenital in origin, studies have demonstrated that new CCMs may appear de novo later in life in both the sporadic and familial forms of the disease.

Sporadic CCMs

Sporadic CCMs are almost always found as solitary lesions with no known genetic predisposition. As mentioned above, the sporadic form is more commonly associated with a DVA. Sporadic CCMs are likely the result of an isolated somatic mutation in a single cell [2]. Such a mutation can result from radiation therapy, and multiple reports describe patients who developed CCMs following radiation treatment. Fortunately, the risk of radiation-induced CCM formation is quite low, and such cases are typically associated with higher doses of radiation (>30 Gy) [14].

Familial CCMs

In contrast to the sporadic form of CCMs, the familial form is characterized by multiple lesions and an autosomal-dominant mode of inheritance with variable penetrance [1, 2]. Indeed, the presence of 3 or more CCMs and a family history of seizures are essentially pathognomonic for the familial form of this disease. In general, seizures are the most common presenting symptom in patients with familial CCMs.

The driver mutations responsible for familial CCM pathogenesis have been localized to 3 distinct gene foci loci on chromosomes 7q (*KRIT1/CCM1*), 7p (*CCM2*), and 3q (*PDCD10/CCM3*) [3, 4]. The proteins encoded by these genes appear to interact with the endothelial cytoskeleton during angiogenesis in the central nervous system, and the loss-of-function mutations may directly drive the development of these lesions.

Clinical Presentation

A significant percentage of CCMs (20–30% of sporadic lesions) are asymptomatic at diagnosis and are found incidentally on MRIs performed for unrelated reasons or symptoms. Interestingly, despite the presence of multiple lesions, not all patients with familial CCM develop symptoms. Indeed, some studies have reported that approximately 40% of patients with the familial form of the disease have remained asymptomatic [11, 13].

When CCMs are symptomatic, the clinical presentation of a specific CCM is associated with its location. CCMs can occur in any location within the central nervous system. It is generally accepted that the prevalence of CCMs in a particular location is in approximate proportion to the volume of the various compartments: 80% supratentorial, 15% brainstem and basal ganglia, and 5% spinal cord. However, a recent meta-analysis of untreated cavernous malformations found that brainstem lesions may comprise a larger percentage than previously thought, up to 35% [15].

Recurrent hemorrhagic-thrombotic cycles are a constant feature of CCMs regardless of whether the lesions are symptomatic. Hemorrhages of various ages, combined with the deposition of hemosiderin in cerebral tissue surrounding the CCM, which results in neuronal dysfunction, are the cause of neurological symptoms. Therefore, the clinical presentation of a specific CCM is directly related to its location as well as the volume and type of hemorrhage (intralesional or extralesional).

Supratentorial/Hemispheric CCMs

Supratentorial/hemispheric CCMs can present with acute hemorrhage, seizures, and progressive neurological dysfunction (Fig. 24.1b) [3, 11, 13, 15]. Seizures are by far the most common clinical manifestation associated with hemispheric CCMs and are the presenting symptom in 40–80% of cases. Despite the prevalence of seizures in patients with hemispheric CCMs, no definitive data are available regarding the risk of new-onset seizures associated with lesions that have been found incidentally. Several studies have attempted to determine the relative risk. They have shown rates for the new onset of seizures of 0.9–2.4% per person-year [9, 16]. It has been well documented that patients with CCMs who present with seizures are at risk of developing epilepsy that may be medically refractory. CCMs likely cause seizures due to induced focal gliosis, hemosiderin deposition, and inflammatory responses of the

brain parenchyma surrounding the CCM. Although focal neurological deficits secondary to mass effect are possible, they are rarely associated with supratentorial lesions unless the lesion is located in the primary motor cortex, basal ganglia, or thalamus.

Brainstem CCMs

Patients with CCMs located in the brainstem most commonly present following an acute hemorrhage, with severe and progressive neurological deficits that include cranial neuropathies and long-tract signs (Fig. 24.2a, b) [4, 13, 15, 17]. Although patients with a first clinically symptomatic hemorrhage event associated with a brainstem CCM typically present with acute neurological deficits, these deficits can improve over time as the hemorrhage becomes organized and absorbed. Recurrent hemorrhages, however, are associated with more severe and permanent neurological impairment. Occasionally, large brainstem lesions can develop that are associated with only minimal deficits; this occurs most frequently with pontine lesions, where the mass gradually displaces the densely packed ascending and descending fiber tracts. Acute mortality due to a brainstem CCM is rare without multiple episodes of symptomatic hemorrhage.

Spinal Cord CCMs

Intramedullary spinal cord CCMs can have variable clinical presentations and can readily be confused with demyelinating diseases, intramedullary spinal neoplasms, and spinal arteriovenous malformations. In general, the clinical presentation of a patient with a spinal cord CCM can be divided into 1 of 3 types: (1) acute onset of

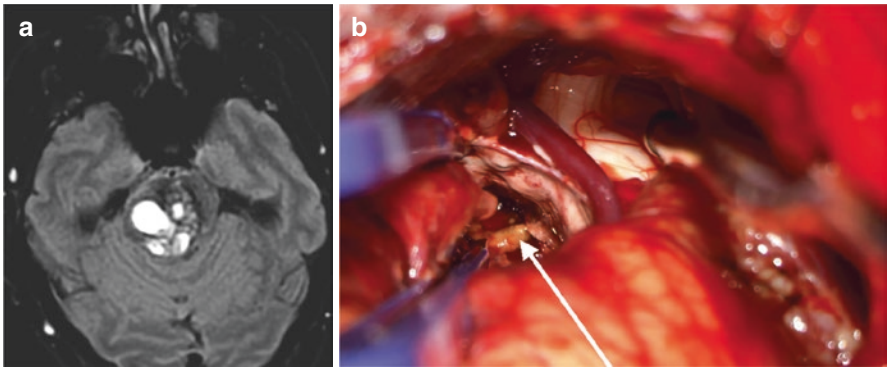

Fig. 24.2 (**a**) T2-weighted axial MRI demonstrating a large pontine brainstem cavernous malformation with associated hemorrhages of various ages. (**b**) Intraoperative surgical microscopic photograph demonstrating the surgical corridor and resection cavity (*arrow*). (*Used with permission from Barrow Neurological Institute, Phoenix, Arizona*)

major neurological deficits, (2) repetitive stepwise deterioration, and (3) slow progressive deterioration [18–21]. Various combinations of these presentations occur frequently. Symptom development in types 1 and 2 is related to episodes of acute hemorrhage with sudden onset of symptoms. In these cases, the severity of neurological deficits is related to the exact location of the lesion (level and position within the cord) as well as the volume and type of hemorrhage (intralesional, extralesional, or both). Presentation in the third group is probably related to minor bleeding episodes (microhemorrhages), focal thrombosis, and gliosis, resulting in the gradual growth of the lesion. Painful dysesthesias are a typical feature in this last group and may be related to the neurotoxic effects of hemosiderin. In general, pain is a common presenting symptom for patients with spinal cord CCMs and has been reported as a significant component in 40–60% of patients [18–21].

Imaging Findings

MRI plays an essential role in the diagnosis and workup for patients with CCMs (Figs. 24.1b and 24.2a) [13]. Computed tomography can help identify acutely hemorrhagic lesions, but MRI remains the most important imaging modality for CCM identification and evaluation. MRI evidence of hemorrhage is seen with any CCM regardless of whether the lesions are symptomatic or not. Hemorrhages of various ages, combined with hemosiderin deposition in cerebral tissue surrounding the cavernous malformation, produce the unique popcorn-like lesions seen on T1- and T2-weighted MRI sequences. Gradient echo and susceptibility-weighted sequences can further help identify small lesions that have not recently hemorrhaged [11, 13]. Some patients with familial CCMs can have a very large number of lesions seen on gradient echo and susceptibility-weighted MRI sequences. Contrasted MRI sequences can be useful for identifying DVAs, which are most commonly associated with sporadic CCMs, and for treatment and surgical approach planning [6, 7]. In general, CCMs are angiographically occult lesions, and catheter angiography should be reserved for cases where a potential arteriovenous malformation is a concern [11].

Differential Diagnosis

Given the classic appearance of CCMs on MRI, the differential diagnosis for CCMs is relatively limited. Some lesions that mimic CCMs on MRI are hemorrhagic or calcified neoplastic lesions, particularly hemorrhagic metastases, oligodendrogliomas, and pleomorphic xanthoastrocytomas. However, these oncological lesions tend to be associated with more perilesional edema. Some large CCMs could be initially mistaken for an arteriovenous malformation, in which case a catheter angiogram would be useful in determining the diagnosis (as discussed above).

Natural History of CCMs: Risk of New and Recurrent Symptomatic Hemorrhage Events

An understanding of the natural history of CCMs is critical to clinical decision-making regarding their management. Unfortunately, the natural history of CCMs is not as straightforward as it may appear, and a thorough understanding of the likely natural history for a given lesion for a specific patient is quite nuanced.

Numerous studies have been published on the natural history of cavernous malformations [4, 5, 9–11, 13, 15, 17]. Hemorrhage rates vary widely from series to series, depending on the definition of hemorrhage, the population being studied, and the methodology used to calculate and report future hemorrhage risk. Although these discrepancies complicate our ability to discern the future hemorrhage risk of a given CCM, it is now generally accepted that the risk of symptomatic hemorrhage or rehemorrhage of a CCM is influenced by the type of CCM, the lesion location, and the symptoms initially associated with that CCM (Table 24.1) [11, 15, 22].

Overall, brainstem CCMs appear to be associated with a greater risk of new and recurrent symptomatic hemorrhage events than supratentorial and hemispheric CCMs. Large case series have reported annual bleeding rates among supratentorial CCMs of 0.25–1.1% [11, 15, 22]. Similar studies have found estimated annual bleeding rates for brainstem lesions to be 2–3% [11, 15, 22].

In addition to CCM location, lesion type and the quality of previous hemorrhage events also affect the natural history of these vascular malformations. Zabramski et al. [13] classified cavernous malformations into four subtypes based on MRI characteristics (Table 24.2). The risk of hemorrhage appears to be greatest with type I and type II lesions, which are also more likely to be symptomatic.

Two recent meta-analyses have further demonstrated that the natural history of CCMs varies on the basis of the symptoms associated with their initial presentation [15, 22]. Both of these studies found that the risk of future CCM hemorrhage was greater among patients who presented with focal neurological deficits than among patients with incidentally discovered lesions. Horne et al. [15] reported the 5-year risk of intracranial hemorrhage of a previously unruptured, nonbrainstem cavernous malformation to be 3.8%; however, the 5-year risk of a recurrent hemorrhage for nonbrainstem lesions was 18.4%. Similarly, Taslimi et al. [22] found that

Table 24.1 Relative risk stratification for cerebral cavernous malformation symptomatic hemorrhage or rehemorrhage

Variable	Higher risk of symptomatic hemorrhage or rehemorrhage	Lower risk of symptomatic hemorrhage or rehemorrhage
Initial clinical presentation	Focal neurological deficit	Asymptomatic
CCM location	Brainstem	Cerebral convexity
CCM imaging subtype	IA > 1B > II	III, IV

Abbreviation: *CCM* cerebral cavernous malformation

Table 24.2 Magnetic resonance imaging classification for cerebral cavernous malformations

Lesion type	Magnetic resonance signal characteristic	Pathologic characteristics	Natural history: risk of hemorrhage
IA	T1: hyperintense focus of hemorrhage T2: hyperintense or hypointense focus of hemorrhage extending through the wall of the hypointense rim that surrounds the lesion	"Overt" extralesional focus of hemorrhage extending outside the lesion capsule	Almost all lesions are symptomatic; high risk of recurrent symptomatic hemorrhage
IB	T1: hyperintense focus of hemorrhage T2: hyperintense or hypointense focus of hemorrhage surrounded by a hypointense rim	Subacute focus of intralesional hemorrhage	Risk of symptomatic hemorrhage related to presentation and location, higher for symptomatic lesions and those in the brainstem
II	T1: reticulated mixed-signal core T2: reticulated mixed-signal core surrounded by a hypointense rim	Loculated areas of hemorrhage and thrombosis of varying age surrounded by gliotic, hemosiderin-stained brain; in large lesions, calcifications may be seen	Risk of symptomatic hemorrhage related to the presentation, higher in symptomatic patients
III	T1: isointense or hypointense T2: hypointense with hypointense rim that magnifies the size of the lesion GRE: hypointense with greater magnification than T2	Chronic resolved hemorrhage with hemosiderin staining within and around the lesion	Rarely symptomatic; lesions have a low risk of symptomatic hemorrhage
IV	T1: poorly seen or not visualized at all T2: poorly seen or not visualized at all GRE: punctate hypointense lesions	Akin to capillary telangiectasias	Rarely symptomatic; very low risk of hemorrhage

Abbreviation: *GRE* gradient echo

hemorrhage rates varied on the basis of initial clinical presentation. These authors reported that the annual incident rate of hemorrhage for incidentally discovered nonbrainstem CCMs was 0.3% per patient-year. In their study, the annual rehemorrhage rates were markedly higher: 6.3% for supratentorial CCMs with a median time to rehemorrhage of 10.5 months [22]. These recent meta-analyses also found that brainstem CCMs were associated with a higher risk of hemorrhage and rehemorrhage than nonbrainstem cerebral lesions. Horne et al. [15] reported the 5-year risk of intracranial hemorrhage of a previously unruptured brainstem CCM to be 8%, compared with 3.8% for nonbrainstem lesions. They also reported an elevated

5-year risk of a recurrent hemorrhage associated with brainstem lesions (30.8%) versus nonbrainstem lesions (18.4%). Similarly, Taslimi et al. [22] found that hemorrhage rates varied on the basis of anatomical location. These authors reported that the annual incident rate of hemorrhage for previously unruptured brainstem CCMs was 2.8% per patient-year, compared with 0.3% for nonbrainstem lesions. Annual rehemorrhage rates were also higher for brainstem CCMs than for nonbrainstem CCMs (32.3% vs. 6.3%).

Importantly, although some smaller studies have suggested possible correlations between rupture risk and demographic characteristics, including sex, larger studies and meta-analyses have reported no independent prognostic significance for risk related to age, sex, or CCM multiplicity [11, 15, 22]. Likewise, some studies have suggested that the presence of a DVA is a risk factor for future hemorrhage, but the data regarding this are not conclusive [7].

Regarding the natural history of familial versus sporadic CCMs, it appears that the natural histories are analogous. Recall that the clinical penetrance of the familial disease is highly variable, with 40–60% of patients reporting being free of symptoms. It is important to consider that, in familial cases, patients almost always have multiple CCMs. Therefore, although the annual risk of hemorrhage per patient may be elevated in familial cases, the annual risk of hemorrhage per lesion is likely equivalent to that of sporadic cases.

Clinical Management and Treatment Considerations

The decision to surgically resect a CCM should consider the clinical presentation, the lesion location, the potential for associated neurosurgical morbidity, and the natural history of the disease. The risk of surgical resection varies greatly with the location of the CCM, which therefore affects surgical decision-making. Guided by the results of numerous surgical series and natural history studies, the Angioma Alliance Scientific Advisory Board published their recommendations for clinical management of cavernous malformations [11]. Our center generally follows this algorithm for surgical decision-making for CCMs, although expanding the Angioma Alliance Scientific Advisory Board guidelines to scenarios not explicitly addressed in their recommendations (Table 24.3).

We recommend nonoperative management for incidentally discovered or asymptomatic CCMs, particularly if they are located in the eloquent cortex, thalamus, basal ganglia, brainstem, or spinal cord. Under certain circumstances, surgical resection can be performed for patients with asymptomatic, sporadic CCMs in easily accessible, noneloquent areas to prevent future hemorrhage in light of particular psychological burdens or lifestyle or career choices. We strongly discourage operating on asymptomatic patients with familial lesions regardless of the location of the CCM because even complete surgical resection will not result in a cure of the underlying genetic disease. For patients with multiple lesions, we recommend genetic testing and the possible use of evolving medical therapies.

Table 24.3 Clinical decision-making recommendations for cerebral cavernous malformations

Presentation, location	Recommendation
Incidentally discovered or asymptomatic	
Any	Single lesion: observation Multiple lesions: observation and genetic testing
Single, first-time seizure	
Any	Single lesion: antiepileptic medication Multiple lesions: antiepileptic medication and genetic testing
Medically refractory epilepsy	
Supratentorial	Single lesion: resection Multiple lesions: resection if a single lesion can be identified as the epileptogenic source; if not, then observation and antiepileptic medication
First hemorrhage with focal neurological deficit	
Noneloquent cerebral cortex or cerebellum	Resection
Deep or eloquent cortex	Observation or resection if clinical presentation and anatomy are favorable[a]
Brainstem	Observation or resection if clinical presentation and anatomy are favorable[a]
Spinal cord	Large hemorrhage: observation or resection if clinical presentation and anatomy are favorable[a] Small hemorrhage with minimal neurological deficit: observation
Recurrent hemorrhage with focal neurological deficit	
Deep or eloquent cortex	Resection if possible
Brainstem	Resection if possible
Spinal cord	Resection if possible

[a]Favorable presentation is defined as a fixed neurological deficit, such that the morbidity associated with the surgical approach would not worsen symptoms. Favorable anatomy is defined as pial or ependymal extension or hematoma cavity providing a surgical corridor

For patients with one or many CCMs who experience a first-time seizure, we recommend starting antiepileptic medications. If patients achieve seizure freedom with antiepileptic therapy, we recommend nonoperative management of the CCM. If patients with a single CCM continue to have medically refractory seizures, we recommend surgical resection of this lesion [23]. A systematic review performed by Englot et al. [24] found that 75% of patients with resected supratentorial CCMs were able to achieve seizure freedom. For patients with multiple CCMs and medically refractory epilepsy, if the epileptogenic focus can be localized to a specific lesion, we recommend resection of that lesion. If the epileptogenic cannot be localized to a particular lesion, we recommend continuing maximal medical therapy.

We recommend surgical resection for patients who present with a first-time hemorrhage from a single lesion in either noneloquent cerebral cortex or cerebellum,

have associated focal neurological deficits, and are medically appropriate surgical candidates. In this scenario, complete surgical resection can eliminate the risk of future hemorrhages and can result in a surgical cure with limited associated surgical morbidity.

For lesions in more surgically challenging anatomical locations, such as deep cerebral structures, brainstem, and spinal cord, additional factors must be considered because of the inherent surgical morbidity associated with accessing these locations [3, 4, 11, 25–29]. Even though future hemorrhages from untreated lesions in these locations would likely result in progressive neurological deterioration, it is important to recognize that resection of these lesions is associated with a high risk of complications. Early postoperative deficits after resection of brainstem CCMs are reported in 40–50% of patients [30]. Therefore, in general, we initially recommend nonoperative management for patients who have experienced only a single bleed with limited neurological sequelae from a CCM in any of the aforementioned locations. However, certain clinical and anatomical scenarios may make surgical resection favorable. If a patient has a fixed neurological deficit, such that there is no additional anticipated neurological morbidity associated with the surgical approach to the lesion, and if the lesion abuts a pial or ependymal surface or the hemorrhage has created a surgical corridor, then resection can be considered to prevent recurrent hemorrhage. If these clinical and anatomical features do not exist, then we recommend nonoperative management. However, if a CCM were to symptomatically hemorrhage multiple times or demonstrate instability on serial follow-up imaging, these findings should factor into clinical decision-making. Recurrent symptomatic hemorrhages from lesions in these locations are another indication for surgical intervention. Despite the high risk associated with surgical treatment of these difficult lesions, well-selected patients can tolerate surgery and have improved neurological outcomes [3, 4, 11, 25–30].

In summary, and given the inherent risks associated with deep cerebral, brainstem, and spinal cord operations, we recommend reserving resection for patients with 1 or more of the following indications: (1) a history of multiple hemorrhages, (2) severe or progressive symptoms, and (3) acute or subacute hemorrhage and significant mass effect. In addition, we typically recommend resection only when either or both of the following anatomical features are also present: (1) the lesion abuts a pial or ependymal surface or (2) the patient has an acute hemorrhage extending outside the lesion capsule (exophytic). High rates of recurrent symptomatic hemorrhages have been reported after incomplete surgical removal, which highlights the importance of complete resection if surgery is performed for lesions in these highly eloquent anatomical locations.

Advances in surgical technologies and techniques, such as intraoperative neuronavigation, tractography, microscope visualization and integration with navigation, mapping techniques, and neurophysiological monitoring, have further facilitated safer resection. In a well-selected patient population, experienced neurovascular or skull base surgeons can achieve acceptable outcomes after surgery for brainstem or deep cerebral cavernous malformations.

Potential Role for Stereotactic Radiosurgery

Stereotactic radiosurgery has been proposed as a treatment option for cavernous malformations in surgically challenging areas. However, the efficacy of this technique is debatable [11, 28]. In general, we recommend against using stereotactic radiosurgery as the primary treatment option for CCMs and recommend considering its use only for cases in which surgery is not an option. A full discussion of the controversial role of radiosurgery for cavernous malformations is beyond the scope of this chapter.

CCMs and Pregnancy

Historically, pregnancy was believed to be associated with an increased risk of hemorrhage in patients with CCMs. However, quantitative data supporting this assumption are scarce. Cavernous malformations have been reported to increase in size during pregnancy, and exacerbation of other symptoms related to acute hemorrhage has been documented. However, few reports in the literature document such events. Importantly, recent publications have studied this issue and found no evidence of increased risk of hemorrhage associated with pregnancy or delivery [12]. On the basis of these and other data, the Angioma Alliance Scientific Advisory Board has stated that "the risk of neurological symptoms during pregnancy is likely not different than the nonpregnant state," and vaginal delivery should not be precluded [11].

Management of symptomatic hemorrhage from cavernous malformations during pregnancy should be based on the severity of the episode and the imaging characteristics of the lesion. In general, the approach to managing a new CCM during pregnancy should account for the additional risk that surgical intervention may pose to the pregnant woman and the fetus, but the treatment algorithm should remain otherwise similar. If symptoms are severe and endanger maternal and fetal life, then surgical resection would likely be warranted. Fortunately, the need for emergency neurosurgical treatment during pregnancy has been rare.

Acknowledgments We thank the staff of Neuroscience Publications at Barrow Neurological Institute for assistance with manuscript preparation.

Disclosures The authors have no personal, financial, or institutional interest in any of the drugs, materials, or devices described in this manuscript.

Financial Support The authors have no financial support for this manuscript to report at this time.

References

1. Baranoski JF, Kalani MY, Przybylowski CJ, Zabramski JM. Cerebral cavernous malformations: review of the genetic and protein-protein interactions resulting in disease pathogenesis. Front Surg. 2016;3:60.
2. Cavalcanti DD, Kalani MY, Martirosyan NL, Eales J, Spetzler RF, Preul MC. Cerebral cavernous malformations: from genes to proteins to disease. J Neurosurg. 2012;116(1):122–32.
3. Davies JM, Kim H, Lawton MT. Surgical treatment of cerebral cavernous malformations. J Neurosurg Sci. 2015;59(3):255–70.
4. Garcia RM, Ivan ME, Lawton MT. Brainstem cavernous malformations: surgical results in 104 patients and a proposed grading system to predict neurological outcomes. Neurosurgery. 2015;76(3):265–77; discussion 77–8.
5. Voigt K, Yasargil MG. Cerebral cavernous haemangiomas or cavernomas. Incidence, pathology, localization, diagnosis, clinical features and treatment. Review of the literature and report of an unusual case. Neurochirurgia (Stuttg). 1976;19(2):59–68.
6. Abe T, Singer RJ, Marks MP, Norbash AM, Crowley RS, Steinberg GK. Coexistence of occult vascular malformations and developmental venous anomalies in the central nervous system: MR evaluation. AJNR Am J Neuroradiol. 1998;19(1):51–7.
7. Mooney MA, Zabramski JM. Developmental venous anomalies. Handb Clin Neurol. 2017;143:279–82.
8. Otten P, Pizzolato GP, Rilliet B, Berney J. 131 cases of cavernous angioma (cavernomas) of the CNS, discovered by retrospective analysis of 24,535 autopsies. Neurochirurgie. 1989;35(2):82–3, 128–31.
9. Del Curling O Jr, Kelly DL Jr, Elster AD, Craven TE. An analysis of the natural history of cavernous angiomas. J Neurosurg. 1991;75(5):702–8.
10. Robinson JR, Awad IA, Little JR. Natural history of the cavernous angioma. J Neurosurg. 1991;75(5):709–14.
11. Akers A, Al-Shahi Salman R, Awad IA, Dahlem K, Flemming K, Hart B, et al. Synopsis of guidelines for the clinical management of cerebral cavernous malformations: consensus recommendations based on systematic literature review by the Angioma Alliance Scientific Advisory Board Clinical Experts Panel. Neurosurgery. 2017;80(5):665–80.
12. Kalani MY, Zabramski JM. Risk for symptomatic hemorrhage of cerebral cavernous malformations during pregnancy. J Neurosurg. 2013;118(1):50–5.
13. Zabramski JM, Wascher TM, Spetzler RF, Johnson B, Golfinos J, Drayer BP, et al. The natural history of familial cavernous malformations: results of an ongoing study. J Neurosurg. 1994;80(3):422–32.
14. Nimjee SM, Powers CJ, Bulsara KR. Review of the literature on de novo formation of cavernous malformations of the central nervous system after radiation therapy. Neurosurg Focus. 2006;21(1):e4.
15. Horne MA, Flemming KD, Su IC, Stapf C, Jeon JP, Li D, et al. Clinical course of untreated cerebral cavernous malformations: a meta-analysis of individual patient data. Lancet Neurol. 2016;15(2):166–73.
16. Josephson CB, Leach JP, Duncan R, Roberts RC, Counsell CE, Al-Shahi Salman R, et al. Seizure risk from cavernous or arteriovenous malformations: prospective population-based study. Neurology. 2011;76(18):1548–54.
17. Gross BA, Lin N, Du R, Day AL. The natural history of intracranial cavernous malformations. Neurosurg Focus. 2011;30(6):E24.
18. Ogilvy CS, Louis DN, Ojemann RG. Intramedullary cavernous angiomas of the spinal cord: clinical presentation, pathological features, and surgical management. Neurosurgery. 1992;31(2):219–29; discussion 29–30.
19. Goyal A, Rinaldo L, Alkhataybeh R, Kerezoudis P, Alvi MA, Flemming KD, et al. Clinical presentation, natural history and outcomes of intramedullary spinal cord cavernous malformations. J Neurol Neurosurg Psychiatry. 2019;90(6):695–703.

20. Kim KM, Chung CK, Huh W, Lee WJ, Park SB, Kim CH, et al. Clinical outcomes of conservative management of spinal cord cavernous angiomas. Acta Neurochir. 2013;155(7):1209–14.
21. Steiger HJ, Turowski B, Hanggi D. Prognostic factors for the outcome of surgical and conservative treatment of symptomatic spinal cord cavernous malformations: a review of a series of 20 patients. Neurosurg Focus. 2010;29(3):E13.
22. Taslimi S, Modabbernia A, Amin-Hanjani S, Barker FG 2nd, Macdonald RL. Natural history of cavernous malformation: systematic review and meta-analysis of 25 studies. Neurology. 2016;86(21):1984–91.
23. Chang EF, Gabriel RA, Potts MB, Garcia PA, Barbaro NM, Lawton MT. Seizure characteristics and control after microsurgical resection of supratentorial cerebral cavernous malformations. Neurosurgery. 2009;65(1):31–7; discussion 7–8.
24. Englot DJ, Han SJ, Lawton MT, Chang EF. Predictors of seizure freedom in the surgical treatment of supratentorial cavernous malformations. J Neurosurg. 2011;115(6):1169–74.
25. Abla AA, Lekovic GP, Turner JD, de Oliveira JG, Porter R, Spetzler RF. Advances in the treatment and outcome of brainstem cavernous malformation surgery: a single-center case series of 300 surgically treated patients. Neurosurgery. 2011;68(2):403–14; discussion 14-5.
26. Baranoski JF, Bajaj A, Przybylowski CJ, Catapano JS, Frisoli FA, Lang MJ, et al. Clip retraction of the tentorium: application of a novel technique for tentorial retraction during supracerebellar transtentorial approaches. J Neurosurg. 2020:1–5.
27. Davies JM, Lawton MT. Improved outcomes for patients with cerebrovascular malformations at high-volume centers: the impact of surgeon and hospital volume in the United States, 2000–2009. J Neurosurg. 2017;127(1):69–80.
28. Lawton MT, Lang MJ. The future of open vascular neurosurgery: perspectives on cavernous malformations, AVMs, and bypasses for complex aneurysms. J Neurosurg. 2019;130(5):1409–25.
29. Mascitelli J, Burkhardt JK, Gandhi S, Lawton MT. Contralateral supracerebellar-infratentorial approach for resection of thalamic cavernous malformations. Oper Neurosurg (Hagerstown). 2018;15(4):404–11.
30. Gross BA, Batjer HH, Awad IA, Bendok BR, Du R. Brainstem cavernous malformations: 1390 surgical cases from the literature. World Neurosurg. 2013;80(1–2):89–93.

Part V
Miscellaneous Conditions and Endovascular Procedures

Chapter 25
Venous Sinus Stenting for Idiopathic Intracranial Hypertension

Abigail P. McCallum and Dale Ding

What Is Idiopathic Intracranial Hypertension?

By general agreement, idiopathic intracranial hypertension (IIH) is a condition of increased intracranial pressure (ICP). IIH most commonly occurs in obese women of childbearing age, and it is characterized by signs and symptoms of elevated ICP in an alert and oriented patient with normal neuroimaging (except those known to be caused by chronically elevated ICP) and normal lumbar puncture (LP) and cerebrospinal fluid (CSF) analysis, with the exception of elevated opening pressure [1].

Symptoms/Diagnosis

IIH is, by nature, a diagnosis of exclusion. It carries a relatively wide variety of symptoms, and thus, differential diagnoses. These differential diagnoses may or may not be effectively excluded depending on the knowledge, experience, and resources of the provider [2]. In 2014, the Neuro-Ophthalmology Research Disease Investigator Consortium (NORDIC) published a multicenter, double-blind, randomized, placebo-controlled study on IIH—the first large prospective study of its kind. The study distinguished between symptoms initially reported by patients on study entry as well as all symptoms reported at study entry, listed by frequency, summarized in Table 25.1. The most common initially reported symptoms were headache, visual loss, headache and visual loss combined, and pulsatile tinnitus.

A. P. McCallum · D. Ding (✉)
Department of Neurological Surgery, University of Louisville School of Medicine, Louisville, KY, USA
e-mail: Abigail.McCallum@uoflhealth.org; Dale.Ding@uoflhealth.org

J. R. Mascitelli, M. J. Binning (eds.), *Introduction to Vascular Neurosurgery*,
https://doi.org/10.1007/978-3-030-88196-2_25

Table 25.1 Frequency of initial symptoms and all symptoms reported at NORDIC study entry

Initial symptoms	Frequency (%)
Headache	35–40
Visual loss	15–20
Headache and visual loss	15–20
Pulsatile tinnitus	10–15
Asymptomatic	5–10
Other	5–10
Diplopia	0–5
All symptoms	
Headache	80–85
Transient visual obscurations	65–70
Back pain	50–55
Pulsatile tinnitus	50–55
Dizziness	50–55
Photophobia	45–50
Neck pain	40–45
Visual loss	30–35
Nocturia	25–30
Cognitive	15–20
Radicular pain	15–20
Diplopia	15–20

Adapted from Wall et al. [1]

Other reported symptoms included transient visual obscurations (TVOs), back pain, dizziness, photophobia, neck pain, nocturia, cognitive problems, and radicular pain [1].

Nomenclature

The constellation of symptoms in IIH can paint a somewhat nebulous clinical picture. Early on, Walter Dandy implied the need for proper nomenclature to describe this condition in his 22-patient case—series published in 1937. Each patient in this series was noted to have signs and symptoms of elevated intracranial pressure without a space-occupying lesion. Patients complained of headache, sometimes nausea, vomiting, diplopia, dizziness, and vision loss. Their symptoms were accompanied by objective findings of bilateral papilledema, sometimes unilateral or bilateral ocular hemorrhages, and elevated ICP on ventricular or LP [3]. This led to the eventual development of diagnostic criteria known as the "Modified Dandy Criteria," which are commonly used today and listed below [4]. Wall and colleagues of the NORDIC IIH Study Group further modified these criteria, amounting to the most common classification schemes currently used.

Modified Dandy Criteria as originally designated by Smith et al. [4]:

1. Signs and symptoms of increased intracranial pressure (headaches, nausea, vomiting, transient obscurations of vision, papilledema).
2. No localizing neurologic signs otherwise, with the single exception being unilateral or bilateral VI nerve paresis.
3. Cerebrospinal fluid which can show increased pressure but with no cytologic or chemical abnormalities otherwise.
4. Normal to small symmetrical ventricles must be demonstrated (originally required ventriculography, but now demonstrated on computed tomography).

Further modified, Modified Dandy Criteria [1]

1. Presence of signs and symptoms of increased ICP.
2. Absence of localizing findings on neurologic examination except those known to occur from increased ICP.
3. Absence of deformity, displacement, or obstruction of the ventricular system and otherwise normal neurodiagnostic studies, except for evidence of increased cerebrospinal fluid pressure (>200 mm water). Abnormal neuroimaging except for empty sella turcica, optic nerve sheath with filled-out CSF spaces, and smooth-walled non-flow-related venous sinus stenosis or collapse should lead to another diagnosis.
4. Awake and alert patient.
5. No other cause of increased ICP present.

The most appropriate nomenclature for the group of disorders which meet or almost meet Modified Dandy Criteria continues to be revisited in the literature, and multiple alternative naming conventions have been proposed [1]. Friedman et al. proposed one such alternative, in which the term "IIH" is reserved for "truly" idiopathic cases of intracranial hypertension, and "pseudotumor cerebri" (PTC) is used to describe the cluster of syndromes for which an identifiable etiology of elevated ICP may be present. In this naming scheme, the authors support the use of the umbrella term PTC syndrome (PTCS). PTCS, by this system, is then subdivided into primary and secondary PTC, with IIH a nested subset of primary PTC, and secondary PTC making up those syndromes with causes such as venous sinus thrombosis, medications, and some medical conditions [5]. This naming scheme avoids the oxymoronic discussion of "secondary causes of IIH," and it attempts to reconcile commonly used historical nomenclature with a modern and evolving understanding of the disease process.

In a letter to the editor titled "The Modified Dandy Criteria for Idiopathic Intracranial Hypertension, No Need to Fix What is not Broken," Michael Wall of the NORDIC study group took exception to this proposed change in nomenclature, implying that "pseudo"-syndromes lack legitimacy in the eyes of researchers and that an unambiguous naming scheme is already provided in the well-accepted Modified Dandy Criteria. The author recommended naming IIH-like conditions with identifiable causes for what they are (e.g., Vitamin A-induced intracranial hypertension). This same letter proposed some additional modifications to the criteria, as listed above, with the intent to publish in their then-upcoming study in 2014 [6].

Fargen and colleagues also proposed the revised terminology "chronic intracranial venous hypertension syndrome" as well as "CIVHS-spectrum disorder" based on their assertion that cerebral venous hypertension is the central cause of the disorder in patients. The "spectrum" was proposed to allow the inclusion of patients who are obviously symptomatic at lower opening-pressures and who respond to pressure-lowering therapies [7].

Pathogenesis

No single unifying theory exists on the pathogenic mechanisms of IIH. The concept of CSF hypersecretion, an early and obvious proposed etiology, was supported in early infusion studies but was not well supported by subsequent hydrodynamics or MRI studies [8–11]. This is despite the fact that one accepted and efficacious treatment for IIH is acetazolamide, a drug which reduces CSF secretion [12]. CSF outflow obstruction may play a role, though there is general agreement that when CSF outflow obstruction is caused by reduced absorption, such as in the setting of subarachnoid hemorrhage or meningitis, overt hydrocephalus is the expected outcome. Lymphatics may play a possible role in CSF outflow in the setting of IIH, but significantly more studies on the physiology of intracranial lymphatics are necessary [5, 8]. Finally, cerebral venous hypertension and venous outflow obstruction, which are inherently connected to the concept of CSF outflow obstruction, are emerging as two increasingly common denominators in studies investigating pathogenetic mechanisms of IIH [8, 13].

Fargen and colleagues take a strong stance on this subject, asserting unequivocally that IIH is caused by intracranial venous hypertension. It is true that a clear connection has been established between cerebral venous pressures and CSF resorption through the arachnoid granulations, with several studies demonstrating a required 3–5-mmHg gradient from the subarachnoid space to venous sinus. Venous hypertension disrupts this gradient, leading to elevated ICP [8, 13]. Disease processes that have the potential to cause venous hypertension are therefore easy to implicate, including obesity and venous sinus stenosis.

Obesity is extremely common in patients with IIH. However, it has been noted that obesity alone, with or without its link to venous hypertension, does not clearly explain IIH because of the uniquely female predominance of the condition which would otherwise be expected to be balanced according to the prevalence of obesity among both male and females populations [5].

Venous sinus stenosis is increasingly regarded as relevant and is discussed in more detail further in this chapter. An understanding of the pathophysiology of venous sinus stenosis in relation to ICP continues to evolve. One current hypothesis suggests that increased ICP leads to external compression of the venous sinuses, leading to venous outflow obstruction and congestion, and therefore a positive feedback loop whereby ICP continues to increase. This hypothesis raises an obvious

question as to whether venous sinus stenosis may be a cause, or simply an effect, of elevated ICP [13].

Other possible pathogenetic mechanisms proposed included the role of hormones, nutritional excess of Vitamin A, and associated disorders such as OSA and PCOS are beyond the scope of discussion of this chapter [8].

Treatments

Treatments for IIH fall into three categories—disease modification, drug treatments, and surgical interventions. In regard to disease modification, weight loss is almost universally agreed upon as beneficial. Weight loss of as little as 3–6% has been reported to be effective [14]. One prospective cohort trial of 25 women showed a significant reduction in ICP, headaches and papilledema with 15% loss of bodyweight [15].

Certain drug treatments have become commonplace and vary in their level of effectiveness. Acetazolamide, a carbonic anhydrase inhibitor that affects ion and water transport across the choroid plexus, reduces CSF secretion. Multiple randomized studies have taken place to assess the efficacy of acetazolamide in treating IIH, most prominently the 2014 IIHTT study [12], a randomized, double-blind, placebo-controlled trial. In this study, 165 patients with IIH and mild visual loss, all following a supervised, low-salt weight-reduction diet and lifestyle modification program were randomized to receive acetazolamide or no acetazolamide. Grade of papilledema, CSF pressure, a "visual quality of life" measure and general quality of life (QOL) measures were significantly improved in the acetazolamide group compared to placebo. However, headache disability and visual acuity scores were not significantly different (though both groups improved), and it was noted that there was increased weight loss in the acetazolamide group, potentially related to increased side effects of the medication such as nausea, vomiting, and loss of taste. Of note the patients were followed for 6 months only [8, 12].

Other medical treatments include topiramate, furosemide, and octreotide. Some promise has been shown in uncontrolled studies for topiramate, an antiepileptic and migraine medication with weak carbonic anhydrase activity [16]. Limited data exist for the use of furosemide, a diuretic, which appears less effective than acetazolamide or topiramate and may cause hypokalemia when used in conjunction with other carbonic anhydrase inhibitors [8, 17]. No blinded or controlled studies exist investigating octreotide, a somatostatin analogue which may, in uncontrolled studies, improve papilledema, headaches, and visual problems in IIH patients [18].

Few well-designed surgical trials exist to support any particular surgical technique over another therefore selection is based on provider preference and local factors.

Optic nerve sheath fenestration is a frequently used intervention for IIH which is indicated when the main symptom is visual disturbance due to papilledema and patients have had poor or refractory response to medical management [17].

CSF diversion, either via ventriculoperitoneal (VP) or lumboperitoneal (LP) shunts, are indicated predominantly in medically refractory patients for which headache is the predominant symptom though both have the potential to improve visual symptoms as well [17]. Little data on difference in outcomes exist between the two types of shunt, though VP shunting appears slightly lower device failure rate as well as a slightly lower complication rate [8, 17].

Venous sinus stenting, an efficient and low complication treatment, is described in further detail in upcoming sections.

What Is Venous Sinus Stenosis?

Studies noting varying degrees of unilateral or bilateral cerebral transverse sinus obstruction or stenosis in IIH patients became increasingly common in the early 2000s; however, the significance of this pathology in relation to IIH as well as a putative pathogenetic relationship was controversial. A possible mechanism was proposed in a 2005 case report describing total resolution of headaches and papilledema at 2 months, in a 28-year-old woman with previously diagnosed IIH and CT venogram demonstrating bilateral cerebral transverse sinus stenosis, after single lumbar puncture. Immediately after lumbar puncture a repeat CT venogram reportedly demonstrated an increase in venous sinus perfusion. From this patient the authors proposed a positive feedback loop in which transient increase in CSF pressure (still of potentially unknown etiology) induces sinus compression, leading to venous outflow obstruction, increase in venous sinus pressure, and consequently further increase in CSF pressure. The authors proposed that the feedback loop persists until either a new equilibrium is reached between ICP and outflow obstruction, or when the limit of deformability of the venous sinus wall is reached. Patients can persist in this new steady state with the myriad of described symptoms. The proposed mechanism provided an explanation of why some patients with IIH appeared to experience long-standing remission with single or serial lumbar punctures, which would not otherwise be expected to be effective [19, 20]. While this explanation is compelling it remains unclear whether venous sinus stenosis results from or causes IIH.

While very few studies exist on venous sinus stenosis in the normal patient population, one relatively large descriptive study of 100 IIH patients provides a significant portion of the information that is currently known about venous sinus stenosis in this population. The study investigated venous sinus pressures in IIH patients as well as those with high suspicion of IIH but with inconsistent opening pressures (e.g., previously documented elevated opening pressure but found to be normal post-angiography during this descriptive study). The group used venous manometry to compare adjacent anatomical and summative gradients in patients with and without “pathological venous outflow obstruction,” measuring at the superior sagittal sinus (SSS), torcula, transverse sinus, sigmoid sinus, internal jugular vein (IJ) below the jugular bulb, and at the superior vena cava–atrial junction. The latter-most

served as the measurement of central venous pressure (CVP). The median total cranial pressure gradient was about 3 mmHg in patients without venous sinus stenosis and 19 mmHg in those with venous sinus stenosis. Median extracranial gradients between the jugular bulb to the right atrio-caval junction were also determined. The intracranial and extracranial gradients were compared using the SSS pressure and the CVP, and an overall pressure gradient of median 4 mmHg was found in patients with normal ICP and no venous stenosis compared to 15 mmHg across all IIH patients [13].

The authors drew several conclusions from these data. They noted firstly that intracranial venous pressures are (unsurprisingly) probably always higher than CVP, including in healthy individuals, but that significant elevation of intracranial venous pressure may be present where stenoses exist. In all the study patients, superior sagittal sinus pressures were highly correlated with opening pressure, and higher OP was highly predictive of pathologic venous sinus pressure gradient, as was the female gender. Interestingly, they did not find BMI to be a predictor of elevated pressure gradient, despite being able to accurately predict patient CVP and SSS pressures based on patient BMI. Regardless, the authors assert that CVP must be the basis on which elevated venous sinus pressures begin to arise and that physiologic venous outflow obstruction, which in this study was almost always at the transverse sinus, may be a significant contributing factor in more than 50% of patient with IIH.

A discussion of the hypothetical role of venous sinus stenosis in IIH would be incomplete without acknowledgment of recent literature which emphasizes the difference between extrinsic and intrinsic types of stenosis. Proponents of usage of this terminology include Patsalides and colleagues, who in several publications have noted the importance of such a distinction [21]. In the setting of venous sinus stenosis, a small subgroup of patients has been demonstrated to have fixed anatomical variations such as a septal band, enlarged arachnoid granulations, chronic thrombosis, trabeculae, or other primary identifiable causes of stenosis [22]. However, since it is clear that not all patients with this intrinsic venous sinus stenosis possess signs or symptoms of elevated ICP or papilledema, it has been suggested that a "second hit" is required for patients with intrinsic venous sinus stenosis to develop IIH [22]. The writers of this paper note in several publications that the majority of IIH patients with stenosis possess extrinsic stenosis, which is proposed to occur via the previously mentioned positive feedback loop which putatively takes mild elevations in ICP and turns them into significant problems.

Venous Sinus Stenting in IIH

Support treatment through venous sinus stenting of both intrinsic and extrinsic venous sinus stenosis in IIH patients continues to increase, though multiple groups continue to hypothesize that stenting of intrinsic stenoses should lead to a greater reduction in ICP than extrinsic stenosis. One study of 13 medically refractory IIH

patients noted that the greatest reductions in ICP occurred in four out of the five patients in the study whose venous sinus stenosis was intrinsic [22, 23]. While this trend was notable, it was not statistically significant. Of note, a larger prospective follow-up study by the same group with 50 patients also did not show a statistically significant difference in ICP reduction between patients with intrinsic vs. extrinsic venous sinus stenosis [24].

These data seem to suggest that either intrinsic or extrinsic stenosis in the setting of IIH may be appropriately treated with venous sinus stenting given the correct circumstances; however, the question is raised as to what degree of stenosis should qualify a patient for venous sinus stenting.

West and colleagues sought to more clearly establish the link between angiographic stenosis and physiologic venous sinus outflow obstruction in patients with IIH. They investigated the use of noninvasive venous imaging, angiography, and venography for detecting a clinically significant pressure gradient associated with venous sinus stenosis. In this study a significant venous pressure gradient was defined as at least 8 mmHg. A gradient of 6 or 7 mmHg was accepted in a few select cases in the study. The study noted some important findings. Firstly, MRV/CTV in this study had a calculated specificity of 1, but a sensitivity of 0.42 only. More than 75% of the patients in the study with negative MRV possessed clinically significant transverse sinus pressure gradients on subsequent angiography. Additionally, during catheter angiography a stenosis of 30–35% was determined to be the "optimal" threshold for sensitivity and specificity in detecting symptomatic venous outflow obstruction, which the authors noted to be a relatively low degree of stenosis compared to other disease processes in the arterial system such as carotid stenosis. The study also demonstrated a correlation between percent stenosis and pressure gradient magnitude with a 3.5-mmHg increase in pressure gradient per 10% increase in stenosis [25]. While the study possessed several limitations including small sample size, risk of measurement bias, and a somewhat arbitrarily selected pressure gradient cutoff of "sometimes" 6–7 mmHg and 8 mmHg strictly speaking, it was valuable in bringing into question the diagnostic utility of noninvasive venous imaging in assisting in ruling out physiologically significant venous outflow obstruction. The wide variability in findings on this subject demonstrate only that percent cutoffs to determine either candidacy for catheter angiography or candidacy for stenting remains largely a matter of institutional preference.

Patient Selection

Fargen et al. published a 2018 literature review outlining eight systematic reviews or meta-analyses and 29 published patient series and provided recommendations for the selection and treatment of IIH patients using venous sinus stenting. The review emphasized the lack of randomized trials and prospective studies available; therefore, an alternate grading scale was developed for the level of evidence on which

recommendations are based. These recommendations rely heavily on expert opinion from supporting available studies [26]. Recommendations qualified as strong if there were multiple available prospective and retrospective case series, moderate if there were several retrospective studies and/or support of expert opinion, and weak if evidence was limited to expert opinion only. Recommendations included discussion of patient selection based on noninvasive imaging, medically refractory symptoms, intracranial pressure and BMI, and also considered recommendations for retreatment of patients with refractory symptoms [26].

In selecting patients, a moderate score was given in recommending venography in patients with ICPs (most commonly determined via LP) greater than 25 cmH2O, and for those who had medically refractory symptoms or were intolerant to attempted medical treatment. Strong recommendations were, unsurprisingly, provided that catheter venography be performed to assess candidacy for stenting, and a moderate recommendation was made that a pressure gradient of 8 mmHg or higher should be present for patients to undergo stenting [26]. It should be noted however that this number was arbitrarily selected by *Ahmed* et al, who set a precedent thence followed by other groups [27, 28].

Of note, the study made a moderate recommendation that it is reasonable to use noninvasive venous imaging as a screening tool to determine candidacy for VSS but qualified based on weak evidence that it is also reasonable to offer diagnostic venography to IIH patients without noninvasive imaging or with negative noninvasive imaging. These recommendations appear to have been made due to the relatively high number of studies which report the use of noninvasive imaging-based selection criteria to determine which patients undergo diagnostic catheter angiography or venography. Multiple of these studies required MRV or CTV for all included patients, and several studies designated percent stenosis cutoffs when deciding to offer diagnostic venography/angiography. While the use of noninvasive imaging techniques appears to be common practice in the currently available literature, a smaller body of studies has pointed out that transverse sinus hypoplasia and stenosis are found with relatively high frequency in the normal population, with unilateral stenosis making up 33% of "healthy" individuals and bilateral stenoses making up approximately 5% [26, 28].

Furthermore, as previously discussed, CTV and MRV have been shown to have mediocre to poor specificity and in certain cases extremely poor sensitivity for predicting symptomatic venous outflow obstruction. In a study of medically refractory IIH patients who underwent catheter angiography regardless of noninvasive venography results, MRV/CTV had a sensitivity of 0.42, and a negative predictive value of 22% for detecting significant venous sinus pressure gradients on manometry [25]. As a result, the utility noninvasive venography is called into significant question. Recommendations supporting the use of noninvasive imaging for screening may be the result of momentum in earlier studies, and habitual practice of experts in a changing environment. It is not the practice of this institution to rely on noninvasive imaging as a screening tool for patients with IIH due to the aforementioned reasons.

Evidence for Venous Sinus Stenting

Transtenotic Gradient

There is little question from the available literature that venous sinus stenting reduces the transtenotic gradient in the vast majority of patients on post-stent venography, with a mean reduction from 20.4 mmHg to 2.4 mmHg following stenting reported in a systematic review and meta-analysis of 241 patients [23]. The response to stenting based on specific types of stenosis remains to be seen. Some authors theorize that secondary deterioration and adjacent stent stenosis are less likely in patients with intrinsic stenosis which may be a more primary cause of elevated ICP compared to patients with extrinsic stenosis [22, 23].

ICP

In this same review, of the 69 patients who underwent post-stent LP, mean ICP reduced from 36.4 to 20.4 cm H2O and all but a single patient (who subsequently was found to have new adjacent stenosis) experience some reduction in ICP. In a prospective pilot study of 10 patients with medically refractory IIH and venous sinus stenosis with a trans-stenosis venous pressure gradient, Liu et al. demonstrated a significant immediate reduction in ICP via ICP monitors implanted at the time of stenting. Patients experienced a mean reduction in ICP of 17 mmHg immediately after stenting, with an additional overnight mean reduction of 8 mmHg [29]. Patsalides and colleagues evaluated opening pressure 3 months before and 3 months after VSS in 50 patients with IIH and a transtenotic gradient of ≥8. They demonstrated a statistically significant reduction in ICP at 3 months post VSS of 45%. Of note, these patients had a concurrent statistically significant decrease in acetazolamide usage and an increase in BMI [24].

Symptoms

Many studies do not clearly delineate which symptoms improve or the manner in which they improve post-stenting. The language used to describe similar symptoms is variable and makes for an unclear picture. Multiple systematic reviews and meta-analyses have been performed in recent years to evaluate the efficacy of VSS with regards to symptomatic improvement. Cumulatively these studies report 78–83% improvement in headache, 87–97% improvement in papilledema, and 95% improvement in tinnitus, with simultaneously low complication rates of 1.6–2.9% major and 1.6–4.4% minor [30–36].

Visual Outcomes

In a non-randomized prospective study by Dinkin et al., ten medically refractory or medically intolerant patients, or those presenting with fulminant vision loss, underwent unilateral venous stenting for a transtenotic gradient of >8 mmHg. This study placed emphasis on the analysis of visual fields and reported mostly observational findings. Of the 25 eyes evaluated, 12 improved in acuity, 4 worsened, and 9 remained stable. Color vision testing improved. Twenty of 25 eyes improved with regard to Humphrey visual fields and mean improvement of +5.34 dB was statistically significant and robust. Likewise, 20 of 24 eyes had papilledema with statistically significant improvement post-stenting. Of the patients who entered the study due to fulminant papilledema and vision loss, all 6 eyes had visual field improvement, none developed optic atrophy. In terms of other factors, 11 of 13 patients had improved headaches, with resolution in four. All with pulse synchronous tinnitus on presentation had resolution had complete resolution of pulse-synchronous tinnitus and all patients with transient visual obscurations improved, majority with total resolution. All the patients also reported improved quality of life [23]. A review and meta-analysis by the same group noted that only a minority of studies offer quantitative data regarding visual acuity, with 58.4% of the 166 eyes with acuity loss exhibiting improvement post-stenting, however, specifics were limited otherwise. Only three studies analyzed visual fields, one of which is summarized above. Since visual field loss contributes significantly to disability in IIH patients, more data on this subject are needed.

Adverse Events

Typical adverse events associated with any standard angiographic procedure, such as contrast allergy or retroperitoneal hematoma are not discussed in detail in this chapter. Headache is the most common side effect of VSS, reported in approximately 30–50% of patients, typically on the side ipsilateral to the side of the stent, typically lasting several days, and thought to be related to dural stretch [37]. The most important adverse events of VSS related directly to stenting include in-stent stenosis, and stent-adjacent stenosis (SAS). In-stent stenosis caused by stent thrombosis is extremely rare with the increasing use of dual antiplatelet therapy, but potentially disastrous. In-stent stenosis (none thrombotic) was reported in 3.4% of patients in a study of 185 patients. SAS is significantly more common than in-stent stenosis, with an incidence ranging from 6 to 18% of patients in various studies [31, 37, 38]. One study evaluating midterm transverse sinus stent patency in 104 patients revealed a SAS in 10% of patients and noted that stent size over 6 mm was a significant independent predictor of the development of SAS [39]. Two solutions to this problem as employed at this institution include stenting to the torcula and

under-sizing the stent to the extent possible. One study of 185 patients reported an overall complication rate of 5.4%, with 1.6% major complications such as subdural hematoma, intracerebral hemorrhage, or subarachnoid hemorrhage (3 patients), all of whom required surgical or procedural intervention as a result (craniotomy or EVD), and minor complications in 3.8% including transient hearing loss, syncopal episode, retroperitoneal hematoma and UTI [31].

Procedural Considerations

For patients with IIH deemed eligible for screening for venous sinus stenosis, it is the practice of this institution that patients first undergo diagnostic cerebral angiography with venous manometry under conscious sedation. Arterial and venous access is gained at the start of the case and a diagnostic arteriogram is obtained in a standard fashion to rule out dural AV-fistula or other vascular abnormality and evaluate dominance of the venous sinuses. Venous manometry is performed with recording of the mean venous pressures (MVPs) at the superior sagittal sinus, torcula, transverse sinus, sigmoid sinus, jugular bulb, and internal jugular vein as previously described [40]. While some institutions perform venous manometry and stenting under general anesthesia in the same sitting, a recent retrospective review of a prospectively maintained database of patients undergoing angiographic evaluation of venous sinus stenosis demonstrated that MVPs and transtenotic gradients were significantly lower in the same patients under general anesthesia compared to under conscious sedation [40].

Patients with gradients ≥8 mmHg under conscious sedation return for venous sinus stenting after premedication with aspirin and clopidogrel. An example is provided in Fig. 25.1. Aspirin reaction unit (ARU) and P2Y12 reaction unit (PRU)

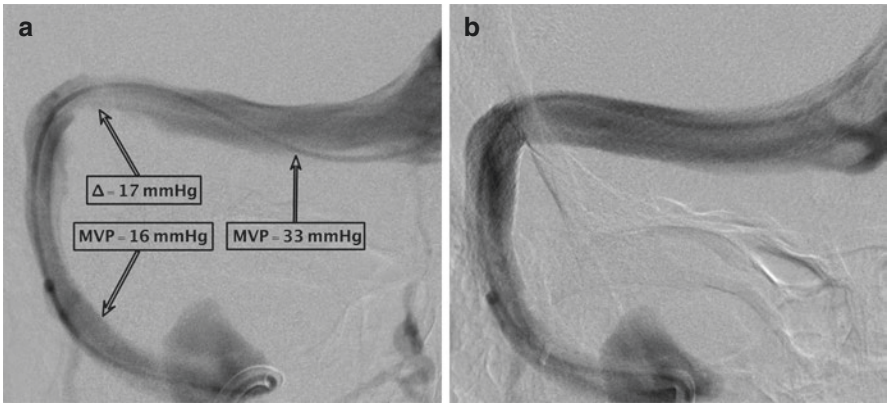

Fig. 25.1 (**a**) Pre-procedural venous sinus manometry indicating venous sinus gradient at the transverse–sigmoid junction. Manometry and stenting are performed at different visits due to differences found in pressure gradients under general anesthesia vs. awake. (**b**) Angiogram post stent placement

levels are obtained on arrival for the procedure. Patients not considered therapeutic according to the laboratory cutoffs receive an additional load of antiplatelet agents. Patients are placed under general anesthesia and received 100 units/kg of heparin after venous access is obtained. It is not the routine practice of this institution to obtain both arterial and venous access during the stenting procedure unless internal jugular access difficulties are anticipated based on prior angiography. Stenting is performed without pressure measurements due to previously mentioned alterations in MVPs and gradients under general anesthesia [40]. Antiplatelet agents are continued for 3 months after stenting. A follow-up diagnostic angiography of the ipsilateral internal carotid artery and external carotid artery with venous manometry under conscious sedation is performed at 3 months post-stenting. If follow-up imaging is satisfactory, both antiplatelet agents are stopped. Patients also undergo another diagnostic angiogram at one-year post-stenting.

Stent selection Stents currently used for this procedure are designed for other anatomical regions. Commonly used devices include those originally intended for the extracranial carotid arteries, the femoral and iliac arteries, and the biliary ducts. There are no studies comparing the type of stent with clinical outcomes. Therefore, stent selection is based largely on appropriate sizing for adequate wall opposition, and provider preference. As previously mentioned, stents greater than 6 mm in diameter may increase the risk of SAS. Number of stents depends on the available lengths and provider preference. It is the practice of this institution to stent from torcula to mid-sigmoid in an effort to prevent stent-adjacent stenosis. However, a greater number of high-radial force stents could in theory contribute to increased severity of post-procedural headaches due to dural stretching and consideration should be made for this when educating patients. A clinical trial is currently recruiting investigating the safety and efficacy of a stent specifically developed for VSS in patients with IIH [41].

Stent laterality Studies suggest that unilateral stenting on the side of the largest initial trans-stenotic gradient in patients with bilateral transverse sinus stenosis results in immediate gradient improvement bilaterally in the majority of patients, as well as a reduction in ICP, improved CSF dynamics, and durable improvement in signs and symptoms of IIH including headache and papilledema [42]. As a result, it is the practice of this institution to perform unilateral stenting first, even in the setting of bilateral transverse sinus stenosis. If patients fail to improve following unilateral stent placement, contralateral stenting is considered at a later date after repeat venous manometry.

Antiplatelet Agents

There is considerable variation regarding the type and duration of antiplatelet therapy in the setting of patients undergoing venous sinus stenting. Practices are well summarized in a systematic review and meta-analysis performed by Dinkin et al. and range from life-long aspirin with or without lifelong clopidogrel, clopidogrel and

aspirin limited duration of (1–3 months), use of aspirin or clopidogrel alone, and use of warfarin in the perioperative period [22]. It is the practice of this institution to administer dual antiplatelet therapy (DAPT), substituting prasugrel 10 mg daily for clopidogrel nonresponders, and dipyridamole 75 mg three times daily for aspirin nonresponders, from 1 week prior to 3 months post-VSS. On the morning of the procedure, medication dosing is adjusted according to morning lab results, and the procedure is not delayed for nonresponders. A follow-up venogram with pressure gradients is performed at 3 months and DAPT use is reassessed at that time. If follow-up venography shows stent patency and no stent-adjacent or in-stent stenosis, DAPT is halted entirely. A long-term venogram is also obtained in 1 year, to confirm lack of stent thrombosis, stenosis, and/or recurrence of venous sinus stenosis or gradients.

Intravascular Ultrasound

This tool may help improve venous stenting procedures by improving diagnostic accuracy, treatment planning, and stent placement. Intravascular ultrasound provides 360° views of the lumen of the venous sinus which can improve the accuracy of measurements regarding length and degree of stenosis as well as whether the stenosis is intrinsic or extrinsic [22, 43]. In one study, IVUS was used to assist in identifying luminal stenosis characteristics and assisting precise venous stent placement. Authors noted that it was possible to evaluate the sinus intraluminal wall and, for example, inspect for immediate adjacent-stent sinus wall collapse, informing them on whether to stent further or in certain circumstances use longer stents [43]. More studies would be required to demonstrate the utility of IVUS in VSS.

Future Directions

Stent Improvement

Currently used devices are designed with higher radial force to allow the opposition of expansion of stiffer, thicker walled, pathological vessels [22]. Likewise, these devices require larger catheters for delivery. As previously mentioned, a clinical trial is currently underway investigating a stent specifically designed for VSS in the setting of IIH [41].

Randomized Controlled Trials

Currently lacking are randomized controlled trials comparing operative procedures to endovascular neurosurgery for the treatment of IIH, though one, called OPEN-UP is currently recruiting patients [44]. Additionally, no RCTs yet exist investigating the choice of antiplatelets/anticoagulants, and duration of use, in this predominantly young population.

References

1. Wall M, Kupersmith MJ, Kieburtz KD, Corbett JJ, Feldon SE, Friedman DI, et al. The idiopathic intracranial hypertension treatment trial: clinical profile at baseline. JAMA Neurol. 2014;71(6):693–701.
2. Wall M. Idiopathic intracranial hypertension. Neurol Clin. 2010;28(3):593–617.
3. Dandy WE. Intracranial pressure without brain tumor. Ann Surg. 1937;106(4):492–513.
4. Smith JL. Whence pseudotumor cerebri? J Clin Neuroophthalmol. 1985;5(1):55–6.
5. Friedman DI, Liu GT, Digre KB. Revised diagnostic criteria for the pseudotumor cerebri syndrome in adults and children. Neurology. 2013;81(13):1159–65.
6. Wall M. The modified Dandy criteria for idiopathic intracranial hypertension, no need to fix what is not broken. In: Friedman DI, editor. Disputes & debates: rapid online correspondence ed. Neurology: Wolters Kluwer; 2014.
7. Coffman SA, Singh J, Wolfe S, Fargen KM. Unexpected occlusion of the contralateral transverse sinus after stenting for idiopathic intracranial hypertension. Interv Neuroradiol. 2018;24(6):718–21.
8. Markey KA, Mollan SP, Jensen RH, Sinclair AJ. Understanding idiopathic intracranial hypertension: mechanisms, management, and future directions. Lancet Neurol. 2016;15(1):78–91.
9. Donaldson JO. Cerebrospinal fluid hypersecretion in pseudotumor cerebri. Trans Am Neurol Assoc. 1979;104:196–8.
10. Malm J, Kristensen B, Markgren P, Ekstedt J. CSF hydrodynamics in idiopathic intracranial hypertension: a long-term study. Neurology. 1992;42(4):851–8.
11. Eisenberg HM, McComb JG, Lorenzo AV. Cerebrospinal fluid overproduction and hydrocephalus associated with choroid plexus papilloma. J Neurosurg. 1974;40(3):381–5.
12. Committee NIIHSGW, Wall M, McDermott MP, Kieburtz KD, Corbett JJ, Feldon SE, et al. Effect of acetazolamide on visual function in patients with idiopathic intracranial hypertension and mild visual loss: the idiopathic intracranial hypertension treatment trial. JAMA. 2014;311(16):1641–51.
13. Fargen KM. Idiopathic intracranial hypertension is not idiopathic: proposal for a new nomenclature and patient classification. J NeuroInterv Surg. 2020;12(2):110.
14. Skau M, Sander B, Milea D, Jensen R. Disease activity in idiopathic intracranial hypertension: a 3-month follow-up study. J Neurol. 2011;258(2):277–83.
15. Sinclair AJ, Burdon MA, Nightingale PG, Ball AK, Good P, Matthews TD, et al. Low energy diet and intracranial pressure in women with idiopathic intracranial hypertension: prospective cohort study. BMJ. 2010;341:c2701.
16. Celebisoy N, Gökçay F, Sirin H, Akyürekli O. Treatment of idiopathic intracranial hypertension: topiramate vs acetazolamide, an open-label study. Acta Neurol Scand. 2007;116(5):322–7.
17. Portelli M, Papageorgiou PN. An update on idiopathic intracranial hypertension. Acta Neurochir. 2017;159(3):491–9.
18. Panagopoulos GN, Deftereos SN, Tagaris GA, Gryllia M, Kounadi T, Karamani O, et al. Octreotide: a therapeutic option for idiopathic intracranial hypertension. Neurol Neurophysiol Neurosci. 2007:1.
19. De Simone R, Marano E, Fiorillo C, Briganti F, Di Salle F, Volpe A, et al. Sudden re-opening of collapsed transverse sinuses and longstanding clinical remission after a single lumbar puncture in a case of idiopathic intracranial hypertension. Pathogenetic implications. Neurol Sci. 2005;25(6):342–4.
20. Matloob SA, Toma AK, Thompson SD, Gan CL, Robertson F, Thorne L, et al. Effect of venous stenting on intracranial pressure in idiopathic intracranial hypertension. Acta Neurochir. 2017;159(8):1429–37.
21. Sundararajan SH, Ramos AD, Kishore V, Michael M, Doustaly R, DeRusso F, et al. Dural venous sinus stenosis: why distinguishing intrinsic-versus-extrinsic stenosis matters. AJNR Am J Neuroradiol. 2021;42(2):288–96.

22. Dinkin MJ, Patsalides A. Venous sinus stenting for idiopathic intracranial hypertension: where are we now? Neurol Clin. 2017;35(1):59–81.
23. Dinkin MJ, Patsalides A. Venous sinus stenting in idiopathic intracranial hypertension: results of a prospective trial. J Neuroophthalmol. 2017;37(2):113–21.
24. Patsalides A, Oliveira C, Wilcox J, Brown K, Grover K, Gobin YP, et al. Venous sinus stenting lowers the intracranial pressure in patients with idiopathic intracranial hypertension. J Neurointerv Surg. 2019;11(2):175–8.
25. West JL, Greeneway GP, Garner RM, Aschenbrenner CA, Singh J, Wolfe SQ, et al. Correlation between angiographic stenosis and physiologic venous sinus outflow obstruction in idiopathic intracranial hypertension. J NeuroInterv Surg. 2019;11(1):90.
26. Fargen KM, Liu K, Garner RM, Greeneway GP, Wolfe SQ, Crowley RW. Recommendations for the selection and treatment of patients with idiopathic intracranial hypertension for venous sinus stenting. J Neurointerv Surg. 2018;10(12):1203–8.
27. Ahmed RM, Wilkinson M, Parker GD, Thurtell MJ, Macdonald J, McCluskey PJ, et al. Transverse sinus stenting for idiopathic intracranial hypertension: a review of 52 patients and of model predictions. AJNR Am J Neuroradiol. 2011;32(8):1408–14.
28. Durst CR, Ornan DA, Reardon MA, Mehndiratta P, Mukherjee S, Starke RM, et al. Prevalence of dural venous sinus stenosis and hypoplasia in a generalized population. J Neurointerv Surg. 2016;8(11):1173–7.
29. Liu KC, Starke RM, Durst CR, Wang TR, Ding D, Crowley RW, et al. Venous sinus stenting for reduction of intracranial pressure in IIH: a prospective pilot study. J Neurosurg. 2017;127(5):1126–33.
30. Puffer RC, Mustafa W, Lanzino G. Venous sinus stenting for idiopathic intracranial hypertension: a review of the literature. J Neurointerv Surg. 2013;5(5):483–6.
31. Starke RM, Wang T, Ding D, Durst CR, Crowley RW, Chalouhi N, et al. Endovascular treatment of venous sinus stenosis in idiopathic intracranial hypertension: complications, neurological outcomes, and radiographic results. Sci World J. 2015;2015:140408.
32. Teleb MS, Cziep ME, Lazzaro MA, Gheith A, Asif K, Remler B, et al. Idiopathic intracranial hypertension. A systematic analysis of transverse sinus stenting. Interv Neurol. 2013;2(3):132–43.
33. Satti SR, Leishangthem L, Chaudry MI. Meta-analysis of CSF diversion procedures and Dural venous sinus stenting in the setting of medically refractory idiopathic intracranial hypertension. AJNR Am J Neuroradiol. 2015;36(10):1899–904.
34. McDougall CM, Ban VS, Beecher J, Pride L, Welch BG. Fifty shades of gradients: does the pressure gradient in venous sinus stenting for idiopathic intracranial hypertension matter? A systematic review. J Neurosurg. 2018;130(3):999–1005.
35. Arac A, Lee M, Steinberg GK, Marcellus M, Marks MP. Efficacy of endovascular stenting in dural venous sinus stenosis for the treatment of idiopathic intracranial hypertension. Neurosurg Focus. 2009;27(5):E14.
36. Lai LT, Danesh-Meyer HV, Kaye AH. Visual outcomes and headache following interventions for idiopathic intracranial hypertension. J Clin Neurosci. 2014;21(10):1670–8.
37. Daggubati LC, Liu KC. Intracranial venous sinus stenting: a review of idiopathic intracranial hypertension and expanding indications. Cureus. 2019;11(2):e4008.
38. Raper D, Buell TJ, Ding D, Chen CJ, Starke RM, Liu KC. Pattern of pressure gradient alterations after venous sinus stenting for idiopathic intracranial hypertension predicts stent-adjacent stenosis: a proposed classification system. J Neurointerv Surg. 2018;10(4):391–5.
39. El Mekabaty A, Pearl MS, Moghekar A, Gailloud P. Mid-term assessment of transverse sinus stent patency in 104 patients treated for intracranial hypertension secondary to dural sinus stenosis. J Neurointerv Surg. 2021;13(2):182–6.
40. Raper DMS, Buell TJ, Chen CJ, Ding D, Starke RM, Liu KC. Intracranial venous pressures under conscious sedation and general anesthesia. J Neurointerv Surg. 2017;9(10):986–9.

41. Venous Sinus Stenting With the River Stent in IIH ClinicalTrials.Gov: U.S. National Library of Mediccine; [updated January 28, 2021; cited 2021 May 3]. Available from: https://clinicaltrials.gov/ct2/show/NCT03556085.
42. Larson A, Rinaldo L, Chen JJ, Cutsforth-Gregory J, Theiler AR, Brinjikji W. Reductions in bilateral transverse sinus pressure gradients with unilateral transverse venous sinus stenting for idiopathic intracranial hypertension. J NeuroInterv Surg. 2021;13(2):187–90: neurintsurg-2020-016170.
43. Yan F, Rajah G, Ding Y, Hua Y, Zhang H, Jiao L. et al. Safety and efficacy of intravascular ultrasound as an adjunct to stenting for cerebral venous sinus stenosis-induced idiopathic intracranial hypertension: a pilot study. J Neurosurg. 2019;132(3):749–54. https://doi.org/10.3171/2018.11.JNS181885. PMID:30835685.
44. Operative procedures vs. endovascular neurosurgery for untreated pseudotumor trial (OPEN-UP) ClinicalTrials.gov: U.S. National Library of Medicine; 2015 [updated 24 July 2020; cited 2021. Clinical Trial]. Available from: https://clinicaltrials.gov/ct2/show/NCT02513914?term=OPEN-UP&draw=2&rank=1.

Chapter 26
Middle Meningeal Embolization for Subdural Hematoma

Alina Mohanty, Justin R. Mascitelli, and Peter Kan

Background

Chronic subdural hematomas (cSDHs) are one of the most common neurosurgical conditions requiring intervention. With the current incidence estimated to be 13.5/100,000 in the general population and as high as 58.1/100,000 in the elderly population, future incidence is expected to rise as the population ages and as anticoagulation and antiplatelet use increase [1–3]. Chronic subdural hematomas develop most commonly after shearing of the bridging veins, usually in the cases of trauma, though they can also develop without a precipitating event. The development and increase in the size of the subdural hematoma are thought to be due to a combination of inflammatory response, angiogenesis, and hemolysis. One such mechanism of rebleeding is the overproduction and oversecretion of tissue plasminogen activator resulting in hyperactive fibrinolysis and clotting cascade dysfunction; as a result, there is increased rebleeding from the capillaries and an enlargement of the hematoma [4, 5]. The formation of a neo-membrane that encapsulates the cSDH, thought to stem from a nonspecific inflammatory response in meningeal cells, contributes to the decreased reabsorption of the hematoma [4]. Neovascularization also contributes to the development and extension of the chronic subdural hematoma; high

A. Mohanty
Department of Neurosurgery, Baylor College of Medicine, Houston, TX, USA
e-mail: Alina.Mohanty@bcm.edu

J. R. Mascitelli
Department of Neurosurgery, University of Texas Health Science Center at San Antonio, San Antonio, TX, USA

P. Kan (✉)
Department of Neurosurgery, University of Texas Medical Branch, Galveston, TX, USA
e-mail: ptkan@utmb.edu

J. R. Mascitelli, M. J. Binning (eds.), *Introduction to Vascular Neurosurgery*,
https://doi.org/10.1007/978-3-030-88196-2_26

concentrations of vascular endothelial growth factor (VEGF) and placental growth factor (PIGF) have been found in hematoma fluid from patients with cSDH [6, 7]. This pathologic neoangiogenesis creates frail and immature microcapillaries that cause microhemorrhages that recurrently bleed, promote, and sustain chronic subdural hematomas.

Presentation

Chronic subdural hematoma is radiographically present as a crescent-shaped collection of fluid in the subdural space, with volume/extent of hematoma better approximated on axial, sagittal, and coronal views. Though the fluid is typically hypodense, the chronic subdural hematoma can also comprise fluid with hyperdense or heterogenous density. Computed tomography (CT) is typically the initial choice of imaging, though magnetic resonance imaging (MRI) can be used to better characterize internal anatomy as well as the size of the subdural hematoma [4]. Though radiographically present, not all chronic subdural hematomas present with symptoms. These asymptomatic chronic subdural hematomas typically are smaller in size with a more benign course and can be managed conservatively: medications studied include corticosteroids, antifibrinolytics, statins, and angiotensin-converting enzyme inhibitors, although none is the standard of care at this time [8]. Symptomatic manifestation of chronic subdural hematomas is often the result of increased intracranial pressure and presents in a wide variety of symptoms including, but not limited to, headaches, changes in mental status, seizures, nausea and vomiting, weakness, sensory disturbances, stroke, or coma [9]. Symptomatic chronic subdural hematomas and those of a larger size, such as those with >10 mm of greatest thickness or those with >5 mm of midline shift, are managed with surgery [2]. Traditional surgery options for hematoma evacuation include burr-hole craniostomy with drainage, twist drill craniostomy with drainage, and craniotomy.

Being male, alcoholic, elderly, and on antiplatelet or anticoagulation medications are risk factors for developing chronic subdural hematoma [9]. Despite both medical and surgical management, recurrence rates of cSDH with conventional techniques of surgical evacuation were recorded to be as high as 37% [10].

Middle Meningeal Artery Embolization

The first recorded case of successful middle meningeal artery (MMA) embolization for treatment of cSDH was by Mandai et al. in 2000. They described a patient with liver cirrhosis and coagulopathy who had chronic subdural hematoma recurrence refractory to the repeated evacuation of the hematoma. Previous studies had shown

arteries originating from branches of the MMA entering the outer membranes of chronic subdural hematomas [11, 12]. Since super-selective angiography on this patient showed similar abnormal microcapillaries on the outer membrane, the authors decided to embolize the MMA to decrease blood supply to the membrane of the chronic subdural hematoma and therefore, prevent or delay recurrence. Immediately after the embolization, CT imaging revealed contrast material in the body of the subdural hematoma. Additionally, complete disappearance of hematoma by 7 months was noted by CT scan with the patient experiencing no permanent neurological deficits [13].

Subsequent case series using MMA embolization for cSDH were published after Mandai's case report that showed no further recurrences of cSDH after the embolization procedure [14–19]. Additionally, retrospective comparison in three trials over this time period showed MMA embolization to be superior to conventional therapy with regard to hematoma recurrence [20–22]. A meta-analysis in 2018 by Srivatsan et al. of these three trials demonstrated that hematoma recurrence rate was significantly decreased in the embolization group compared with conventional treatment group (2.1% vs. 27.7%; odds ratio = 0.087; 95% confidence interval, 0.026–0.292; $P < 0.001$; $I^2 = 0\%$), with similar surgical complication rates between groups (2.1% vs. 4.4%) [23]. Since that meta-analysis was published, further case series with greater sample sizes have been published demonstrating the efficacy of MMA embolization for cSDH. A series by Kan et al. across 15 centers showed a 97.4% success rate in 154 embolizations with 6.5% of patients requiring further intervention for continued hematoma expansion [24]. Link et al. had a 91% success rate in 60 cases without any procedural complications [25]. A summary of select published series and a summary of published meta-analyses on MMA embolization for cSDH are given in Tables 26.1 and 26.2, respectively.

Anatomy

The middle meningeal artery supplies greater than two-thirds of the dura. The MMA classically originates from the first part, the mandibular segment, of the internal maxillary, a terminal branch of the external carotid artery, though anatomic variants of the MMA include origins from portions of the internal carotid artery or even the basilar artery [38, 39]. Extracranially, the MMA passes through the roots of the auriculotemporal nerve before entering the cranium through the foramen spinosum. The MMA gives off two basal branches that supply the dura of the temporal fossa – the petrosal and cavernous branches – before dividing into the anterior and posterior divisions [38, 39]. Possible anastomoses include those with the ascending pharyngeal artery, branches of the ophthalmic artery such as the recurrent meningeal artery of the ophthalmic artery and the dural branches of the ophthalmic artery (Fig. 26.1), the posterior meningeal artery, and the mastoid branches of the occipital artery [38].

Table 26.1 Select published series using MMA embolization for treatment of cSDH

Study	Patients	Embolizations	Mean age	Embolization method	Outcomes	Study population
Mino [16]	4	4/4 successfully embolized	73	Gelatin sponge and Guglielmi detachable coils	No recurrences	Repeated recurrences of cSDH or progressive re-accumulation of the hematoma in a short period of time after burr-hole surgery
Matsumoto [20]	4	4/4 successfully embolized	65.8	*N*-butyl-2-cyanoacrylate (NBCA) or platinum coils	No recurrences	Refractory cSDH with 2 or more recurrences
Hashimoto [18]	5	5/5 successfully embolized	71.4	*N*-butyl-2-cyanoacrylate (NBCA), polyvinyl alcohol particles	No recurrences	Refractory cSDH either after or before burr-hole irrigation: 3/5 (60%) In patients with risk for recurrence: 2/5 (40%)
Tempaku [15]	5	5/5 successfully embolized	83	Polyvinyl alcohol particles, transfemoral or transbrachial approach	No recurrences	Recurrent cSDH after burr-hole surgery with irrigation and drainage
Ishihara [14]	7	7/7 successfully embolized	–	*N*-butyl-2-cyanoacrylate (NBCA)	No recurrences	Third recurrence of cSDH or second recurrence with risk factors
Waqas [26]	8	8/8 successfully embolized	63.6	Onyx	No recurrences, complete hematoma resolution in 3/8 (37.5%) and >50% resolution in 5/8 (62.5%) patients	**Primary treatment: 6/8 (75%)**, Recurrent cSDH: 2/8 (25%)
Saito [27]	8	8/8 successfully embolized	79	*N*-butyl-2-cyanoacrylate (NBCA), transfemoral or transbrachial approach	7/8 (87.5%) no recurrences	Two or more ipsilateral recurrences of cSDH within 3 months and cases with high risks of recurrence in which could not discontinue antithrombotic or anticoagulant therapy, 7/8 (87.5%) received embolization with concomitant burr-hole drainage surgery

Okuma [28]	17	17/17 successfully embolized	76.4	N-butyl-2-cyanoacrylate (NBCA) or trisacryl gelatin microspheres, followed by burr hole and irrigation	No recurrences	Harbored ≥2 risk factors for intractable cSDH
Yajima [29]	18	18/18 successfully embolized	78.7	N-butyl-2-cyanoacrylate (NBCA), transfemoral approach	No recurrences	Most treated initially by burr-hole irrigation/drainage who developed third recurrence or had risk factors for recurrence of cSDH
Nakagawa [30]	20	28/28 successfully embolized	78.3	N-butyl-2-cyanoacrylate (NBCA), followed by burr-hole irrigation and drainage surgery	No recurrences	Persistent ipsilateral CSDH recurrence after two previous burr-hole irrigation and drainage surgeries
Ng [31]	21	22/25 successfully embolized	77.4	Polyvinyl alcohol particles, transfemoral approach	21/22 (95.5%) no recurrences, hematoma volume resorption (HVR) higher in the surgical treatment and embolization group (mean difference 17.5 mL, $p = 0.015$)	Embolization procedure as an adjuvant treatment to surgical treatment in those who required surgery because of one or more symptoms attributable to cSDH, excluded if past history of cSDH surgery
Kim [22]	20	26/26 successfully embolized	72.4	Polyvinyl alcohol particles, transfemoral approach	25/26 (96.2%) no recurrences	After burr-hole and drainage surgery in high-risk surgical candidates with recurrence of cSDH

(continued)

Table 26.1 (continued)

Study	Patients	Embolizations	Mean age	Embolization method	Outcomes	Study population
Catapano [32]	35	40/41 successfully embolized	68	Onyx, microspheres, N-butyl cyanoacrylate (NBCA), mostly transradial approach	26/41 (63.4%) with complete cSDH resolution overall: 22/29 (75.8%) with complete resolution after embolization of both anterior and posterior branches, 4/12 (33.3%) complete resolution after embolization of either anterior or posterior branch. 1/41 (2.4%) treatment failure	Previous failed surgery: 9/35 (25.7%), failed conservative management 6/35 (17.1%), adjunct embolization along with surgery 2/35 (5.7%)
Rajah [33]	46	44/46 successfully embolized	71.7	Onyx, transradial approach	38/44 (86.4%) with complete or partial cSDH resolution. 5/44 (11.4%) needed rescue surgery	Recurrent cSDH: 5/46 (10.9%), adjunct procedure within 24 hours of burr-hole evacuation: 4/46 (8.7%), **primary treatment: 37/46 (80.4%)**
Link [25]	49	60/60 successfully embolized	69	Polyvinyl alcohol particles, transfemoral approach	41/45 (91.1%) had improvement of symptoms and reduction in size. 4/45 (8.9%) needed further surgery	Recurrent cSDH after surgical evacuation: 8/60 (13.3%), prophylaxis after surgical evacuation: 10/60 (16.7%), **previously untreated cSDH: 42/60 (70.0%)**
Ban [21]	72	72/72 successfully embolized	69.3	Polyvinyl alcohol particles	71/72 (98.6%) no recurrences. 1/72 (1.4%) needed rescue surgery	**Asymptomatic patients: 27/72 (37.5%)**, symptomatic patients with adjunctive hematoma evacuation: 45/72 (62.5%)

Shotar [34]	89	91/104 successfully embolized	74	Triacryl gelatin microspheres with or without coils, N-butyl cyanoacrylate (NBCA), or coiling, mostly transfemoral approach	85/89 (95.5%) no recurrences	After burr-hole surgery in those with recurrent cSDH: 22/89 (24.7%). After burr-hole surgery with an independent recurrence risk factor: 85/89 (95.5%)
Joyce [35]	121: 70 patients between ages of 65–79, 51 patients with ages ≥80	148/151 successfully embolized (3 failed cases out of 87 cases between ages of 65–79)	72.3: mean age of patients aged 65–79, 85.2: mean age of patients ≥80 years	Embosphere Microsphere particles + coils, polyvinyl alcohol particles, Onyx, N-butyl-2-cyanoacrylate (NBCA), mostly transfemoral approach	cSDH stability or improvement was observed in 73/80 (91.3%) of those aged 65–79 and 57/58 (98.3%) of those aged ≥80. 4/87 (4.6%) needed further surgery in the 65–79 group	As rescue treatment after prior evacuation (craniotomy/burr hole): 32/87 (36.8%) between ages of 65–79, 21/64 (32.8%) in those ≥80 years; as prophylactic treatment: 13/87 (14.9%) between ages of 65–79, 4/64 (6.3%) in those ≥80 years
Kan [24]	138	150/154 successfully embolized	69.8	Particles and coils, particles, liquid embolics, mostly transfemoral approach	144/154 (93.5%) no recurrences, 109/154 (70.8%) of patients with at least 50% reduction in cSDH thickness, 9/135 (6.5%) needed further surgery	Prior evacuation surgery (craniotomy/burr holes): 46/138 (33.3%), prior subdural hematoma: 66/138 (47.8%). **Primary treatment: 92/138 (66.7%)**

Abbreviations: *cSDH* chronic subdural hematoma

Table 26.2 Select published meta-analyses using MMA embolization for treatment of cSDH

Study and year	Groups	Number of studies included	Patients	Recurrence rates	Complications
Haldrup 2020 [36]	MMA embolization for primary cSDH versus MMA embolization for recurrent cSDH	18	191	Recurrence rate for patients treated with MMA embolization for recurrent cSDH: 2.4%, 95% CI (0.5%; 11.0%), vs recurrence rate for patients treated with MMA embolization for primary cSDH: 4.1%, 95% CI (1.4%; 11.4%). Odds Ratio for recurrence for primary versus recurrent cSDH patients: 1.7 (95% CI 0.3; 11.1)	–
Jumah 2020 [37]	MMA embolization versus with conventional treatments for refractory or cSDH	11	177	MMA embolization had a 26% ($p < 0.001$, 95% CI 21%–31%, $I^2 = 0$) lower risk of hematoma recurrence (2.7% in the MMAE group)	Need for surgical rescue was 20% less ($p < 0.001$, 95% CI = 12%–27%, $I^2 = 12.4$) and complications were 3.6% less ($p = 0.008$, 95% CI 1%–6%, $I^2 = 0$) in embolization group compared to conventional treatment group
Srivatsan 2018 [23]	MMA embolization versus conventional surgery	3	96	Recurrence rate in the embolization group: 2.1% versus 27.7% in conventional treatment group (odds ratio = 0.087; 95% confidence interval, 0.026–0.292; $P < 0.001$; $I^2 = 0\%$)	Surgical complication rate in embolization group: 2.1% versus 4.4% in conventional treatment group (odds ratio = 0.563; 95% confidence interval, 0.107–2.96; $P = 0.497$; $I^2 = 27.5\%$)

Abbreviations: *MMA* middle meningeal artery, *cSDH* chronic subdural hematoma

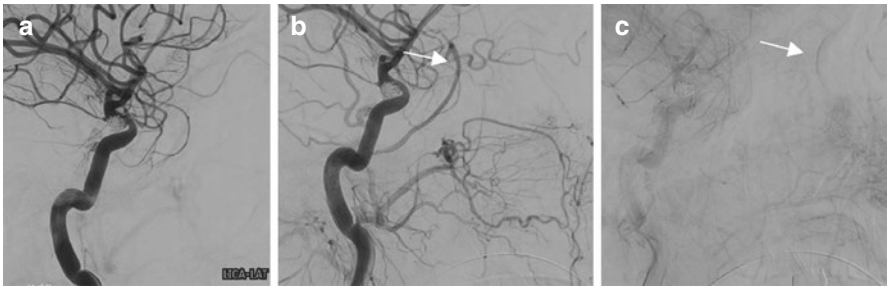

Fig. 26.1 (**a**) Absent ophthalmic artery and choroidal blush after internal carotid artery injection in one patient (**b**) with the meningo-opthalmic variant, visualized with the ophthalmic artery arising off of the middle meningeal artery and the corresponding (**c**) choroidal blush

Procedure

The procedure can be performed with little to no sedation and local anesthesia rather than general anesthesia if the patient is amenable. Common femoral or radial artery access is obtained and a guide catheter is placed into the proximal external carotid or distal common carotid artery. Prior to proceeding, it is important to confirm that the ophthalmic artery arises from the internal carotid artery. Next, a microcatheter is advanced into the MMA for super-selective angiography. Patients with chronic refractory subdural hematoma can have "cotton-wool" staining on MMA angiography; this is thought to represent the sinusoids of the MMA vasculature penetrating into the dura mater, with the "cotton-wool" appearance possibly being due to pathologic neovascularization (Fig. 26.2) [18, 24, 28, 40]. Collaterals such as the lacrimal and petrous branches must be identified at this time with super-selective angiography prior to MMA embolization so that the catheter tip can be placed distal to the artery prior to embolization. We recommend embolization distal to the bifurcation separately in the frontal and parietal branches. Embolic agents commonly used for MMA embolization include particles, Onyx, N-butyl cyanoacrylate (NBCA), other liquid embolics (e.g., SQUID), and coils. Larger particles (250–500 microns) have the advantage of not penetrating unseen anastomoses; liquid embolics not only have the advantage of distal penetration but also have the danger of penetrating unseen anastomoses, potentially leading to stroke or cranial nerves injury; coils can be used for safe proximal MMA occlusion if dangerous anastomoses are seen, making particle or liquid embolics unsuitable for embolization. Embolization is continued until anterograde flow stasis is observed with no contrast opacification in the frontal and parietal branches. Common carotid angiography is then repeated to ensure patency of all intracranial vessels. Initial postoperative CT imaging can be obtained after 24 hours to check for new hemorrhages. CT imaging to check the status of the cSDH should be obtained after 3 months since studies have shown that resolution of the chronic subdural hematoma happens over time and most often occurs 4–6 weeks after MMA embolization (Fig. 26.3) [21, 24].

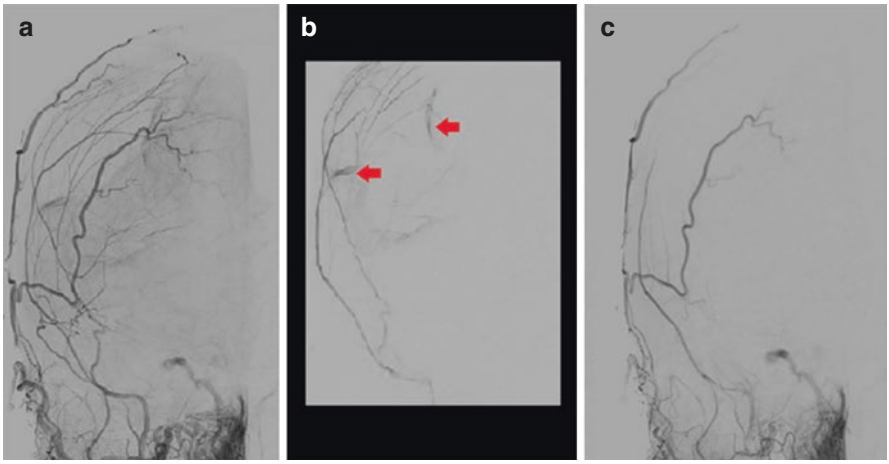

Fig. 26.2 (**a**) Preoperative anteroposterior right ECA angiogram, and (**b**) anteroposterior MMA angiogram showing cotton-staining from the MMA into the subdural collection (arrows). (**c**) post-MMA-embolization anteroposterior ECA angiogram demonstrating resolution of the staining around the occluded MMA. *Abbreviations:* ECA external carotid artery, MMA middle meningeal artery

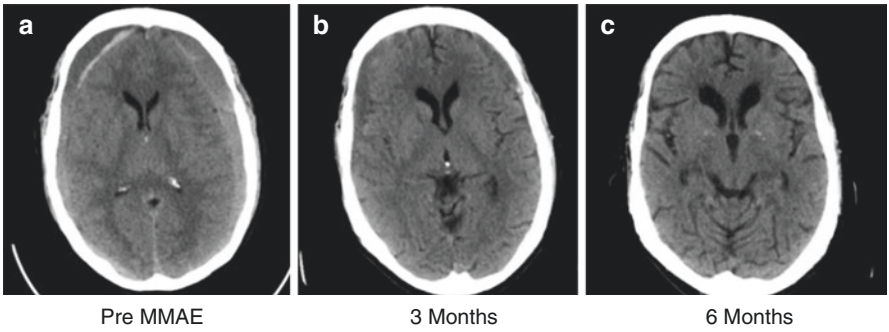

Fig. 26.3 CT scans of a patient who underwent bilateral MMA embolizations. (**a**) Preoperative CT scan showed bilateral CSDHs. (**b**) CT scan 3 months after embolization showed significant reduction in size of CSDHs bilaterally. (**c**) CT scan 6 months after embolization showed complete resolution of bilateral CSDHs. *Abbreviations:* MMA middle meningeal artery, CSDH chronic subdural hematoma

Risks, Complications, and Contraindications

As mentioned earlier, two of the greatest periprocedural risks include embolization of dangerous collaterals such as the petrosal branch and lacrimal branch. The petrosal branch supplies the vasa vasorum of cranial nerve VII as the nerve travels through the petrous bone, and therefore embolization of this branch can lead to facial paralysis. Similarly, branches of the MMA such as the meningo-lacrimal

branch can form collaterals with branches of the ophthalmic artery. Embolization of any branches that form collaterals with the ophthalmic artery can result in blindness. Consequently, after identifying these branches on initial superselective angiography, the microcatheter tip should be placed distally to these branches. In the case that the catheter tip is unable to be distally placed, either discontinuation of the embolization or coil embolization of the proximal trunk should be considered. The series by Kan et al. of 154 embolizations found that 8.5% of their cases had such collaterals, of which unintentional embolizations were avoided in all by keeping the microcatheter tip distal to the collateral [24]. Other complications include stroke, hemorrhage, access site complications such as hematoma and arterial injury, as well as recurrence of the subdural hematoma. In the same series by Kan et al. as above, the complication rate for ischemic stroke was 0.6% and the rate of hemorrhagic stroke was 1.7% [24]. The other case series by Link et al. with 60 cases had no procedural complications [25].

Contraindications to middle meningeal embolization include poor vascular access to the MMA and contradictions to angiography, such as severe renal failure. Other relative contraindications include pregnancy, significant allergic reaction to contrast material, and coagulopathy.

Future Directions

Embolization of the middle meningeal artery for chronic subdural hematoma is a new but promising alternative or adjunct to conventional evacuation surgeries. One major benefit of embolization is the ability to avoid general anesthesia and its associated complications, especially in the elderly population with multiple comorbidities in whom chronic subdural hematoma often occurs. Additionally, it is less invasive and might avoid some of the morbidity associated with more invasive evacuation procedures such as craniotomy. Most importantly, MMA embolization provides a method to treat refractory cases of chronic subdural hematomas that have often failed multiple treatment attempts with conventional methods. There are multiple ongoing randomized controlled trials that will determine in which situations and patient populations MMA embolization treatment will be superior or comparable to conventional methods. For example, Embolization of the Middle Meningeal Artery With ONYX™ Liquid Embolic System for Subacute and Chronic Subdural Hematoma (EMBOLISE) will compare embolization with Onyx and adjunctive burr-hole surgery to conventional burr-hole surgery alone in patients with severe presentation of cSDH requiring surgery and will compare MMA embolization to observation only in patients with a less severe presentation [41]. Another trial, the SQUID Trial for the Embolization of the Middle Meningeal Artery for Treatment of Chronic Subdural Hematoma (STEM), will compare MMA embolization with SQUID liquid embolic along with burr-hole drainage and standard medical therapy to burr-hole drainage and standard medical therapy [42]. Whether MMA embolization replaces traditional methods such as burr-hole drainage as a first-line treatment,

whether it is used in conjunction with those traditional treatments, or whether it is used solely for refractory cases of chronic subdural hematoma is yet to be seen.

References

1. Link TW, Schwarz JT, Paine SM, Kamel H, Knopman J. Middle meningeal artery embolization for recurrent chronic subdural hematoma: a case series. World Neurosurg. 2018;118:e570–4.
2. Fiorella D, Arthur AS. Middle meningeal artery embolization for the management of chronic subdural hematoma. J Neurointerv Surg. 2019;11:912–5.
3. Mehta V, Harward SC, Sankey EW, Nayar G, Codd PJ. Evidence based diagnosis and management of chronic subdural hematoma: a review of the literature. J Clin Neurosci. 2018;50:7–15.
4. Sahyouni R, Goshtasbi K, Mahmoodi A, Tran DK, Chen JW. Chronic subdural hematoma: a historical and clinical perspective. World Neurosurg. 2017;108:948–53.
5. Katano H, Kamiya K, Mase M, Tanikawa M, Yamada K. Tissue plasminogen activator in chronic subdural hematomas as a predictor of recurrence. J Neurosurg. 2006;104:79–84.
6. Weigel R, Hohenstein A, Schilling L. Vascular endothelial growth factor concentration in chronic subdural hematoma fluid is related to computed tomography appearance and exudation rate. J Neurotrauma. 2014;31:670–3.
7. Kalamatianos T, Stavrinou LC, Koutsarnakis C, Psachoulia C, Sakas DE, Stranjalis G. PlGF and sVEGFR-1 in chronic subdural hematoma: implications for hematoma development. J Neurosurg. 2013;118:353–7.
8. Roh D, Reznik M, Claassen J. Chronic subdural medical management. Neurosurg Clin N Am. 2017;28:211–7.
9. Yang W, Huang J. Chronic subdural hematoma: epidemiology and natural history. Neurosurg Clin N Am. 2017;28:205–10.
10. Desai VR, Scranton RA, Britz GW. Management of recurrent subdural hematomas. Neurosurg Clin N Am. 2017;28:279–86.
11. Tanaka T, Fujimoto S, Saitoh K, Satoh S, Nagamatsu K, Midorikawa H. Superselective angiographic findings of ipsilateral middle meningeal artery of chronic subdural hematoma in adults. No Shinkei Geka. 1998;26:339–47.
12. Tanaka T, Fujimoto S, Saito K, Kaimori M. Histological study of operated cases of chronic subdural hematoma in adults: relationship between dura mater and outer membrane. No Shinkei Geka. 1997;25:701–5.
13. Mandai S, Sakurai M, Matsumoto Y. Middle meningeal artery embolization for refractory chronic subdural hematoma. Case report J Neurosurg. 2000;93:686–8.
14. Ishihara H, Ishihara S, Kohyama S, Yamane F, Ogawa M, Sato A, Matsutani M. Experience in endovascular treatment of recurrent chronic subdural hematoma. Interv Neuroradiol. 2007;13 Suppl 1:141–4.
15. Tempaku A, Yamauchi S, Ikeda H, Tsubota N, Furukawa H, Maeda D, Kondo K, Nishio A. Usefulness of interventional embolization of the middle meningeal artery for recurrent chronic subdural hematoma: five cases and a review of the literature. Interv Neuroradiol. 2015;21:366–71.
16. Mino M, Nishimura S, Hori E, Kohama M, Yonezawa S, Midorikawa H, Kaimori M, Tanaka T, Nishijima M. Efficacy of middle meningeal artery embolization in the treatment of refractory chronic subdural hematoma. Surg Neurol Int. 2010;1:78.
17. Takahashi K, Muraoka K, Sugiura T, Maeda Y, Mandai S, Gohda Y, Kawauchi M, Matsumoto Y. Middle meningeal artery embolization for refractory chronic subdural hematoma: 3 case reports. No Shinkei Geka. 2002;30:535–9.
18. Hashimoto T, Ohashi T, Watanabe D, et al. Usefulness of embolization of the middle meningeal artery for refractory chronic subdural hematomas. Surg Neurol Int. 2013;4:104.

19. Hirai S, Ono J, Odaki M, Serizawa T, Nagano O. Embolization of the middle meningeal artery for refractory chronic subdural haematoma. Usefulness for patients under anticoagulant therapy. Interv Neuroradiol. 2004;10 Suppl 2:101–4.
20. Matsumoto H, Hanayama H, Okada T, Sakurai Y, Minami H, Masuda A, Tominaga S, Miyaji K, Yamaura I, Yoshida Y. Which surgical procedure is effective for refractory chronic subdural hematoma? Analysis of our surgical procedures and literature review. J Clin Neurosci. 2018;49:40–7.
21. Ban SP, Hwang G, Byoun HS, Kim T, Lee SU, Bang JS, Han JH, Kim C-Y, Kwon O-K, Oh CW. Middle meningeal artery embolization for chronic subdural hematoma. Radiology. 2018;286:992–9.
22. Kim E. Embolization therapy for refractory hemorrhage in patients with chronic subdural hematomas. World Neurosurg. 2017;101:520–7.
23. Srivatsan A, Mohanty A, Nascimento FA, Hafeez MU, Srinivasan VM, Thomas A, Chen SR, Johnson JN, Kan P. Middle meningeal artery embolization for chronic subdural hematoma: meta-analysis and systematic review. World Neurosurg. 2019;122:613–9.
24. Kan P, Maragkos GA, Srivatsan A, et al. Middle meningeal artery embolization for chronic subdural hematoma: a multi-center experience of 154 consecutive embolizations. Neurosurgery. 2020. https://doi.org/10.1093/neuros/nyaa379.
25. Link TW, Boddu S, Paine SM, Kamel H, Knopman J. Middle meningeal artery embolization for chronic subdural hematoma: a series of 60 cases. Neurosurgery. 2019;85:801–7.
26. Waqas M, Vakhari K, Weimer PV, Hashmi E, Davies JM, Siddiqui AH. Safety and effectiveness of embolization for chronic subdural hematoma: systematic review and case series. World Neurosurg. 2019;126:228–36.
27. Saito H, Tanaka M, Hadeishi H. Angiogenesis in the septum and inner membrane of refractory chronic subdural hematomas: consideration of findings after middle meningeal artery embolization with low-concentration n-butyl-2-cyanoacrylate. NMC Case Rep J. 2019;6:105–10.
28. Okuma Y, Hirotsune N, Sato Y, Tanabe T, Muraoka K, Nishino S. Midterm follow-up of patients with middle meningeal artery embolization in intractable chronic subdural hematoma. World Neurosurg. 2019;126:e671–8.
29. Yajima H, Kanaya H, Ogino M, Ueki K, Kim P. Middle meningeal artery embolization for chronic subdural hematoma with high risk of recurrence: a single institution experience. Clin Neurol Neurosurg. 2020;197:106097.
30. Nakagawa I, Park HS, Kotsugi M, et al. Enhanced hematoma membrane on DynaCT images during middle meningeal artery embolization for persistently recurrent chronic subdural hematoma. World Neurosurg. 2019;126:e473–9.
31. Ng S, Derraz I, Boetto J, Dargazanli C, Poulen G, Gascou G, Lefevre P-H, Molinari N, Lonjon N, Costalat V. Middle meningeal artery embolization as an adjuvant treatment to surgery for symptomatic chronic subdural hematoma: a pilot study assessing hematoma volume resorption. J Neurointerv Surg. 2020;12:695–9.
32. Catapano JS, Ducruet AF, Nguyen CL, Baranoski JF, Cole TS, Majmundar N, Wilkinson DA, Fredrickson VL, Cavalcanti DD, Albuquerque FC. Middle meningeal artery embolization for chronic subdural hematoma: an institutional technical analysis. J Neurointerv Surg. 2020. https://doi.org/10.1136/neurintsurg-2020-016552.
33. Rajah GB, Waqas M, Dossani RH, et al. Transradial middle meningeal artery embolization for chronic subdural hematoma using Onyx: case series. J Neurointerv Surg. 2020;12:1214–8.
34. Shotar E, Meyblum L, Premat K, et al. Middle meningeal artery embolization reduces the post-operative recurrence rate of at-risk chronic subdural hematoma. J Neurointerv Surg. 2020;12:1209–13.
35. Joyce E, Bounajem MT, Scoville J, et al. Middle meningeal artery embolization treatment of nonacute subdural hematomas in the elderly: a multiinstitutional experience of 151 cases. Neurosurg Focus. 2020;49:E5.
36. Haldrup M, Ketharanathan B, Debrabant B, Schwartz OS, Mikkelsen R, Fugleholm K, Poulsen FR, Jensen TSR, Thaarup LV, Bergholt B. Embolization of the middle meningeal

artery in patients with chronic subdural hematoma-a systematic review and meta-analysis. Acta Neurochir. 2020;162:777–84.
37. Jumah F, Osama M, Islim AI, Jumah A, Patra DP, Kosty J, Narayan V, Nanda A, Gupta G, Dossani RH. Efficacy and safety of middle meningeal artery embolization in the management of refractory or chronic subdural hematomas: a systematic review and meta-analysis. Acta Neurochir. 2020;162:499–507.
38. Bonasia S, Smajda S, Ciccio G, Robert T. Middle meningeal artery: anatomy and variations. AJNR Am J Neuroradiol. 2020;41:1777–85.
39. Seker A, Martins C, Rhoton AL. Meningeal anatomy. In: Pamir MN, Black PM, Fahlbusch R (eds) (2010) Meningiomas: a comprehensive text. Saunders/Elsevier, Philadelphia, p. 11–51.
40. Link TW, Rapoport BI, Paine SM, Kamel H, Knopman J. Middle meningeal artery embolization for chronic subdural hematoma: endovascular technique and radiographic findings. Interv Neuroradiol. 2018;24:455–62.
41. National Institutes of Health. Embolization of the middle meningeal artery with ONYX™ liquid embolic system for subacute and chronic subdural hematoma. 2020. https://ClinicalTrials.gov/show/NCT04402632. Accessed 28 Nov 2020.
42. National Institutes of Health. The SQUID trial for the embolization of the middle meningeal artery for treatment of chronic subdural hematoma (STEM). 2020. https://ClinicalTrials.gov/show/NCT04410146. Accessed 28 Nov 2020.

Chapter 27
Embolization of Head, Neck, and Spinal Tumors

Fazeel M. Siddiqui, Gary Rajah, Joseph J. Gemmete, Neeraj Chaudhary, Augusto Elias, and Aditya S. Pandey

Introduction

Management of head, neck, and spine tumors can be complex and requires a multidisciplinary approach. Vascular tumors can be treated with preoperative embolization followed by resection. The main goals of tumor embolization are to keep the operative field dry by controlling surgically inaccessible blood vessels, shortening the operative procedural time and the duration of general anesthesia, decreasing operative blood loss and transfusion requirements, and making the overall procedure safer for the patient [1, 2]. Palliative embolization is also an option for surgically unresectable tumors by reducing tumor size and clinical symptoms as well as controlling bleeding from highly vascular nasopharyngeal tumors and advanced head and neck cancers [3–5]. Intra-arterial delivery of chemotherapeutic agents is

F. M. Siddiqui
Interventional Neurology, Metro Health- University of Michigan Health, Grand Rapids, MI, USA

G. Rajah
Interventional Neurosurgery, Munson Health, Traverse City, MI, USA
e-mail: grajah@mhc.net

J. J. Gemmete · N. Chaudhary
Department of Radiology, University of Michigan, Ann Arbor, MI, USA
e-mail: gemmete@med.umich.edu; neerajc@med.umich.edu

A. Elias
Interventional Neuroradiology, Metro Health- University of Michigan Health, Grand Rapids, MI, USA
e-mail: Augusto.elias@metrogr.org

A. S. Pandey (✉)
Department of Neurosurgery, University of Michigan, Ann Arbor, MI, USA
e-mail: adityap@med.umich.edu

J. R. Mascitelli, M. J. Binning (eds.), *Introduction to Vascular Neurosurgery*,
https://doi.org/10.1007/978-3-030-88196-2_27

another evolving indication that has been studied extensively in head and neck cancers as well as pediatric retinoblastomas. The purpose of this chapter is to review the endovascular techniques, and their application for the treatment of intracranial and extracranial tumors.

Pathophysiology

Tumor vascularity is derived from angiogenesis or the formation of new blood vessels supplying the tumor bed. The extensive vascularity of tumors involves the hypertrophy of parent arteries and the development of small new arteries and capillaries from the parent arteries that supply the region of the tumor origin. As the tumor invades the surrounding tissue, it also recruits secondary arterial supply from arteries supplying the invaded tissue [3]. Angiogenesis is dependent on expression of the vascular permeability factor/vascular endothelial growth factor (VEGF) in tumor tissue. Significant elevation of VEGF gene expression is associated with highly vascular tumors and promotes the permeability of tumor vessels [6, 7]. Tumor embolization is particularly useful in tumors with high vascularity. The primary arterial supply of tumors is treated by embolization of the arterial pedicles and capillary bed of the tumor with the goal of partial or complete angiographic devascularization. If the tumor has secondary vascularization from recruitment of intracranial inaccessible vessels, trans-tumor embolization via external carotid feeders can be performed utilizing embolizing agents that can deeply penetrate the tumor tissue. Direct tumor embolization via a direct percutaneous approach is also an attractive option. Sudden massive devascularization can lead to necrosis and edema with worsening of mass effect, tumoral hemorrhage, and worsening of symptoms [8]. Hence, careful selection of the embolic material and timing of operative resection is the key for successful outcome.

Principles of Cerebral Angiography for Head, Neck, and Spine Tumors

The principles of cerebral angiography for head and neck tumors are based on detailed knowledge of the arterial anatomy of the head and neck. Based on initial cross-sectional CT/MRI imaging, the expected arterial supply to the tumor can be determined. However, a complete cerebral angiography including bilateral angiograms of both external carotid arteries, internal carotid arteries, thyrocervical trunks, and vertebral arteries should be obtained to identify the arterial supply to the tumor as well as collaterals prior to embolization. Sometimes, super-selective catheterization of feeding arteries is necessary for determination of dangerous anastomoses and arterial-venous shunts [8].

Although most tumors amenable to endovascular embolization have arterial supply from the branches of the external carotid artery, many dangerous anastomoses exist between the extracranial and intracranial circulation. During tumor embolization, the collateral milieu can change, and dangerous anastomoses may appear which were not originally present. Knowledge of these arterial anastomoses is especially important to prevent cranial nerve injury, blindness, and acute ischemic stroke. Furthermore, the use of repeated control angiography during the embolization to identify these anastomoses is key to performing a safe embolization [8]. Table 27.1 describes the common intracranial and extracranial anastomosis and cranial nerves at risk.

Tumors can also create arterial-venous shunts with no normal capillary bed. Embolization of these shunts should be performed with coils or large particles to

Table 27.1 Major intracranial and extracranial anastomosis and cranial nerves at risk [8, 55–57]

Major extracranial artery	Anastomosing branch	Major intracranial artery	Anastomosing branch	Cranial nerves at risk
Superior thyroid artery	NA	NA	NA	X, superior laryngeal nerve br. (superior laryngeal a.)
Lingual artery	NA	NA	NA	Extracranial segment of XII
Ascending pharyngeal artery	NMT	Cavernous ICA VA	MHT Vertebral segmental br.	IV (via MHT), V, VI (jugular br. and via MHT), VII, VIII, IX (jugular br.), X (jugular br.), XI (jugular br. and musculospinal br.), XII (hypoglossal br.)
	Inferior tympanic a.	Petrous ICA	Caroticotympanic a.	
	Superior pharyngeal a.	Cavernous ICA Petrous ICA Lacerum ICA	ILT Mandibular br. Carotid canal br.	
	Muscular br.	VA	Vertebral segmental br.	
Posterior auricular artery	Stylomastoid br.[a]	VA	Posterior meningeal a.	VII (stylomastoid br.)
Occipital artery	Muscular br.	VA	Vertebral segmental br. PICA can originate from occipital a. in rare cases.	VII (stylomastoid br.)
	Stylomastoid br.[a]	VA	Posterior meningeal a.	
Facial artery	Angular a.	ICA	OA (dorsal nasal a.)	Rare association

(continued)

Table 27.1 (continued)

Major extracranial artery	Anastomosing branch	Major intracranial artery	Anastomosing branch	Cranial nerves at risk
Internal maxillary artery	Middle meningeal a. (cavernous br.)	ICA	ILT (tentorial br.) MHT	III (via ILT), V (artery of foramen rotundum), VI (via ILT) V (cavernous br. Of MMA), VI, VII (petrous br. Of MMA)
	Middle meningeal a. (sphenoidal br.)	ICA	OA	
	Middle meningeal a. (frontal br.)	ICA	OA (anterior falcine artery)	
	Accessory meningeal a. (artery of foramen ovale)	ICA	ILT (posteromedial br.)	
	Vidian a.	Petrous ICA	Vidian a.	
	Anterior deep temporal a.	ICA	OA (distal lacrimal a.)	
	Artery of foramen rotundum	ICA	ILT (anterolateral br.)	
	Infraorbital a.	ICA	OA (dorsal nasal a.)	
	Sphenoplatetine a.	ICA	OA (anterior and posterior ethmoidal br.)	
	Greater palatine a.	ICA	OA (posterior ethmoidal br.)	
Superficial temporal artery	Frontal br.	ICA	OA (supraorbital br.)	Rare association

NMT neuromeningeal trunk, *MHT* meningohypophyseal trunk, *ILT* inferiolateral trunk, *ICA* internal carotid artery, *VA* vertebral artery, *NA* not applicable, *OA* ophthalmic artery, *MMA* middle meningeal artery, *PICA* posterior inferior cerebellar artery

[a]Stylomastoid branch can arise from either the posterior auricular artery or occipital artery

prevent nontarget embolization into the pulmonary system, or worse, into the arterial system if a right-to-left shunt is present.

For spinal tumors, complete spinal angiography should be performed with careful attention to the origin of radiculo-medullary vessels prior to embolization.

Embolization Techniques

Many embolization techniques exist today for tumor devascularization prior to surgical resection or as an adjunctive treatment for palliation of clinical symptoms. The three major embolization techniques include trans-arterial, direct percutaneous puncture, and/or a combination of both. The mainstays of current endovascular

embolic agents include liquid embolic agents such as Onyx (Medtronic), Phil (MicroVention), NBCA glue (Cordis Neurovascular), and Squid (Balt). Coil embolization as well as particulate embolic agents includes polyvinyl alcohol (PVA), Embospheres, and gelfoam. Table 27.2 describes the characteristics and specific advantages and disadvantages of commonly used embolic agents. The operator's comfort with each embolic agent as well as tumor location and catheter position determine which agent is appropriate for the individual case. Direct percutaneous puncture of the tumor with subsequent embolization with liquid embolic agents remains another option for tumors, inaccessible from an intra-arterial approach.

There are two different paradigms for traditional tumor embolization. The first is devascularization via deep liquid embolic penetration into the tumor, which typically requires distal catheter placement or travel of the liquid embolic agent. The two liquid embolic agents, widely available are glue and Onyx. The polymerization time of glue measured in time elapsed to flow arrest can be modified by the addition of glacial acid [9]. Onyx, on the other hand, comes in two concentrations (Onyx 18 and Onyx 34), with Onyx 18, being less viscous, travels farther [10].

The second treatment paradigm is the occlusion of all the arterial pedicles to soften the tumor and prevent large volume blood loss during surgical resection. If there are deep arterial pedicles that are difficult to reach during surgery, these should be targeted with embolization and are most useful for the surgeons performing the resection.

Lastly, the location of the arterial tumor pedicles will determine which embolic agents can be utilized. Typically, particles that are 300 microns in size or larger will need a microcatheter with at least an inner diameter of 0.021 inches to prevent blockage in the hub, and thus distal intracranial lesions maybe better suited to liquid embolic agents with microcatheters of inner diameter of 0.017 inches or smaller. There is more control and visualization with an Onyx or Squid injection when compared to particulate material or glue. Apollo microcatheters (Medtronic) are detachable tip catheters that can be useful if the tip of the microcatheter has been glued in place. Gentle, long duration backward traction on the detachable catheter will allow the tip to break free. Dual lumen balloons (Scepter XC, Microvention) can also provide some help with forward penetration, while minimizing the reflux of liquid embolic agents such as Onyx.

Embolization of head or neck lesions can either be performed with the patient awake or under general anesthesia. Performing the procedure awake allows for accurate assessment of the patient's neurological status; however, motion from patient movement can make visualization of dangerous anastomoses and the embolic material more difficult. With general anesthesia, the patient's neurological exam is lost, and the operator is dependent on provocative testing with Amytal and lidocaine for determining dangerous anastomoses; however, visualization of these small arterial connections on the angiogram is easier given the lack of motion [11]. Injection of dimethyl sulfoxide (DMSO), a solvent for Onyx, in an awake patient can cause discomfort resulting in motion artifact and making visualization of the embolic agent difficult. This can be alleviated with injection of intra-arterial preservative-free lidocaine. Furthermore, during surgical resection, Onyx can spark

Table 27.2 Characteristics of commonly used embolic agents

Embolic agent	Composition	Solvent/ carrier	Catheter compatibility	Tumor types	Advantages and disadvantages	Permanence
Onyx (18, 34)	Polyvinyl ethanol copolymer mixed tantalum powder	DMSO	Marathon, Echelon, Apollo, Headway Duo, Scepter XC balloon microcatheter	Head, neck, and spine tumors	Fine control Deeper penetration with Onyx 18 Visibility DMSO toxicity Proximal reflux Operative fire hazard Need for shaker	Yes
NBCA glue (customizable concentrations)	N-Butyl-Cyanoacrylate	Dextrose 5%	Headway Duo, Marathon, Magic microcatheters	Head, neck, and spine tumors	Deeper penetration Custom concentration Average visualization Catheter gluing	Yes
Squid (12, 18)	Polyvinyl ethanol copolymer mixed with micro-ionized tantalum	DMSO	Marathon, Echelon, Apollo, Headway Duo, Scepter XC balloon catheter	Head, neck, and spine tumors (limited use)	Fine control Better visibility Lower viscosity Longer injection times (when compared to Onyx)	Yes
Phil (25%, 30%, 35%)	No tantalum. Hydroxyethyl methacrylate (PHEMA), covalently bonded to iodine.	DMSO	Marathon, Echelon, Apollo, Headway Duo, Scepter XC balloon catheter	Head, neck, and spine tumors (limited use)	Fine control Better visibility No shaking Prefilled syringes Nonmetallic Avoid streak artifact during imaging High embolic capacity	Yes

Coils	Platinum coils, hydrogel coils, fibered coils	NA	Depends on coil size, but usually 017-025 microcatheter.	Head, neck, and spine tumors	Relatively predictable deployment, useful for vessel sacrifice or tumor pedicle takedown. Can be used as a marker for operative level Can be used adjunctively to help keep other embolic agents in place.	Yes, but collaterals can develop easily overtime
PVA particles	Polyvinyl alcohol particles. Many sizes.	NA	017-035 catheters can be used based on the size of the particles	Predominately in the neck via ECA branches. Less control makes them not ideal for intracranial use.	Easy to use Excellent for nasopharyngeal tumors. Good penetration with smaller sizes Low visibility High risk for intracranial use Lack of control	No
Embospheres (40–120, 100–300, 300–500,500–700, 700–900, 900–1200 microns)	Trisacryl cross-linked with gelatin	NA	017-035 microcatheters based on size of particles	Predominately in the neck via ECA branches. Less control makes them not ideal for intracranial use.	Easy to use Excellent for nasopharyngeal tumors. Good penetration with smaller sizes Low visibility High risk for intracranial use Lack of control	No

DMSO dimethyl-sulfoxide, *NBCA* N-Butyl-Cyanoacrylate, *NA* not applicable

with a unipolar Bovie. This can be prevented with a bipolar unit; however, the surgeon should be warned prior to the operation. If the embolic agent is not seen on fluoroscopy, keep in mind, there may be high flow arterial venous shunts causing nontarget embolization to the lungs. If this is the case, reassess the situation and consider upsizing the particulate material, using coils to occlude the shunt, or injecting liquid embolic agents that have a continuous cohesive column such as Onyx or Squid.

Typical Setup for Head and Neck Tumor Embolization

Access under ultrasound guidance with placement of a 6F sheath, radial or femoral. 6F Benchmark sheath (Penumbra) or Envoy guide catheter (Cordis Neurovascular) can be used. Although a 5F diagnostic catheter can be used as a guide for straightforward external carotid artery (ECA) related tumors with a 0.021 microcatheter such as a Nautica (Medtronic), these limits repeat angiographic runs or roadmap images for selection of arterial supply to the tumor.

1. Standard coiling catheters can be used unless POD coils or RUBY coils (Penumbra) are being used for larger vessel sacrifice [12]. These require 025 PX Slim or Lantern catheters. An Amplatzer plug or MVP plug for vessel takedown may require a larger microcatheter or guide catheter for deployment. An awake balloon test occlusion (BTO) should be done prior to vessel sacrifice.
2. If glue is used, 5% dextrose (D5) solution and N-Butyl-Cyanoacrylate (NBCA) along with lipiodol should be placed on a separate table along with glacial acetic acid (GAA). The concentration of NBCA used for injection depends on the distance of the catheter from the tumor and the amount of arterial-venous shunting. The catheter is primed with D5 to make sure that no ionic solution meets the glue mixture resulting in premature polymerization. Glue can be injected using the push technique or sandwich technique to avoid excessive reflux and gluing of the microcatheter to the vessel wall. Glue injections can be prolonged with a wedged microcatheter position. Furthermore, a larger diameter guide catheter is recommended when injecting glue through the microcatheter. This approach would prevent fragmentation and any nontarget embolization of glue stuck to the microcatheter when pulling through the guide catheter. Prolonged glue injection can also be obtained by flooding the arterial bed of the tumor with D5 injected through the guide catheter during the glue injection. This will prevent premature polymerization of the glue; however, the glue can fragment with this technique, making precise deposition difficult.
3. If liquid embolic agents other than NBCA are utilized, catheter compatibility with the carrier DMSO must be kept in mind. The authors typically use a Headway Duo (Microvention) for distal embolization with Onyx or a Scepter XC dual lumen balloon for intracranial embolization. Echelon, Marathon, and Apollo (Medtronic) microcatheters are also compatible with DMSO. The mara-

thon microcatheter is the only semi flow directed microcatheter compatible with the use of Onyx. Magic (Balt) catheters are true flow directed microcatheters and can be used with glue for very distal, tortuous work. This catheter requires a 0.008–0.0010 in diameter microwire given its smaller inner luminal diameter.

4. The injection of Onyx should be done under a blank negative roadmap. The injection can be performed by slowly building the Onyx plug around the microcatheter which may take up to 20 minutes depending on the size of the vessel and if the microcatheter is in a wedged position. Onyx can also be injected using the pressure cooker technique or by inflating a double lumen DSMO compatible balloon catheter, making sure it is occlusive, and then injecting the Onyx under flow arrest. Large arterial pedicles supplying the tumor are more easily occluded with coils or the heavier Onyx 34.
5. A distal access catheter-like DAC 038 (Stryker) or Phenom plus catheter can be utilized to provide distal microcatheter control and minimize Onyx cast deflection during microcatheter removal.
6. Pearl: If a catheter is glued in place, one must consider the location, intracranial versus extracranial, the size, tortuosity and fragility of the vessel, and the type of embolic agent used. Usually a long slow pull, over several minutes can release Onyx from the microcatheter. Problems from pulling the microcatheter can arise when there is reflux of a large portion of Onyx around the microcatheter or when embolization was performed in a tortuous vessel. Glue, on the other hand, is different as it may not release given its adhesive properties and if a vessel is torn with removal of the microcatheter, it is essential to have a balloon microcatheter in place to prevent life threatening extravasation. Finally, catheters fixated at the tumor can be left in situ and cut at the access site and then removed during surgical excision of the tumor. If necessary, cut downs can be done to shorten the catheter or surgical removal. Otherwise, aspirin 81 mg can be started depending on location to prevent embolic risk from retained catheters. A venous-retained catheter is much more forgiving than an arterial one.
7. Particulate embolization with PVA or spherical embolic agents can be performed through a variety of microcatheters depending on the size of the embolic agent. After placement of a microcatheter in peri-tumoral location, nonspherical PVA is usually suspended in a 70% contrast solution. PVA 250-350 microns in size are usually used to prevent nontarget embolization through arterial anastomoses. The solution is injected with a 1-cc syringe using small puffs under negative roadmap to provide optimal control. Spherical agents (i.e., Embospheres, Beadblock, etc.) are suspended in a similar manner, with the size of the embolic agent determined by the catheter position and goals of the embolization. Smaller particles may provide a higher degree of tumor devascularization; however, this must be weighed with the possible increased risk of nontarget embolization through arterial anastomoses, the risk of bleeding into the tumor from more complete necrosis, and the theoretical increase risk of cranial nerve injury given the distal penetration into vasa nervorum. Following embolization with particulate material, a Gelfoam pledget (cigar shape) can be pushed or a coil placed through the microcatheter to occlude the arterial pedicle.

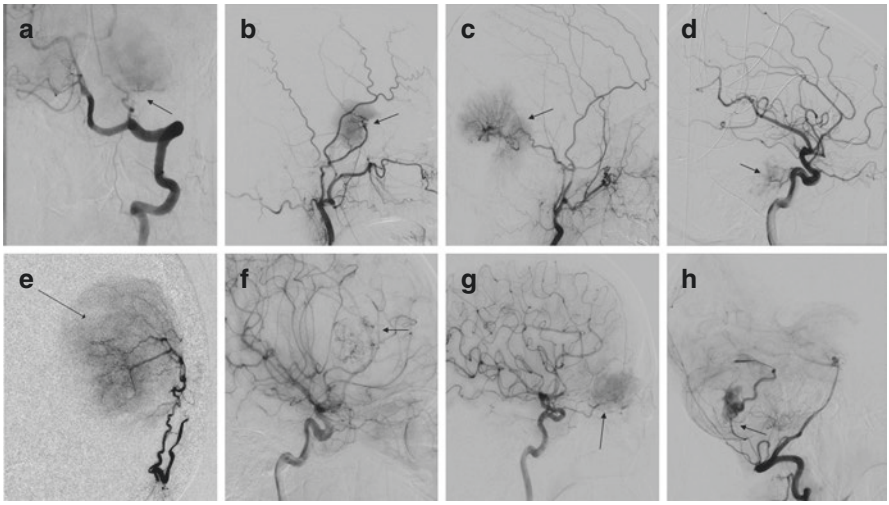

Fig. 27.1 Variation in the blood supply of meningiomas and other intracranial hypervascular tumors. (**a**) Left Posterior fossa meningioma supplied by posterior meningeal artery of vertebral artery. (**b**) Right sphenoid wing meningioma supplied by anterior division of middle meningeal artery. (**c**) Left middle cranial fossa meningioma supplied by petrous-squamosal branch of left middle meningeal artery. (**d**) Petroclival meningioma supplied by left meningiohypophyseal branch of internal carotid artery. (**e**) Left occipital meningioma supplied by left occipital artery. (**f**) Right frontal metastasis from malignant melanoma supplied by prefrontal branch of right middle cerebral artery. Notice a significant midline shift of anterior cerebral artery from tumor mass effect. (**g**) Left orbit plasmacytoma supplied by ophthalmic artery. (**h**) Left cerebellar cystic hemangioblastoma supplied by left posterior inferior cerebellar artery with a large draining vein into transverse sinus

8. For hypervascular tumors with arterial supply from the internal carotid artery (ICA) or vertebral artery (VA), embolization can be extremely difficult due to the small size of the artery making microcatheter catheterization nearly impossible (Fig. 27.1f–h). Furthermore, injection of any embolic agent into an artery arising off the ICA or VA runs the risk of nontarget embolization into the intracranial circulation causing either blindness or an acute ischemic stroke.

Typical Setup for Direct/Percutaneous Tumor Embolization

Direct percutaneous embolization of tumors under fluoroscopic, ultrasound, or CT guidance is an acceptable and safer method for technically challenging cases in which conventional transarterial embolization is impossible because of the small size of the arterial feeders or involvement of branches arising from the ICA or VA.

Complete devascularization of the tumor can be obtained with decreased risk to the patient by using a direct tumoral injection of nBCA or Onyx. The authors perform percutaneous injection of n-BCA or Onyx by placing an 18-gauge, short

guiding needle into the tumor using imaging guidance and then coaxially introducing a 20-gauge spinal needle. After the needle is correctly placed within the vascular bed of the tumor, constant reflux of blood is observed. The contrast agent is injected through the needle and a tumorgram is obtained to assess for arterial reflux, venous drainage, potential for extravasation, and to determine which vascular compartment of the tumor will be filled with n-BCA or Onyx. The injection of the embolic agent is then performed using a negative roadmap. The procedure is stopped after complete devascularization is achieved, as determined by non-visualization of intratumoral flow, or if the risk for potential arterial reflux into the intracranial circulation is high.

Typical Setup for Spinal Tumor Embolization

The authors prefer a 5 or 6F sheath with femoral access for spinal angiography. Spinal angiography can also be performed from a radial approach; however, the currently available catheters may make this more difficult. A comprehensive diagnostic spinal angiogram should be performed prior to embolization to identify large segmental arteries and their radicular components. This is done in a true AP projection since the anterior spinal artery will course in the midline which is identified by the spinal process. Glucagon can be given to stop bowel movements per interventionalist preference. The authors also prefer general anesthesia to control breath holds and limit respiration artifact. A Mickelson, Cobra or Sim 1 catheter can be utilized for angiography depending on the anatomy. Preoperative cross-sectional imaging reviewed prior to the angiogram can provide valuable information about the anatomy and location of the takeoff of the anterior spinal artery. Spinal angiography is easiest with a radiopaque ruler placed on the patient to keep track of spinal levels. Careful, judicial recording of the volume of contrast utilized is also important given the multiple levels that must be interrogated. Typically, a 5F Mickelson catheter is stable enough to run a microcatheter coaxially for embolization. If needed, a large 6F guide catheter can be used, but often these are too large to directly engage the paraspinal artery ostium. Provocative testing can be utilized prior to embolization of an arterial pedicle supplying the tumor.

Commonly Treated Tumors

Head and neck tumors typically amenable to endovascular embolization can be broken down into cranial and neck lesions (Table 27.3). Cranial lesions include meningiomas, hemangiopericytoma, hemangioblastoma, juvenile nasopharyngeal angiofibroma, sarcomas, and hypervascular metastases.

Neck tumors amenable to endovascular embolization include carotid body tumors, paragangliomas, sarcomas, and carcinomas. Neck tumor embolization can

Table 27.3 Highly vascular head and neck tumors treated with preoperative embolization

Cranial tumors	Target vessels/typical blood supply	Angiographic pattern	Timing of surgery	Preferred embolization techniques
Juvenile nasopharyngeal angiofibroma	Branches of ECA, typically internal maxillary artery branches (the sphenopalatine and descending palatine branches), the anterior division of the APA, and the AMA.	Highly vascular tumor	2–4 days	Gelfoam/PVA/Embospheres/Onyx
Hemangiopericytoma	ICA and VA as well as ECA	Highly vascular with blood supply from pial feeders of ICA and VA. Corkscrew arteries, fluffy tumor stain and lack of early draining veins	1–6 days	If the dominant supply to the tumor is a large ECA feeder, polyvinyl alcohol (PVA; 150–250 μm) or Embospheres (100–300 μm). Transtumoral embolization with Onyx via small MMA feeders can be considered if pial feeders from ICA and VA are the primary source of blood supply.
Metastatic lesions	Branches of ICA/VA	Highly vascular metastasis, most commonly RCC	1–6 days	Highly vascular brain metastasis can be embolized if microcatheter can be navigated distally into the feeder, and superselective angiography shows no staining of the adjacent normal brain territories. Provocative testing can be performed prior to embolization. Precise embolization with Onyx or NBCA glue is recommended over embospheres or PVA.

Meningiomas	*Branches of ICA and ECA*		1–7 days	Any embolic material can be used at the interventionalist discretion. Small diameter embospheres should be avoided in feeders with dangerous collaterals to intracranial vessels. Proximal arterial pedicle control is sometimes preferred over deep penetration especially when Onyx is used.
Anterior fossa	Artery of the falx and the ethmoidal arteries	The angiographic pattern of meningioma can vary from multiple vessels supply from ICA and ECA with long-lasting tumor stain, fewer vessels with weak tumor stain or no visible vasculature		
Middle fossa	Artery of the foramen rotundum, the vidian arteries, the middle meningeal and accessory meningeal artery, and the ascending pharyngeal artery	Meningiomas can also develop many irregular corkscrew-like vessels, with dense, well-defined and long-lasting tumor stain, but early venous drainage (HPC pattern).		
Posterior fossa	Posterior meningeal artery, the occipital artery, and the anterior meningeal branch of the vertebral artery	Secondary angiogenesis leads to the recruitment of intracranial vessels and pial arterial feeders.		
Hemangioblastoma	Branches of vertebrobasilar system	Highly vascular	1–7 days to 21 days	Onyx or NBCA glue, although other embolysates have been used in various case series
Neck tumors				
Glomus tumors (paragangliomas)				
Carotid body tumor	Branches of ECA, most commonly ascending pharyngeal artery and occipital arteries	Characteristic splaying of the carotid bifurcation with high vascularity	Immediately after embolization	PVA, embospheres, Onyx
Glomus vagale and jugulare tumors	Higher branches of ECA	Highly vascular tumors in the higher cervical region or skull base.		

ECA external carotid artery, *APA* ascending pharyngeal artery, *AMA* accessory meningeal artery, *PVA* polyvinyl alcohol, *ICA* internal carotid artery, *VA* vertebral artery, *NBCA* N-Butyl-Cyanoacrylate, *RCC* renal cell carcinoma

also be performed to control tumor hemorrhage and epistaxis. This is a form of palliative embolization for base of tongue lesions or pharyngeal lesions. Neck tumors often get blood supply from ECA branches such as the sphenopalatine, internal maxillary artery, and facial arteries. Lower neck lesions can be supplied by superior thyroid vessels, as well as thyrocervical trunk contributions depending on which cervical triangle the tumor is within.

Spine tumors, amenable to endovascular embolization include large meningiomas, sarcomas, and hypervascular metastases such as renal cell carcinoma. These lesions are typically supplied by paraspinal arteries. Large radicular and segmental arteries supplying the cord must be identified and preserved prior to and during tumor embolization.

Other endovascular techniques include catheter directed microinjection of chemotherapy for tumors such as head and neck cancers and retinoblastoma. Use of catheter directed therapies for blood–brain barrier disruption for chemotherapy of glioblastomas is currently investigational.

Meningioma

Meningiomas are the most frequently diagnosed primary brain tumor accounting for 33.8% of all primary brain and central nervous system tumors [13]. The incidence of symptomatic meningiomas is estimated to be 2 per 100,000 person-years [14]. Approximately 90% of meningiomas are benign, 6% are atypical, and 2% are anaplastic [15]. Meningiomas are primarily fed by branches of ECA, and ICA and in the setting of posterior fossa meningioma, the VAs. Convexity, parasagittal, and sphenoid wing meningiomas are primarily supplied by middle meningeal artery branches and olfactory groove meningiomas are supplied by branches of the ethmoidal arteries from the ophthalmic artery along with dural branches of the internal carotid artery. Lateral posterior fossa meningiomas are generally supplied by branches of the occipital and ascending pharyngeal artery, whereas posteromedial posterior fossa meningiomas are typically fed by meningeal branches of the vertebral artery and the posterior meningeal artery. Clival and tentorial meningiomas may receive their blood supply from various feeders such as the tentorial artery, ascending pharyngeal artery, cavernous internal carotid artery, and middle meningeal artery [16] (Fig. 27.1a–e).

Preoperative embolization is currently advocated for large meningiomas because of their vascularity, to reduce blood loss and promote complete resection of the tumor which has been known to reduce recurrence rates [17].

A matched analysis of 76 of patients undergoing surgery with and without embolization demonstrated that the mean value of estimated blood loss, 1403 ml vs. 1852 ml, and the number of transfusions, 1325 ml vs. 1747 ml, were lower in embolized patients than in nonembolized patients [18]. Several other studies have also shown reduction in operative blood loss in patients receiving preoperative embolization [3].

The safety of preoperative embolization for meningiomas is well established by many studies. A retrospective analysis of preoperative embolization of 167 cranial base meningiomas showed excellent success rates in 91% of patients embolized without any permanent neurological complications [19]. A systematic review of 36 studies comprising 459 patients showed that among patients receiving preoperative embolization for meningiomas, only 4.6% sustained complications as a direct result of the embolization [20].

Some areas of meningioma are not as amenable to embolization as others. For instance, anterior cranial fossa meningioma (Optic sheath meningiomas, orbital meningiomas, Cribriform plate, and planum sphenoidale Meningiomas) would require embolization of the branches of the ophthalmic artery or posterior ethmoidal artery with dangerous collaterals to retinal artery [3]. Placing vision at risk for embolization of a tumor is rarely indicated as there are other ways to ensure hemostasis during removal. On the other hand, convexity, parasagittal, and lateral sphenoid wing meningiomas are often good targets for embolization as the middle meningeal artery is easily accessed and safe to embolize beyond the orbital contributing segment. Embolization of posterior fossa meningiomas and clival meningiomas with feeders from the vertebral artery or basilar artery are also high risk for neurological complications [3]. Figure 27.2 describes an example of preoperative embolization of a large temporo-occipital meningioma. Final operative pictures demonstrate a devascularized tumor with remarkably low blood loss.

Hemangiopericytoma

Hemangiopericytomas (HPCs) are rare dural-based neoplasms (previously classified as a type of meningioma) and account for less than 1% of all intracranial tumors. Intracranial HPCs are highly hypervascular, with a high risk for local recurrence and tendency to metastasize both within the craniospinal axis as well as to extraneural sites [21]. Preoperative embolization of HPC can be technically challenging because of the predominant blood supply is from pial feeders of ICA or VA. Transarterial embolization with Onyx or glue is preferred for small ECA feeders versus occlusion of the pial feeders from ICA/VA. If large feeders from ECA arterial branches are present, those can be embolized with particulate material utilizing PVA or Embospheres [21]. In a series of fifteen patients with pathologically confirmed HPC, more extensive devascularization percentages were achieved for HPCs with primarily ECA blood supply than with HPCs supplied via the ICA/VA circulation (76% versus 58%). There was a trend toward greater devascularization of ICA/VA-dominant HPCs embolized with Onyx (70%) versus PVA (33.3%) [21]. Direct percutaneous tumor embolization of HPC has also reported with histocryl, glue, or alcohol in few case reports [22, 23].

Hemangioblastoma

Hemangioblastomas (HB) are benign, highly vascular tumors, commonly located in cerebellum, spinal cord, or brainstem. These tumors comprise up to 2.5% of CNS neoplasms and 7-12% of posterior fossa lesions in adult patients [24]. Nearly one-third of patients with these tumors have von Hippel-Lindau disease (VHL), this is especially true for tumors that arise from spinal cord [25]. Both liquid and particulate embolic materials have been used to embolize arterial feeders in HB patients prior to surgical resection. In a retrospective study comparing outcomes between embolized patients ($n = 46$) and non-embolized controls ($n = 79$), Liu et al. demonstrated greater intraoperative blood loss and blood transfusion requirements within non-embolized patients, yet no difference in complication rates [26]. In a series of 10 patients with solid large cerebellar HB, embolization was successful in 90% of the patients, achieving total resection with minimum blood loss [27]. However, a systematic review of 23 studies, comprising 111 patients that underwent preoperative embolization and 392 patients without embolization, did not show an increase rate of gross total tumor resection, a decrease estimated blood loss, or other complications. The risk of embolization related complications including stroke and hemorrhage were much higher in this group, partly related to the blood supply from branches of vertebrobasilar system [28]. Figure 27.1h shows a left VA angiogram demonstrating angiographic blush of tumor with arterial supply from posterior inferior cerebellar artery. Notice the brisk arterial venous shunt. Embolization was not performed in this case due to high risk for stroke and inadvertent embolization to lungs via the arterial venous shunt.

Although embolization has some role in the treatment of HB, careful preoperative planning and studying of feeders is needed prior to any attempted embolization.

Glomus tumors (Paragangliomas)

Paragangliomas, or glomus tumors, are derived from neural crest cells and are a rare entity, comprising 0.6% of all neoplasms in the head and neck region [29]. They are highly vascular, benign tumors that are capable of local invasion into the surrounding structures. The most common location for these tumors is along the temporal bone involving the tympanic nerve or jugular fossa, followed by the carotid bifurcation and vagus nerve [1]. The carotid body tumor demonstrates the typical angiographic appearance involving the “splaying” of the carotid bifurcation [30] (Fig. 27.3b). All paragangliomas demonstrate a strong angiographic contrast blush indicating their hypervascularity [1]. Arterial supply to these tumors often involves branches from the ECA and ICA, but almost all patients have some supply from the ascending pharyngeal arteries [31]. Clinical presentation for these tumors varies based on location. Preoperative arterial embolization is reserved for large head and neck paragangliomas. Tikkakoski et al. compared blood loss and operative time between patients embolized before surgical excision with that of non-embolized patients and showed a significantly lower amount of blood loss (588

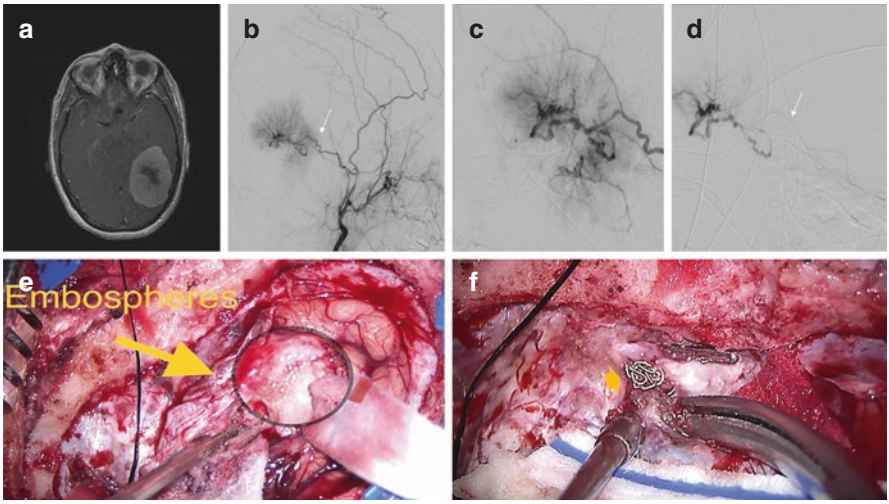

Fig. 27.2 A 50-year-old female who presented with exertional headaches. Intracranial imaging demonstrated a large left temporo-occipital mass, likely meningioma. Given the size and vascularity of the mass, preoperative embolization was performed prior to surgical resection. (**a**) Axial contrast-enhanced T1-weighted image shows a 7-cm hypervascular mass in the left temporo-occipital region. (**b** and **c**) Lateral left external carotid angiogram and super-selective left middle meningeal artery angiogram shows a large hypervascular mass (white arrow) with arterial supply off the petro-squamosal and petrous branches of middle meningeal artery (white arrow in Fig. 27.2b). (**d**) Microcatheterization of the petro-squamosal branch of middle meningeal artery with embolization of the tumor with embospheres (300-500 microns). (**e** and **f**) Intraoperative photographs demonstrate devascularized tumor with embospheres (Fig. 27.2e) and embolized coil (Fig. 27.2f, thick yellow arrow). The estimate blood loss at the time of surgery was 200 ml. (Courtesy, Dr. Bryan Figueroa)

versus 1374 ml, $P = 0.04$) and operation time in the embolization group [32]. White et al. described a case series of 38 patients that underwent selective arterial embolization of their paraganglioma using PVA particles ranging in size from 100 to 1000 microns. The tumor subtypes treated were carotid body (n = 20), glomus vagale (n = 10), and glomus jugulare (n = 8). Post-embolization angiography revealed an average decrease in blood flow to tumor of 75% [33]. To prevent inadvertent proximal reflux of embolic agents, distal catheter placement is preferred with embolization performed under continuous fluoroscopic monitoring. PVA, embospheres, or gelfoam have all been used successfully. Figure 27.3 shows a case of carotid body tumor in a 63-year-old woman treated with Onyx embolization prior to surgical resection.

Direct percutaneous placement of needles into a carotid body tumor with embolization using Onyx or glue has also been described [34].

Furthermore, a comparison of transarterial particulate embolization to direct percutaneous embolization of carotid body tumors showed a decrease in operative blood loss, blood transfusion requirement, and operative time with less complications in the direct puncture group [35]. Proximal embolization of feeding vessels is not recommended because ICA collaterals can develop around the tumor [31].

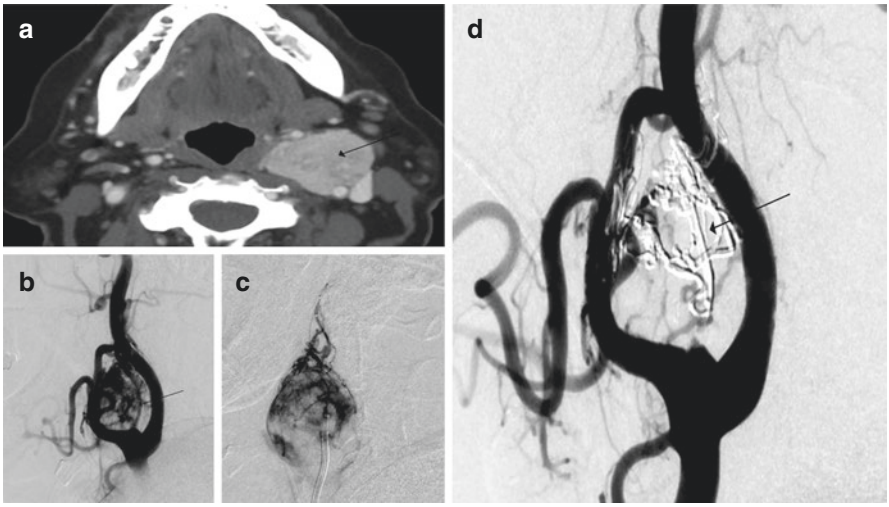

Fig. 27.3 A 63-year-old female who presented with hoarseness from a left neck mass consistent with a carotid body tumor. Given the hypervascularity preoperative embolization was performed prior to surgical resection. (**a**) Axial contrast-enhanced CT of the neck shows a hypervascular mass (black arrow) splaying the left carotid bifurcation. (**b**) Lateral left common carotid angiogram shows a hypervascular mass (black arrow) splaying the carotid bifurcation. (**c**) Lateral left ascending pharyngeal angiogram with injection of the odontoid branch show filling of this hypervascular mass. (**d**) Lateral left common carotid angiogram after the intra-arterial injection of Onyx and particles in the odontoid branch, artery of the carotid body, and small branches off the facial artery shows near complete devascularization of the mass. Onyx is identified in the arterial vessels supply of the mass (black arrow)

Juvenile Nasopharyngeal Angiofibroma

Juvenile nasopharyngeal angiofibroma (JNAs) accounts for 0.5% of all head and neck tumors and predominantly occur in adolescent males [36, 37]. Patients generally present with nasal obstruction and recurrent epistaxis. The tumors arise from the lateral margin of the posterior nasal cavity, adjacent to the sphenopalatine foramen. The major arterial supply to these tumors is typically the ipsilateral internal maxillary, facial, ascending pharyngeal, and recurrent meningeal artery with occasional additional arterial supply from branches of the internal carotid or contralateral external carotid system [3]. The morbidity and mortality associated with this tumor are related to its prominent vascularity and its propensity for aggressive local growth [37]. Preoperative embolization of JNAs has been shown to decrease intraoperative blood loss during surgical resection. Moulin et al. demonstrated a statistically significant difference in blood loss between embolized and non-embolized surgical groups of patients with high-grade tumors [38]. The benefit of embolization is less clear for smaller, less vascular tumors. Surgical resection of the tumor should be performed from 24 to 72 hours after the embolization to achieve optimal

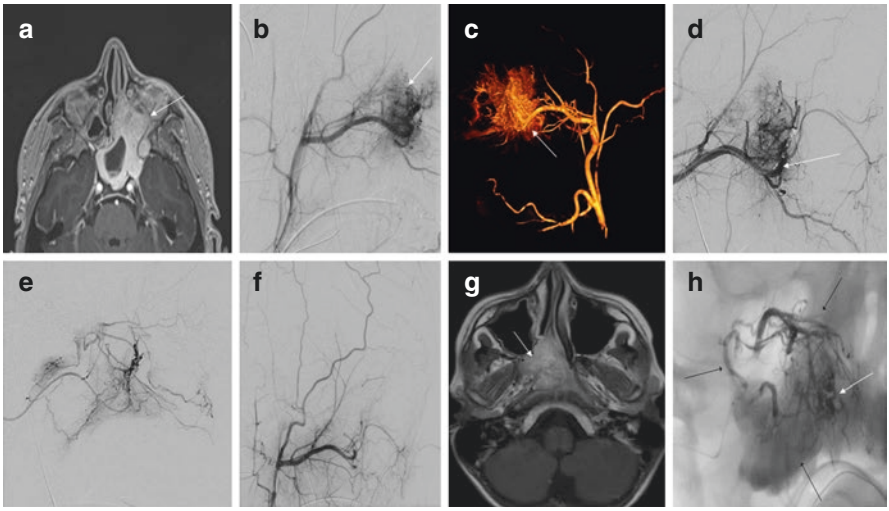

Fig. 27.4 Juvenile angiofibroma in an 18 yo boy (Fig. 27.4a–f) embolized with Embospheres (500-700 micron) and gelfoam and 13 yo boy (**g**, **h**) embolized with Onyx. (**a**) Axial contrast-enhanced T1-weighted image shows a mass within the left posterior nasal pharynx extending into the sphenopalatine foramen (white arrow). (**b** and **c**) Lateral left external carotid artery angiogram (Fig. 27.4b) and 3-D reconstructed images (Fig. 27.4c) shows a hypervascular mass (white arrow) with artery supply off multiple branches of the distal internal maxillary artery. (**d** and **e**) Microcatheter placement (XT-27) in sphenopalatine artery (white arrow) followed embosphere embolization (Fig. 27.4e). (**f**) Lateral left external carotid artery angiogram demonstrated complete devascularization of tumor. (**g**) Axial contrast-enhanced T1-weighted image shows a mass within the right posterior nasal pharynx extending into the sphenopalatine foreman (black arrow). (**h**) Frontal spot fluoroscopy image shows the Onyx cast within arterial feeders to the tumor and tumor parenchyma (black arrows)

devascularization of the tumor [29]. Figure 27.4 describes examples of JNA embolization in an 18-year-old and a 13-year-old boy with embospheres and Onyx respectively.

Direct percutaneous puncture of the tumor with embolization using Onyx has also been described as is associated with a decrease in intraoperative blood loss and transfusion requirements [39, 40].

Embolization of Spinal Tumors

Preoperative embolization of hypervascular spinal tumors has been shown to significantly reduce blood loss when compared to the non-embolized group [41]. In a series of thirty-seven patients who underwent preoperative spinal tumor embolization (24 metastatic and 13 primary lesions), only one complication resulted in transient lower extremity weakness and was attributed to post-embolization swelling that fully resolved after surgical resection. After embolization, tumor blush was

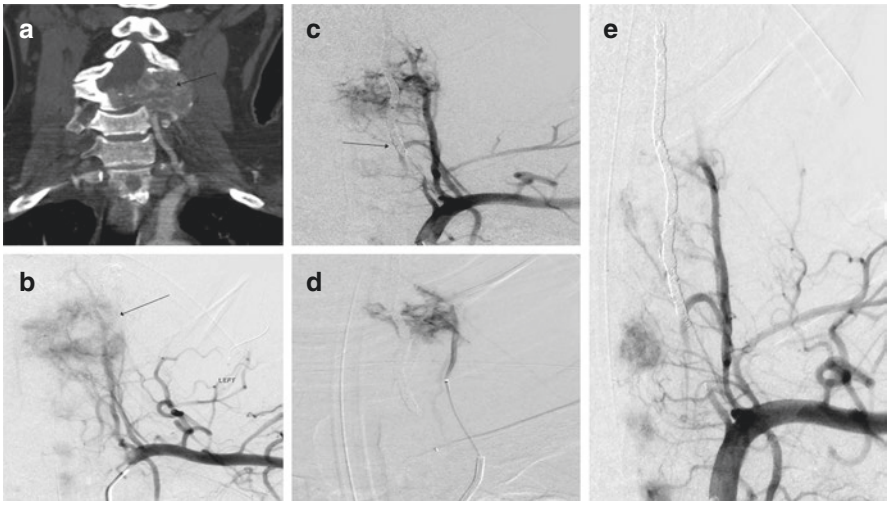

Fig. 27.5 A 69-year-old male with a history of renal cell carcinoma presented with myelopathy and cervical neck pain from a large tumor involving the C5 vertebral body. Preoperative embolization was performed prior to surgical resection and spinal instrumentation. (**a**) Contrast-enhanced coronal CTA of the cervical spine shows a hypervascular mass (black arrow) surrounding the left vertebral artery with boney destruction of C5. (**b**) Frontal left subclavian artery angiogram shows a hypervascular mass at C5 (black arrow) with arterial supply off multiple small branches of the left vertebral artery, thyrocervical trunk, and ascending cervical artery. (**c**) Frontal left subclavian artery angiogram after occlusion of the left vertebral artery with coils and plugs (black arrow) shows persistent arterial supply to the tumor from the thyrocervical trunk and ascending cervical artery. (**d**) Frontal ascending cervical artery angiogram shows filling of the hypervascular mass at C5. (**e**) Frontal left subclavian artery angiogram after occlusion of the left vertebral artery with coils and plugs and embolization of the left thyrocervical trunk and ascending pharyngeal artery with 500–700-micron size embospheres shows near complete devascularization of the mass. The estimate blood loss at the time of surgery was 700 mls

reduced by 83% on average. Average pre- and postoperative modified Rankin Scale scores were 2.10 and 1.36, respectively ($p = 0.03$). Metastatic renal cell carcinoma was the most common tumor type (n = 16%, 43%) followed by hemangioma (n = 4%, 11%) and metastatic thyroid carcinoma (n = 4%, 11%). Onyx or NBCA glue were the preferred embolic agents [42].

Figure 27.5 describes a case of renal cell carcinoma with cervical metastasis, treated with coils and embospheres prior to resection.

Intra-arterial Chemotherapy for Head and Neck Tumors

Head and neck cancers are a challenge to manage. Traditional cancer treatments achieve good locoregional tumor control rates while causing severe side effects. Most head and neck cancer tend to recur at the primary site or in regional neck

lymph nodes, while distant dissemination occurs late and is a less frequent cause of morbidity and death. Therapy with chemotherapeutic drugs administered intravenously is limited because either the concentrations at the tumor site are too low or the total dosages are too high and toxic. The concept of intra-arterial chemotherapy for head and neck cancers has been around for several decades [43, 44]. The blood supply to head and neck tumors is primarily derived from branches of the external carotid artery. Theoretically, super-selective chemotherapy through the arterial feeders of ECA can deliver higher concentrations of pharmacologic agents, while minimizing systemic side effects. With the development of advanced catheter techniques and angiographic imaging, protocols for intra-arterial chemotherapy were developed and showed initial promise. Intra-arterial infusion of high-dose cisplatin with systemic neutralization by intravenous sodium thiosulfate (RADPLAT) was a theoretically attractive approach to the treatment of advanced head and neck cancer. However, multicenter trials have failed to show benefit of RADPLAT, hampered by significant neurological side effects with no overall benefit in mortality [45–47]. Advances in nanotechnology research, specifically using nanoparticle albumin-bound paclitaxel, to safely deliver high concentrations of intra-arterial chemotherapy, have been explored. However, these techniques remain investigational [48].

Intra-arterial chemotherapy for retinoblastomas Retinoblastoma is the most common primary intraocular neoplasm in children. Intra-arterial chemotherapy for the treatment of retinoblastoma was introduced in 1958. However, the first successful selective ophthalmic artery infusion was performed by Yamane et al. by occluding the internal carotid artery, distal to the ostium of ophthalmic artery with a balloon and infusing melphalan near the ostium of the ophthalmic artery [49]. Later, Gobin et al. introduced direct catheterization of the ophthalmic artery and super-selective intra-arterial chemotherapy. The evolution of intra-arterial chemotherapy contributed to increased safety and efficacy of this treatment [50]. A systemic review of 23 studies, published between 2011 and 2019 evaluated the technical success rate of intra-arterial chemotherapy, globe salvage rate, and ocular and systemic complications, as well as the occurrence of deaths, metastasis, and secondary neoplasms. The technical success rate of intra-arterial chemotherapy ranged from 91% to 100% with an ocular salvage between 60 and 80%. Eyelid edema and erythema were the most reported ocular complications while the most common systemic complications were nausea, vomiting, and neutropenia. Overall, intra-arterial chemotherapy was safe and effective in salvaging the globe without compromising survival [51].

Intra-arterial Chemotherapy for Intracranial Neoplasm

Intra-arterial chemotherapy for intracranial neoplasms including gliomas, lymphomas, and CNS metastasis has been studied. However, its role in intracranial neoplasms is still investigational.

Complications

Complications arising from head and neck tumor embolization can be related to access site complications as with any endovascular procedure such as hand or leg ischemia, and retroperitoneal hematoma. More specific complications related to coil or liquid embolic injection will depend on the site of the tumor. Embolization in the presence of AV shunts can result in pulmonary embolism as well as venous sinus occlusion. Skin erythema, alopecia, and cataracts can happen from radiation doses that exceed 3 Gy at one session. An acute ischemic stroke is possible from embolic material migrating through arterial anastomoses into the intracranial circulation as well as from embolization of parasitized intracranial arterial feeders to tumors with inadvertent reflux of embolic material into the parent vessel. Embolization of the arterial supply to cranial nerves with small particles or liquid embolic agents can cause permanent cranial nerve injury. Blindness can occur from embolization involving collaterals of the ophthalmic artery, just as hoarseness, swallowing difficulties, or tongue paralysis can occur with tumors near the vascular supply of these cranial nerves. Skin necrosis of the scalp can result from overzealous embolization of occipital or superficial temporal artery branches prior to surgical resection and this may require a plastic surgery consultation with flap reconstruction. Direct percutaneous injection of Onyx can lead to inadvertent skin tattooing which can be cosmetically challenging to the patient.

Numerous trials have assessed the overall risk of embolization for different types of tumors, with intracranial meningioma embolization carrying a 5.6% risk of ischemia/hemorrhage in one large study with PVA particles. Small particles (50 micron) were discouraged [52]. Available stroke techniques can be utilized for amenable off target liquid embolic retrieval in emergencies, but this should always be weighed with the possible aggravation of the situation [53].

Perioperative Timing

Careful consideration of timing should be included in all head and neck tumor embolization procedures. The goal of the procedure should be clearly defined. If the tumor is causing life-threatening blood loss or oropharyngeal bleeding, its emergent. However, if tumor resection is elective, then usually embolization can be performed 48 hours prior to removal to allow for maximal thrombosis of the occluded vessels, tumor softening, necrosis [54]. Removal of the tumor later may result in the development of collateral vessels supplying the tumor and an increase in intraoperative blood loss. Steroids may be necessary for both large masses near airway and in the head to prevent swelling that could lead to further mass effect post embolization.

Conclusion

Careful planning, knowledge of arterial collaterals, and good patient selection ensures that endovascular embolization of head and neck tumors can be of benefit in decreasing operative blood loss, transfusion requirements, and operative time for surgical resection. Embolization may also have a palliative role in relieving clinical symptoms in patients that are not surgical candidates.

References

1. Gupta R, Thomas AJ, Horowitz M. Intracranial head and neck tumors: endovascular considerations, present and future. Neurosurgery. 2006;59(5 Suppl 3):S251–60; discussion S3–13.
2. American Society of Interventional and Therapeutic Neuroradiology. Head, neck, and brain tumor embolization. AJNR Am J Neuroradiol. 2001;22(8 Suppl):S14–5.
3. Qureshi AI, et al. Intracranial and head and neck tumors: embolization and chemotherapy. In: Textbook of interventional neurology. Cambridge; New York: Cambridge University Press; 2011. p. 312.
4. Facchini G, et al. Palliative embolization for metastases of the spine. Eur J Orthop Surg Traumatol. 2016;26(3):247–52.
5. Sittel C, et al. Superselective embolization as palliative treatment of recurrent hemorrhage in advanced carcinoma of the head and neck. Ann Otol Rhinol Laryngol. 2001;110(12):1126–8.
6. Berkman RA, et al. Expression of the vascular permeability factor/vascular endothelial growth factor gene in central nervous system neoplasms. J Clin Invest. 1993;91(1):153–9.
7. Dvorak HF, et al. Distribution of vascular permeability factor (vascular endothelial growth factor) in tumors: concentration in tumor blood vessels. J Exp Med. 1991;174(5):1275–8.
8. Lazzaro MA, et al. Endovascular embolization of head and neck tumors. Front Neurol. 2011;2:64.
9. Gounis MJ, et al. Effect of glacial acetic acid and ethiodized oil concentration on embolization with N-butyl 2-cyanoacrylate: an in vivo investigation. Am J Neuroradiol. 2002;23(6):938–44.
10. Siekmann R. Basics and principles in the application of onyx LD liquid embolic system in the endovascular treatment of cerebral arteriovenous malformations. Interv Neuroradiol. 2005;11(Suppl 1):131–40.
11. Deveikis JP. Sequential injections of amobarbital sodium and lidocaine for provocative neurologic testing in the external carotid circulation. Am J Neuroradiol. 1996;17(6):1143–7.
12. Kinariwala JP, et al. Therapeutic occlusion of the vertebral artery using a new penumbra occlusion device system and ruby coils (penumbra): a technical note. Brain Circulation. 2020;6(1):52.
13. Wiemels J, Wrensch M, Claus EB. Epidemiology and etiology of meningioma. J Neuro-Oncol. 2010;99(3):307–14.
14. Radhakrishnan K, et al. The trends in incidence of primary brain tumors in the population of Rochester, Minnesota. Ann Neurol. 1995;37(1):67–73.
15. Chamberlain MC. Intracerebral meningiomas. Curr Treat Options Neurol. 2004;6(4):297–305.
16. Huang RY, et al. Imaging and diagnostic advances for intracranial meningiomas. Neuro-Oncology. 2019;21(Suppl 1):i44–61.
17. Manelfe C, Lasjaunias P, Ruscalleda J. Preoperative embolization of intracranial meningiomas. AJNR Am J Neuroradiol. 1986;7(5):963–72.
18. Zhang XB, Jin ZY. [Clinical application of presurgical embolization of meningiomas]. Zhongguo Yi Xue Ke Xue Yuan Xue Bao, 2003;25(2):168–71.

19. Rosen CL, et al. Outcome analysis of preoperative embolization in cranial base surgery. Acta Neurochir. 2002;144(11):1157–64.
20. Shah AH, et al. The role of preoperative embolization for intracranial meningiomas. J Neurosurg. 2013;119(2):364–72.
21. Hanak BW, et al. Preoperative embolization of intracranial hemangiopericytomas: case series and introduction of the transtumoral embolization technique. J Neurointerv Surg. 2016;8(10):1084–94.
22. Casasco A, et al. Major complications of percutaneous embolization of skull-base tumors. AJNR Am J Neuroradiol. 1999;20(1):179–81.
23. Casasco A, et al. Devascularization of craniofacial tumors by percutaneous tumor puncture. AJNR Am J Neuroradiol. 1994;15(7):1233–9.
24. Brundl E, et al. Surgical resection of sporadic and hereditary hemangioblastoma: our 10-year experience and a literature review. Surg Neurol Int. 2014;5:138.
25. Ammerman JM, et al. Long-term natural history of hemangioblastomas in patients with von Hippel-Lindau disease: implications for treatment. J Neurosurg. 2006;105(2):248–55.
26. Liu AH, et al. Clinical effectiveness of preoperative embolization for cerebellar hemangioblastoma. Asian Pac J Cancer Prev. 2013;14(9):5179–83.
27. Sultan A, et al. The value of preoperative embolization in large and giant solid cerebellar hemangioblastomas. Interv Neuroradiol. 2016;22(4):482–8.
28. Ampie L, et al. Safety and outcomes of preoperative embolization of intracranial hemangioblastomas: a systematic review. Clin Neurol Neurosurg. 2016;150:143–51.
29. Gemmete JJ, et al. Embolization of vascular tumors of the head and neck. Neuroimaging Clin N Am. 2009;19(2):181–98, Table of Contents.
30. Lack EE, et al. Paragangliomas of the head and neck region: a clinical study of 69 patients. Cancer. 1977;39(2):397–409.
31. Persky MS, et al. Combined endovascular and surgical treatment of head and neck paragangliomas--a team approach. Head Neck. 2002;24(5):423–31.
32. Tikkakoski T, et al. Preoperative embolization in the management of neck paragangliomas. Laryngoscope. 1997;107(6):821–6.
33. White JB, Link MJ, Cloft HJ. Endovascular embolization of paragangliomas: a safe adjuvant to treatment. J Vasc Interv Neurol. 2008;1(2):37–41.
34. Shah HM, et al. Preliminary experience with the percutaneous embolization of paragangliomas at the carotid bifurcation using only ethylene vinyl alcohol copolymer (EVOH) Onyx. J Neurointerv Surg. 2012;4(2):125–9.
35. Griauzde J, et al. A comparison of particulate and Onyx embolization in preoperative devascularization of carotid body tumors. Neuroradiology. 2013;55(9):1113–8.
36. Davis KR. Embolization of epistaxis and juvenile nasopharyngeal angiofibromas. AJR Am J Roentgenol. 1987;148(1):209–18.
37. Gullane PJ, et al. Juvenile angiofibroma: a review of the literature and a case series report. Laryngoscope. 1992;102(8):928–33.
38. Moulin G, et al. Juvenile nasopharyngeal angiofibroma: comparison of blood loss during removal in embolized group versus nonembolized group. Cardiovasc Intervent Radiol. 1995;18(3):158–61.
39. Gao M, et al. A comparison of particulate and onyx embolization in preoperative devascularization of juvenile nasopharyngeal angiofibromas. Neuroradiology. 2013;55(9):1089–96.
40. Gemmete JJ, et al. Usefulness of percutaneously injected ethylene-vinyl alcohol copolymer in conjunction with standard endovascular embolization techniques for preoperative devascularization of hypervascular head and neck tumors: technique, initial experience, and correlation with surgical observations. AJNR Am J Neuroradiol. 2010;31(5):961–6.
41. Westbroek EM, et al. Comparison of complete and near-complete endovascular embolization of hypervascular spine tumors with partial embolization. J Neurosurg Spine. 2020;1(aop):1–7.
42. Awad AW, et al. The efficacy and risks of preoperative embolization of spinal tumors. J Neurointerv Surg. 2016;8(8):859–64.

43. Sullivan RD. Continuous intra-arterial infusion chemotherapy of head and neck cancer. Trans Am Acad Ophthalmol Otolaryngol. 1962;66:111–7.
44. Espiner HJ, Vowles KD, Walker RM. Cancer chemotherapy by intra-arterial infusion. A preliminary report concerning tumours of the head and neck. Lancet. 1962;1(7222):177–81.
45. Foote RL, et al. A pilot study of high-dose intraarterial cisplatin chemotherapy with concomitant accelerated radiotherapy for patients with previously untreated T4 and selected patients with T3N0-N3M0 squamous cell carcinoma of the upper aerodigestive tract. Cancer. 2005;103(3):559–68.
46. Rasch CR, et al. Intra-arterial versus intravenous chemoradiation for advanced head and neck cancer: results of a randomized phase 3 trial. Cancer. 2010;116(9):2159–65.
47. Homma A, et al. Intra-arterial chemoradiotherapy for head and neck cancer. Jpn J Clin Oncol. 2016;46(1):4–12.
48. Damascelli B, et al. Feasibility and efficacy of percutaneous transcatheter intraarterial chemotherapy with paclitaxel in albumin nanoparticles for advanced squamous-cell carcinoma of the oral cavity, oropharynx, and hypopharynx. J Vasc Interv Radiol. 2007;18(11):1395–403.
49. Yamane T, Kaneko A, Mohri M. The technique of ophthalmic arterial infusion therapy for patients with intraocular retinoblastoma. Int J Clin Oncol. 2004;9(2):69–73.
50. Abramson DH, et al. A phase I/II study of direct intraarterial (ophthalmic artery) chemotherapy with melphalan for intraocular retinoblastoma initial results. Ophthalmology. 2008;115(8):1398–404, 1404 e1.
51. Pekacka A. The role of intraarterial chemotherapy in the management of retinoblastoma. J Ophthalmol. 2020;2020:3638410.
52. Carli D, et al. Complications of particle embolization of meningiomas: frequency, risk factors, and outcome. Am J Neuroradiol. 2010;31(1):152–4.
53. Gungor D, Oğuz Ş, Dinc H. Mechanical removal of a refluxed Onyx piece from the middle cerebral artery using the Solitaire Stent: technical report. Interv Neuroradiol. 2017;23(3):293–6.
54. Cho AA, Annen M. Endovascular embolization of complex hypervascular skull base tumors. Oper Tech Otolaryngol Head Neck Surg. 2014;25(1):133–42.
55. Geibprasert S, et al. Dangerous extracranial-intracranial anastomoses and supply to the cranial nerves: vessels the neurointerventionalist needs to know. AJNR Am J Neuroradiol. 2009;30(8):1459–68.
56. Lasjaunias PL, Berenstein A, Raybaud C. Surgical neuroangiography. Berlin; New York: Springer-Verlag; 1987. p. 1, 3–5.
57. Harrigan MR, Deveikis JP. Handbook of cerebrovascular disease and neurointerventional technique. In: Contemporary medical imaging. 2nd ed. Dordecht: Humana Press; 2013. p. xvii, 850 pages.

Chapter 28
Balloon Test Occlusion, Wada Test and Inferior Petrosal Sinus Sampling

Ali Al Balushi and Jared Knopman

Balloon Test Occlusion

Introduction

Balloon test occlusion (BTO) is an invasive endovascular diagnostic procedure that is done to predict the risk of ischemic stroke in patients planned for therapeutic vessel sacrifice. It is aimed to evaluate the angiographic, clinical, and physiologic effects of temporarily occluding the vessel to determine the tolerability of permanent occlusion. There are many indications for therapeutic vessel sacrifice. These include treatment of cervical and intracranial vascular lesions not amenable to vessel-preserving endovascular or microsurgical techniques, like giant cervical or intracranial aneurysms and pseudoaneurysms, carotid cavernous fistulas, arterial dissections, tumor encasement and bleeding from iatrogenic, traumatic or tumor-related vessel injury [1, 2]. Vessel sacrifice without an occlusion test carries 17–30% risk of ischemic stroke and 12% mortality rate [2, 3]. There are multiple modifications to the standard BTO technique aimed to improve the positive predictive value and decrease the false negative rate. These techniques include hypotensive challenge, stump pressure measurement, neurophysiologic monitoring, venous phase delay evaluation, transcranial Doppler (TCD) evaluation of flow velocity, computed tomography (CT) or magnetic resonance imaging (MRI) perfusion, evaluation of cerebral blood flow with technetium Tc99m hexamethylpropyleneamine oxime, single-photon emission CT, positron-emission tomography (PET), and xenon-enhanced CT. The false negative rate of the standard BTO is 3%–15%, decreased to

A. Al Balushi · J. Knopman (✉)
Department of Neurological Surgery, Weill Cornell Medical College/New York Presbyterian Hospital, New York City, NY, USA
e-mail: aka4002@med.cornell.edu; jak9030@med.cornell.edu

J. R. Mascitelli, M. J. Binning (eds.), *Introduction to Vascular Neurosurgery*,
https://doi.org/10.1007/978-3-030-88196-2_28

3%–10% with the addition of different modifications like cerebral blood flow evaluation [4–6]. BTO is most commonly done for the internal carotid artery (ICA) but the vertebral artery can also be tested. Although this test is done mostly for arteries, it can also be done for venous sinuses in which the assessment is based on angiographic and physiologic data like intra-sinus venous pressure, as clinical effect of sinus occlusion may not be evident until several hours or days after occlusion [7, 8].

Finally, selective BTO without and with neurophysiologic monitoring can also be considered for intracranial arterial branches to determine the feasibility of vessel sacrifice in the evaluation of distal fusiform or mycotic aneurysms that are not amenable for targeted embolization.

Technique

Different techniques for BTO are described and practiced. The main principle is the evaluation of the ability of collateral circulation to maintain the cerebral perfusion of the affected vascular territory during the temporary occlusion. The procedure is done under local anesthesia with the patient awake for the neurologic deficits to be accurately evaluated, however, in emergency situations like life-threatening bleeding from iatrogenic or traumatic vessel injury, it can be done under general anesthesia and clinical exam is substituted by either angiographic evaluation alone or in combination with various other techniques described below. A baseline neurologic examination assessing cranial nerves, language, memory, visual, motor, and sensory function is recorded prior to the procedure. Pacing electrodes are attached to the patient's chest and atropine is kept ready at the bedside in case exaggerated vagal response during balloon inflation results in bradycardia and/or hypotension. Arterial access is established through the contralateral common femoral artery with a 6-French sheath. Activated clotting time (ACT) is checked and weight-based IV unfractionated heparin is given to achieve an ACT of 2–3 times the baseline. IV heparin is not given to patients with active or recent bleeding but all flush lines contain heparinized saline (5000 units in 1 L of normal saline). A complete diagnostic cerebral angiogram including bilateral common carotids, internal carotids, external carotids, and vertebral arteries is first performed with a 5-French diagnostic catheter. Information about the integrity of circle of Willis, collateral status, normal variants, and atherosclerotic plaques are obtained. The 5-French diagnostic catheter is then removed. For BTO of the ICA, a 6-French guide catheter is advanced into the common carotid artery of the desired BTO side and remains connected to continuous heparinized saline drip. Then, using a roadmap technique, a nondetachable balloon is advanced over the micro-wire through the guide catheter into the distal cervical or the horizontal segment of the petrous ICA. An alternative to the use of the guide catheter and nondetachable balloon system is to use a double lumen balloon guide catheter with the balloon positioned in the distal cervical ICA segment.

The balloon is gently inflated under fluoroscopy. Biplane angiography with contrast injection through the guide catheter is then obtained to confirm that the balloon is occlusive and that no anterograde flow past the balloon exists. The balloon remains inflated for a total of 15–30 minutes. If the sacrifice of the carotid artery is planned for an intracranial component or the common carotid artery is to be sacrificed, it is important to place the balloon across the ophthalmic segment to ensure that a false negative "pass" is not obtained due to external carotid artery retrograde flow via the ophthalmic artery. The patient is instructed to report any neurologic deficits and objective clinical examination is performed immediately after balloon inflation and then every 5 minutes. At the completion of the test, the balloon is deflated and removed. After balloon deflation, diagnostic angiography through the guide catheter is performed to ensure no vessel injury or distal embolization has occurred. Many centers adopt additional monitoring techniques, including neurophysiologic monitoring with continuous EEG to evaluate for slowing or change in the electrical activity of the involved hemisphere, especially in intubated patients. Another modification of the BTO technique is additional access from the other common femoral artery or right radial artery with a 5-French sheath and using a 5-French diagnostic catheter to catheterize the contralateral ICA before balloon inflation. After the balloon is inflated, biplane angiography with contrast injection through the contralateral ICA and later the dominant vertebral artery can be performed to evaluate the crossover of contrast to the affected territory. This will evaluate the degree of perfusion and venous phase delay compared to the other hemisphere. If any subjective or objective neurologic abnormalities are detected, the balloon is immediately deflated and angiography is performed through the guide catheter. At this point the test is considered a failure indicating that vessel sacrifice is high risk and would likely result in an ischemic stroke if no extracranial–intracranial bypass is performed prior to occlusion. After deflation, the balloon is slowly withdrawn inside the guide catheter and removed and post-BTO angiography is obtained. The guide catheter, diagnostic catheter, and sheaths are then removed and hemostasis is achieved by closure device and/or manual compression. Vertebral BTO is done in a similar fashion. The patient is then observed in the recovery room or ICU if vessel sacrifice follows the BTO.

Modifications of the Balloon Test Occlusion

Stump Pressure Measurements

To measure stump pressure while the balloon is inflated, double lumen balloon catheter is used for the BTO and the lumen distal to the balloon is connected to a pressure transducer. A maintained post-occlusion mean stump pressure of more than 60% of baseline mean arterial pressure (MAP) indicates adequate collateral perfusion; however, this method is shown to be inconsistent [9].

Hypotensive Challenge

Reduction of the MAP by 30% of the baseline after 20 minutes of tolerated balloon inflation while monitoring the neurologic examination or neurophysiologic monitoring is another method to assess the tolerance of balloon test occlusion. It has an overall low false negative rate, 5.3% reported in one study [10].

Transcranial Doppler

Ipsilateral middle cerebral artery (MCA) peak systolic velocity measurement before and after balloon inflation is a helpful method to determine if the patient can tolerate vessel sacrifice. An immediate drop in ipsilateral MCA peak systolic velocity after balloon inflation to 65% or more of the baseline velocity indicates good collateral reserve, while a drop to less than 54% correlates with a high risk of ischemia after vessel sacrifice [1].

Venous Phase Delay

Evaluation of the ipsilateral venous phase after contralateral ICA contrast injection while the balloon is inflated is used in many centers as the preferred angiographic run. Compared to the contralateral venous phase, ipsilateral venous phase delay of less than 0.5 second was found to have 98% positive predictive value of successful BTO while delay less than 2 seconds correlated with 95% of successful tests. A delay of 3 seconds or more indicates poor tolerability of permanent occlusion [9, 11]. The venous phase delay evaluation method carries the advantage of very short balloon inflation time of 60–90 seconds only. Combined with TCD, the positive predictive value of this method is further augmented [11].

Cerebral Perfusion Assessment

Evaluation of cerebral blood flow (CBF) in patients who tolerate the standard BTO is another useful method to enhance the positive predictive value and reduce false negative rate of the test. There are different methods to calculate the CBF including SPECT, CT Perfusion with Acetazolamide challenge, Xenon CT perfusion, PET, and MR perfusion. Essentially, the techniques provide information about changes in regional cerebral perfusion during BTO compared to baseline. These imaging-based techniques require the angiography suite be equipped with the capability to perform the imaging or the patient needs to be transported to different imaging suites with balloon and catheter in the major vessel which increases the risk of vessel injury.

Neurophysiologic Monitoring

The addition of neurophysiologic monitoring is particularly useful in patients who are sedated or in whom neurologic examination cannot be reliably evaluated. Electroencephalography (EEG), somatosensory, and brainstem-evoked potentials (SSEP and BSEP) are examples of neurophysiologic monitoring data sources. The most commonly used neurophysiologic method is continuous EEG which shows electrographic evidence of ischemia at CBF level of less than 10 mL/100 g/min even when clinical deficits are not yet evident [9]. SSEP similarly shows evidence of reduction of amplitude and prolongation of central conduction time at CBF level less than 15 mL/100 g/min [8, 9].

Complications

Possible complications of the BTO procedure are intimal damage resulting in dissections, pseudoaneurysms, distal thromboembolism, vessel rupture, vasospasm, and access site complications. The complication rate of BTO is less than 3.5% and the mortality rate is 0% [5, 8].

Wada Test

Introduction

Juhn Wada performed the first intracarotid sodium amobarbital injection in the 1940s to investigate the mechanisms of interhemispheric spread of an epileptic focus in human seizures [12]. He noticed temporary loss of function in the injected hemisphere, for example, aphasia in the hemisphere harboring language centers. In 1960, Wada described the technique in collaboration with Rasmussen and used this test to lateralize language dominance. Wada test or intracarotid amobarbital test (IAT) is performed as part of the presurgical evaluation for patients with refractory focal epilepsy with the main aim of lateralizing language and memory function in either cerebral hemisphere to determine the feasibility and extent of surgical resection and predict postoperative neurologic dysfunction [13, 14]. Typical patients undergoing epilepsy surgery are those with identifiable brain lesions like temporal lobe epilepsy due to mesial temporal sclerosis, tumors, arteriovenous malformation, or focal cortical dysplasia; however, other patients with a defined epileptic focus without imaging abnormalities may also be considered [15]. Anterior temporal lobectomy and amygdalohippocampectomy are the most commonly performed epilepsy surgeries and given that language and memory are localized in the temporal

lobe, Wada testing provides valuable information that guides the surgical planning [16]. Similarly, with frontal lobe lesions, language localization provides essential information. Wada testing is performed in collaboration with a team consisting of an epileptologist, neurophysiologist, and neuropsychologist, in addition to neurophysiology technical staff. Sodium amobarbital is a short-acting barbiturate drug that potentiates GABA-mediated inhibition in the brain, thereby explaining its temporary anesthetic effects on the hemispheric neurons supplied by the ipsilateral injected carotid artery [17].

Technique

The procedure is performed with the patient awake and connected to continuous EEG monitoring. Sedative medications are not given as they would interfere with memory evaluation and EEG interpretation. The patient is given instructions about how the test will be conducted. A baseline neurologic and neuropsychological examination is established, and a baseline awake EEG is obtained. The patient is then brought to the angiography room and placed in a supine position. A 4- or 5-French sheath is inserted in either common femoral artery under local anesthesia and a 4- or 5-French diagnostic catheter is used to catheterize the internal carotid artery supplying the hemisphere of surgical interest. Diagnostic cerebral angiography is performed to evaluate the cerebral vascular anatomy. The catheter positioned in the proximal cervical internal carotid artery is then connected to continuous heparinized saline drip using a 3-way stopcock, and the angiography table is moved away from the x-ray machine. The team is asked to enter the room at this stage. A 50-mL syringe containing 500 mg amobarbital in 50 mL of normal saline is prepared. Using a 3-way stopcock, a 10-mL syringe is connected to the 3-way and used to draw up 10 mL (100 mg amobarbital). The 3-way stopcock is connected to the catheter. As the team is ready for the test with the neuropsychologist, epileptologist, and neurophysiology staff in the room at bedside, the patient is asked by the neuropsychologist to keep the arms up and loudly count down from 10 to 1. At this time, 100 mg of amobarbital (10 mL) is infused over 3–5 seconds. The lock is then opened to the saline drip and another 3 mL of amobarbital is prepared in the 10-mL syringe by aspirating from the 50-mL syringe through the 3-way stopcock, in case if it is needed. The effects of amobarbital are immediate, and clinical signs of contralateral arm drift, hemiplegia, and ipsilateral gaze deviation develop soon after injection. Also, the cEEG shows background attenuation in the affected hemisphere. At this stage, the catheter is removed. Over the next 5–10 minutes, a series of neuropsychologic tests are carried out evaluating different domains of language and memory. After 30–45 minutes when the clinical and electrographic effects of amobarbital resolve, a neurologic exam is carried out and then the procedure continues with catheterizing the contralateral ICA in the same fashion. At the end of the procedure, the catheter and sheath are removed and hemostasis is obtained by a closure device and/or manual compression. It is important to mention that careful evaluation of the

initial angiographic images before amobarbital infusion is critical. For example, if a brisk anterior communicating artery flow is present, a slower infusion is given to avoid significant crossover to the contralateral hemisphere. Similarly, if the diagnostic angiogram demonstrates carotid-basilar anastomosis like persistent primitive trigeminal artery variant, then the drug delivery must be given past this variant to avoid infusing amobarbital into the brainstem, which if happened would suppress the critical respiratory and cardiac centers. In this case, the ACT is checked and weight-based unfractionated heparin is given intravenously to achieve ACT of 2–3 times the baseline. While in the proximal cervical internal carotid artery, the diagnostic catheter is then connected to continuous heparinized saline drip and a microcatheter is advanced through the diagnostic catheter over a microwire to the internal carotid artery past the variant artery and amobarbital is infused through the microcatheter.

Similar to Wada testing, spinal provocative testing utilizing neurophysiological monitoring, also known as a spinal Wada test, can be done for patients with spinal cord arteriovenous malformation (AVM) in whom the spinal arteries originate from the same feeding pedicle to determine the safety of embolization and/or resection. Smaller doses of amobarbital or lidocaine are infused selectively through a microcatheter positioned in the AVM feeding pedicle [18].

Current Role in Epilepsy Presurgical Evaluation

The Wada test has long been considered the gold standard test against which newer modalities have been compared [19]. New noninvasive imaging-based tests that are cheaper, less resource- and personnel- intensive are increasingly utilized to replace Wada testing. These tests include functional MRI (fMRI), magnetoencephalography (MEG), transcranial magnetic stimulation (TMS), and positron-emission tomography (PET). The fMRI, specifically, has been shown to carry a very high concordance rate with Wada testing and is considered by many centers as the new gold standard for eloquent cortex lateralization, including language areas [20, 21]. With the increased utilization of fMRI, the performance of Wada tests has declined significantly over the past 2 decades despite significantly increased numbers of epilepsy surgeries [14, 19]. The Wada test remains a valuable tool especially in patients who are unable to undergo fMRI due to claustrophobia or metal implants and in those with atypical language localization in both hemispheres on fMRI [20].

Alternative Agents

Amobarbital is the standard drug used in Wada test. However, because of its global shortage, alternative short-acting agents have been studied and found to be safe alternatives including etimodate, propofol, methohexital, and pentobarbital [22]. Methohexital is a short-acting barbiturate sedative that was shown to yield

comparative results to amobarbital during Wada test [23]. It has a shorter half-life than amobarbital. It is given as a 3-mg initial bolus followed by additional 2 mg if needed [24].

Complications

Overall, the Wada test has a very low complication rate of about 1% [8, 14]. These complications include carotid artery injury resulting in dissection, cerebral ischemia from thromboembolism and femoral access site complications.

Inferior Petrosal Sinus Sampling

Introduction

Bilateral inferior petrosal sinus sampling (IPSS) is a dynamic neuroendovascular test technique used to sample central venous blood directly and simultaneously from the inferior petrosal sinuses in conjunction with peripheral venous blood sampling to measure adrenocorticotropic hormone (ACTH) levels in the course of evaluating the etiology of Cushing's disease, or ACTH-dependent hypercortisolism [25]. IPSS also helps to lateralize the side of ACTH hypersecretion if the source is from the pituitary gland [26]. The anterior pituitary gland drains into the cavernous sinus, which in turn drains into the internal jugular veins through ipsilateral inferior petrosal sinuses. Patients undergoing IPSS often present with symptoms and signs of hypercortisolism to the endocrinologists who run diagnostic tests to confirm the diagnosis and evaluate the source of cortisol excess. The IPSS test is indicated in patients who are diagnosed with ACTH-dependent hypercortisolism. ACTH-dependent hypercortisolism accounts for 80% of all causes of endogenous hypercortisolism and includes ACTH-secreting pituitary tumors and ectopic ACTH-hypersecretion from tumors in the lungs, pancreas, or small bowel but they may occur anywhere in the body, or rarely from ectopic corticotrophin-releasing hormone (CRH) production [27]. Surgical resection of the hypersecreting tumor is the mainstay of treatment of ACTH-dependent hypercortisolism. MRI of the brain with thin cuts through the sella turcica is obtained to look for pituitary tumors. In patients with MRI evidence of pituitary adenoma, the tumor may not necessarily be the source of ACTH overproduction given that nonfunctioning incidentalomas are found in up to 10% of the general population. Similarly, normal imaging does not rule out a pituitary source of ACTH hypersecretion as 40% of confirmed cases of Cushing disease have a normal MRI [28].

The IPSS technique requires time and utilization of resources for the collection of samples according to the protocol for blood sample collections of central and

Table 28.1 IPSS test collection samples and reporting

Sampling location	Test	Before CRH administration		After CRH administration			
		–5 minutes	0 minutes	2 minutes	5 minutes	10 minutes	15 minutes
Right IPSS	ACTH						
	Prolactin						
Left IPSS	ACTH						
	Prolactin						
Peripheral	ACTH						
	Prolactin						
	Cortisol						

peripheral ACTH and cortisol levels before and after stimulation with peripheral intravenous CRH. Measuring prolactin hormone levels helps to increase the diagnostic accuracy of the IPSS test and biochemically confirm accurate collection site [29, 30]. The IPSS procedure requires teamwork with every team member receiving clear instructions about their role prior to the start, and the samples are properly labeled, handled, stored, and later sent to the laboratory. The lab should be notified ahead of time to prepare to receive the samples. The lab results are released in a table format with each result corresponding to its location and collection time relevant to CRH stimulation. Table 28.1 shows a sample of the collection and reporting protocol used at our institution.

Technique

The patient is placed in a supine position. Under local anesthesia, venous access is established through the bilateral common femoral veins. A 5-French sheath is placed on one side and a 6-French sheath is placed on the other side. A baseline ACT is checked after venous access and weight-based unfractionated heparin can be given intravenously through the sheath after the second sheath is inserted. The larger (6 French) sheath is also used for peripheral blood sample collection. Under fluoroscopic guidance, a 5-French guide catheter is advanced over the guidewire via the 6-French sheath through the inferior vena cava into the distal internal jugular vein of the same sheath side, for convenience and to avoid side confusion. The guidewire is then removed and the catheter is connected to continuous heparinized saline drip (5000 units of IV unfractionated heparin in 1 L of normal saline). Next, under fluoroscopic guidance, a microcatheter is advanced over a microwire to the proximal inferior petrosal sinus, the microwire is then removed. A diagnostic run through the microcatheter is obtained to ensure proper positioning of the microcatheter. The microcatheter is then connected to continuous heparinized saline drip. Next, using the contralateral femoral 5-French sheath, a 5-French guide catheter is

advanced over the guidewire through the inferior vena cava into the distal segment of the other internal jugular vein. The guidewire is then removed and the catheter is connected to continuous heparinized saline drip. Next, under fluoroscopic guidance, a microcatheter is advanced over a microwire through the guide catheter to the proximal inferior petrosal sinus of the opposite side, the microwire is then removed. A diagnostic run through the microcatheter is obtained to ensure proper positioning of the microcatheter (Fig. 28.1). The microcatheter is then connected to continuous heparinized saline drip. The team is made ready for the start of the collection at the predetermined time intervals. At the team leader's instruction, the saline drips are disconnected from the microcatheters and the 6-French sheath, and the team withdraws 2 mL of blood waste at the same time from each site: two central samples from the microcatheters and one peripheral sample from the 6-French femoral sheath. Immediately and synchronously on instruction, another 2 mL is collected from each site at the different time intervals: baseline, and then 2, 5, 10, and 15 minutes after administration of intravenous CRH (1 mcg/kg, max 100 mcg). The blood samples are labeled with their respective location and timing and placed in an ice container to be delivered to the laboratory. At the end of the procedure, the microcatheters and guide catheters are removed under fluoroscopy, one at a time. The femoral venous sheaths are then removed and hemostasis is achieved via closure device and/or manual compression.

Fig. 28.1 bilateral inferior petrosal sinuses sampling (injection from microcatheter in left inferior petrosal sinus, arrow)

Interpretation

A ratio of central to peripheral ACTH of 2.0 or more at baseline or 3.0 or more after CRH stimulation is consistent with Cushing's disease, i.e., pituitary source [26]. The overall sensitivity and specificity of IPSS are 96–100% and 100%, respectively [26, 31]. IPSS with CRH stimulation test is the most accurate and reliable test differentiating pituitary from non-pituitary ACTH-dependent causes of ACTH hypersecretion and is considered the gold standard [31].

Complications

The IPSS procedure has a very low complication risk of less than 1% with the most common complication being access site hematoma [25]. Difficulties catheterizing the inferior petrosal sinuses or improper positioning of the catheter decreases the diagnostic yield of the procedure.

Conclusion

The neuroendovascular diagnostic techniques described in this chapter are powerful tools that provide important information and guide treatment decisions. For example, in patients who pass balloon test occlusion, the parent vessel can be subsequently sacrificed either endovascularly or surgically depending on the indication and urgent nature of the vessel sacrifice. Basic understanding of the indications, technical aspects, and interpretations of balloon test occlusion, Wada testing, and IPSS procedures cannot be overemphasized.

References

1. Sorteberg A, Bakke SJ, Boysen M, Sorteberg W. Angiographic balloon test occlusion and therapeutic sacrifice of major arteries to the brain. Neurosurgery. 2008;63(4):651–61. https://doi.org/10.1227/01.NEU.0000325727.51405.D5.
2. Chaudhary N, Gemmete JJ, Thompson BG, Pandey AS. Intracranial endovascular balloon test occlusion-indications, methods, and predictive value. Neurosurg Clin N Am. 2009;20(3):369–75. https://doi.org/10.1016/j.nec.2009.01.004.
3. American Society of Interventional and Therapeutic Neuroradiology. Carotid artery balloon test occlusion. AJNR Am J Neuroradiol. 2001;22(8 Suppl):S8–9.
4. Linskey ME, Jungreis CA, Yonas H, et al. Stroke risk after abrupt internal carotid artery sacrifice: accuracy of preoperative assessment with balloon test occlusion and stable xenon-enhanced CT. AJNR Am J Neuroradiol. 1994;15(5):829–43.

5. Mathis JM, Barr JD, Jungreis CA, et al. Temporary balloon test occlusion of the internal carotid artery: experience in 500 cases. AJNR Am J Neuroradiol. 1995;16(4):749–54.
6. Matsubara N, Izumi T, Okamoto S, et al. Multimodal assessment for balloon test occlusion of the internal carotid artery. J Neuroendovasc Therapy. 2016;10(3):108–15. https://doi.org/10.5797/jnet.oa.2015-0012.
7. Ernemann U, Löwenheim H, Freudenstein D, Koerbel A, Heininger A, Tatagiba M. Hemodynamic evaluation during balloon test occlusion of the sigmoid sinus: clinical and technical considerations. AJNR Am J Neuroradiol. 2005;26(1):179–82.
8. Hurst RW, Rosenwasser R. Neurointerventional management: diagnosis and treatment. 2nd ed. New York: Informa Healthcare; 2012. 254p.
9. Elias AE, Chaudhary N, Pandey AS, Gemmete JJ. Intracranial endovascular balloon test occlusion: indications, methods, and predictive value. Neuroimaging Clin N Am. 2013;23(4):695–702. https://doi.org/10.1016/j.nic.2013.03.015.
10. Standard SC, Ahuja A, Guterman LR, et al. Balloon test occlusion of the internal carotid artery with hypotensive challenge. AJNR Am J Neuroradiol. 1995;16(7):1453–8.
11. Sorteberg A. Balloon occlusion tests and therapeutic vessel occlusions revisited: when, when not, and how. AJNR Am J Neuroradiol. 2014;35(5):862–5. https://doi.org/10.3174/ajnr.A3852.
12. Wada J, Rasmussen T. Intracarotid injection of sodium amytal for the lateralization of cerebral speech dominance: experimental and clinical observations. J Neurosurg. 1960;17:266–82.
13. Rosenow F, Lüders H. Presurgical evaluation of epilepsy. Brain. 2001;124(9):1683–700.
14. Haag A, Knake S, Hamer HM, et al. The Wada test in Austrian, Dutch, German, and Swiss epilepsy centers from 2000 to 2005: a review of 1421 procedures. Epilepsy Behav. 2008;13(1):83–9. https://doi.org/10.1016/j.yebeh.2008.02.012.
15. Manford M. Recent advances in epilepsy. J Neurol. 2017;264(8):1811–24. https://doi.org/10.1007/s00415-017-8394-2.
16. Ramey WL, Martirosyan NL, Lieu CM, Hasham HA, Lemole GM Jr, Weinand ME. Current management and surgical outcomes of medically intractable epilepsy. Clin Neurol Neurosurg. 2013;115(12):2411–8. https://doi.org/10.1016/j.clineuro.2013.09.035.
17. Mathers DA, Wan X, Puil E. Barbiturate activation and modulation of GABA(A) receptors in neocortex. Neuropharmacology. 2007;52(4):1160–8. https://doi.org/10.1016/j.neuropharm.2006.12.004.
18. Niimi Y, Sala F, Deletis V, Setton A, de Camargo AB, Berenstein A. Neurophysiologic monitoring and pharmacologic provocative testing for embolization of spinal cord arteriovenous malformations. AJNR Am J Neuroradiol. 2004;25(7):1131–8.
19. Baxendale S. The Wada test. Curr Opin Neurol. 2009;22(2):185–9. https://doi.org/10.1097/WCO.0b013e328328f32e.
20. Bauer PR, Reitsma JB, Houweling BM, Ferrier CH, Ramsey NF. Can fMRI safely replace the Wada test for preoperative assessment of language lateralisation? A meta-analysis and systematic review. J Neurol Neurosurg Psychiatry. 2014;85(5):581–8. https://doi.org/10.1136/jnnp-2013-305659.
21. Janecek JK, Swanson SJ, Sabsevitz DS, et al. Language lateralization by fMRI and Wada testing in 229 patients with epilepsy: rates and predictors of discordance. Epilepsia. 2013;54(2):314–22. https://doi.org/10.1111/epi.12068.
22. Patel A, Wordell C, Szarlej D. Alternatives to sodium amobarbital in the Wada test. Ann Pharmacother. 2011;45(3):395–401. https://doi.org/10.1345/aph.1P476.
23. Conradi N, Rosenberg F, Biermann L, Haag A, Hermsen A, Gorny I, von Podewils V, Gurschi M, Keil F, Hattingen E, Menzler K, Bauer S, Schubert-Bast S, Knake S, Rosenow F, Strzelczyk A. Advantages of methohexital over amobarbital in determining hemispheric language and memory lateralization in the Wada test – a retrospective study. Epilepsy Behav. 2020;113:107551. https://doi.org/10.1016/j.yebeh.2020.107551. Epub 2020 Nov 24.
24. Loddenkemper T, Möddel G, Dinner DS, Kim H, Schuele SU, Alexopoulos AV, Kotagal P, Lüders HO. Language assessment in Wada test: comparison of methohexital and amobarbital. Seizure. 2009;18(9):656–9. https://doi.org/10.1016/j.seizure.2009.08.002. Epub 2009 Oct 1.

25. Miller DL, Doppman JL. Petrosal sinus sampling: technique and rationale. Radiology. 1991;178(1):37–47. https://doi.org/10.1148/radiology.178.1.1845785.
26. Oldfield EH, Doppman JL, Nieman LK, et al. Petrosal sinus sampling with and without corticotropin-releasing hormone for the differential diagnosis of Cushing's syndrome [published correction appears in N Engl J Med 1992;326(17):1172]. N Engl J Med. 1991;325(13):897–905. https://doi.org/10.1056/NEJM199109263251301.
27. Losa M, Allora A, Panni P, Righi C, Mortini P. Bilateral inferior petrosal sinus sampling in adrenocorticotropin-dependent hypercortisolism: always, never, or sometimes? J Endocrinol Investig. 2019;42(8):997–1000. https://doi.org/10.1007/s40618-019-1006-5.
28. Newell-Price J, Bertagna X, Grossman AB, Nieman LK. Cushing's syndrome. Lancet. 2006;367(9522):1605–17. https://doi.org/10.1016/S0140-6736(06)68699-6.
29. Grant P, Dworakowska D, Carroll P. Maximizing the accuracy of inferior petrosal sinus sampling: validation of the use of prolactin as a marker of pituitary venous effluent in the diagnosis of Cushing's disease. Clin Endocrinol. 2012;76(4):555–9. https://doi.org/10.1111/j.1365-2265.2011.04257.x.
30. Sharma ST, Raff H, Nieman LK. Prolactin as a marker of successful catheterization during IPSS in patients with ACTH-dependent Cushing's syndrome. J Clin Endocrinol Metab. 2011;96(12):3687–94. https://doi.org/10.1210/jc.2011-2149.
31. Kola B, Grossman AB. Dynamic testing in Cushing's syndrome. Pituitary. 2008;11(2):155–62. https://doi.org/10.1007/s11102-007-0079-x.

Index

J. R. Mascitelli, M. J. Binning (eds.), *Introduction to Vascular Neurosurgery*,
https://doi.org/10.1007/978-3-030-88196-2